

JSCSEN 89(11) 1401-1524 (2024)

ISSN 1820-7421(Online)

Journal of the Serbian Chemical Society

Electronic

VOLUME 89

NO 11

BELGRADE 2024

Available on line at



www.shd.org.rs/JSCS/

The full search of JSCS
is available through

DOAJ DIRECTORY OF
OPEN ACCESS
JOURNALS
www.doaj.org

The **Journal of the Serbian Chemical Society** (formerly Glasnik Hemijskog društva Beograd), one volume (12 issues) per year, publishes articles from the fields of chemistry. The **Journal** is financially supported by the **Ministry of Education, Science and Technological Development of the Republic of Serbia**.

Articles published in the **Journal** are indexed in **Clarivate Analytics products: Science Citation Index-Expanded™** – accessed via **Web of Science®** and **Journal Citation Reports®**.

Impact Factor announced on 28 June, 2023: **1.000**; **5-year Impact Factor: 1.100**.

Articles appearing in the **Journal** are also abstracted by: **Scopus, Chemical Abstracts Plus (CAplusSM), Directory of Open Access Journals, Referativnii Zhurnal (VINITI), RSC Analytical Abstracts, EuroPub, Pro Quest and Asian Digital Library.**

Publisher:

Serbian Chemical Society, Karnegijeva 4/III, P. O. Box 36, 1120 Belgrade 35, Serbia
tel./fax: +381-11-3370-467, E-mails: **Society** – shd@shd.org.rs; **Journal** – jscs@shd.org.rs
Home Pages: **Society** – <http://www.shd.org.rs/>; **Journal** – <http://www.shd.org.rs/JSCS/>
Contents, Abstracts and full papers (from Vol 64, No. 1, 1999) are available in the electronic form at the Web Site of the **Journal** (<http://www.shd.org.rs/JSCS/>).

Internet Service:

Former Editors:

Nikola A. Pušin (1930–1947), **Aleksandar M. Leko** (1948–1954),
Panta S. Tutundžić (1955–1961), **Miloš K. Mladenović** (1962–1964),
Đorđe M. Dimitrijević (1965–1969), **Aleksandar R. Despić** (1969–1975),
Slobodan V. Ribnikar (1975–1985), **Dragutin M. Dražić** (1986–2006).

Editor-in-Chief:

BRANISLAV Ž. NIKOLIĆ, Serbian Chemical Society (E-mail: jscs-ed@shd.org.rs)

Deputy Editor:

DUŠAN SLADIĆ, Faculty of Chemistry, University of Belgrade

Sub editors:

Organic Chemistry

DEJAN OPSENICA, Institute of Chemistry, Technology and Metallurgy, University of Belgrade

Biochemistry and

Biotechnology

JÁNOS CSANÁDI, Faculty of Science, University of Novi Sad

Inorganic Chemistry

OLGICA NEDIĆ, INEP – Institute for the Application of Nuclear Energy, University of Belgrade

Theoretical Chemistry

BILJANA GLIŠIĆ, Faculty of Science, University of Kragujevac

Physical Chemistry

IVAN JURANIĆ, Serbian Chemical Society

Electrochemistry

LJILJANA DAMJANOVIĆ-VASILJIĆ, Faculty of Physical Chemistry, University of Belgrade

Analytical Chemistry

SNEŽANA GOJKOVIĆ, Faculty of Technology and Metallurgy, University of Belgrade

Polymers

RADA BAOŠIĆ, Faculty of Chemistry, University of Belgrade

Thermodynamics

BRANKO DUNJIĆ, Faculty of Technology and Metallurgy, University of Belgrade

Chemical Engineering

MIRJANA KIJEVCANIN, Faculty of Technology and Metallurgy, University of Belgrade

Materials

TATJANA KALUĐEROVIĆ RADOIČIĆ, Faculty of Technology and Metallurgy, University of Belgrade

Metallic Materials and

Metallurgy

RADA PETROVIĆ, Faculty of Technology and Metallurgy, University of Belgrade

Environmental and

Geochemistry

ANA KOSTOV, Mining and Metallurgy Institute Bor, University of Belgrade

History of and

Education in Chemistry

VESNA ANTIĆ, Faculty of Agriculture, University of Belgrade

English Language

DRAGICA TRIVIĆ, Faculty of Chemistry, University of Belgrade

Editors:

LYNNE KATSIKAS, Serbian Chemical Society

VLATKA VAJS, Serbian Chemical Society

JASMINA NIKOLIĆ, Faculty of Technology and Metallurgy, University of Belgrade

Technical Editors:

VLADIMIR PANIĆ, Institute of Chemistry, Technology and Metallurgy, University of Belgrade

MARIO ZLATOVIĆ, Faculty of Chemistry, University of Belgrade

Journal Manager &

Web Master:

MARIO ZLATOVIĆ, Faculty of Chemistry, University of Belgrade

Office:

VERA ČUŠIĆ, Serbian Chemical Society

Editorial Board

From abroad: R. Adžić, Brookhaven National Laboratory (USA); A. Casini, University of Groningen (The Netherlands); G. Cobb, Baylor University (USA); D. Douglas, University of British Columbia (Canada); G. Inzelt, Etvos Lorand University (Hungary); J. Kenny, University of Perugia (Italy); Ya. I. Korenman, Voronezh Academy of Technology (Russian Federation); M. D. Lechner, University of Osnabrueck (Germany); S. Macura, Mayo Clinic (USA); M. Spiteller, INFU, Technical University Dortmund (Germany); M. Stratakis, University of Crete (Greece); M. Swart, University de Girona (Cataluna, Spain); G. Vunjak-Novaković, Columbia University (USA); P. Worsfold, University of Plymouth (UK); J. Zagal, Universidad de Santiago de Chile (Chile).

From Serbia: B. Abramović, V. Antić, R. Baošić, V. Bešković, J. Csanadi, Lj. Damjanović-Vasiljić, A. Dekanski, V. Dondur, B. Dunjić, M. Đuran, B. Glišić, S. Gojković, I. Gutman, B. Jovančičević, I. Juranić, T. Kaluđerović Radiočić, L. Katsikas, M. Kijevcanin, A. Kostov, V. Leovac, S. Milonjić, V.B. Mišković-Stanković, O. Nedić, B. Nikolić, J. Nikolić, D. Opsenica, V. Panić, M. Petkovska, R. Petrović, I. Popović, B. Radak, S. Ražić, D. Sladić, S. Sovilj, S. Šerbanović, B. Šolaja, Ž. Tešić, D. Trivić, V. Vajs, M. Zlatović.

Subscription: The annual subscription rate is 150.00 € including postage (surface mail) and handling. For Society members from abroad rate is 50.00 €. For the proforma invoice with the instruction for bank payment contact the Society Office (E-mail: shd@shd.org.rs) or see JSCS Web Site: <http://www.shd.org.rs/JSCS/>, option Subscription.

Godišnja pretplata: Za članove SHD: 2.500,00 RSD, za penzionere i studente: 1000,00 RSD, a za ostale: 3.500,00 RSD; za organizacije i ustanove: 16.000,00 RSD. Uplate se vrše na tekući račun Društva: 205-13815-62, poziv na broj 320, sa naznakom "pretplata za JSCS".

Nota: Radovi čiji su svi autori članovi SHD prioritetno se publikuju.

Odlukom Odbora za hemiju Republičkog fonda za nauku Srbije, br. 66788/1 od 22.11.1990. godine, koja je kasnije potvrđena odlukom Saveta Fonda, časopis je uvršten u kategoriju međunarodnih časopisa (M-23). Takođe, aktom Ministarstva za nauku i tehnologiju Republike Srbije, 413-00-247/2000-01 od 15.06.2000. godine, ovaj časopis je proglašen za publikaciju od posebnog interesa za nauku. **Impact Factor** časopisa objavljen 28. juna 2023. godine je 1,000, a petogodišnji **Impact Factor** 1,100.



CONTENTS*

Organic Chemistry

- H. S. Aziz, I. Q. M. Al-Araj, L. R. Abdul-Raheem and A. A. Ahmed:* Synthesis and biological evaluation of some new heterocyclic derivatives from substituted thiopyrimidine 1401
- M. Nassiri Koopaei, M. Monavari, N. Vousooghi, S. Moshirabadi, M. J. Assarzadeh, M. Amini and A. Almasirad:* Synthesis and *in silico* ADMET evaluation of new thiazole and thiazolidine-4-one derivatives as non-ulcerogenic analgesic and anti-inflammatory agents 1411

Biochemistry and Bioengineering

- B. Karayavuz, S. K. Vagolu, D. Kart, T. Tönjum and O. Unsal-Tan:* Synthesis, antimicrobial and antifungal evaluation of new 4-(furan-2-ylmethyl)-6-methylpyridazin-3(2*H*)-ones 1423

Theoretical Chemistry

- W. López-Orozco, L. H. Mendoza-Huizar, G. A. Álvarez-Romero, J. M. Torres-Valencia and M. Sanchez-Zavala:* Chemical reactivity of alliin and its molecular interactions with the protease Mpro of SARS-CoV-2 1433
- A. Belhassan, G. Salgado, L. H. Mendoza-Huizar, H. Zaki, S. Chtita, T. Lakhlifi, M. Bouachrine, L. Gerli Candia and W. Cardona:* Identification of musk compounds as inhibitors of the main SARS-CoV-2 protease by molecular docking and molecular dynamics studies 1447

Analytical Chemistry

- A. Redžepović-Dorđević, M. Dodevska, M. Jovetić and M. Ačanski:* Fiber and microelements content in various types of wheat bread 1461
- M. Niculescu, M.-C. Pascariu, A. Racu and B.-O. Taranu:* Thermal behavior of polymeric nickel(II) oxalate complex obtained through nickel(II) nitrate/ethylene glycol reaction 1475

Thermodynamics

- N. Chakraborty, P. Thakur, K. C. Juglan and A. H. Syed:* Thermophysical investigation of glycol ethers in mannitol solutions at various temperatures 1489

History of and Education in Chemistry

- F. Stašević, A. Bubanja, A. Maksimović and J. Đurđević Nikolić:* Chemistry educational outcomes and standards in Serbia and Montenegro. Analysis of the teachers' attitudes and high school students' achievements 1507

Published by the Serbian Chemical Society
Karnegijeva 4/III, P.O. Box 36, 11120 Belgrade, Serbia
Printed by the Faculty of Technology and Metallurgy
Karnegijeva 4, P.O. Box 35-03, 11120 Belgrade, Serbia

* For colored figures in this issue please see electronic version at the Journal Home Page:
<http://www.shd.org.rs/JSCS/>



J. Serb. Chem. Soc. 89 (11) 1401–1410 (2024)
JSCS–5795

Synthesis and biological evaluation of some new heterocyclic derivatives from substituted thiopyrimidine

HADIL S. AZIZ, INTISAR Q. M. AL-ARAJ*, LINDA R. ABDUL-RAHEEM
and AMENA A. AHMED

Chemistry Department, College of Education for Pure Sciences, University of Mosul, Mosul, Iraq

(Received 13 August, revised 9 September 2023, accepted 30 June 2024)

Abstract: This study aimed at creation of a few new heterocyclic compounds that include sulfur and nitrogen atoms. Also, some chalcones, thiazolidine and Schiff base derivatives have been prepared. The spectroscopic data (IR, ¹H- and ¹³C-NMR) have verified the structure of the produced molecules. Interesting findings were obtained when several synthetic substances were physiologically tested against a range of pathogenic Gram-positive and Gram-negative bacteria.

Keywords: thiazolidine; chalcones; Schiff bases; cyclization; pathogenic bacteria.

INTRODUCTION

Cyclic organic compounds, known as heterocyclic compounds, at least have one heteroatom other than carbon in the cyclic ring structure. The three most prevalent heteroatoms are oxygen, nitrogen and sulfur.¹ The most significant natural organic heterocyclic compounds are usually found in large quantities in the products of both plants and animals.² The use of heterocyclic compounds is widespread in the fields of agrochemical, pharmaceutical and veterinary applications.³ Numerous heterocyclic substances are extremely beneficial and necessary for human life.⁴ Hormones, vital amino acids, antibiotics, alkaloids, haemoglobin, vitamins, dyes and pigments are only a few examples of the many substances with heterocyclic structures.⁵ Many pharmaceuticals and agrochemicals contain at least one heterocyclic unit; heterocycles play an important role in many natural products.⁶ Important building blocks for novel materials with interesting electrical, mechanical or biological properties incorporate heterocyclic systems.⁷

Pyrimidine has two nitrogen atoms and a six-membered heterocyclic structure.⁸ It is essential component of nucleic acid and widely distributed in nature in

*Corresponding author. E-mail: Mahmood_intisar@uomosul.edu.iq
<https://doi.org/10.2298/JSC230813067A>



the form of N-substituted sugar derivatives (nucleosides).⁹ Cytosine, thymine and uracil are pyrimidines that contribute to the distinctive three-dimensional structure of RNA and the double helix of DNA.¹⁰ Pyrimidine and its derivatives are one of the most significant heterocyclic nitrogenous cycles. They are important enough to a variety of biological activities.¹¹ The ring system of pyrimidine is found in several vitamins, antibiotics, alkaloids and nucleic acids and their derivatives.¹²

Thiazolidine is a chemical compound found in many pharmaceutical drugs. It has been shown to have anti-inflammatory and antioxidant properties.¹³ Thiazolidine has been studied for its potential use as a treatment for conditions such as arthritis and diabetes.¹⁴ Also, it may help improve cognitive function and memory retention.¹⁵ Its derivatives also exhibit anti-inflammatory and anti-tumor properties,¹⁶ that make them promising candidates for treating chronic inflammatory and certain types of diseases.¹⁷ After all, thiazolidine and its derivatives have shown great promise as a versatile class of drugs with diverse therapeutic applications.¹⁸

Chalcones are natural compounds found in plants and they have gained significant attention due to their diverse biological activities.¹⁹ They have potential in reducing inflammation, treating cancer and managing diabetes.²⁰ These compounds employ their medicinal properties by affecting various signaling pathways and enzymes, leading to a wide range of therapeutic effects.²¹ Interestingly, chalcones are also present in some food sources like green tea, apples and onions.²² Some studies suggest that incorporating chalcones into our diet may offer health benefits like reducing the risk of cardiovascular diseases. Overall, chalcones hold promising prospects for developing new drugs and improving health outcomes.²³

Schiff bases are a significant class of the most frequently used organic compounds. They have several uses in a wide range of industries.^{24–26} A variety of enzymatic processes appear to use Schiff bases as significant intermediates.^{27,28} Schiff bases, derived from heterocyclic compounds, are molecules of interest as their chemical and biological properties suggest such compounds as probable antibacterial candidates.

In this paper, we present synthesis of some novel heterocyclic compounds with new substituents as well as antibacterial activity for some compounds with different functional groups.

EXPERIMENTAL

General

The chemicals were obtained from two different commercial sources, BDH and Fluka without any further purification, while substituted thiopyrimidine (**1**)²⁹ was previously prepared and purified before usage. Melting points (MP) were calculated on the Electro-Thermal IA1900. IR (Shimadzu FT-IR-8400) spectrometer operating in the 4000–400 cm⁻¹ range with

KBr disks were used. $^1\text{H-NMR}$ and $^{13}\text{C-NMR}$ spectrum were captured using a Varian Agilent USA 400 MHz, 100 MHz respectively, coupling constants (J) are provided in Hz, while chemical shifts (δ) are given in ppm. Spectrometer at the Laboret Centre, University of Tehran. Thin layer chromatography (TLC) was used to monitor and confirm the compounds purity on TLC aluminium sheets.

General procedure

Synthesis of compound 2.³⁰ A solution of 1-amino-4-methyl-6-phenylpyrimidine-2-(1*H*)-thione (**1**, 0.01 mol), in absolute ethanol (30 mL) and potassium hydroxide (8 g) was stirred for 35 min, then 0.01 mol of bromo ethyl acetate was gradually added. The reaction mixture was refluxed for 8 h, then, the progress of the reaction was monitored through TLC. After that, the mixture was mixed with crushed ice, ether was used to extract the product (4×30 mL) and after the solvent was evaporated at low pressure, column chromatography (5 petrol:1 EtOAc) was used to purify and to give the ester compound **2**.

Synthesis of compound 3.³¹ To a solution of the ester compound **2** (0.01 mol) and 50 mL of absolute ethanol, 0.01 mol of hydrazine hydrate (85 %) was added. The mixture of the reaction was refluxed for 2 h, using a water bath. When TLC showed no ester was left, the mixture was cooled and the acid hydrazide was formed. Then, the resulting precipitate was filtered, washed with water and recrystallized from ethanol to give the compound **3**.

Synthesis of compounds 4–6.³² The acid hydrazide **3** (0.01 mol) was dissolved in ethanol (30 mL), then *p*-nitrobenzaldehyde (0.01 mol) in ethanol (25 mL) was added and followed by few drops of acetic acid to get a clear solution. After refluxing the mixture for 4 h, the progress of the reaction was monitored through TLC, cooling the mixture resulted the precipitate which was filtered and purified using column chromatography (5 hexane:1 EtOAc) to give compound **4**. The above experiment was repeated, worked up and purified as mentioned above using 0.01 mol of acid hydrazide with 0.01 mol of 2,4-dimethoxybenzaldehyde and with 0.01 mol of 4-*N,N*-dimethylaminobenzaldehyde to give compounds **5** and **6**, respectively.

Synthesis of substituted thiazolidines 7–9.³³ In the presence of pyridine (20 mL), a mixture of compound **4** (0.01 mol) and thioglycolic acid (0.01 mol) was refluxed for 5 h. The TLC indicated that no starting materials were left, the mixture was cooled and concentrated. Purifying the crud product with column chromatography (10 hexane:2 EtOAc) gave the title compound **7**. The above experiment was repeated, worked upon and purified as above using 0.01 mol of thioglycolic acid each separately with 0.01 mol of compounds **5** and **6** to give compounds **8** and **9**, respectively.

Synthesis of compound 10.³⁴ A mixture of 1-amino-4-methyl-6-phenyl pyrimidine-2-(1*H*)thione (**1**, 0.01 mol) in 30 mL of ethanol and 0.01 mol of phenyl isothiocyanate was refluxed using the steam bath for 8 h. When TLC confirmed the reaction was completed, the mixture was cooled and stored overnight in the refrigerator. The filtration process was carried out and of the resulting solid was purified by column chromatography (5 petrol:1 EtOAc) to get compound **10**.

Synthesis of compound 11.³⁵ To a mixture of an equimolar of compound **10** (0.01 mol) and malonic acid (0.01 mol), 30 mL of acetyl chloride was added and then refluxed for 3 h. The progress of the reaction was monitored through TLC, then, the reaction mixture was cooled, filtered and the crude product was purified by column chromatography (5 hexane:1 EtOAc) to give compound **11**.

Synthesis of chalcone 13.³⁶ A solution of 1-amino-4-methyl-6-phenyl pyrimidine-2-(1*H*)thione (**1**, 0.01 mol) in THF (20 mL) was stirred while acetyl chloride (10 mL) was being added dropwise at 0 °C. The mixture was left to reach the room temperature, then it was

refluxed for 3 h. When the TLC revealed that the reaction was completed, crushed ice was added, then, an aqueous solution of (10 %) NaHCO₃ was used to neutralize the reaction mixture. The resulted precipitate was firstly filtered, washed with water and recrystallized from ethanol to produce compound **12**.

In order to prepare compound **13**, a flask with a magnetic stirrer was filled with 10 mL of 10 % sodium hydroxide solution along with 25 mL of ethanol, 0.01 mol of compound **12** and 0.01 mol of *p*-nitrobenzaldehyde. The mixture was stirred for 10 h at room temperature. The formed precipitate was then filtered, washed with cold water until it almost became neutral and dried before the crude product was purified using column chromatography (5 hexane:1 EtOAc) to give compound **13**.

*Synthesis of compound 14.*³⁶ Compound **13** (0.01 mol) and a nucleophilic reagent (thiourea, 0.01 mol) were dissolved in ethanol and sodium hydroxide was added (2 g NaOH and 10 mL ethanol). The mixture was stirred for 7–8 h. TLC proved that the reaction was complete. The produced solid was filtered off, totally dissolved in water and precipitated with HCl. The obtained precipitate was then filtered, washed with water, dried and recrystallized from ethanol/dioxan to obtain the target compound.

RESULTS AND DISCUSSION

Organic compounds based on substituted thiopyrimidines have many different applications in the field of synthetic organic chemistry. They are also significant in medicinal chemistry. The structures of the newly prepared compounds have been established after the target compounds were produced. The intermediates and final products were each characterized by FT-IR and ¹H-NMR and ¹³C-NMR. Compound **1** was used as starting material to obtain the target compounds.

In Fig. 1 esterification of compound **1** *via* reaction with CH₂BrCO₂Et in the presence of ethanol to give the corresponding ester **2** is presented. The structure was confirmed by ¹H-NMR which showed a quartet at δ 4.09 ppm and a triplet at δ 1.31 ppm related to methylene and methyl group for the ester **2**, respectively. In addition, ¹³C-NMR presented signal at δ 168.6 ppm due to C=O group and signal at 61.2 ppm refer to (CH₂ adjacent to O), IR spectrum presented the key band of carbonyl group at 1745 cm⁻¹ for the ester. Treatment of an ester **2** with N₂H₄·H₂O in absolute ethanol was carried out successfully to synthesized acid hydrazide **3**. The obtained spectral data confirmed the formation of the desired product. The protons of amino group appeared as a doublet at 3.80 ppm in the acid hydrazide **3** demonstrating the elimination of the ester protons. The efficient reaction of substituted benzaldehydes with acid hydrazide **3** in ethanol gave the substituted hydrazones **4–6**, respectively. IR spectra revealed bands corresponding to the azomethine (CH=N) group and the other groups substituted on the aldehyde such as NO₂, OCH₃ and N(CH₃)₂ which confirm the coupling with aldehyde happened successfully. The ¹H-NMR for compound **4** presented a singlet at 8.44 ppm belonging to the proton of azomethine group, while for compound **5** it was a singlet at 3.79 ppm related to OCH₃ groups, also a singlet at 8.27 ppm belongs to

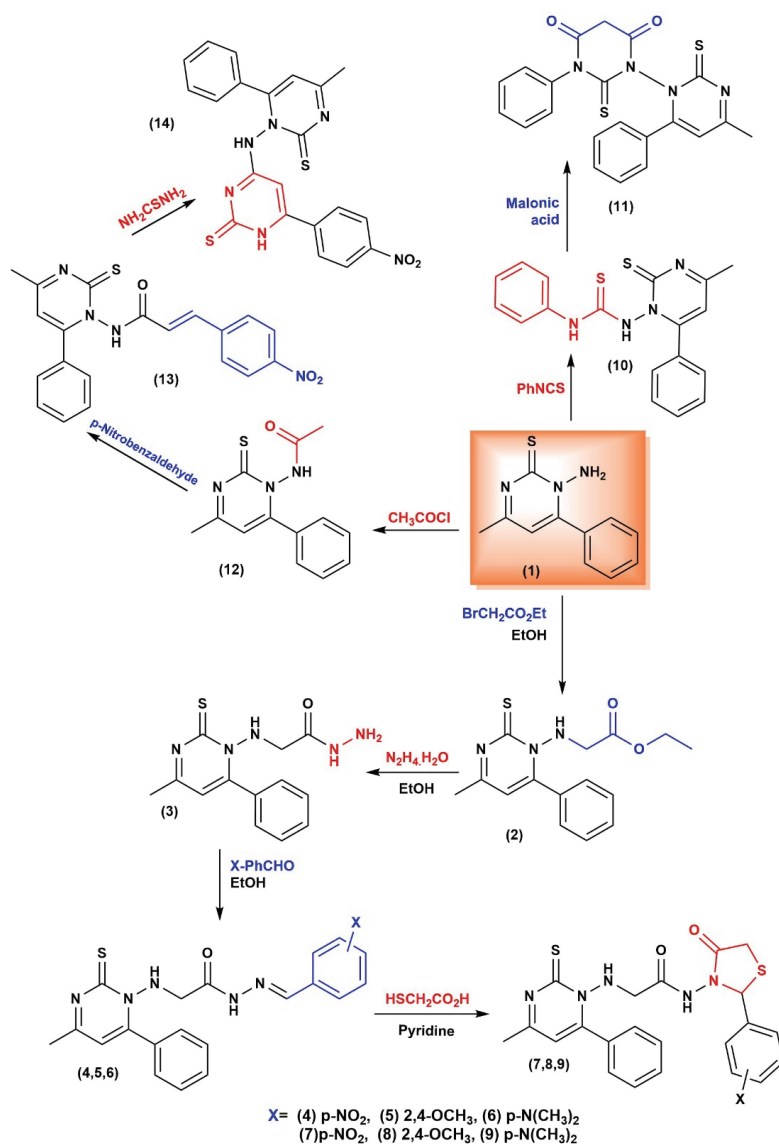


Fig. 1. Synthesis of compounds 2–14.

the proton of $\text{CH}=\text{N}$ group. For compound 6, the $^1\text{H-NMR}$ data showed a singlet at 2.89 ppm referring to 6 protons of two methyl groups (*N,N*-dimethyl group) and a singlet at 8.40 ppm for $\text{CH}=\text{N}$ proton. Also, $^{13}\text{C-NMR}$ showed signals at δ 148.6 and 41.9 ppm related to $\text{CH}=\text{N}$ and two CH_3 groups, respectively. On the other hand, a new five membered heterocyclic compounds were formed by refluxing substituted hydrazones 4–6 with thioglycolic acid in pyridine again the

resulting compounds were verified by ^1H -, ^{13}C -NMR and IR. Compound **7** showed two doublets at 3.38 and 3.34 ppm for methylene group within the thiazolidine ring. The IR spectrum also confirmed the structure of **7** by showing an asymmetric and symmetric stretching for NO_2 group at 1518 and 1345 cm^{-1} , respectively. Also, compounds **8** and **9** were confirmed by ^1H -, ^{13}C -NMR and IR spectra which showed the essentially required peaks as presented in compound **7**. The second line consisted of two steps, the first one was formation of compound **10** by the reaction of compound **1** with phenyl isothiocyanate in ethanol. IR showed band at 1485 cm^{-1} belonging to $\text{C}=\text{S}$, ^{13}C -NMR also confirmed the formation of **10** with a signal at δ 180.5 ppm that refer to carbon in $\text{C}=\text{S}$ group. Treatment of equimolar of **10** and malonic acid in the presence of acetyl chloride gave the target compound **11** which offered two bands for two carbonyl groups at 1734 and 1676 cm^{-1} , respectively. Similarly, ^{13}C -NMR showed two signals at δ 164.4 and 161.5 ppm due to two ($\text{C}=\text{O}$) groups, ^1H -NMR gave a singlet at 2.97 ppm that belongs to CH_2 adjacent to $\text{C}=\text{O}$ group. The last line included three steps, the first step was the synthesis of **12** through the reaction of compound **1** with acetyl chloride, ^1H -NMR showed a singlet at 2.01 ppm for acetyl protons, ^{13}C -NMR gave signal at 166.4 ppm belonging to $\text{C}=\text{O}$ and 20.5 ppm for CH_3 adjacent to $\text{C}=\text{O}$. IR spectrum showed band at 1735 cm^{-1} for carbonyl group. Secondly, the reaction between compound **12** and *p*-nitrobenzaldehyde produced compound **13**. Again, the structure of the resulted compound was confirmed by ^1H -NMR spectrum which showed two doublets at 7.79 and 7.03 ppm belonging to the α and β protons, respectively. In addition, ^{13}C -NMR indicate the formation of structure by signal for $\text{C}=\text{O}$ at 166.1 and 122.2, 146.7 ppm of α and β carbon, respectively. IR revealed a band at 1703 cm^{-1} due to the carbonyl group. Finally, the cyclization of chalcone **13** *via* adding thiourea to give new substituted six membered heterocyclic ring compound **14** was carried out successfully. ^1H -NMR spectrum showed a singlet at 9.02 ppm for the proton in the new-formed substituted thiopyrimidine ring.

The biological study

The disc diffusion method was used to test the antibacterial efficacy of some synthesized compounds against two bacterial strains, *Staphylococcus aureus* (Gram-positive) and *Escherichia coli* (Gram-negative). DMSO was used as a solvent for both the control and the selected samples. For the initial assessment of the invitro antibacterial activity, a total of five compounds were carefully chosen from Fig. 1, taking into consideration the structural properties of the compounds obtained, namely compounds **11** and **14**. These compounds were deemed to be the final products. In addition, compounds **2**, **6** and **8** were also included in the selection process due to their involvement as either intermediate or final products in the various transformation steps outlined in the scheme. These five compounds

showed significant activities and could largely inhibit the bacteria growth. According to the results shown in Table I, five different concentrations have been taken (12.5, 25, 50, 100 and 200 mg/mL) to determine the optimal dose or therapeutic rang of the screened compounds.

TABLE I. Biological activity of some prepared compounds

Compound	Concentration, g/L	Bacteria	
		<i>S. aureus</i>	<i>E. coli</i>
14	200	12	24
	100	8	19
	50	0	16
	25	0	14
	12.5	0	5
2	200	21	20
	100	19	18
	50	17	14
	25	13	12
	12.5	9	5
6	200	9	18
	100	0	16
	50	0	12
	25	0	10
	12.5	9	5
11	200	10	23
	100	8	19
	50	0	17
	25	0	12
	12.5	0	7
8	200	23	25
	100	21	20
	50	15	17
	25	13	14
	12.5	6	8
Amikacin (amk)	20 mg/disc	21	20

At 200 mg/mL for compound **8** (23 mm) and compound **2** (21 mm), *S. aureus* was inhibited, whereas compounds **14**, **11** and **6** (12, 10 and 9 mm, respectively) at 200 mg/mL of concentration *E. coli* was inhibited. Compounds **8**, **14** and **11** had inhibition zones of 25, 24 and 23 mm, while compounds **2** and **6** at 200 mg/mL have 20 and 18 mm, respectively. It is thought to be that those compounds exhibiting high activity are attributed to the multi-functional groups (highly containing of nitrogen and sulfur) and the structure possessed by these particular compounds.³⁷

Chemically, it has been observed that antimicrobial activity can be enhanced by introducing different constituents at different positions of the heterocyclic ring

(thiazolidinone (**8**), pyrimidine thion (**14**)).^{38,39} Several studies indicated that the bacterial death could occur via either inhibiting DNA gyrase which is mainly responsible for bacterial chromosome replication and transcription⁴⁰ or likely by inhibition of Mur ligases action which is responsible for peptidoglycan biosynthesis, a crucial molecule that is giving the shape and rigidity to the cell wall envelope 1.⁴¹

CONCLUSION

Synthesizing heterocyclic compounds containing multi-functional groups with interesting biological activity could help develop new medicinal compounds for treatment of complex infections and diseases. New heterocyclic compounds have been successfully synthesized using substituted thiopyrimidine as a starting material. The initial biological screening of some synthesized compounds (**2**, **6**, **8**, **11** and **14**) against two pathogenic bacteria namely, *S. aureus* and *E. coli* showed interesting biological properties. Compounds **8** and **14** presented the highest inhibition activity compared to control. The reason behind that antibacterial activity of these compounds could be related to inhibition of the essential enzymes (DNA gyrase or Mur ligases) for the bacterial growth. In addition, the type and position of substituents on the hetero-ring play a significant role in the activity. Spectral data have been used to elucidate and confirm the structure of the prepared compounds. Biological screening for some prepared compounds has been evaluated. The outcomes revealed that the bioactivity of some synthesized molecules could be employed in the field of pharmaceutical chemistry.

SUPPLEMENTARY MATERIAL

Additional data and information are available electronically at the pages of journal website: <https://www.shd-pub.org.rs/index.php/JSCS/article/view/12544>, or from the corresponding author on request.

Acknowledgement. The authors gratefully acknowledge the Chemistry Department-College of Education for Pure Science-University of Mosul for providing the necessary resources to carry out this study.

ИЗВОД

СИНТЕЗА И ИСПИТИВАЊЕ БИОЛОШКЕ АКТИВНОСТИ НЕКИХ ХЕТЕРОЦИКЛИЧНИХ ДЕРИВАТА СУПСТИТУИСАНИХ ТИОПИРИМИДИНА

HADIL S. AZIZ, INTISAR Q. M. AL-ARAJ, LINDA R. ABDUL-RAHEEM и AMENA A. AHMED

Chemistry Department, College of Education for Pure Sciences, University of Mosul, Mosul, Iraq

Током овог истраживања осмишљено је неколико нових хетероцикличних једињења који садрже атоме азота и сумпора. Такође, синтетисано је и неколико деривата чалкона, тиазолидина и Шифових база. Спектроскопским подацима (IC, ¹H- и ¹³C-NMR) поврђена је структура добијених молекула. Интересантни резултати су добијени из биолошких тестова према палети патогених Грам-позитивних и Грам-негативних бактерија.

(Примљено 13. августа, ревидирано 9. септембра 2023, прихваћено 30. јуна 2024)

REFERENCES

1. N. N. Makhova, L. I. Belen'kii, G. A. Gazieva, I. L. Dalinger, L. S. Konstantinova, V. V. Kuznetsov, A. N. Kravchenko, M. M. Krayushkin, O. A. Rakitin, A. M. Starosotnikov, L. L. Fershtat, S. A. Shevelev, V. Z. Shirinian, V. N. Yarovenko, *Russ. Chem. Rev.* **89** (2020) 55 (<https://dx.doi.org/10.1070/RCR4914>)
2. A. Z. A. Tlais, G. M. Fiorino, A. Polo, P. Filannino, R. Di Cagno, *Molecules* **25** (2020) 2987 (<https://dx.doi.org/10.3390/molecules25132987>)
3. H. Kumari, H. Kumar, K. Sharma, *IARS' Int. Res. J.* **12** (2023) 1839 (<https://dx.doi.org/10.51611/iars.irj.v12i02.2022.213>)
4. M. M. Heravi, V. Zadsirjan, *RSC Adv.* **10** (2020) 44247 (<https://dx.doi.org/10.1039/D0RA09198G>)
5. M. N. Patel, P. S. Karia, P. A. Vekariya, A. P. Patidar. *Arab. J. Chem.* **12** (2019) 2983 (<https://dx.doi.org/10.1016/j.arabjc.2015.06.031>)
6. A. Lattanzi, *Chem. Rec.* **23** (2023) 1 (<https://dx.doi.org/10.1002/tcr.202300066>)
7. R. Arivazhagan, C. Sridevi, A. Prakasam, *J. Mol. Struct.* **1232** (2021) 129956 (<https://dx.doi.org/10.1016/j.molstruc.2021.129956>)
8. E. Zarenezhad, M. Farjam, A. Iraj, *J. Mol. Struct.* **1230** (2021) 129833 (<https://doi.org/10.1016/j.molstruc.2020.129833>)
9. S. Bhilare, H. Shet, Y. S. Sanghvi, A. R. Kapdi, *Molecules* **25** (2020) 1645 (<https://dx.doi.org/10.3390/molecules25071645>)
10. W. K. Olson, S. Li, T. Kaukonen, A. V. Colasanti, Y. Xin, X. J. Lu, *Biochemistry* **58** (2019) 2474 (<https://dx.doi.org/10.1021/acs.biochem.9b00122>)
11. A. Ramírez-Trinidad, K. Carrillo-Jaimes, J. A. Rivera-Chávez, E. Hernández-Vázquez, *Med. Chem. Res.* **32** (2023) 144 (<https://dx.doi.org/10.1007/s00044-022-02997-6>)
12. S. Singh, S. Ahmad, D. Mehta, S. Alam, *Pharm. Sci. Technol.* **3** (2019) 40 (<https://dx.doi.org/10.11648/j.pst.20190302.12>)
13. P. Srivastava, G. Teli, P. A. Chawla, *Lett. Drug Des. Discov.* **20** (2023) 894 (<https://dx.doi.org/10.2174/1570180819666220523142245>)
14. N. Long, A. Le Gresley, S. P. Wren, *ChemMedChem* **16** (2021) 1717 (<https://dx.doi.org/10.1002/cmde.202100177>)
15. N. Trotsko, J. Golus, P. Kazimierzak, A. Paneth, A. Przekora, G. Ginalska, M. Wujec, *Eur. J. Med. Chem.* **189** (2020) 112045 (<https://dx.doi.org/10.1016/j.ejmech.2020.112045>)
16. S. R. Atta-Allah, N. S. M- Ismail, I. F. Nassar, *Lett. Drug Des. Discov.* **18** (2021) 525 (<https://dx.doi.org/10.2174/1570180817999201123164201>)
17. M. Rashid, N. Shrivastava, A. Husain, *J. Chilean Chem. Soc.* **65** (2020) 4817 (<http://dx.doi.org/10.4067/S0717-97072020000204817>)
18. A. Amin, T. Qadir, A. Salhotra, P. K. Sharma, I. Jeelani, H. Abe, *Curr. Bioact. Compd.* **18** (2022) 77 (<https://dx.doi.org/10.2174/1573407218666220303100501>)
19. S. Rocha, A. Sousa, D. Ribeiro, C. M. Correia, V. L. M. Silva, C. M. M. Santos, A. M. S. Silva, A. N. Araújo, E. Fernandes, M. Freitas, *Food Funct.* **10** (2019) 5510 (<https://dx.doi.org/10.1039/C9FO01298B>)
20. M. C. Egbujor, S. Saha, B. Buttari, E. Profumo, L. Saso. *Expert Rev. Clin. Pharmacol.* **14** (2021) 465 (<https://dx.doi.org/10.1080/17512433.2021.1901578>)
21. M. Rudrapal, J. Khan, A. A. Bin Dukhyil, R. M. I. I. Alarousy, E. I. Attah, T. Sharma, S. J. Khairnar, A. R. Bendale, *Molecules* **26**(2021) 7177 (<https://dx.doi.org/10.3390/molecules26237177>)

22. R. de A. M. Neto, C. B. R. Santos, S. V. C. Henriques, L. de O. Machado, J. N. Cruz, C. H. T. de P. da Silva, a Silva, L. B. Federico, E. H. C. de Oliveira, M. P. C. de Souza, P. N. B. da Silva, C- A. Tafte, I. M. Ferreira, M, R. F. Gomes, *J. Biomol. Struct. Dyn.* **40** (2022) 2204 (<https://dx.doi.org/10.1080/07391102.2020.1839562>)
23. M. A. El-Hashash, S. A. Rizk, S. R. Atta-Allah, *Molecules* **20** (2015) 22069 (<https://dx.doi.org/10.3390/molecules201219827>)
24. A. A. Ahmed, I. Q. Mahmood, H. S. Aziz, *Int. J. Drug Delivery Technol.* **12** (2022) 1087 (<https://dx.doi.org/10.25258/ijddt.12.3.27>)
25. A. Mermer, N. Demirbas, H. Uslu, A. Demirbas, S. Ceylan, Y. Sirin, *J. Mol. Struct.* **1181** (2019) 412 (<https://dx.doi.org/10.1016/j.molstruc.2018.12.114>)
26. S. M. Gomha, H. A. Ahmed, M. Shaban, T. Z. Abolibda, M. S. Khushaim, K. A. Alharbi, *Materials* **14** (2021) 3718 (<https://dx.doi.org/10.3390/ma14133718>)
27. A. A. Hamed, I. A. Abdelhamid, G. R. Saad, N. A. Elkady, M. Z. Elsabee, *Int. J. Biol. Macromol.* **153** (2020) 492 (<https://dx.doi.org/10.1016/j.ijbiomac.2020.02.302>)
28. I. Q. M. Alaraj, R. A. Saeed, L. Reyadh, A. A. Ahmed, *J. Turkish Chem. Soc. Sect. Chem.* **11** (2024) 425 (<https://dx.doi.org/10.18596/jotcsa.1371936>)
29. A. A. Ahmed, N. G. Ahmed, A. K. Ahmad, *Pak. J. Sci. Ind. Res. Ser. A: Phys. Sci.* **63** (2020) 1 (<https://dx.doi.org/10.52763/PJSIR.PHYS.SCI.63.1.2020.1.11>)
30. S. A. Abdul Husseina, A. A.M. Kubbab, *Der. Pharma. Chem.* **7** (2015) 250 (<https://www.derpharmachemica.com/pharma-chemica/synthesis-characterization-and-antimicrobial-activity-of-new-25disubstituted134thiadiazole-derivatives.pdf>)
31. K. K. Bedia, O. Elçin, U. Seda, K. Fatma, S. Nathaly, R. Sevim, A. Dimoglo, *Eur. J. Med. Chem.* **41** (2006) 1253 (<https://dx.doi.org/10.1016/j.ejmech.2006.06.009>)
32. S. Senthilkumar, J. Seralathan, G. Muthukumaran, *J. Mol. Struct.* **1226** (2021) 129354 (<https://dx.doi.org/10.1016/j.molstruc.2020.129354>)
33. M. A. Gouda, A. A. Abu-Hashem, *Arch. Pharm. (Weinheim)* **344** (2011) 170 (<https://dx.doi.org/10.1002/ardp.201000165>)
34. M. Amir, K. Shikha, *Eur. J. Med. Chem.* **39** (2004) 535 (<https://dx.doi.org/10.1016/j.ejmech.2004.02.008>)
35. A. A. Aly, R. El-Sayed, *Chem. Papers* **60** (2006) 56 (<https://dx.doi.org/10.2478/s11696-006-0010-3>)
36. T. A. Farghaly, G. S. Masaret, Z. A. Muhammad, M. F. Harras, *Bioorg. Chem.* **98** (2020) 103761 (<https://dx.doi.org/10.1016/j.bioorg.2020.103761>)
37. P. Ngamsurach, P. Praipipat, *RSC Adv.* **12** (2022) 26435 (<https://doi.org/10.1039/D2RA04611C>)
38. K. Omar, A. Geronikaki, P. Zoumpoulakis, C. Camoutsis, M. Soković, A. Ćirić, J. Glamočlija, *Bioorg. Med. Chem.* **18** (2010) 426 (<https://dx.doi.org/10.1016/j.bmc.2009.10.041>)
39. T. Chaban, Y. Matiichuk, Z. Chulovska, O. Tymoshuk, I. Chaban, V. Matiychuk, *Arch. Pharm.* **354** (2021) 2100037 (<https://dx.doi.org/10.1002/ardp.202100037>)
40. C. J. Galvin, M. Hobson, J. X. Meng, A. Ierokomos, *J. Biol. Chem.* **299** (2023) 103003 (<https://dx.doi.org/10.1016/j.jbc.2023.103003>)
41. C. Tratat, A. Petrou, A. Geronikaki, M. Ivanov, M. Kostić, M. Soković, I. S. Vizirianakis, N. F. Theodoroula, M. Haroun, *Molecules* **27** (2022) 1930 (<https://dx.doi.org/10.3390/molecules27061930>).

SUPPLEMENTARY MATERIAL TO
**Synthesis and biological evaluation of some new heterocyclic
derivatives from substituted thiopyrimidine**

HADIL S. AZIZ, INTISAR Q. M. AL-ARAJ*, LINDA R. ABDUL-RAHEEM
and AMENA A. AHMED

Chemistry Department, College of Education for Pure Sciences, University of Mosul, Mosul, Iraq

J. Serb. Chem. Soc. 89 (11) (2024) 1401–1410

4-Methyl-6-phenyl-2-thioxopyrimidin-1(2H)-yl ethyl glycinate (2)

Yield: 70 %, colorless oil; IR (KBr, cm^{-1}): 3101, 2950, 2845, 1745, 1217, 1166; $^1\text{H-NMR}$ (400 MHz, DMSO-d_6), (δ , ppm): 8.28 (1H, s, C-H thiopyrimidine), 7.46 (2H, dd, $J=7.4, 1.5$ Hz, Ar-H), 7.29 (2H, t, $J=7.2$ Hz, Ar-H), 7.26 – 7.19 (1H, m, Ar-H), 5.50 (1H, m, N-H), 4.09 (2H, q, $J=6.0$ Hz, CH_2 ester), 3.60 (2H, d, $J=33.5$ Hz, CH_2 next to NH), 2.88 (3H, s, CH_3 thiopyrimidine), 1.31 (3H, t, $J=6.0$ Hz, CH_3 ester). $^{13}\text{C-NMR}$ (100 MHz, DMSO-d_6), (δ , ppm): 176.3, 168.6, 166.6, 160.9, 134.5, 129.4, 128.8, 127.6, 110.3, 61.2, 57.3, 24.8, 14.7.

2-((4-Methyl-6-phenyl-2-thioxopyrimidin-1(2H)-yl) amino) aceto hydrazide (3)

Yield: 75 %, solid powder (white); M.p.: 153 – 155 °C; IR (KBr, cm^{-1}): 3315, 2920, 2850, 1681, 1150; $^1\text{H-NMR}$ (400 MHz, DMSO-d_6), (δ , ppm): 8.17 (1H, s, NH next to NH_2), 7.41 – 7.36 (2H, m, Ar-H), 7.25 (2H, dd, $J=10.9, 4.2$ Hz, Ar-H), 7.22 – 7.18 (3H, m, Ar-H), 4.22 (1H, s, N-H) 3.80 (2H, d, $J=15.8$ Hz, NH_2), 3.56 (1H, s, CH_2 next to C=O), 2.90 (1H, s, CH_2 next to C=O), 2.68 (3H, s, CH_3). $^{13}\text{C-NMR}$ (100 MHz, DMSO-d_6), (δ , ppm): 176.3, 172.3, 166.6, 160.9, 134.5, 129.4, 128.8, 127.6, 110.3, 53.3, 24.8.

2-((4-methyl-6-phenyl-2-thioxopyrimidin-1(2H)-yl)amino)-N'-(4-nitrobenzylidene)-acetohydrazide. (4)

Yield: 86 %, solid powder (yellow); M.p.: 200 – 201 °C; IR (KBr, cm^{-1}): 3213, 2933, 2864, 1697, 1672, 1541, 1373, 1158; $^1\text{H-NMR}$ (400 MHz, DMSO-d_6), (δ , ppm): δ 9.83 (1H, s, NH next to C=O), 8.44 (1H, s, CH=N), 8.22 (1H, s, CH thiopyrimidine), 8.08 (2H, d, $J=7.5$ Hz, Ar-H), 7.78 (2H, d, $J=7.5$ Hz, Ar-H), 7.41 (2H, dd, $J=7.5, 1.5$ Hz, Ar-H), 7.30 (2H, t, $J=7.4$ Hz, Ar-H), 7.26 – 7.20 (1H, m, Ar-H), 3.75 (1H, s, CH_2), 3.61 (1H, s, CH_2), 3.49 (1H, s, NH), 2.92 (3H, s, CH_3). $^{13}\text{C-NMR}$ (100 MHz, DMSO-d_6), (δ , ppm): 176.3, 166.6, 163.9, 160.9, 148.6, 148.0, 139.9, 134.5, 129.4, 128.8, 128.0, 127.6, 124.5, 110.3, 53.6, 24.8.

N'-(2,4-dimethoxybenzylidene)-2-((4-methyl-6-phenyl-2-thioxopyrimidin-1(2H)-yl)amino)acetohydrazide. (5)

Yield: 69 %, solid powder (pale yellow); M.p.: 108–110 °C; IR (KBr, cm^{-1}): 3188, 2939, 2835, 1681, 1602, 1207; $^1\text{H-NMR}$ (400 MHz, DMSO-d_6), (δ , ppm): 10.41 (1H, s, NH next to C=O), 8.49 (1H, s, CH thiopyrimidine), 8.27 (1H, s, CH=N), 7.48 (1H, d, $J=7.4$ Hz, Ar-CH),

* Corresponding author. E-mail: Mahmood_intisar@uomosul.edu.iq

7.44 (2H, dd, $J=7.4, 1.2$ Hz, Ar-CH), 7.29 (2H, t, $J=7.4$ Hz, Ar-CH), 7.22 (1H, m, Ar-CH), 6.61 – 6.58 (2H, m, Ar-CH), 6.00 (1H, s, NH), 3.79 (6H, s, OCH₃), 3.69 (1H, CH₂), 3.51 (1H, CH₂), 3.06 (3H, s, CH₃). ¹³C-NMR (100 MHz, DMSO-d₆), (δ , ppm): 176.3, 166.6, 163.9, 162.8, 161.0, 160.9, 149.8, 134.5, 129.7, 129.4, 128.8, 127.6, 117.5, 110.3, 107.0, 100.3, 56.8, 56.0, 53.6, 24.8.

N'-(4-(dimethyl amino) benzylidene)-2-((4-methyl-6-phenyl-2-thioxopyrimidin-1(2H)-yl)amino)aceto hydrazide (6)

Yield: 77 %, solid powder (orang); M.p.: 229-231 °C; IR (KBr, cm⁻¹): 3201, 2923, 2836, 1675, 1634, 1150; ¹H-NMR (400 MHz, DMSO-d₆), (δ , ppm): 10.93 (1H, s, NH next to C=O), 8.54 (1H, s, CH thiopyrimidine), 8.40 (1H, s, CH=N), 7.49 (2H, dd, $J=7.4, 1.2$ Hz, Ar-CH), 7.37 (2H, d, $J=7.5$ Hz, Ar-CH), 7.30 (2H, t, $J=7.2$ Hz, Ar-CH), 7.26 – 7.20 (1H, m, Ar-CH), 6.64 (2H, d, $J=7.5$ Hz, Ar-CH), 5.73 (1H, s, NH), 3.56 (1H, s, CH₂), 3.43 (1H, s, CH₂), 2.96 (3H, s, CH₃), 2.89 (6H, s, N-CH₃). ¹³C-NMR (100 MHz, DMSO-d₆), (δ , ppm): 176.3, 166.6, 163.9, 160.9, 153.9, 148.6, 134.5, 129.4, 128.8, 128.8, 127.6, 121.0, 111.0, 110.3, 53.6, 41.9, 24.8.

2-((4-methyl-6-phenyl-2-thioxopyrimidin-1(2H)-yl) amino)-N-(2-(4-nitrophenyl)-4-oxothiazolidin-3-yl) acetamide (7)

Yield: 80 %, solid powder (white); M.p.: 226-228 °C; IR (KBr, cm⁻¹): 3223, 2929, 2846, 1732, 1518, 1345, 1280, 712; ¹H-NMR (400 MHz, DMSO-d₆), (δ , ppm): 9.29 (1H, s, NH), 8.45 (1H, s, CH thiopyrimidin), 8.25 (2H, d, $J=7.5$ Hz, Ar-H), 7.57 (2H, d, $J=7.7$ Hz, Ar-H), 7.39 (2H, dd, $J=7.4, 1.2$ Hz, Ar-H), 7.28 (2H, t, $J=7.2$ Hz, Ar-H), 7.24 – 7.20 (1H, m, Ar-H), 6.92 (1H, s, CH thiazolidine), 3.51 (1H, s, NH), 3.48 (2H, s, CH₂ next to C=O), 3.38 (1H, d, $J=12.4$ Hz, CH next to C=O), 3.34 (1H, d, $J=12.6$ Hz, CH next S), 3.05 (3H, s, CH₃). ¹³C-NMR (100 MHz, DMSO-d₆), (δ , ppm): 176.3, 172.3, 168.3, 166.6, 160.9, 148.6, 148.2, 134.5, 129.4, 128.8, 127.6, 125.7, 123.9, 110.3, 67.6, 52.8, 33.3, 24.8.

Dimethoxyphenyl)-4-oxothiazolidin-3-yl)-2-((4-methyl-6-phenyl-2-thioxopyrimidin-1(2H)-yl) amino) acetamide (8)

Yield: 69 %, solid powder (white); M.p.: 289-290 °C; IR (KBr, cm⁻¹): 3013, 2932, 2825, 1674, 1264, 1172, 1028, 720; ¹H-NMR (400 MHz, DMSO-d₆), (δ , ppm): 9.39 (1H, s, NH next to C=O), 8.47 (1H, s, CH thiopyrimidine), 7.41 (2H, dd, $J=7.4, 1.5$ Hz, Ar-H), 7.28 (2H, dd, $J=12.1, 4.6$ Hz, Ar-H), 7.26 (1H, d, $J=7.5$ Hz, Ar-H), 7.23 (1H, dd, $J=5.2, 3.8$ Hz, Ar-H), 6.63 (1H, d, $J=1.4$ Hz, Ar-H), 6.60 (1H, dd, $J=7.5, 1.4$ Hz, Ar-H), 6.47 (1H, s, C-H thiazolidine), 4.10 (1H, s, NH), 3.80 (6H, s, OCH₃), 3.50 (2H, s, CH₂ next to C=O), 3.40 (1H, br.d, $J=12.3$ Hz, CH next to C=O), 3.36 (1H, br.d, $J=12.4$ Hz, CH next to S), 3.04 (3H, s, CH₃). ¹³C-NMR (100 MHz, DMSO-d₆), (δ , ppm): 176.3, 172.3, 168.3, 166.6, 161.3, 160.9, 155.6, 134.5, 129.7, 129.4, 128.8, 127.6, 120.0, 110.3, 107.4, 100.8, 61.4, 56.8, 56.0, 52.8, 33.3, 24.8.

N-(2-(4-(dimethylamino)phenyl)-4-oxothiazolidin-3-yl)-2-((4-methyl-6-phenyl-2-thioxopyrimidin-1(2H)-yl)amino)acetamide (9)

Yield: 75 %, solid powder (pale pink); M.p.: 247-249 °C; IR (KBr, cm⁻¹): 3372, 3221, 3062, 2953, 2848, 1715, 1290, 731; ¹H-NMR (400 MHz, DMSO-d₆), (δ , ppm): 8.45 (1H, s, C-H thiopyrimidine), 7.80 (1H, s, NH), 7.41 (2H, dd, $J=7.3, 1.5$ Hz, Ar-H), 7.25 (2H, dd, $J=10.7, 4.5$ Hz, Ar-H), 7.23 – 7.21 (1H, m, Ar-H), 7.10 (2H, d, $J=7.5$ Hz, Ar-H), 6.68 – 6.65 (3H, m, Ar-H + C-H thiazolidine), 5.12 (1H, s, NH), 3.57 (1H, s, CH₂ next to NH), 3.37 (1H, br.d, $J=12.4$ Hz, CH₂ next to C=O), 3.34 (1H, s, CH₂ next to NH), 3.33 (1H, br.d, $J=8.8$ Hz, CH₂ next to S), 3.04 (3H, s, CH₃), 2.90 (6H, s, N(CH₃)₂). ¹³C-NMR (100 MHz, DMSO-d₆), (δ ,

ppm): 176.3, 172.3, 168.3, 166.6, 160.9, 155.3, 134.6, 133.7, 129.4, 128.8, 127.6, 127.5, 111.4, 110.3, 67.6, 52.8, 41.9, 33.3, 24.8.

1-(4-methyl-6-phenyl-2-thioxopyrimidin-1(2H)-yl)-3-phenylthiourea (10)

Yield: 88 %, solid powder (pale green); M.p.: 157-159 °C; IR (KBr, cm⁻¹): 3172, 2920, 2837, 1560, 1485, 1372; ¹H-NMR (400 MHz, DMSO-d₆), (δ, ppm): 9.86 (1H, s, NH), 8.39 (1H, s, C-H thiopyrimidine), 7.52 (2H, dd, *J* = 7.4, 1.2 Hz Ar-H), 7.32 (2H, t, *J* = 7.4 Hz, Ar-H), 7.29 – 7.24 (4H, m, Ar-H), 7.22 – 7.17 (1H, m, Ar-H), 7.13 – 7.08 (2H, m, Ar-H), 2.90 (3H, s, CH₃). ¹³C-NMR (100 MHz, DMSO-d₆), (δ, ppm): 180.5, 176.2, 166.6, 162.9, 139.2, 134.5, 129.4, 129.0, 128.8, 127.6, 124.5, 121.5, 113.2, 24.8.

5-(4-methyl-6-phenyl-2-thioxopyrimidin-1(2H)-yl)-1-phenyl-6-thioxopiperidine-2,4-dione(11)

Yield: 65 %, solid powder (pale brown); M.p.: 87-89 °C; IR (KBr, cm⁻¹): 3020, 2978, 2840, 1734, 1647, 1550-1392, 1502; ¹H-NMR (400 MHz, DMSO-d₆), (δ, ppm): 8.68 (1H, s, thiopyrimidine), 7.49 (2H, br.dd, *J* = 7.5, 1.4 Hz, Ar-H), 7.45 (2H, br.dd, *J* = 7.4, 1.3 Hz, Ar-H), 7.37 (2H, t, *J* = 7.5 Hz, Ar-H), 7.29 (2H, t, *J* = 7.5 Hz, Ar-H), 7.23 – 7.19 (1H, m, Ar-H), 7.15 – 7.10 (1H, m, Ar-H), 3.03 (3H, s, CH₃), 2.89 (2H, s, CH₂ Aliph. ring). ¹³C-NMR (100 MHz, DMSO-d₆), (δ, ppm): 181.5, 169.2, 164.9, 164.5, 164.4, 161.5, 137.4, 134.6, 130.5, 129.9, 129.7, 129.4, 129.2, 127.8, 110.5, 43.6, 24.8.

N-(4-methyl-6-phenyl-2-thioxopyrimidin-1(2H)-yl) acet amide (12)

Yield: 85 %, solid powder (brown); M.p.: 184-186 °C; IR (KBr, cm⁻¹): 3207, 2983, 2841, 1735, 1595-1404; ¹H-NMR (400 MHz, DMSO-d₆), (δ, ppm): 9.05 (1H, s, NH), 8.26 (1H, s, CH thiopyrimidine), 7.36 (2H, dd, *J* = 7.3, 1.3 Hz, Ar-H), 7.23 (2H, t, *J* = 7.2 Hz, Ar-H), 7.20 – 7.15 (1H, m, Ar-H), 2.88 (3H, s, CH₃ thiopyrimidine), 2.01 (3H, s, CH₃ next to C=O). ¹³C-NMR (100 MHz, DMSO-d₆), (δ, ppm): 176.2, 166.6, 166.5, 134.5, 129.3, 128.8, 127.7, 113.2, 24.8, 20.5.

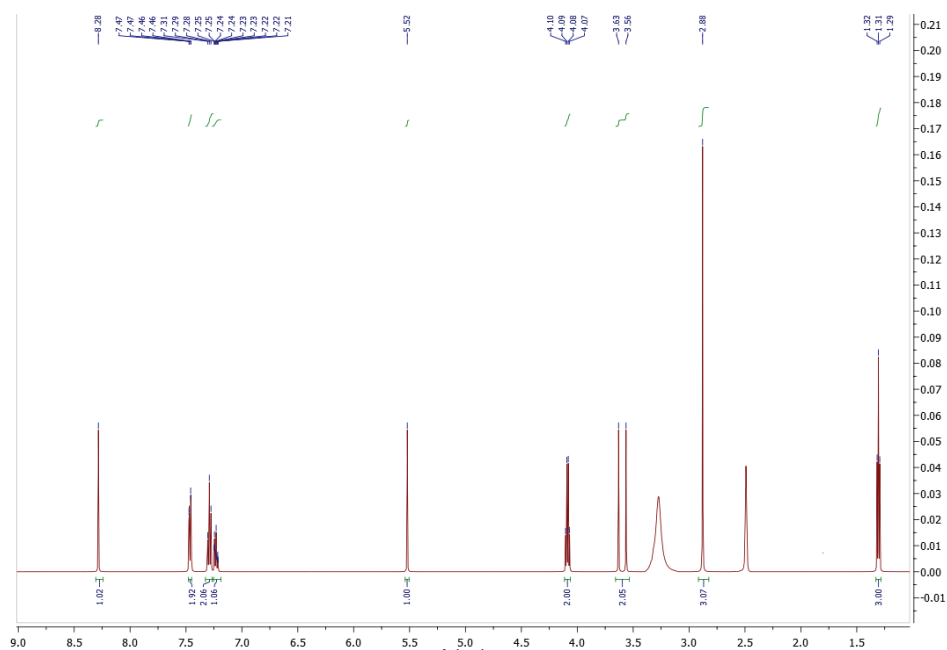
N-(4-methyl-6-phenyl-2-thioxopyrimidin-1(2H)-yl)-3-(4-nitrophenyl) acrylamide (13)

Yield: 70 %, solid powder (Pale brown); M.p.: 178-180 °C; IR (KBr, cm⁻¹): 3116, 2935, 2866, 1703, 1628; ¹H-NMR (400 MHz, DMSO-d₆), (δ, ppm): 9.55 (1H, s, NH), 8.41 (1H, s, C-H thiopyrimidine), 8.17 (2H, d, *J* = 7.5 Hz, Ar-H), 7.79 (1H, d, *J* = 15.2 Hz, β-CH), 7.55 (2H, d, *J* = 7.7 Hz, Ar-H), 7.42 (2H, dd, *J* = 7.4, 1.5 Hz, Ar-H), 7.26 (2H, t, *J* = 7.3 Hz, Ar-H), 7.22 – 7.17 (1H, m, Ar-H), 7.03 (1H, d, *J* = 15.2 Hz, α-CH), 3.06 (3H, s, CH₃). ¹³C-NMR (100 MHz, DMSO-d₆), (δ, ppm): 176.2, 166.6, 166.1, 162.9, 147.8, 146.7, 142.4, 134.5, 129.4, 129.1, 128.8, 127.6, 124.5, 122.2, 113.2, 24.8.

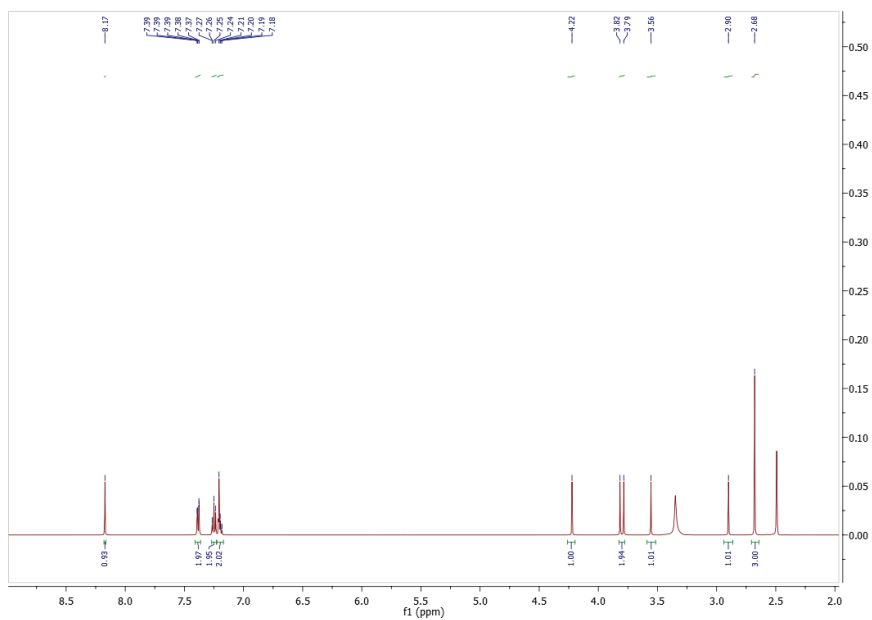
4-methyl-1-((6-(4-nitrophenyl)-2-thioxo-1,2-dihydropyrimidin-4-yl) amino)-6-phenylpyrimidine-2(1H)-thione (14)

Yield: 81 %, solid powder (pale green); M.p.: 81-82 °C; IR (KBr, cm⁻¹): 3428, 2930, 1632, 1593; ¹H-NMR (400 MHz, DMSO-d₆), (δ, ppm): 9.02 (1H, s, C-H heterocyclic ring), 8.88 (1H, s, C-H thiopyrimidine), 8.21 (2H, d, *J* = 7.5 Hz, Ar-H), 7.73 (2H, d, *J* = 7.5 Hz, Ar-H), 7.49 (2H, dd, *J* = 7.4, 1.3 Hz, Ar-H), 7.24 (2H, t, *J* = 7.4 Hz, Ar-H), 7.20 – 7.12 (1H, m, Ar-H), 2.96 (3H, s, CH₃). ¹³C-NMR (100 MHz, DMSO-d₆), (δ, ppm): 176.2, 175.8, 166.6, 163.8, 162.9, 148.8, 146.8, 142.3, 134.5, 129.4, 128.8, 127.8, 127.6, 124.1, 113.2, 98.4, 24.8.

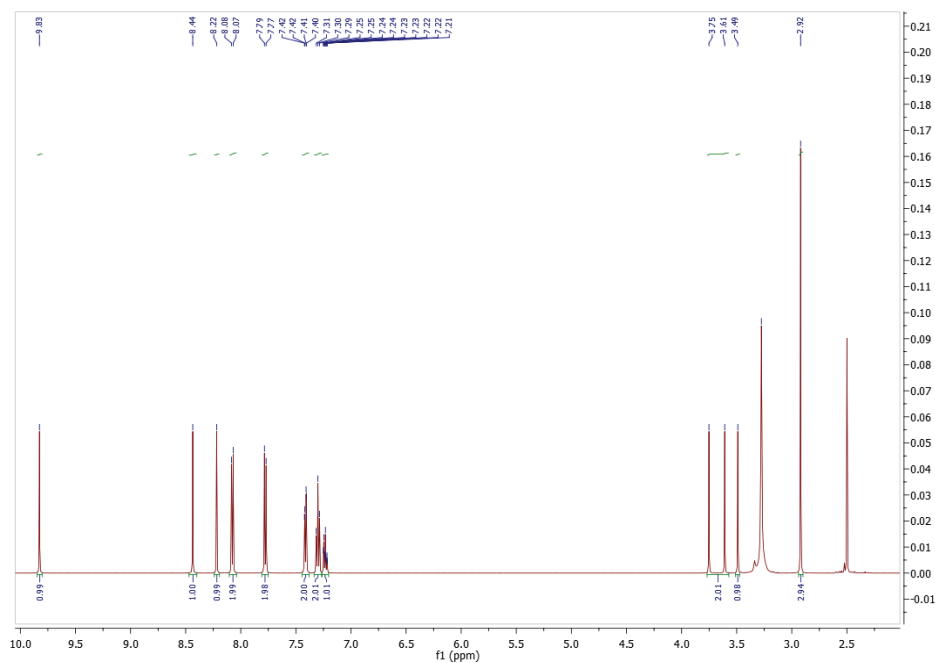
Note: The signal at 2.5 ppm in all spectra is related to the deuterated solvent (DMSO-d₆), and the signal around 3.3 ppm is due to the moisture in (DMSO-d₆).



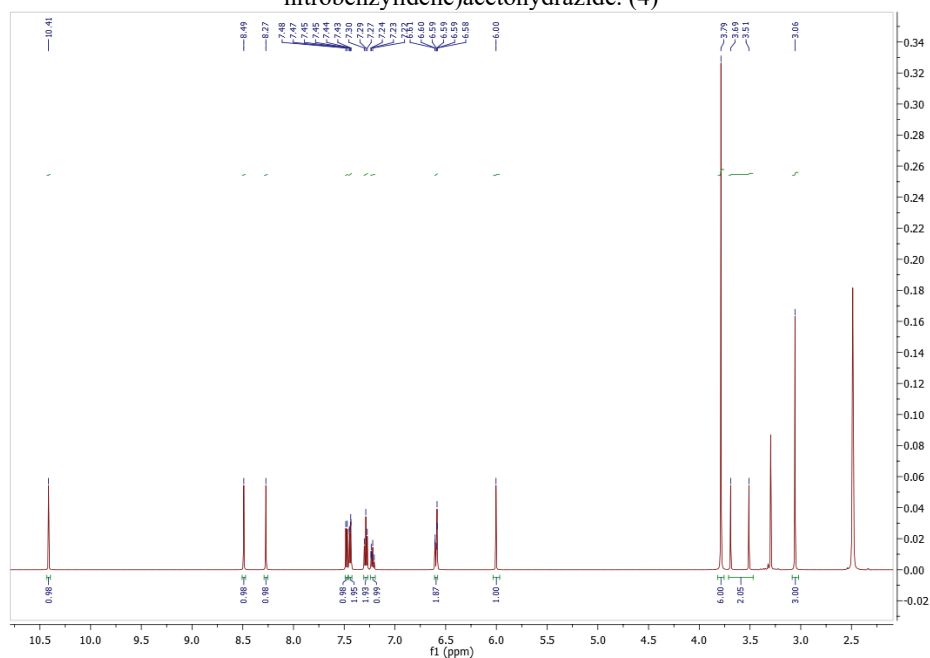
¹H-NMR for 4-Methyl-6-phenyl-2-thioxopyrimidin-1(2H)-yl ethyl glycinate (2)



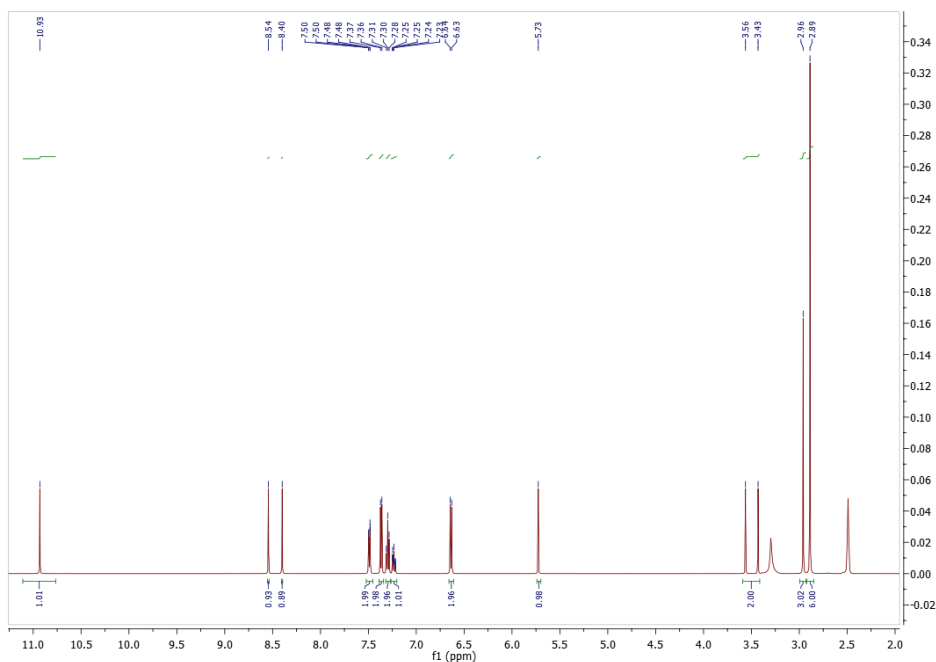
¹H-NMR for 2-((4-Methyl-6-phenyl-2-thioxopyrimidin-1(2H)-yl) amino) aceto hydrazide (3)



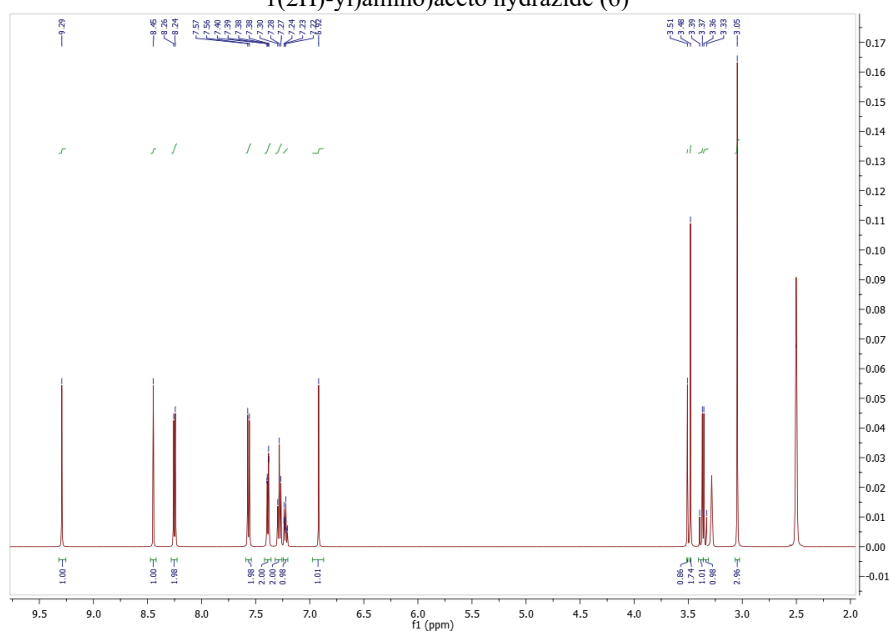
$^1\text{H-NMR}$ for 2-((4-methyl-6-phenyl-2-thioxopyrimidin-1(2H)-yl)amino)-N'-(4-nitrobenzylidene)acetohydrazide. (4)



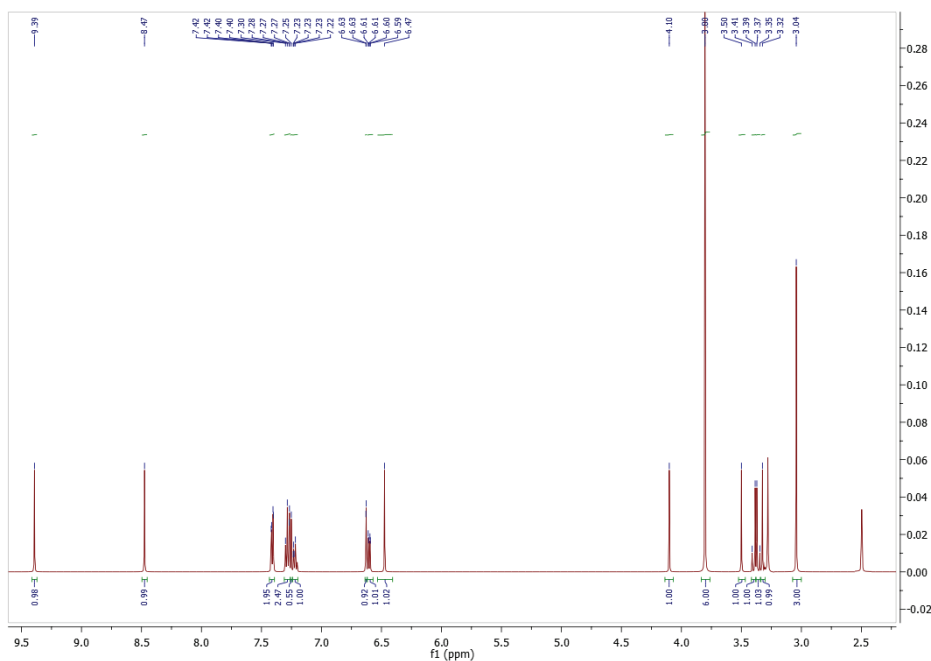
$^1\text{H-NMR}$ for N'-(2,4-dimethoxybenzylidene)-2-((4-methyl-6-phenyl-2-thioxopyrimidin-1(2H)-yl)amino)acetohydrazide. (5)



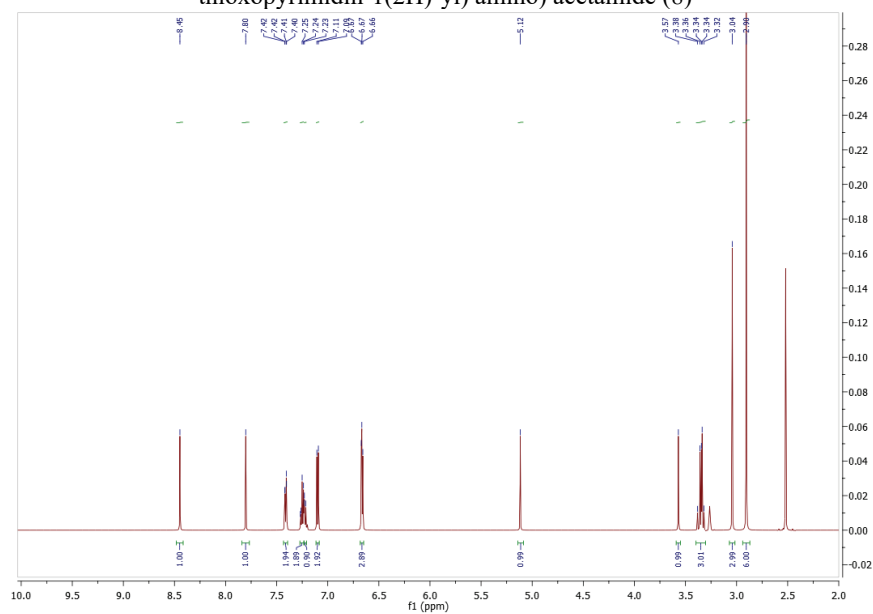
$^1\text{H-NMR}$ for N' -(4-(dimethyl amino) benzylidene)-2-((4-methyl-6-phenyl-2-thioxopyrimidin-1(2H)-yl)amino)aceto hydrazide (6)



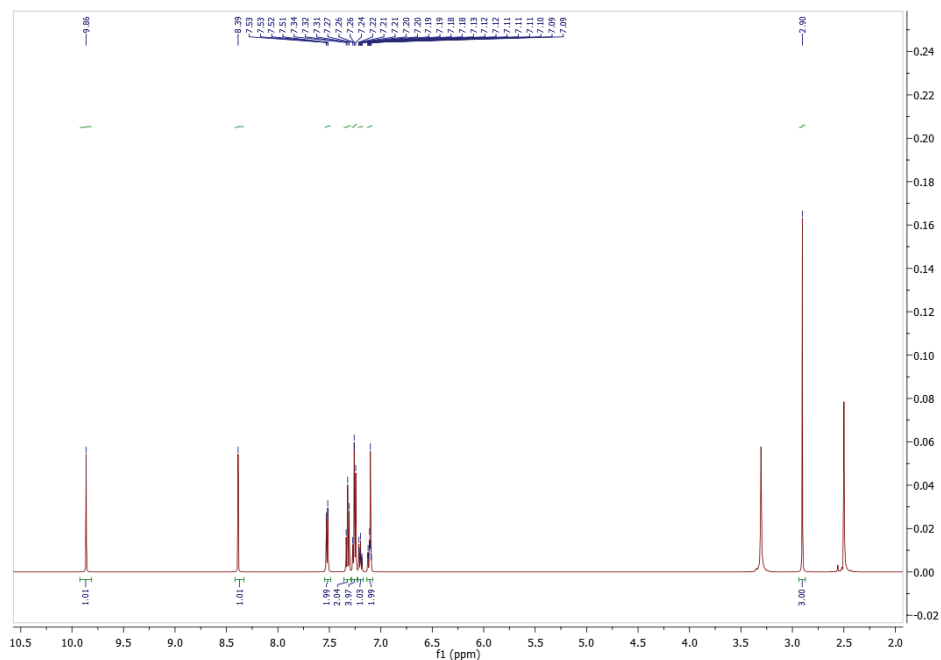
$^1\text{H-NMR}$ for 2-((4-methyl-6-phenyl-2-thioxopyrimidin-1(2H)-yl) amino)- N -(2-(4-nitrophenyl)-4-oxothiazolidin-3-yl) acetamide (7)



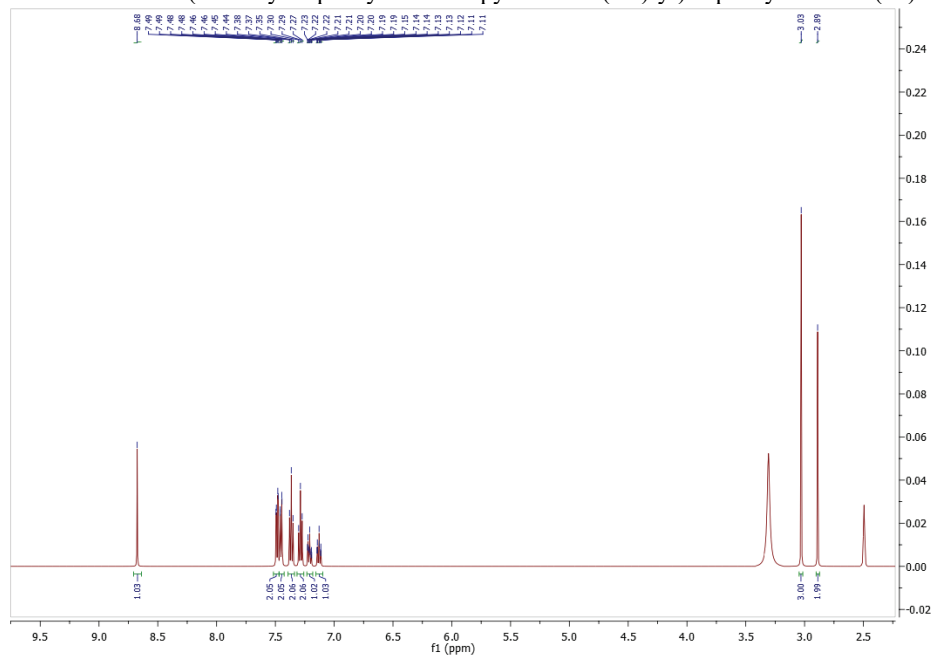
¹H-NMR for dimethoxyphenyl)-4-oxothiazolidin-3-yl)-2-((4-methyl-6-phenyl-2-thioxopyrimidin-1(2H)-yl) amino) acetamide (8)



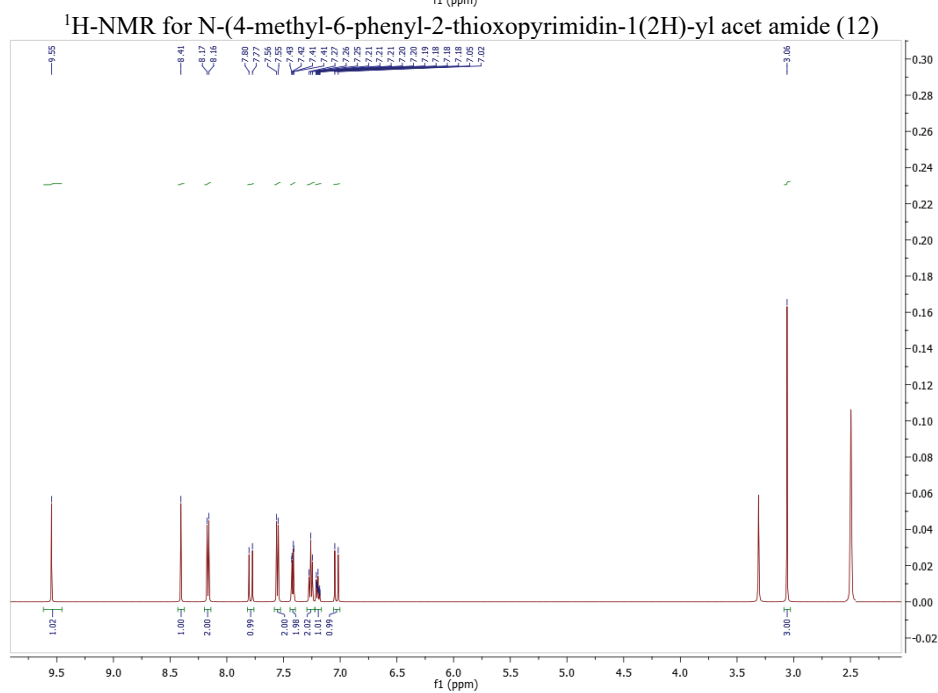
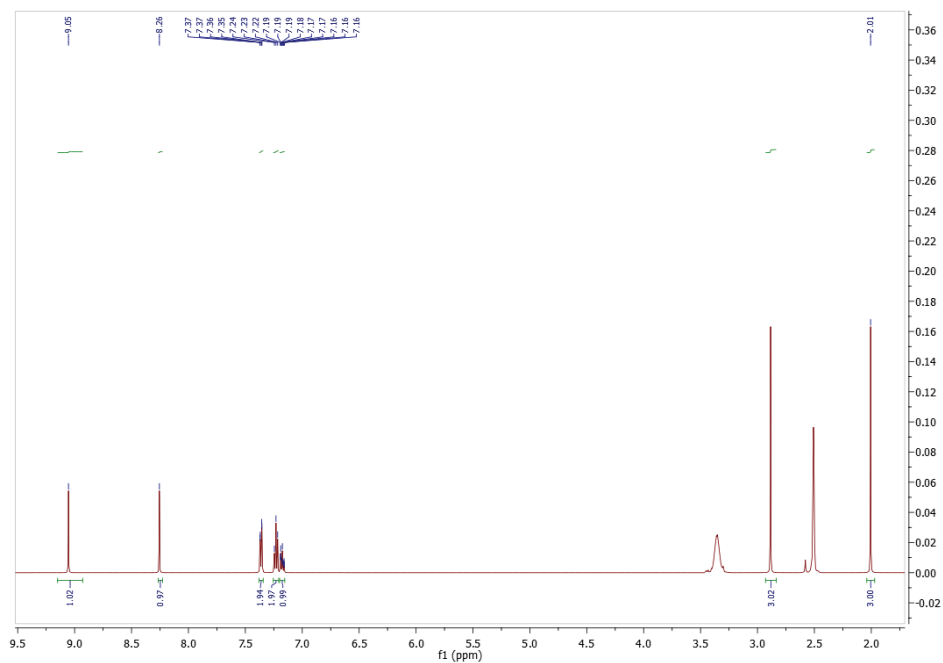
¹H-NMR for N-(2-(4-(dimethylamino)phenyl)-4-oxothiazolidin-3-yl)-2-((4-methyl-6-phenyl-2-thioxopyrimidin-1(2H)-yl)amino)acetamide (9)

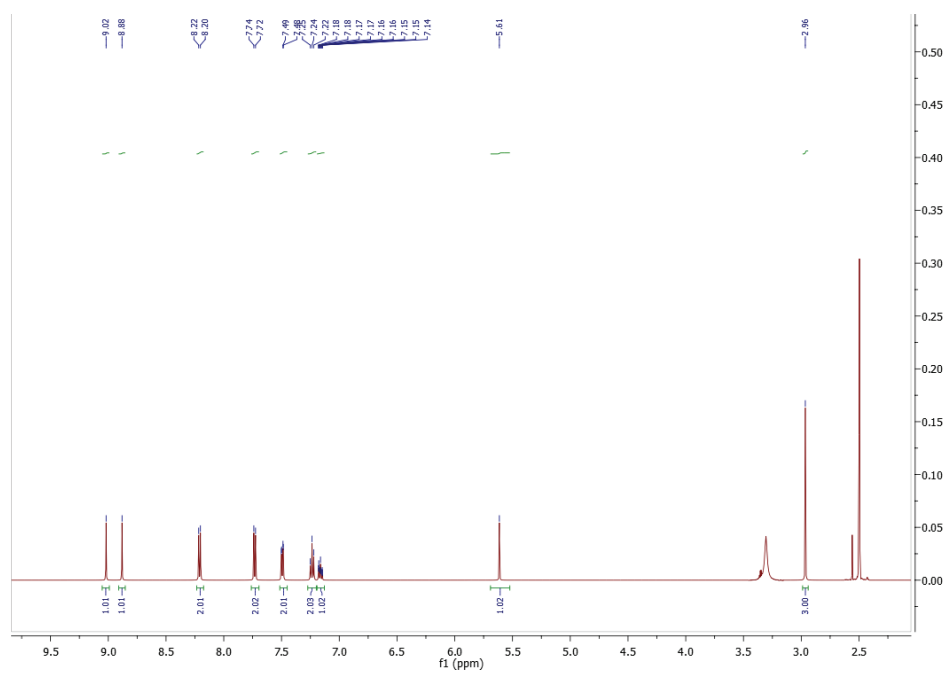


$^1\text{H-NMR}$ for 1-(4-methyl-6-phenyl-2-thioxopyrimidin-1(2H)-yl)-3-phenylthiourea (10)

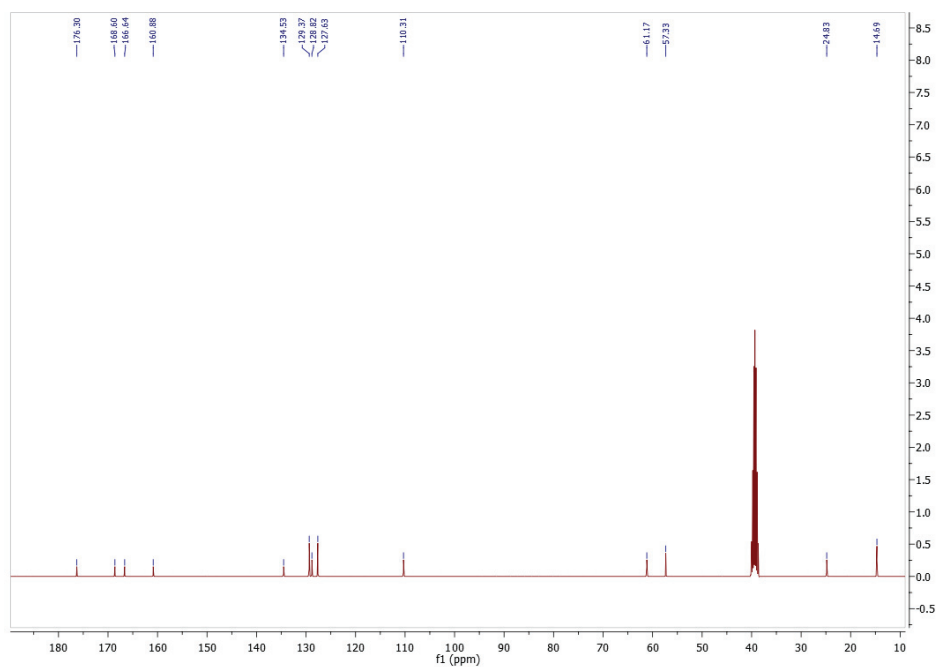


$^1\text{H-NMR}$ for 5-(4-methyl-6-phenyl-2-thioxopyrimidin-1(2H)-yl)-1-phenyl-6-thioxopiperidine-2,4-dione (11)

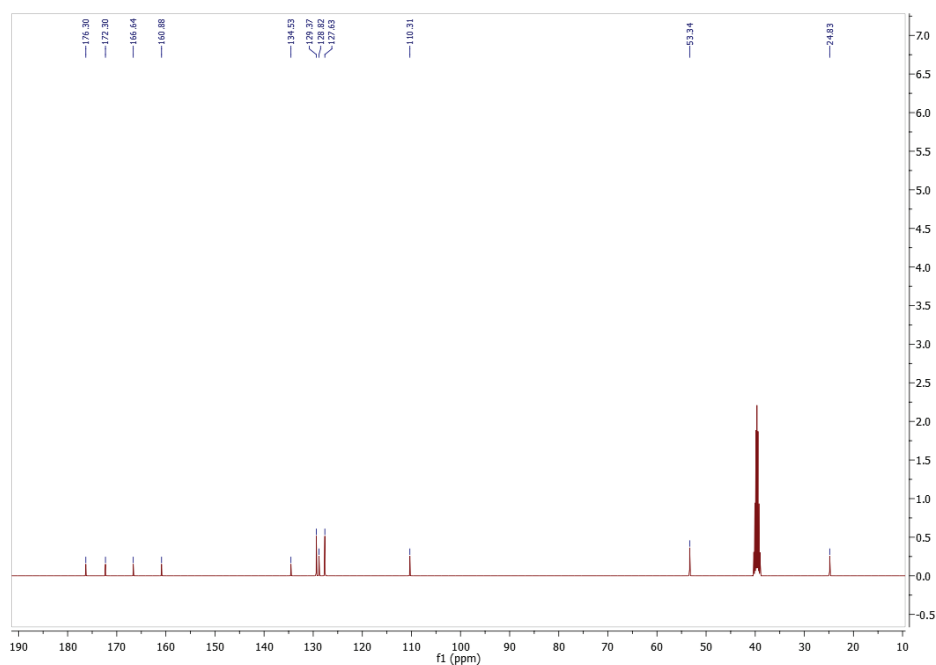




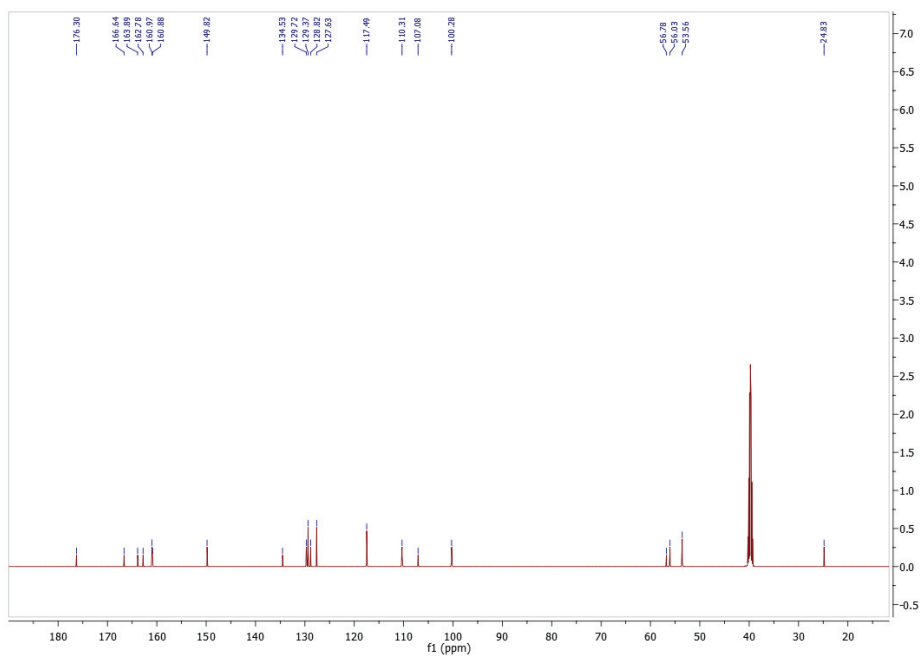
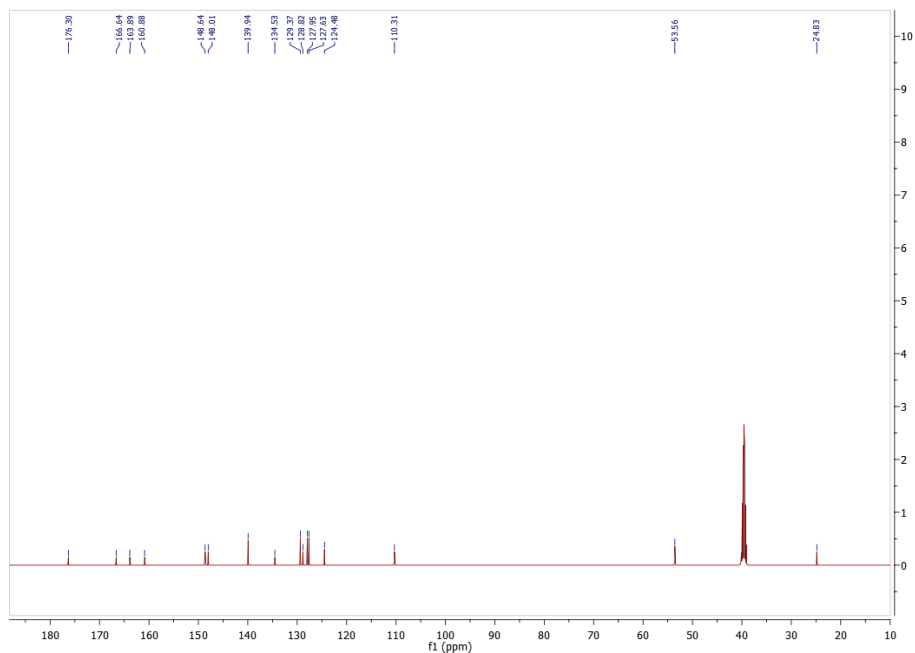
$^1\text{H-NMR}$ for 4-methyl-1-((6-(4-nitrophenyl)-2-thioxo-1,2-dihydropyrimidin-4-yl) amino)-6-phenylpyrimidine-2(1H)-thione (14)

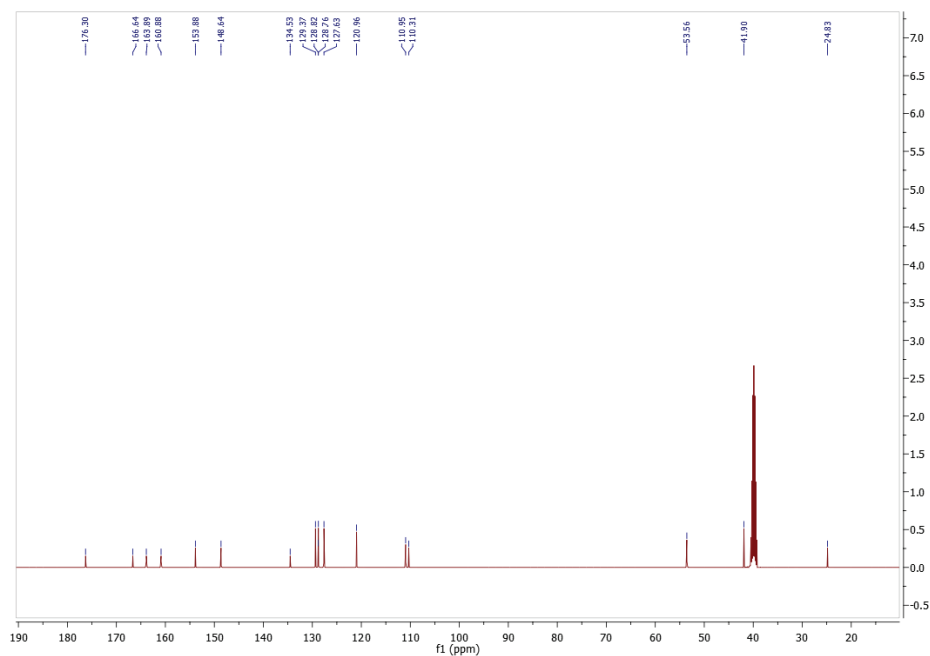


$^{13}\text{C-NMR}$ for 4-Methyl-6-phenyl-2-thioxopyrimidin-1(2H)-yl ethyl glycinate (2)

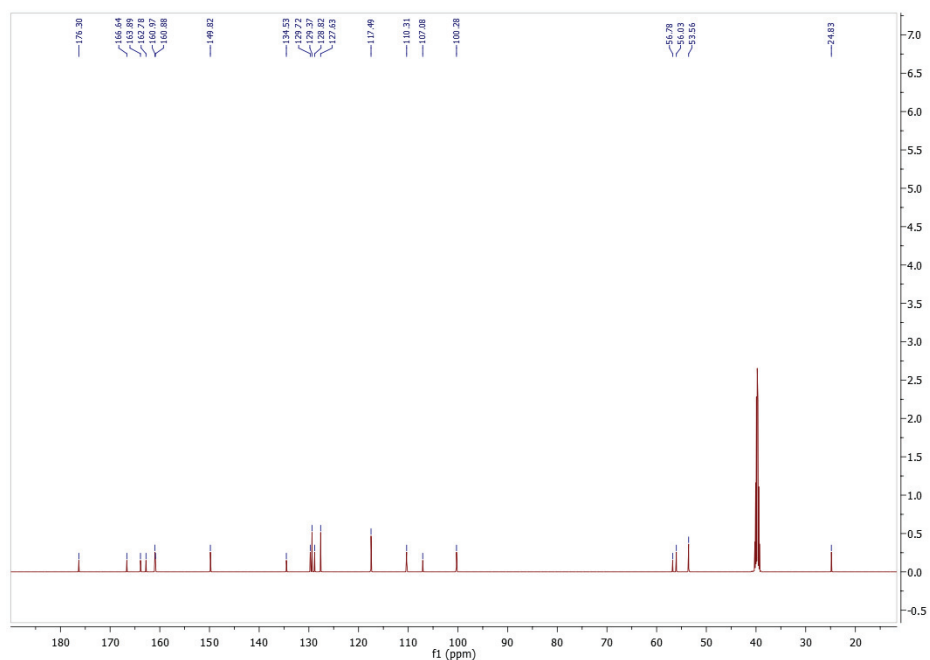


$^{13}\text{C-NMR}$ for 2-((4-Methyl-6-phenyl-2-thioxopyrimidin-1(2H)-yl) amino) aceto hydrazide (3)

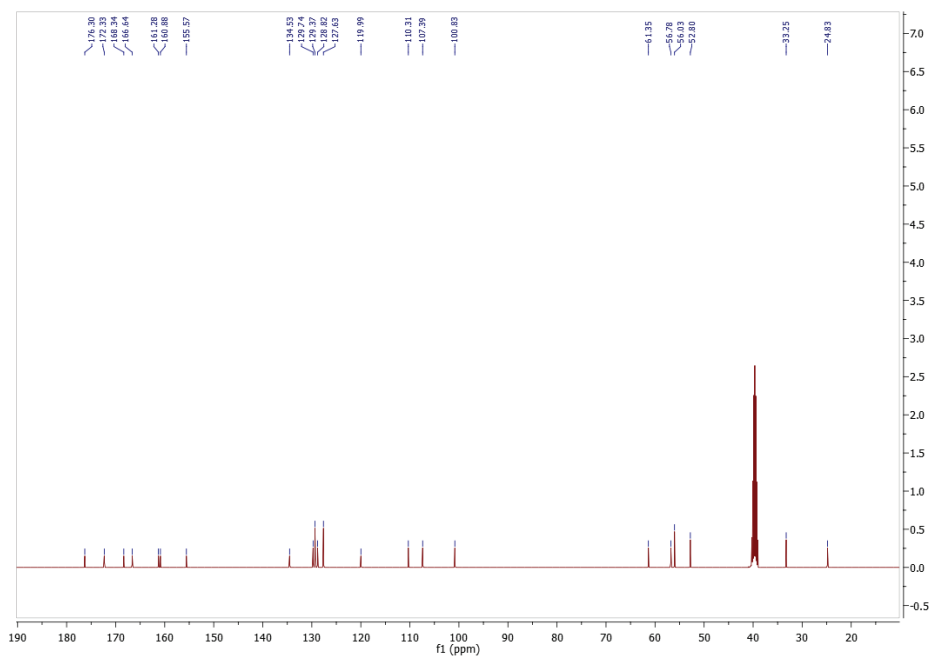




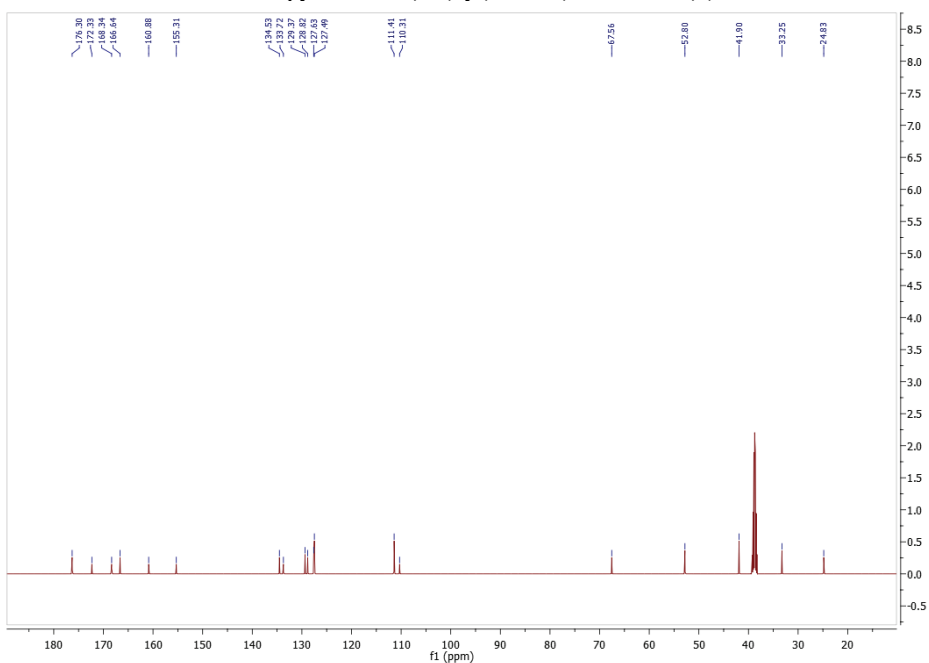
^{13}C -NMR for N' -(4-(dimethyl amino) benzylidene)-2-((4-methyl-6-phenyl-2-thioxopyrimidin-1(2H)-yl)amino)aceto hydrazide (6)



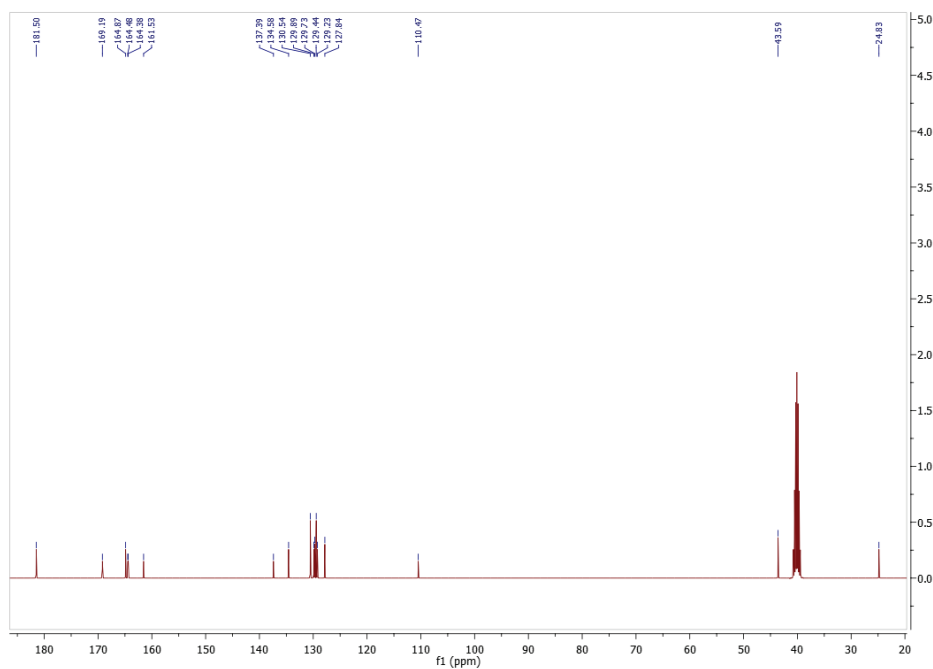
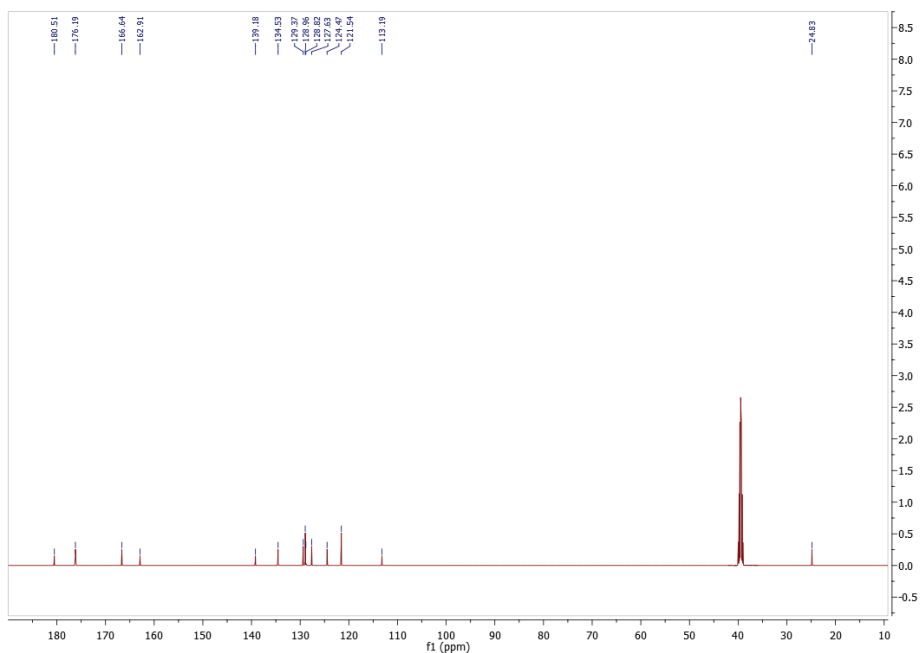
^{13}C -NMR for 2-((4-methyl-6-phenyl-2-thioxopyrimidin-1(2H)-yl) amino)-N-(2-(4-nitrophenyl)-4-oxothiazolidin-3-yl) acetamide (7)

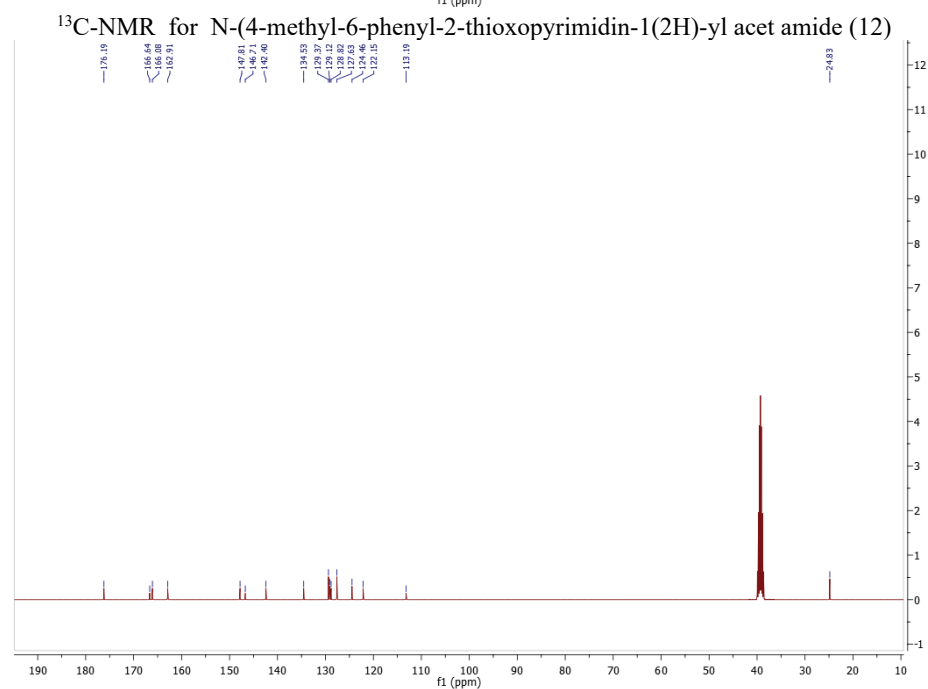
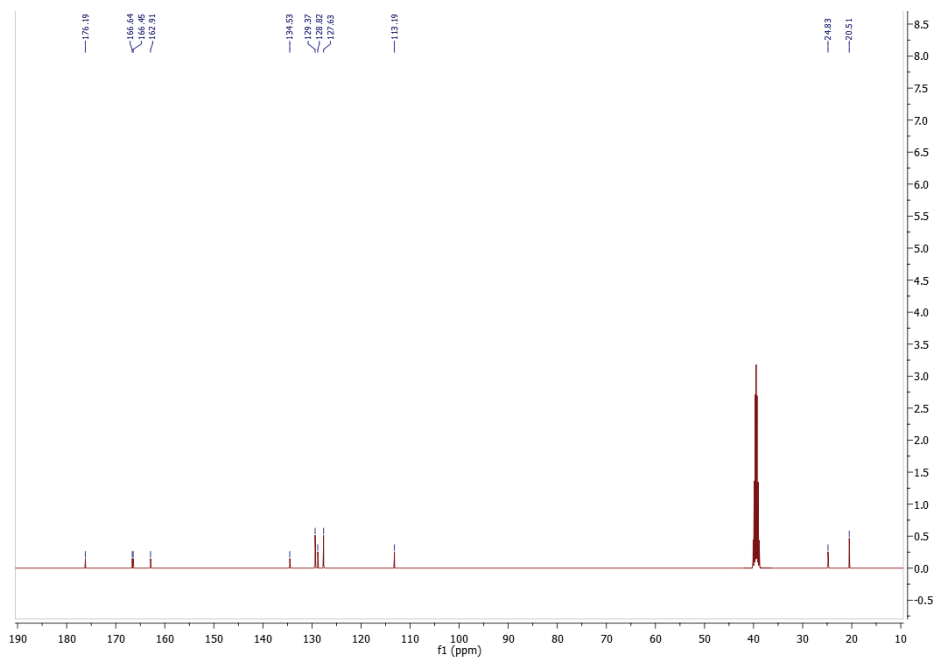


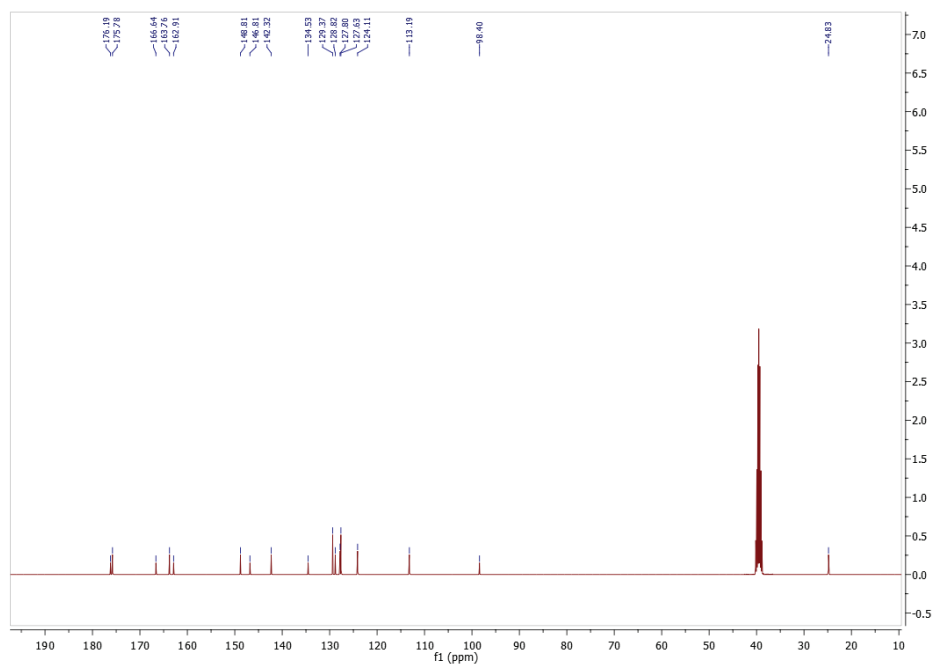
¹³C-NMR for dimethoxyphenyl)-4-oxothiazolidin-3-yl)-2-((4-methyl-6-phenyl-2-thioxopyrimidin-1(2H)-yl) amino) acetamide (8)



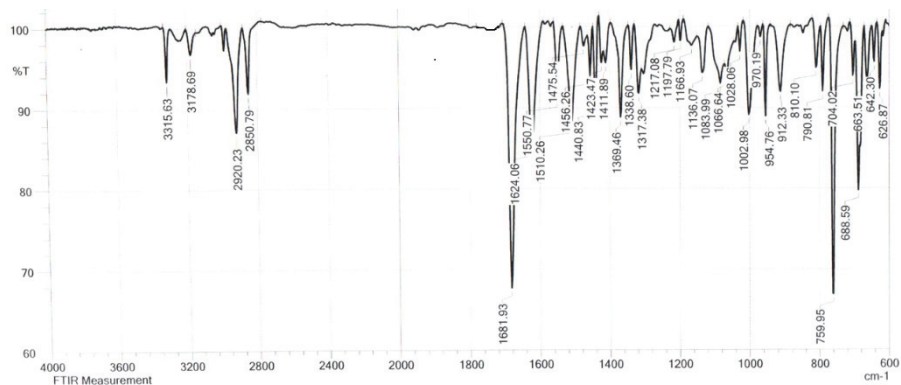
¹³C-NMR for N-(2-(4-(dimethylamino)phenyl)-4-oxothiazolidin-3-yl)-2-((4-methyl-6-phenyl-2-thioxopyrimidin-1(2H)-yl)amino)acetamide (9)



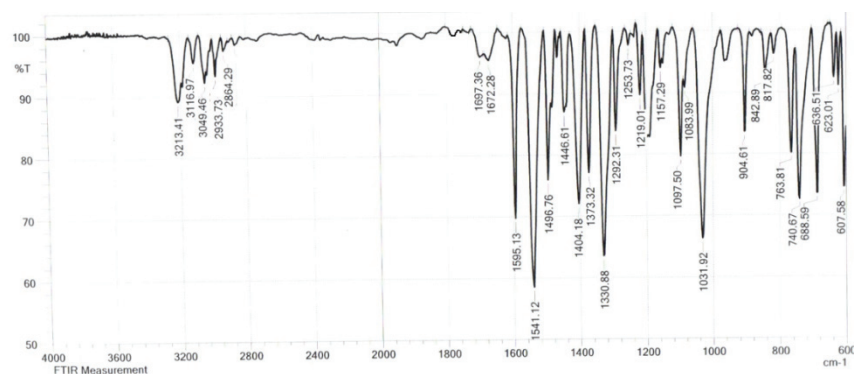




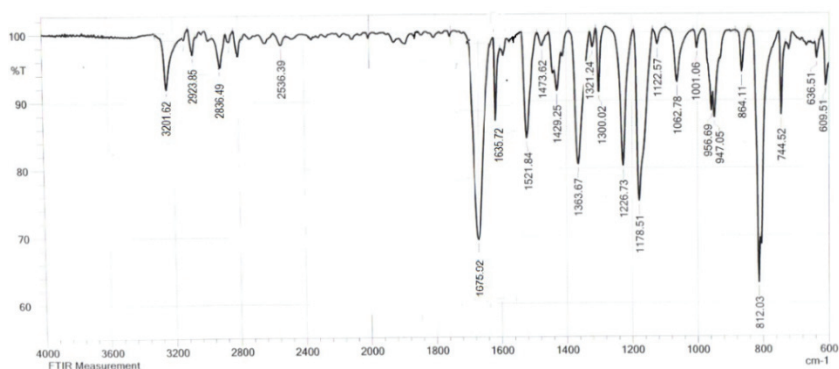
^{13}C -NMR for 4-methyl-1-((6-(4-nitrophenyl)-2-thioxo-1,2-dihydropyrimidin-4-yl) amino)-6-phenylpyrimidine-2(1H)-thione (14)



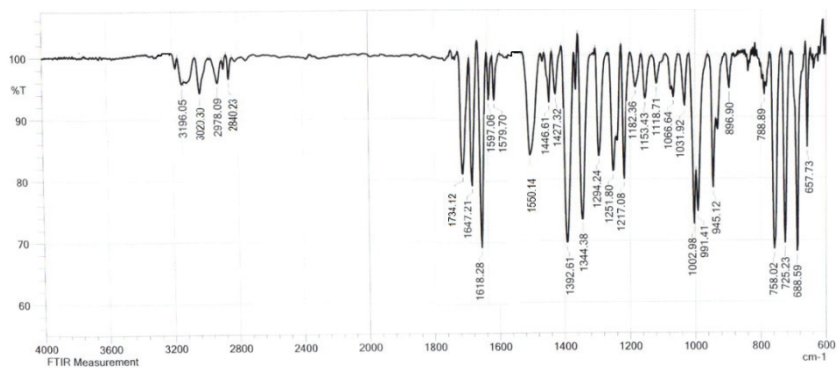
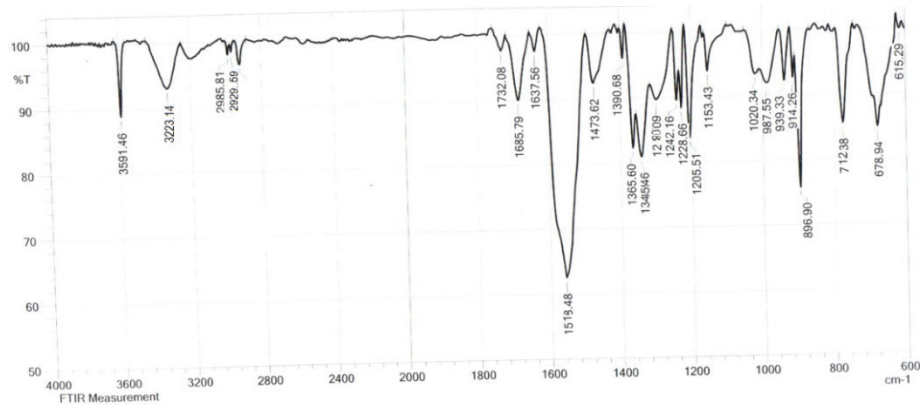
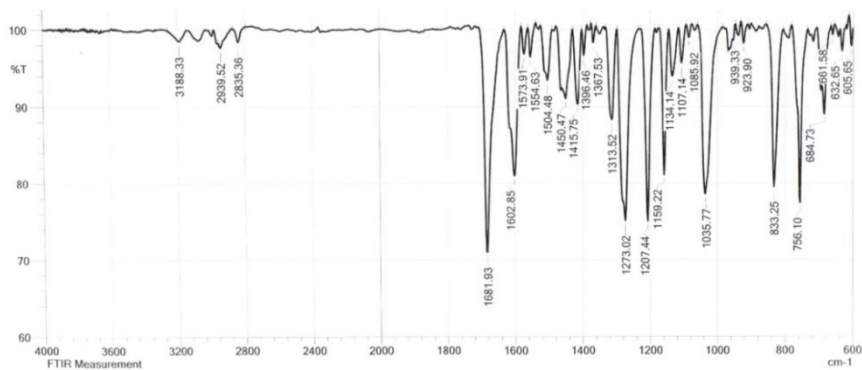
IR spectrum for 2-((4-Methyl-6-phenyl-2-thioxopyrimidin-1(2H)-yl) amino) aceto hydrazide (3)

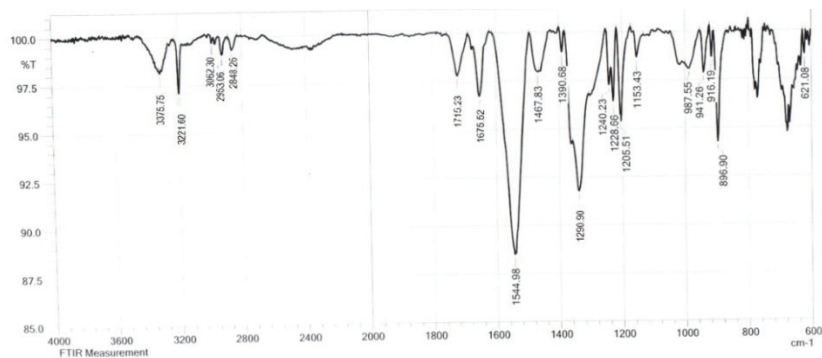


IR spectrum for 2-((4-methyl-6-phenyl-2-thioxopyrimidin-1(2H)-yl)amino)-N'-(4-nitrobenzylidene)acetohydrazide. (4)

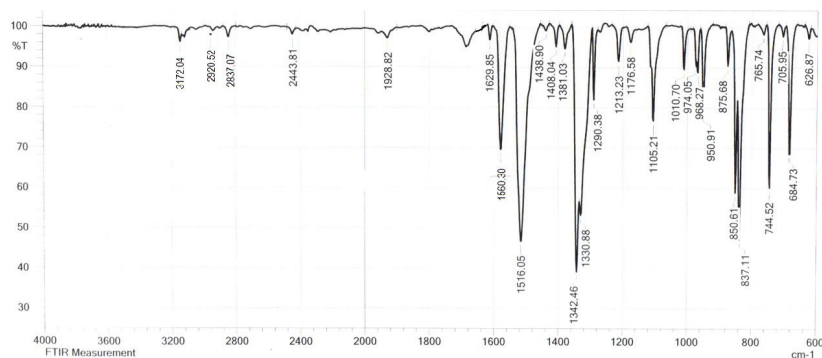


IR spectrum for N'-(2,4-dimethoxybenzylidene)-2-((4-methyl-6-phenyl-2-thioxopyrimidin-1(2H)-yl)amino)acetohydrazide.(5)

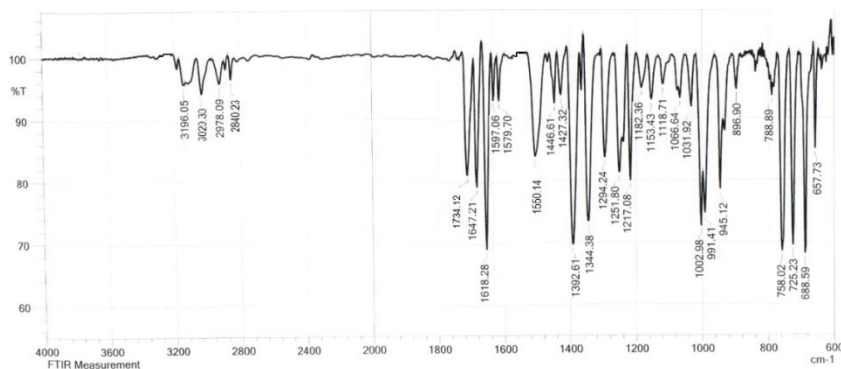




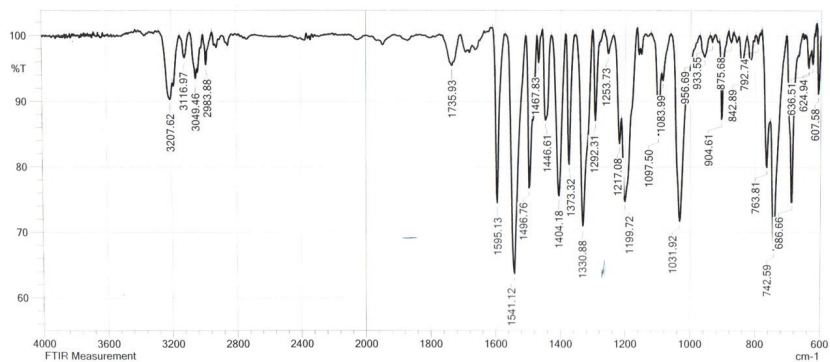
IR spectrum for N-(2-(4-(dimethylamino)phenyl)-4-oxothiazolidin-3-yl)-2-((4-methyl-6-phenyl-2-thioxypyrimidin-1(2H)-yl)amino)acetamide (9)



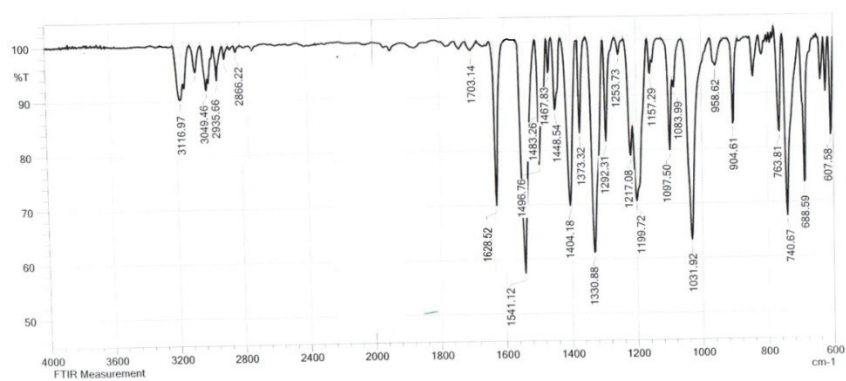
IR spectrum for 1-(4-methyl-6-phenyl-2-thioxypyrimidin-1(2H)-yl)-3-phenylthiourea (10)



IR spectrum for 5-(4-methyl-6-phenyl-2-thioxypyrimidin-1(2H)-yl)-1-phenyl-6-thioxopiperidine-2,4-dione(11)



IR spectrum for N-(4-methyl-6-phenyl-2-thioxopyrimidin-1(2H)-yl) acet amide (12)



IR spectrum for N-(4-methyl-6-phenyl-2-thioxopyrimidin-1(2H)-yl)-3-(4-nitrophenyl) acrylamide (13)



J. Serb. Chem. Soc. 89 (11) 1411–1422 (2024)
JSCS–5796

Synthesis and *in silico* ADMET evaluation of new thiazole and thiazolidine-4-one derivatives as non-ulcerogenic analgesic and anti-inflammatory agents

MANSUR NASSIRI KOOPAEI¹, MAHSHID MONAVARI², NASIM VOUSOOGHI^{3,4},
SADAF MOSHIRABADI⁵, MOHAMMAD JAVAD ASSARZADEH⁵, MOHSEN AMINI^{1,6}
and ALI ALMASIRAD^{5*}

¹Department of Medicinal Chemistry, Faculty of Pharmacy, Tehran University of Medical Sciences, Tehran, Iran, ²Department of Pharmacology and Toxicology, Faculty of Pharmacy, Tehran Medical Sciences, Islamic Azad University, Tehran, Iran, ³Department of Applied Cell Sciences, School of Advanced Technologies in Medicine, Tehran University of Medical Sciences, Tehran, Iran, ⁴Research Center for Cognitive and Behavioral Sciences, Tehran University of Medical Sciences, Tehran, Iran, ⁵Department of Medicinal Chemistry, Faculty of Pharmacy, Tehran Medical Sciences, Islamic Azad University, Tehran, Iran and ⁶Pharmaceutical Sciences Research Center (PSRC), The Institute of Pharmaceutical Sciences (TIPS), Tehran University of Medical Sciences, Tehran, Iran.

(Received 29 October 2023, revised 12 February, accepted 23 June 2024)

Abstract: A series of 1,3-thiazoline-4-one derivatives bearing 2-phenoxyphenyl moiety, were synthesized as potential new analgesic and anti-inflammatory agents. The structures were confirmed by FT-IR, NMR and mass spectra. The abdominal constriction (writing) test was selected to evaluate analgesic activity and the results showed that nearly all of them were active, and the most potent was **10m** with 96 % inhibition when compared to the control. The best compounds were selected to investigate the anti-inflammatory activity by carrageenan induced rat paw edema test. The results showed that compounds **8** and **10h** were active from the 2nd to 5th hour of assessment. The ulcerogenic evaluation of two selected compounds showed that they are comparable with the vehicle control group and without any ulcerogenic effect potential. The target compounds showed an acceptable *in silico* ADME profile.

Keywords: thiazoline; fenamate; writing test; carrageenan induced edema; cyclooxygenase.

INTRODUCTION

Non-steroidal anti-inflammatory drugs (NSAIDs) are important medications for the treatment of arthritis. NSAIDs alleviate the pain and swelling related to

* Corresponding author. E-mail: almasirad.a@iaups.ac.ir
<https://doi.org/10.2298/JSC231029064N>



arthritis by prevention of the arachidonic acid metabolism through the cyclooxygenase (COX) enzyme pathway and, as a result, thereby, the production of prostaglandins (PGs), which stimulate pain receptors.^{1,2}

Additionally, there is a close relationship between some leukotrienes (LTs), as the 5-lipoxygenase metabolites and the induction of hyperalgesia seen in the inflammation pathway by lowering the sensitivity of C fibers.^{3,4}

The LTs and PGs are involved in the acute ulcer caused by NSAIDs. Therefore, compounds that, in turn, inhibit both 5-LO and COX alleviate side effects and potentiate the pharmacological activity in the treatment of inflammation. There are some findings about the induction of dual 5-LOX/COX inhibitory activity of known NSAID, mefenamic acid, and its corresponding fenamate-like derivatives by changing their acidic moiety to hydrazone or different heterocyclic rings.^{1,5–10} Besides the anti-inflammatory activity of fenamate-like structures, antiepileptic and CCK-B antagonistic effects have been reported in compounds bearing these moieties.^{11,12}

However, thiazoline-4-one is another moiety with known biological activities including antimicrobial,¹³ antiparasitic,¹⁴ antidiabetic,¹⁵ antiviral,¹⁶ anticancer,¹⁷ antioxidant,¹⁸ antiseizure¹⁹ and anti-inflammatory properties²⁰ (Fig. 1). Amongst different thiazolidinones, the arylidene substituted derivatives are more attractive for medicinal chemists due to their pharmacological potential. The 4-arylidene conjugated with carbonyl moiety of this kind of heterocyclic ring can prepare an electrophilic position to the nucleophilic groups in different proteins and enzymes²¹. On this basis and using molecular hybridization of previously reported active compounds **1–3** (Fig. 2),²² herein the new 5-arylidene thiazoline-4-ones bearing fenamate-like structure **10a–n** were designed and synthesized, and their biological activities were evaluated.

EXPERIMENTAL

Chemistry

Thin layer chromatography was applied to control the reaction and purity of the products. Melting points were taken on an electrothermal IA 9300 capillary melting-point apparatus (Ontario, Canada) and are uncorrected. FT-IR spectra were recorded on Shimadzu FT-IR-8400 instrument in KBr disk. ¹H-NMR spectra were recorded on Bruker AC-400 MHz FT NMR (Brucker, Rheinstetten, Germany). ¹³C-NMR spectra were recorded on a Varian Unity INOVA 500 MHz spectrometer. Mass spectra were obtained using a Finnigan Mat TSQ-70 spectrometer at 70 eV (Finnigan Mat, Bremen, Germany) and a 5973 network mass selective detector (Agilent technology). Elemental analysis was performed with a Perkin-Elmer model 240-c apparatus (Perkin Elmer, Norwalk, CT, USA). The results of the elemental analyses (C, H, N) were within ±0.4 % of the calculated amount. Compound **6** was synthesized as reported previously.²³

Analytical and spectral data of the synthesized compounds are given in Supplementary material to this paper.

Synthesis of 2-(2-phenoxybenzylidene)thiosemicarbazide (7)

A suspension of 2-phenoxybenzaldehyde **6** (1 g, 5 mmol), thiosemicarbazide (0.45 g, 5 mmol) and ethanol (10 mL) was refluxed for 3 h. After cooling, the resulting thiosemicarbazone was removed by filtration and washed with water to give compound **7**.

Synthesis of 2-(2-phenoxybenzylidene)-2-(4-phenylthiazol-2-yl)hydrazine (8)

A mixture of thiosemicarbazone **7** (1 g, 3.7 mmol), phenacyl chloride (0.57 g, 3.7 mmol) and dry sodium acetate (1.5 g, 18 mmol) was dissolved in 15 mL of dry 1,4-dioxan. The solution was heated under reflux for 12 h. The mixture was cooled and diluted with water to give compound **8**.

Synthesis of 2-(2-(2-phenoxybenzylidene)hydrazinyl)thiazol-4(5H)-one (9)

A mixture of thiosemicarbazone **7** (1 g, 3.7 mmol), and ethyl bromoacetate (0.4 mL, 3.7 mmol), dry sodium acetate (1.2 g, 14.7 mmol) was dissolved in 15 mL of dry 1,4-dioxan. The solution was heated under reflux for 15 h. The mixture was cooled and diluted with water to give compound **9**.

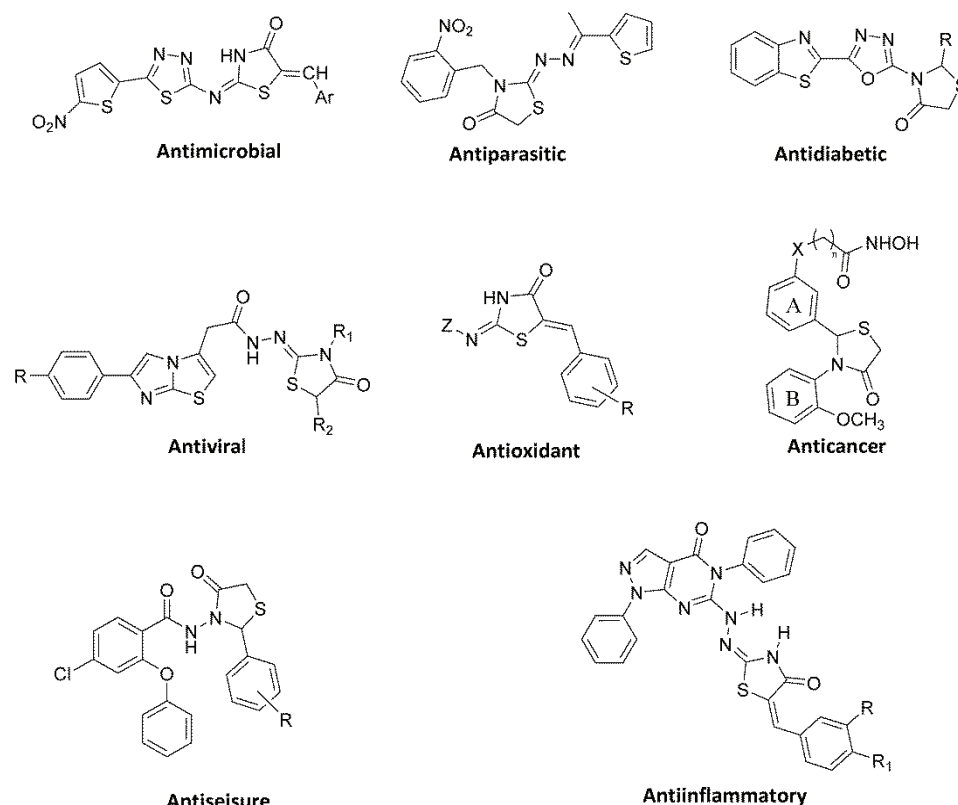


Fig. 1. Biologically active compounds bearing thiazolidinone ring.

General procedure for the preparation of 1,3-thiazoline-4-ones (10a–n)

A mixture of thiazolone **9** (1 g, 3.2 mmol) in glacial acetic acid (10 mL), corresponding aldehydes (3.4 mmol), and anhydrous sodium acetate (1 g, 12.8 mmol) were stirred under reflux for 18 h. The end of the reaction was observed by TLC, then cold water was added to the reaction mixture, and the resulting precipitate was filtered, washed by water and crystallized by ethanol. The structural parameters of **10a–n** were evaluated by FT-IR, NMR and mass spectra and have been reported at supplementary material.

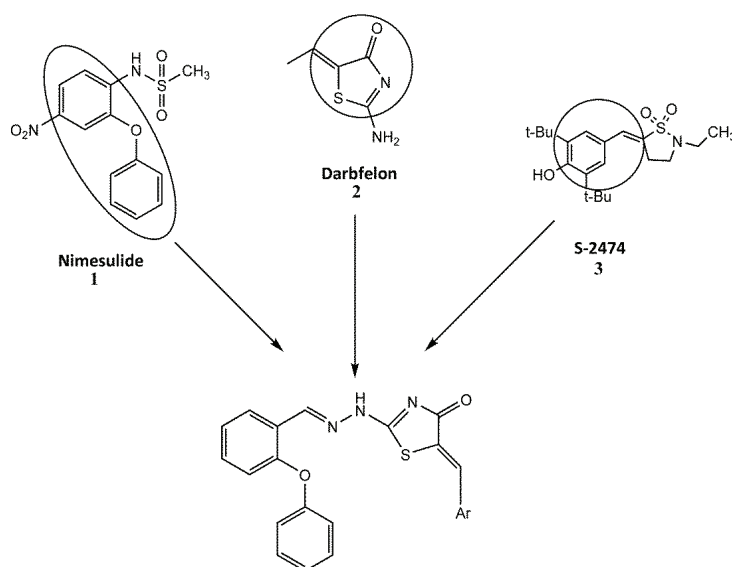


Fig. 2. The design of compounds **10a–n** according to the pharmacophoric pattern of well-known analgesic agents.

RESULTS AND DISCUSSION

Compound **6** was prepared by the reaction of salicylaldehyde **4** with bromobenzene **5** in dry DMF.²³ The reaction of **6** with thiosemicarbazide gave the thiosemicarbazone **7**. Treatment of **7** with phenacylchloride afforded compound **8**.²⁵ The thiazolidinone **9** was obtained through the cyclization of **7** by ethyl bromoacetate. The final derivatives (**10a–n**) were prepared *via* the reaction of **9** with different aldehydes (Fig. 3, Table I).²⁶

The thiazolidinone ring formation was confirmed through the FT-IR spectrum by finding of carbonyl at 1712 cm^{-1} and aliphatic CH_2 at 3.85 ppm in $^1\text{H-NMR}$. The structures of target compounds were confirmed by finding carbonyl vibrations over 1700 cm^{-1} and in $^1\text{H-NMR}$, olefinic CH, which was found in some compounds separately from the aromatic protons over 7.50 ppm and the imine proton $\text{N}=\text{CH}$ that was well defined between 8.50–8.90 ppm. The imine proton has appeared as two singlet signals in **10a–c**, **10e**, **10g–i** and **10k–n** that proves the formation of both *Z* and *E* isomers. However, the chemical shift of the

olefinic proton in different compounds put an emphasis on the *Z* configuration formation of the target derivatives over this band.²⁷

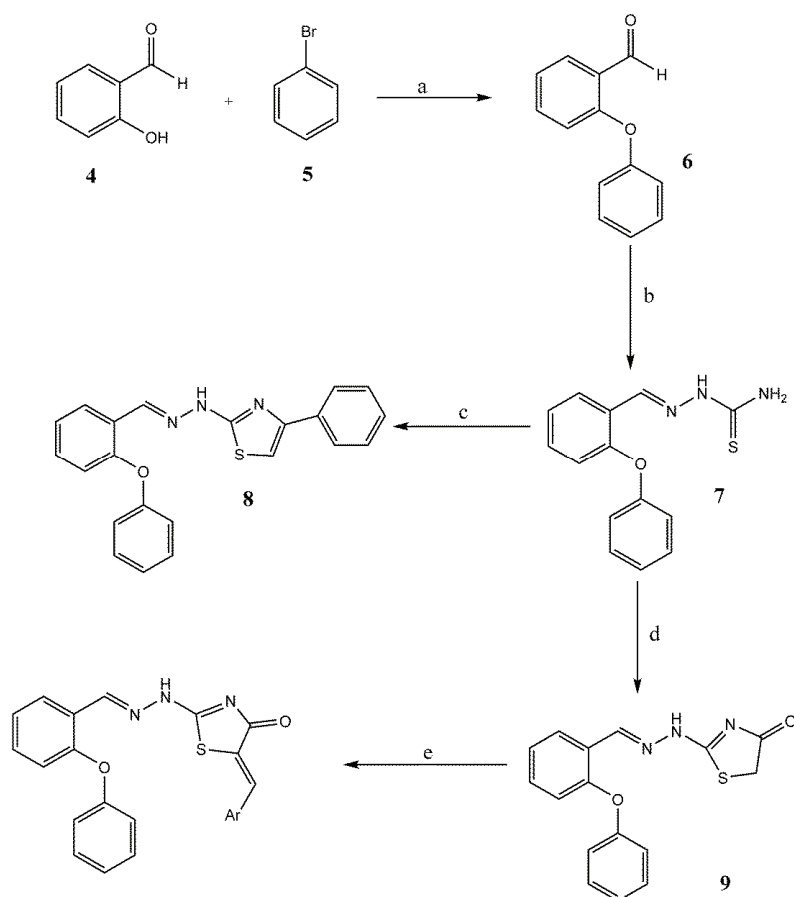
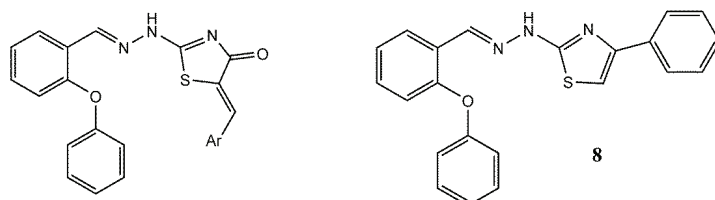


Fig. 3. Synthesis of compounds **10a-10s**: a) Cu, CuCl, K₂CO₃, DMF, reflux; b) NH₂NHCSNH₂, EtOH, reflux; c) Ph-COCH₂Cl, 1,4-dioxan, reflux; d) BrCH₂CO₂Et, 1,4-dioxan, reflux; e) ArCHO, AcONa, AcOH, reflux.

As seen in Table II, nearly all the target compounds showed significant analgesic activity in comparison to control, and amongst them, **10m** was more potent than mefenamic acid.

SAR studies showed that bioisosteric replacement of phenyl with some heterocyclic moieties (compounds **10k-m**) can lead to more potent compounds. In general, substituted phenyl ring is better than unsubstituted ring. Both electron-donating and withdrawing groups on the para position of the phenyl ring are tolerable. The comparison of **10e** and **10f** proves that substitution on para position of phenyl ring with electron donating groups is preferable to ortho.

TABLE I. The physical data of compounds **10a–n**

Compound	Ar	Melting point, °C	Yield, %	<i>M_w</i>	Mol. formula
8	–	136–137	51	371	C ₂₂ H ₁₇ N ₃ OS
10a	Phenyl	249–251	42	399	C ₂₃ H ₁₇ N ₃ O ₂ S
10b	4-Fluorophenyl	186–188	50	417	C ₂₃ H ₁₆ N ₃ FO ₂ S
10c	4-Chlorophenyl	227–229	51	433.5	C ₂₃ H ₁₆ N ₃ ClO ₂ S
10d	4-Bromophenyl	273–275	67	478	C ₂₃ H ₁₆ N ₃ BrO ₂ S
10e	2-Hydroxyphenyl	169–171	45	415	C ₂₃ H ₁₇ N ₃ O ₃ S
10f	4-Hydroxyphenyl	213–215	50	415	C ₂₃ H ₁₇ N ₃ O ₃ S
10g	4-Methylphenyl	205–207	50	413	C ₂₄ H ₁₉ N ₃ O ₂ S
10h	4-Methoxyphenyl	174–176	71	429	C ₂₄ H ₁₉ N ₃ O ₃ S
10i	4-Thiomethylphenyl	213–215	62	445	C ₂₄ H ₁₉ N ₃ O ₂ S ₂
10j	4-Nitrophenyl	251–253	47	444	C ₂₃ H ₁₆ N ₄ O ₄ S
10k	Furyl	186–188	37	389	C ₂₁ H ₁₅ N ₃ O ₃ S
10l	2-Pyridyl	209–211	36	400	C ₂₂ H ₁₆ N ₄ O ₂ S
10m	3-Pyridyl	260–262	42	400	C ₂₂ H ₁₆ N ₄ O ₂ S
10n	2-Phenoxyphenyl	219–221	50	491	C ₂₉ H ₂₁ N ₃ O ₃ S

TABLE II. The effects of compounds **10a–n** and mefenamic acid in the abdominal constrictions induced by acetic acid in mice

Compound	Constriction No. (mean ± SEM) ^a	Inhibition, % ^b	<i>P</i> value
Control	63.5±16.77	–	–
Mefenamic acid	8.16±3.31	87.13	< 0.001
8	08.17±02.31	87.13	< 0.001
10a	83.17±23.57	30.97	> 0.05
10b	34.00±03.41	46.45	< 0.001
10c	16.50±06.75	74.01	< 0.001
10d	26.50±12.69	58.26	< 0.001
10e	20.00±03.41	68.5	< 0.001
10f	11.00±02.53	82.67	< 0.001
10g	20.67±03.88	67.44	< 0.001
10h	13.17±06.01	79.25	< 0.001
10i	25.67±14.69	59.57	< 0.001
10j	25.33±07.39	60.11	< 0.001
10k	20.00±05.33	68.5	< 0.001
10l	21.50±03.45	66.14	< 0.001
10m	02.17±01.72	96.58	< 0.001
10n	15.00±04.24	76.38	< 0.001

^aNumber of animals in each group *n* = 6; ^binhibition obtained by comparison with vehicle control group

The pharmacological evaluation of the synthesized compounds showed that most of them were active anti-inflammatory agents in comparison to control, and the activity profile of compound **10h** was similar to mefenamic acid (Table III).

TABLE III. The anti-inflammatory activity of the selected compounds in the carrageenan-induced paw edema model in rat expressed as increase in paw volume \pm SEM in %; number of animals in each group: $n = 6$; *** $p < 0.001$, ** $p < 0.01$, * $p < 0.05$ compared to control group

Compound	Time, h				
	1	2	3	4	5
Control	30.29 \pm 3.146	49.87 \pm 2.10	52.67 \pm 2.61	50.87 \pm 2.33	46.37 \pm 1.85
Mefenamic acid	21.18 \pm 1.34	27.37 \pm 1.64***	25.7 \pm 1.88***	22.66 \pm 1.43***	19.69 \pm 0.70***
8	14.72 \pm 0.87***	21.81 \pm 1.09***	32.71 \pm 1.60***	37.83 \pm 0.80**	33.12 \pm 1.27**
10c	23.37 \pm 1.86	30.46 \pm 1.54***	36.15 \pm 0.82***	41.25 \pm 0.65	35.21 \pm 0.44*
10f	20.54 \pm 1.52	32.63 \pm 2.76**	41.74 \pm 3.49	49.38 \pm 4.51	46.07 \pm 4.15
10h	22.14 \pm 1.94	26.00 \pm 2.43***	29.98 \pm 3.75***	30.85 \pm 5.27**	27.44 \pm 5.27**
10m	23.32 \pm 1.39	32.56 \pm 4.43**	34.12 \pm 5.22*	33.06 \pm 6.59*	29.08 \pm 6.53**
10n	30.53 \pm 1.79	34.34 \pm 3.15**	39.13 \pm 1.21*	44.98 \pm 2.97	42.47 \pm 2.58

However, only compound **8** was effective from 1st to 5th hour. It could be deduced by comparing the results that both electron-withdrawing and donating groups on the benzylidene moiety are tolerable. The effectiveness of **10m** emphasizes the possibility of the replacement of phenyl with other heteroaromatic ring systems. Compounds **10c** and **10k** were evaluated for their acute ulcerogenic activity. A significant reduction in ulcerogenic activity without any stomach ulceration was observed in the both compounds compared to indomethacin (Table IV). However, indomethacin as the standard drug displayed a high score of 4 as shown in Table IV. In contrast, neither **10c** nor **10k** induced significant ulceration in comparison to control. The anti-oxidative activity of thiazolidinone and thiazoline rings could be the reason for their low ulcerogenic properties.²⁸

In silico ADMET evaluation

Eight pharmacokinetic parameters for forecasting oral bioavailability were calculated by the Swiss ADME online program (www.swissadme.ch).²⁹ As shown in Table S-I (supplementary material), all compounds except **10i**, **10j** and **10n** have high GI absorptions.

One of several tools for evaluating properties such as toxicity risk, log p , log s , fragment-based drug-likeness, and overall drug score is Osiris property explorer (OPE, <https://www.organic-chemistry.org/prog/peo/>), which is a web-based program. The OPE study demonstrated that except for compound **8**, which showed high risks of tumorigenic effects, compound **10f**, which showed high risk of reproductive effects, and compound **10k** which showed the high risk of mutagenic

effects, all compounds are supposed to be non-mutagenic, non-tumorigenic, non-irritant with no reproductive effects. The potential drug-likeness values of all compounds were positive (3.04–5.67) except for **10j** which was negative; hence, their similarity to traded drugs was more than that of the commercial chemicals Table S-II (Supplementary material). Another tool for assessing the ADMET properties of compounds is a comprehensive platform called admetSAR3.0, which is utilized for search, prediction, and optimization purposes.³⁰ Due to the admetSAR3.0, all compounds except for **8**, **10g**, **10h**, **10m** and **10n** which display low oral bioavailability, are expected to exhibit high oral absorption. Comparing the SwissADME online program with admetSAR3.0, both tools are an indicator of a poor oral bioavailability of derivative **10m**. Furthermore, admetSAR3.0, providing a more comprehensive and precise assessment, reveals poor oral absorption for compounds **8**, **10g**, **10h** and **10n**. Regarding the toxicity risks predicting by admetSAR3.0, all compounds, excluding **8**, are anticipated to be non-carcinogenic, non-irritant with no respiratory toxicity. Compound **8** stands out as carcinogenic. Additionally, a comparison between OPE and admetSAR3.0 tools, reveals the mutual carcinogenicity of compound **8**. OPE also highlights compound **10c** for tumorigenicity. According to admetSAR3.0, compounds **8**, **10a**, **10g**, **10h**, **10k** and **10m** are supposed to have no reproductive toxicity. Conversely, other compounds are anticipated to exhibit harmful reproductive effects. Notably, while OPE identifies compound **10h** with high risks for reproductive effects, admetSAR3.0 categorizes this derivative as posing low risk Table S-III (Supplementary material).

TABLE IV. The ulcerogenic activity observed on gastric mucosa of rats; number of animals in each group: $n = 6$; ulcerogenic activity = the mean score of control and each treated group, *** $p < 0.001$ as compared to indomethacin group

Compound	Ulcerogenic activity (mean \pm SEM)
Control	0.00 \pm 0.00
Indomethacin	3.67 \pm 0.21
10c	0.00 \pm 0.00***
10k	0.00 \pm 0.00***

Pharmacological evaluations

All ethical manners for the use of laboratory animals were considered carefully, and the study protocol was approved by the IAU-TMS ethical committee. The analgesic activity was determined *in vivo* by the acetic acid induced abdominal constriction (writhing) test on mice, and all the procedures, statistical analysis, and calculation of inhibition percent were performed conforming to our previously expressed research.⁵ In writhing test, significant reduction in constrictions, when compared to control, is an accepted parameter showing the analgesic

potency of a compound and the procedure was explained in Supplementary material.

The most potent compounds in the previous test were selected for further evaluation. Anti-inflammatory activity was assessed by carrageenan-induced rat paw edema test.^{6,23} In the mentioned test, the ability of compound to significantly inhibit the paw edema induced by carrageenan could be considered as an important parameter of anti-inflammatory activity and the procedure was described in Supplementary material. Ulcerogenic potential of the two selected target compounds **10c** and **10k** were evaluated and scored by the method of Cioli on Wistar rats.³¹ The method of performance and other situations and scoring system (no lesion: 0 to more than one large ulcer: 4), were chosen as the previously described procedures.^{27,32,33} In this experiment the mucosal damage induced by high dose orally administered reference drug and **10c** and **10k** were evaluated according to the mentioned scoring order and the method was illustrated in Supplementary material.

CONCLUSION

New 1,3-thiazoline-4-one derivatives with 2-phenoxyphenyl and different arylidene moieties were synthesized, their analgesic and anti-inflammatory activities were screened *in vivo*. The results revealed that most of them (**10b–n**) were effective analgesic agents in comparison to control, and their activities were comparable or higher than for mefenamic acid. Most of the evaluated compounds and mefenamic acid were inactive at the 1st hour of evaluation, but compound **8** was active at this hour. Some of the final products (**8**, **10h** and **10m**) were efficient anti-inflammatory agents when compared to the control, and they were active at the 2nd to 5th hour of assessment, similar to mefenamic acid. The acute gastric ulcerogenic activity of the selected derivatives (**10c** and **10k**) was evaluated and, unlike indomethacin, their severity index was same as for the control group.

SUPPLEMENTARY MATERIAL

Additional data and information are available electronically at the pages of journal website: <https://www.shd-pub.org.rs/index.php/JSCS/article/view/12641>, or from the corresponding author on request.

Acknowledgement. Authors would like to thank the late professor Abbas Shafiee for his considerable help that made this work possible.

ИЗВОД

СИНТЕЗА И *IN SILICO* ИСПИТИВАЊЕ АДМЕТ ОСОБИНА СЕРИЈЕ НОВИХ ДЕРИВАТА ТИАЗОЛА И ТИАЗОЛИДИН-4-ОНА КАО НЕ-УЛЦЕРОГЕНСКИХ АНАЛГЕТИКА И АНТИ-ИНФЛАМАТОРНИХ АГЕНАСА

MANSUR NASSIRI KOOPAEI¹, MAHSHID MONAVARI², NASIM VOUSOOGHI^{3,4}, SADAF MOSHIRABADI⁵, MOHAMMAD JAVAD ASSARZADEH⁵, MOHSEN AMINI^{1,6} и ALI ALMASIRAD⁵

¹Department of Medicinal Chemistry, Faculty of Pharmacy, Tehran University of Medical Sciences, Tehran, Iran, ²Department of Pharmacology and Toxicology, Faculty of Pharmacy, Tehran Medical Sciences, Islamic Azad University, Tehran, Iran, ³Department of Applied Cell Sciences, School of Advanced Technologies in Medicine, Tehran University of Medical Sciences, Tehran, Iran, ⁴Research Center for Cognitive and Behavioral Sciences, Tehran University of Medical Sciences, Tehran, Iran, ⁵Department of Medicinal Chemistry, Faculty of Pharmacy, Tehran Medical Sciences, Islamic Azad University, Tehran, Iran и ⁶Pharmaceutical Sciences Research Center (PSRC), The Institute of Pharmaceutical Sciences (TIPS), Tehran University of Medical Sciences, Tehran, Iran

Синтетисана је нова серија деривата 1,3-тиазолин-4-она, која садржи 2-феноксифенилну групу, као потенцијално нових аналгетичких и анти-инфламаторних агенаса. Структуре једињења су потврђене FT-IR, NMR и масеним спектрима. Тест абдоминалне пункције је одабран за испитивање аналгетичке активности. Добијени резултати показују да су скоро сва једињења активна, и да је дериват **10m** најактивнији са 96 % инхибиције у поређењу са контролним једињењем. Најактивнија једињења су одабрана да им се испита анти-инфламаторна активност тестом едема изазваног карагенаном на шапи пацова. Резултати показују да су једињења **8** и **10h** активна од 2. до 5. сата тестирања. Испитивање улцерогене активности два одабрана једињења су упоредива са контролном групом и не показују потенцијал за улцерогенску активност. Циљана једињења показују прихватљиве *in silico* ADME профиле.

(Примљено 29. октобра, ревидирано 12. фебруара 2023, прихваћено 23. јуна 2024)

REFERENCES

1. A. Almasirad, M. Tajik, D. Bakhtiari, A. Shafiee, M. Abdollahi M, M. J. Zamani, R. Khorasani, H. Esmaily, *J. Pharm. Pharma. Sci.* **8** (2005) 419 ([https://sites.ualberta.ca/~csps/JPPS8\(3\)/A.Shafiee/mefenamic.htm](https://sites.ualberta.ca/~csps/JPPS8(3)/A.Shafiee/mefenamic.htm))
2. M. Shekarchi, L. navidpour, A. Rajabi-Khorami, M. Shekarchi, A. Partoazar, H. Shafaroodi, N. Rahmanipour, A. Shafiee, M. Shekarchi, *Iran. J. Pharm. Res.* **10** (2011) 369 (<https://www.ncbi.nlm.nih.gov/pmc/articles/PMC3828903/>)
3. S. Nikfar, M. Abdollahi, F. Etemad, M. Sharifzadeh, *Gen. Pharmacol.* **29** (1997) 583 ([https://doi.org/10.1016/S0306-3623\(96\)00575-7](https://doi.org/10.1016/S0306-3623(96)00575-7))
4. C. Charlier, C. Michaux. *Eur. J. Med. Chem.* **38** (2003) 645 ([https://doi.org/10.1016/S0223-5234\(03\)00115-6](https://doi.org/10.1016/S0223-5234(03)00115-6))
5. A. Almasirad, R. Hosseini, H. Jalalizadeh, Z. Rahimi-Moghaddam, N. Abaeian, M. Janafrooz, M. Abbaspour, V. Ziaee, A. Dalvandi, A. Shafiee, *Biol. Pharma. Bull.* **29** (2006) 1180 (<https://doi.org/10.1248/bpb.29.1180>)
6. A. Rineh, N. Mahmoodi, M. Abdollahi, A. Foroumadi, M. Sorkhi, A. Shafiee, *Arch. Pharm. Chem. Life Sci.* **340** (2007) 409 (<https://doi.org/10.1002/ardp.200700045>)
7. A. Shafiee, A. Rineh, A. Kebriaeezadeh, A. Foroumadi, V. Sheibani, M. R. Afarinesh, *Med. Chem. Res.* **18** (2009) 758 (<https://doi.org/10.1007/s00044-009-9165-0>)

8. D. H. Boschelli, D. T. Connor, D. A. Bornemeier, R. D. Dyer, J. A. Kennedy, P. J. Kuipers, G. C. Okonkwo, D. J. Schrier, C. D. Wright, *J. Med. Chem.* **36** (1993) 1802 (<https://doi.org/10.1021/jm00065a002>)
9. D.P. Wallach, V.R. Brown, *Biochem. Biophys. Acta (BBA) – Lipids Lipid. Met.* **663** (1981) 361 ([https://doi.org/10.1016/0005-2760\(81\)90165-X](https://doi.org/10.1016/0005-2760(81)90165-X))
10. A. Almasirad, A. Shafiee, M. Abdollahi, A. Neoparast, N. Shahrokhinejad, N. Vousooghi, S. A. Tabatabai, R. Khorasani, *Med. Chem. Res.* **20** (2011) 435 (<https://doi.org/10.1007/s00044-010-9335-0>)
11. A. Almasirad, S.A.Tabatabai, M. Faizi, A. Kebriaeezadeh, N. Mehrabi, A. Dalvandi, A. Shafiee. *Bioorg. Med. Chem. Lett.* **14** (2004) 6057 (<https://doi.org/10.1016/j.bmcl.2004.09.072>)
12. A. Almasirad, M. Sheikha, R. Hosseini, S. A. Tabatabai, A. Shafiee, *Arch. Pharm.* **337** (2004) 193 (<https://doi.org/10.1002/ardp.200300822>)
13. A. Khomami, M. Rahimi, A. Tabei, P. Saniee, A. Mahboubi, A. Foroumadi, N. Nassiri-Koopaei, A. Almasirad, *Mini. Rev. Med. Chem.* **19** (2019) 239 (<https://doi.org/10.2174/1389557518666181017142630>)
14. S. Carradori, D. Secci, B. Bizzarri, P. Chimenti, C. De-Monte, P. Guglielmi, C. Campestre, D. Rivanera, C. Bordon, L. Jones-Brando, *J. Enzyme Inhib. Med. Chem.* **32** (2017) 746 (<https://doi.org/10.1080/14756366.2017.1316494>)
15. R. Bhutani, D. P. Pathak, G. Kapoor, A. Husain, M. A. Iqbal, *Bioorg. Chem.* **83** (2019) 6 (<https://doi.org/10.1016/j.bioorg.2018.10.025>)
16. N. U. Güzeldemirci, E. Pehlivan, L. Naesens, *Marmara Pharm. J.* **22** (2018) 237 (<https://doi.org/10.12991/mpj.2018.61>)
17. F. Yang, S. Peng, Y. Li, L. Su, Y. Peng, J. Wu, H. Chen, M. Liu, Z. Yi, Y. Chen, *Org. Biomol. Chem.* **14** (2016) 1727 (<https://doi.org/10.1039/c5ob02250a>)
18. M. Djukic, M. Fesatidou, I. Xenikakis, A. Geronikaki, V. T. Angelova, V. Savic, M. Pasic, B. Krilovic, D. Djukic, B. Gobeljic, M. Pavlica, A. Djuric, I. Stanojevic, D. Vojvodic, L. Saso. *Chem. Biol. Interact.* **286** (2018) 119 (<https://doi.org/10.1016/j.cbi.2018.03.013>)
19. M. Faizi, R. Jahani, S. A. Ebadi, S. A. Tabatabai, E. Rezaee, M. Lotfaliei, M. Amini, A. Almasirad, *EXCLI J.* **16** (2017) 52 (<https://doi.org/10.17179/excli2016-692>)
20. G. N. Tageldin, S. M. Fahmy, H. M. Ashour, M. A. Khalil, R. A. Nassra, I. M. Labouta, *Bioorg. Chem.* **80** (2018) 164 (<https://doi.org/10.1016/j.bioorg.2018.06.013>)
21. D. Kaminsky D, A. Kryshchysyn, R. Lesyk, *Eur. J. Med. Chem.* **140** (2017) 542 (<https://doi.org/10.1016/j.ejmech.2017.09.031>)
22. K. Oda, T. Hida, T. Sakata, M. Nagai, Y. Sugata, T. Masui, H. Nogusa, *Org. Process. Res. Dev.* **12** (2008) 442 (<https://doi.org/10.1021/op800008w>)
23. A. Almasirad, M. Nassiri Koopaei, A. Shafiee, N. Nassiri-Koopaei, M. J. Assarzadeh, A. Tabei, M. Ghadimi, *J. Pharm. Health. Sci.* **1** (2013) 137 (<https://sid.ir/paper/188761/en>)
24. M. Nassiri Koopaei, M. J. Assarzadeh, A. Almasirad, S. F. Ghasemi-Niri, M. Amini, A. Kebriaeezadeh, N. Nassiri-Koopaei, M. Ghadimi, A. Tabei, *Iran. J. Pharm. Res.* **12** (2013) 721 (<https://doi.org/10.22037/ijpr.2013.1366>)
25. S. Bondock, W. Khalifa, A. A. Fadda, *Eur. J. Med. Chem.* **42** (2007) 948 (<https://doi.org/10.1016/j.ejmech.2006.12.025>)
26. A. Almasirad, N. Vousooghi, S. A. Tabatabai, A. Kebriaeezadeh, A. Shafiee, *Acta Chim. Slov.* **54** (2007) 317 ([https://acta-arhiv.chem-soc.si/54/graph/acta-54\(2\)-GA.htm](https://acta-arhiv.chem-soc.si/54/graph/acta-54(2)-GA.htm))

27. K. Omar, A. Geronikaki, P. Zoumpoulakis, C. Camoutsis, M. Soković, A. Ćirić, J. Glamočlija, *Bioorg. Med. Chem.* **18** (2010) 426 (<https://doi.org/10.1016/j.bmc.2009.10.041>)
28. M. H. Shih, F. Y. Ke, *Bioorg. Med. Chem.* **12** (2004) 4633 (<https://doi.org/10.1016/j.bmc.2004.06.033>)
29. A. Daina, O. Michielin, V. Zoete, *Sci. Rep.* **7** (2017) 42717 (<https://doi.org/10.1038/srep42717>)
30. Gu Y . Gu, Z. Yu, Y. Wang, L. Chen, C. Lou, C. Yang, W. Li, G. Liu, Y . Tang, *Nucleic Acids Res.* **22** (2024) gkae298 (<https://doi.org/10.1093/nar/gkae298>)
31. S. M. I. Badr, *Turkish J. Chem.* **35** (2011) 131 (<https://doi.org/10.3906/kim-1001-473>)
32. C. Anamaria, D. Leonte, L. Vlase, L. Csaba Bencze, S. Imre, G. Marc, B. Apan, C. Mogoşan, V. Zaharia, *Molecules* **23** (2018) 2425 (<https://doi.org/10.3390/molecules23102425>)
33. M. J. Assarzadeh, A. Almasirad, A. Shafiee, M. Nassiri Koopaei, M. Abdollahi, *Med. Chem. Res.* **23** (2014) 948 (<https://doi.org/10.1007/s00044-013-0697-y>).

SUPPLEMENTARY MATERIAL TO
**Synthesis and *in silico* ADMET evaluation of new thiazole and
thiazolidine-4-one derivatives as non-ulcerogenic analgesic and
anti-inflammatory agents**

MANSUR NASSIRI KOOPAEI¹, MAHSHID MONAVARI², NASIM VOUSOOGHI^{3,4},
SADAF MOSHIRABADI⁵, MOHAMMAD JAVAD ASSARZADEH⁵, MOHSEN AMINI^{1,6}
and ALI ALMASIRAD^{5*}

¹Department of Medicinal Chemistry, Faculty of Pharmacy, Tehran University of Medical Sciences, Tehran, Iran, ²Department of Pharmacology and Toxicology, Faculty of Pharmacy, Tehran Medical Sciences, Islamic Azad University, Tehran, Iran, ³Department of Applied Cell Sciences, School of Advanced Technologies in Medicine, Tehran University of Medical Sciences, Tehran, Iran, ⁴Research Center for Cognitive and Behavioral Sciences, Tehran University of Medical Sciences, Tehran, Iran, ⁵Department of Medicinal Chemistry, Faculty of Pharmacy, Tehran Medical Sciences, Islamic Azad University, Tehran, Iran and ⁶Pharmaceutical Sciences Research Center (PSRC), The Institute of Pharmaceutical Sciences (TIPS), Tehran University of Medical Sciences, Tehran, Iran

J. Serb. Chem. Soc. 89 (11) (2024) 1411–1422

Synthesis of (2-phenoxybenzylidene)thiosemicarbazide (7)

The yield was 1.0 g (69%), mp 203–205°C (EtOH); IR (KBr): $\nu_{\text{cm}^{-1}}$, 3426, 3264 (NH₂ NH), 3165 (CH, aromatic, alkene), 1606 (C=N), 1365 (C=S). ¹H NMR (DMSO-*d*₆, 400MHz): 11.41 (bs, 1H, NH), 8.36 (s, 1H, CH=N), 8.20 (d, J=8.0Hz, 1H, aromatic), 7.95 (bs, 2H, NH₂), 7.45–6.93(m, 8H, aromatic).

Synthesis of (2-phenoxybenzylidene)-2-(4-phenylthiazol-2-yl)hydrazine (8)

Yield (51%), IR (KBr): $\nu_{\text{cm}^{-1}}$, 3298 (NH), 3165 (CH, aromatic, alkene), 1686 (C=N). ¹H NMR (DMSO-*d*₆, 400MHz): 12.20 (bs, 1H, NH), 8.31 (s, 1H, CH=N), 7.95 (d, J=7.6Hz, 1H, aromatic), 7.84 (d, J=8.4Hz, 2H, aromatic), 7.43–7.38 (m, 4H, aromatic), 7.33 (s, 1H, thiazole), 7.31–7.13 (m, 4H, aromatic), 7.01 (d, J=8.0Hz, 2H, aromatic), 6.94 (d, J=8.0Hz, 1H, aromatic). ¹³C NMR (125 MHz, DMSO-*d*₆): δ = 168.49, 157.62, 154.47, 136.28, 131.22, 130.60, 129.52, 129.05, 128.00, 126.38, 126.07, 125.99, 124.87, 123.86, 120.22, 118.40, 118.30, 104.25. MS: m/z (%) 371 (M⁺, 29), 356 (6), 328 (4), 269 (15), 198 (71), 181 (100), 168 (29), 152 (17), 134 (35), 77 (93),

51(44).Anal. Calcd. for C₂₂H₁₇N₃OS: C, 71.15; H, 4.58; N, 11.32. Found: C, 71.20; H, 4.63; N, 11.27.

* Corresponding author. E-mail: almasirad.a@iaups.ac.ir

2-(2-(2-phenoxybenzylidene)hydrazinyl)thiazol-4(5H)-one (9)

The yield was 1.0 g (71%), mp 214–218°C (EtOH); IR (KBr): vcm^{-1} , 3441 (NH), 3052 (CH, aromatic, alkene), 1712 (C=O), 1641 (C=N). ^1H NMR (DMSO- d_6 , 400MHz): 11.95 (bs, 1H, NH), 8.48 (s, 1H, CH=N), 7.99 (d, 1H, $J=7.2\text{Hz}$, aromatic), 7.50–6.97 (m, 8H, aromatic), 3.85 (s, 2H, CH_2 , thiazolone). Anal. Calcd. for $\text{C}_{16}\text{H}_{13}\text{N}_3\text{O}_2\text{S}$: C, 61.73; H, 4.18; N, 13.50. Found: C, 61.68; H, 4.14; N, 13.54.

2-(2-(2-phenoxybenzylidene)hydrazinyl)-5-(benzylidene)thiazol-4(5H)-one (10a)

Yield (42%), IR (KBr): vcm^{-1} , 3411 (NH), 3059 (CH aromatic, alkene), 1719 (C=O), 1643 (C=N). ^1H NMR (DMSO- d_6 , 400MHz): 12.61 (bs, 1H, NH), 8.67, 8.53 (s, 1H, CH=N, E/Z isomers, 23% & 67%), 7.85–7.01 (m, 15H, aromatic, alkene). ^{13}C NMR (125 MHz, DMSO- d_6): $\delta=$ 168.59, 157.81, 134.45, 134.21, 131.38, 130.70, 130.64, 130.30, 130.14, 129.70, 129.34, 129.12, 128.38, 124.96, 124.31, 124.10, 123.92, 118.95, 118.31. MS: m/z (%) 399 (M^+ , 9), 307 (95), 230 (38), 219 (8), 197 (18), 181 (35), 134 (100), 104 (12), 90 (40), 77 (22), 51 (14). Anal. Calcd. for $\text{C}_{23}\text{H}_{17}\text{N}_3\text{O}_2\text{S}$: C, 69.17; H, 4.26; N, 10.52. Found: C, 69.23; H, 4.31; N, 10.45.

2-(2-(2-phenoxybenzylidene)hydrazinyl)-5-(4-fluorophenyl)thiazol-4(5H)-one (10b)

Yield (50%), IR (KBr): vcm^{-1} , 3444 (NH), 1716 (C=O), 1641 (C=N). ^1H NMR (DMSO- d_6 , 400MHz): 8.59, 8.52 (s, 1H, CH=N, E/Z isomers, 55% & 45%), 8.09–6.95 (m, 15H, =CH alkene, aromatic). ^{13}C NMR (125 MHz, DMSO- d_6): $\delta=$ 161.88, 157.63, 155.59, 133.09, 132.66, 132.59, 130.69, 130.63, 127.74, 125.72, 124.90, 124.77, 124.32, 123.93, 120.40, 118.96, 118.32, 118.22, 116.89, 116.71, 116.55, 116.37. MS: m/z (%) 417 (M^+ , 2), 397 (3), 343 (10), 323 (6), 311 (18), 237 (78), 218 (17), 197 (90), 181 (100), 152 (34), 141 (22), 123 (42), 108 (68), 95 (37), 77 (40), 51 (28). Anal. Calcd. for $\text{C}_{23}\text{H}_{16}\text{N}_3\text{FO}_2\text{S}$: C, 66.18; H, 3.83; N, 10.07. Found: C, 66.24; H, 3.77; N, 10.02.

2-(2-(2-phenoxybenzylidene)hydrazinyl)-5-(4-chlorobenzylidene)thiazol-4(5H)-one (10c)

Yield (51%), IR (KBr): vcm^{-1} , 3420 (NH), 3031 (CH aromatic, alkene), 1717 (C=O), 1643 (C=N). ^1H NMR (DMSO- d_6 , 400MHz): 8.62, 8.53 (s, 1H, CH=N, E/Z isomers, 54% & 46%), 8.08 (dd, $J=9.2\text{Hz}$, $J=2.0\text{Hz}$, 1H, aromatic), 7.85 (d, $J=8.4\text{Hz}$, 2H, aromatic), 7.72–7.06 (m, 9H, aromatic, alkene), 7.01 (d, $J=8.4\text{Hz}$, 2H, aromatic). ^{13}C NMR (125 MHz, DMSO- d_6): $\delta=$ 167.89, 157.56, 155.71, 152.61, 134.75, 133.22, 132.96, 131.93, 130.63, 129.99, 129.73, 129.44, 128.20, 127.79, 125.53, 124.84, 123.97, 120.30, 118.38. MS: m/z (%) 433 (M^+ , 9), 375 (25), 340 (22), 324 (17), 255 (22), 197 (44), 181 (100), 168 (62), 152 (21), 139 (90), 124 (25), 111 (56), 77 (38), 51 (22). Anal. Calcd. for $\text{C}_{23}\text{H}_{16}\text{N}_3\text{ClO}_2\text{S}$: C, 63.66; H, 3.69; N, 9.68. Found: C, 63.69; H, 3.75; N, 9.61.

2-(2-(2-phenoxybenzylidene)hydrazinyl)-5-(4-Bromobenzylidene)thiazol-4(5H)-one (10d)

Yield (67%), IR (KBr): vcm^{-1} , 3422 (NH), 3031 (CH aromatic, alkene), 1716 (C=O), 1645 (C=N). ^1H NMR (DMSO- d_6 , 400MHz): 12.65 (bs, 1H, NH), 8.53 (s, 1H, CH=N), 8.07–6.96 (m, 14H, =CH alkene, aromatic). ^{13}C NMR (125 MHz, DMSO- d_6): $\delta=$ 167.00, 156.89, 133.53, 133.29, 132.70, 132.40, 132.12, 130.72, 130.65, 130.22, 129.47, 128.38, 124.97, 124.94, 124.79, 124.38, 123.64, 119.43, 119.01. MS: m/z (%) 479 ($\text{M}^+ + 2$, 5), 477 (M^+ , 5), 392 (21), 311 (11), 297 (32), 284 (22), 254 (22), 213 (75), 211 (75), 196 (94), 181 (100), 165 (37), 152 (40), 133 (25), 115 (23), 89 (85), 77 (84). Anal. Calcd. for $\text{C}_{23}\text{H}_{16}\text{N}_3\text{BrO}_2\text{S}$: C, 57.74; H, 3.34; N, 8.78. Found: C, 57.69; H, 3.37; N, 8.82.

2-(2-(2-phenoxybenzylidene)hydrazinyl)-5-(2-hydroxybenzylidene)thiazol-4(5H)-one (10e)

Yield (45%), IR (KBr): vcm^{-1} , 3419 (OH,NH), 3031 (=CH aromatic, alkene), 1712 (C=O), 1630 (C=N). ^1H NMR (DMSO- d_6 , 400MHz): 12.85 (bs, 1H, NH), 10.79 (s, 1H, OH), 8.74, 8.61 (s, 1H, CH=N, E/Z isomers, 65% & 35%), 7.80 (d, $J=7.71$, 1H, aromatic), 7.72-7.63(m, 2H, aromatic), 7.53-7.02 (m, 11H, =CH aromatic, alkene), 6.96 (d, 1H, $J=8.0\text{Hz}$, aromatic). ^{13}C NMR (125 MHz, DMSO- d_6): $\delta=$ 163.72, 158.31, 156.85, 155.84, 133.08, 132.28, 130.73, 130.65, 129.99, 129.38, 127.83, 127.53, 124.81, 124.41, 123.98, 123.45, 120.07, 119.43, 119.03, 118.36, 116.86. MS: m/z (%) 415 (M^+ , 8), 398 (6), 322 (11), 255 (13), 196 (21), 181 (100), 165 (37), 152 (14), 121 (30), 77 (60), 51 (30). Anal. Calcd. for $\text{C}_{23}\text{H}_{17}\text{N}_3\text{O}_3\text{S}$: C, 66.50; H, 4.09; N, 10.12. Found: C, 66.56; H, 4.04; N, 10.15.

2-(2-(2-phenoxybenzylidene)hydrazinyl)-5-(4-hydroxybenzylidene)thiazol-4(5H)-one (10f)

Yield (50%), IR (KBr): vcm^{-1} , 3354 (OH, NH), 3025 (=C.H aromatic, alkene) 1710 (C=O), 1636 (C=N). ^1H NMR (DMSO- d_6 , 400MHz): 12.55 (bs, 1H, NH), 10.08 (bs, 1H,OH), 8.61 (s, 1H, CH=N), 8.38 (d, 1H, $J=6.4\text{Hz}$, aromatic), 8.06-6.75 (m, 10H, aromatic), 7.57 (s, 1H, alkene), 6.87 (d, $J=8.8\text{Hz}$, 2H, aromatic). ^{13}C NMR (125 MHz, DMSO- d_6): $\delta=$ 165.89, 159.80, 157.65, 155.58, 133.10, 132.59, 130.69, 130.63, 129.96, 127.84, 124.94, 124.31, 123.92, 120.43, 118.94, 118.31, 116.72, 116.25, 116.17. MS: m/z (%) 415 (M^+ , 62), 398 (16), 339 (37), 322 (100), 225 (9), 196 (25), 181 (96), 165 (14), 150 (71), 121 (25), 77 (26), 51 (12). Anal. Calcd. for $\text{C}_{23}\text{H}_{17}\text{N}_3\text{O}_3\text{S}$: C, 66.50; H, 4.09; N, 10.12. Found: C, 66.47; H, 4.06; N, 10.09.

2-(2-(2-phenoxybenzylidene)hydrazinyl)-5-(4-methylbenzylidene)thiazol-4(5H)-one (10g)

Yield (50%), IR (KBr): vcm^{-1} , 3438 (NH), 3027 (=CH aromatic, alkene), 1712 (C=O), 1642 (C=N). ^1H NMR (DMSO- d_6 , 400MHz): 12.55 (bs, 1H, NH), 8.54, 8.44 (s, 1H, CH=N, E/Z isomers, 41% & 35%), 8.08 (d, 1H, $J=8\text{Hz}$, aromatic), 7.78-6.99 (m, 13H, , aromatic, alkene), 2.36 (s, 3H, CH₃). ^{13}C NMR (125 MHz, DMSO- d_6): $\delta=$ 165.23, 157.76, 155.31, 141.20, 140.00, 132.73, 131.91, 131.65, 130.62, 130.28, 130.24, 130.17, 129.93, 128.30, 124.99, 123.82, 118.82, 118.73, 118.18, 21.53. MS: m/z (%) 413 (M^+ , 66), 398 (12), 337 (42), 320 (100), 255 (10), 196 (19), 181 (92), 148 (62), 119 (19), 77 (21), 51 (10). Anal. Calcd. for $\text{C}_{24}\text{H}_{19}\text{N}_3\text{O}_2\text{S}$: C, 69.73; H, 4.60; N, 10.16. Found: C, 69.680; H, 4.65; N, 10.11.

2-(2-(2-phenoxybenzylidene)hydrazinyl)-5-(4-methoxybenzylidene)thiazol-4(5H)-one (10h)

Yield (71%), IR (KBr): vcm^{-1} , 3430 (NH), 3040 (=C.H aromatic, alkene), 1712 (C=O), 1624 (C=N). ^1H NMR (DMSO- d_6 , 400MHz): 12.50 (bs, 1H, NH), 8.60, 8.45 (s, 1H, CH=N, E/Z isomers, 70% & 30%), 8.11-6.96 (m, 14H, aromatic, alkene), 3.83 (s, 3H, CH₃). ^{13}C NMR (125 MHz, DMSO- d_6): $\delta=$ 162.01, 160.88, 157.47, 155.62, 132.24, 130.70, 130.63, 130.11, 129.26, 127.02, 126.64, 124.33, 123.94, 120.64, 120.39, 118.95, 118.33, 115.27, 114.84, 55.82. MS: m/z (%) 429 (M^+ , 80), 398 (35), 367 (60), 336 (100), 225 (10), 203 (15), 196 (12), 181 (87), 164 (55), 152 (45), 121 (25), 77 (35), 51 (16). Anal. Calcd. for $\text{C}_{24}\text{H}_{19}\text{N}_3\text{O}_3\text{S}$: C, 67.13; H, 4.42; N, 9.79. Found: C, 67.17; H, 4.38; N, 9.74.

2-(2-(2-phenoxybenzylidene)hydrazinyl)-5-(4-thiomethylbenzylidene)thiazol-4(5H)-one (10i)

Yield (62%), IR (KBr): vcm^{-1} , 3416 (NH), 3050 (CH aromatic.alkene), 1711 (C=O), 1644 (C=N). ^1H NMR DMSO- d_6 , 400MHz): 12.55 (bs, 1H, NH), 8.61, 8.49 (s, 1H, CH=N,E/Z isomers, 51% & 49%), 8.09 (d, 1H, $J=7.6\text{Hz}$, aromatic), 7.78-6.95 (m, 13H, aromatic, alkene), 2.53 (s, 3H, CH₃). ^{13}C NMR (125 MHz, DMSO- d_6): $\delta=$ 162.01, 160.88, 157.47, 155.62, 132.24, 130.70, 130.63, 130.11, 127.02, 126.64, 124.92, 124.33, 123.94, 120.64, 120.39, 118.95, 118.33, 115.27, 114.84, 55.82. MS: m/z (%) 445 (M^+ , 9%), 353 (44),

197 (63), 181 (100), 139 (68), 123 (29), 51 (81). Anal. Calcd. for C₂₄H₁₉N₃O₂S₂: C, 64.71; H, 4.26; N, 9.43. Found: C, 64.67; H, 4.29; N, 9.47.

2-(2-(2-phenoxybenzylidene)hydrazinyl)-5-(4-nitrobenzylidene)thiazol-4(5H)-one (10j)

Yield (47%), IR (KBr): $\nu_{\text{cm}^{-1}}$, 3429 (NH), 3106, 3064 (CH aromatic, alkene), 1720 (C=O), 1645 (C=N), 1513, 1342 (NO₂). ¹H NMR (DMSO-d₆, 400MHz): 8.61 (s, 1H, CH=N), 8.36 (d, *J*=8.0Hz, 2H, aromatic), 8.08 (d, *J*=8.4Hz, 1H, aromatic), 7.90 (d, *J*=8.0Hz, 2H, aromatic), 7.65 (s, 1H, alkene), 7.61-7.13 (m, 6H, aromatic), 7.07 (d, *J*=8Hz, 2H, aromatic). ¹³C NMR (125 MHz, DMSO-d₆): δ = 166.86, 157.62, 155.59, 147.24, 140.99, 133.08, 131.03, 130.81, 130.64, 128.83, 127.67, 125.75, 124.87, 124.68, 124.61, 124.50, 123.94, 120.38, 118.34. MS: *m/z* (%) 444 (M⁺, 36), 397 (15), 351 (92), 305 (12), 275 (8), 196 (37), 181 (100), 149 (20), 135 (15), 89 (42), 77 (28), 51 (12). Anal. Calcd. for C₂₃H₁₆N₄O₄S: C, 62.16; H, 3.60; N, 12.61. Found: C, 62.21; H, 3.64; N, 12.64.

2-(2-(2-phenoxybenzylidene)hydrazinyl)-5-((furan-2-yl)methylene)thiazol-4(5H)-one (10k)

Yield (37%), IR (KBr): $\nu_{\text{cm}^{-1}}$, 3423 (NH), 1709 (C=O), 1623 (C=N). ¹H NMR (DMSO-d₆, 400MHz): 12.45 (bs, 1H, NH), 8.6, 8.32 (s, 1H, CH=N, E/Z isomer, 29% & 71%), 8.08 (s, 1H, Furan), 7.94 (s, 1H, aromatic), 7.53-6.93 (m, 9H, aromatic, alkene), 6.74 (s, 1H, furan), 6.68 (s, 1H, furan). ¹³C NMR (125 MHz, DMSO-d₆): δ = 167.68, 157.59, 155.65, 150.30, 149.59, 147.18, 146.67, 133.15, 130.64, 125.65, 124.92, 123.97, 119.69, 118.35, 117.53, 117.07, 116.25, 113.74, 112.93. MS: *m/z* (%) 389 (M⁺, 22), 296 (17), 287 (62), 196 (7), 181 (35), 153 (11), 124 (100), 121 (10), 96 (35), 80 (20), 70 (13), 52 (29). Anal. Calcd. for C₂₁H₁₅N₃O₃S: C, 64.78; H, 3.85; N, 10.79. Found: C, 64.72; H, 3.79; N, 10.74.

2-(2-(2-phenoxybenzylidene)hydrazinyl)-5-((pyridine-2-yl)methylene)thiazol-4(5H)-one (10l)

Yield (36%), IR (KBr): $\nu_{\text{cm}^{-1}}$, 3421 (NH), 3055 (CH aromatic, alkene), 1721 (C=O), 1638 (C=N). ¹H NMR (DMSO-d₆, 400MHz): 12.45 (bs, 1H, NH), 8.83 (d, 1H, *J*=4.8Hz, Pyridin), 8.61, 8.43 (s, 1H, CH=N, E/Z isomers, 68% & 32%), 8.06 (m, 1H, pyridin), 7.93 (m, 2H, pyridin), 7.81 (d, *J*=7.2Hz, 1H, aromatic), 7.66 (s, 1H, alkene), 7.55-7.13 (m, 6H, aromatic), 7.02 (d, *J*=8.0Hz, 2H, aromatic). ¹³C NMR (125 MHz, DMSO-d₆): δ = 168.08, 157.60, 155.63, 152.56, 152.37, 149.77, 137.73, 133.09, 130.64, 128.17, 127.67, 127.63, 126.26, 125.73, 124.91, 123.96, 123.77, 120.35, 119.69, 118.34. MS: *m/z* (%) 400 (M⁺, 38), 307 (100), 269 (8), 204 (41), 196 (28), 181 (95), 161 (20), 152 (15), 135 (73), 115 (8), 77 (30), 51 (21). Anal. Calcd. for C₂₂H₁₆N₄O₂S: C, 66.00; H, 4.00; N, 14.00. Found: C, 66.07; H, 4.05; N, 13.97.

2-(2-(2-phenoxybenzylidene)hydrazinyl)-5-((pyridine-3-yl)methylene)thiazol-4(5H)-one (10m)

Yield (42%), IR (KBr): $\nu_{\text{cm}^{-1}}$, 3430 (NH), 1718 (C=O), 1636 (C=N). ¹H NMR (DMSO-d₆, 400MHz): 8.96, 8.87 (s, 1H, CH=N, E/Z isomers, 15% & 85%), 8.69 (m, 2H, Pyridine), 8.23 (d, 1H, *J*=8.0Hz, pyridin), 8.11-7.15 (m, 9H, aromatic, pyridine, alkene), 7.01 (d, *J*=8.0Hz, 2H, aromatic). ¹³C NMR (125 MHz, DMSO-d₆): δ = 168.21, 157.61, 155.66, 151.68, 150.36, 136.30, 134.78, 133.26, 130.76, 130.64, 127.91, 125.96, 125.55, 124.96, 124.83, 124.18, 123.95, 120.40, 119.70, 118.34. MS: *m/z* (%) 400 (M⁺, 50), 307 (100), 280 (7), 218 (8), 196 (23), 181 (94), 162 (15), 152 (12), 135 (50), 91 (18), 77 (21), 51 (15). Anal. Calcd. for C₂₂H₁₆N₄O₂S: C, 66.00; H, 4.00; N, 14.00. Found: C, 66.03; H, 4.06; N, 14.05.

2-(2-(2-phenoxybenzylidene)hydrazinyl)-5-(2-phenoxybenzylidene)thiazol-4(5H)-one (10n)

Yield (50%), IR (KBr): $\nu_{\text{cm}^{-1}}$, 3419 (NH), 3032 (CH aromatic, alkene), 1716 (C=O), 1638 (C=N). ¹H NMR DMSO-d₆, 400MHz): 8.60, 8.51 (s, 1H, CH=N, E/Z isomers, 28% & 72%), 8.06 (d, 1H, *J*=7.2Hz, aromatic), 7.76-6.96 (m, 18H, aromatic, alkene). ¹³C NMR (125

MHz, DMSO-*d*₆): δ = 169.97, 157.63, 156.94, 155.78, 155.61, 133.15, 132.03, 130.70, 130.64, 129.46, 127.77, 125.68, 125.59, 124.94, 124.79, 124.34, 123.94, 120.41, 119.45, 118.97, 118.32, MS: m/z (%) 491 (M⁺, 8), 398 (25), 311 (16), 218 (31), 196 (25), 181 (100), 165 (15), 119 (12), 77 (25). Anal. Calcd. for C₂₉H₂₁N₃O₃S: C, 70.87; H, 4.27; N, 8.55. Found: C, 70.83; H, 4.29; N, 8.51.

Pharmacological evaluations

Male NMRI mice weighing 20–25 g and male Wistar rats (100–150 g) (Pasteur Institute of Iran) were used for analgesic activity evaluation by abdominal constriction test. Mefenamic acid was prescribed (30 mg/kg) and target compounds were injected in an equal molar ratio to 30 mg/kg of reference drug, 30 min after the animals were injected ip with acetic acid (0.6 %, 0.1 ml/10 g). All the procedures, statistical analysis and calculation of inhibition percent were performed conforming to our previously expressed research.¹ Wistar male rats were used in carrageenan-induced rat paw edema test and the selected doses were similar to the writing test and other situations, estimation of increment in paw volume and statistical analysis were done similarly as reported earlier (Table III).^{2,3}

The results were expressed as the mean \pm SEM of 6 animals per group. The data were statistically analyzed by one-way analysis of variance (ANOVA) followed by Tukey multicomparison test. Differences with P<0.05 between experimental groups were considered statistically significant. In ulcerogenic test, suspension of indomethacin, 60 mg/kg and compounds in an equal molar ratio to indomethacin dose, in 0.5 % aqueous sodium carboxymethyl cellulose as vehicle, were administered orally to test animals. The control group animals received the same volumes of dosing vehicle.

Insilico ADMET Evaluation

Lipinski's rule of five important parameters for oral absorption of synthesized compounds states that the molecular weight of the target compound should be \leq 500. The number of hydrogen bond donors should be \leq 5 and the number of hydrogen bond acceptors should be \leq 10. The topological polar surface area should be \leq 140. The number of rotatable bonds should be \leq 10. If a compound violates two aforesaid rules, it will lead to poor oral absorption.⁴

For determining drug-likeness, a fragment list was created by shredding 3300 traded drugs as well as 15000 commercially available chemicals of Fluka company yielding a complete list of all available fragments. The occurrence frequency of every one of the fragments was determined within the collection of traded drugs and within the supposedly non-drug-like collection of Fluka compounds. While 80% of the traded drugs have a positive drug-likeness value, the big majority of Fluka chemicals account for a negative value. The drug-score combines drug-likeness, clogp, clogs, molecular weight, and toxicity risks in one functional value that might be used to judge the compound's overall potential to qualify for a drug.⁵

Another tool for assessing the ADMET properties of compounds is a comprehensive platform called admetSAR3.0, which is utilized for search, prediction, and optimization purposes. Within the search module, there are over 370,000 high-quality experimental ADMET data entries available, covering 104,652 unique compounds. Moreover, it includes a chemical structure similarity search function to aid in comparison. In the prediction module, admetSAR3.0 covers an expanded range of endpoints, including 119 ADMET-related endpoints across five categories: basic properties, ADME properties, human health toxicities, environmental risk assessment, and cosmetic risk assessment. Within the optimization

module, it optimizes ADMET properties via scaffold hopping and transformation rules. In ADMETopt, more than 50,000 distinct scaffolds from the ChEMBL and Enamine databases assist in matching similar scaffolds. Finally, the updated interface of admetSAR3.0 represents users with succinct result presentations along with practical assistance.⁶

Table S-I: The significant pharmacokinetic parameters for acceptable oral bioavailability of the synthesized compounds **8**, **10a-10n**

Compound	MW ^a (g/mol)	NROTB ^b	HBA ^c	HBD ^d	TPSA ^e (Å ²)	ClogP ^f	GI absorption	LV ^g
8	371.45	6	3	1	74.75	5.01	High	0
10a	399.46	6	4	1	88.35	4.55	High	0
10b	417.46	6	5	1	88.35	4.80	High	0
10c	433.91	6	4	1	88.35	5.01	High	0
10d	478.36	6	4	1	88.35	5.09	High	1
10e	415.46	6	5	2	108.58	4.02	High	0
10f	415.46	6	5	2	108.58	4.08	High	0
10g	413.49	6	4	1	88.35	4.83	High	0
10h	429.49	7	5	1	97.58	4.49	High	0
10i	445.56	7	4	1	113.65	5.04	Low	0
10j	444.47	7	6	2	138.01	2.74	Low	0
10k	389.43	6	5	1	101.49	3.90	High	0
10l	400.45	6	5	1	101.24	3.84	High	0
10m	400.45	6	5	1	101.24	3.84	High	0
10n	491.56	8	5	1	97.58	5.73	Low	1

^aMolecular weight; ^bNumber of rotatable bonds; ^cNumber of hydrogen bond acceptors; ^dNumber of hydrogen bond donors; ^eTopological polar surface area; ^fConsensus log P_{ow} (logarithm of partition coefficient of compound between n-octanol and water); ^gLipinski's violation

Table S-II: The toxicity risks, drug-likeness, and drug-score of target compounds **8**, **10a-10n**

Compound d	Toxicity Risks ¹				Drug-Likeness	Drug-Score
	M ²	T ³	I ⁴	R ⁵		
8	-	+	-	-	4.54	0.16
10a	-	-	-	-	3.92	0.36
10b	-	-	-	-	4.01	0.34
10c	-	-	-	-	5.67	0.3
10d	-	-	-	-	3.04	0.27
10e	-	-	-	-	5.13	0.38
10f	-	-	-	+	5.14	0.23
10g	-	-	-	-	3.56	0.33
10h	-	-	-	-	5.16	0.35
10i	-	-	-	-	5.1	0.3
10j	-	-	-	-	-5.25	0.19
10k	+	-	-	-	4.69	0.25
10l	-	-	-	-	5.03	0.44
10m	-	-	-	-	5.48	0.44
10n	-	-	-	-	5.04	0.23

¹Ranked according to (-) no risk, (±) medium risk, (+) high risk; M², Mutagenic; T³, Tumorigenic; I⁴, Irritant; R⁵, Reproductive effective.

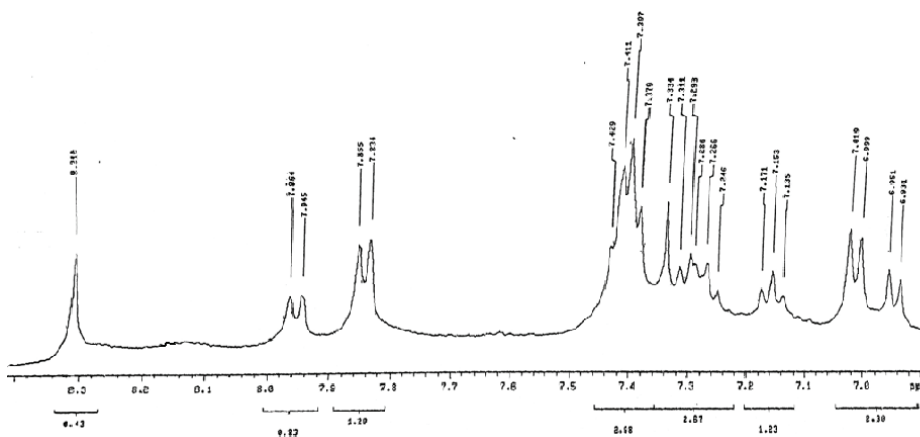
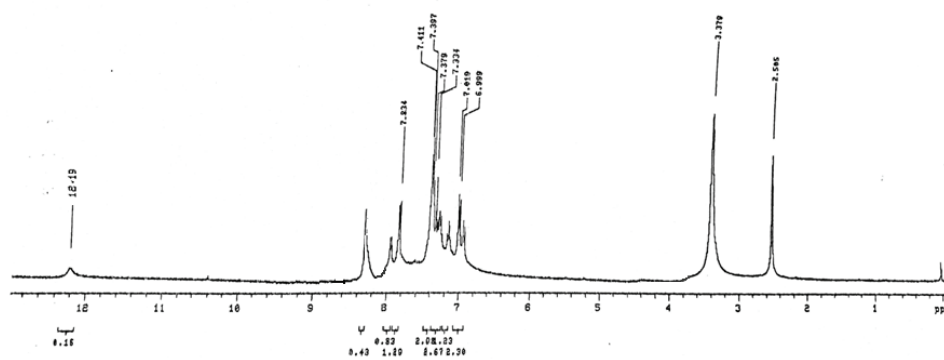
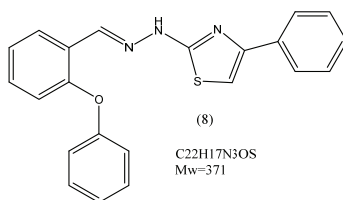
Table S-III: Human oral bioavailability and toxicity risks of target compounds **8, 10a-10n**

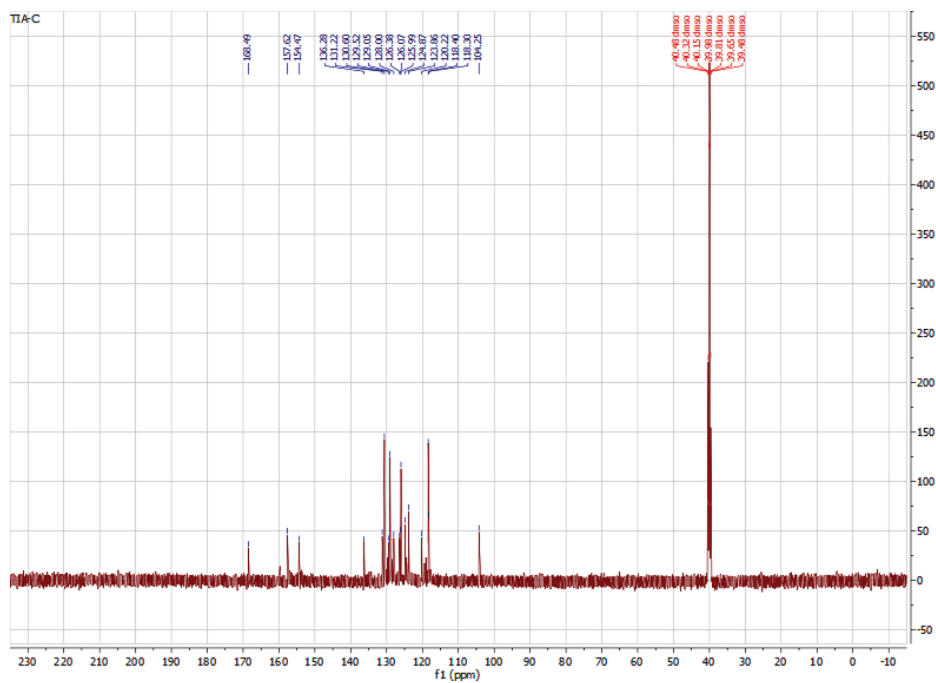
Compound	Human oral bioavailability	Toxicity Risks ¹			
		Carcinogenicity	Skin irritation	Reproductive toxicity	Respiratory toxicity
8	Low	+	-	-	-
10a	High	-	-	-	-
10b	High	-	-	+	-
10c	High	-	-	+	-
10d	High	-	-	+	-
10e	High	-	-	+	-
10f	High	-	-	+	-
10g	Low	-	-	-	-
10h	Low	-	-	-	-
10i	High	-	-	+	-
10j	High	-	-	+	-
10k	High	-	-	-	-
10l	High	-	-	+	-
10m	Low	-	-	-	-
10n	Low	-	-	+	-

¹Ranked according to (-) low risk and (+) high risk.

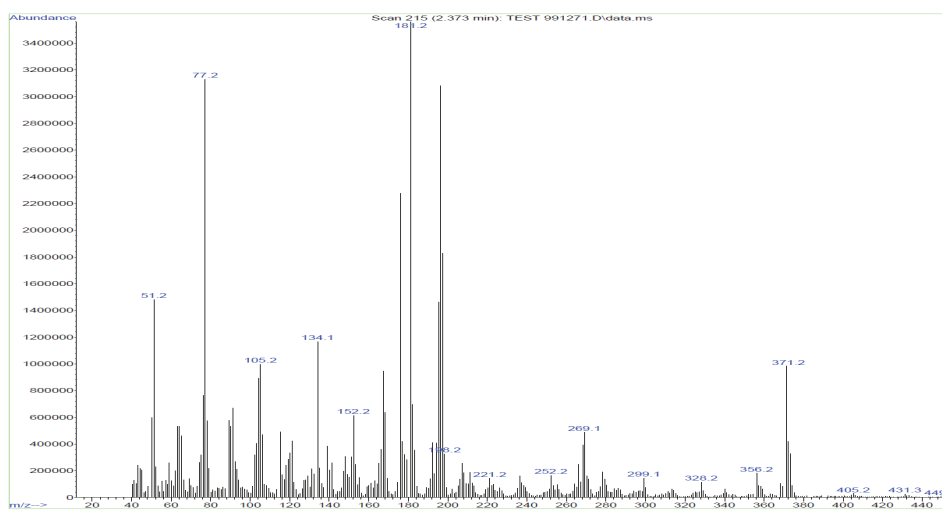
REFERENCES

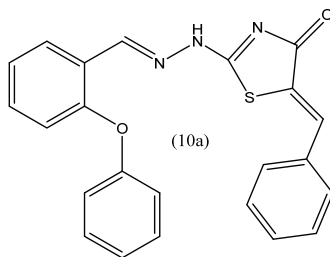
1. A. Almasirad, R. Hosseini, H. Jalalizadeh, Z. Rahimi-Moghaddam, N. Abaeian, M. Janafrooz, M. Abbaspour, V. Ziaee, A. Dalvandi, A. Shafiee, *Biol. Pharma. Bull.* **29** (2006) 1180 (<https://doi.org/10.1248/bpb.29.1180>)
2. A. Rineh, N. Mahmoodi, M. Abdollahi, A. Foroumadi, M. Sorkhi, A. Shafiee, *Arch. Pharm. Chem. Life. Sci.* **340** (2007) 409 (<https://doi.org/10.1002/ardp.200700045>)
3. A. Almasirad, M. Nassiri Koopaei, A. Shafiee, N. Nassiri-Koopaei, M. J. Assarzadeh, A. Tabei, M. Ghadimi, *J. Pharm. Health. Sci.* **1** (2013) 137 (<https://sid.ir/paper/188761/en>)
4. M. Faizi, R. Jahani, S. A. Ebadi, S. A. Tabatabai, E. Rezaee, M. Lotfaliei, M. Amini, A. Almasirad, *EXCLI. J.* **16** (2017) 52 (<https://doi.org/10.17179/excli2016-692>)
5. <https://www.organic-chemistry.org/prog/peo/>
6. Gu Y. Gu, Z. Yu, Y. Wang, L. Chen, C. Lou, C. Yang, W. Li, G. Liu, Y. Tang, *Nucleic Acids Res.* **22** (2024) gkae298 (<https://doi.org/10.1093/nar/gkae298>).



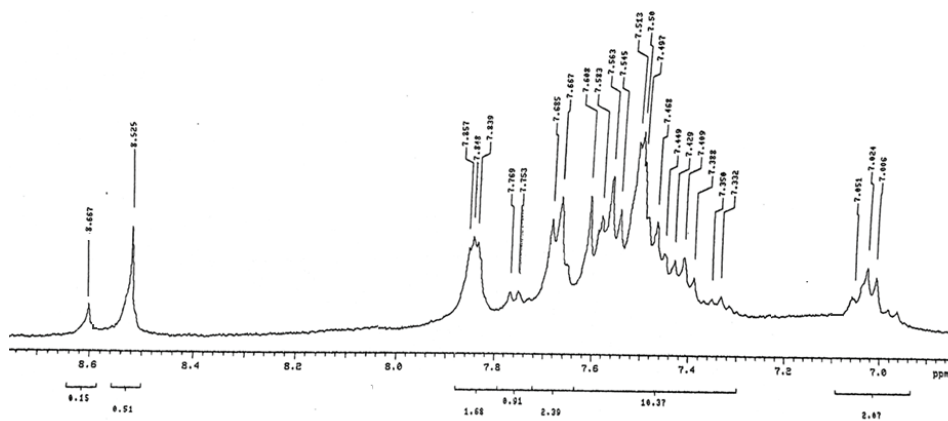
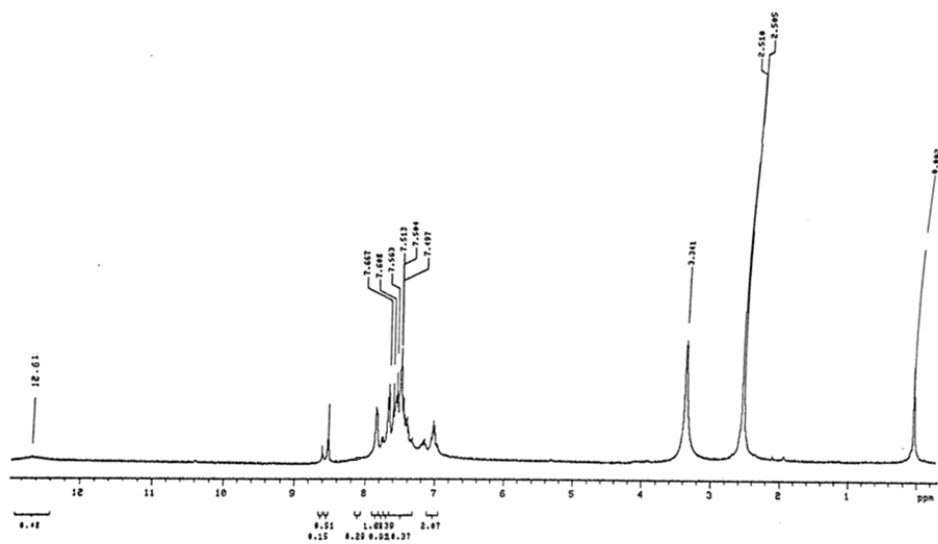


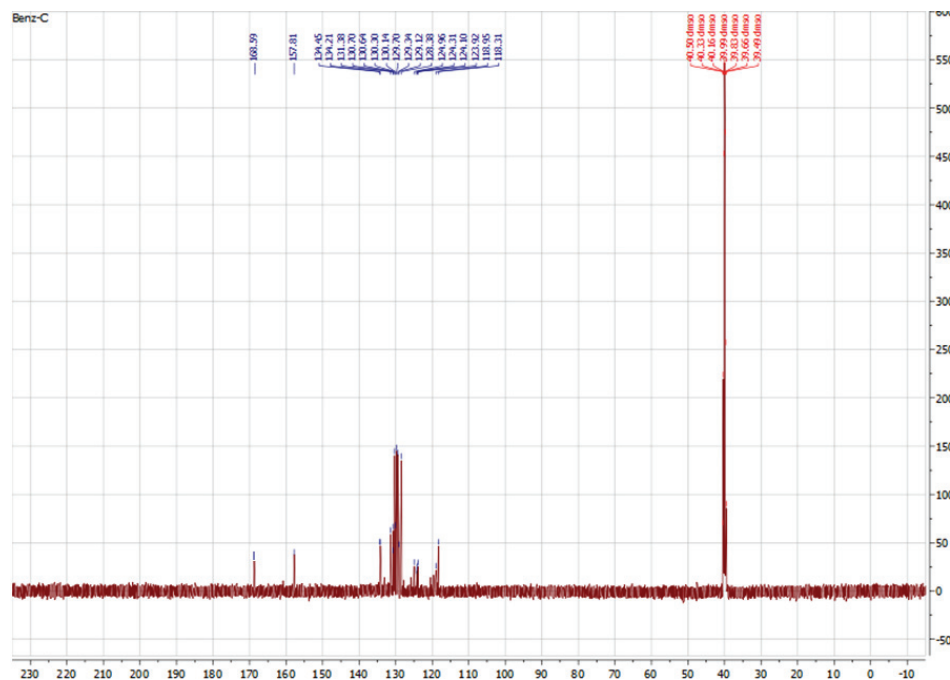
File : C:\MSDCHEM\3\DATA\Snapshot\TEST 991271.D
Operator :
Acquired : 23 Jul 2007 22:08 using AcqMethod test.M
Instrument : MSD
Sample Name : Thia
Misc Info :
Vial Number : 1



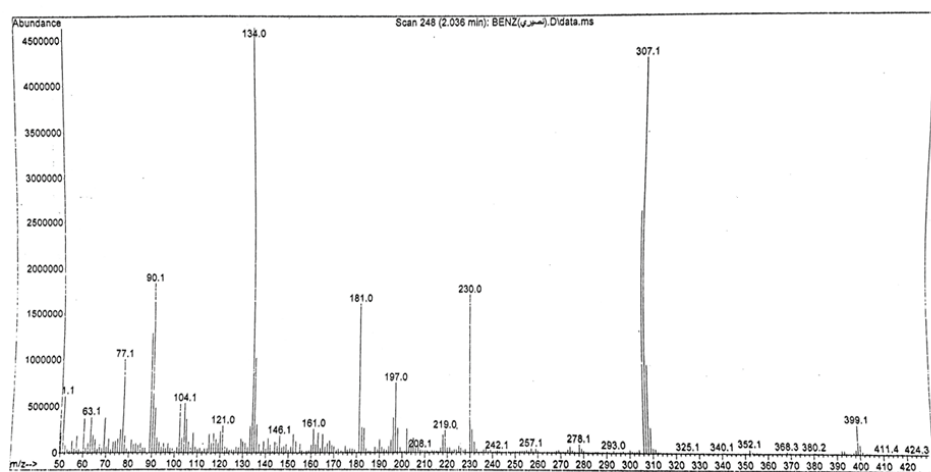


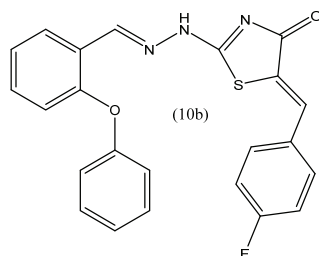
C₂₃H₁₇N₃O₂S
Mw=399



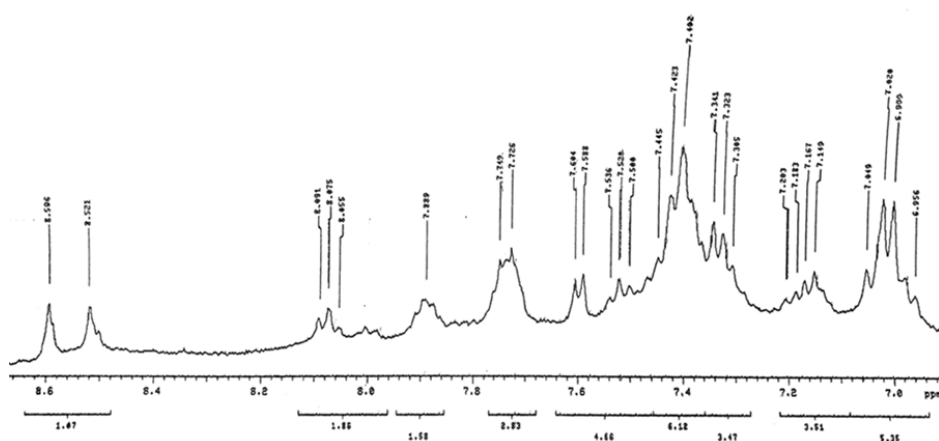
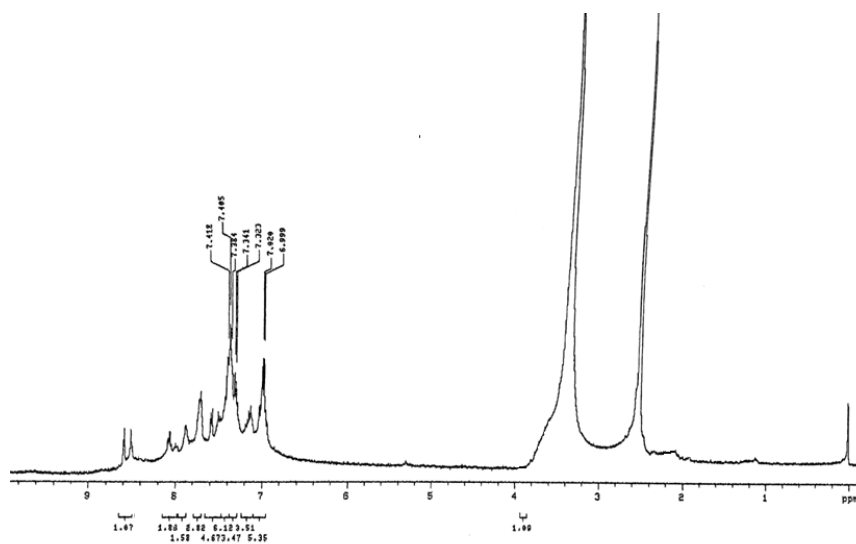


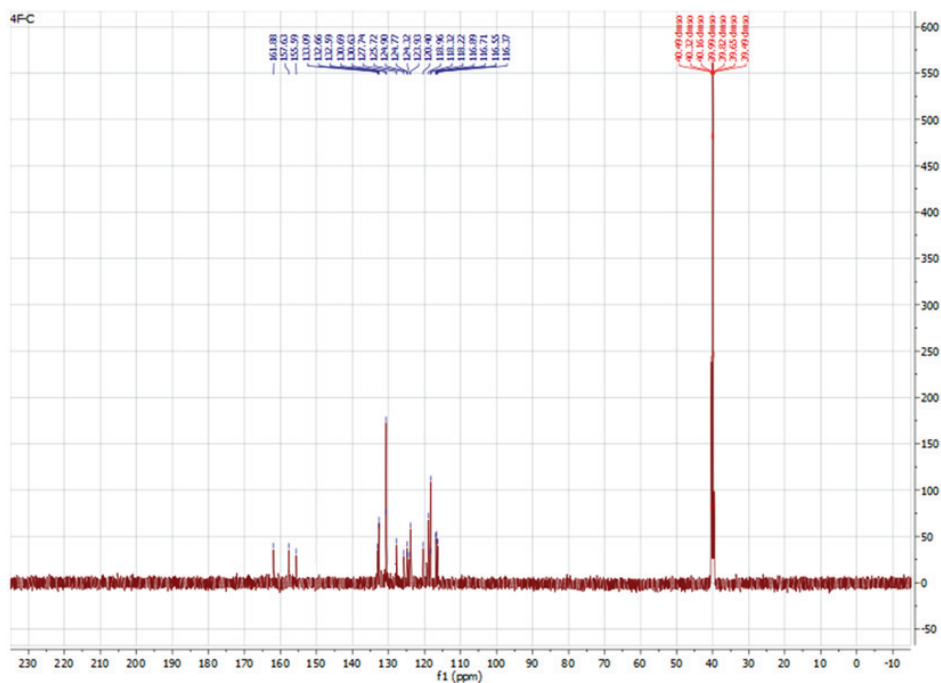
File : C:\msdchem\13\DATA\BENZ(بِنز),D
 Operator : ahoupai
 Acquired : 13 Dec 2010 13:20 using AcqMethod test dp.M
 Instrument : MSD Direct Probe
 Sample Name: benz
 Misc info :
 Vial Number: 1



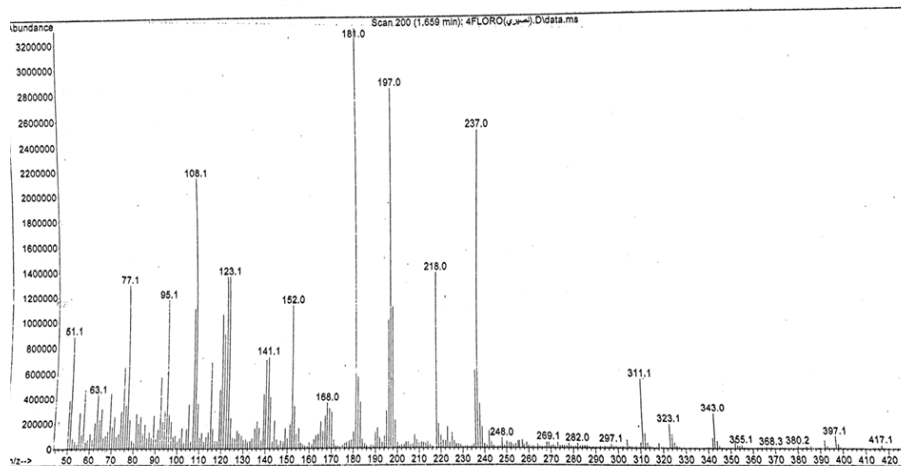


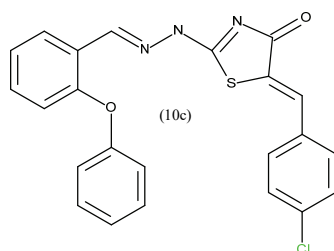
C₂₃H₁₆N₃FO₂S
 Mw=417



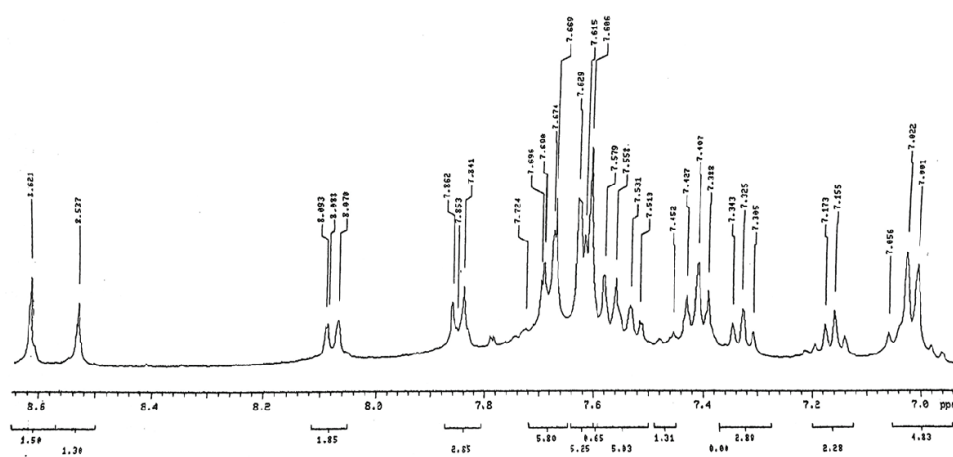


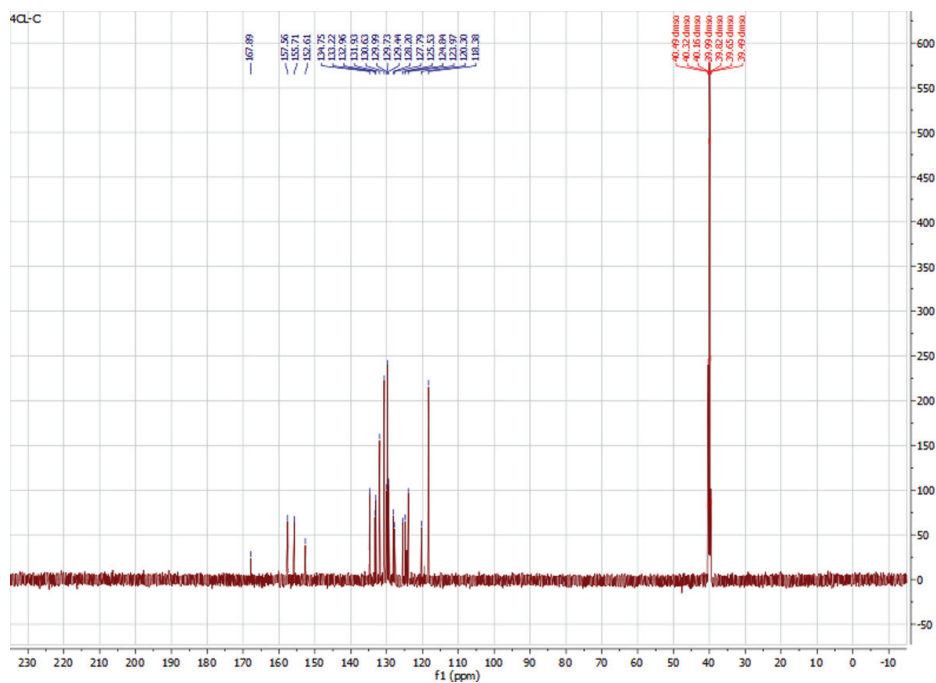
File : C:\msdchem\3\DATA\4FLORO(4FC).D
 Operator : shoupa
 Acquired : 13 Dec 2010 12:43 using AcqMethod test dp.M
 Instrument : MSD Direct Probe
 Sample Name : 4floro
 Misc Info :
 Vial Number : 1



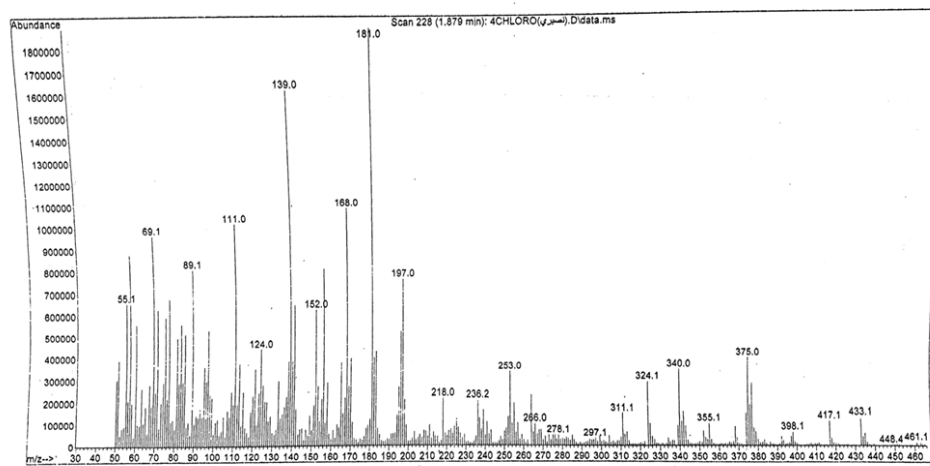


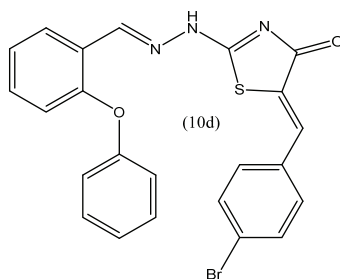
C₂₃H₁₆N₃ClO₂S
Mw=433.5



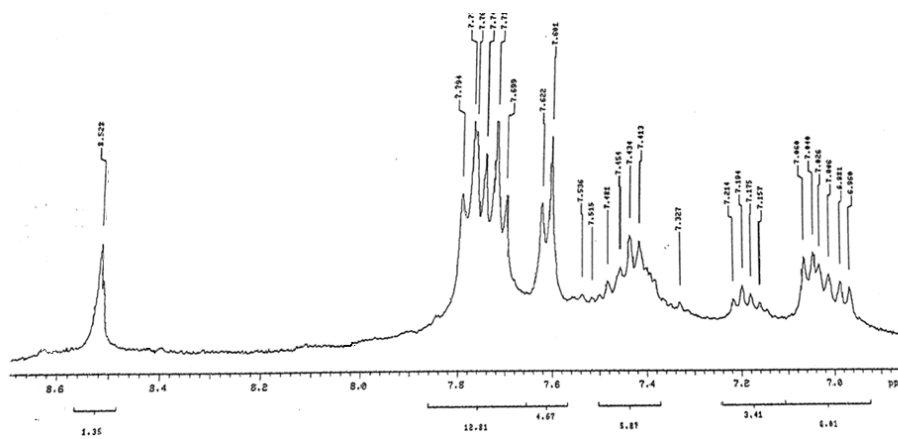
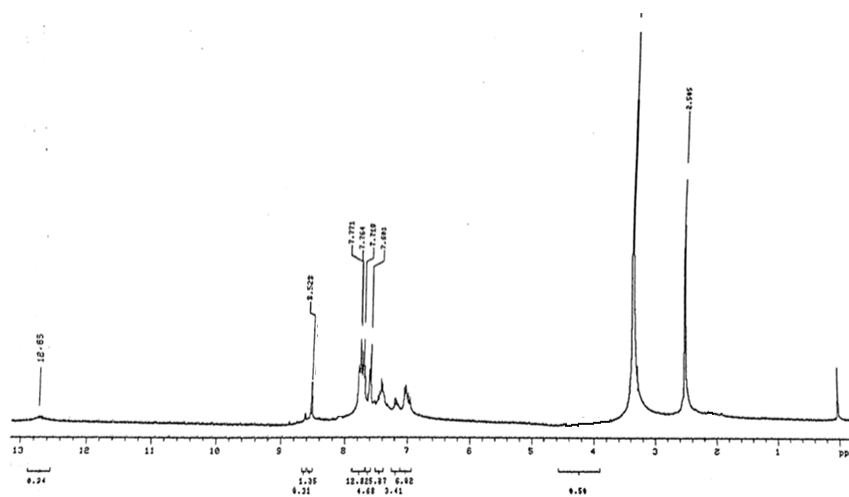


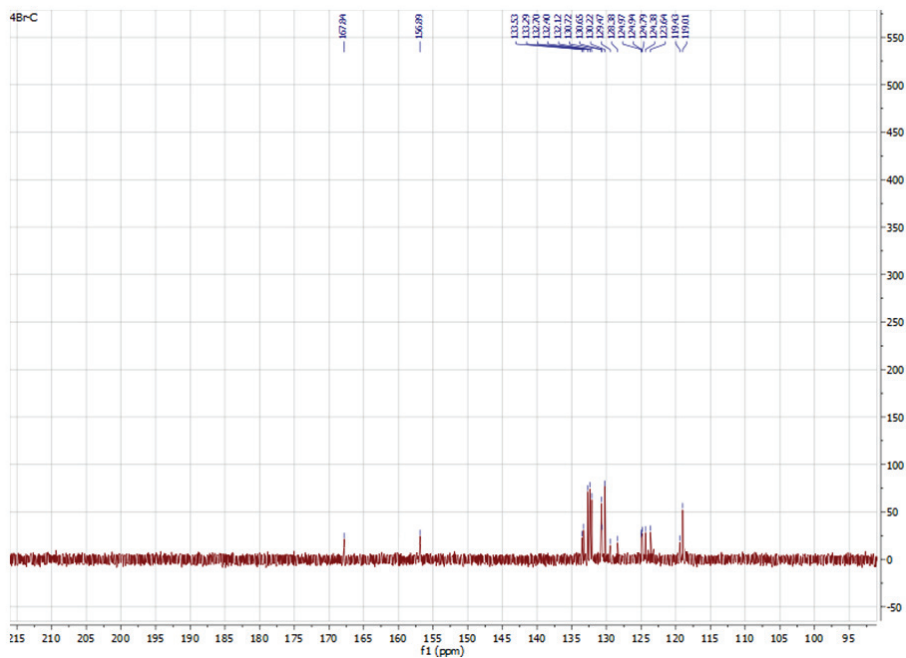
File :C:\msdchem\3\DATA\4CHLORO(تسويي).D
 Operator : ahoupal
 Acquired : 13 Dec 2010 12:54 using AcqMethod: test dp.M
 Instrument : MSD Direct Probe
 Sample Name: 4chloro
 Misc Info :
 Vial Number: 1



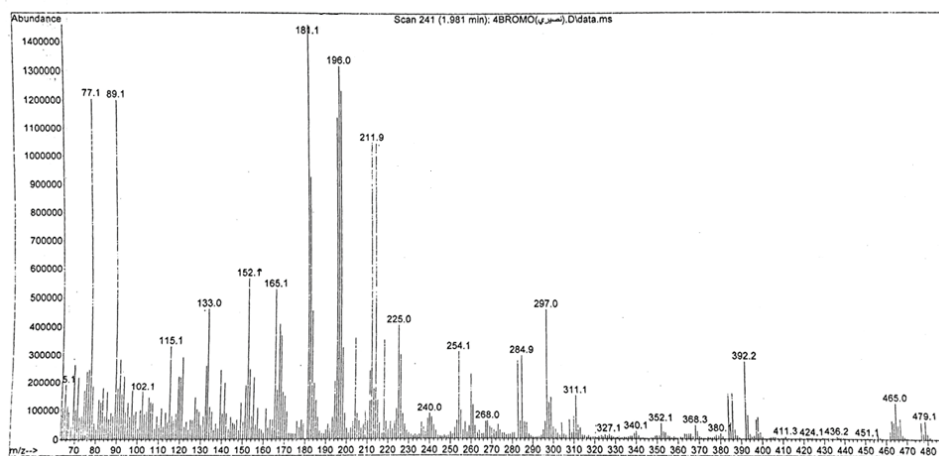


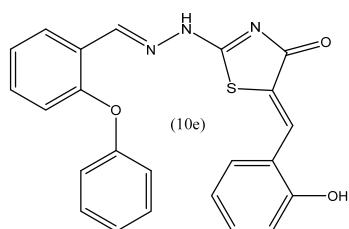
C₂₃H₁₆N₃BrO₂S
Mw=478



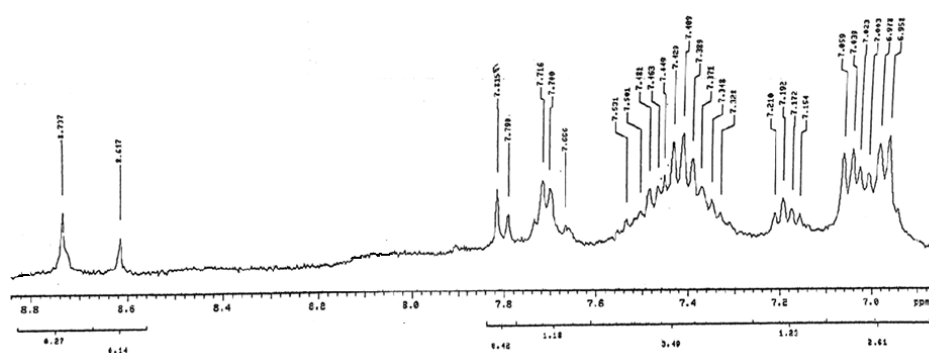
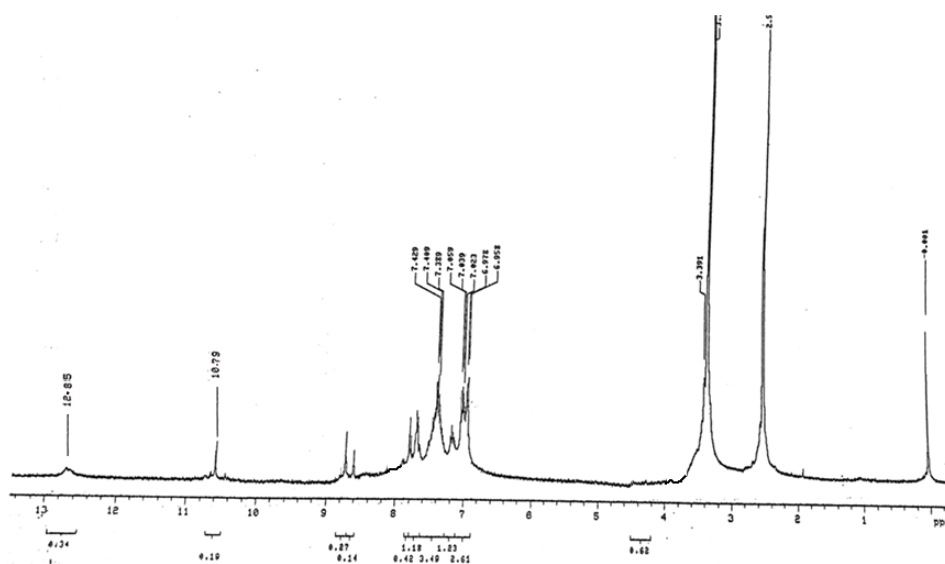


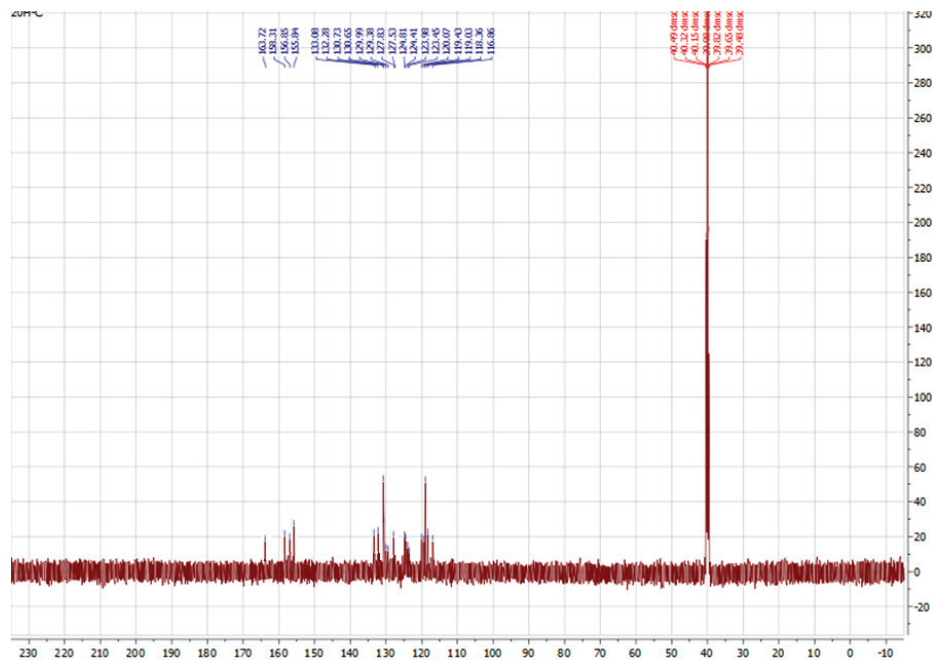
File : C:\msdchem\3\DATA\4BROMO(تصويري).D
 Operator : ahoupai
 Acquired : 13 Dec 2010 12:34 using AcqMethod test dp.M
 Instrument : MSD Direct Probe
 Sample Name: 4boromo
 Misc Info :
 Vial Number: 1



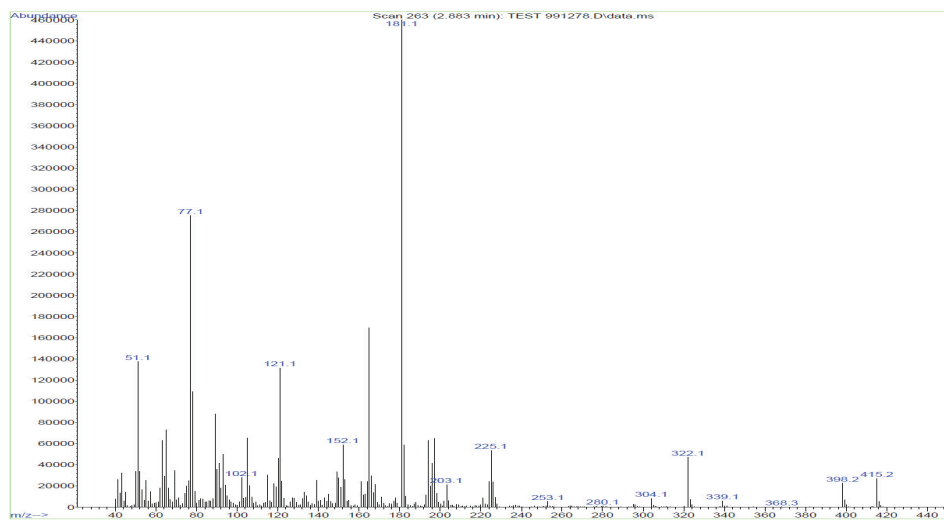


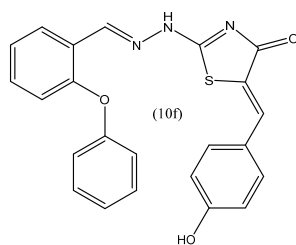
C₂₃H₁₇N₃O₃S
Mw=415



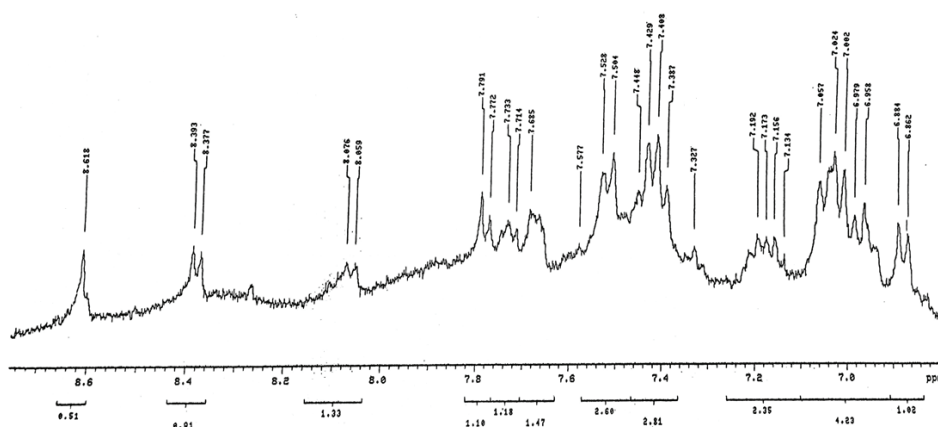
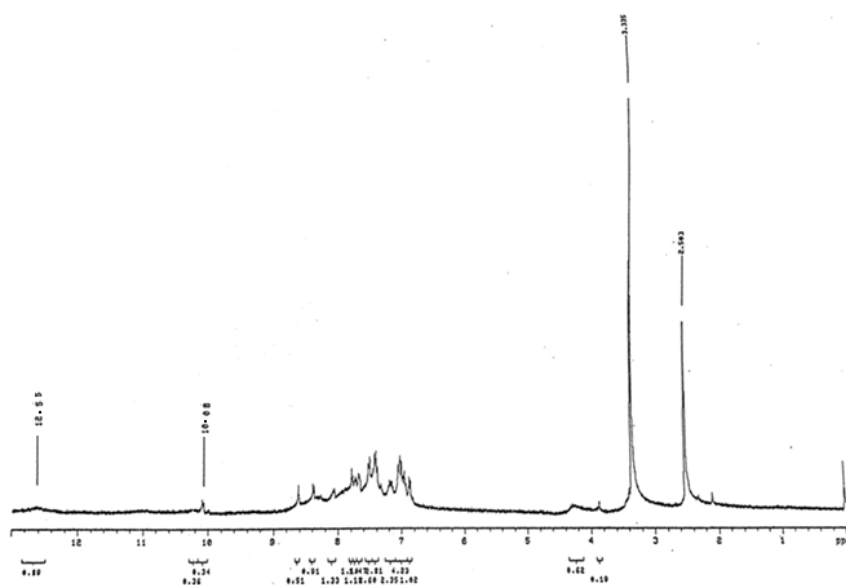


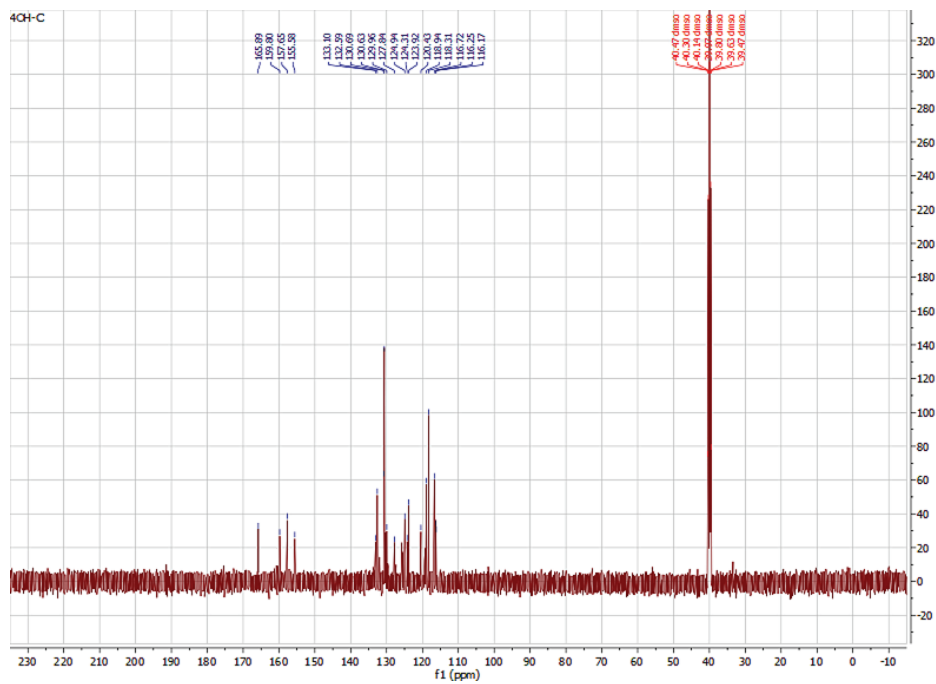
File : C:\MSDCHEM\3\DATA\Snapsho\TEST 991278.D
 Operator :
 Acquired : 23 Jul 2007 23:25 using AcqMethod test.M
 Instrument : MSD
 Sample Name : 2OH
 Misc Info :
 Vial Number : 1



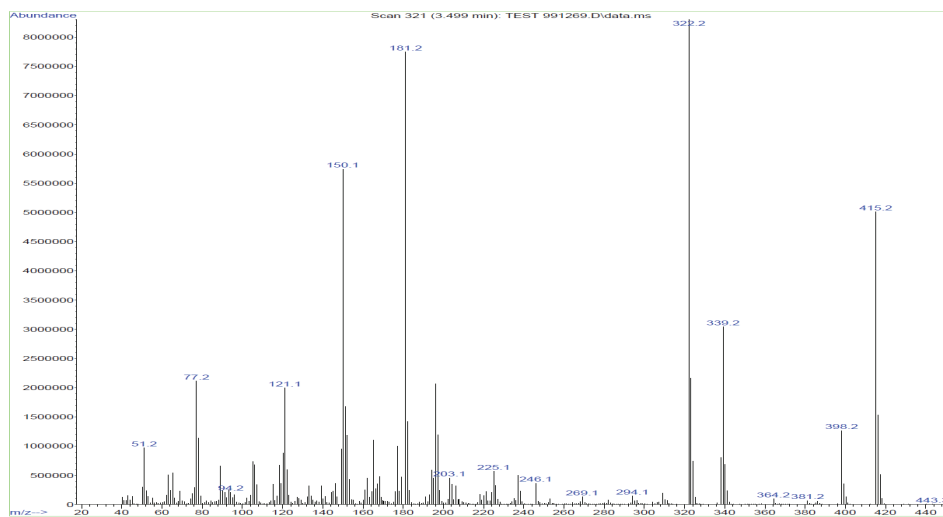


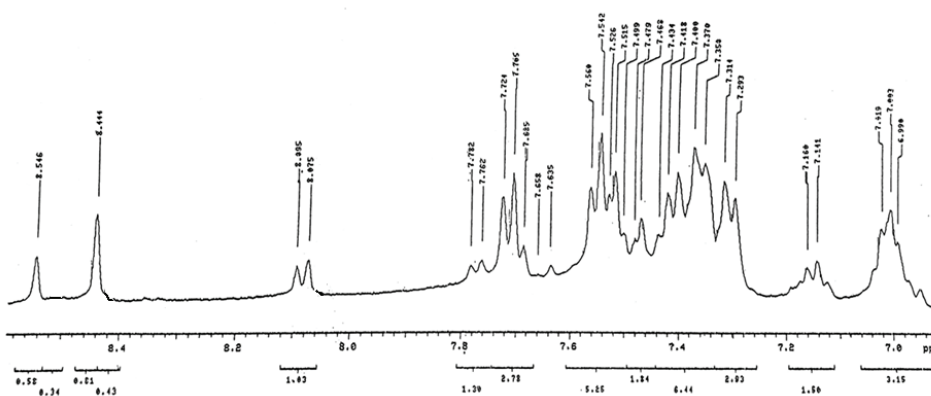
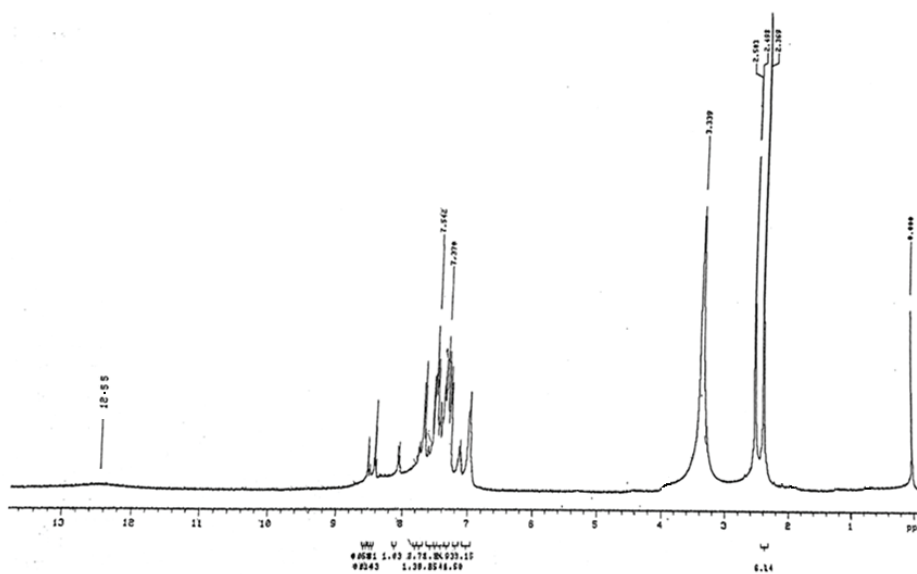
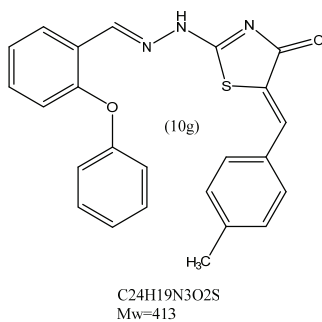
C₂₃H₁₇N₃O₃S
Mw=415

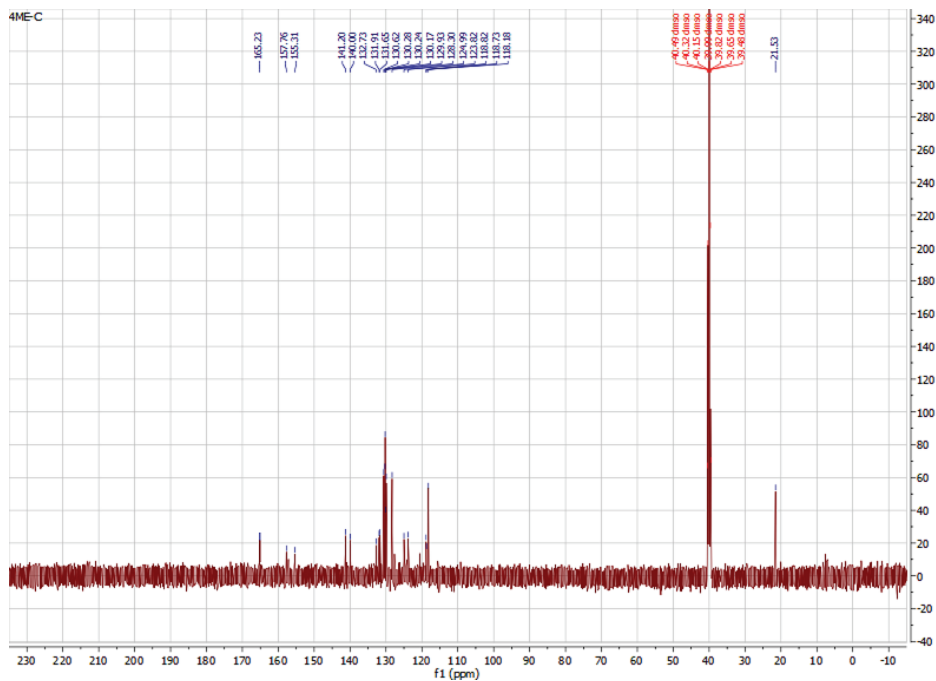




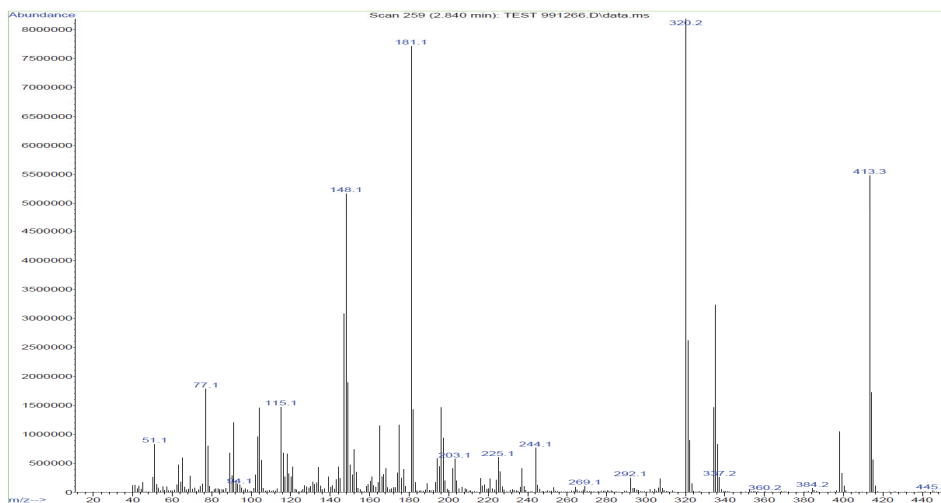
File :C:\MSDCHEM\3\DATA\Snapshot\TEST 991269.D
Operator :
Acquired : 23 Jul 2007 21:41 using AcqMethod test.M
Instrument : MSD
Sample Name: 4OH
Misc Info :
Vial Number: 1

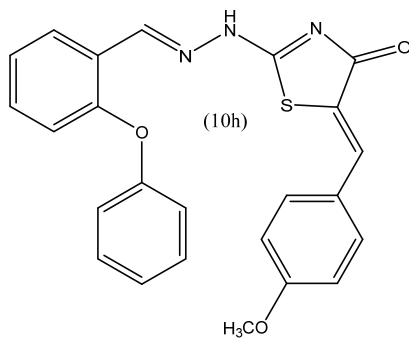




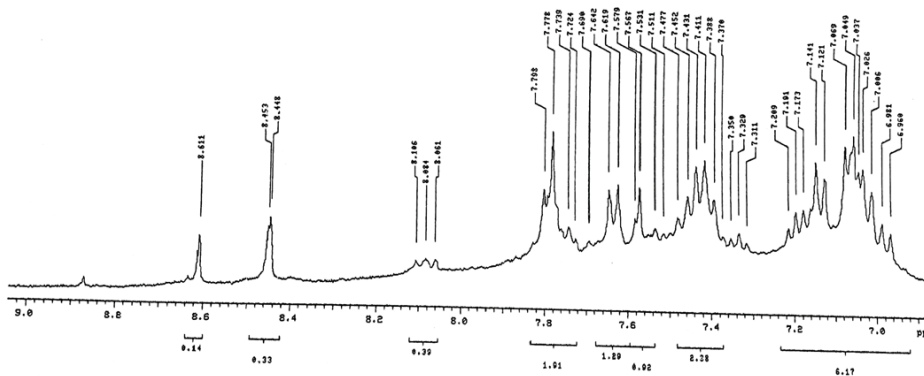
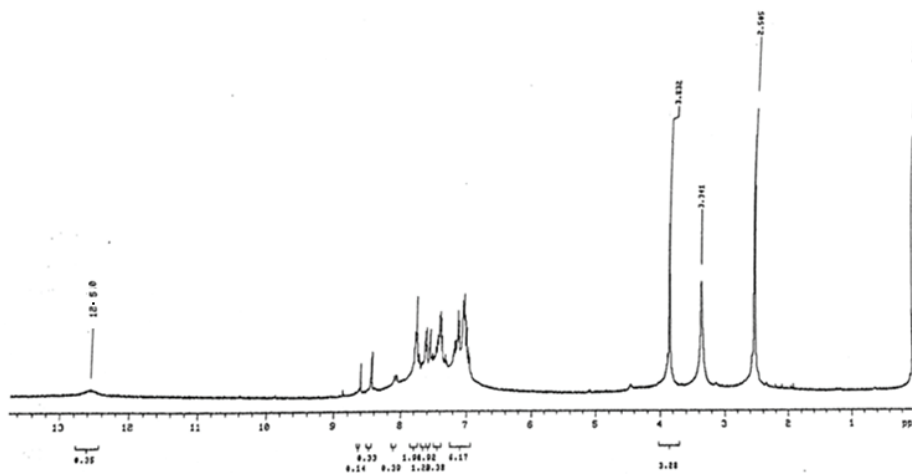


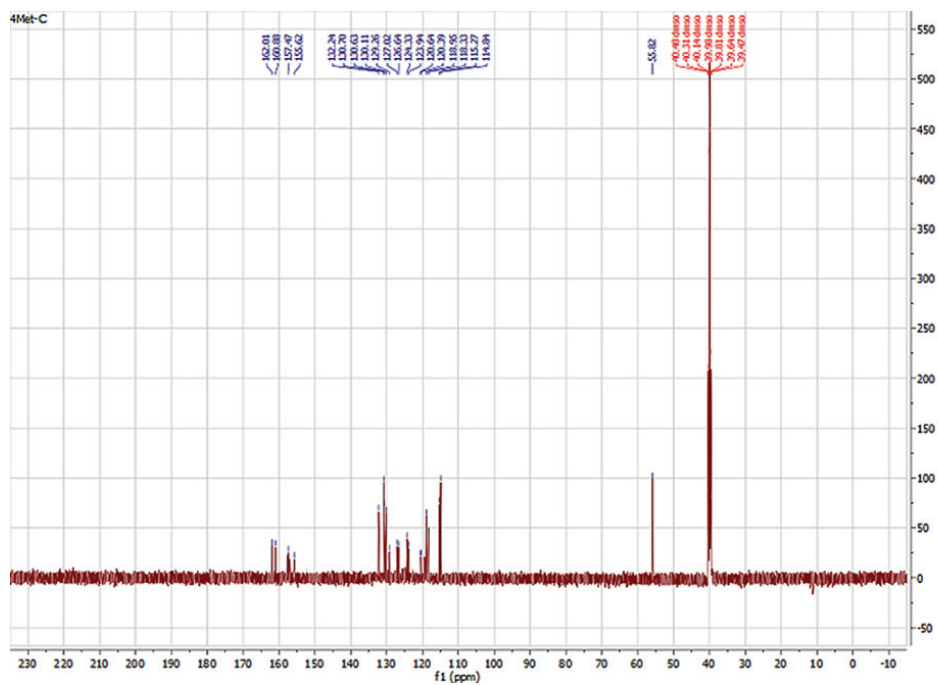
File : C:\MSDCHEM\3\DATA\Snapshot\TEST 991266.D
Operator :
Acquired : 23 Jul 2007 21:03 using AcqMethod test.M
Instrument : MSD
Sample Name: 4CH3
Misc Info :
Vial Number: 1



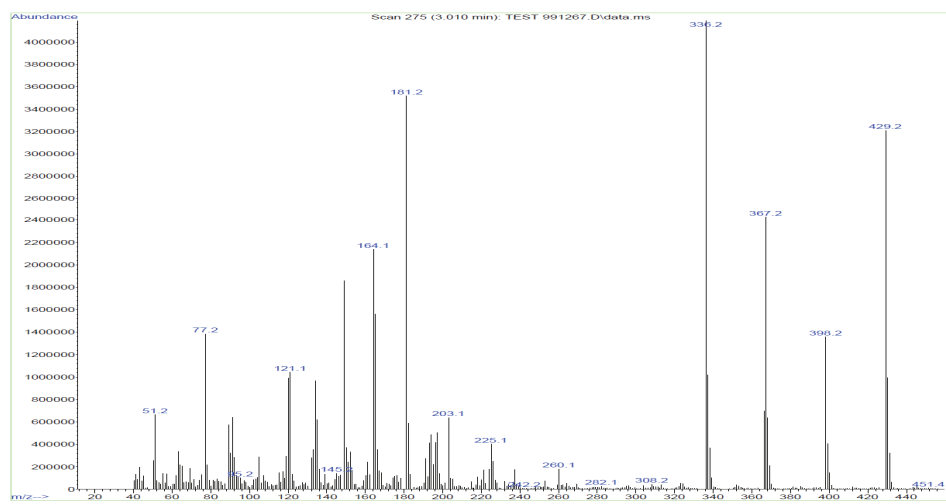


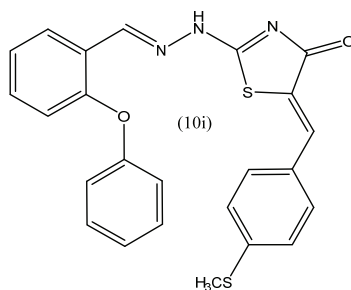
$C_{24}H_{19}N_3O_3S$
MW: 429.49



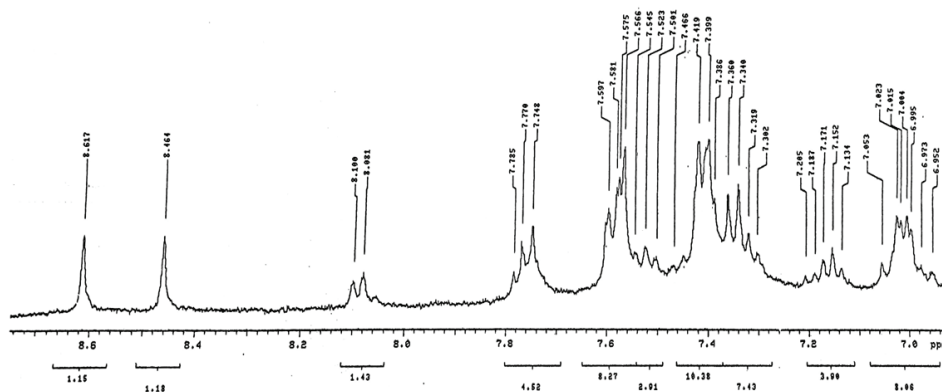
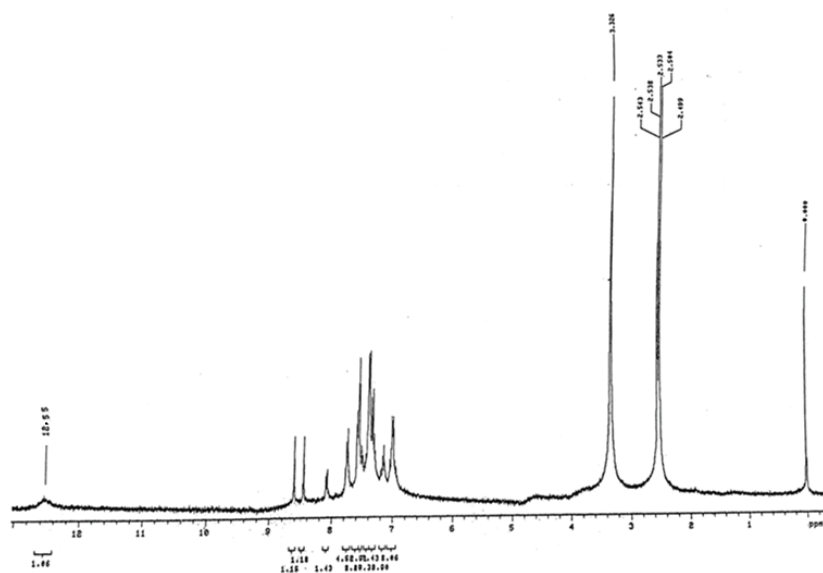


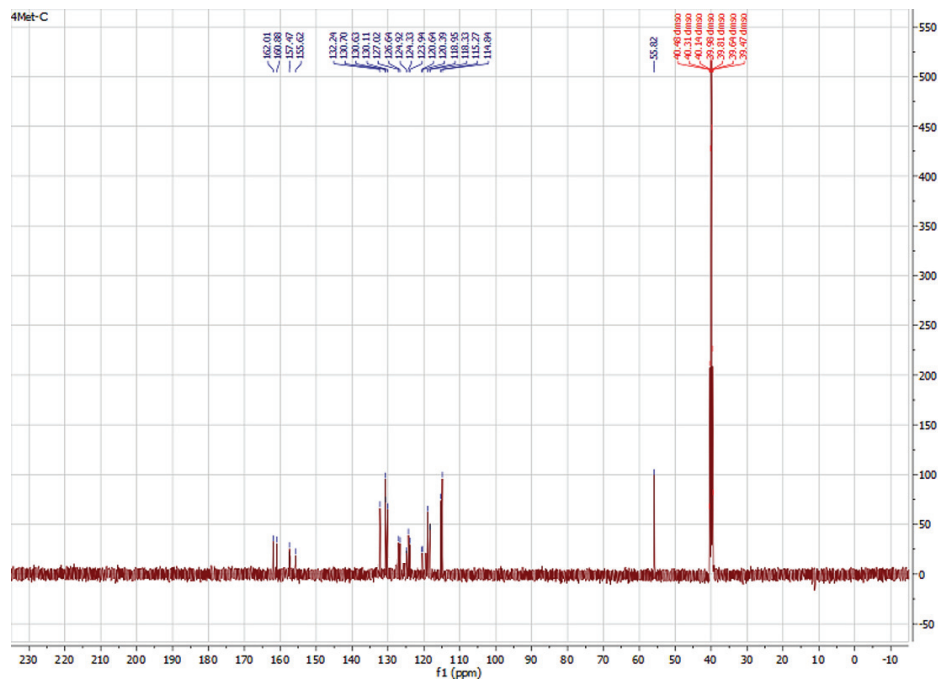
File : C:\MSDCHEM\3\DATA\Snapshot\TEST 991267.D
 Operator :
 Acquired : 23 Jul 2007 21:15 using AcqMethod test.M
 Instrument : MSD
 Sample Name : 4OCH3
 Misc Info :
 Vial Number : 1



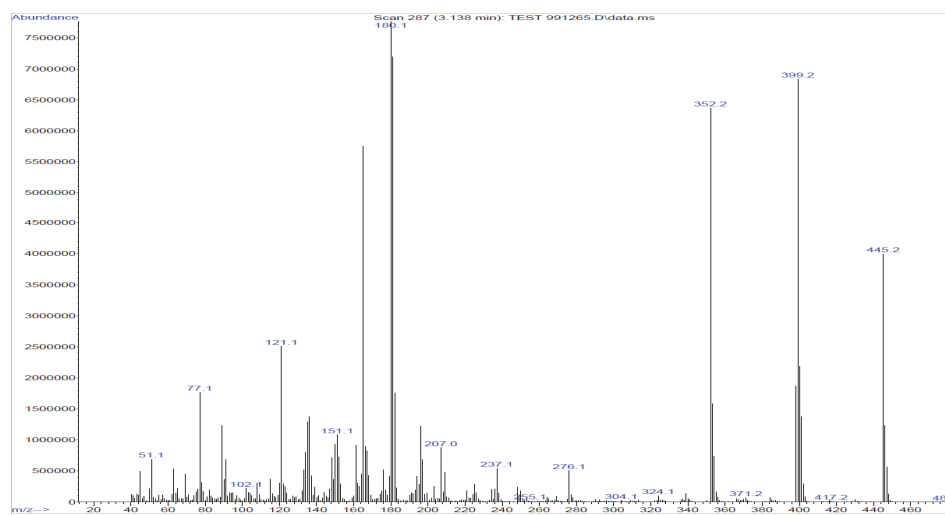


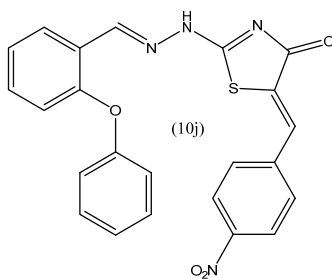
C₂₄H₁₉N₃O₂S₂
Mw=445



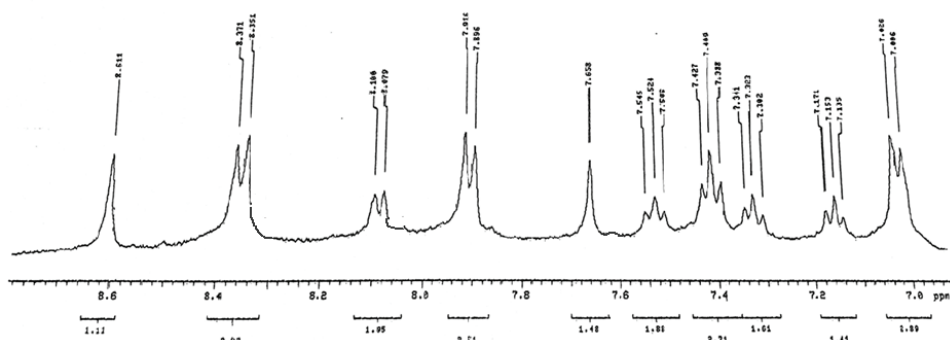
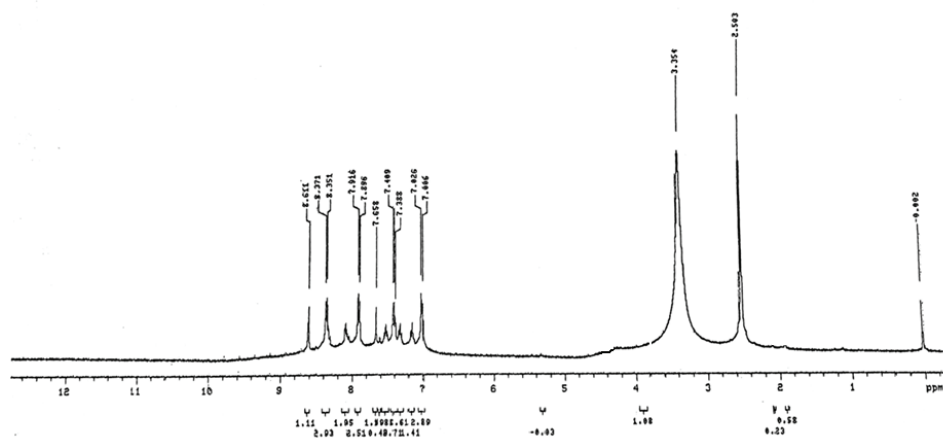


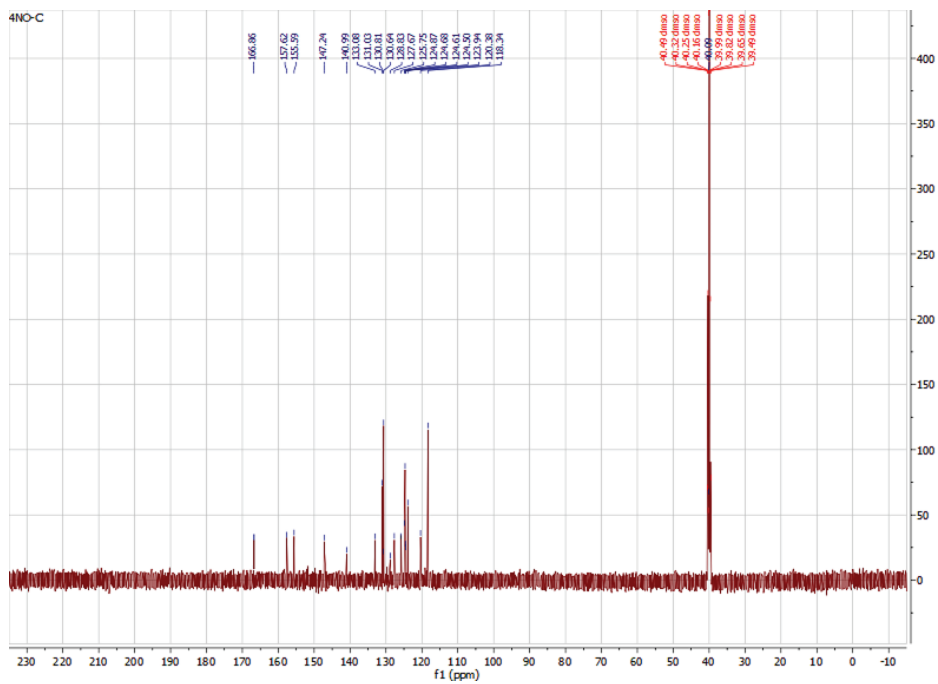
File :C:\MSDCHEM\3\DATA\Snapshot\TEST 991265.D
Operator :
Acquired : 23 Jul 2007 20:50 using AcqMethod test.M
Instrument : MSD
Sample Name: 4SCH3
Misc Info :
Vial Number: 1



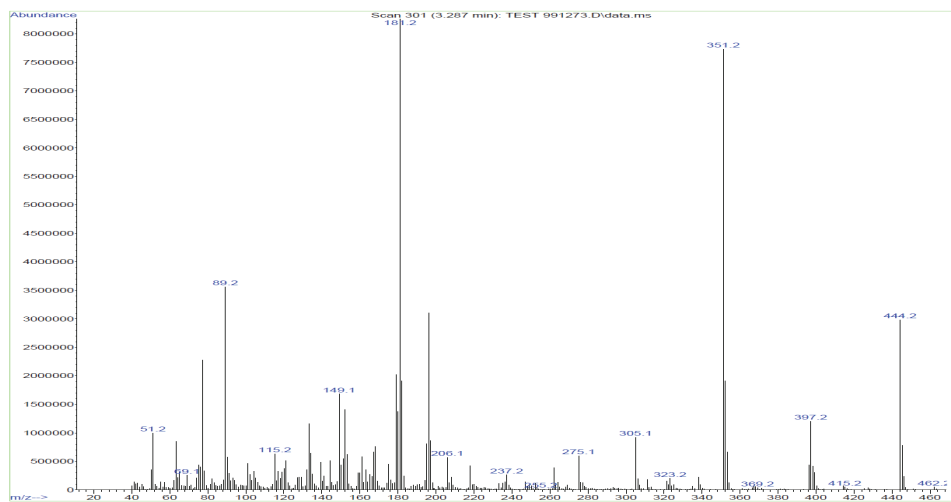


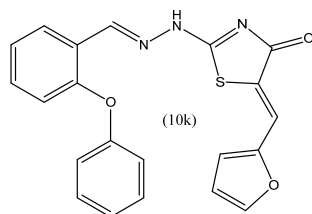
C₂₃H₁₆N₄O₄S
 Mw=444



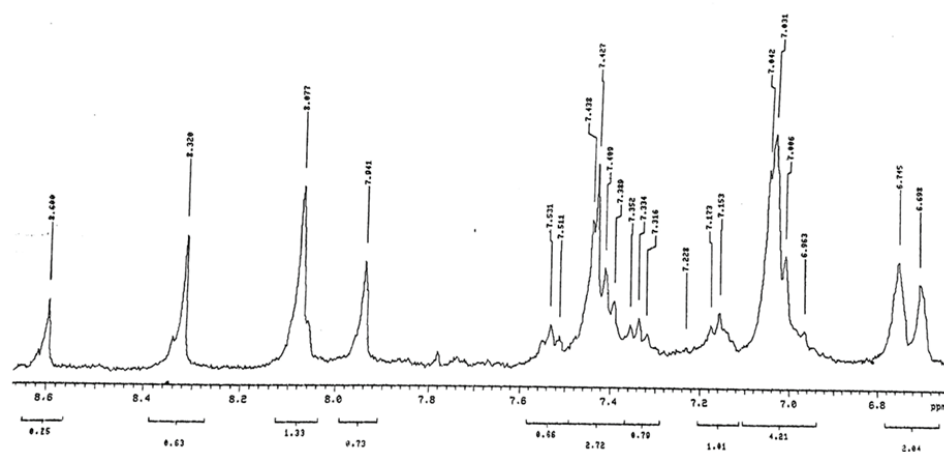
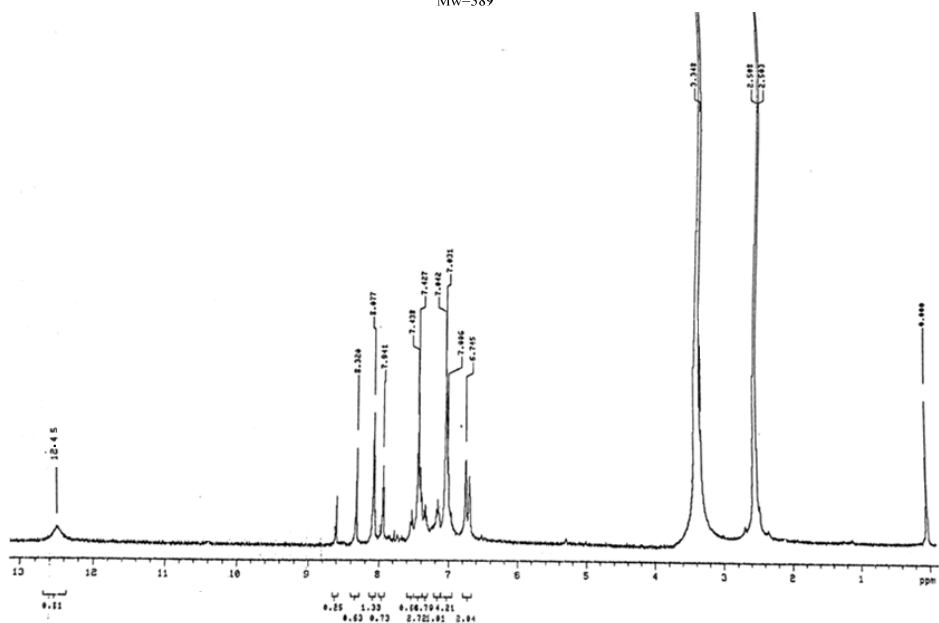


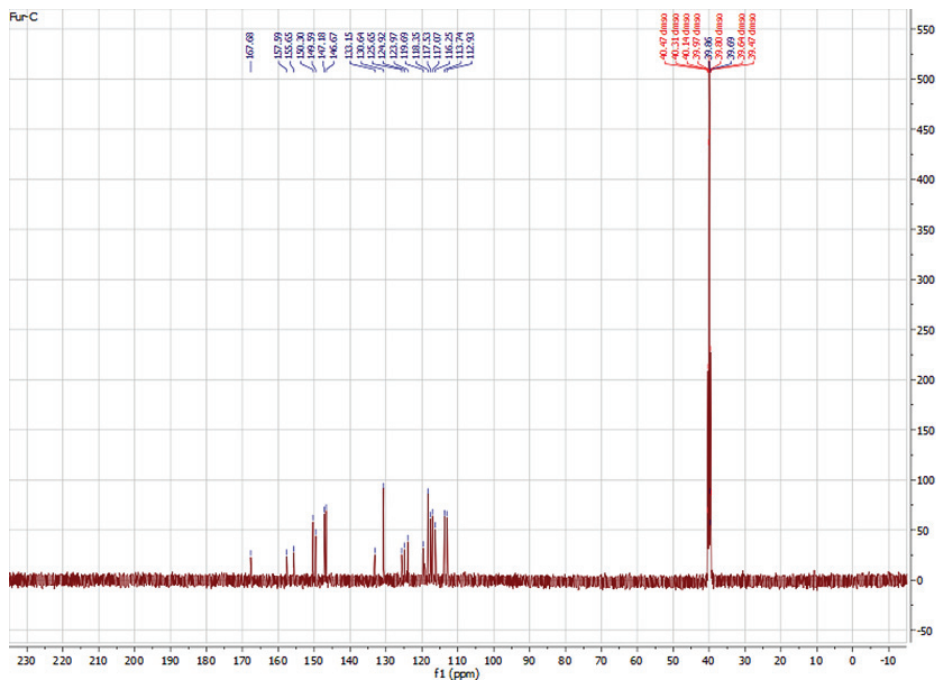
File : C:\MSDCHEM\3\DATA\Snapshot\TEST 991273.D
 Operator :
 Acquired : 23 Jul 2007 22:31 using AcqMethod test.M
 Instrument : MSD
 Sample Name: 4NO2
 Misc Info :
 Vial Number: 1



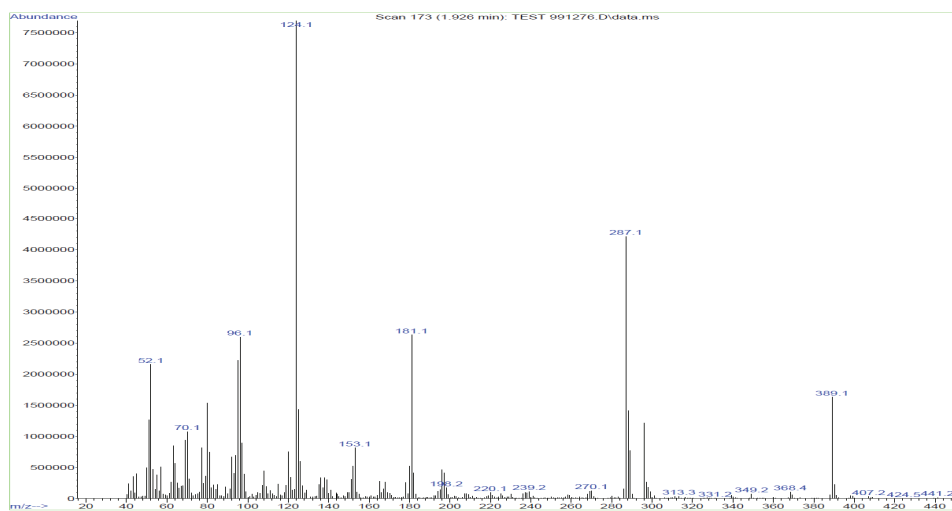


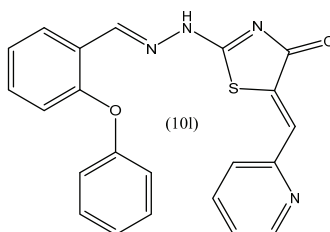
C₂₁H₁₅N₃O₃S
M_w=389



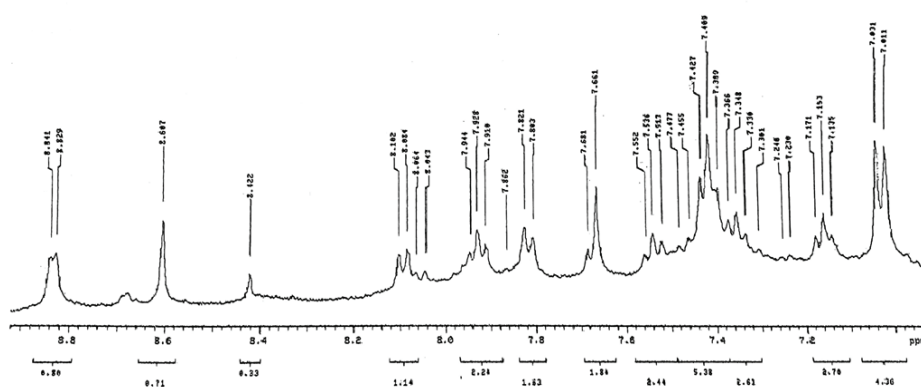
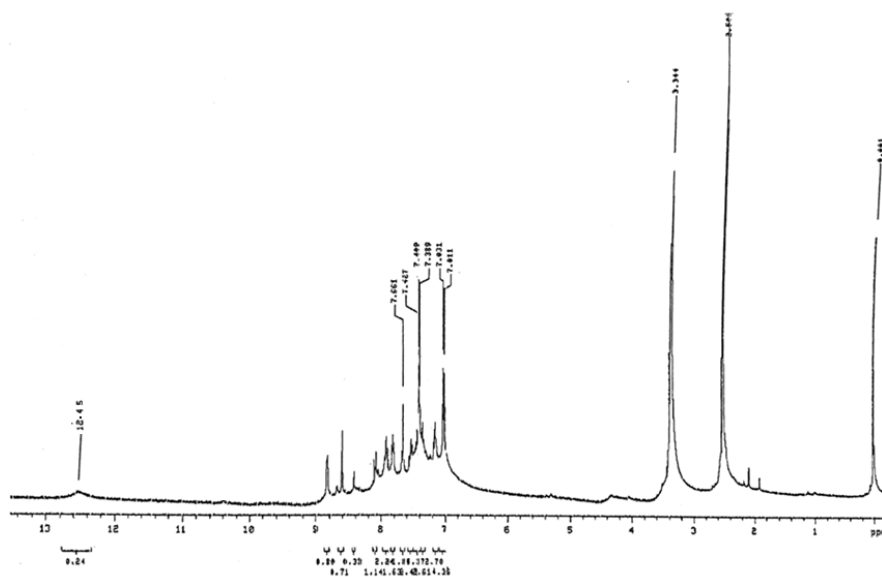


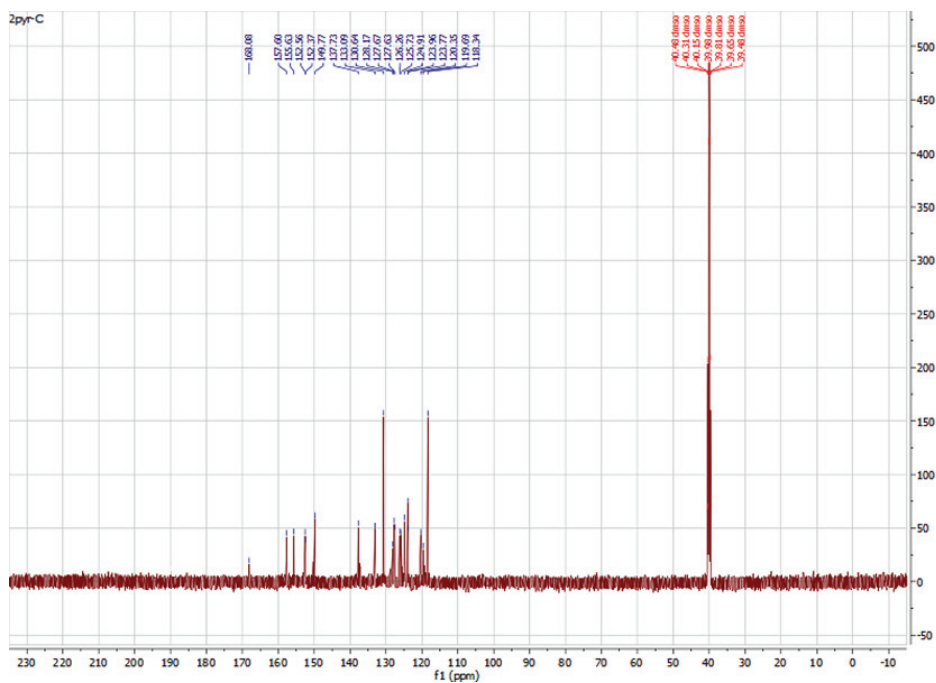
File : C:\MSDCHEM\3\DATA\Snapshot\TEST 991276.D
Operator :
Acquired : 23 Jul 2007 23:05 using AcqMethod test.M
Instrument : MSD
Sample Name: Fur
Misc Info :
Vial Number: 1



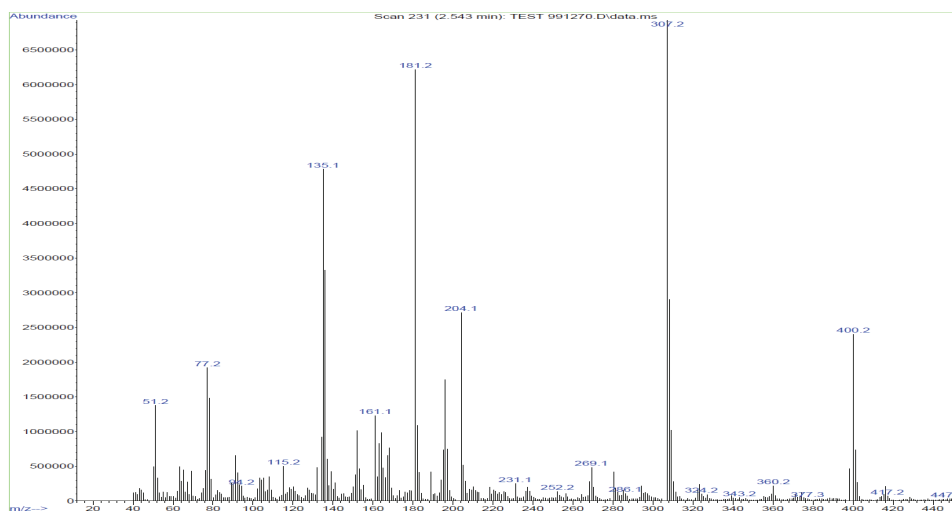


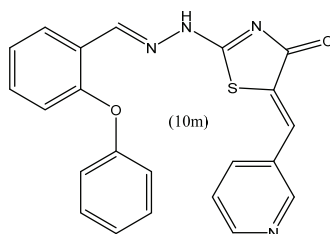
C₂₂H₁₆N₄O₂S
Mw=400



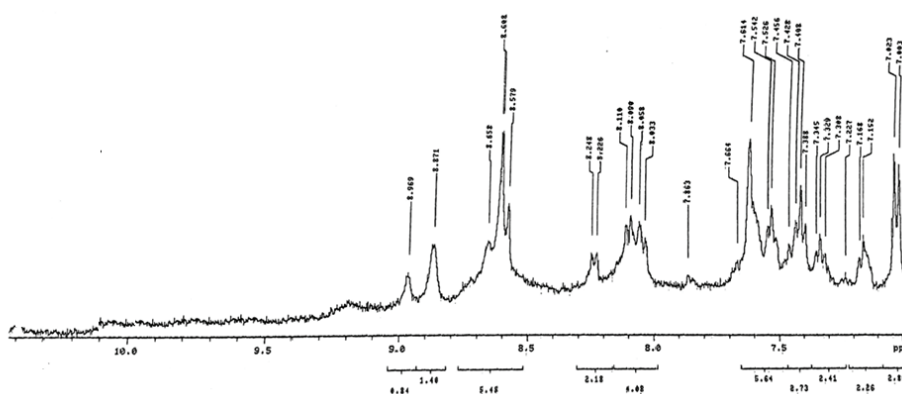
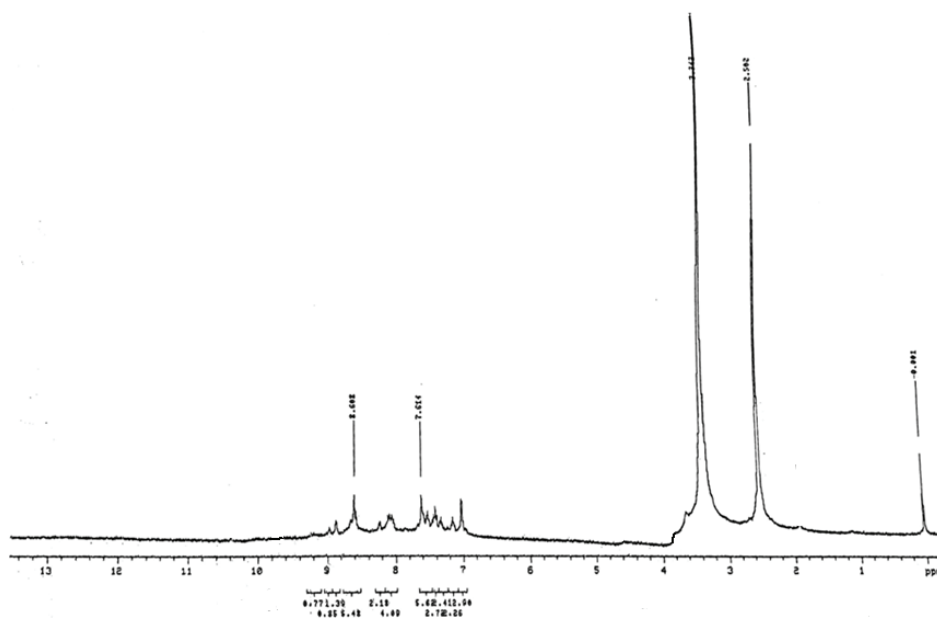


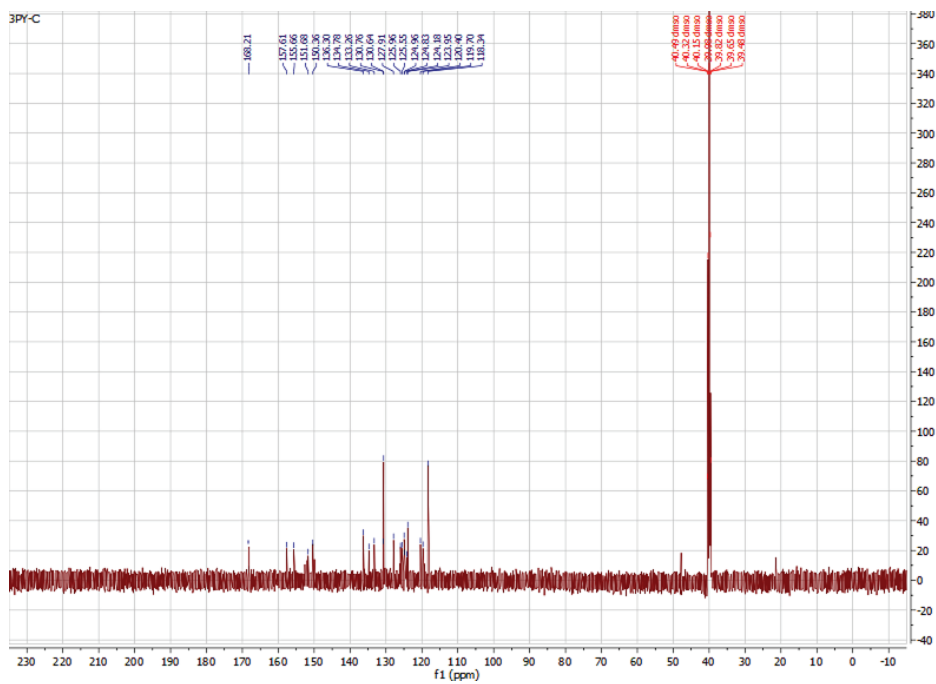
File : C:\MSDCHEM3\DATA\Snapshot\TEST 991270.D
Operator :
Acquired : 23 Jul 2007 21:57 using AcqMethod test.M
Instrument : MSD
Sample Name: 2Pyr
Misc Info :
Vial Number: 1



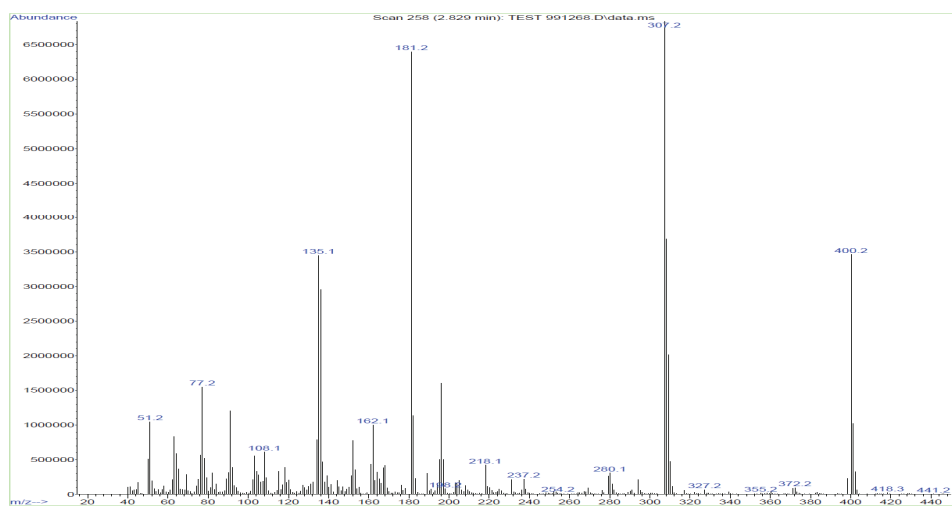


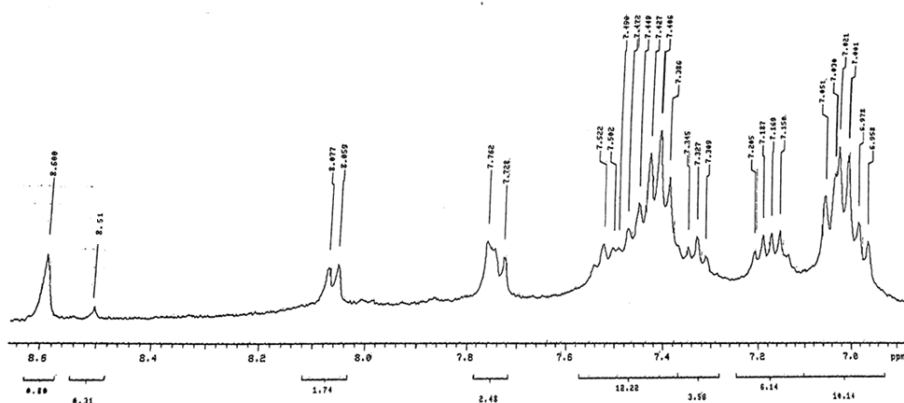
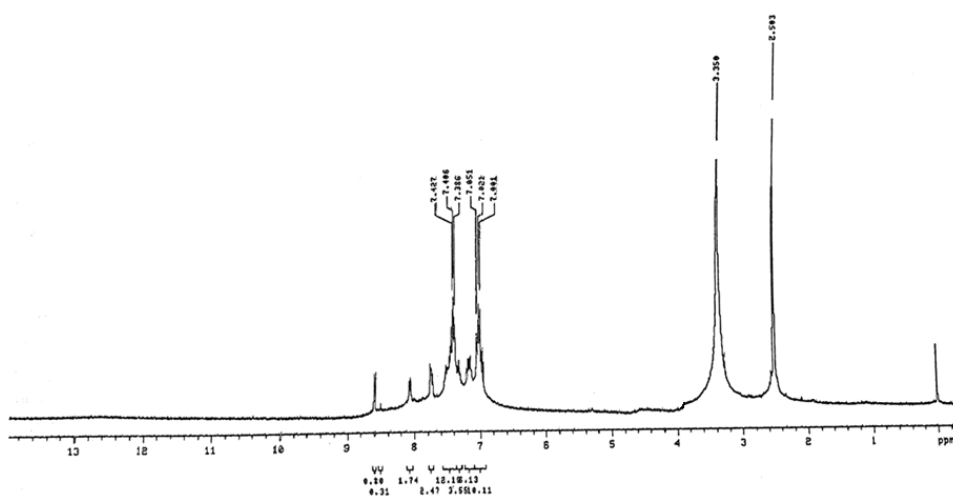
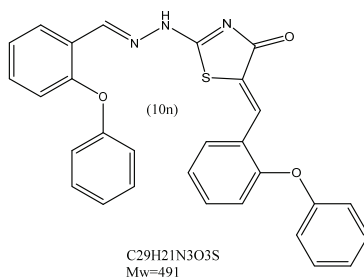
C₂₂H₁₆N₄O₂S
M_w=400

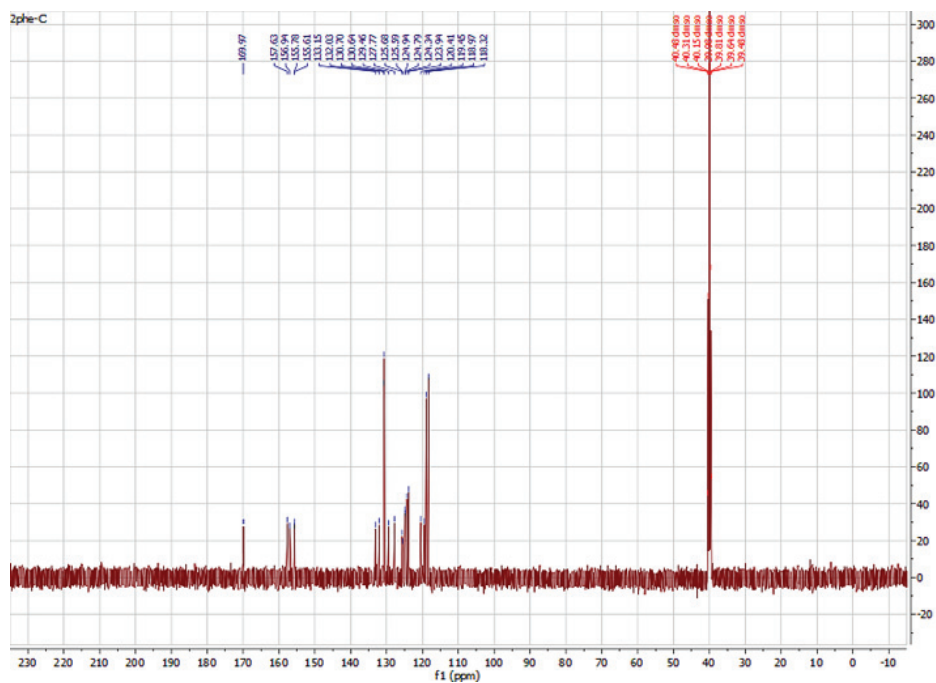




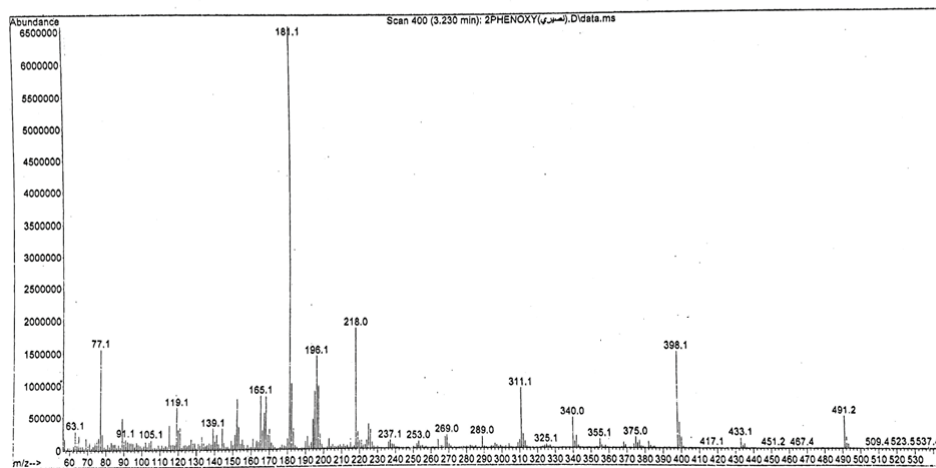
File : C:\MSDCHEM\3\DATA\SnapShot\TEST 991268.D
Operator :
Acquired : 23 Jul 2007 21:28 using AcqMethod test.M
Instrument : MSD
Sample Name: 3Pyr
Misc Info :
Vial Number: 1







File : C:\msdchem\3\DATA\2PHENOXY(متصوري).D
 Operator : ahoupal
 Acquired : 13 Dec 2010 13:03 using AcqMethod test dp.M
 Instrument : MSD Direct Probe
 Sample Name : 2phenoxy
 Misc Info :
 Vial Number: 1





J. Serb. Chem. Soc. 89 (11) 1423–1431 (2024)
JSCS–5797

Synthesis, antimycobacterial and antifungal evaluation of new 4-(furan-2-ylmethyl)-6-methylpyridazin-3(2H)-ones

BURCU KARAYAVUZ¹, SIVA KRISHNA VAGOLU², DIDEM KART³,
TONE TØNJUM^{2,4} and OYA UNSAL-TAN^{1*}

¹Department of Pharmaceutical Chemistry, Faculty of Pharmacy, Hacettepe University, Ankara, Turkey, ²Unit for Genome Dynamics, Department of Microbiology, University of Oslo, Oslo, Norway, ³Department of Pharmaceutical Microbiology, Faculty of Pharmacy, Hacettepe University, Ankara, Turkey and ⁴Unit for Genome Dynamics, Department of Microbiology, Oslo University Hospital, Oslo, Norway

(Received 24 April, revised 12 July 2023, accepted 31 March 2024)

Abstract: This study reports the synthesis and evaluation of a series of new pyridazin-3-ones with furan moieties **5a–j** and **6a–f**, to test for their antimycobacterial and antifungal activities. The structures of the target compounds were confirmed by elemental analysis and spectroscopic techniques (IR, mass, ¹H- and ¹³C-NMR). Amongst the compounds tested, **5e**, **5g**, **5i** and **6e** exhibited highest activity against *Mycobacterium tuberculosis*, while **5h**, **6d** and **6f** showed moderate *in vitro* antifungal activities against *Candida albicans* and *Candida parapsilosis*.

Keywords: pyridazinone; furan; biological activity.

INTRODUCTION

Tuberculosis (TB), the main leading infectious killer globally, is a contagious disease caused by *Mycobacterium tuberculosis* (Mtb). According to the WHO report in 2022, TB was responsible for the deaths of 1.6 million people in 2021. The number of TB deaths increased in 2020 and 2021, breaking the downward trend between 2005 and 2019. The fight against TB has been delayed since the beginning of the pandemic.¹ Current treatment of drug-sensitive tuberculosis is a 6-month regimen of 4 first-line drugs (isoniazide, rifampicin, ethambutol and pyrazinamide). Treatment of cases with drug-resistant Mtb requires 18–24 months of therapy with the addition of second-line drugs.^{2–5} Mtb can survive in nutrient and oxygen deprived conditions, and the disease most often becomes latent. The ability of Mtb to enter latency makes it very difficult to eradicate. The reactivation of latent TB infection accounts for the majority of new TB cases, par-

* Corresponding author. E-mail: oyaunsal@hacettepe.edu.tr
<https://doi.org/10.2298/JSC230424040K>

ticularly in countries with low TB incidence.⁶ Considering the compliance problem in treatment, the increase in drug-resistant cases and the emergence of many individuals with latent TB, new effective antitubercular agents are needed.⁷ Pyridazine-3(2*H*)-ones have attracted ample attention in the field of medicinal chemistry due to their diverse pharmacological properties such as antimycobacterial,^{8,9} antibacterial,¹⁰ antifungal,¹¹ antiviral,¹² anti-inflammatory,¹³ anticancer¹⁴ and anticonvulsant¹⁵ activities. Pyridazine-3(2*H*)-ones also hold the advantage that they are easy to modify from the different positions of the ring. It has been reported in the literature that many compounds with a pyridazin-3(2*H*)-one skeleton exhibited antimycobacterial potential. In particular, 2,6-disubstituted pyridazin-3(2*H*)-ones have been found to have strong antimycobacterial activities as summarized in Fig. 1.^{8,16–19}

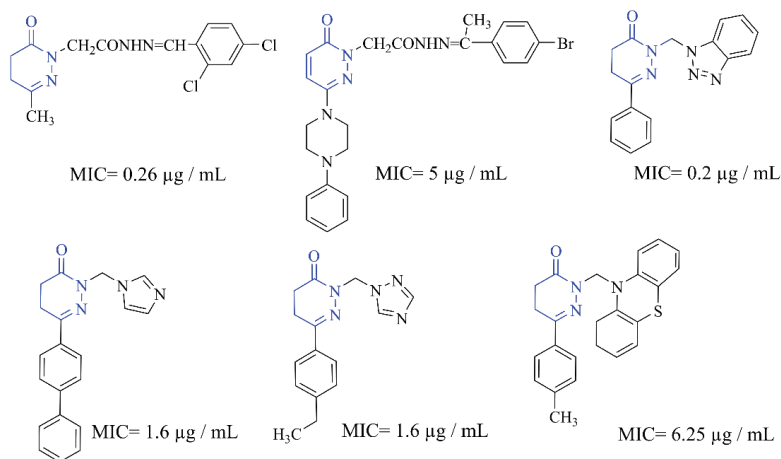


Fig. 1. Some 2,6-disubstituted pyridazin-3(2*H*)-ones with antimycobacterial.

On the other hand, its effects on various microorganisms make the furan an important moiety. Furan and nitrofur structures have long been demonstrated to be active in the development of new compounds with antimycobacterial^{20–27} and antifungal^{28–30} activity (Fig. 2).

The aim of this study was to synthesize a set of new 4-(furan-2-ylmethyl)-6-methyl-pyridazin-3(2*H*)-ones, which are the hybridization product of furan and pyridazin-3(2*H*)-one ring, and test them for antimycobacterial and antifungal activity.

EXPERIMENTAL

Chemistry

The melting points were measured using the Thomas–Hoover capillary melting point apparatus (Philadelphia, PA, USA); the data are uncorrected. ATR-FTIR spectra were acquired using a Spectrum BX FTIR spectrometer (Perkin Elmer) with MIRacle ATR attach-

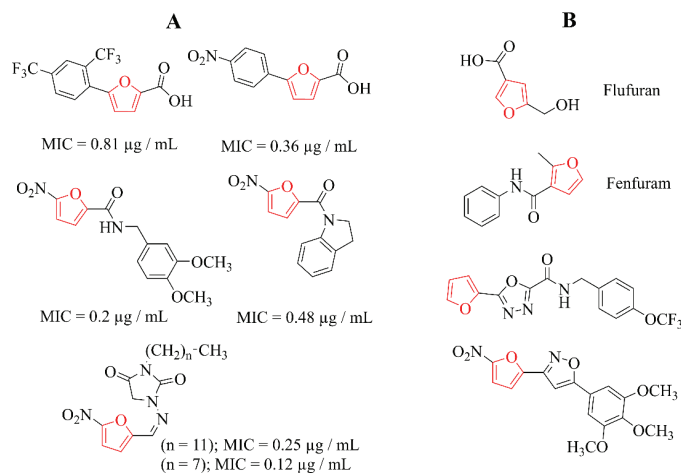


Fig. 2. Furan/nitrofurans compounds with: A) antimycobacterial and B) antifungal activity.

ment (Pike Technologies), and they were published in cm^{-1} . The ^1H and ^{13}C -NMR spectra (DMSO- d_6 /CDCl $_3$) were recorded on a Varian Mercury 400 FT NMR or Bruker Avance Neo 500 MHz spectrophotometer using TMS as an internal reference (chemical shift represented in δ / ppm). The ESI-MS spectra were obtained using a micromass ZQ-4000 single quadrupole mass spectrometer. Elemental analyses (C, H and N) were carried out using a Leco CHNS 932 analyzer.

Synthetic procedures

6-Methyl-4,5-dihydropyridazine-3(2H)-one (1). 50 mmol of hydrazine hydrate was added to a solution of 50 mmol of levulinic acid in 60 mL of ethanol and heated under reflux at 120 °C for 2 h. After evaporation of the solvent, the resulting solid was filtered and washed with ether to get the desired compound⁸.

4-(2-Furylmethyl)-6-methylpyridazin-3(2H)-one (2). 3.36 g (30 mmol) of **1** was dissolved in a 5 % KOH solution (35 mL) in ethanol. 2.48 mL (30 mmol) of furfural was added and refluxed for 4 h. Some of the solvent was removed and the mixture was concentrated. Subsequently, the solution poured into ice water was acidified with 2 M HCl (pH 2). The precipitated solid was crystallized from ethyl acetate. Yield, 3.51 g (62 %).

General procedure for the preparation of 2-chloro-N-arylacetamides (**3a–j**) and 2-chloro-1-(4-arylpiperazin-1-yl)ethanones (**4a–f**)

Various aryl amines (10 mmol) or N-arylpiperazines were dissolved in 10 ml of acetone. Potassium carbonate (20 mmol) was added and mixed in an ice bath for 5 min. Chloroacetyl chloride (12 mmol) was added dropwise under a fume hood. The reaction mixture was removed from the ice bath and stirred for 1 h at room temperature. When the reaction was complete, the mixture was poured into ice water, the precipitated solid was filtered off and desired intermediate compounds were obtained.³¹ The details for **3a–j** and **4a–f** are given in Supplementary material to this paper.

General procedure for the preparation of 2-[5-(furan-2-ylmethyl)-3-methyl-6-oxopyridazin-1(6H)-yl]-N-(aryl)acetamides (5a–j) and 4-(furan-2-ylmethyl)-6-methyl-2-[2-oxo-2-(4-aryl)piperazin-1-yl]ethyl]pyridazin-3(2H)-ones (6a–f)

The mixture of **2** (2 mmol) and potassium carbonate (4 mmol) in 20 mL of acetonitrile was refluxed for 30 min. Subsequently, **3a–j** or **4a–f** was added and mixture was refluxed for 4–6 h. When the reaction was complete, it was poured into ice water and extracted with ethyl acetate. After the ethyl acetate phase was dried with anhydrous sodium sulfate and filtered, the excess solvent was removed. It was purified by column chromatography with the appropriate ethyl acetate: *n*-hexane solvent system.

Biological studies

In-vitro M. tuberculosis MABA assay. Antimycobacterial activities of synthesized compounds against Mtb H37Rv strain were tested using microplate alamar blue assay (MABA) technique. In antimycobacterial activity studies, isoniazid was used as reference compound. The minimum inhibitor concentration (MIC) values of the compounds are given in Table I in $\mu\text{g} / \text{mL}$. Mtb H37Rv was inoculated from a freezer stock into 7H9+OADC and grown to mid-log phase. Logarithmically growing Mtb was then inoculated into Sauton's medium in 96 well plates with wells containing increasing concentrations of test compounds at an OD_{600} of 0.0008, corresponding to approximately 4×10^5 CFU/mL in 200 μL per well. Plates were incubated at 37 °C for 1 week, at which point 32.5 μL of a resazurin–tween mixture (8:5 ratio of 0.6 mM resazurin in 1XPBS to 20 % Tween 80) was added and the plate was incubated at 37 °C overnight. Production of fluorescent resorufin was used as an indication to determine the MIC of the compounds.

Antifungal activity. Antifungal activity of the target compounds and fluconazole was tested against the American Type Culture Collection (ATCC) strains of *Candida albicans* (ATCC 90028), *Candida krusei* (ATCC 6258) and *Candida parapsilosis* (ATCC 90018). MIC values ($\mu\text{g}/\text{mL}$), were determined by broth microdilution method according to Clinical and Laboratory Standards Institute (CLSI) reference documents.³² Briefly, the strains which were stored at –80 °C in glycerol were thawed and subcultured twice onto Sabouraud dextrose agar before the test. Broth microdilution was performed using RPMI 1640 broth (ICN-Flow, with glutamine, without bicarbonate and with pH indicator) buffered to pH 7.0 with 3-*N*-morpholinopropanesulfonic acid (MOPS). The inoculum densities were prepared from 24 h subcultures. The final test concentration of fungi was $0.5\text{--}2.5 \times 10^3$ cfu/mL. Fluconazole was dissolved at a concentration of 64–0.0625 $\mu\text{g}/\text{mL}$ in sterile deionized distilled water. The target compounds were dissolved in dimethyl sulfoxide and diluted with distilled water until their final twofold concentrations of the compounds in microtiter plate wells ranged from 1024–0.25 $\mu\text{g}/\text{mL}$. After 48 h incubation at 35 °C, the plates were checked visually for the growth of fungi and the MIC values were calculated. The MIC values of the compounds were determined from three independent experiments.

RESULTS AND DISCUSSION

Chemistry

The title compounds **5a–j** and **6a–f** were synthesized via the pathway shown in Fig 3. 6-methyl-4,5-dihydropyridazine-3(2H)-one **1**, used as starting material, was synthesized by heating levulinic acid and hydrazine hydrate in ethanol. The reaction of **1** with furfural in the presence of potassium hydroxide gave 4-(2-

furylmethyl)-6-methylpyridazin-3(2H)-one **2**. The intermediate compounds (**3a–j** and **4a–f**) were gained by reacting chloroacetyl chloride with the appropriate arylamines/*N*-arylpiperazines. The target compounds, **5a–j** and **6a–f** were obtained by *N*-alkylation with **3a–j** and **4a–f** in the presence of potassium carbonate. Characterization of newly synthesized compounds (**2**, **5a–j** and **6a–f**) was performed using IR, ¹H- and ¹³C-NMR, mass spectral data as well as elemental analysis. Spectral data details and spectra are presented in the Supplementary material.

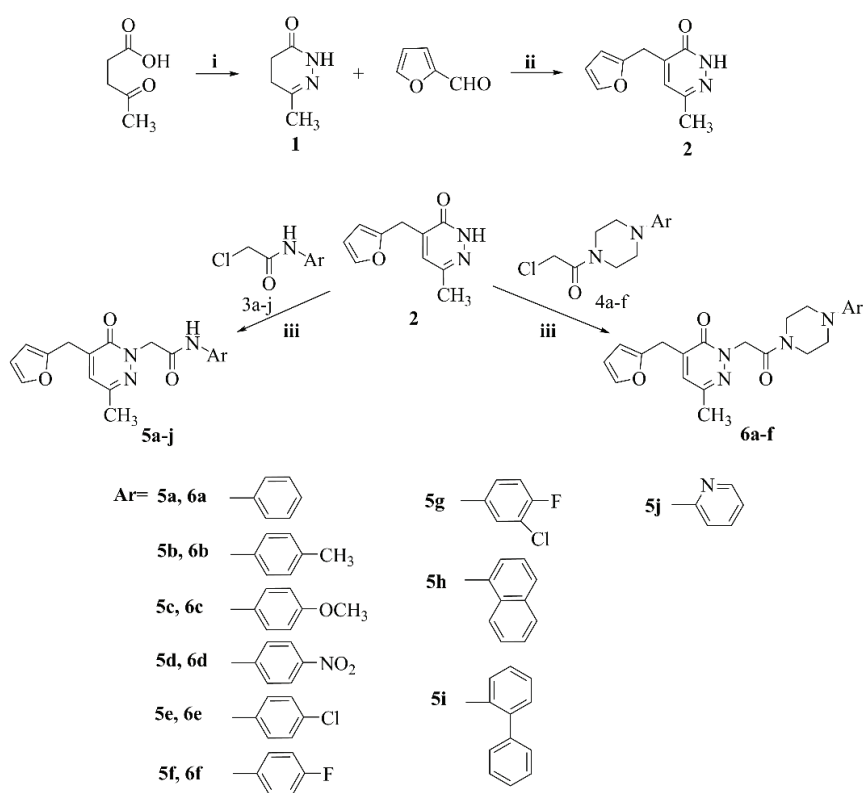
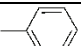
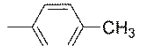
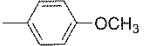
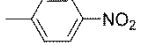
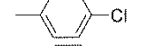
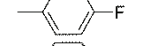
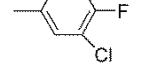
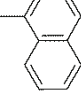
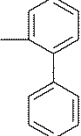
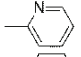
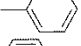
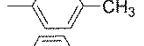

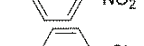




Fig. 3. Synthesis of the target compounds. Reagents and conditions: *i*. $\text{NH}_2\text{NH}_2 \cdot \text{H}_2\text{O}$, reflux, *ii*. 5% KOH /ethanol, HCl , reflux and *iii*. K_2CO_3 , reflux.

Biological activity

2-Substituted-4-(furan-2-ylmethyl)-6-methyl-pyridazin-3(2H)-ones (**5a–j** and **6a–f**) were tested for their antimycobacterial activities against Mtb reference strain H37Rv in comparison with isoniazid. These components were also tested with regard to their antifungal activities against strains of the yeast species *C. albicans*, *C. krusei* and *C. parapsilosis* in comparison with fluconazole. The MIC values of the compounds against these organisms were reported in Table I.

TABLE I. Antimycobacterial and antifungal activities of the compounds

Compd.	Ar	MIC / $\mu\text{g mL}^{-1}$			
		<i>M. tuberculosis</i> H37Rv	<i>C. albicans</i> ATCC 90028	<i>C. krusei</i> ATCC 6258	<i>C. parapsilosis</i> ATCC 90018
5a		64.8	256	256	256
5b		67.6	256	256	256
5c		70.8	256	512	512
5d		36.9	256	256	256
5e		17.9	256	512	256
5f		34.2	256	256	256
5g		19.9	256	256	256
5h		37.4	128	256	128
5i		20.1	256	256	256
5j		65.1	256	256	128
6a		39.3	256	256	256
6b		42.9	256	256	256
6c		42.3	512	256	256
6d		46.03	128	256	64
6e		22.56	256	256	256
6f		41.1	128	256	128
Isoniazid		0.02			
Fluconazole			1	32	1

The highest activity against Mtb H37Rv was found for **5e**, **5g**, **5i** and **6e** (MIC 15–25 $\mu\text{g/mL}$). Chlorine substitution (**5e**, **5g**, **6e**) to the phenyl ring caused an increase in activity for both series (**5a–j** and **6a–f**). For 2-[5-(furan-2-yl-methyl)-3-methyl-6-oxopyridazin-1(6H)-yl]-N-(aryl)acetamide derivatives (**5a–j**), it was observed that the activity increased with the replacement of small groups

such as phenyl (**5a**, $MIC = 64.8 \mu\text{g/mL}$) and pyridine (**5j**, $MIC = 65 \mu\text{g/mL}$) with larger groups such as biphenyl (**5i**, $MIC = 20 \mu\text{g/mL}$) and naphthyl (**5h**, $MIC = 37.4 \mu\text{g/mL}$). In addition, for the same series, introducing the electron donating groups to the phenyl ring (**5b** and **5c**, $MIC: 65\text{--}70 \mu\text{g/mL}$) did not contribute to the activity. No significant increase in the antimycobacterial activity of **6a–f** bearing the piperazine ring was observed.

The antifungal activity tests against three fungi strains (*C. albicans* ATCC 90028, *C. krusei* ATCC 6258 and *C. parapsilosis* ATCC 90018) showed that **5h**, **6d** and **6f** proved to exhibit some moderate *in vitro* antifungal activities against *C. albicans* and *C. parapsilosis* ($MIC: 64\text{--}128 \mu\text{g/mL}$). However, all compounds were inactive against *C. krusei* ($MIC \geq 256 \mu\text{g/mL}$). Electron withdrawing groups (F and NO_2) on the phenyl ring slightly improved the activity. These activities are the only modest ones in comparison with fluconazole, the standard ($MIC = 1 \mu\text{g/mL}$).

CONCLUSION

In summary, a series of new pyridazin-3-ones having furan moiety **5a–j** and **6a–f** was designed and synthesized to assess their antimycobacterial and antifungal activities. The structures of the target compounds were characterized using elemental analysis and spectroscopic methods (IR, mass, ^1H - and ^{13}C -NMR). Amongst the tested compounds, **5e**, **5g**, **5i** and **6e** showed highest activity against *M. tuberculosis* and all chlorine-bearing compounds were found to be in this group. For antifungal activity, **5h**, **6d**, and **6f** exhibited weak *in vitro* antifungal activities against *C. albicans* and *C. parapsilosis*. Further modifications of pyridazin-3-ones are required to enable even lower MICs and therapeutic potential.

SUPPLEMENTARY MATERIAL

Additional data and information are available electronically at the pages of journal website: <https://www.shd-pub.org.rs/index.php/JSCS/article/view/12361>, or from the corresponding author on request.

Acknowledgements. TT acknowledges financial support by the Research Council of Norway (RCN project numbers #261669 and #309592) and EU JPI-AMR (RCN project number 298410).

ИЗВОД

СИНТЕЗА И ИСПИТИВАЊЕ АНТИМИКОБАКТЕРИЈСКЕ И АНТИФУНГАЛНЕ
 АКТИВНОСТИ НОВИХ ДЕРИВАТА 4-(ФУРАН-2-ИЛМЕТИЛ)-
 -6-МЕТИЛПИРИДАЗИН-3(2H)-ОНА

BURCU KARAYAVUZ¹, SIVA KRISHNA VAGOLU², DIDEM KART³, TONE TONJUM^{2,4} и OYA UNSAL-TAN¹

¹Department of Pharmaceutical Chemistry, Faculty of Pharmacy, Hacettepe University, Ankara, Turkey, ²Unit for Genome Dynamics, Department of Microbiology, University of Oslo, Oslo, Norway, ³Department of Pharmaceutical Microbiology, Faculty of Pharmacy, Hacettepe University, Ankara, Turkey и ⁴Unit for Genome Dynamics, Department of Microbiology, Oslo University Hospital, Oslo, Norway.

Током истраживања извршена је синтеза и евалуацији серије нових деривата 4-(фуран-2-илметил)-6-метилпиридазин-3(2H)-она **5a–j** и **6a–f** и испитана је њихова антимикобактеријска и антифунгална активност. Структуре циљних једињења потврђене су елементарном анализом и спектроскопским техникама (IR, масеном спектрометријом, ¹H и ¹³C-NMR). Међу тестираним једињењима, **5e**, **5g**, **5i** и **6e** су показале највећу активност против *Mycobacterium tuberculosis*, док су **5h**, **6d** и **6f** показале умерену *in vitro* антифунгалну активност против *C. albicans* and *C. parapsilosis*.

(Примљено 24. априла, ревидирано 12. јула 2023, прихваћено 31. марта 2024)

REFERENCES

1. World Health Organization, *Global Tuberculosis Report*, 2022
2. M. M. Sirim, V. S. Krishna, D. Sriram, O. Unsal Tan, *Eur. J. Med. Chem.* **188** (2020) 112010 (<https://doi.org/10.1016/j.ejmech.2019.112010>)
D. Falzon, H. J. Schünemann, E. Harausz, L. González-Angulo, C. Lienhardt, E. Jaramillo, K. Weyer, *Eur. Respir. J.* **49** (2017) 1 (<http://dx.doi.org/10.1183/13993003.02308-2016>)
3. A. Koch, H. Cox, V. Mizrahi, *Curr. Opin. Pharmacol.* **42** (2018) 7 (<https://doi.org/10.1016/j.coph.2018.05.013>)
4. V. Dartois, *Nat. Rev. Microbiol.* **12** (2014) 159 (<https://doi.org/10.1038/nrmicro3200>)
5. H. Getahun, A. Matteelli, R. E. Chaisson, M. Raviglione, *N. Eng. J. Med.* **372** (2015) 2127 (<https://doi.org/10.1056/NEJMRA1405427>)
6. G. Grüber, *Prog. Biophys. Mol. Biol.* **152** (2020) 2 (<https://doi.org/10.1016/J.PBIOMOLBIO.2020.02.003>)
7. O. U. Tan, K. Ozadali, P. Yogeewari, D. Sriram, A. Balkan, *Med. Chem. Res.* **21** (2012) 2388 (<http://dx.doi.org/10.1007/s00044-011-9770-6>)
8. D. Mantu, M. C. Luca, C. Moldoveanu, G. Zbancioc, I. I. Mangalagiu, *Eur. J. Med. Chem.* **45** (2010) 5164 (<http://dx.doi.org/10.1016/J.EJMECH.2010.08.029>)
9. H. B. V. Sowmya, T. S. Kumara, G. Nagendrapa, J. P. Jasinski, S. P. Millikan, G. Jose, Dileep R., P. S. Sujan Ganapathy, *J. Mol. Struct.* **1054** (2013) 179 (<http://dx.doi.org/10.1016/J.MOLSTRUC.2013.09.046>)
10. G. Zhou, P. C. Ting, R. Aslanian, J. Cao, D. W. Kim, R. Kuang, J. F. Lee, J. Schwerdt, H. Wu, R. J. Herr, A. J. Zych, J. Yang, S. Lam, S. Wainhaus, T. A. Black, P. M. McNicholas, Y. Xu, S. S. Walker, *Bioorg. Med. Chem. Lett.* **21** (2011); 2890 (<http://dx.doi.org/10.1016/J.BMCL.2011.03.083>)
11. D. Li, P. Zhan, H. Liu, C. Pannecouque, J. Balzarini, E. De Clercq, X. Liu, *Bioorg. Med. Chem.* **21** (2013); 2134 (<http://dx.doi.org/10.1016/J.BMC.2012.12.049>)
12. J. Singh, D. Sharma, R. Bansal, *Future Med. Chem.* **9** (2016) 95 (<http://dx.doi.org/10.4155/FMC-2016-0194>)

13. X. Zhang, J. Luo, Q. Li, Q. Xin, L. Ye, Q. Zhu, Z. Shi, F. Zhan, B. Chu, Z. Liu, Y. Jiang, *Eur. J. Med. Chem.* **226** (2021) 113812 (<http://dx.doi.org/10.1016/J.EJMECH.2021.113812>)
14. A. A. Siddiqui, S. Partap, S. Khisal, M. Shahar Yar, R. Mishra, *Bioorg. Chem.* **99** (2020) 103584 (<http://dx.doi.org/10.1016/J.BIOORG.2020.103584>)
15. S. Utku, M. Gökçe, G. Aslan, G. Bayram, *Turkish J. Chem.* **35** (2011); 331 (<http://dx.doi.org/10.3906/kim-1009-63>)
16. M. Asif, M. Imran, *Anal. Chem. Lett.* **10** (2020) 414 (<http://dx.doi.org/10.1080/22297928.2020.1776633>)
17. M. Asif, A. Singh, S. A. Khan, A. Husain, *Brazilian J. Pharm. Sci.* **54** (2018); 1 (<http://dx.doi.org/10.1590/S2175-97902018000300040>)
18. M. Asif, A. Imran, M. Imran, *IJPSR* **11** (2020) 826 ([http://dx.doi.org/10.13040/IJPSR.0975-8232.11\(2\).826-31](http://dx.doi.org/10.13040/IJPSR.0975-8232.11(2).826-31))
19. L. R. Chiarelli, M. Mori, G. Beretta, A. Gelain, E. Pini, J. C. Sammartino, G. Stelitano, D. Barlocco, L. Costantino, M. Lapillo, G. Poli, I. Caligiuri, F. Rizzolio, M. Bellinzoni, T. Tuccinardi, S. Villa, F. Meneghetti, *J. Enzyme Inhib. Med. Chem.* **34** (2019) 823 (<http://dx.doi.org/10.1080/14756366.2019.1589462>)
20. L. R. Chiarelli, M. Mori, D. Barlocco, G. Beretta, A. Gelain, E. Pini, M. Porcino, G. Mori, G. Stelitano, L. Costantino, M. Lapillo, D. Bonanni, G. Poli, T. Tuccinardi, S. Villa, F. Meneghetti, *Eur. J. Med. Chem.* **155** (2018) 754 (<http://dx.doi.org/10.1016/j.ejmech.2018.06.033>)
21. R. P. Tangallapally, R. Yendapally, R. E. Lee, K. Hevener, V. C. Jones, A. J. M. Lenaerts, M. R. McNeil, Y. Wang, S. Franzblau, R. E. Lee, *J. Med. Chem.* **47** (2004) 5276 (<http://dx.doi.org/10.1021/jm049972y>)
22. Y. L. Fan, J. B. Wu, X. Ke, Z. P. Huang, *Bioorg. Med. Chem. Lett.* **28** (2018) 3064 (<https://doi.org/10.1016/j.bmcl.2018.07.046>)
23. R. P. Tangallapally, D. Sun, N. Budha, R. E. Lee, A. J. M. Lenaerts, N. Budha, R. E. Lee, *Bioorg. Med. Chem. Lett.* **17** (2007) 6638 (<http://dx.doi.org/10.1016/j.bmcl.2007.09.048>)
24. N. R. Tawari, R. Bairwa, M. K. Ray, M. G. R. Rajan, M. S. Degani, *Bioorg. Med. Chem. Lett.*, **20** (2010); 6175 (<http://dx.doi.org/10.1016/j.bmcl.2010.08.127>)
25. N. H. Zuma, J. Aucamp, D. D. N'Da, *Eur. J. Pharm. Sci.* **140** (2019) 105092 (<https://doi.org/10.1016/j.ejps.2019.105092>)
26. N. H. Zuma, F. J. Smit, R. Seldon, J. Aucamp, A. Jordaan, D. F. Warner, D. D. N'Da, *Bioorg. Chem.* **96** (2020) 103587 (<https://doi.org/10.1016/j.bioorg.2020.103587>)
27. Z. Yang, Y. Sun, Q. Liu, A. Li, W. Wang, W. Gu, *J. Agric. Food Chem.* **69** (2021) 13373 (<https://doi.org/10.1021/acs.jafc.1c03857>)
28. A. Evidente, G. Cristinzio, B. Punzo, A. Andolfi, A. Testa, D. Melck, *Chem. Biodivers.* **6** (2009) 328 (<http://dx.doi.org/10.1002/CBDV.200800292>)
29. O. S. Trefzger, N. V. Barbosa, R. L. Scapolatempo, A. R. das Neves, M. L. F. S. Ortale, D. B. Carvalho, A. M. Honorato, M. R. Fragoso, C. Y. K. Shuiguemoto, R. T. Perdomo, M. F. C. Matos, M. R. Chang, C. C. P. Arruda, A. C. M. Baroni, *Arch. Pharm.* **353** (2020) 1900241 (<http://dx.doi.org/10.1002/ARDP.201900241>)
30. G. B. Wang, L. F. Wang, C. Z. Li, J. Sun, G. M. Zhou, D. C. Yang, *Res. Chem. Intermed.* **38** (2012) (<https://doi.org/10.1007/s11164-011-0327-6>)
31. Clinical and Laboratory Standards Institute (CLSI), *Ref. Method Broth Dilution Antifung. Susceptibility Test. Yeasts. Approv. Stand.*, 2008 (https://clsi.org/media/1461/m27a3_sample.pdf).

SUPPLEMENTARY MATERIAL TO

**Synthesis, antimycobacterial and antifungal evaluation of new
4-(furan-2-ylmethyl)-6-methylpyridazin-3(2H)-ones**

BURCU KARAYAVUZ¹, SIVA KRISHNA VAGOLU², DIDEM KART³,
TONE TØNJUM^{2,4} and OYA UNSAL-TAN^{1*}

¹Department of Pharmaceutical Chemistry, Faculty of Pharmacy, Hacettepe University, Ankara, Turkey, ²Unit for Genome Dynamics, Department of Microbiology, University of Oslo, Oslo, Norway, ³Department of Pharmaceutical Microbiology, Faculty of Pharmacy, Hacettepe University, Ankara, Turkey and ⁴Unit for Genome Dynamics, Department of Microbiology, Oslo University Hospital, Oslo, Norway

J. Serb. Chem. Soc. 89 (11) (2024) 1423–1431

4-(2-Furylmethyl)-6-methylpyridazin-3(2H)-one (**2**). m.p. 126–127 °C. IR; 3124 (N–H), 2960, 2842 (C–H), 1648 (C=O), 1609, 1562, 1505, 1473, 1434 (C=N ve C=C). ¹H-NMR (DMSO-d₆, 400 MHz); δ 2.18 (3H; s; –CH₃), 3.80 (2H; s; –CH₂–), 6.20 (1H; d; furan H₃, J = 3.2 Hz), 6.39 (1H; dd; furan H₄, J₁ = 3.2 Hz, J₂ = 2 Hz), 6.98 (1H; s; pyridazinone H₅), 7.56 (1H; d; furan H₅, J = 1.6 Hz), 12.76 (1H; s; NH) ppm. ¹³C-NMR (DMSO-d₆, 100 MHz); δ 20.21 (CH₃), 27.20 (CH₂), 107.38, 110.61 (furan C₃, C₄), 131.08 (pyridazinone C₅), 139.11 (pyridazinone C₄), 142.17 (furan C₅), 144.11 (pyridazinone C₆), 150.89 (furan C₂), 160.18 (pyridazinone CO) ppm. ESI-MS (*m/z*): 191.27 [M+H]⁺, 213.27 [M+Na]⁺ (100%). Anal. Calcd. For C₁₀H₁₀N₂O₂: C, 63.15; H, 5.30; N, 14.73. Found: C, 62.96; H, 5.34; N, 14.70.

2-[5-(Furan-2-ylmethyl)-3-methyl-6-oxopyridazin-1(6H)-yl]-N-phenylacetamide (**5a**)

Yield 45 %; m.p. 124–125 °C. IR; 3265 (N–H), 3088 (C–H), 1671, 1658 (C=O), 1613, 1600, 1553, 1501, 1446 (C=N ve C=C). ¹H-NMR (CDCl₃, 400 MHz); δ 2.30 (3H; s; –CH₃), 3.95 (2H; s; –CH₂–), 4.95 (2H; s; CH₂CONH), 6.21 (1H; d; furan H₃, J = 3.2 Hz), 6.35–6.36 (1H; dd; furan H₄, J₁ = 3 Hz, J₂ = 2 Hz), 6.85 (1H; s; pyridazinone H₅), 7.05 (1H; t; Ar–H₄), 7.23–7.27 (2H; m; Ar–H₃,₅, ve CHCl₃), 7.38 (1H; dd; furan H₅, J₁ = 2 Hz, J₂ = 0.8 Hz), 7.48 (2H; d; Ar–H₂,₆, J = 7.6 Hz), 8.95 (1H; s; NH) ppm. ¹³C-NMR (CDCl₃, 100 MHz); δ 20.94 (CH₃), 28.34 (CH₂), 57.83 (CH₂CO), 108.15, 110.63 (furan C₃, C₄), 119.83, 124.25, 128.84, 131.17, 137.70, 140.16, 142.26, 145.76 (aromatic carbons), 150.14 (furan C₂), 160.59 (pyridazinone CO), 165.19 (CONH) ppm. ESI-MS (*m/z*): 324.34 [M+H]⁺, 346.30 [M+Na]⁺ (% 100). Anal. calcd. for C₁₈H₁₇N₃O₃: C, 66.66; H, 5.30; N, 13.00. Found: C, 67.01; H, 5.43; N, 13.00.

2-[5-(Furan-2-ylmethyl)-3-methyl-6-oxopyridazin-1(6H)-yl]-N-4-methylphenylacetamide (**5b**)

Yield 39 %; m.p. 112 °C. IR; 3271 (N–H), 3072 (C–H), 1702, 1640 (C=O), 1607, 1546, 1515, 1446 (C=N ve C=C). ¹H-NMR (DMSO-d₆, 400 MHz); δ 2.23 (3H; s; –CH₃), 2.25 (3H;

* Corresponding author. E-mail: oyaunsal@hacettepe.edu.tr

s; $-\text{CH}_3$), 3.85 (2H; s; $-\text{CH}_2-$), 4.83 (2H; s; CH_2CONH), 6.22 (1H; d; furan H_3 , $J = 2.8$ Hz), 6.40–6.42 (1H; dd; furan H_4 , $J_1 = 3.2$ Hz, $J_2 = 2$ Hz), 7.05 (1H; s; pyridazinone H_5), 7.11 (2H; d; Ar- $\text{H}_{3',5'}$, $J = 8.4$ Hz), 7.45 (2H; d; Ar- $\text{H}_{2',6'}$, $J = 8.8$ Hz), 7.58 (1H; d; furan H_5 , $J = 1.2$ Hz), 10.18 (1H; s; NH) ppm. ^{13}C -NMR (DMSO- d_6 , 100 MHz); δ 20.27, 20.40 (CH_3), 27.59 (CH_2), 54.73 (CH_2CO), 107.54, 110.64 (furan C_3 , C_4), 119.00, 129.15, 130.93, 132.27, 136.22, 138.79, 142.24, 143.85 (aromatic carbons), 150.73 (furan C_2), 159.09 (pyridazinone CO), 164.90 (CONH) ppm. ESI-MS (m/z): 338.35 $[\text{M}+\text{H}]^+$, 360.31 $[\text{M}+\text{Na}]^+$ (% 100). Anal. calcd. for $\text{C}_{19}\text{H}_{19}\text{N}_3\text{O}_3$: C, 67.64; H, 5.68; N, 12.46. Found: C, 67.42; H, 5.74; N, 12.41.

2-[5-(Furan-2-ylmethyl)-3-methyl-6-oxopyridazin-1(6H)-yl]-N-(4-methoxyphenyl)acetamide (5c)

Yield 38 %; m.p. 73 °C. IR; 3268 (N–H), 1649 (C=O), 1600, 1546, 1463, 1440, 1415 (C=N ve C=C). ^1H -NMR (DMSO- d_6 , 400 MHz); δ 2.23 (3H; s; $-\text{CH}_3$), 3.72 (3H; s; $-\text{OCH}_3$), 3.85 (2H; s; $-\text{CH}_2-$), 4.81 (2H; s; CH_2CONH), 6.22 (1H; d; furan H_3 , $J = 3.2$ Hz), 6.41 (1H; t; furan H_4), 6.88 (2H; d; Ar- $\text{H}_{3',5'}$, $J = 9.2$ Hz), 7.05 (1H; s; pyridazinone H_5), 7.48 (2H; d; Ar- $\text{H}_{2',6'}$, $J = 9.2$ Hz), 7.58 (1H; m; furan H_5), 10.12 (1H; s; NH) ppm. ^{13}C -NMR (DMSO- d_6 , 100 MHz); δ 20.27 (CH_3), 27.60 (CH_2), 54.66 (CH_2CO), 55.12 (OCH_3), 107.54, 110.64 (furan C_3 , C_4), 113.89, 120.51, 130.91, 131.88, 138.79, 142.24, 143.83, 155.25 (aromatic carbons), 150.74 (furan C_2), 159.09 (pyridazinone CO), 164.65 (CONH) ppm. ESI-MS (m/z): 354.29 $[\text{M}+\text{H}]^+$, 376.26 $[\text{M}+\text{Na}]^+$ (% 100). Anal. calcd. for $\text{C}_{19}\text{H}_{19}\text{N}_3\text{O}_4$: C, 64.58; H, 5.42; N, 11.89. Found: C, 64.31; H, 5.56; N, 11.66.

2-[5-(Furan-2-ylmethyl)-3-methyl-6-oxopyridazin-1(6H)-yl]-N-(4-nitrophenyl)acetamide (5d)

Yield 37 %; m.p. 165–166 °C. IR; 3227 (N–H), 1719, 1648 (C=O), 1595, 1576, 1503 (C=N ve C=C). ^1H -NMR (CDCl_3 , 400 MHz); δ 2.35 (3H; s; $-\text{CH}_3$), 3.97 (2H; s; $-\text{CH}_2-$), 5.02 (2H; s; CH_2CONH), 6.20 (1H; dd; furan H_3 , $J_1 = 3.2$ Hz, $J_2 = 0.8$ Hz), 6.36 (1H; dd; furan H_4 , $J_1 = 1.6$ Hz, $J_2 = 0.8$ Hz), 6.98 (1H; s; pyridazinone H_5), 7.37 (1H; dd; furan H_5 , $J_1 = 1.6$ Hz, $J_2 = 0.8$ Hz), 7.48–7.52 (2H; m; Ar- $\text{H}_{2',6'}$), 7.96–8.00 (2H; m; Ar- $\text{H}_{3',5'}$), 9.95 (1H; s; NH) ppm. ^{13}C -NMR (CDCl_3 , 100 MHz); δ 20.95 (CH_3), 28.48 (CH_2), 58.09 (CH_2CO), 108.12, 110.68 (furan C_3 , C_4), 119.10, 124.64, 131.95, 139.83, 142.35, 143.28, 143.62, 146.33 (aromatic carbons), 149.91 (furan C_2), 160.77 (pyridazinone CO), 165.79 (CONH) ppm. ESI-MS (m/z): 369.27 $[\text{M}+\text{H}]^+$, 391.21 $[\text{M}+\text{Na}]^+$ (% 100). Anal. calcd. for $\text{C}_{18}\text{H}_{16}\text{N}_4\text{O}_5$: C, 58.69; H, 4.38; N, 15.21. Found: C, 58.26; H, 4.25; N, 15.11.

2-[5-(Furan-2-ylmethyl)-3-methyl-6-oxopyridazin-1(6H)-yl]-N-(4-chlorophenyl)acetamide (5e)

Yield 46 %; m.p. 131 °C. IR; 3277 (N–H), 3082 (C–H), 1708, 1649 (C=O), 1551, 1489, 1421, 1400 (C=N ve C=C). ^1H -NMR (DMSO- d_6 , 400 MHz); δ 2.24 (3H; s; $-\text{CH}_3$), 3.85 (2H; s; $-\text{CH}_2-$), 4.85 (2H; s; CH_2CONH), 6.22 (1H; d; furan H_3 , $J = 3.2$ Hz), 6.40–6.41 (1H; dd; furan H_4 , $J_1 = 3.2$ Hz, $J_2 = 2$ Hz), 7.06 (1H; s; pyridazinone H_5), 7.37 (2H; d; Ar- $\text{H}_{3',5'}$, $J = 8.8$ Hz), 7.58–7.61 (3H; m; Ar- $\text{H}_{2',6'}$ and furan H_5), 10.43 (1H; s; NH) ppm. ^{13}C -NMR (DMSO- d_6 , 100 MHz); δ 20.24 (CH_3), 27.59 (CH_2), 54.86 (CH_2CO), 107.54, 110.64 (furan C_3 , C_4), 120.57, 126.95, 128.71, 131.02, 137.66, 138.80, 142.25, 143.95 (aromatic carbons), 150.71 (furan C_2), 159.08 (pyridazinone CO), 165.37 (CONH) ppm. ESI-MS (m/z): 358.24 $[\text{M}+\text{H}]^+$, 380.21 $[\text{M}+\text{Na}]^+$ (% 100), 382.20 $[\text{M}+\text{Na}+2]^+$. Anal. calcd. for $\text{C}_{18}\text{H}_{16}\text{ClN}_3\text{O}_3$: C, 60.42; H, 4.51; N, 11.74. Found: C, 60.12; H, 4.43; N, 11.66.

2-[5-(Furan-2-ylmethyl)-3-methyl-6-oxopyridazin-1(6H)-yl]-N-(4-fluorophenyl)acetamide (5f)

Yield 55 %; m.p. 132 °C. IR; 3294 (N–H), 3095 (C–H), 1703, 1645 (C=O), 1598, 1557, 1537, 1409 (C=N ve C=C). ¹H-NMR (DMSO-d₆, 400 MHz); δ 2.24 (3H; s; –CH₃), 3.85 (2H; s; –CH₂–), 4.85 (2H; s; CH₂CONH), 6.22 (1H; d; furan H₃, *J* = 2.8 Hz), 6.40–6.41 (1H; dd; furan H₄, *J*₁ = 2.6 Hz, *J*₂ = 1.6 Hz), 7.06 (1H; s; pyridazinone H₅), 7.13–7.18 (2H; t; Ar–H_{3,5}), 7.57–7.60 (3H; m; Ar–H_{2,6} and furan H₅), 10.34 (1H; s; NH) ppm. ¹³C-NMR (DMSO-d₆, 100 MHz); δ 20.26 (CH₃), 27.59 (CH₂), 54.75 (CH₂CO), 107.54, 110.64 (furan C₃, C₄), 115.36, 120.76, 130.99, 135.11, 138.80, 142.24, 143.92, 156.83 (aromatic carbons), 150.72 (furan C₂), 159.14 (pyridazinone CO), 165.12 (CONH) ppm. ESI-MS (*m/z*): 342.29 [M+H]⁺, 364.26 [M+Na]⁺ (% 100). Anal. calcd. for C₁₈H₁₆FN₃O₃: C, 63.34; H, 4.72; N, 12.31. Found: C, 63.23; H, 4.79; N, 12.15.

2-[5-(Furan-2-ylmethyl)-3-methyl-6-oxopyridazin-1(6H)-yl]-N-(3-chloro-4-fluorophenyl)acetamide (5g)

Yield 39 %; m.p. 140–141 °C. IR; 3280 (N–H), 3076 (C–H), 1711, 1644 (C=O), 1593, 1555, 1538, 1400 (C=N ve C=C). ¹H-NMR (CDCl₃, 400 MHz); δ 2.32 (3H; s; –CH₃), 3.95 (2H; s; –CH₂–), 4.95 (2H; s; CH₂CONH), 6.19 (1H; dd; furan H₃, *J*₁ = 3 Hz, *J*₂ = 0.6 Hz), 6.35 (1H; dd; furan H₄, *J*₁ = 3 Hz, *J*₂ = 1.8 Hz), 6.92 (2H; ; pyridazinone H₅ and Ar–H₆), 7.13–7.15 (1H; m; Ar–H₅), 7.37 (1H; dd; furan H₅, *J*₁ = 2 Hz, *J*₂ = 0.8 Hz), 7.63 (1H; dd; Ar–H₂, *J*₁ = 6.8 Hz *J*₂ = 2.4 Hz), 9.41 (1H; s; NH) ppm. ¹³C-NMR (CDCl₃, 100 MHz); δ 20.92 (CH₃), 28.42 (CH₂), 57.84 (CH₂CO), 108.09, 110.64 (furan C₃, C₄), 116.20, 119.16, 120.74, 121.64, 131.60, 134.46, 139.89, 142.27, 146.00, 153.27, 155.71 (aromatic carbons), 150.02 (furan C₂), 160.64 (pyridazinone CO), 165.24 (CONH) ppm. ESI-MS (*m/z*): 398.18 [M+Na]⁺ (% 100), 400.17 [M+Na+2]⁺. Anal. calcd. for C₁₈H₁₅ClFN₃O₃: C, 57.53; H, 4.02; N, 11.18. Found: C, 57.41; H, 3.91; N, 11.06.

2-[5-(Furan-2-ylmethyl)-3-methyl-6-oxopyridazin-1(6H)-yl]-N-(naphthalen-1-yl)acetamide (5h)

Yield 41 %; m.p. 165 °C. IR; 3303 (N–H), 2956 (C–H), 1671, 1651 (C=O), 1603, 1544, 1504, 1467, 1434 (C=N ve C=C). ¹H-NMR (CDCl₃, 400 MHz); δ 2.33 (3H; s; –CH₃), 4.01 (2H; s; –CH₂–), 5.10 (2H; s; CH₂CONH), 6.22 (1H; d; furan H₃, *J* = 3.2 Hz), 6.34 (1H; dd; furan H₄, *J*₁ = 3.4 Hz, *J*₂ = 2 Hz), 6.87 (1H; s; pyridazinone H₅), 7.36–7.37 (1H; dd; furan H₅, *J*₁ = 1.8 Hz, *J*₂ = 1.2 Hz), 7.43–7.56 (3H; m; Ar–H), 7.65 (1H; d; Ar–H *J* = 8.4 Hz), 7.84 (1H; d; Ar–H *J* = 7.6 Hz), 7.98 (1H; d; Ar–H *J* = 8.4 Hz), 8.14 (1H; d; Ar–H *J* = 7.2 Hz), 9.39 (1H; s; NH) ppm. ¹³C-NMR (CDCl₃, 100 MHz); δ 20.96 (CH₃), 28.29 (CH₂), 58.34 (CH₂CO), 108.22, 110.65 (furan C₃, C₄), 119.21, 120.73, 125.26, 125.74, 125.91, 126.12, 126.37, 128.64, 131.28, 132.47, 133.96, 140.36, 142.31, 146.10 (aromatic carbons), 150.05 (furan C₂), 160.80 (pyridazinone CO), 165.79 (CONH) ppm. ESI-MS (*m/z*): 374.29 [M+H]⁺, 396.25 [M+Na]⁺ (% 100). Anal. calcd. for C₂₂H₁₉N₃O₃: C, 70.76; H, 5.13; N, 11.25. Found: C, 70.47; H, 5.14; N, 11.23.

2-[5-(Furan-2-ylmethyl)-3-methyl-6-oxopyridazin-1(6H)-yl]-N-((1,1'-biphenyl)-2-yl)acetamide (5i)

Yield 45 %; m.p. 158–159 °C. IR; 3288 (N–H), 3045 (C–H), 1697, 1642 (C=O), 1522, 1475, 1449, 1437, 1418 (C=N ve C=C). ¹H-NMR (CDCl₃, 400 MHz); δ 2.14 (3H; s; –CH₃), 3.82 (2H; s; –CH₂–), 4.79 (2H; s; CH₂CONH), 6.22 (1H; d; furan H₃, *J* = 3.2 Hz), 6.39 (1H; dd; furan H₄, *J*₁ = 3 Hz, *J*₂ = 1.8 Hz), 6.66 (1H; s; pyridazinone H₅), 7.14–7.19 (2H; m; Ar–H), 7.23–7.26 (2H; m; Ar–H), 7.34–7.38 (4H; m; Ar–H), 7.43 (1H; m; furan H₅), 7.75

(1H; s; NH), 8.36 (1H; d; Ar-H $J = 8.4$ Hz) ppm. $^{13}\text{C-NMR}$ (CDCl_3 , 100 MHz); δ 20.92 (CH_3), 28.15 (CH_2), 56.20 (CH_2CO), 108.32, 110.70 (furan C_3 , C_4), 121.30, 124.51, 127.75, 128.44, 128.84, 129.17, 130.03, 130.50, 132.38, 134.28, 137.97, 140.35, 142.29, 145.50 (aromatic carbons), 150.12 (furan C_2), 159.74 (pyridazinone CO), 165.03 (CONH) ppm. ESI-MS (m/z): 400.27 $[\text{M}+\text{H}]^+$, 422.25 $[\text{M}+\text{Na}]^+$ (% 100). Anal. calcd. for $\text{C}_{24}\text{H}_{21}\text{N}_3\text{O}_3$: C, 72.16; H, 5.30; N, 10.52. Found: C, 72.08; H, 5.39; N, 10.30.

2-[5-(Furan-2-ylmethyl)-3-methyl-6-oxopyridazin-1(6H)-yl]-N-(pyridin-2-yl)acetamide (5j)

Yield 44 %; m.p. 178 °C. IR: 3264 (N-H), 3087, 2983, 2949 (C-H), 1671, 1658 (C=O), 1613, 1600, 1553, 1501, 1445 (C=N ve C=C). $^1\text{H-NMR}$ (CDCl_3 , 400 MHz); δ 2.28 (3H; s; $-\text{CH}_3$), 3.97 (2H; s; $-\text{CH}_2-$), 4.99 (2H; s; CH_2CONH), 6.21 (1H; dd; furan H_3 , $J_1 = 3.2$ Hz, $J_2 = 0.8$ Hz), 6.36 (1H; dd; furan H_4 , $J_1 = 3$ Hz, $J_2 = 2$ Hz), 6.79 (1H; s; pyridazinone H_5), 7.03 (1H; ddd; Ar-H $J_1 = 7.4$ Hz, $J_2 = 5$ Hz, $J_3 = 0.8$ Hz), 7.39 (1H; m; furan H_5), 7.68 (1H; ddd; Ar-H $J_1 = 8.6$ Hz, $J_2 = 7.2$ Hz, $J_3 = 1.4$ Hz), 8.19 (1H; d; Ar-H $J = 8.4$ Hz), 8.28 (1H; ddd; Ar-H; $J_1 = 5.1$ Hz, $J_2 = 2$ Hz, $J_3 = 0.8$ Hz), 9.18 (1H; s; NH) ppm. $^{13}\text{C-NMR}$ (CDCl_3 , 100 MHz); δ 21.00 (CH_3), 28.23 (CH_2), 56.51 (CH_2CO), 108.25, 110.61 (furan C_3 , C_4), 114.37, 120.03, 130.80, 138.42, 140.56, 142.24, 145.55, 147.77, 150.25, 151.09 (aromatic carbons), 160.32 (pyridazinone CO), 165.57 (CONH) ppm. ESI-MS (m/z): 325.31 $[\text{M}+\text{H}]^+$, 347.27 $[\text{M}+\text{Na}]^+$ (% 100). Anal. calcd. for $\text{C}_{17}\text{H}_{16}\text{N}_4\text{O}_3$: C, 62.95; H, 4.97; N, 17.27. Found: C, 62.66; H, 4.92; N, 16.97.

4-(Furan-2-ylmethyl)-6-methyl-2-[2-oxo-2-(4-phenylpiperazin-1-yl)ethyl]pyridazin-3(2H)-one (6a)

Yield 40 %; m.p. 124 °C. IR: 3116, 2982, 2828 (C-H), 1647 (C=O), 1605, 1535, 1493, 1443 (C=N ve C=C). $^1\text{H-NMR}$ (DMSO-d_6 , 500 MHz); δ 2.22 (3H; s; $-\text{CH}_3$), 3.12–3.14 (4H; m; piperazine), 3.59–3.66 (4H; m; piperazine), 3.84 (2H; s; $-\text{CH}_2-$), 4.99 (2H; s; CH_2CO), 6.22 (1H; d; furan H_3 , $J = 3.05$), 6.41 (1H; m; furan H_4), 6.83 (1H; m; Ar-H), 6.98 (2H; d; Ar-H $J = 8.25$), 7.05 (1H; s; pyridazinone H_5), 7.25 (2H; m; Ar-H), 7.58 (1H; s; furan H_5) ppm. $^{13}\text{C-NMR}$ (DMSO-d_6 , 125 MHz); δ 20.73 (CH_3), 28.14 (CH_2), 44.43, 48.88 (piperazine carbons), 53.25 (CH_2CO), 108.00, 111.13 (furan C_3 , C_4), 116.42, 119.88, 129.48, 131.35, 139.19, 142.72, 144.17 (aromatic carbons), 151.26 (furan C_2), 159.57 (pyridazinone CO), 165.20 (CH_2CON) ppm. ESI-MS (m/z): 393.31 $[\text{M}+\text{H}]^+$, 415.30 $[\text{M}+\text{Na}]^+$ (% 100). Anal. calcd. for $\text{C}_{22}\text{H}_{24}\text{N}_4\text{O}_3$: C, 67.33; H, 6.16; N, 14.28. Found: C, 67.24; H, 6.10; N, 14.21.

4-(Furan-2-ylmethyl)-6-methyl-2-[2-oxo-2-(4-(4-methylphenyl)piperazin-1-yl)ethyl]pyridazin-3(2H)-one (6b)

Yield 47 %; m.p. 140 °C. IR: 3127, 3105, 2982, 2810 (C-H), 1679, 1649 (C=O), 1605, 1537, 1512, 1445 (C=N ve C=C). $^1\text{H-NMR}$ (CDCl_3 , 400 MHz); δ 2.27 (6H; d; $-\text{CH}_3$), 3.11–3.19 (4H; m; piperazine), 3.64–3.67 (2H; m; piperazine), 3.78–3.80 (2H; m; piperazine), 3.93 (2H; s; $-\text{CH}_2-$), 4.99 (2H; s; CH_2CO), 6.19 (1H; d; furan H_3 , $J = 3.2$), 6.35 (1H; dd; furan H_4 , $J_1 = 2.8$ Hz, $J_2 = 1.6$ Hz), 6.78 (1H; s; pyridazinone H_5), 6.83–6.86 (2H; m; Ar- $\text{H}_{2,6}$), 7.10 (2H; d; Ar- $\text{H}_{3,5}$, $J = 8$ Hz), 7.38 (1H; m; furan H_5) ppm. $^{13}\text{C-NMR}$ (CDCl_3 , 100 MHz); δ 20.46 (CH_3), 21.00 (CH_3), 28.25 (CH_2), 42.10, 44.88, 50.00 (piperazine carbons), 52.96 (CH_2CO), 108.06, 110.58 (furan C_3 , C_4), 117.16, 130.23, 140.08, 142.11, 144.67, 148.77 (aromatic carbons), 150.57 (furan C_2), 160.04 (pyridazinone CO), 164.71 (CH_2CON) ppm. ESI-MS (m/z): 429.28 $[\text{M}+\text{Na}]^+$ (% 100). Anal. calcd. for $\text{C}_{23}\text{H}_{26}\text{N}_4\text{O}_3$: C, 67.96; H, 6.45; N, 13.78. Found: C, 67.83; H, 6.51; N, 13.68.

4-(Furan-2-ylmethyl)-6-methyl-2-[2-oxo-2-(4-(4-methoxyphenyl)piperazin-1-yl)ethyl]pyridazin-3(2H)-one (6c)

Yield 47 %; m.p. 121–122 °C. IR; 3047, 2996, 2838 (C–H), 1671, 1641 (C=O), 1599, 1510, 1463, 1447 (C=N ve C=C). ¹H-NMR (CDCl₃, 400 MHz); δ 2.26 (–CH₃), 3.04–3.12 (4H; m; piperazine), 3.64–3.66 (2H; m; piperazine), 3.77–3.80 (5H; m; piperazine and –OCH₃), 3.93 (2H; s; –CH₂–), 4.99 (2H; s; CH₂CO), 6.19 (1H; d; furan H₃, *J* = 2.8 Hz), 6.35 (1H; dd; furan H₄, *J*₁ = 3 Hz, *J*₂ = 1.8 Hz), 6.78 (1H; s; pyridazinone H₅), 6.84–6.92 (4H; m; Ar–H), 7.37 (1H; m; furan H₅) ppm. ¹³C-NMR (CDCl₃, 100 MHz); δ 20.98 (CH₃), 28.24 (CH₂), 42.22, 44.99, 50.93 (piperazine carbons), 52.96 (CH₂CO), 55.54 (OCH₃), 108.04, 110.57 (furan C₃, C₄), 114.54, 119.08, 130.58, 140.08, 142.10, 144.67, 145.18, 154.50 (aromatic carbons), 150.57 (furan C₂), 160.05 (pyridazinone CO), 164.71 (CH₂CON) ppm. ESI-MS (*m/z*): 423.42 [M+H]⁺, 445.39 [M+Na]⁺ (% 100). Anal. calcd. for C₂₃H₂₆N₄O₄: C, 65.39; H, 6.20; N, 13.26 Found: C, 65.17; H, 6.20; N, 13.16.

4-(Furan-2-ylmethyl)-6-methyl-2-[2-oxo-2-(4-(4-nitrophenyl)piperazin-1-yl)ethyl]pyridazin-3(2H)-one (6d)

Yield 51 %; m.p. 153–154 °C. IR; 2879 (C–H), 1673, 1650 (C=O), 1595, 1505, 1483, 1434 (C=N ve C=C). ¹H-NMR (DMSO-d₆, 500 MHz); δ 2.22 (3H; s; –CH₃), 3.52–3.54 (2H; m; piperazine), 3.62 (4H; m; piperazine), 3.72 (2H; m; piperazine), 3.84 (2H; s; –CH₂–), 5.00 (2H; s; CH₂CO), 6.22 (1H; dd; furan H₃, *J*₁ = 3.2 Hz, *J*₂ = 0.7 Hz), 6.41 (1H; dd; furan H₄, *J*₁ = 3.1 Hz, *J*₂ = 1.9 Hz), 7.03–7.05 (3H; m; pyridazinone H₅ ve Ar–H_{2,6}), 7.58 (1H; dd; furan H₅, *J*₁ = 1.8 Hz, *J*₂ = 0.8 Hz), 8.09 (2H; m; Ar–H_{3,5}) ppm. ¹³C-NMR (DMSO-d₆, 125 MHz); δ 20.72 (CH₃), 28.14 (CH₂), 43.71, 46.21, 46.42 (piperazine carbons), 53.25 (CH₂CO), 107.99, 111.13 (furan C₃, C₄), 113.06, 126.21, 131.37, 137.50, 139.20, 142.71, 144.20, 154.80 (aromatic carbons), 151.28 (furan C₂), 159.57 (pyridazinone CO), 165.52 (CH₂CON) ppm. ESI-MS (*m/z*): 460.38 [M+Na]⁺ (% 100). Anal. calcd. for C₂₂H₂₃N₅O₅: C, 60.40; H, 5.30; N, 16.01 Found: C, 60.35; H, 5.38; N, 15.79.

4-(Furan-2-ylmethyl)-6-methyl-2-[2-oxo-2-(4-(4-chlorophenyl)piperazin-1-yl)ethyl]pyridazin-3(2H)-one (6e)

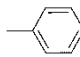
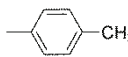
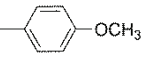
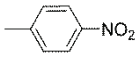
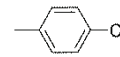
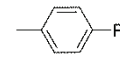
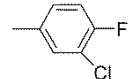
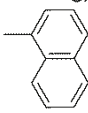
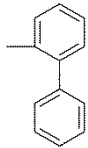
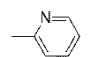
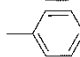
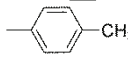
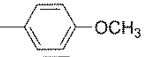
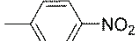
Yield 51 %; m.p. 146–147 °C. IR; 3047, 2935 (C–H), 1677, 1649 (C=O), 1537, 1497, 1467, 1451, 1432 (C=N ve C=C). ¹H-NMR (CDCl₃, 400 MHz); δ 2.25 (3H; s; –CH₃), 3.13–3.21 (4H; m; piperazine), 3.65–3.67 (2H; m; piperazine), 3.77–3.80 (2H; m; piperazine), 3.92 (2H; s; –CH₂–), 4.98 (2H; s; CH₂CO), 6.19 (1H; d; furan H₃, *J* = 2.8 Hz), 6.35 (1H; dd; furan H₄, *J*₁ = 3.2 Hz, *J*₂ = 2 Hz), 6.78 (1H; s; pyridazinone H₅), 6.82–6.84 (2H; m; Ar–H_{2,6}), 7.21–7.26 (2H; m; Ar–H_{3,5}), 7.37 (1H; d; furan H₅, *J* = 1.6 Hz) ppm. ¹³C-NMR (CDCl₃, 100 MHz); δ 20.98 (CH₃), 28.23 (CH₂), 41.90, 44.71, 49.40 (piperazine carbons), 52.92 (CH₂CO), 108.06, 110.57 (furan C₃, C₄), 117.96, 125.59, 129.13, 130.61, 140.07, 142.11, 144.71, 149.46 (aromatic carbons), 150.53 (furan C₂), 160.03 (pyridazinone CO), 164.79 (CH₂CON) ppm. ESI-MS (*m/z*): 427.38 [M+H]⁺, 449.35 [M+Na]⁺ (% 100), 451.34 [M+Na+2]⁺. Anal. calcd. for C₂₂H₂₃ClN₄O₃: C, 61.90; H, 5.43; N, 13.12 Found: C, 61.79; H, 5.57; N, 12.91.



4-(Furan-2-ylmethyl)-6-methyl-2-[2-oxo-2-(4-(4-fluorophenyl)piperazin-1-yl)ethyl]pyridazin-3(2H)-one (6f)

Yield 50 %; m.p. 105 °C. IR; 2921, 2855 (C–H), 1667, 1644 (C=O), 1606, 1507, 1446 (C=N ve C=C). ¹H-NMR (CDCl₃, 400 MHz); δ 2.26 (3H; s; –CH₃), 3.08–3.16 (4H; m; piperazine), 3.65–3.67 (2H; m; piperazine), 3.78–3.80 (2H; m; piperazine), 3.93 (2H; s; –CH₂–), 4.99 (2H; s; CH₂CO), 6.19 (1H; d; furan H₃, *J* = 3.2), 6.35 (1H; dd; furan H₄, *J*₁ = 3

Hz, $J_2 = 1.8$ Hz), 6.78 (1H; s; pyridazinone H₅), 6.87–6.90 (2H; m; Ar–H_{2',6'}), 6.96–7.00 (2H; m; Ar–H_{3',5'}), 7.37 (1H; dd; furan H₅, $J_1 = 2$ Hz, $J_2 = 0.8$ Hz) ppm. ¹³C-NMR (CDCl₃, 100 MHz); δ 20.99 (CH₃), 28.23 (CH₂), 42.10, 44.88, 50.46 (piperazine carbons), 52.95 (CH₂CO), 108.06, 110.58 (furan C₃, C₄), 115.73, 118.76, 130.62, 140.08, 142.12, 144.73, 147.53, 156.52, 158.90 (aromatic carbons), 150.53 (furan C₂), 160.06 (pyridazinon CO), 164.76 (CH₂CON) ppm. ESI-MS (m/z): 411,46 [M+H]⁺, 433,43 [M+Na]⁺ (% 100). Anal. calcd. for C₂₂H₂₃FN₄O₃: C, 64.38; H, 5.65; N, 13.65 Found: C, 64.11; H, 5.77; N, 13.47.

TABLE S-I. Yields, melting points and literature melting points of 2-Chloro-*N*-arylacetamides (**3a-j**) and 2-chloro-1-(4-arylpiperazin-1-yl)ethanones (**4a-f**)

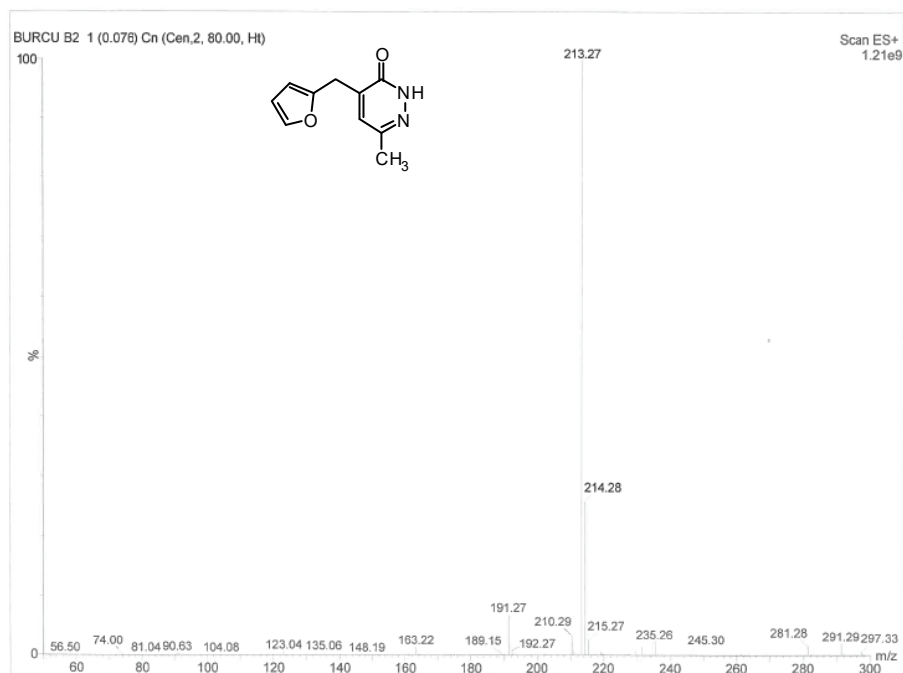
Compound	Ar	Yield (%)	M.p. [Lit M.p.] (° C)
3a		94.9	133 [132] ¹
3b		96.8	119 [130] ²
3c		96.0	119 [119-120] ³
3d		92.0	118 [118] ²
3e		93.2	148 [150] ²
3f		94.2	131 [130-131] ⁴
3g		92.4	75 [75-77] ⁵
3h		90.1	150 [154] ⁶
3i		86.2	152 [152-153] ⁶
3j		83.4	175 [178-180] ⁷
4a		67.6	75 [77] ⁸
4b		83.2	75 [60-1] ⁹
4c		81.4	106 [109-111] ¹⁰
4d		78.28	104 [100-101] ¹¹

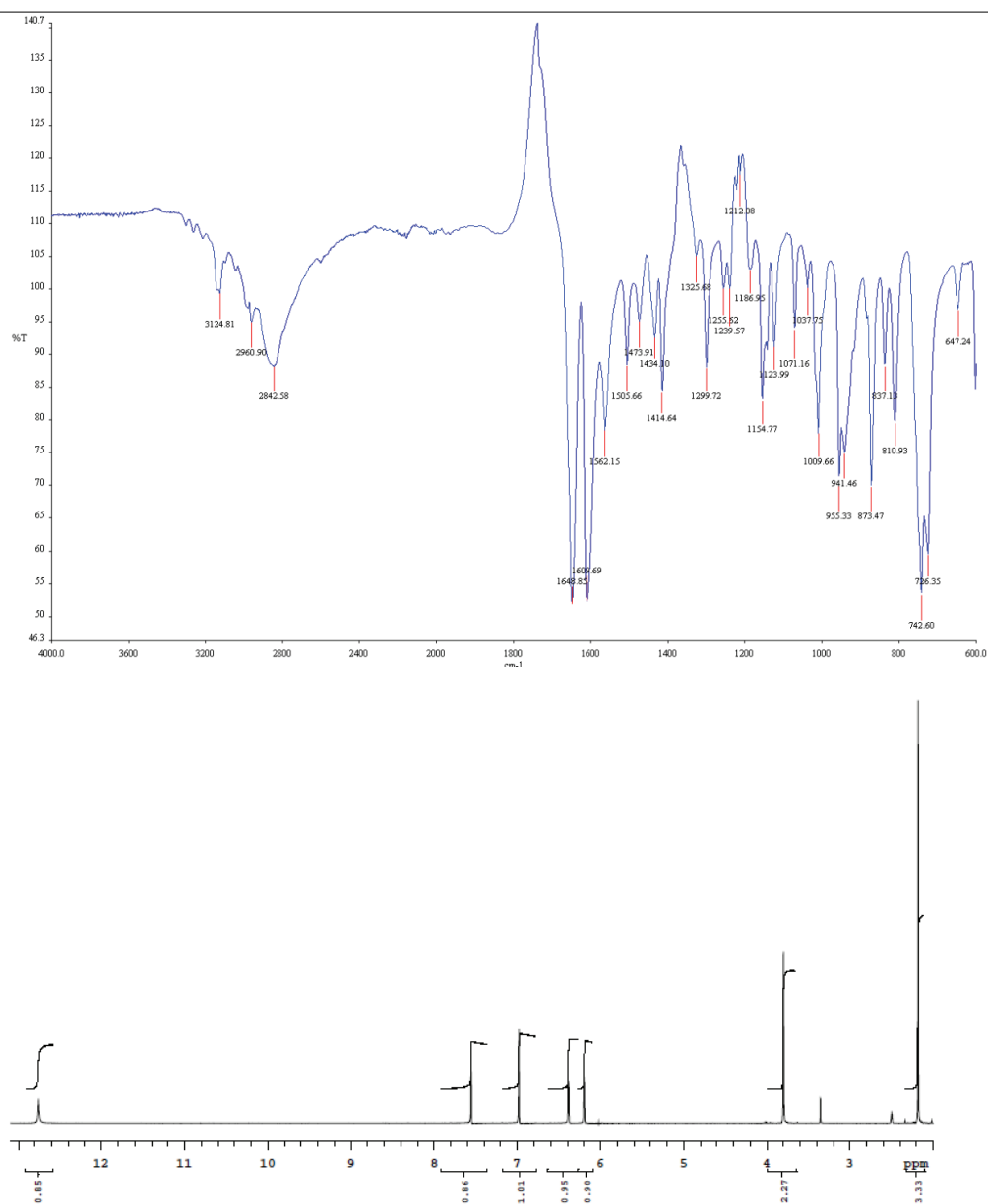
4e		77.17	81 [84-85] ¹²
4f		85.13	104 [95] ¹³

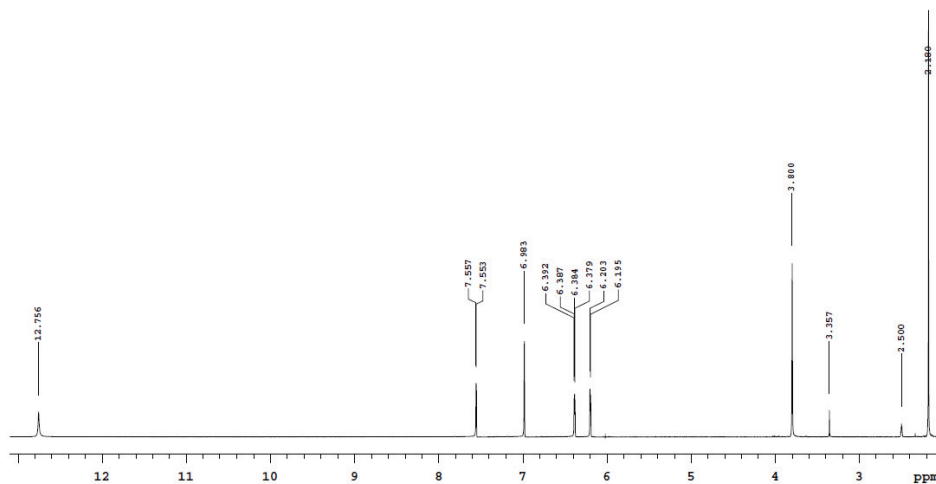
REFERENCES

- N. P. Sahu, C. Pal, N. B. Mandal, S. Banerjee, M. Raha, A. P. Kundu, A. Basu, M. Ghosh, K. Roy, S. Bandyopadhyay, *Bioorganic Med. Chem.* **10** (2002) 1687–1693 ([https://doi.org/10.1016/S0968-0896\(02\)00046-9](https://doi.org/10.1016/S0968-0896(02)00046-9))
- A. D. Desai, K. H. Chikhalia, *E-Journal Chem.* **2** (2005) 15–20 (<https://doi.org/10.1155/2005/575290>)
- I. N. Peixoto, H. D. S. Souza, B. F. Lira, D. F. Silva, E. O. Lima, J. M. Barbosa-Filho, P. F. de Athayde-Filho, *J. Braz. Chem. Soc.* **27** (2016) S1–S19 (<https://doi.org/10.5935/0103-5053.20160063>)
- P. G. Baraldi, D. Preti, M. A. Tabrizi, F. Fruttarolo, G. Saponaro, S. Baraldi, R. Romagnoli, A. R. Moorman, S. Gessi, K. Varani, P. A. Borea, *Bioorganic Med. Chem.* **15** (2007) 2514–2527 (<https://doi.org/10.1016/j.bmc.2007.01.055>)
- D. C. P. Singh, S. R. Hashim, R. G. Singhal, *E-Journal Chem.* **8** (2011) 635–642 (<https://doi.org/10.1155/2011/482831>)
- V. Pace, L. Castoldi, W. Holzer, *Chem. Commun.* **49** (2013) 8383–8385 (<https://doi.org/10.1039/c3cc44255a>)
- V. Patil, K. Tilekar, S. Mehendale-Munj, R. Mohan, C. S. Ramaa, *Eur. J. Med. Chem.* **45** (2010) 4539–4544 (<http://dx.doi.org/10.1016/j.ejmech.2010.07.014>)
- R. K. Sharma, Y. Younis, G. Mugumbate, M. Njoroge, J. Gut, P. J. Rosenthal, K. Chibale, *Eur. J. Med. Chem.* **90** (2015) 507–518 (<https://doi.org/10.1016/j.ejmech.2014.11.061>)
- N. Sati, S. Kumar, S. Sati, *Int. J. Drug Design & Discovery* **2(1)** (2011) 419–424
- D. Szkatuła, E. Krzyżak, P. Stanowska, M. Duda, B. Wiatrak, *Int. J. Mol. Sci.* **22(2021)** 7678 (<https://doi.org/10.3390/ijms22147678>)
- S. Gupta, D. Pandey, D. Mandalapu, V. Bala, V. Sharma, M. Shukla, et al., *MedChemComm* **7(11)** (2016) 2111–2121 (<http://dx.doi.org/10.1039/C6MD00426A>)
- K. Kamiński, B. Wiklik, J. Obniska, *Med. Chem. Res.* **24** (2015) 3047–3061 (<https://doi.org/10.1007/s00044-015-1360-6>)
- B. Begam, K. Singh, A. Rahman, *Indian J. Heterocyclic Chem.*, **26** (2016) 147.

4-(2-FURYLMETHYL)-6-METHYLPYRIDAZIN-3(2H)-ONE (2)

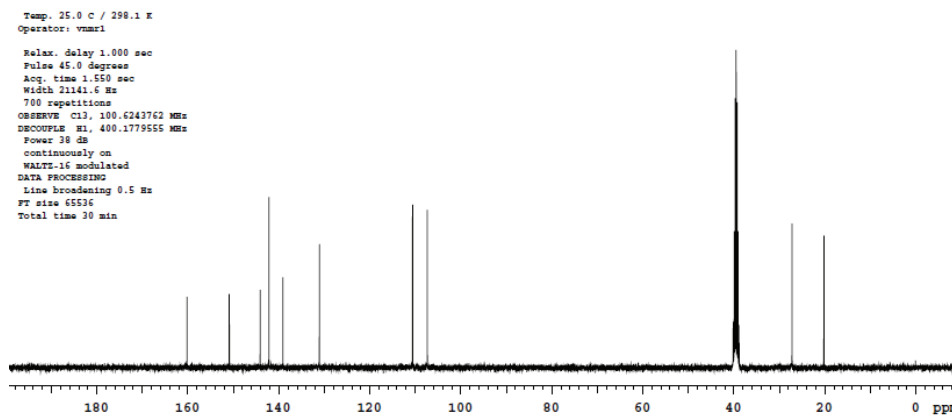


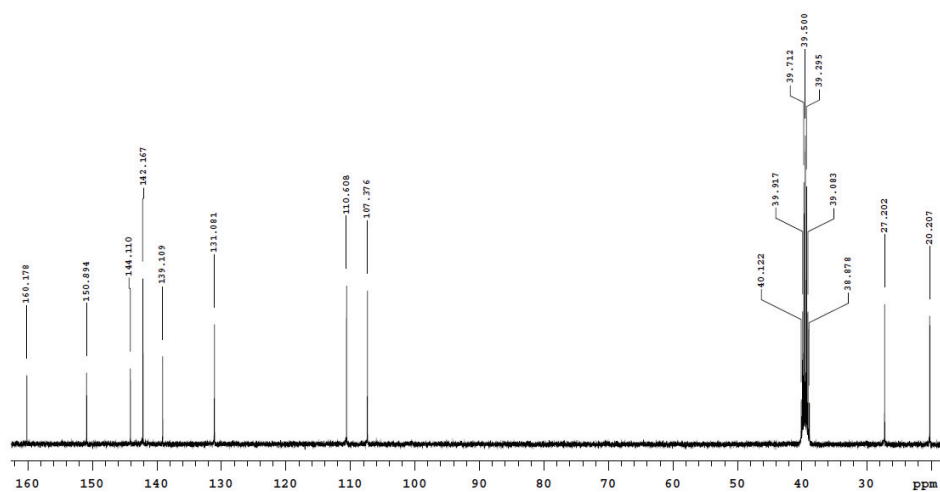


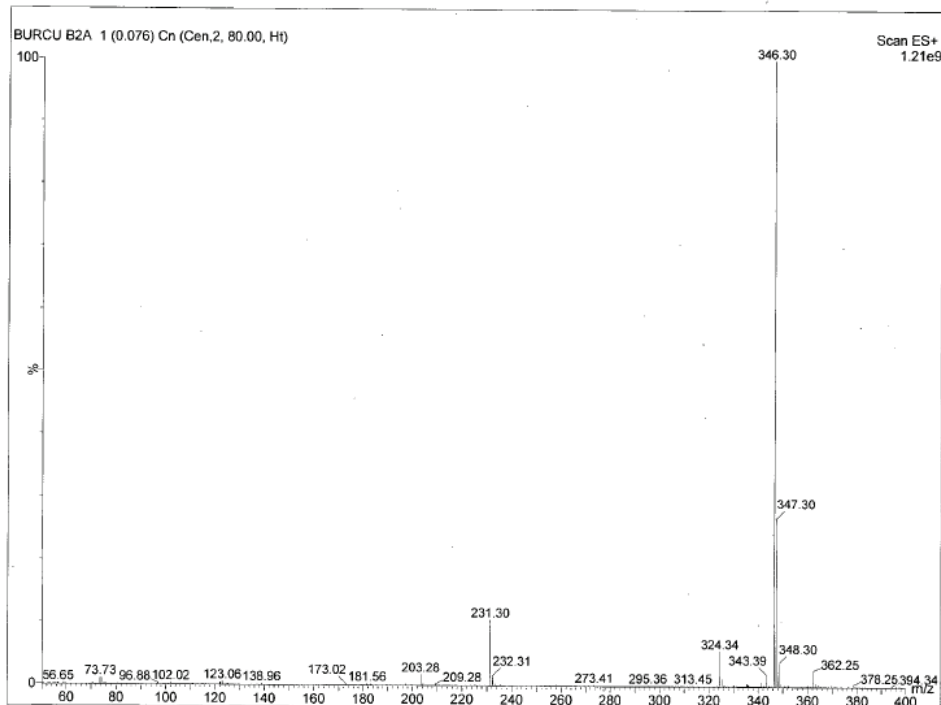
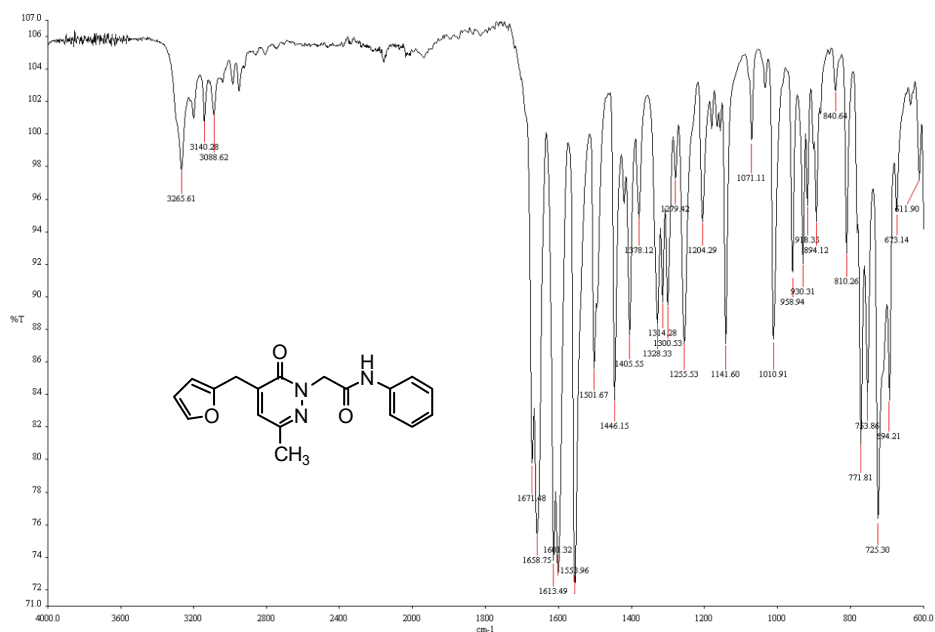


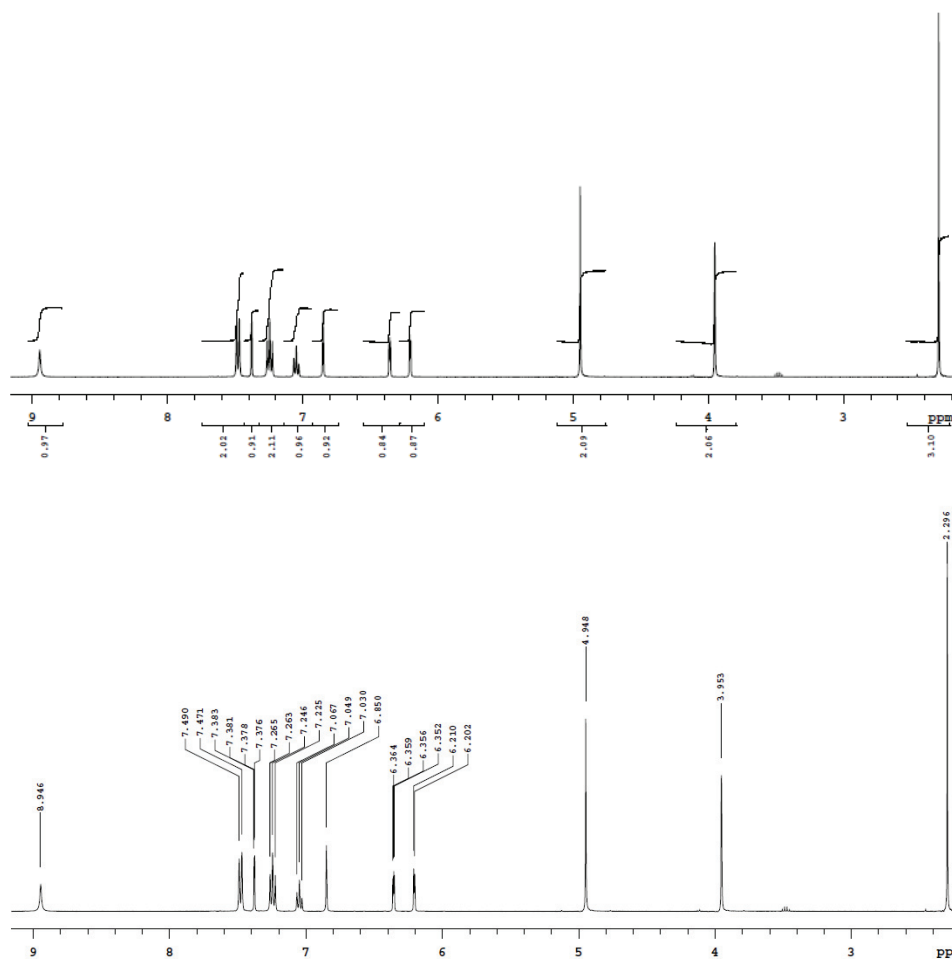
S2

Sample Name:
S2
Data Collected on:
mercury400-mercury400
Archive directory:
/home/vmmr1/vmmr1s/data
Sample directory:
S2_20210220_01
Fidfile: CARBON_01
Pulse Sequence: CARBON (zgpg2)
Solvent: dmsc
Data collected on: Feb 20 2021





2-[5-(FURAN-2-YLMETHYL)-3-METHYL-6-OXOPYRIDAZIN-1(6H)-YL]-N-PHENYLACETAMIDE (**5a**)





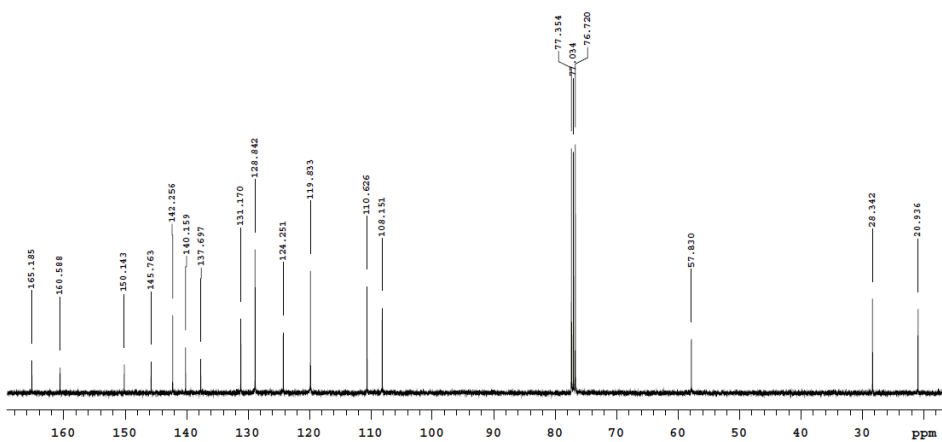
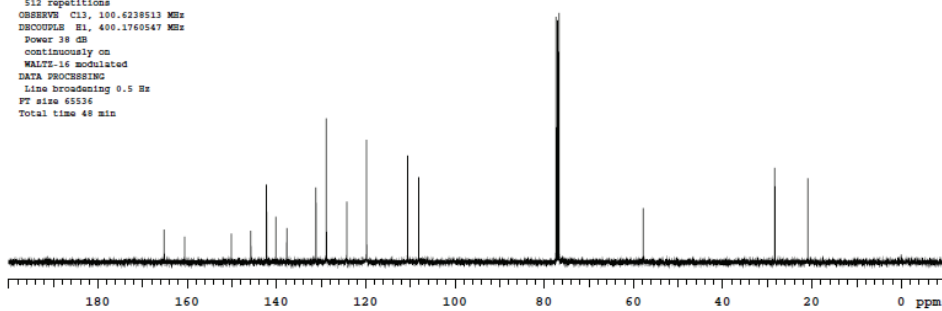
B2A

Sample Name:
B2A
Data Collected on:
mercury400-mercury400
Archive directory:
/home/vmari/vmariya/data
Sample directory:
B2A 20201130 01
FidFile: current

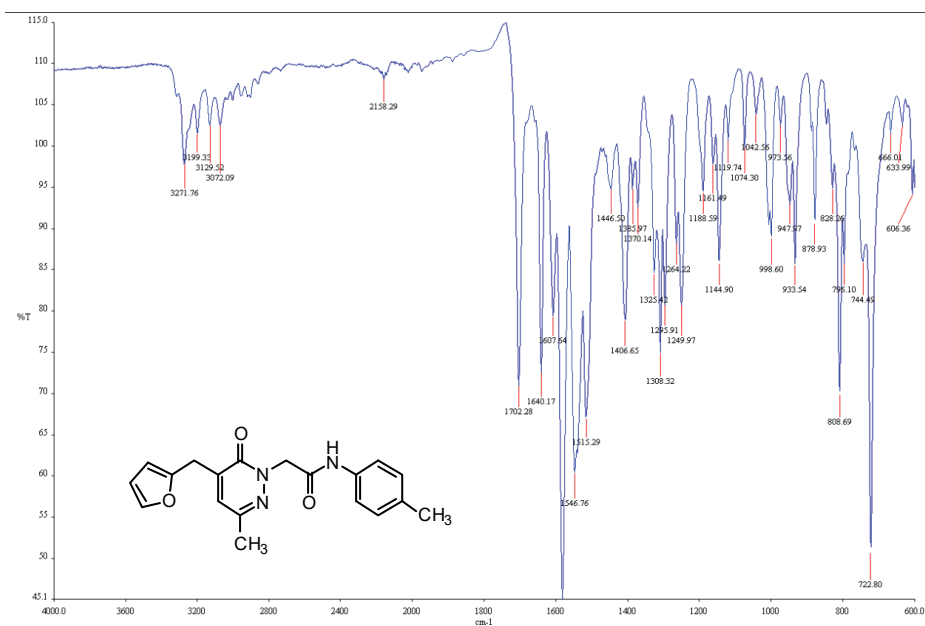
Pulse Sequence: CARBON (s2pul)
Solvent: cdcl3
Data collected on: Nov 30 2020

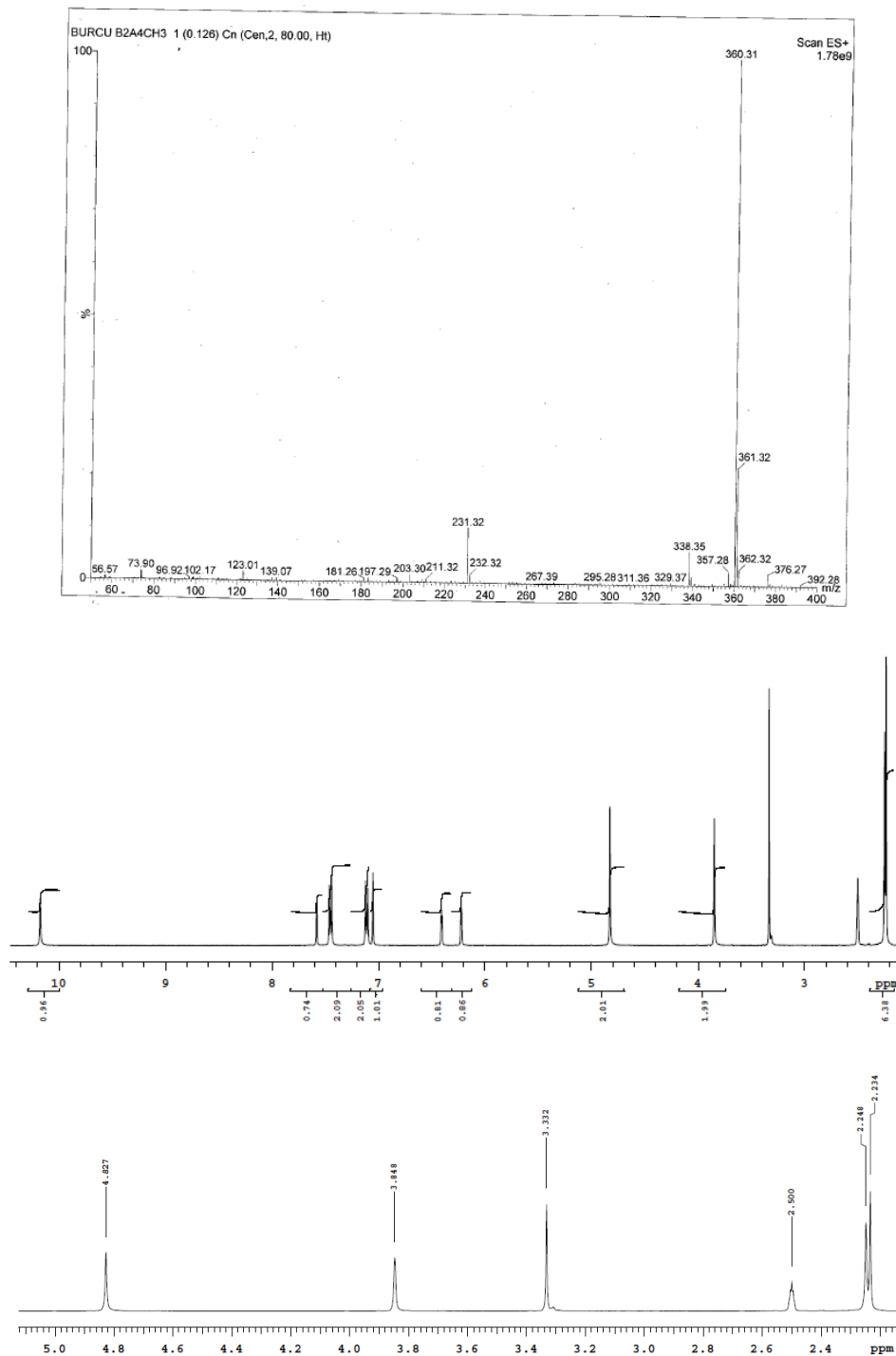
Temp. 35.0 C / 298.1 K
Operator: vmari

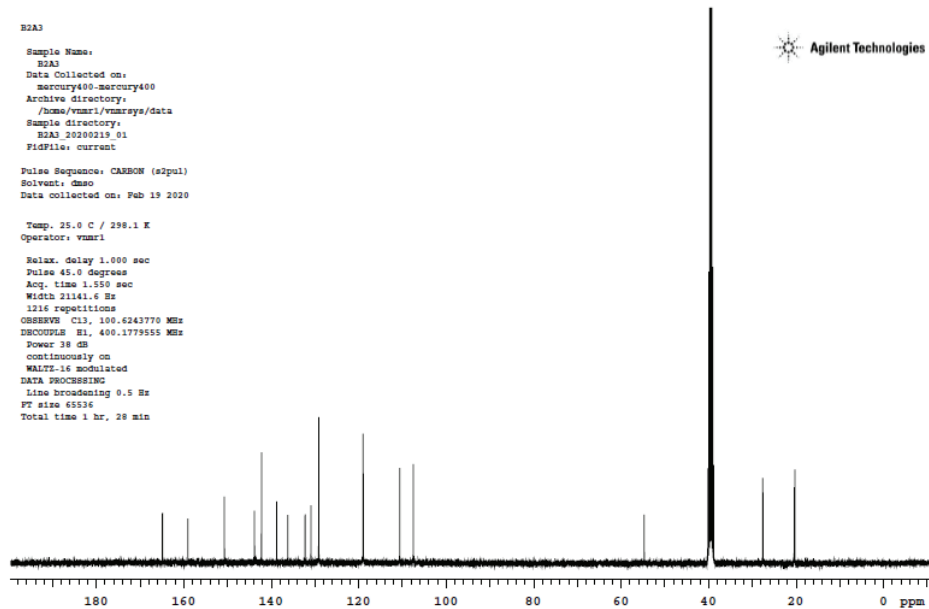
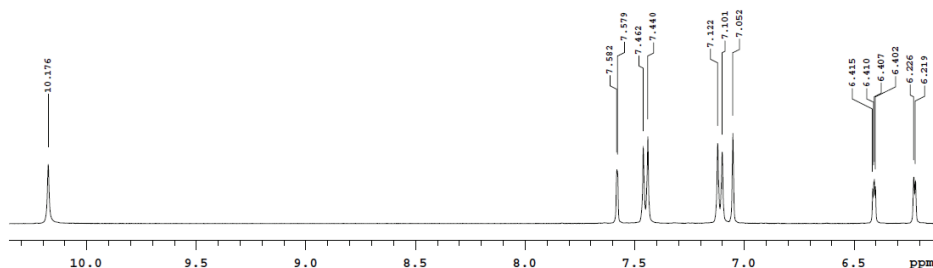
Relax. delay 1.000 sec
Pulse 45.0 degrees
Acq. time 1.550 sec
Width 21141.6 Hz
512 repetitions
OBSERVE Ch1, 100.6238513 MHz
DECOUPLE H1, 400.1760447 MHz
Power 38 dB
continuously on
WALTZ-16 modulated
DATA PROCESSING
Line broadening 0.5 Hz
FT size 65536
Total time 48 min



2-[5-(FURAN-2-YLMETHYL)-3-METHYL-6-OXOPYRIDAZIN-1(6H)-YL]-N-(4-METHYLPHENYL)ACETAMIDE (5B)





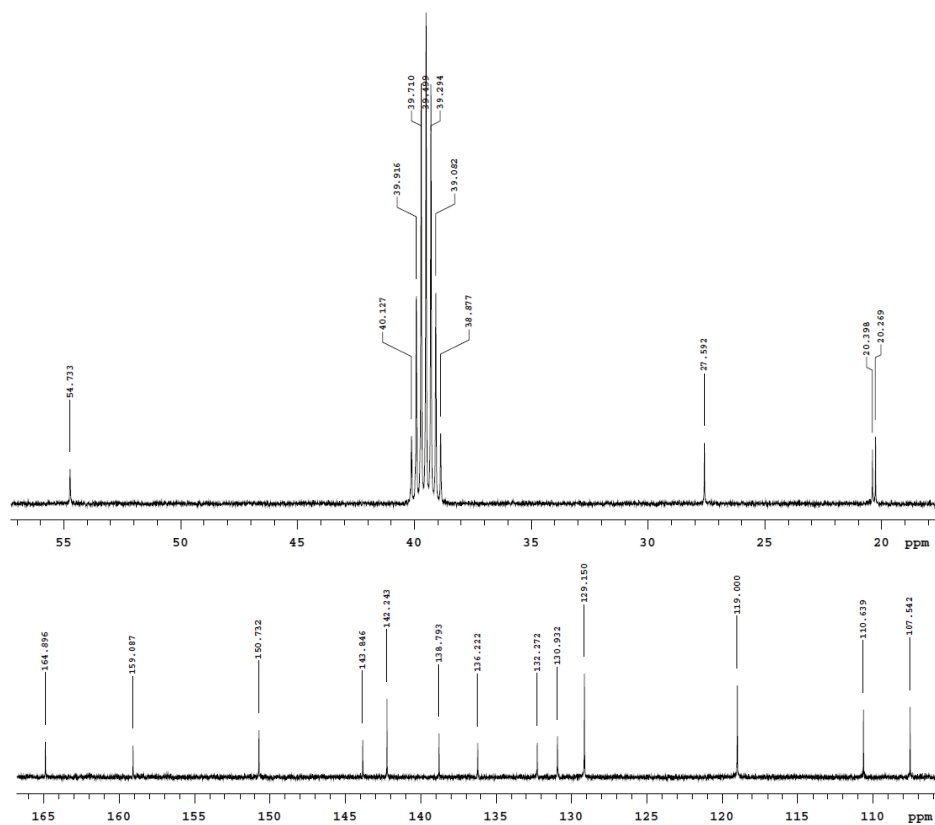


B2A3
 Sample Name:
 B2A3
 Data collected on:
 mercury400-mercury400
 Archive directory:
 /home/vnmr1/vnmrns/data
 Sample directory:
 B2A3_20200219_01
 FidFile: current

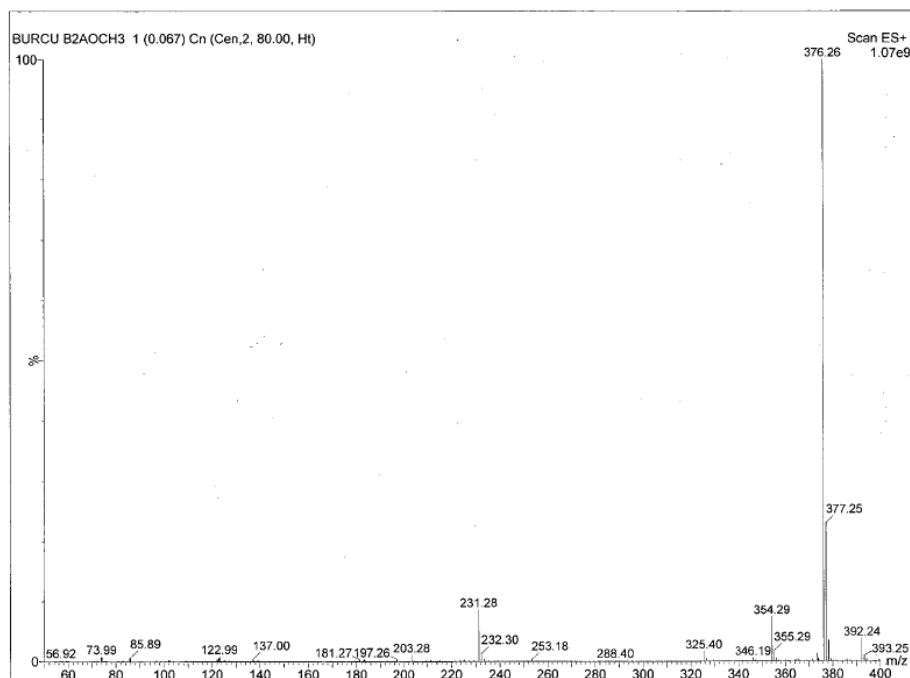
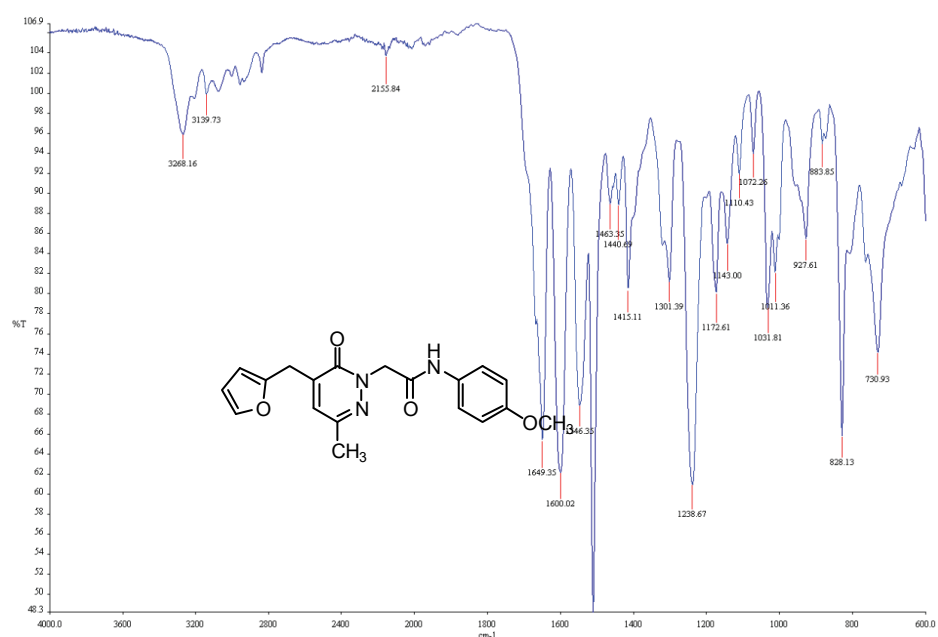
 Pulse Sequence: CARBON (zgpg3)
 Solvent: dmsd
 Data collected on: Feb 19 2020

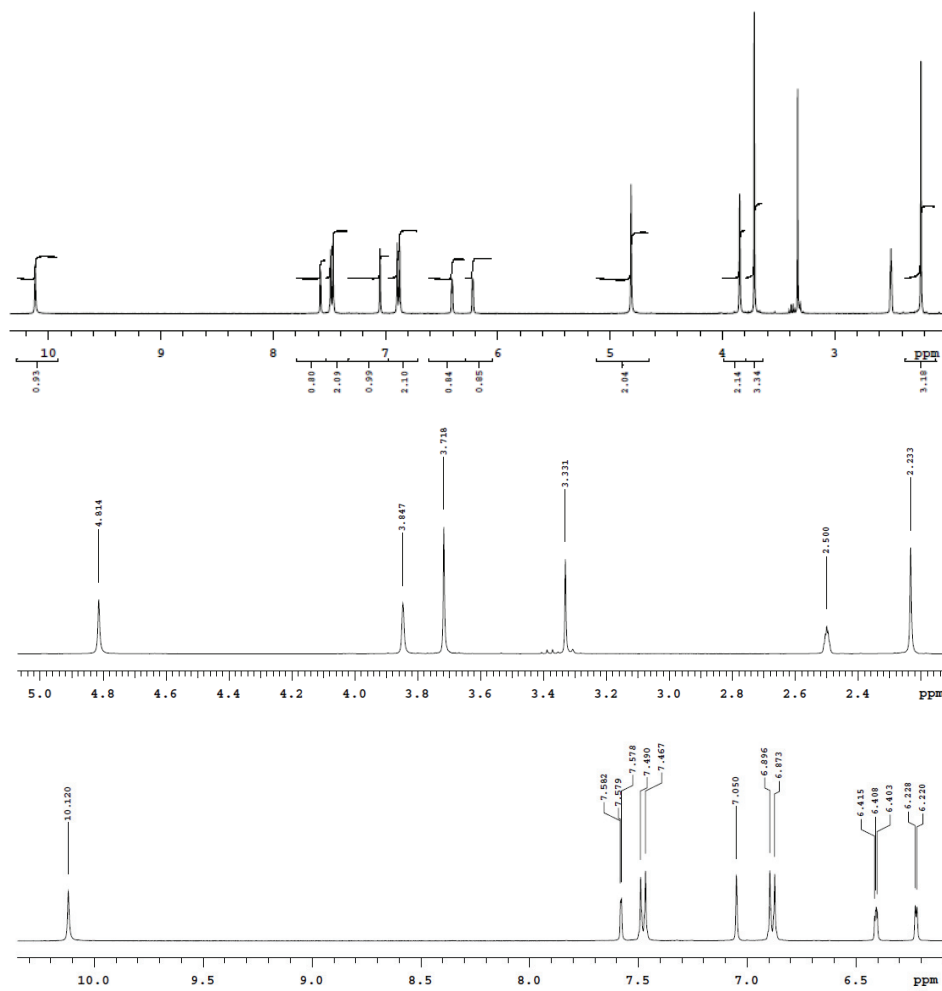
 Temp. 25.0 C / 298.1 K
 Operator: vnmr1

 Relax. delay 1.000 sec
 Pulse 45.0 degrees
 Acq. time 1.550 sec
 Width 21141.6 Hz
 1216 repetitions
 OBSERVE C13, 100.6243770 MHz
 DECOUPLE H1, 400.1779555 MHz
 Power 28 dB
 continuously on
 WALTZ-16 modulated
 DATA PROCESSING
 Line broadening 0.5 Hz
 FT size 65536
 Total time 1 hr, 28 min

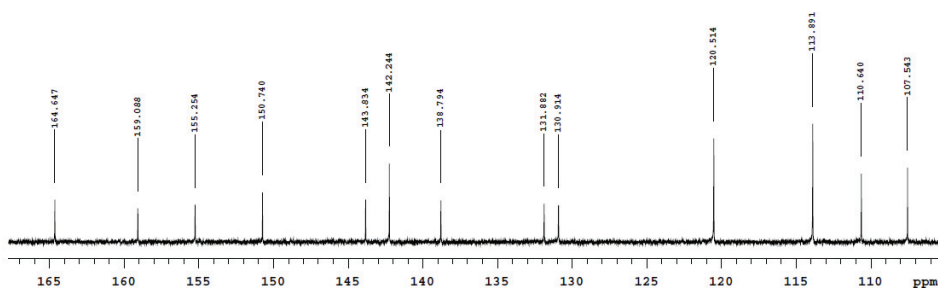
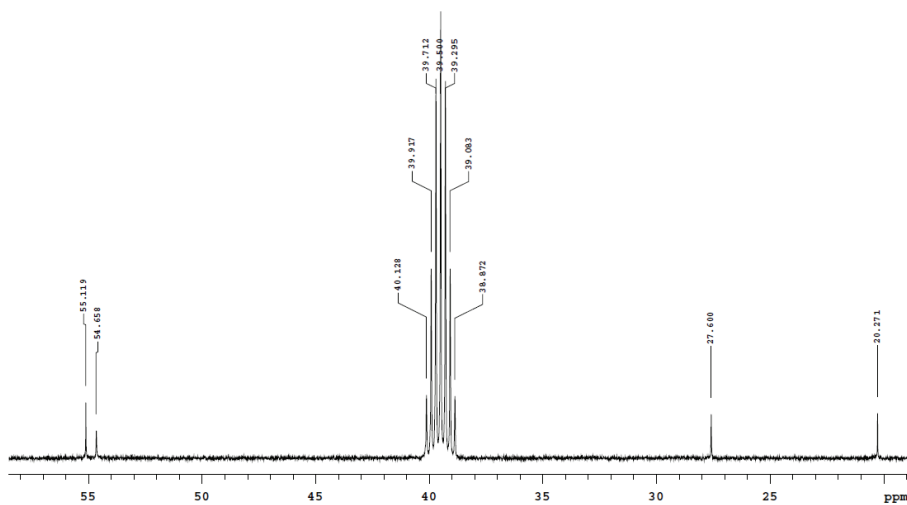
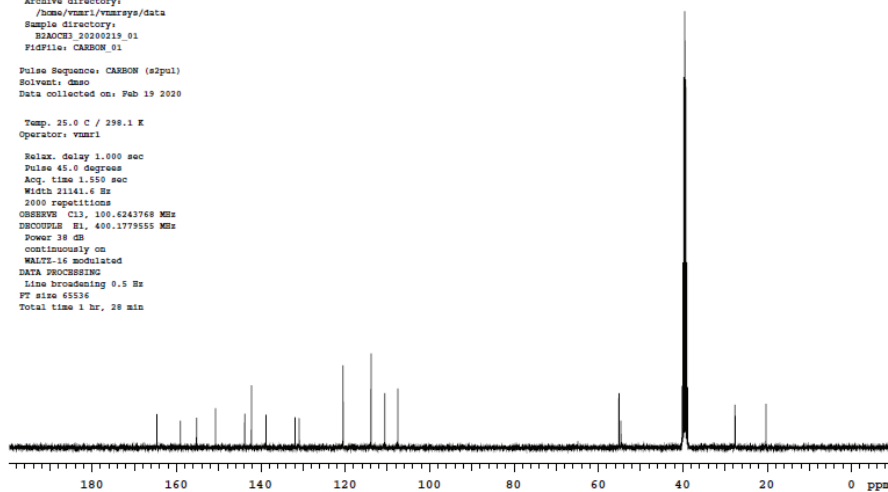


2-[5-(FURAN-2-YLMETHYL)-3-METHYL-6-OXOPYRIDAZIN-1(6H)-YL]-N-(4-METHOXYPHENYL)ACETAMIDE (5C)

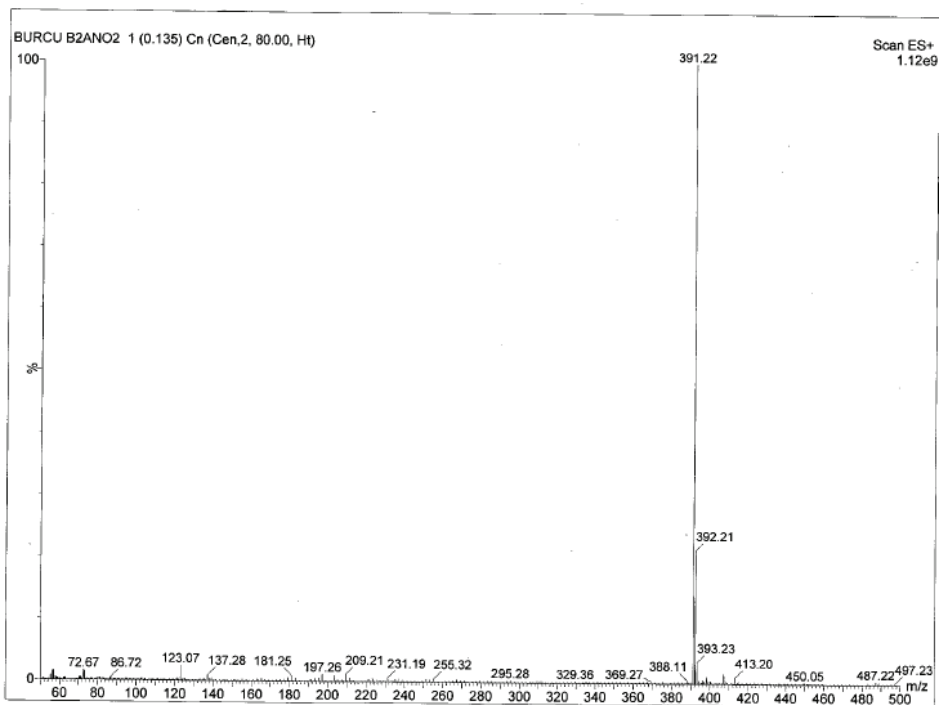
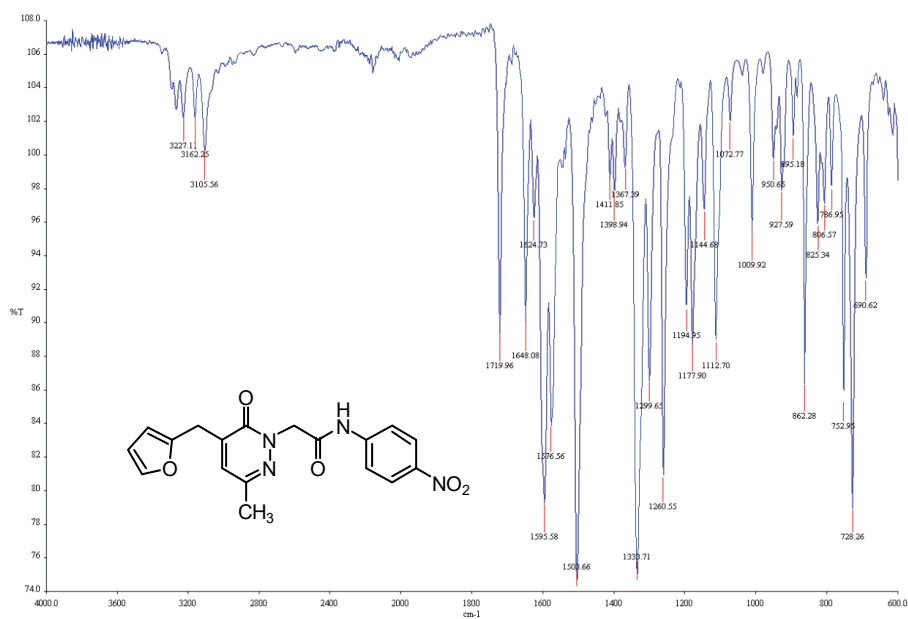


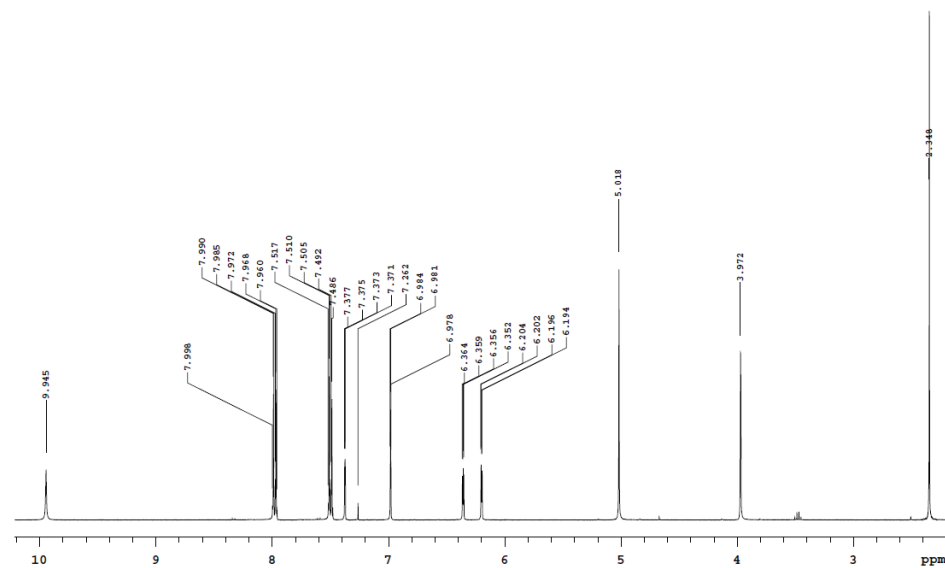
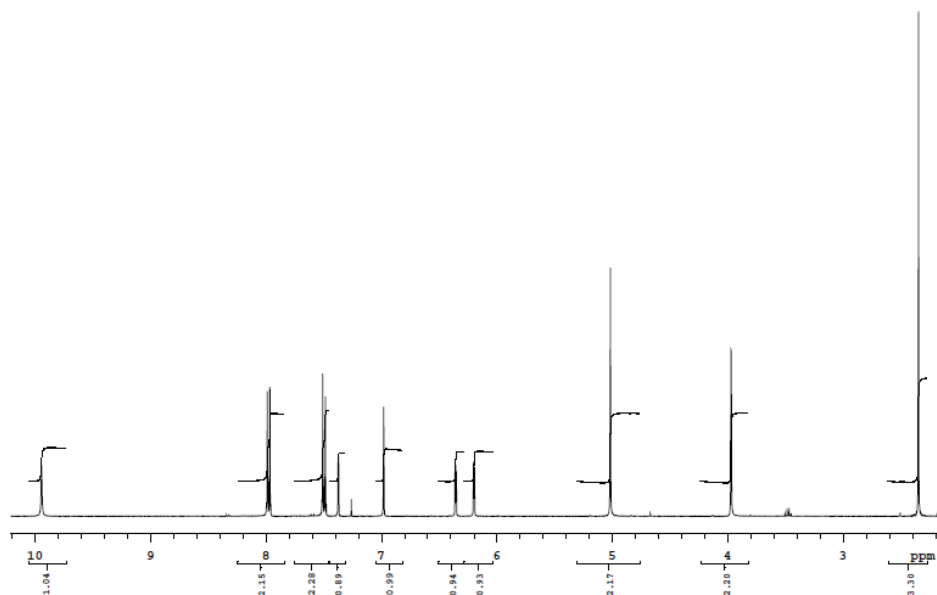


B2AOCB3
 Sample Name:
 B2AOCB3
 Data Collected on:
 Mercury160-mercury400
 Archive directory:
 /home/vmar1/vmarsys/data
 Sample directory:
 B2AOCB3_20200219_01
 Fidfile: CARBON_01
 Pulse Sequence: CARBON (e2pul)
 Solvent: dmsc
 Data collected on: Feb 19 2020
 Temp: 25.0 C / 298.1 K
 Operator: vmar1
 Relax. delay 1.000 sec
 Pulse 45.0 degrees
 Acq. time 1.550 sec
 Width 21141.6 Hz
 2000 repetitions
 OBSERVE CH3, 100.6243768 MHz
 PRODUCE H1, 400.1779555 MHz
 Power 38 dB
 continuously on
 WALTZ-16 modulated
 DATA PROCESSING
 Line broadening 0.5 Hz
 PF size 65536
 Total time 1 hr, 28 min

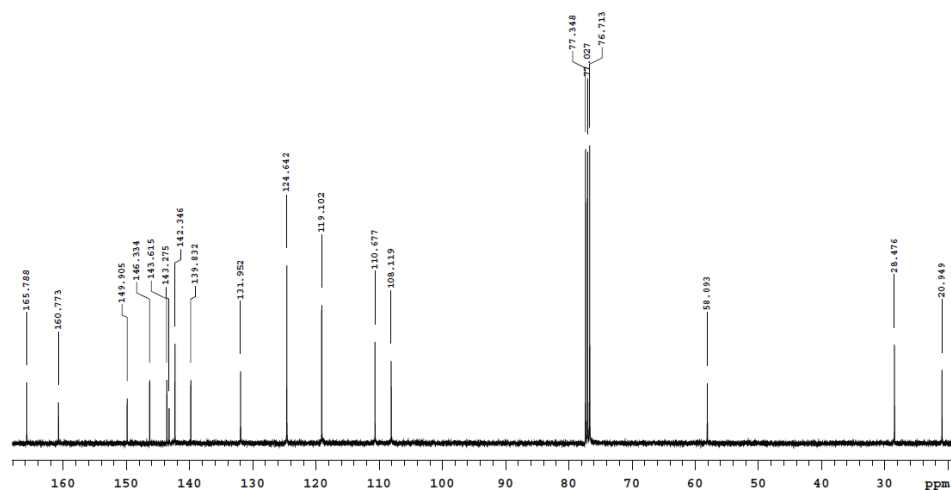
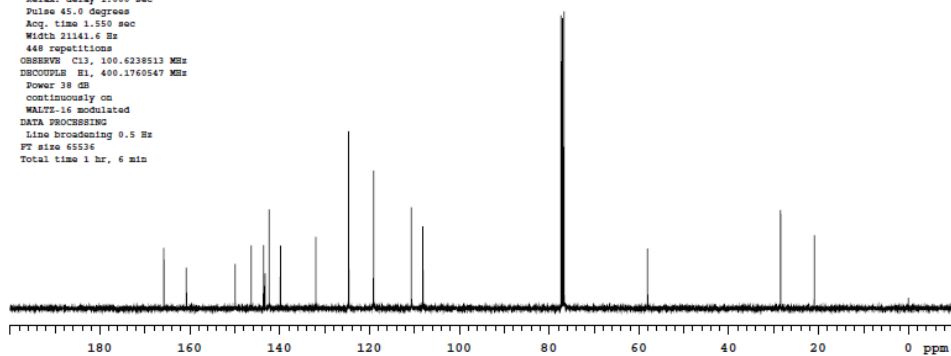


2-[5-(FURAN-2-YLMETHYL)-3-METHYL-6-OXOPYRIDAZIN-1(6H)-YL]-N-(4-NITROPHENYL)ACETAMIDE (5D)

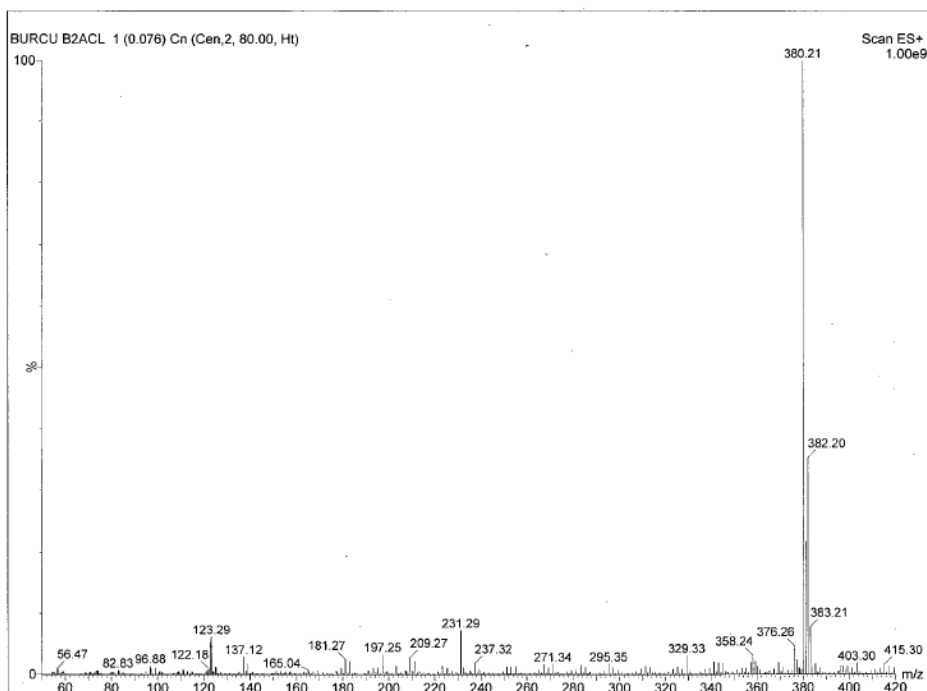
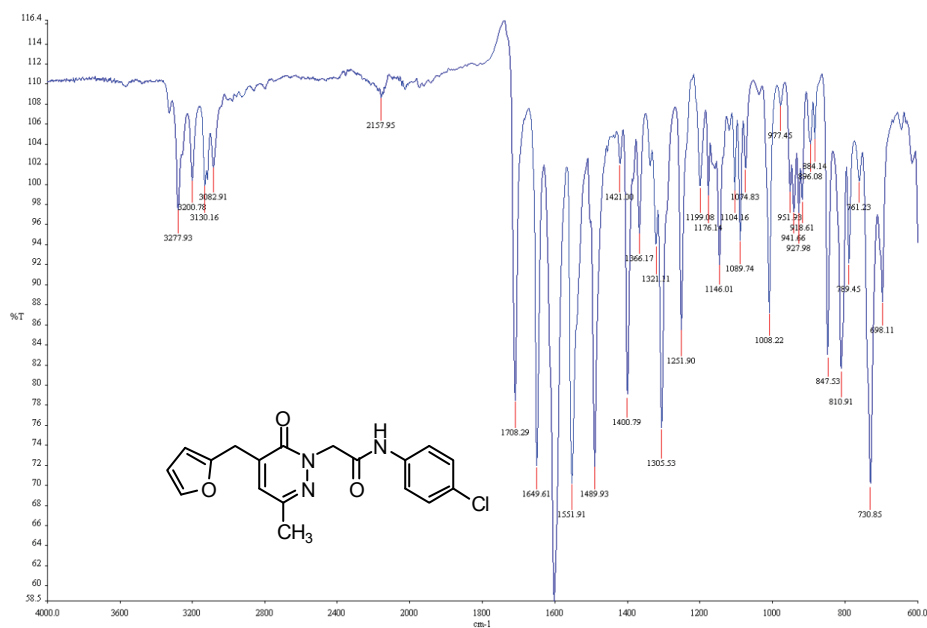


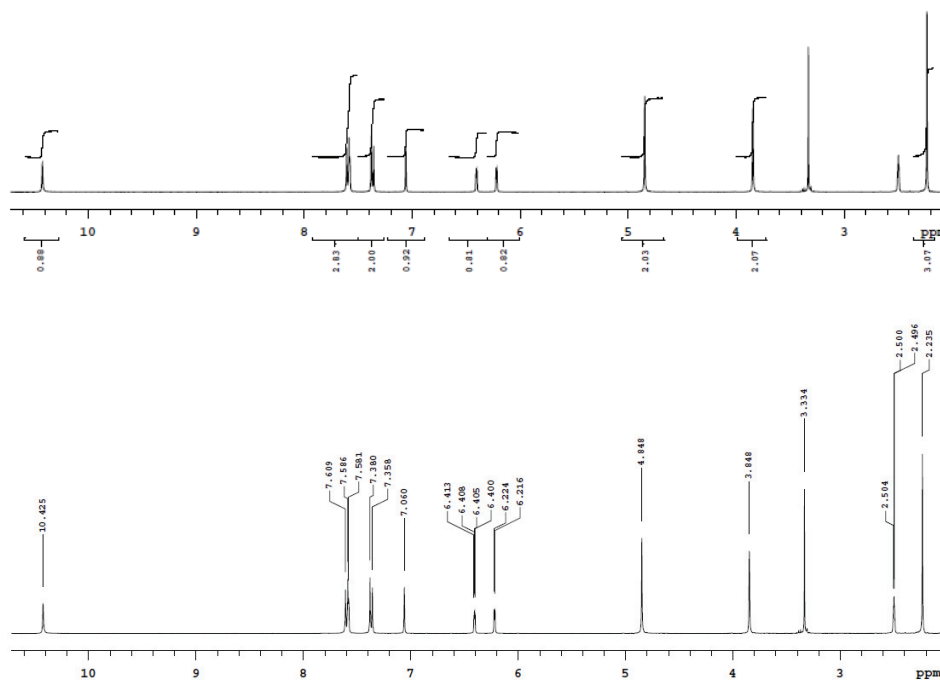


E2AN02
Sample Name:
E2AN02
Data Collected on:
Mercury400-mercury400
Archive directory:
/home/vmari/vmarrays/data
Sample directory:
E2AN02_20201130_01
FidFile: current
Pulse Sequence: CARBON (s2pul)
Solvent: cdcl3
Data collected on: Nov 30 2020
Temp: 25.0 C / 298.1 K
Operator: vmari
Relax. delay 1.000 sec
Pulse 45.0 degrees
Acq. time 1.550 sec
Width 21141.6 Hz
448 repetitions
OBSERVE C13, 100.6238513 MHz
PROCURSE H1, 400.1760547 MHz
Power 38 dB
continuously on
WALTZ-16 modulated
DATA PROCESSING
Line broadening 0.5 Hz
FT size 65536
Total time 1 hr, 6 min

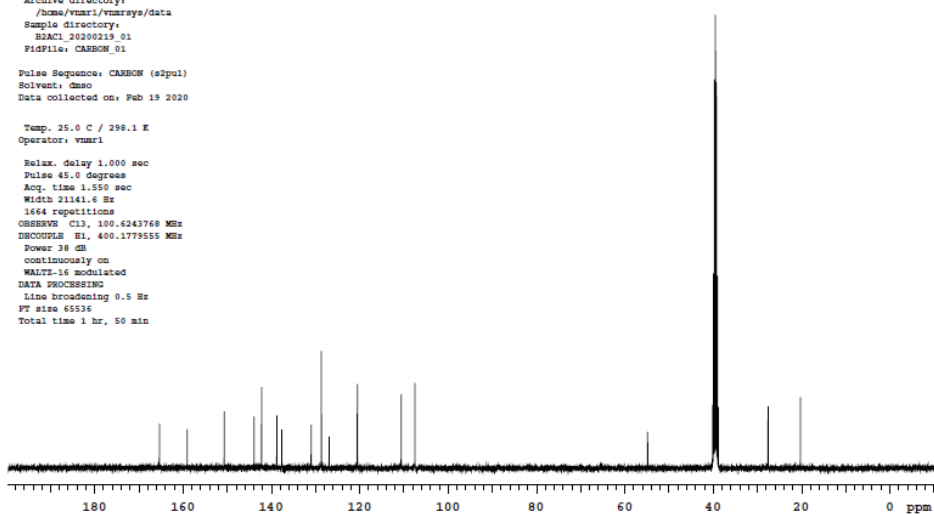


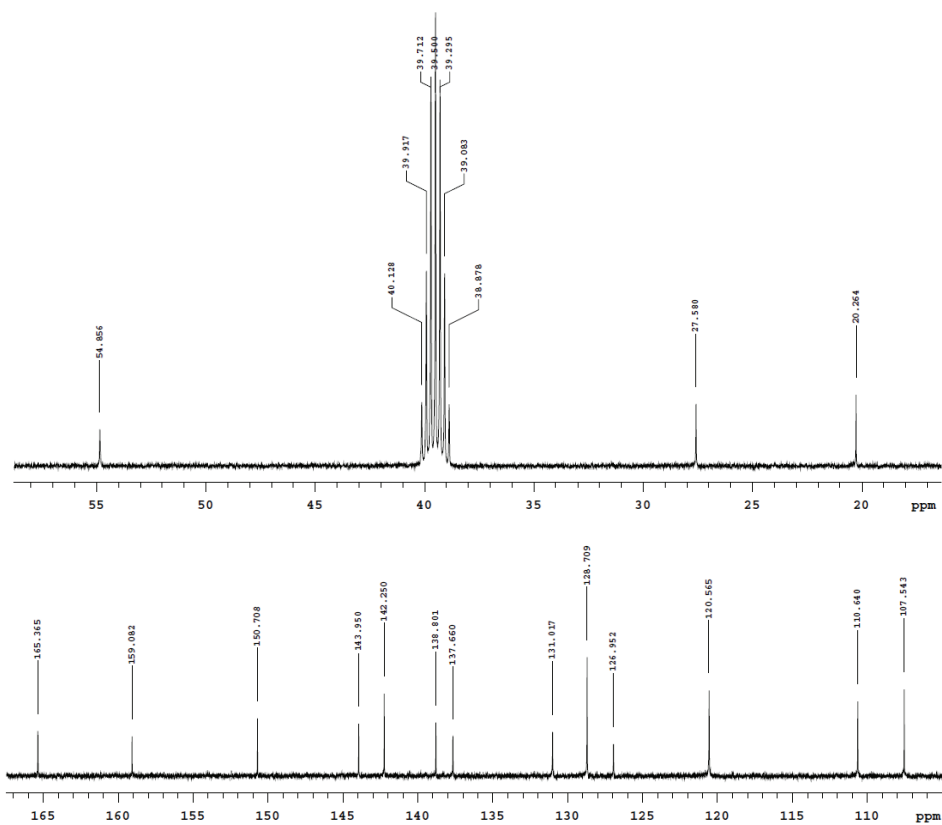
2-[5-(FURAN-2-YLMETHYL)-3-METHYL-6-OXOPYRIDAZIN-1(6H)-YL]-N-(4-CHLOROPHENYL)ACETAMIDE (5E)



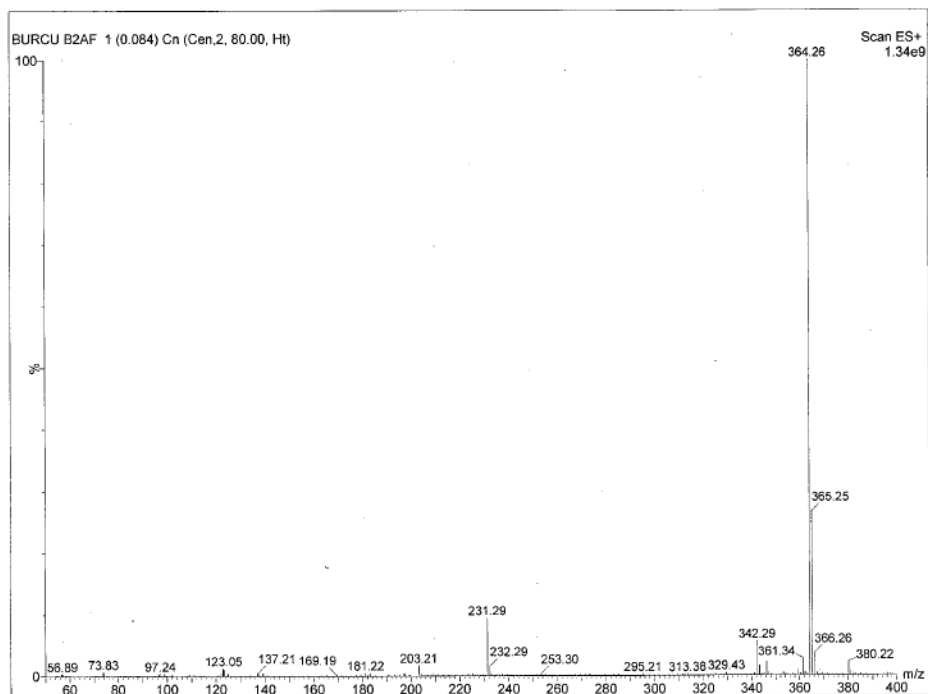
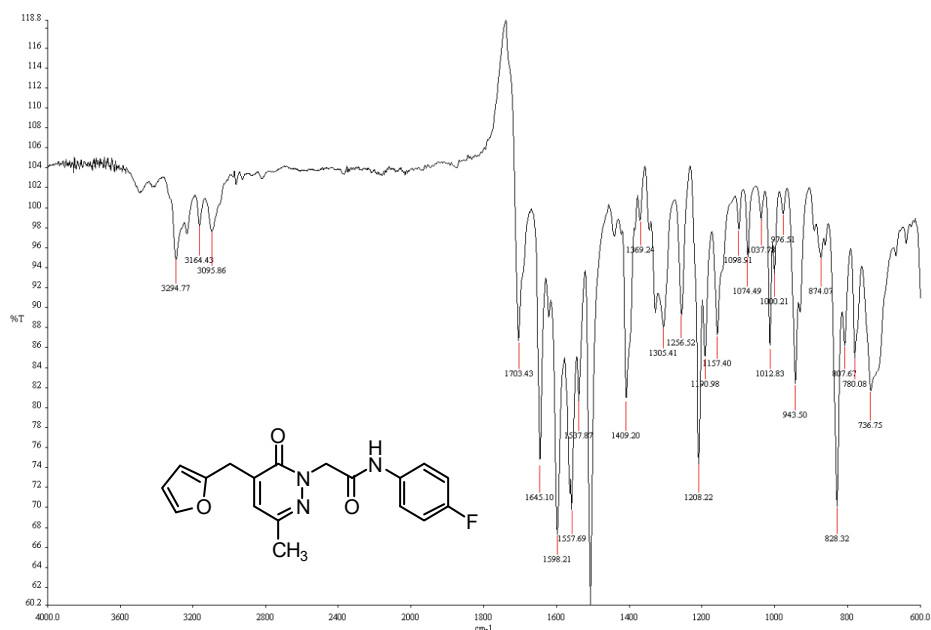


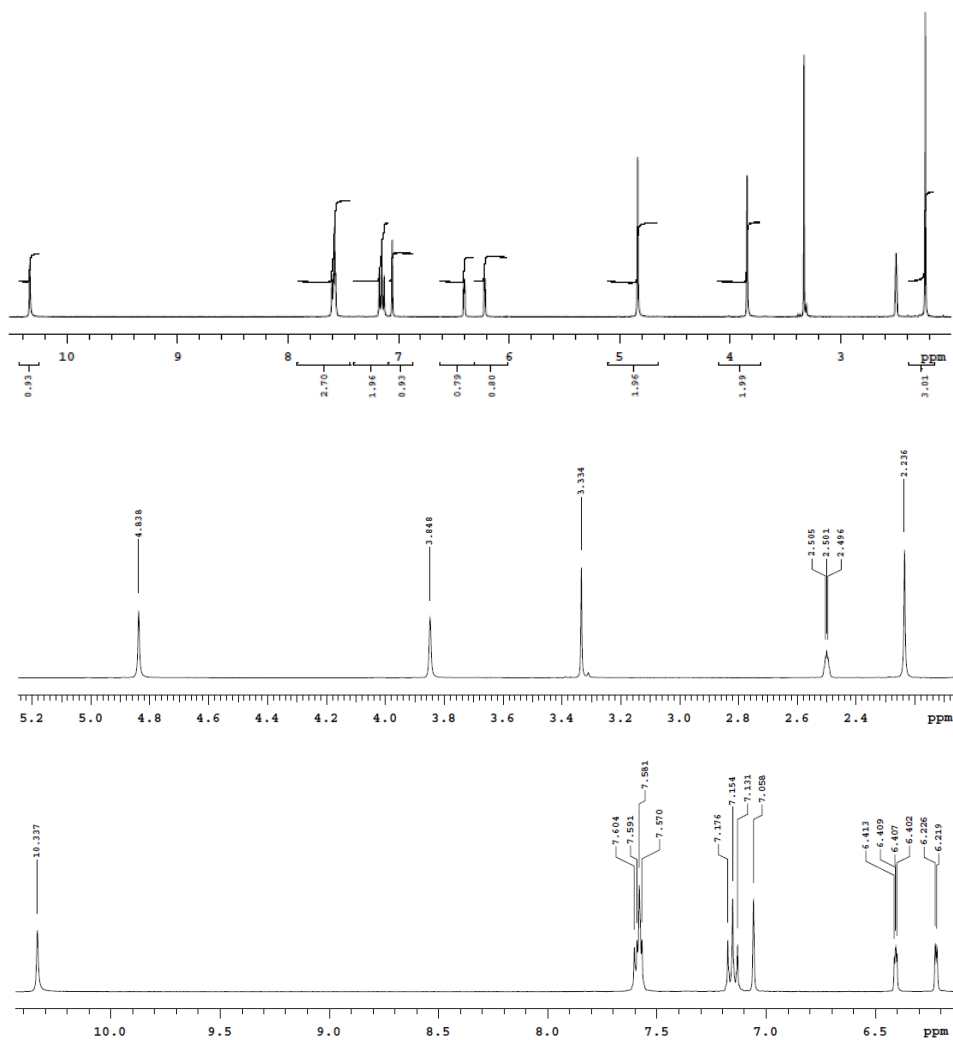
B2AC1
 Sample Name:
 B2AC1
 Data Collected on:
 mercury400-mercury400
 Archive directory:
 /home/vmari/vmrays/data
 Sample directory:
 B2AC1_20200219_01
 F1dFile: CARBON_01
 Pulse Sequence: CARBON (s2pul)
 Solvent: dmsc
 Data collected on: Feb 19 2020
 Temp: 25.0 C / 298.1 K
 Operator: vmari
 Relax. delay 1.000 sec
 Pulse 45.0 degrees
 Acq. time 1.550 sec
 Width 21141.6 Hz
 1664 repetitions
 OBSERVE C13, 100.6243768 MHz
 DECOUPLE H1, 400.1779555 MHz
 Power 18 dB
 continuously on
 WALTZ-16 modulated
 DATA PROCESSING
 Line broadening 0.5 Hz
 FT size 65536
 Total time 1 hr, 50 min

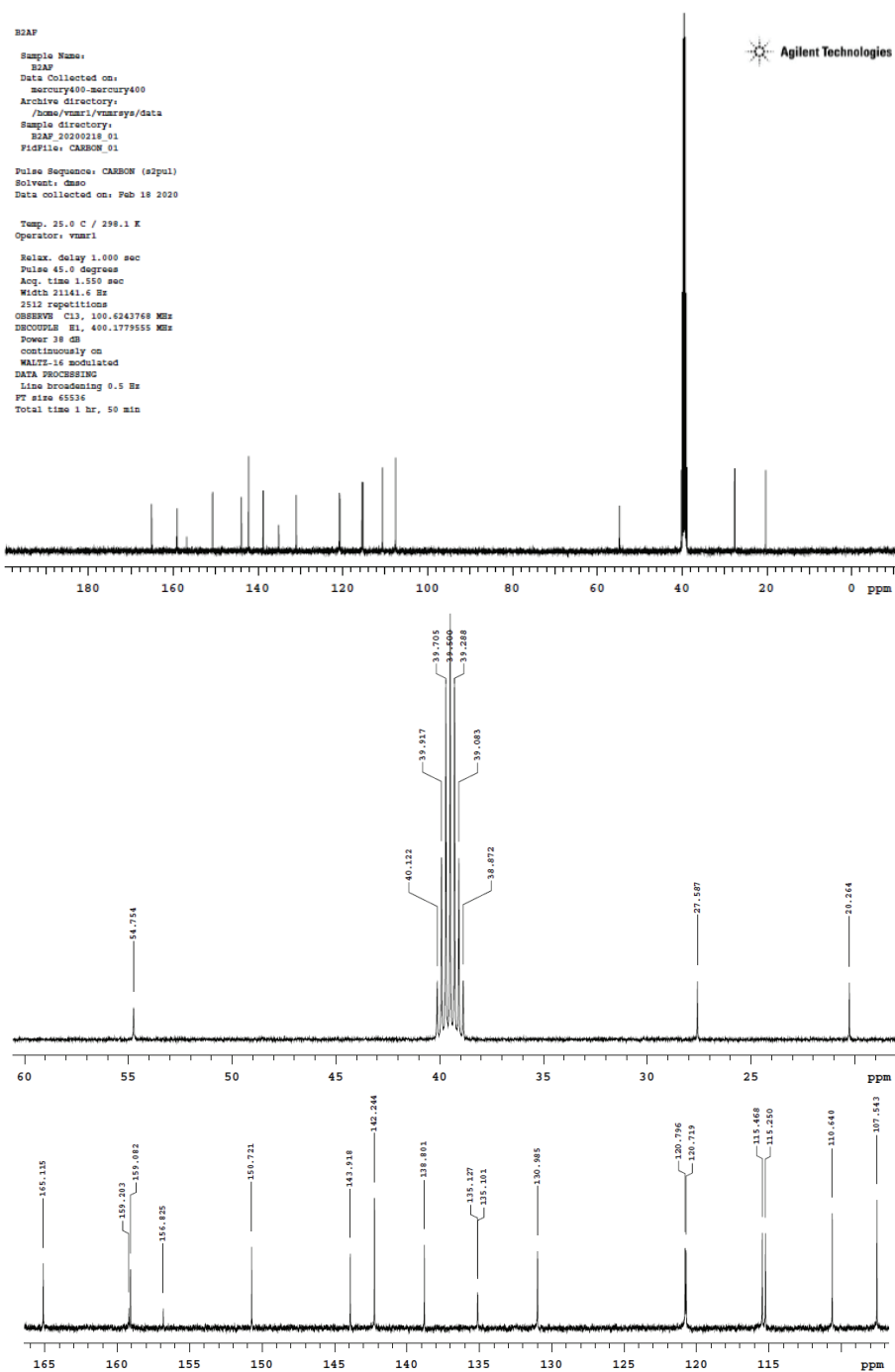




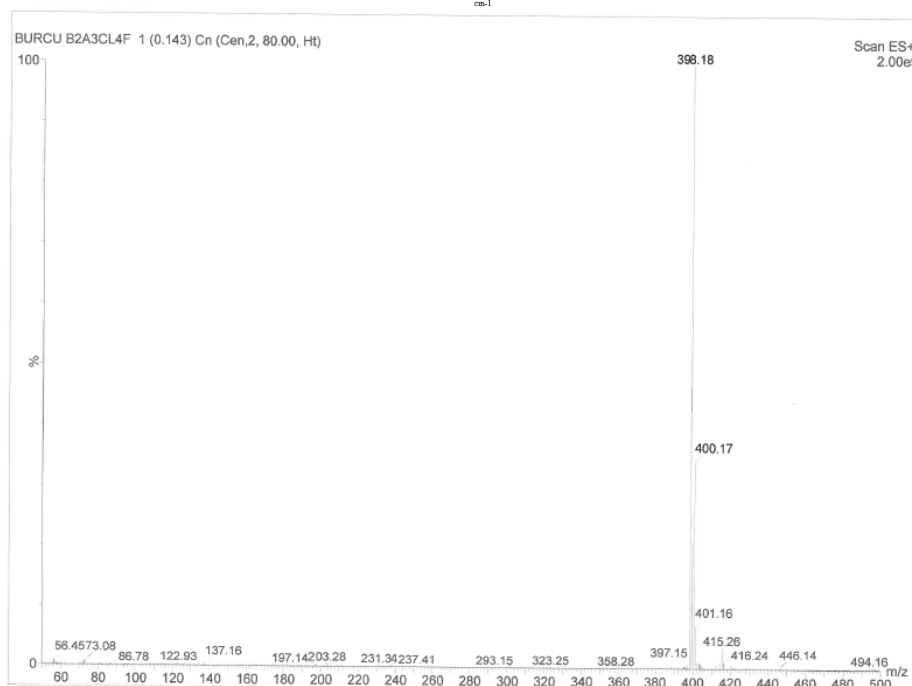
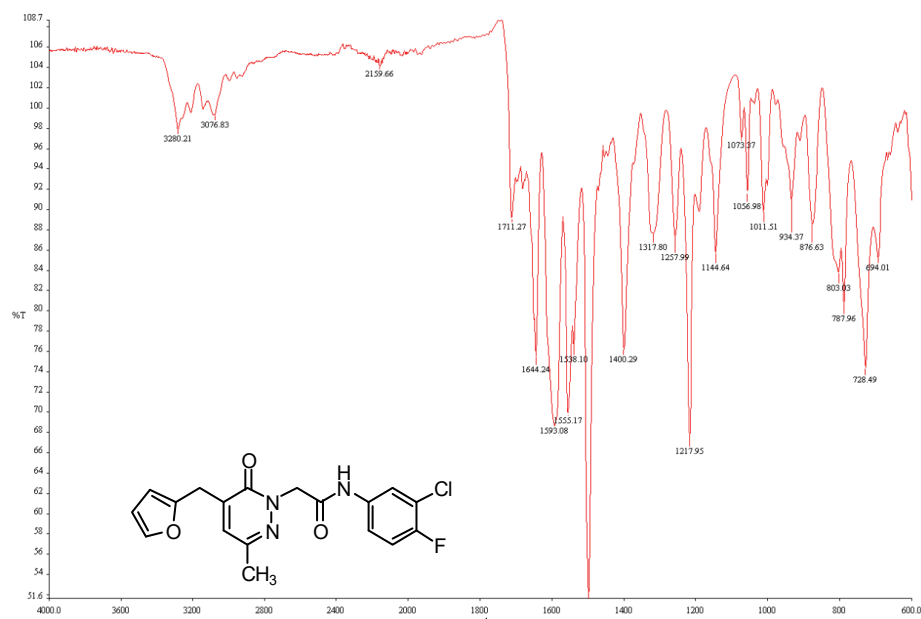
2-[5-(FURAN-2-YLMETHYL)-3-METHYL-6-OXOPYRIDAZIN-1(6H)-YL]-N-(4-FLUOROPHENYL)ACETAMIDE (5F)

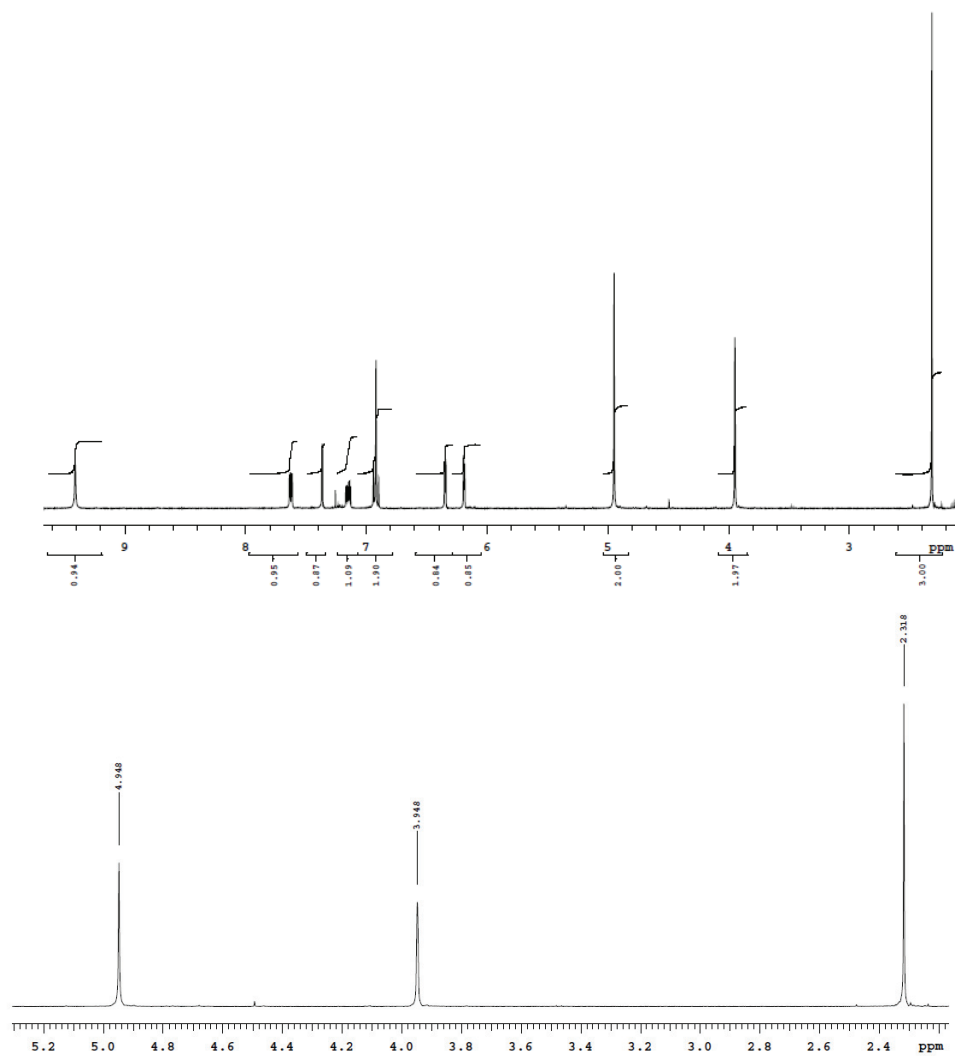


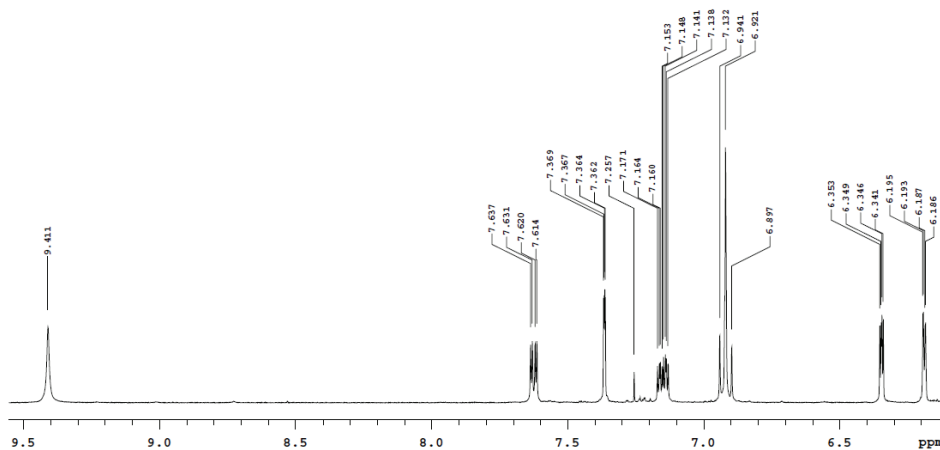




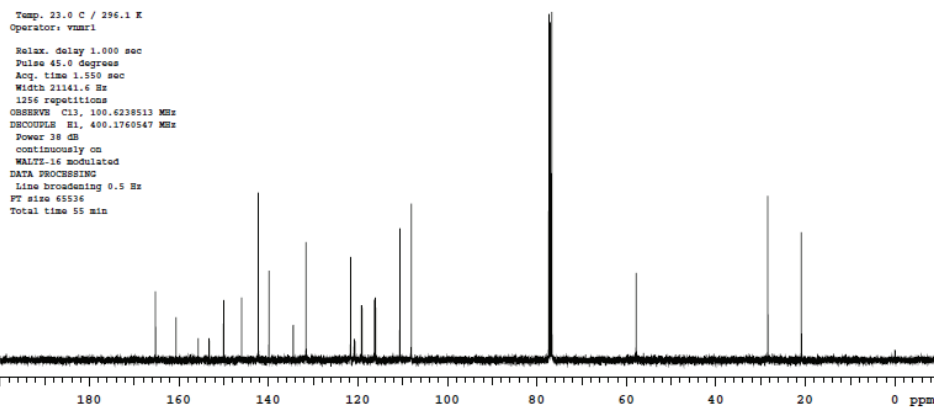
2-[5-(FURAN-2-YLMETHYL)-3-METHYL-6-OXOPYRIDAZIN-1(6H)-YL]-N-(3-CHLORO-4-FLUOROPHENYL)ACETAMIDE (5G)

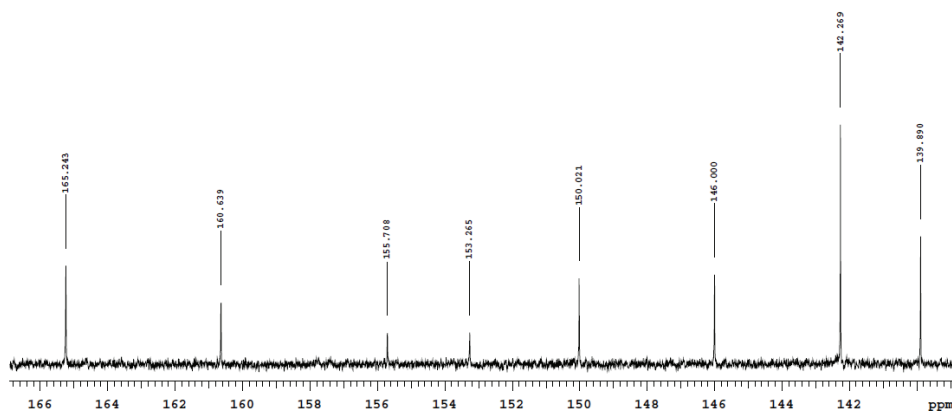
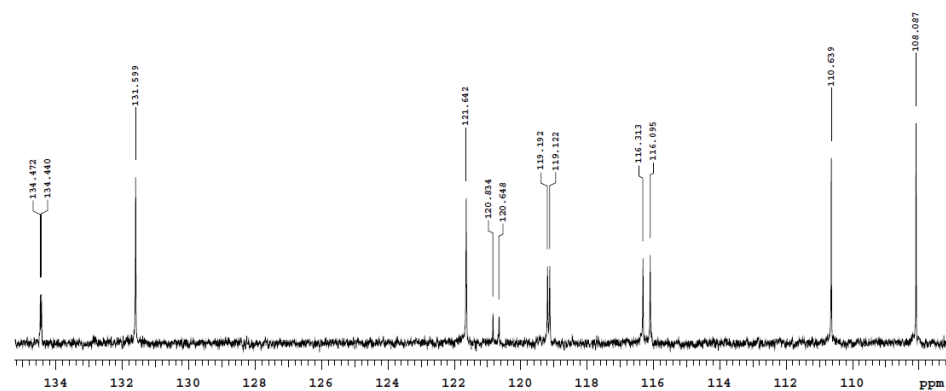
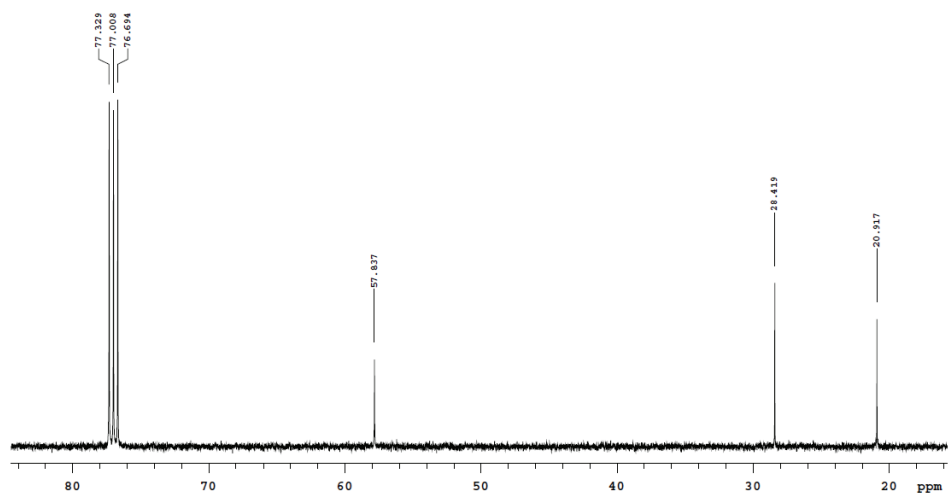




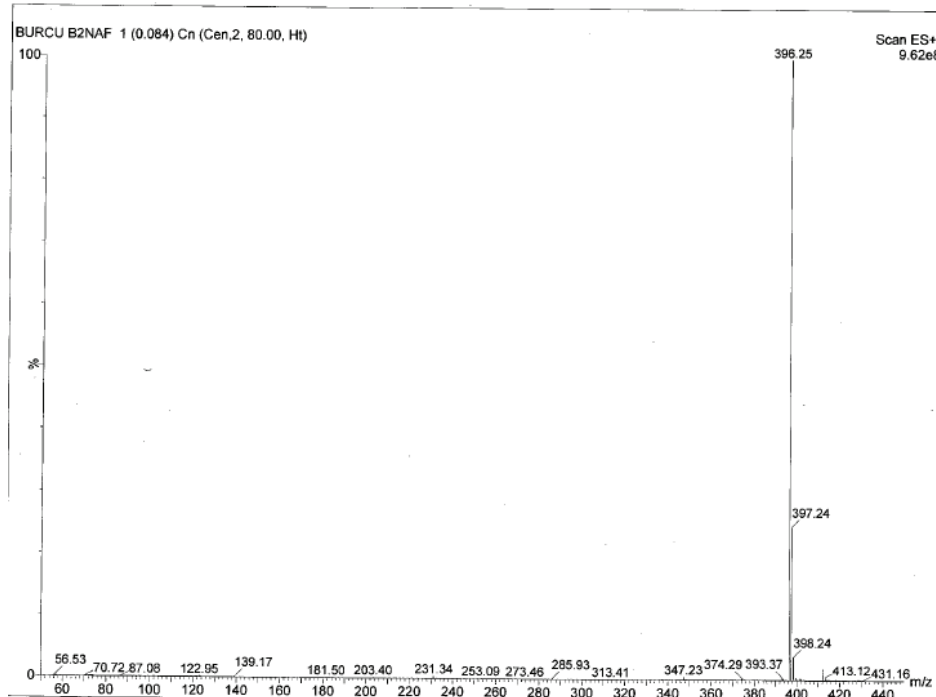
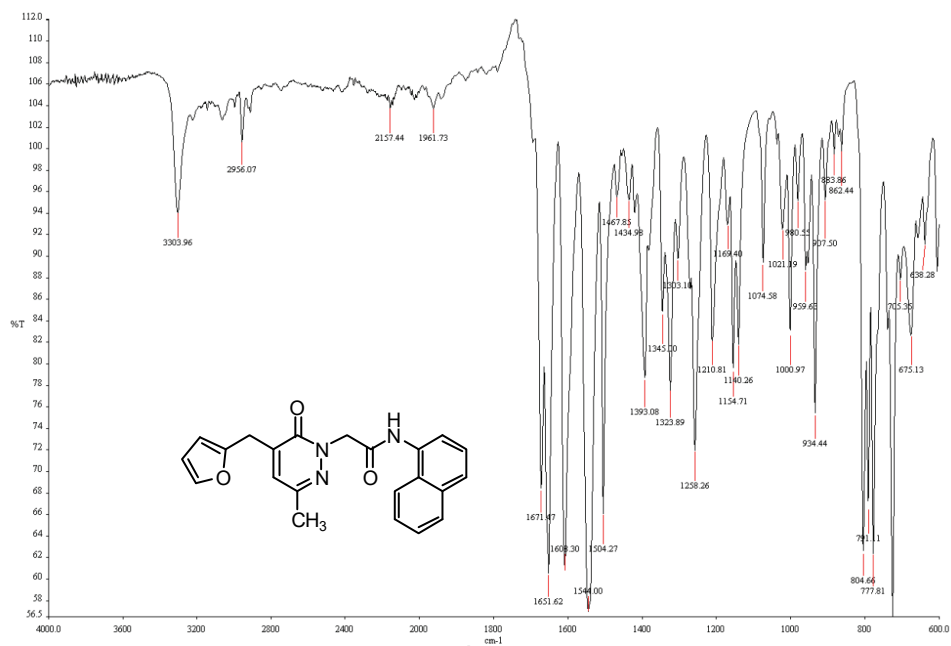


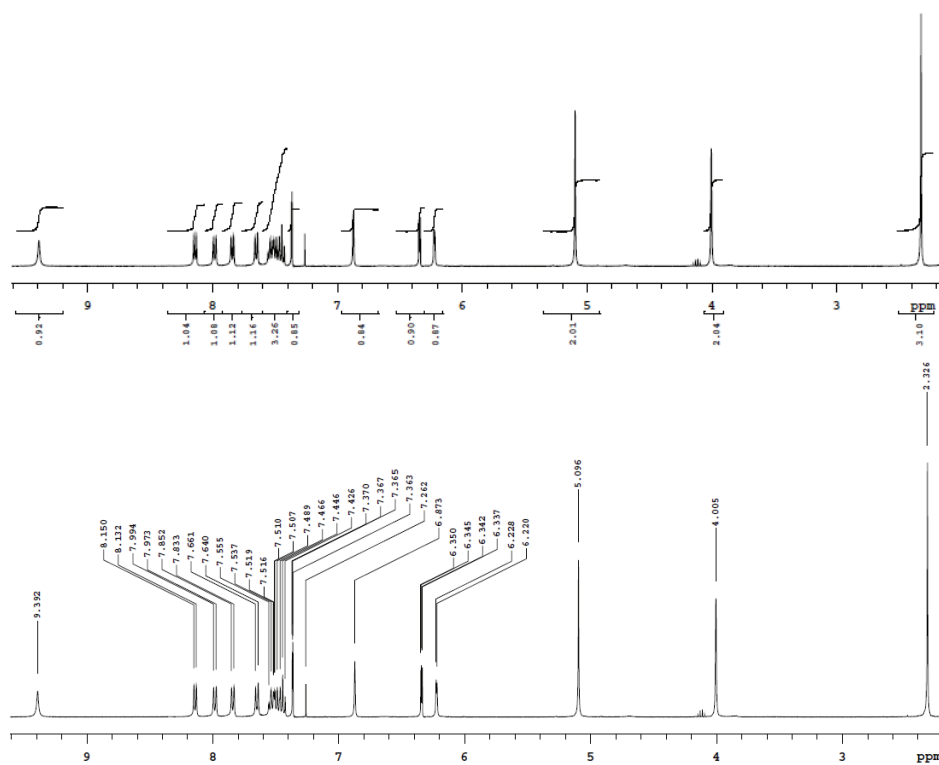
B2A3C14F
 Sample Name: B2A3C14F
 Data Collected on: mercury400-mercury400
 Archive directory: /home/vnmri/vnmrsw/data
 Sample directory: B2A3C14F_20210221_01
 FidFile: CARBON_01
 Pulse Sequence: CARBON (zgpg3)
 Solvent: cdcl3
 Data collected on: Feb 21 2021

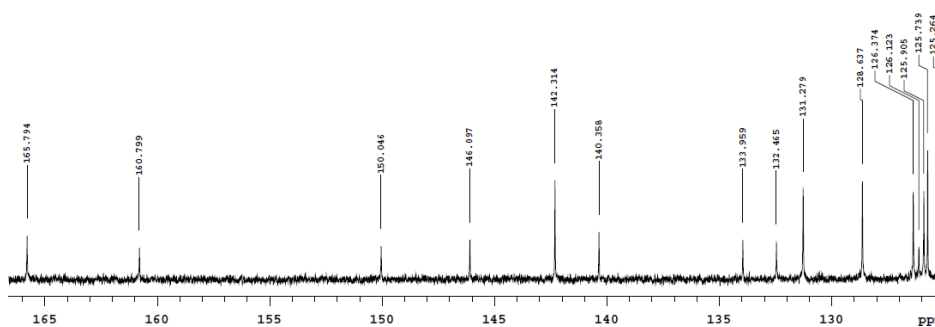
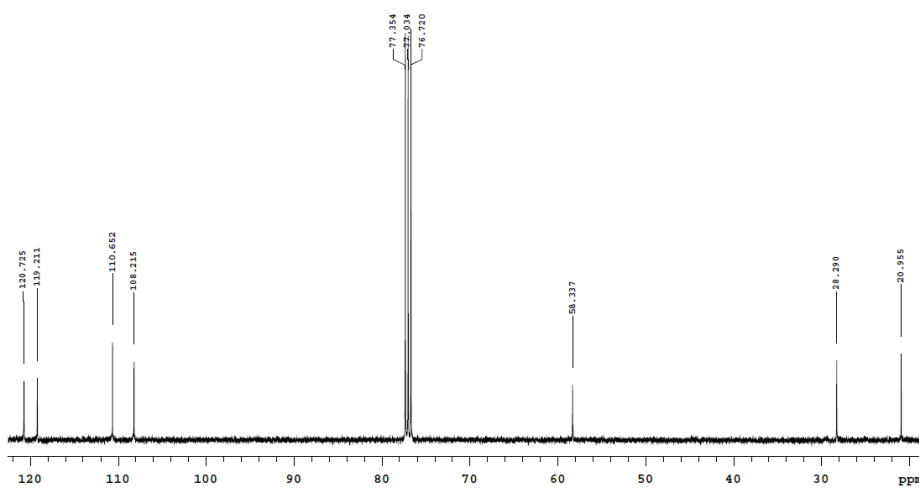
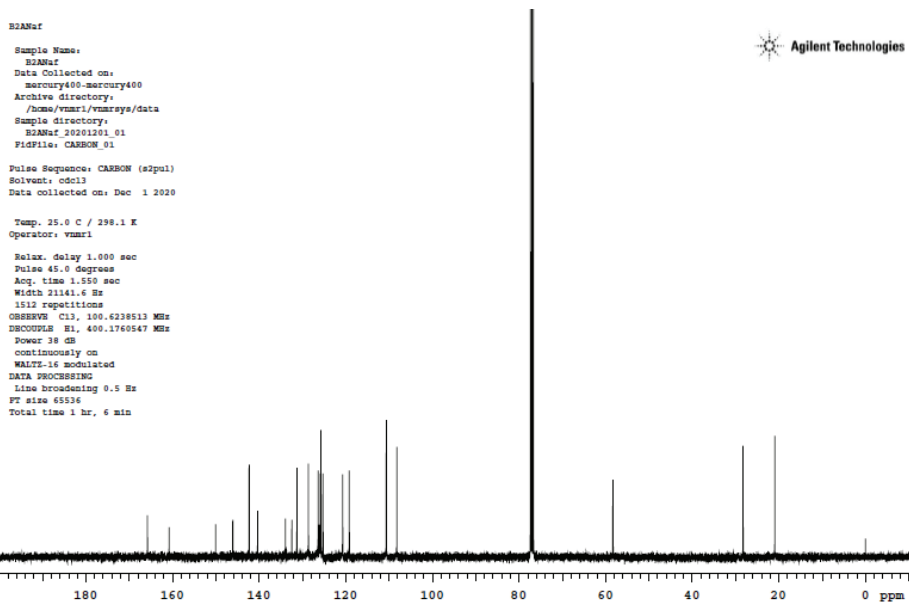




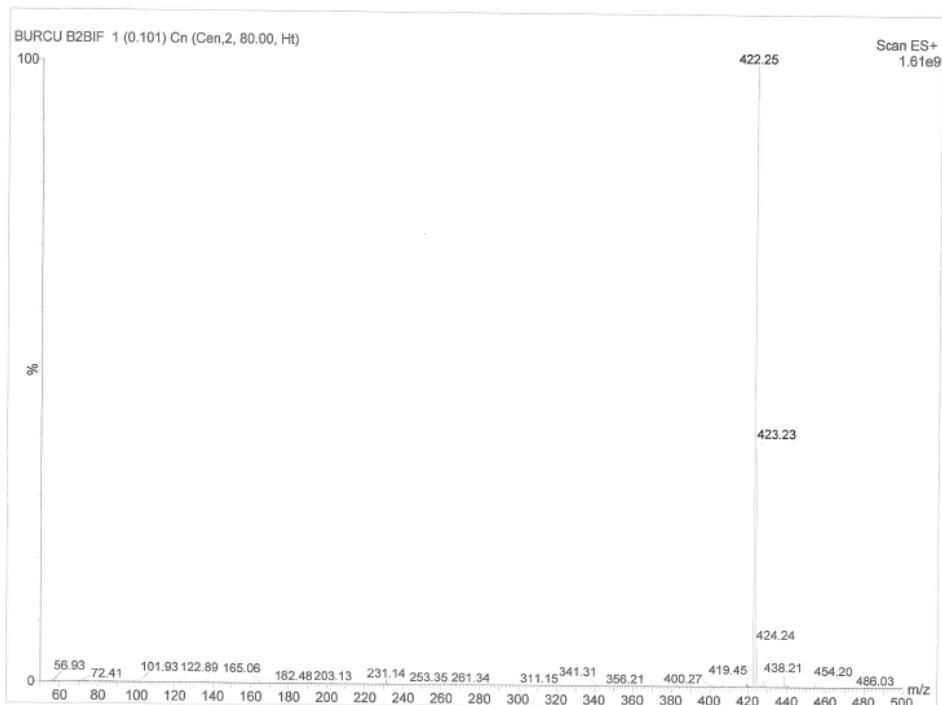
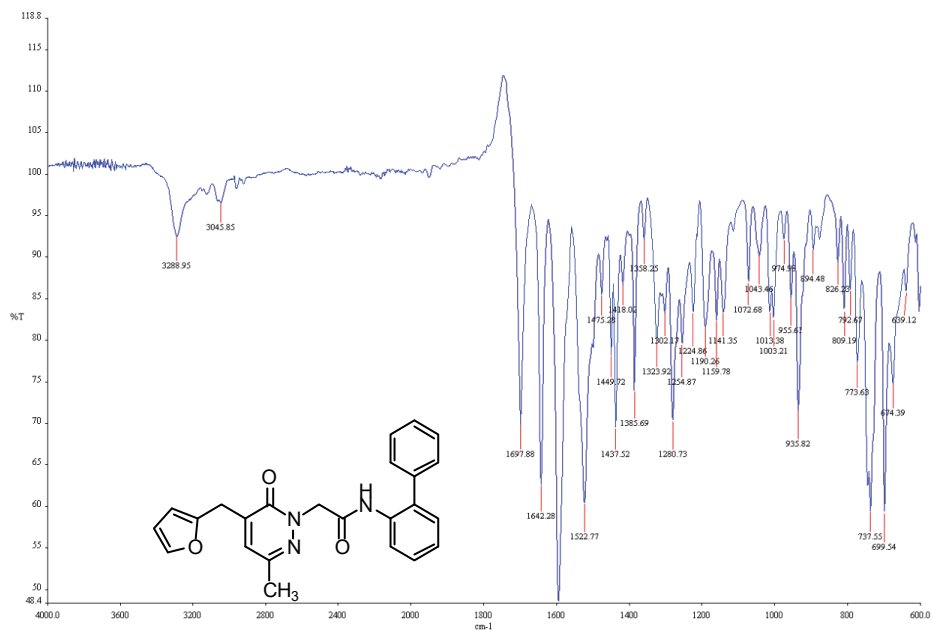
2-[5-(FURAN-2-YLMETHYL)-3-METHYL-6-OXOPYRIDAZIN-1(6H)-YL]-N-(NAPHTHALEN-1-YL)ACETAMIDE (5H)

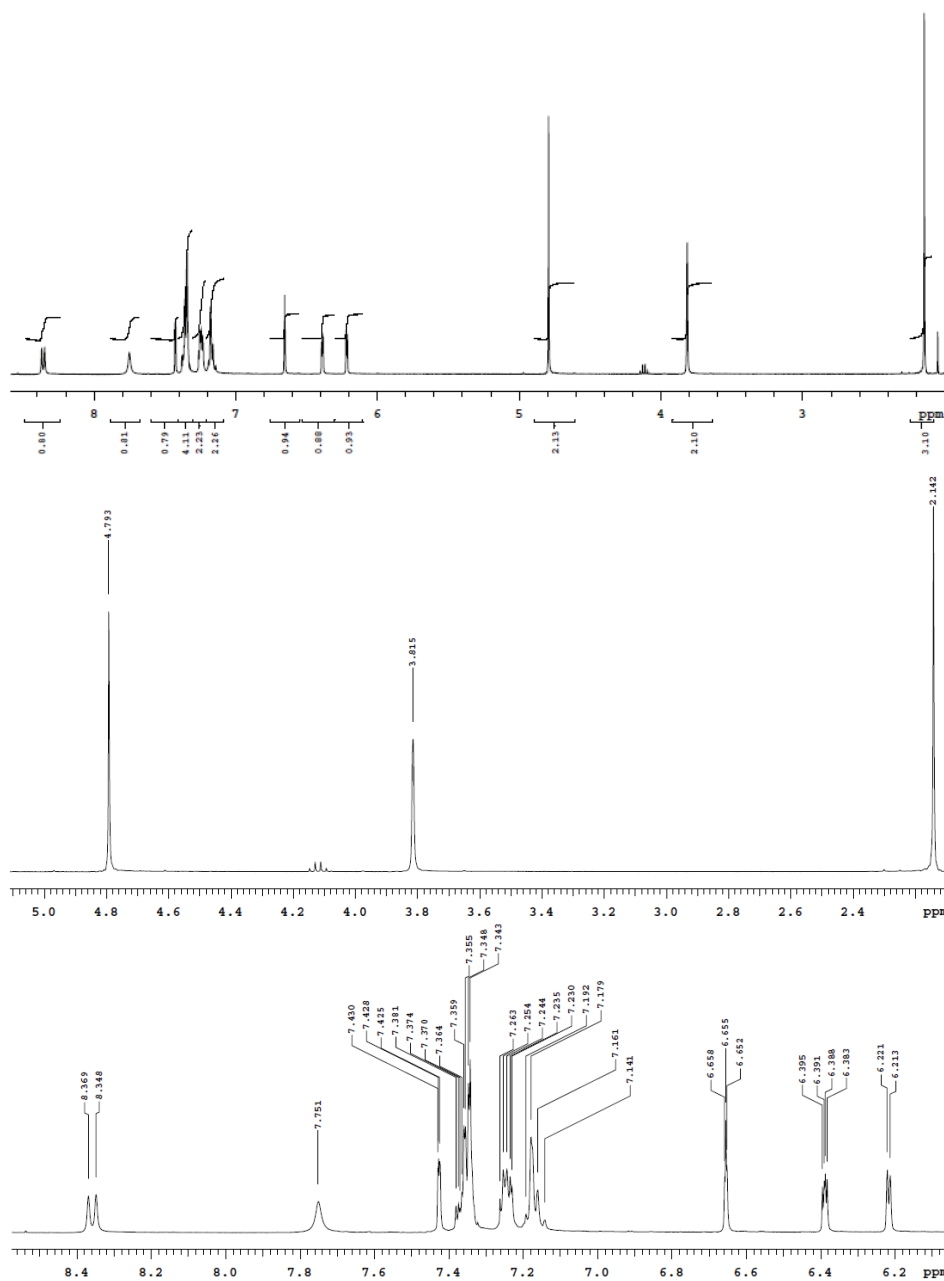


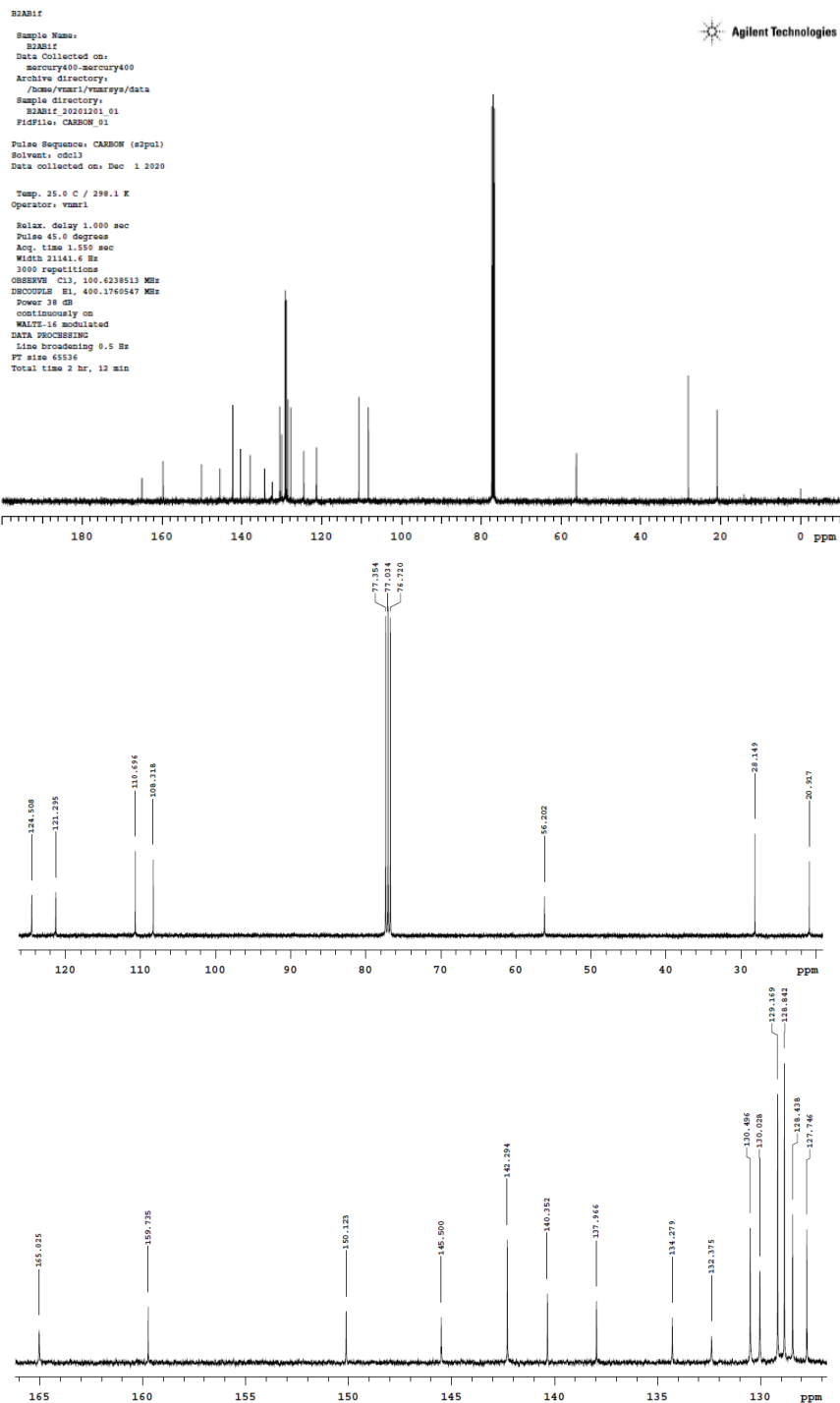




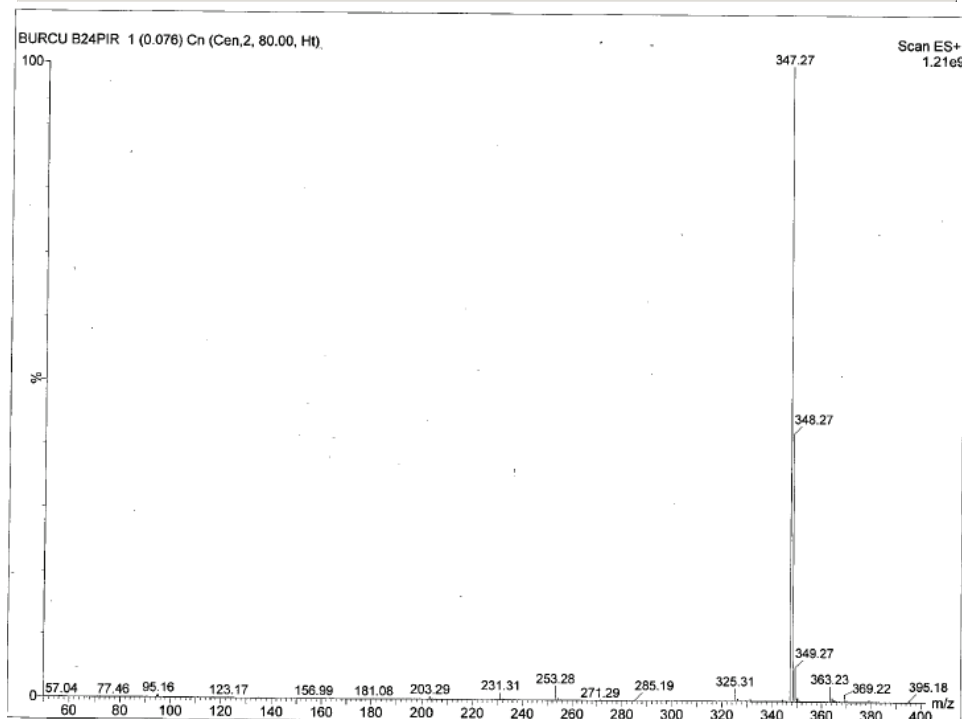
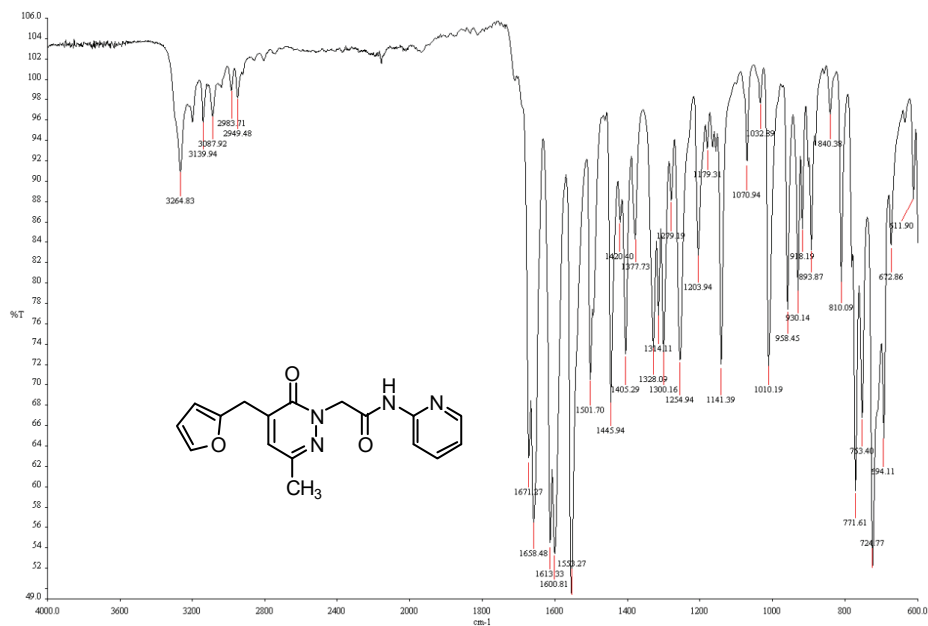
2-[5-(FURAN-2-YLMETHYL)-3-METHYL-6-OXOPYRIDAZIN-1(6H)-YL]-N-((1,1'-BIPHENYL)-2-YL)ACETAMIDE (5I)

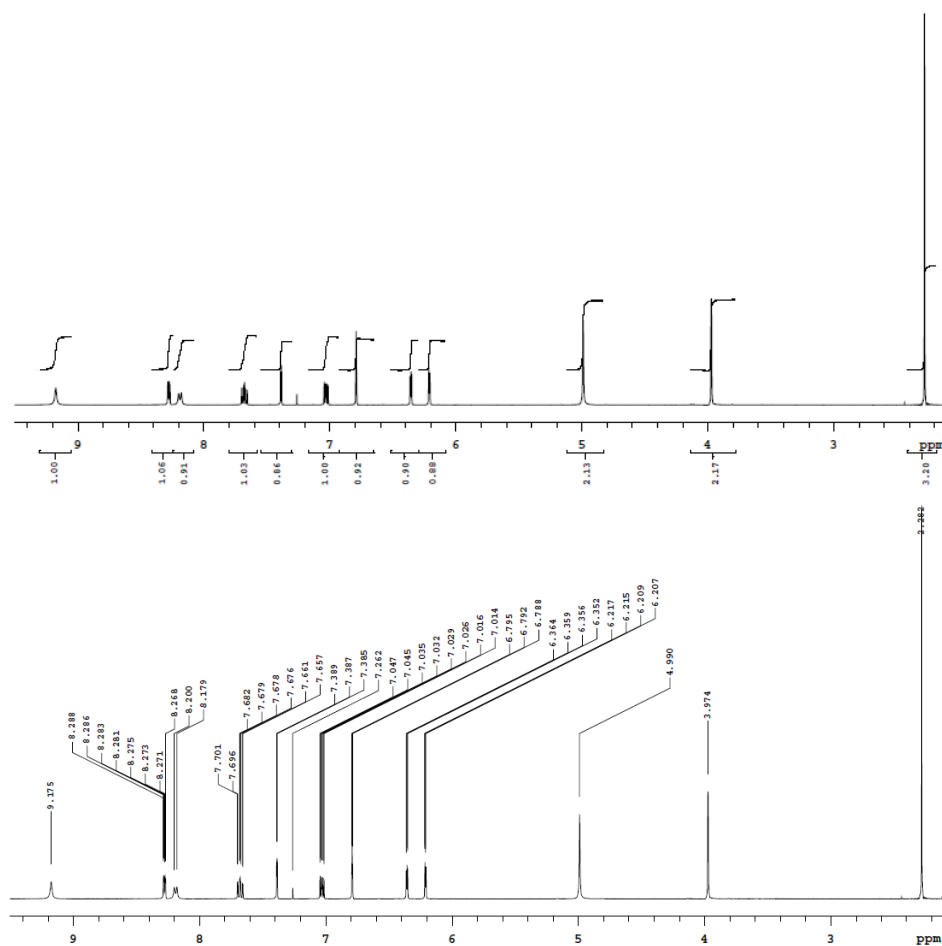






2-[5-(FURAN-2-YLMETHYL)-3-METHYL-6-OXOPYRIDAZIN-1(6H)-YL]-N-(PYRIDIN-2-YL)ACETAMIDE (5J)





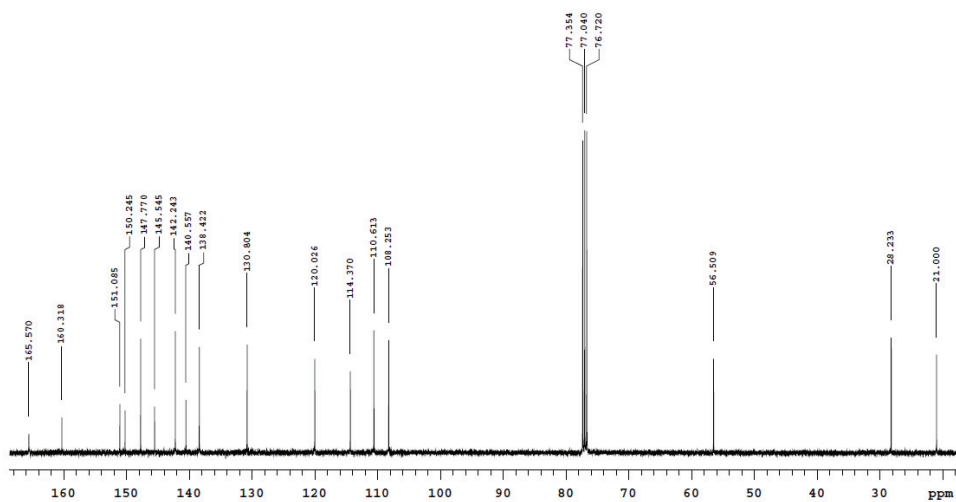
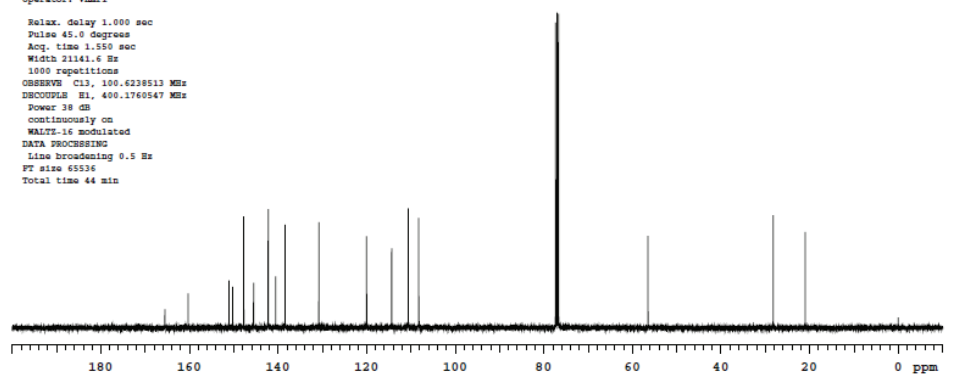
B2APir

Sample Name:
B2APir
Data Collected on:
mercury400-mercury400
Archive directory:
/home/vmr1/vmrays/data
Sample directory:
B2APir_20201201_01
FidFile: CARBON_01

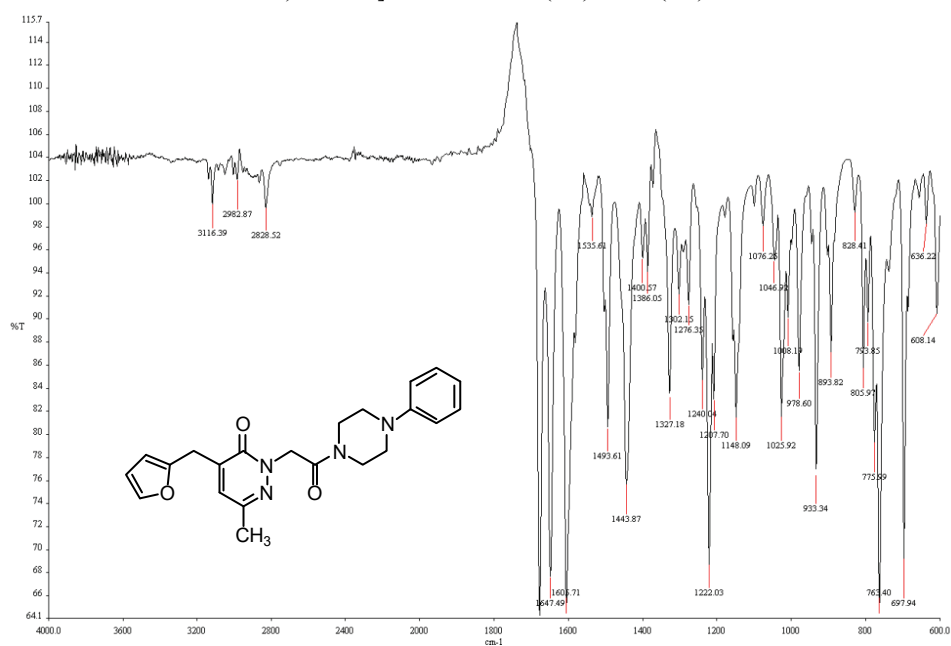
Pulse Sequence: CARBON (s2pul)
Solvent: cdcl3
Data collected on: Dec 1 2020

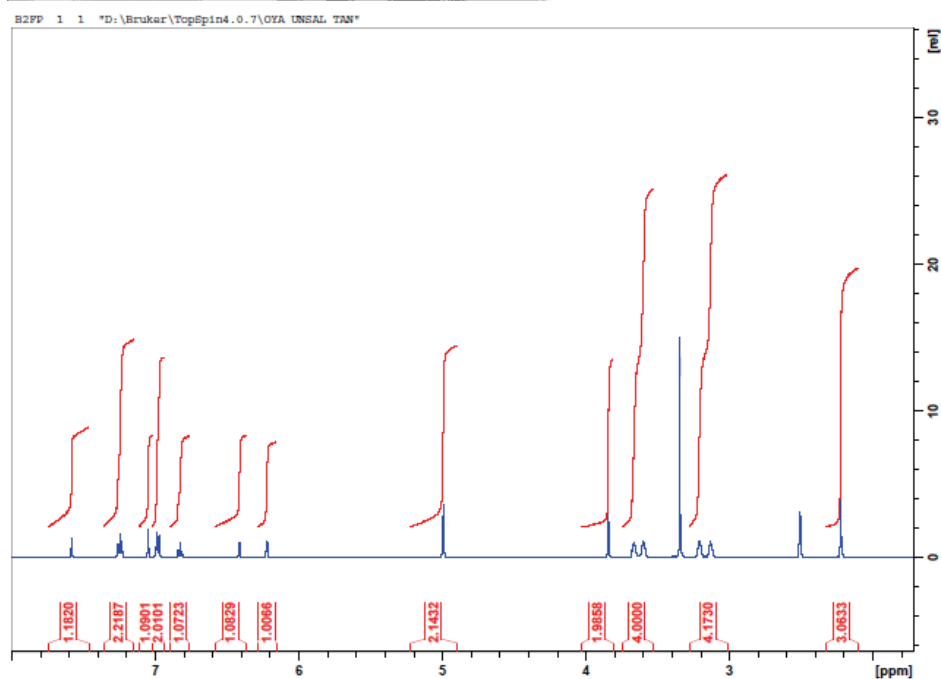
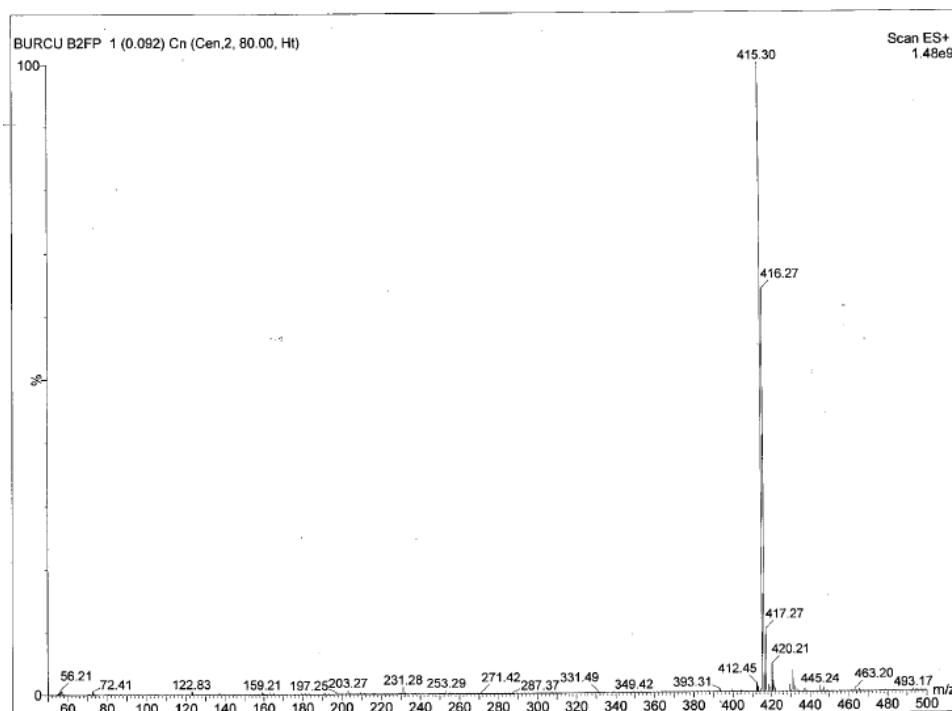
Temp. 25.0 C / 298.1 K
Operator: vmr1

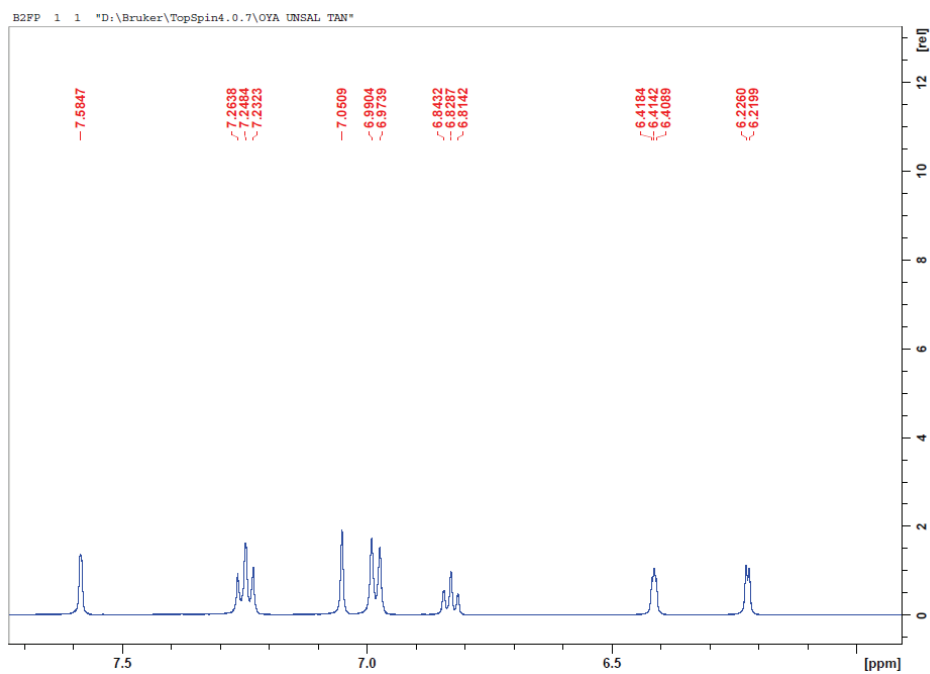
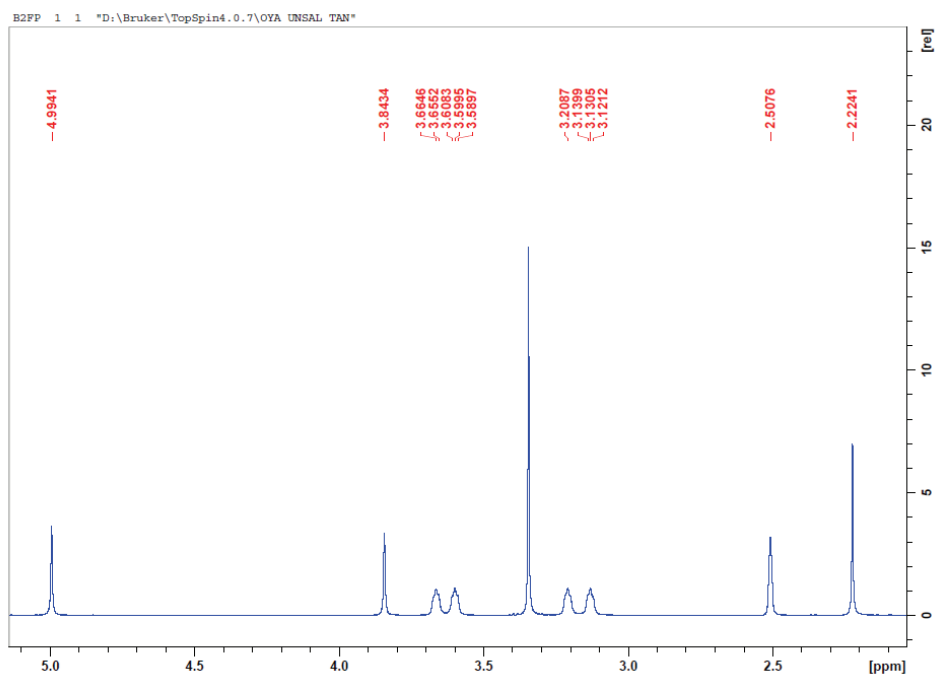
Relax. delay 1.000 sec
Pulse 45.0 degrees
Acq. time 1.550 sec
Width 21141.6 Hz
1000 repetitions
CROSSPO 123, 100.6228513 MHz
DECOUPLR H1, 400.1760547 MHz
Power 38 dB
continuously on
WALTZ-16 Modulated
DATA PROCESSING
Line broadening 0.5 Hz
FT size 65536
Total time 44 min



4-(FURAN-2-YLMETHYL)-6-METHYL-2-[2-OXO-2-(4-PHENYLPYPERAZIN-1-YL)ETHYL]PYRIDAZIN-3(2H)-ONE (6A)







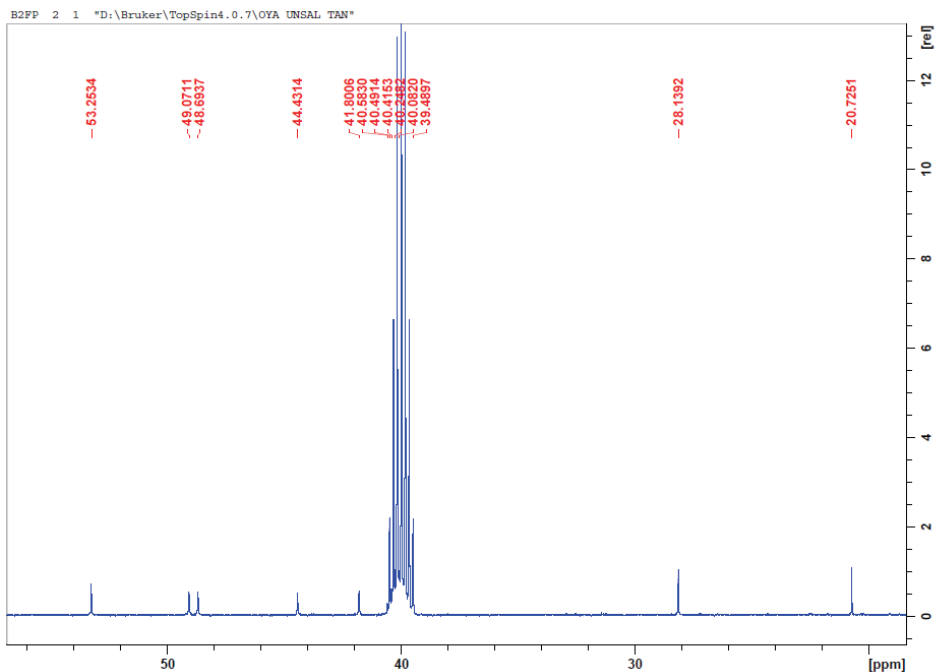
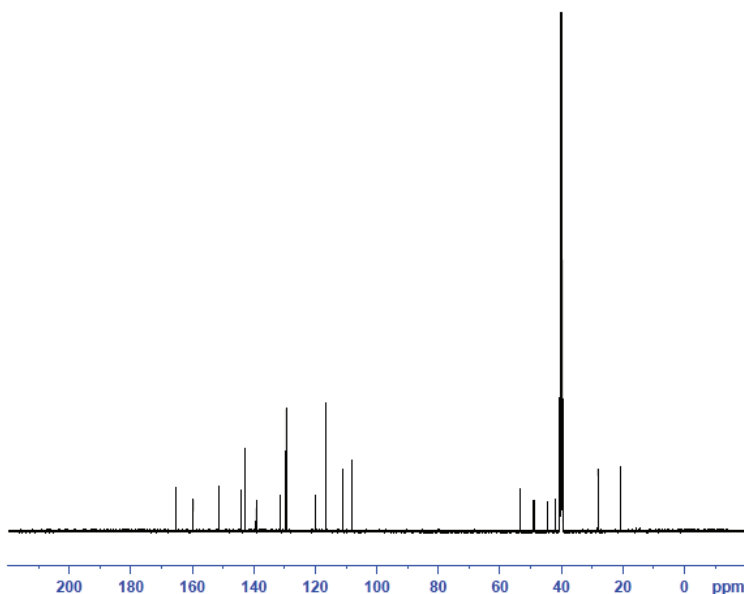


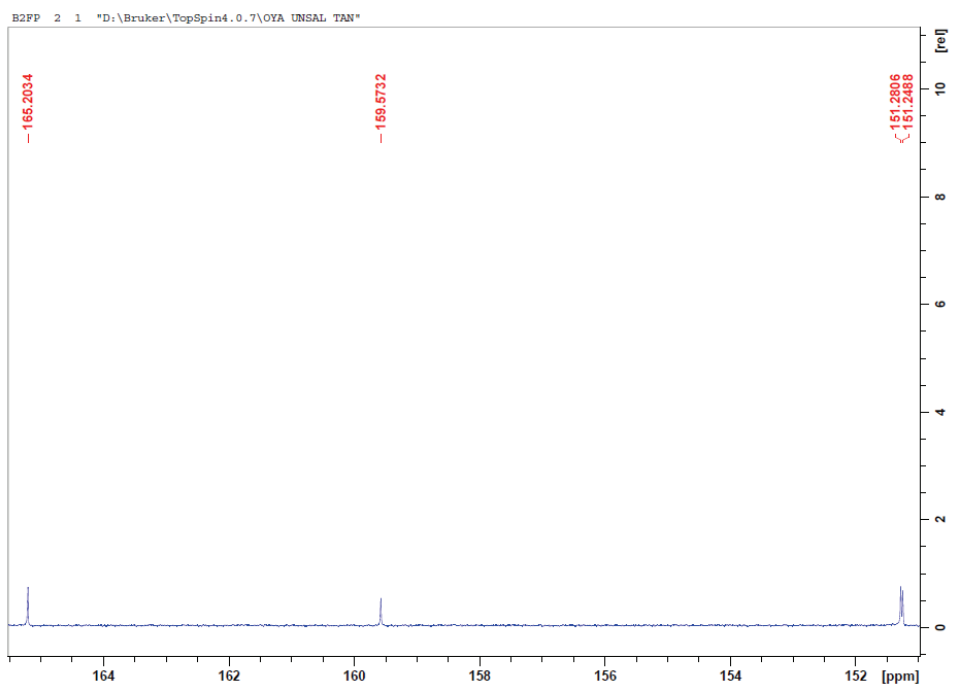
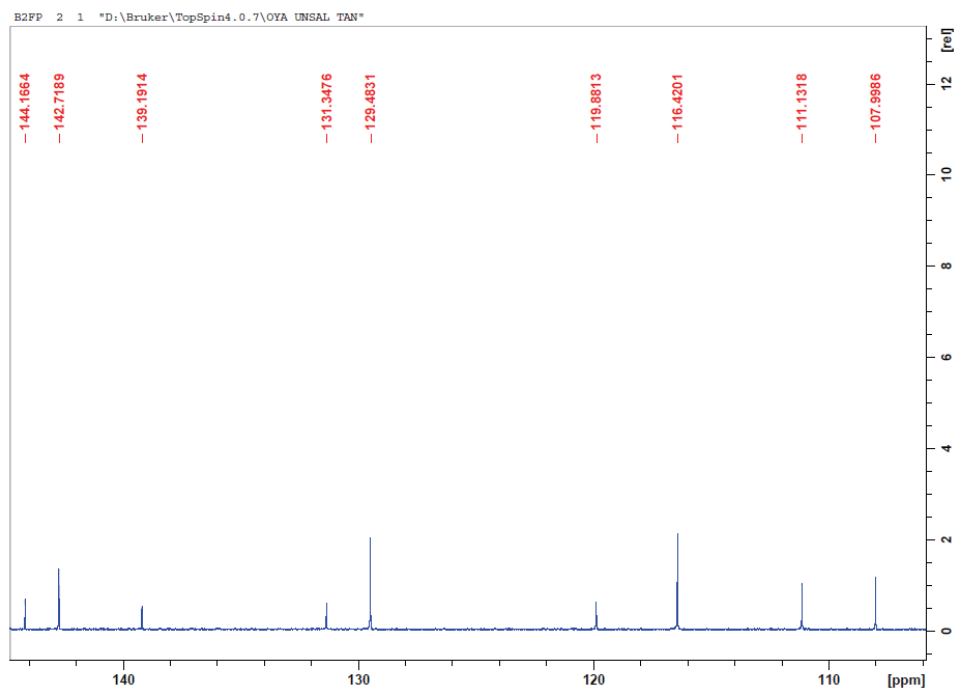
```

Current Data Parameters
NAME      B2FP
EXPRO    2
PROCNO   1

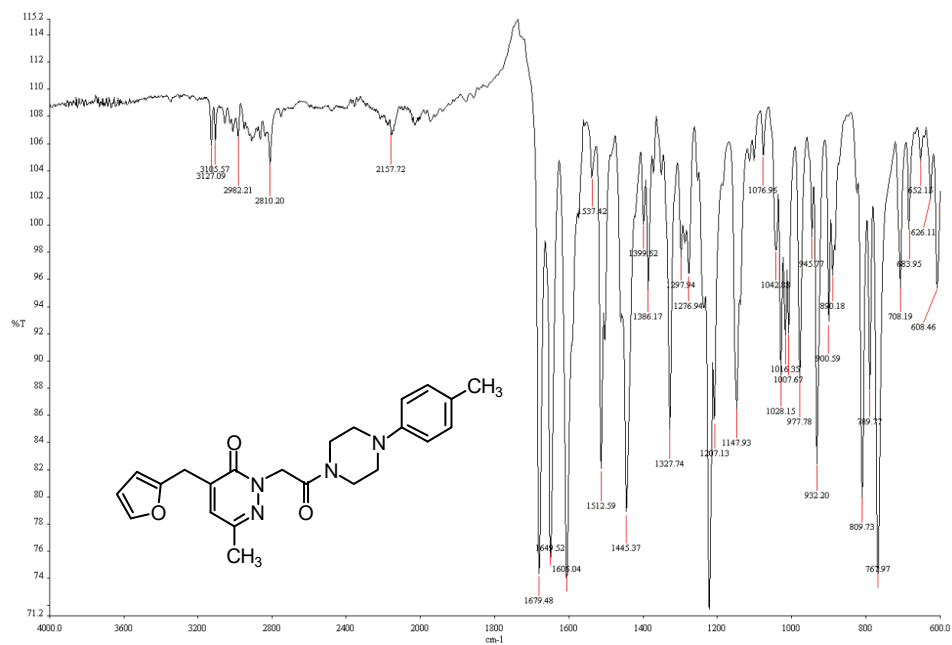
F2 - Acquisition Parameters
Date_    20201022
Time     10.30 h
INSTRUM  Avance
PROBHD   Z151574_0038 (
PULPROG  zgpg30
TD       65536
SOLVENT  DMSO
NS       1500
DS       4
SWH      30120.482 Hz
FIDRES   0.919204 Hz
AQ       1.0878977 sec
RG       101
DW       16.600 usec
DE       6.50 usec
TE       297.7 K
D1       2.0000000 sec
D11      0.0300000 sec
TDO      1
SFO1     125.7703643 MHz
NUC1     13C
PC       3.33 usec
P1       10.00 usec
PLW1     85.18099976 W
SFO2     500.1320005 MHz
NUC2     1H
CPDPRG2  waltz65
PCPD2    80.00 usec
PLW2     24.0428927 W
PLW12    0.24043000 W
PLW13    0.12093000 W

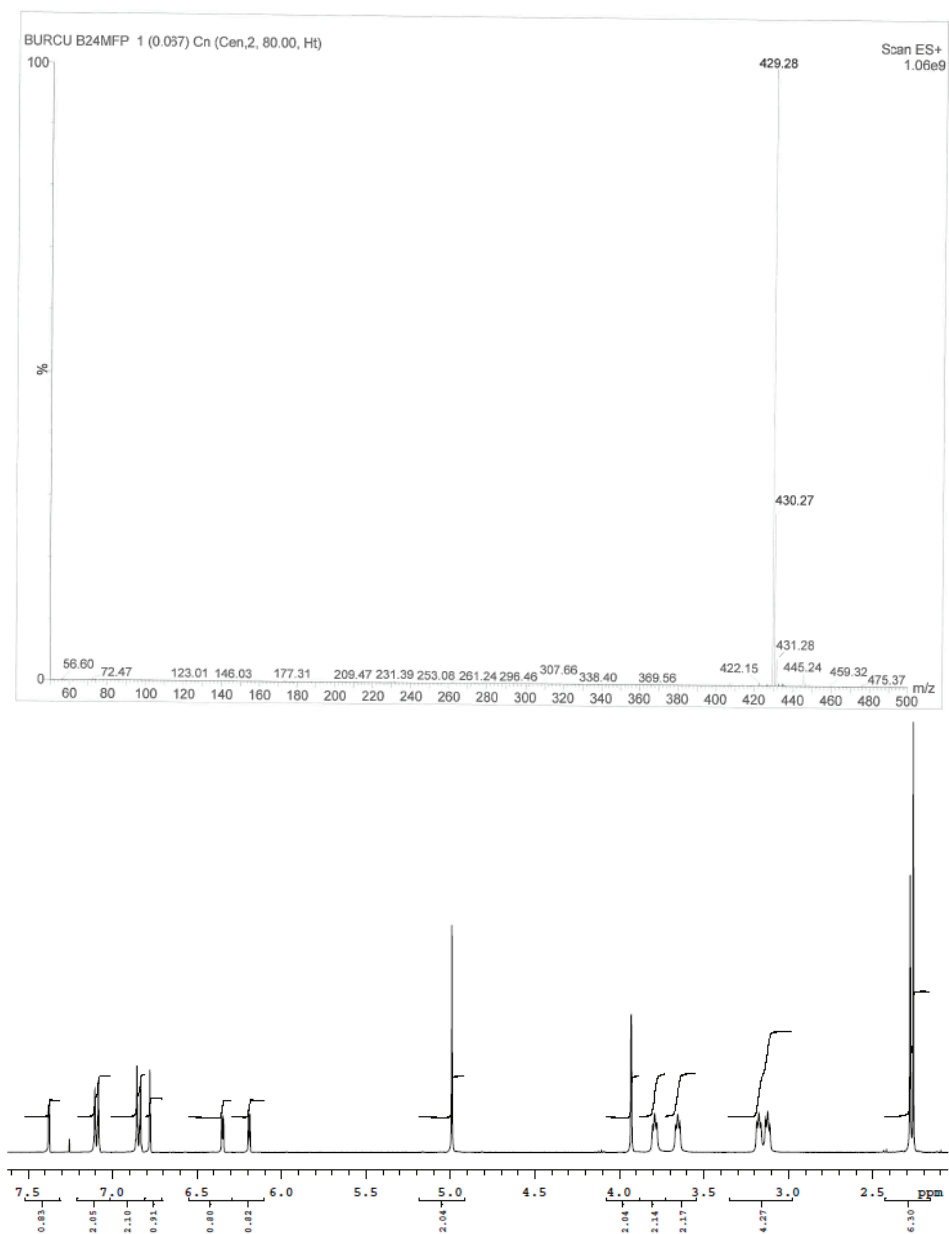
F2 - Processing parameters
SI       32768
SF       125.7577885 MHz
WDW      EM
SSB      0
LB       1.00 Hz
GB       0
PC       1.40
    
```

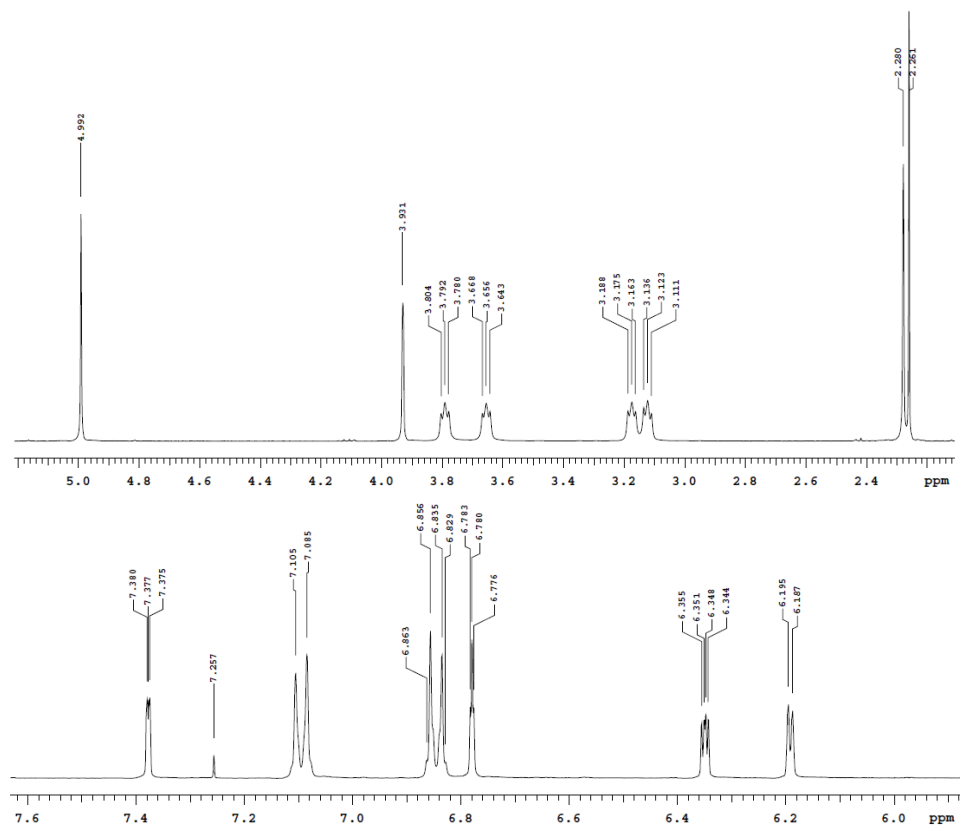




4-(FURAN-2-YLMETHYL)-6-METHYL-2-[2-OXO-2-(4-(4-METHYLPHENYL)PIPERAZIN-1-YL)ETHYL]PYRIDAZIN-3(2H)-ONE (6B)







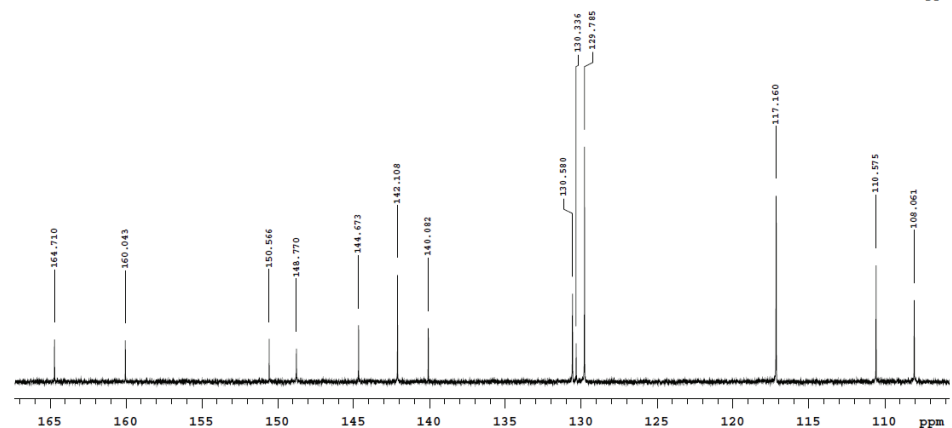
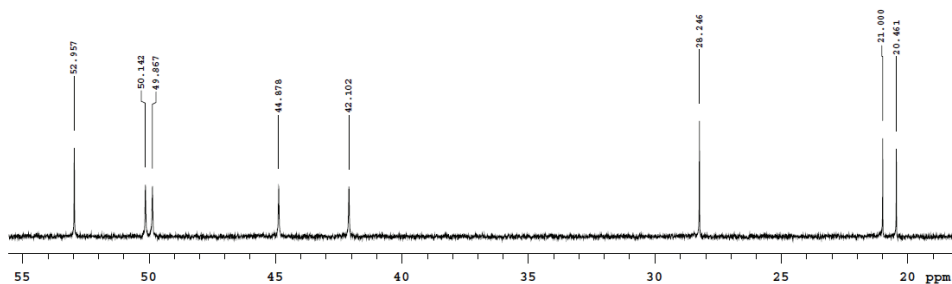
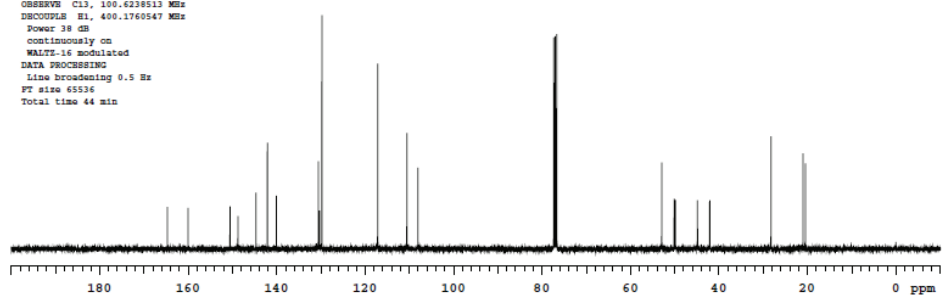
S24MFP
 Sample Name:
 S24MFP
 Data Collected on:
 mercury400-mercury400
 Archive directory:
 /home/vnmr1/vnmrsys/data
 Sample directory:
 S24MFP_20210221_01
 FIDFile: CARBON_01



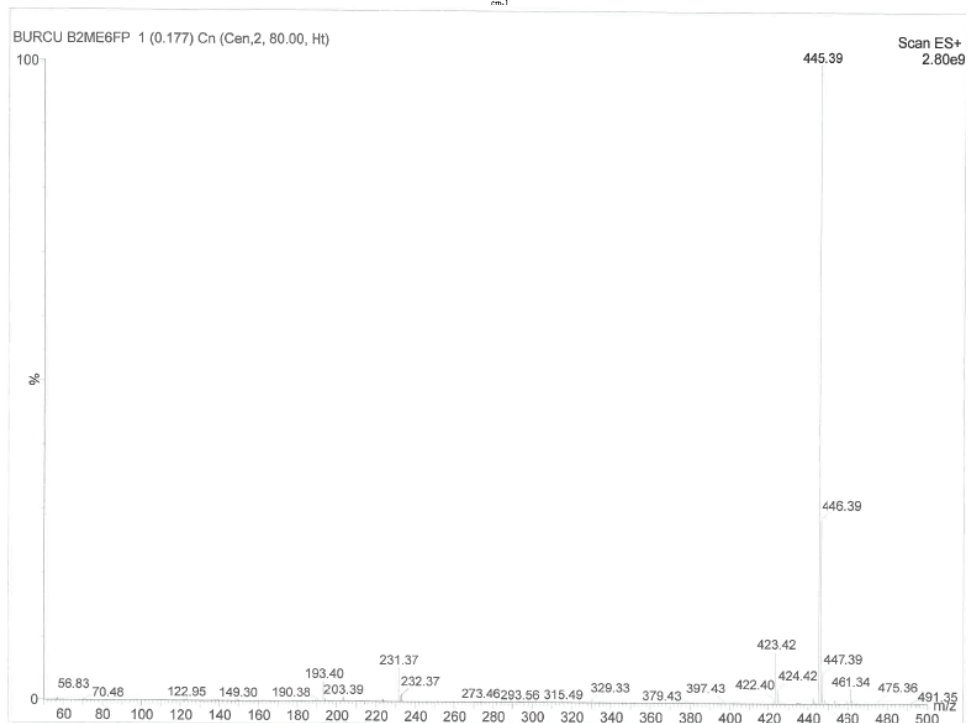
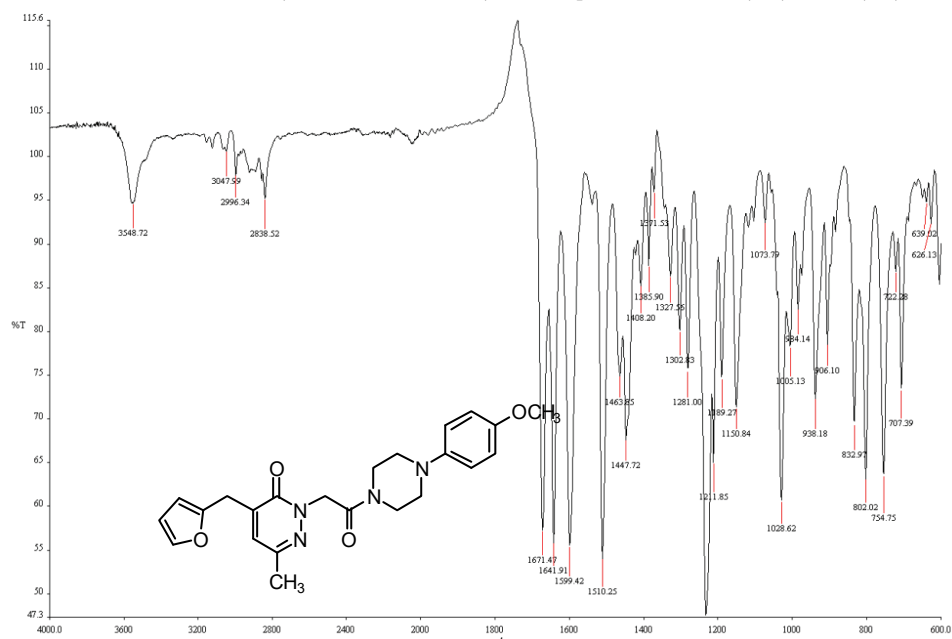
Pulse Sequence: CARBON (s2pul)
 Solvent: cdcl3
 Data collected on: Feb 21 2021

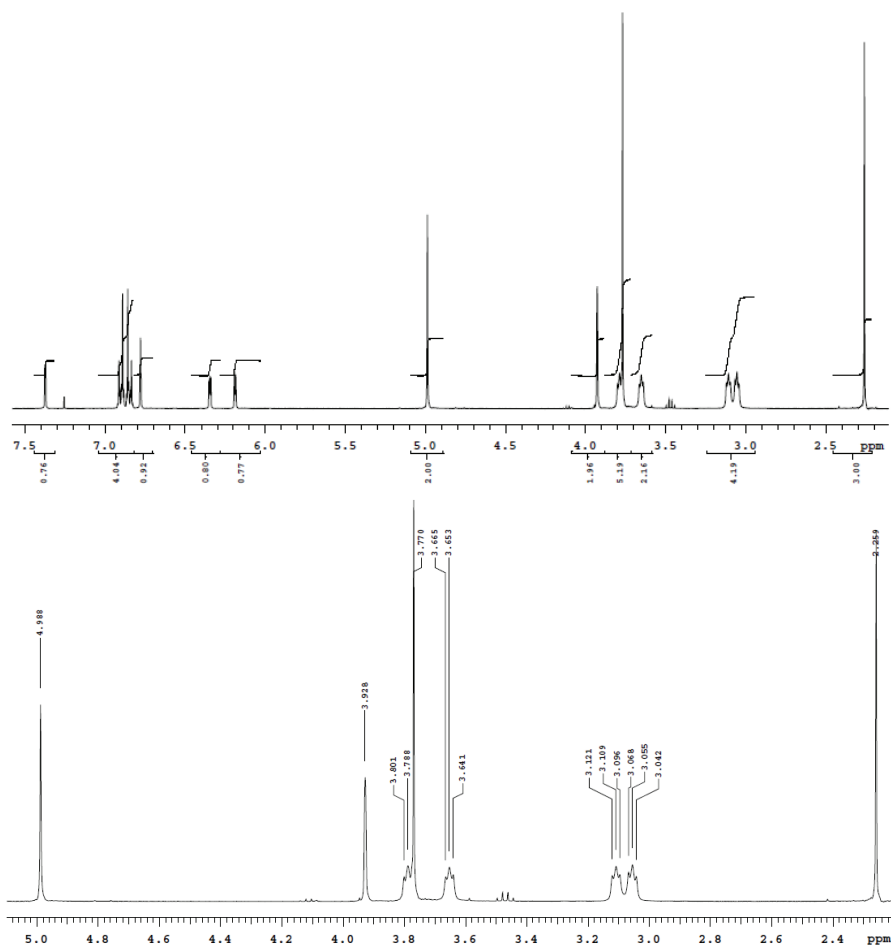
Temp. 23.0 C / 296.1 K
 Operator: vnmr1

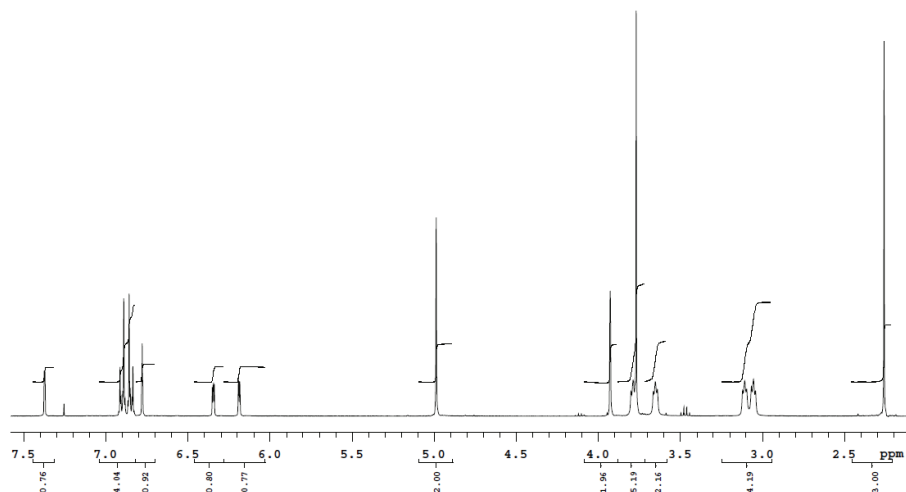
Relax. delay 1.000 sec
 Pulse 45.0 degrees
 Acq. time 1.550 sec
 Width 21141.6 Hz
 1000 repetitions
 OBSERVE C13, 100.6238513 MHz
 DECOUPLE H1, 400.1760547 MHz
 Power 38 dB
 Continuously on
 WALTZ-16 modulated
 DATA PROCESSING
 Line broadening 0.5 Hz
 FT size 65536
 Total time 44 min



4-(FURAN-2-YLMETHYL)-6-METHYL-2-[2-OXO-2-(4-(4-METHOXYPHENYL)PIPERAZIN-1-YL)ETHYL]PYRIDAZIN-3(2H)-ONE (6C)







E2MeOPF

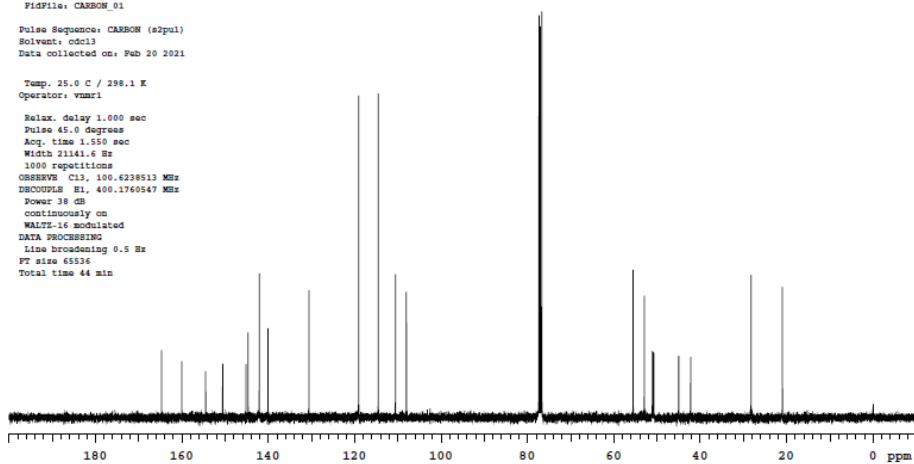
Sample Name:
E2MeOPF
Data Collected on:
mercury400-mercury400
Archive directory:
/home/vmr1/vmr1s/data
Sample directory:
E2MeOPF_20210220_01
FidFile: CARBON_01

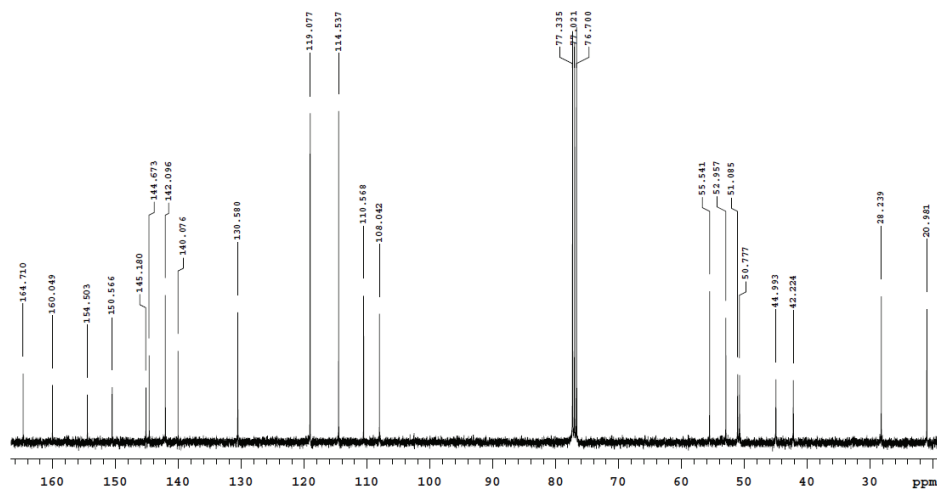


Pulse Sequence: CARBON (s2pul)
Solvent: cdcl3
Data collected on: Feb 20 2021

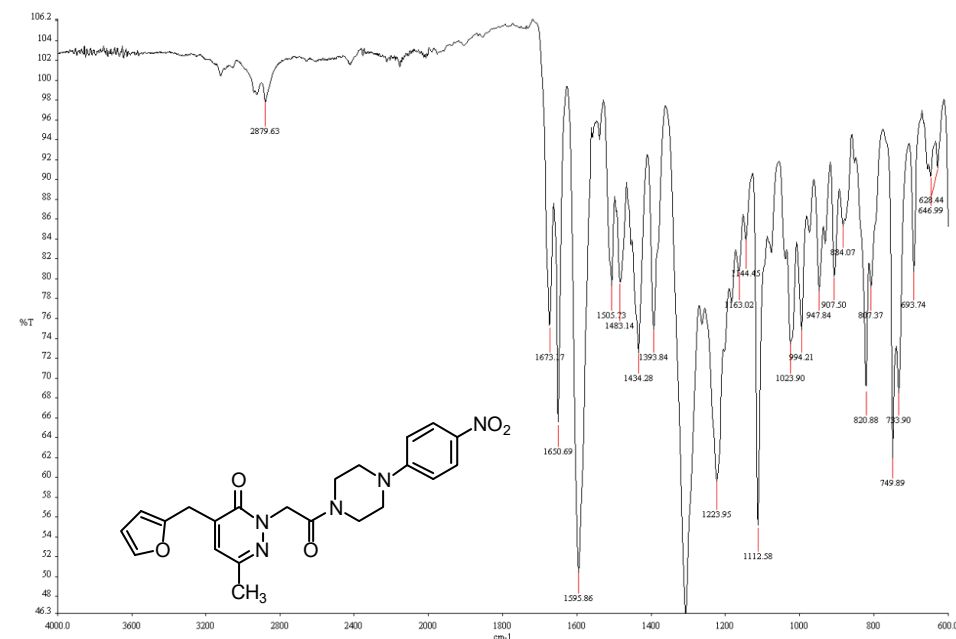
Temp: 25.0 C / 298.1 K
Operator: vmr1

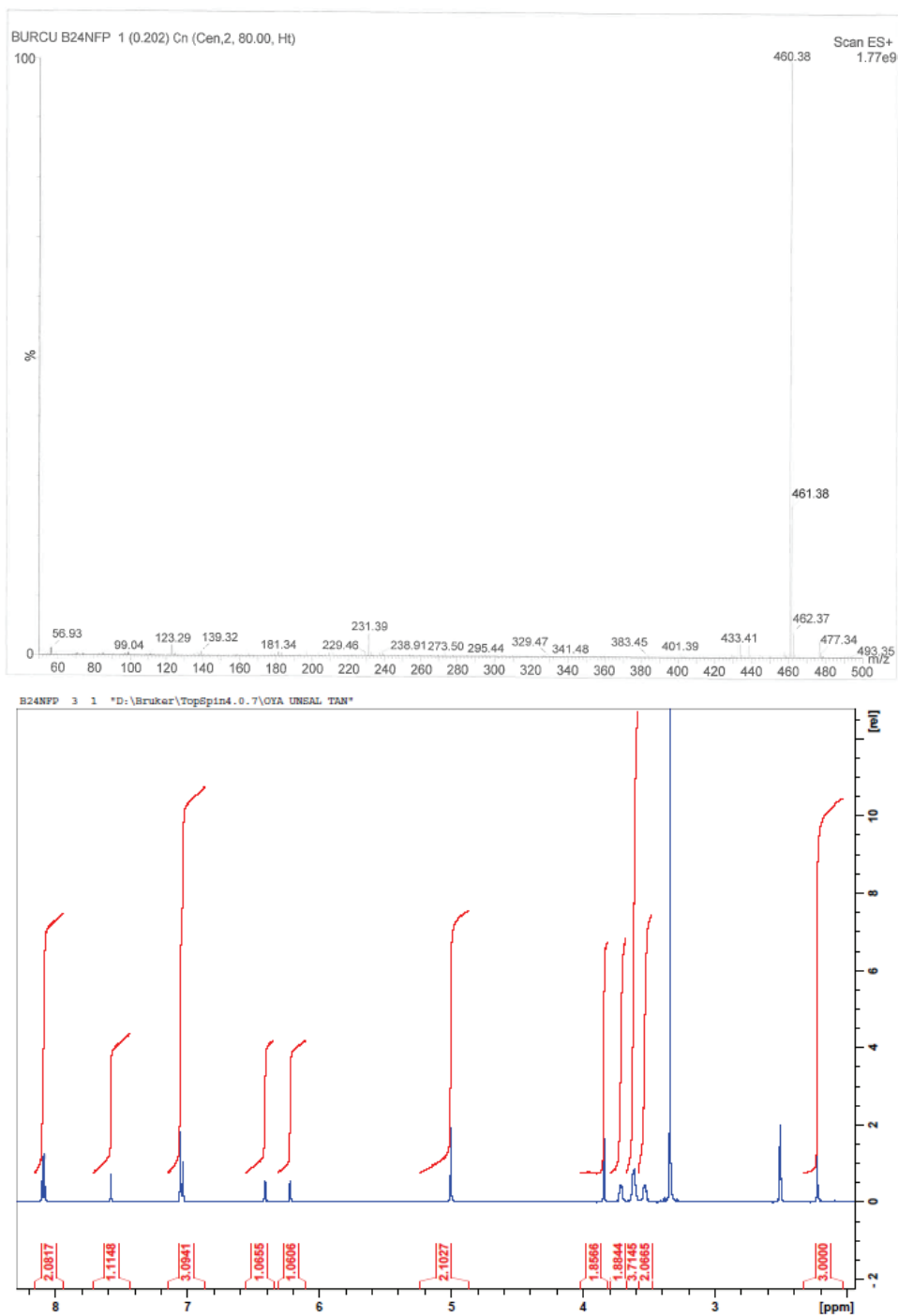
Relax. delay 1.000 sec
Pulse 45.0 degree
Acq. time 1.550 sec
Width 21141.6 Hz
1000 repetitions
OBSERVE ch1, 100.6238513 MHz
NUC1 ch1, 100.6238513 MHz
Power 38 dB
continuously on
WALTZ-16 modulated
DATA PROCESSING
Line broadening 0.5 Hz
FT size 65536
Total time 44 min

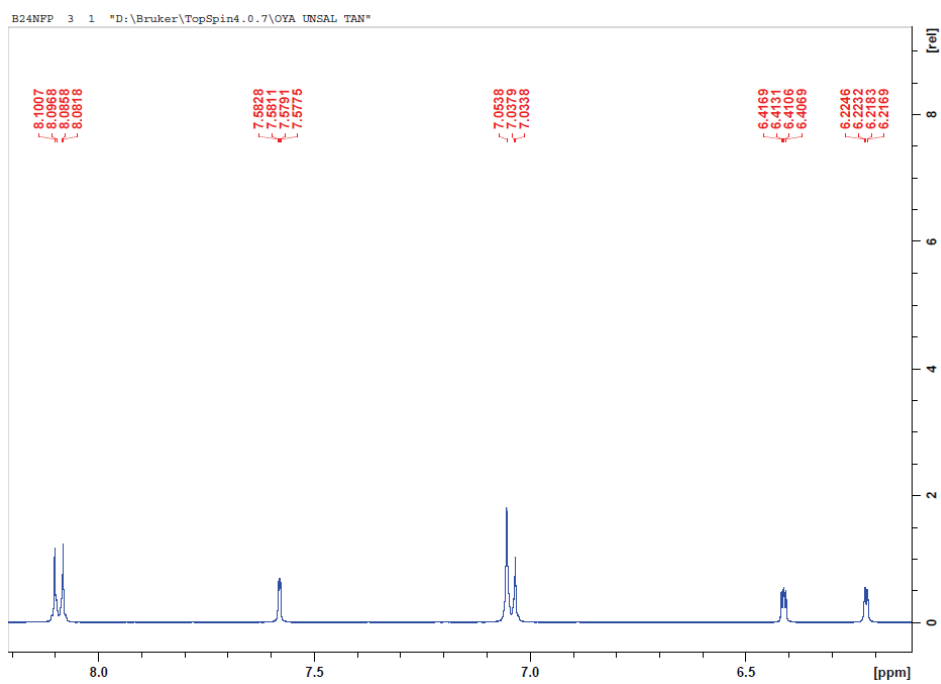
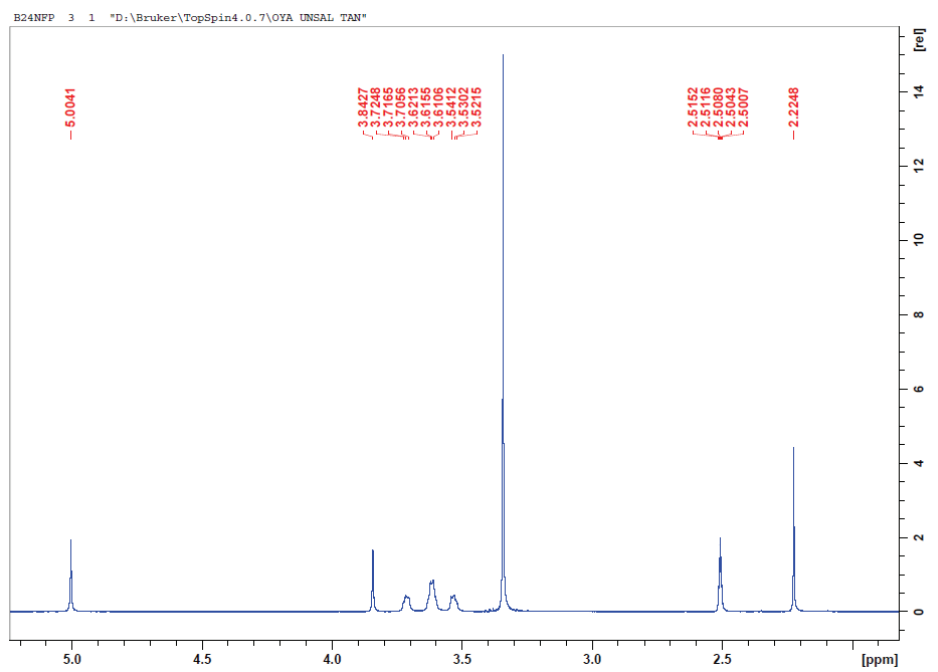




4-(FURAN-2-YLMETHYL)-6-METHYL-2-[2-OXO-2-(4-(4-NITROPHENYL)PIPERAZIN-1-YL)ETHYL]PYRIDAZIN-3(2H)-ONE (6D)







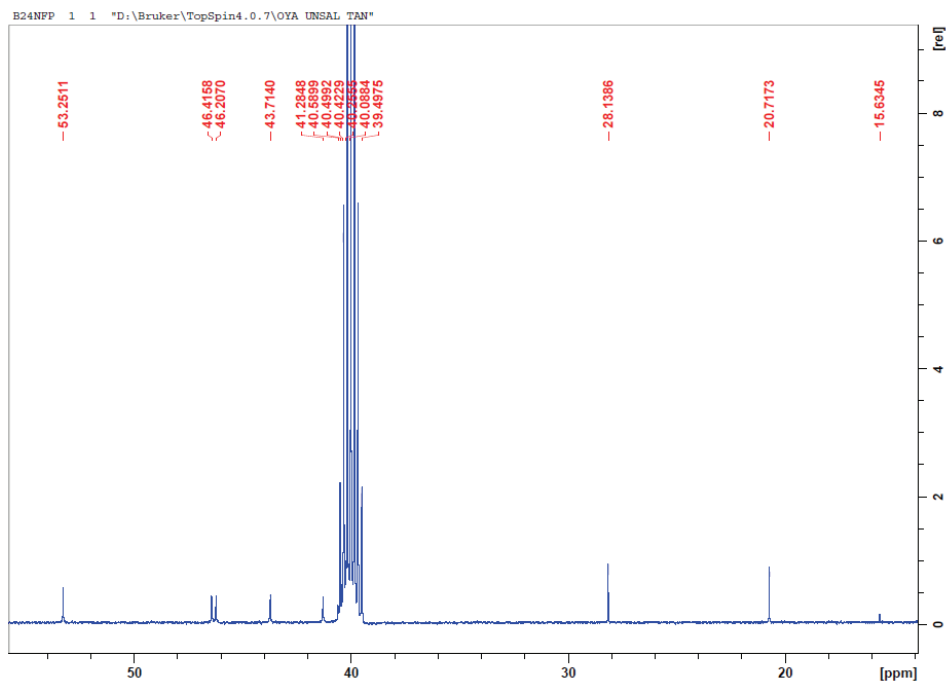
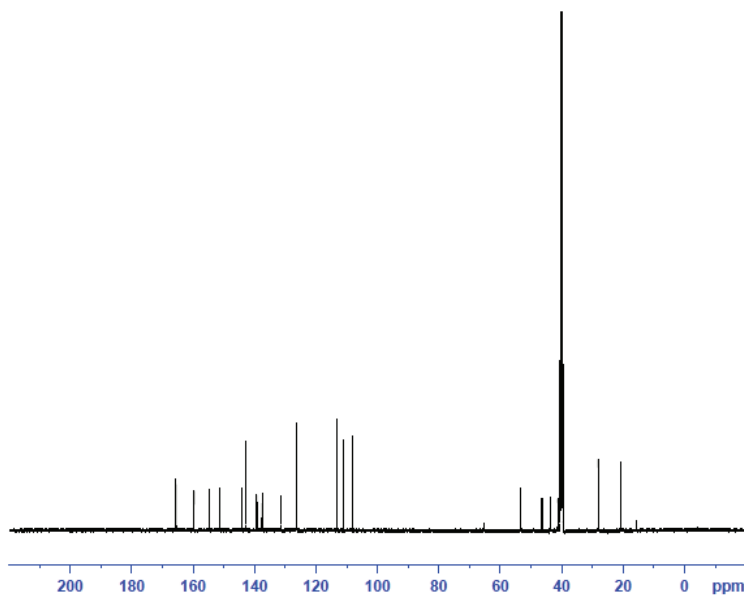


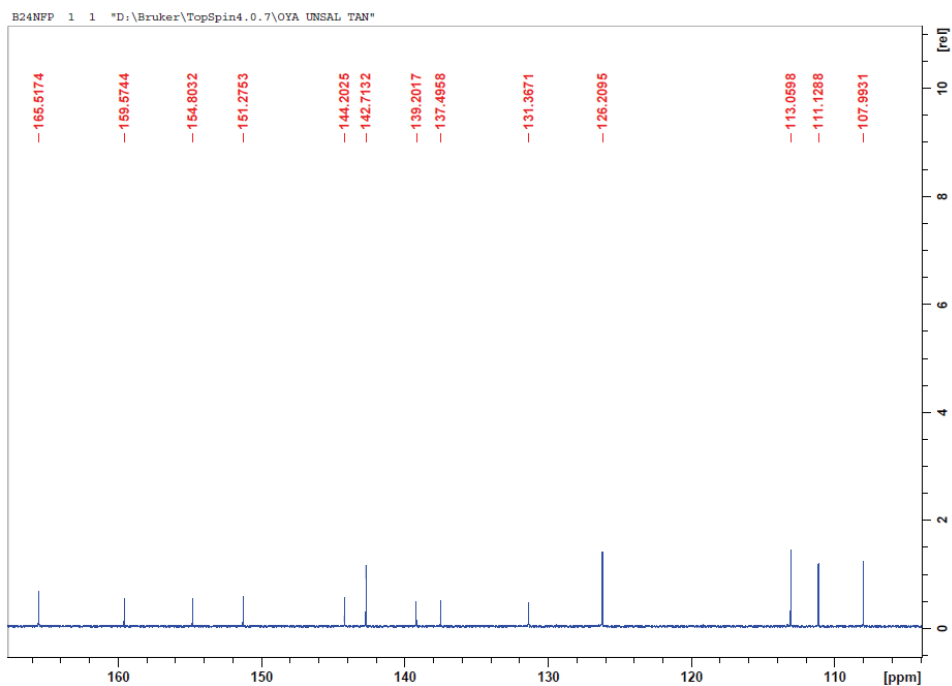
```

Current Data Parameters
NAME      B24NFP
EXPNO    1
PROCNO   1

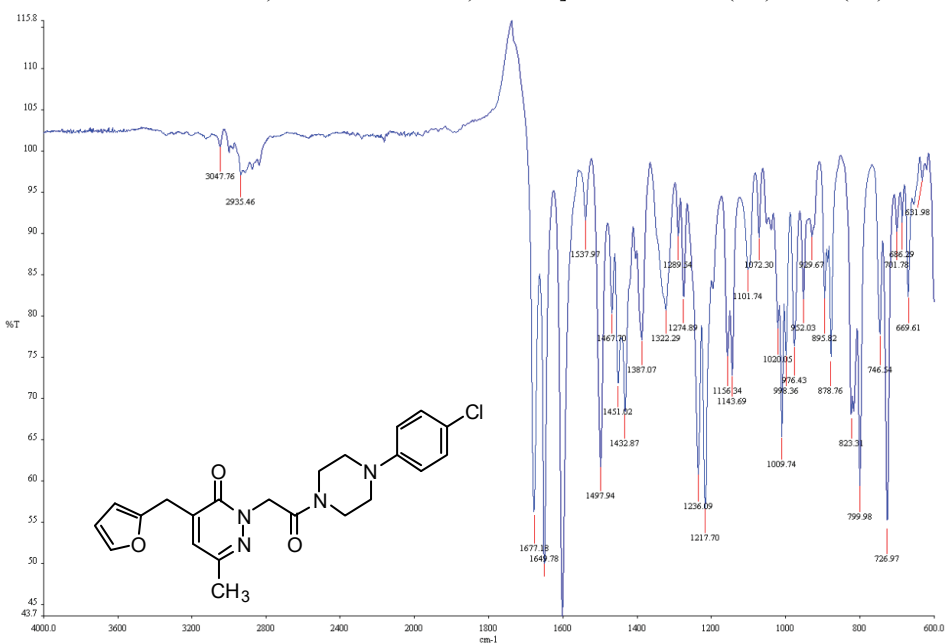
F2 - Acquisition Parameters
Date_    20201022
Time     12.00 h
INSTRUM  Avance
PROBHD   Z151574_0038 (
PULPROG  zgpg30
TD       65536
SOLVENT  DMSO
NS       1600
DS       4
SWH      30120.482 Hz
FIDRES   0.919204 Hz
AQ       1.0878977 sec
RG       101
DW       16.600 usec
DE       6.50 usec
TE       299.2 K
D1       2.00000000 sec
D11      0.03000000 sec
TD0      1
SFO1     125.7703643 MHz
NUC1     13C
PQ       3.32 usec
P1       10.00 usec
PLW1     85.18099976 W
SFO2     500.1320005 MHz
NUC2     1H
CPDPRG2  waltz65
PCPD2    80.00 usec
PLM2     24.0429927 W
PLM12    0.24043000 W
PLM13    0.12093000 W

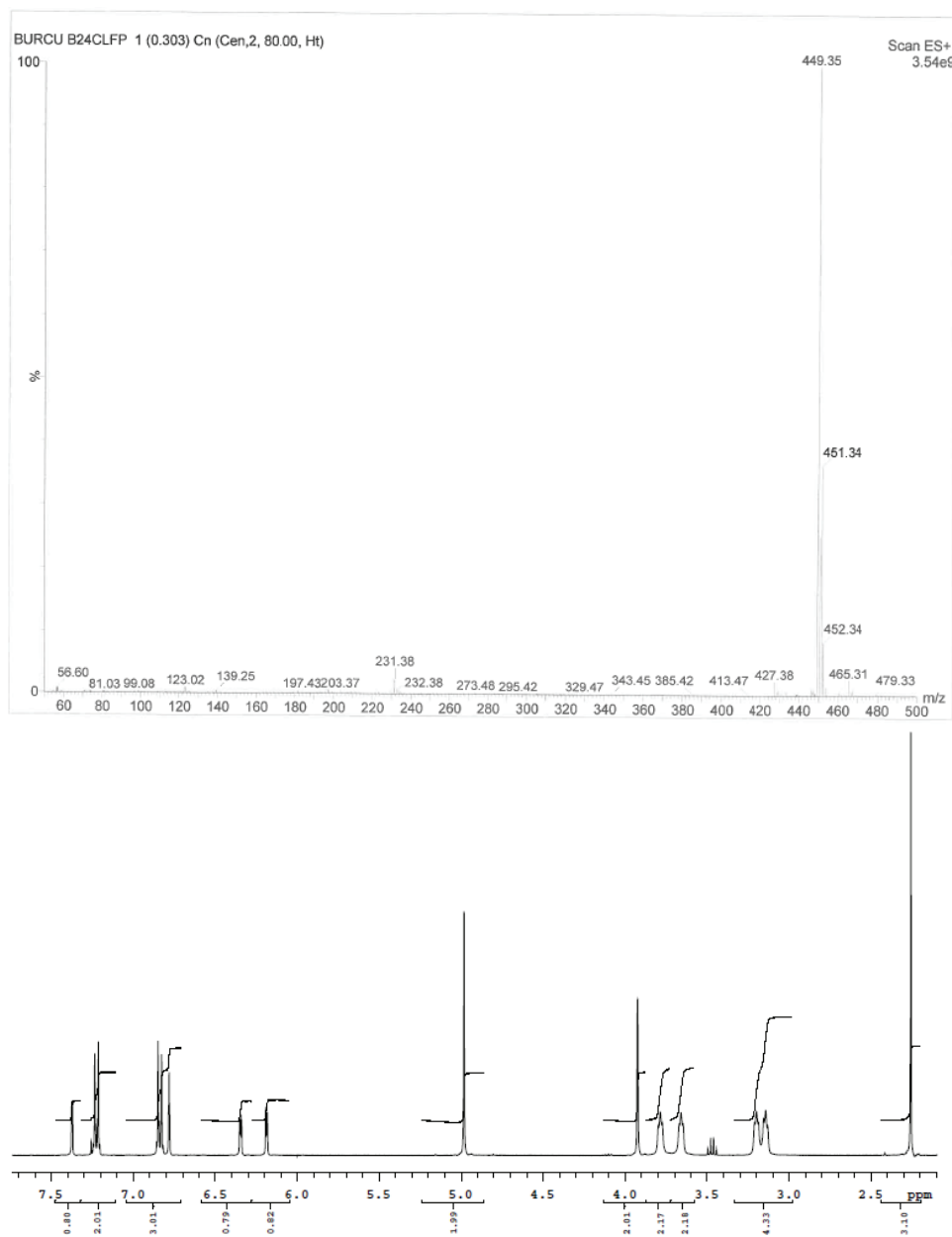
F2 - Processing parameters
SI       32768
SF       125.7577885 MHz
WDW      EM
SSB      0
LB       1.00 Hz
GB       0
PC       1.40
    
```

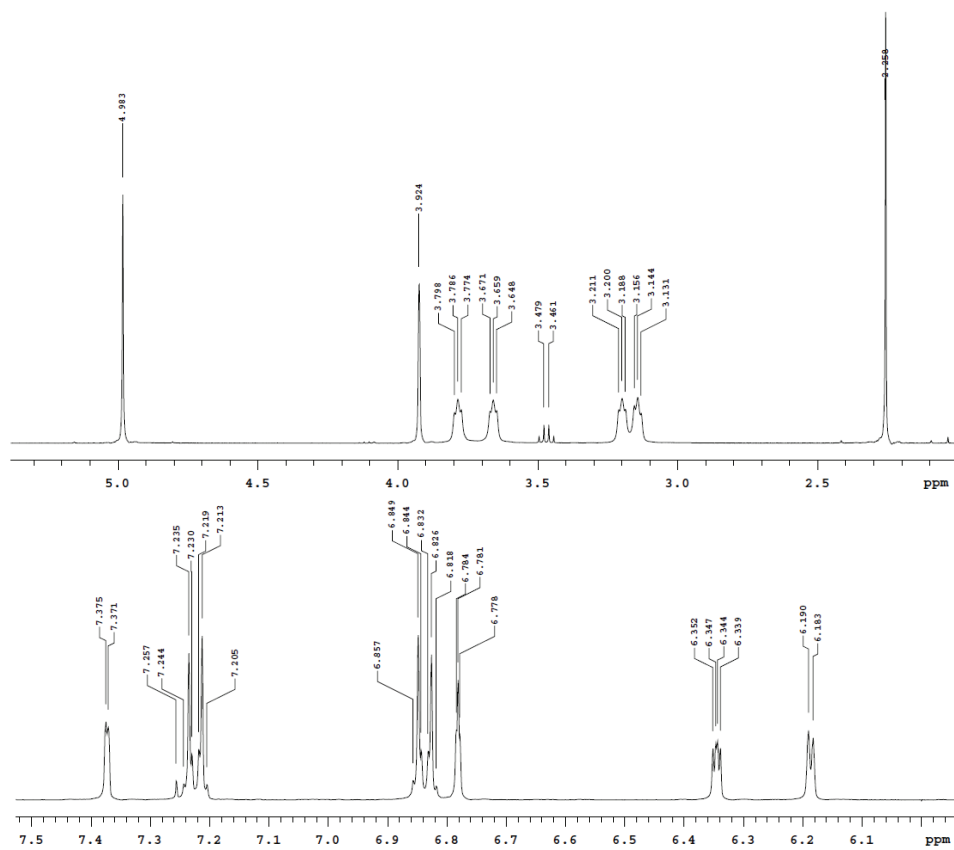




4-(FURAN-2-YLMETHYL)-6-METHYL-2-[2-OXO-2-(4-CHLOROPHENYL)PIPERAZIN-1-YL]ETHYL]PYRIDAZIN-3(2H)-ONE (6E)







B24CLFP

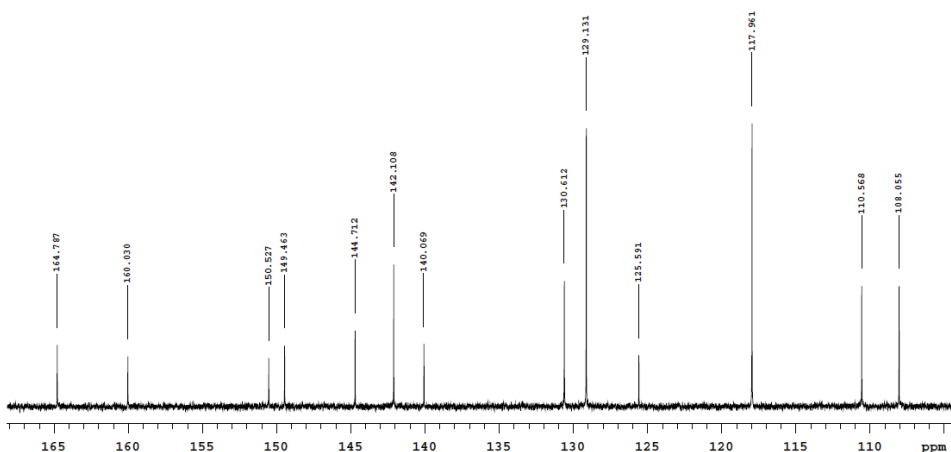
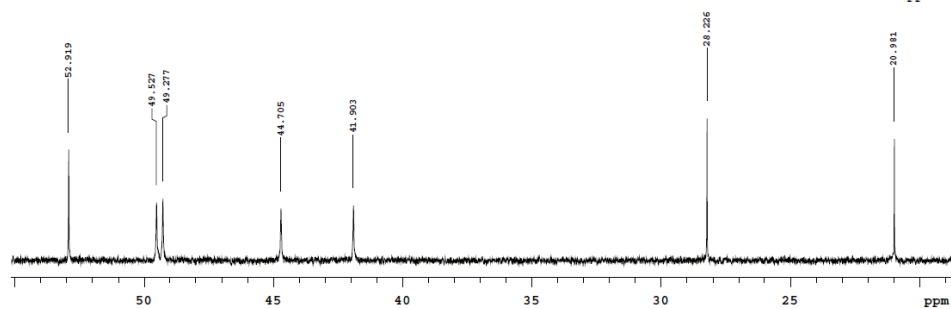
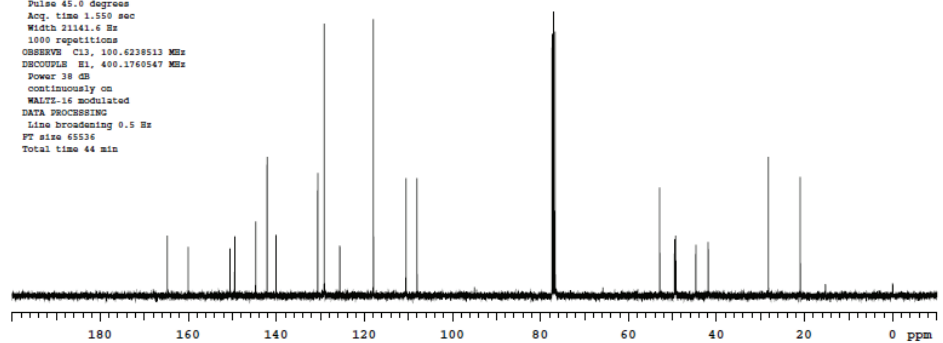
Sample Name:
B24CLFP
Data Collected on:
mercury400-mercury400
Archive directory:
/home/vnmr1/vnmrsys/data
Sample directory:
B24CLFP_20210220_01
FidFile: CARBON_01



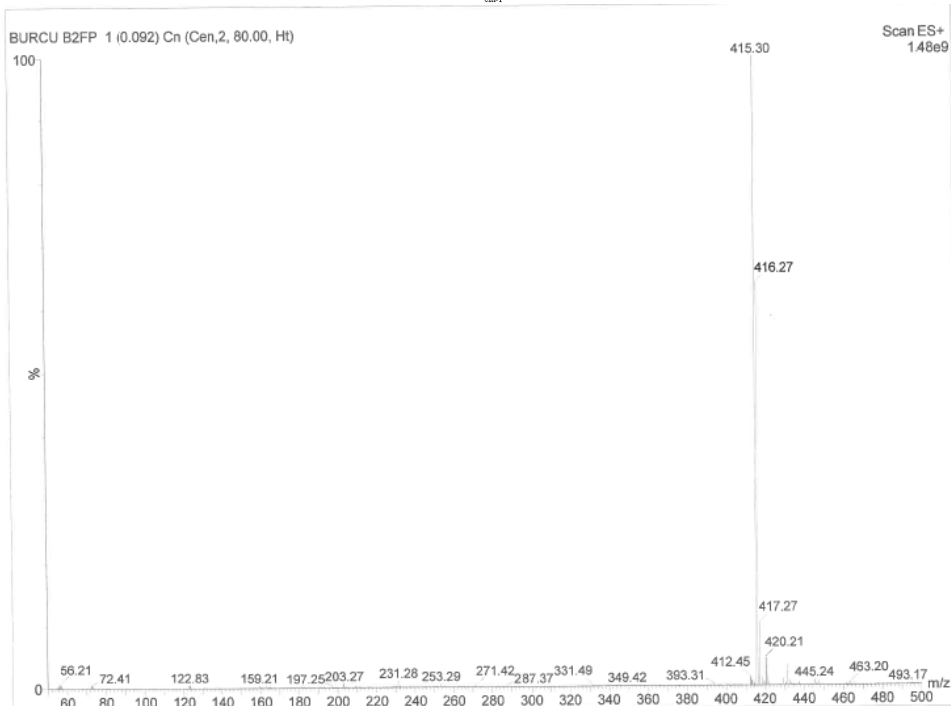
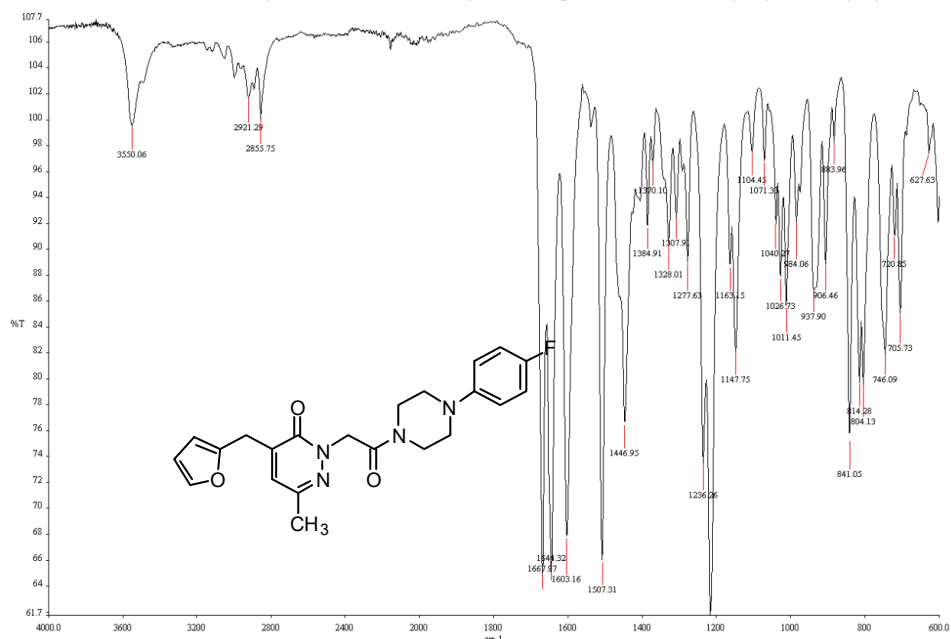
Pulse Sequence: CARBON (s2pul)
Solvent: cdcl3
Data collected on: Feb 20 2021

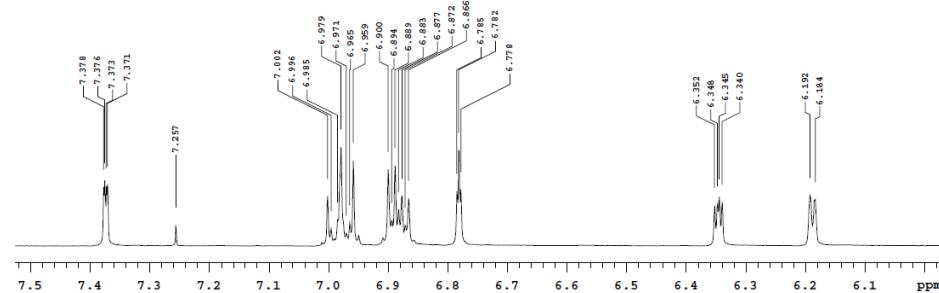
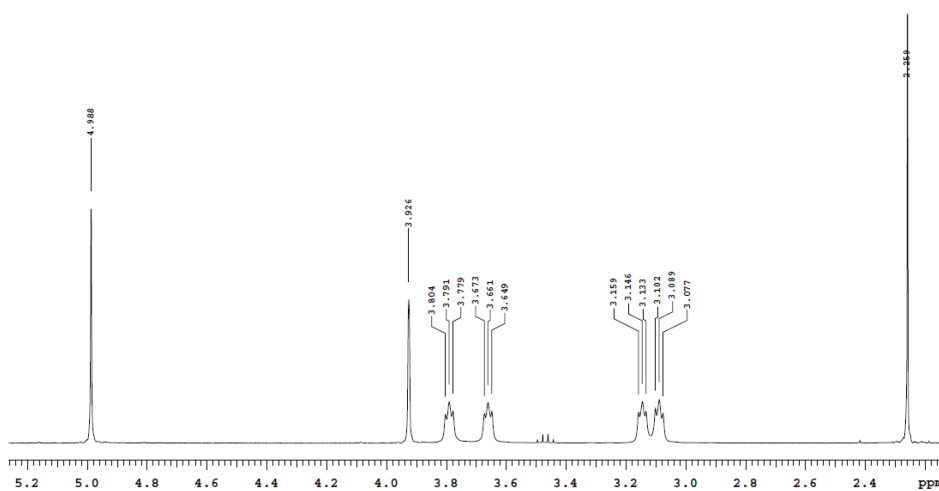
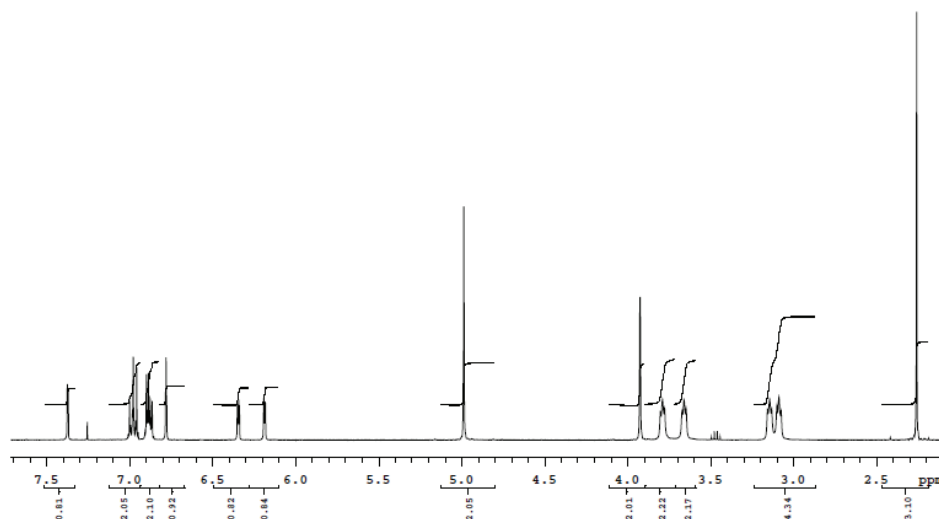
Temp. 25.0 C / 298.1 K
Operator: vnmr1

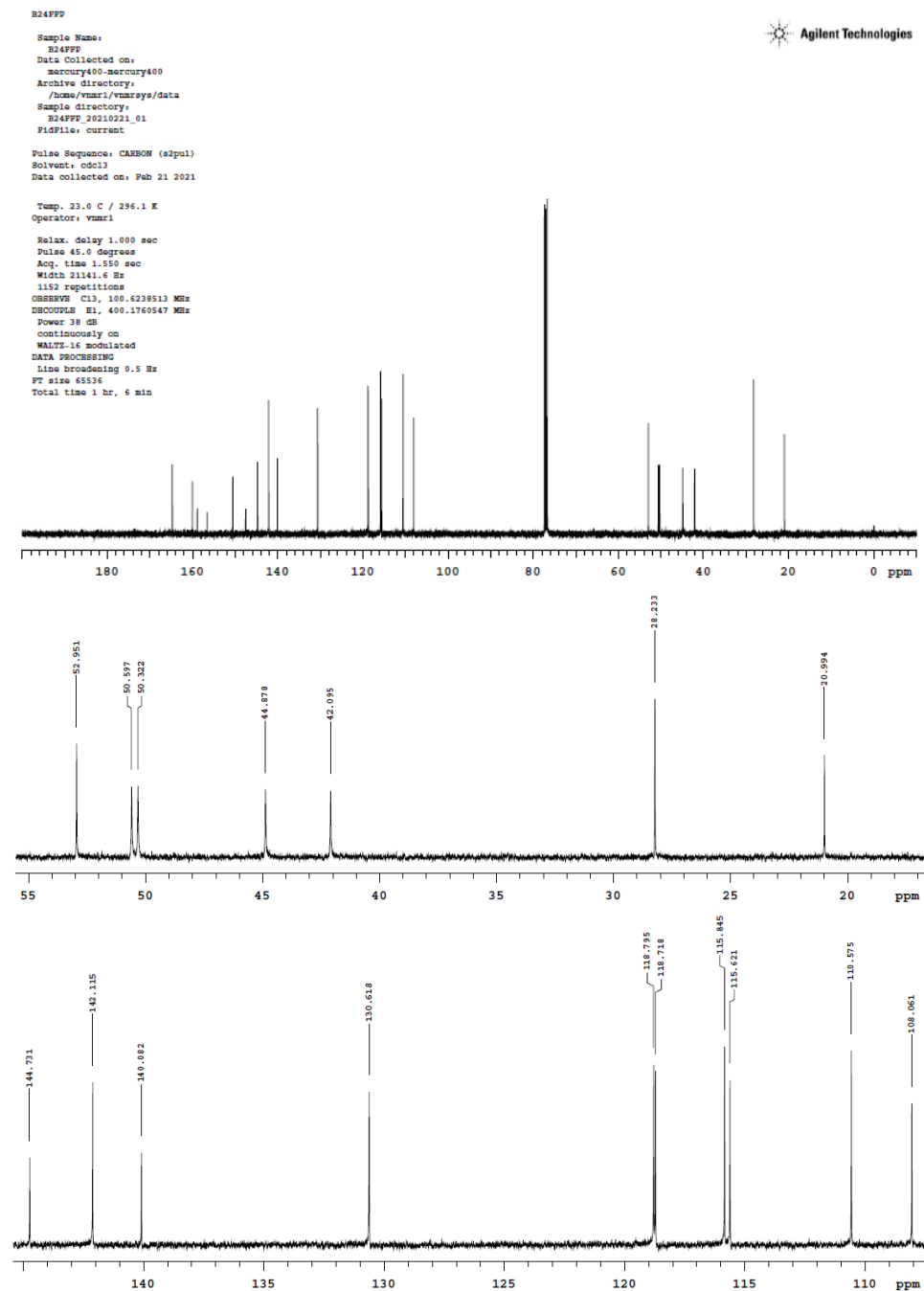
Relax. delay 1.000 sec
Pulse 45.0 degrees
Acq. time 1.550 sec
Width 21141.6 Hz
1600 repetitions
OBSERVE C13, 100.6238513 MHz
DECOUPLE H1, 400.1760547 MHz
Power 38 dB
continuously on
WALTZ-16 modulated
DATA PROCESSING
Line broadening 0.5 Hz
FT size 65536
Total time 44 min

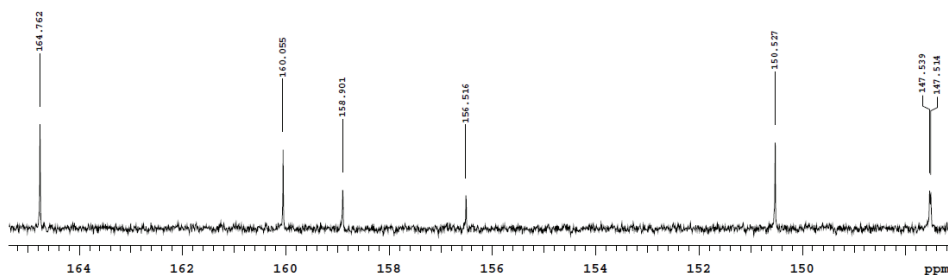


4-(FURAN-2-YLMETHYL)-6-METHYL-2-[2-OXO-2-(4-(4-FLUOROPHENYL)PIPERAZIN-1-YL)ETHYL]PYRIDAZIN-3(2H)-ONE (6F):











J. Serb. Chem. Soc. 89 (11) 1433–1445 (2024)
JSCS–5798

Chemical reactivity of alliin and its molecular interactions with the protease M^{pro} of SARS-CoV-2

WENDOLYNE LÓPEZ-OROZCO, LUIS HUMBERTO MENDOZA-HUIZAR*, GIAAN ARTURO ÁLVAREZ-ROMERO, JESÚS MARTÍN TORRES-VALENCIA and MARICRUZ SANCHEZ-ZAVALA

Academic Area of Chemistry, Universidad Autónoma del Estado de Hidalgo, Carretera Pachuca-Tulancingo, 42184, Mineral de la Reforma, Hidalgo, Mexico

(Received 17 August, revised 9 September, accepted 11 October 2023)

Abstract: In the present work, a computational study of the chemical reactivity of alliin at the X/DGDZVP level of theory (where X is B3LYP, M06, M06L or wB97XD) was performed. The distribution of active sites on alliin was determined by evaluating the Fukui function. For electrophilic attacks, the more reactive sites are on the carbon atoms of the prop-2-ene moiety. The more active sites for nucleophilic attacks are located on the thioether group. In the case of free radical attacks, the more reactive sites are on the carbonyl, thioether and prop-2-ene moieties. Additionally, the molecular docking study revealed that, alliin is able to dock to the protease M^{pro} of SARS-CoV-2 through interactions with the catalytic CYS145-HSD164 dyad *via* van der Waals interactions, with MET49 with interactions alkyl-type ions and with PHE140 by hydrogen bonds. Also, the molecular dynamic study indicates that alliin remains in the pocket site. Last result suggests that this molecule is a potential candidate for further *in vitro* evaluation as a drug for the treatment of the major protease-based SARS-CoV-2 virus.

Keywords: Fukui function; molecular docking; non-covalent.

INTRODUCTION

Alliin (2-amino-3-prop-2-enylsulfanylpropanoic acid), is the most important sulfur compound present in garlic *Allium sativum*.¹ It is well known that alliin is a bioactive compound with medicinal activity, and its organosulfur compounds serve as important storage peptides and synthetic intermediates.² Alliin has shown anticarcinogenic³ and antibiotic activity.⁴ In addition, alliin exhibit cardio and neuroprotective actions and is able to suppress inflammatory responses.² Also, its antiviral activity has been studied for herpes simplex type 1 and 2, influenza type 3, vaccinia virus, stomatitis, vesicular and human rhinovirus; however,

*Corresponding author. E-mail: hhuizar@uaeh.edu.mx
<https://doi.org/10.2298/JSC230817078L>



at working concentrations, it has presented cytotoxicity by which is necessary to extend the study.⁵ Additionally, alliin and its derived sulfoxides have shown a mechanism of action that prevents the formation of free radicals by electron capture, which gives rise to its antioxidant activity.⁶ Also, it has been evaluated as an inhibitor of SARS-CoV-2 M^{Pro} through molecular docking analysis⁷ and molecular dynamics.⁷ It was found that the formation of hydrogen bonds between this serine-type protease and alliin in the active site regions inhibits the COVID-19 outbreak.⁷ Here, it is important to mention that the ΔG energy change of antigen–receptor binding represents the basis of the virus–host interaction at the cell surface, which allows the virus to enter its host cell. Thus, in order to infect a host cell, a virus must have an antigen (for example, the spike glycoprotein of SARS-CoV-2) that has a negative ΔG of binding to the host cell receptor (*e.g.*, the ACE2 receptor for SARS-CoV-2). Thus, thermodynamic and kinetic studies play an important role in the evaluation of antiviral agents because of the complexes formed by virus receptors with the study agent.^{8,9} In this sense, these kinds of studies related to the formation of the alliin–M^{Pro} complex have allowed to evaluate the binding of the complex for different Omicron variants of SARS-CoV-2.¹⁰ Since the binding ΔG plays an important role in determining the stability of the complex with which viral infectivity and mutability may be evaluated. Thus, the bioinformatics studies reported in the literature suggest that alliin may be used alone or in combination with the main therapeutic drug, which would be an efficient therapy to eradicate SARS-CoV-2 with the lowest side effects and toxicity.^{7,11} Nevertheless, no drugs have been developed based on the potential of this bioactive molecule because it is necessary more information related to the alliin–receptor binding. Additionally, we consider that the determination of alliin electronic properties would allow understanding the therapeutic effect towards different diseases. In this sense, to the best of our knowledge, only different sulfur derivatives of alliin have been studied from theoretical point of view employing semiempirical methods¹² and *ab initio* methods in order to investigate their structural properties, vibrational modes and electronic structure.¹³ Thus, in the present work, we evaluated the global and local reactivity parameters of alliin, the binding energy of the complex alliin–M^{Pro}, and validate the docking analysis with a molecular dynamic study. We believe that this type of study contributes to a better understanding of the chemical behaviour of this important bioactive compound.

Theory

Within the framework of density functional theory, it is possible to derive parameters that can be used to analyse the reactivity of a molecular system, such as: the electronic chemical potential (μ), electronegativity (χ), hardness (η) and the electrophilicity index (ω):¹⁴

$$\mu = \left(\frac{\partial E}{\partial N} \right)_{v(r)} = -\frac{1}{2}(I + A) = \frac{1}{2}(\varepsilon_L + \varepsilon_H) \quad (1)$$

$$\chi = -\mu \quad (2)$$

$$\eta = \left(\frac{\partial \mu}{\partial N} \right)_{v(r)} = \left(\frac{\partial^2 E}{\partial N^2} \right)_{v(r)} = (I - A) = (\varepsilon_L - \varepsilon_H) \quad (3)$$

$$\omega = \frac{\mu^2}{2\eta} \quad (4)$$

In these equations, E , N and $v(r)$ are the energy, the number of electrons and the external potential exerted by the nuclei, respectively. I is the ionization potential and A corresponds to the electronic affinity. ε_L is the energy of the lowest unoccupied molecular orbital (LUMO), while ε_H is the energy of the highest occupied molecular orbital (HOMO).¹⁵ The electronic chemical potential is related with the electronic escape tendency.¹⁶ The hardness is related to the stability of molecular systems¹⁷ because it allows measuring the chemical susceptibility of the species to accept electrons.¹³ The electrophilicity index suggests a good nucleophile for higher values, while it indicates the presence of a good electrophile at higher values. In addition, it is possible to define the powers of electroacceptance (ω^-) and electrodonation (ω^+):¹³

$$\omega^- = \frac{(\mu^-)^2}{2\eta} = \frac{(-\frac{1}{4}(3I + A))^2}{2(I - A)} = \frac{(-\frac{1}{4}(3\varepsilon_L + \varepsilon_H))^2}{2(\varepsilon_L - \varepsilon_H)} \quad (5)$$

$$\omega^+ = \frac{(\mu^+)^2}{2\eta} = \frac{(-\frac{1}{4}(I + 3A))^2}{2(I - A)} = \frac{(-\frac{1}{4}(\varepsilon_L + 3\varepsilon_H))^2}{2(\varepsilon_L - \varepsilon_H)} \quad (6)$$

Also, the Fukui function (FF), $f(r)$, is a local parameter commonly used to identify the regions of increased activity on a molecular system,¹⁸ and is defined as follows:¹⁸

$$f(r) = \left(\frac{\partial \rho(r)}{\partial N} \right)_{v(r)} = \left(\frac{\partial \mu(r)}{\partial v(r)} \right) \quad (7)$$

where $\rho(r)$ is the electron density. Note that Eq. (7) allows us to identify the regions in which the electron density is modified by varying the number of electrons, which is useful for identifying the molecular regions most susceptible to nucleophilic and electrophilic attacks.¹⁹ Also, it is possible to evaluate FF using different approaches which are: a) frozen core approximation (FC)¹⁸, b) finite differences (FD)¹⁸ and c) finite differences employing atomic charges (FDAC).²⁰ Under the FC approximation, FF is evaluated as:

$$f^-(r) = \varphi_H^*(r)\varphi_H(r) = \rho_H(r) \quad (8)$$

$$f^+(r) = \varphi_L^*(r)\varphi_L(r) = \rho_L(r) \quad (9)$$

where $f^-(r)$ and $f^+(r)$ correspond to electrophilic and nucleophilic attacks, respectively, $\rho_H(r)$ is the electron density of the HOMO orbital, and $\rho_L(r)$ is the electron density of the LUMO orbital. In the case of FD and FDAC approximations, it is possible to define the FF for the electrophilic, the nucleophilic and the free radical attacks $f^0(r)$. Thus, in the FD approximation, FF is determined as:

$$f^-(r) = \rho_N(r) - \rho_{N-1}(r) \quad (10)$$

$$f^+(r) = \rho_{N+1}(r) - \rho_N(r) \quad (11)$$

$$f^0(r) = \frac{1}{2}(\rho_{N+1}(r) - \rho_{N-1}(r)) \quad (12)$$

where $\rho_{N+1}(r)$, $\rho_N(r)$ and $\rho_{N-1}(r)$ correspond to the electron density of the anionic, neutral and cationic species, respectively. In the third approximation (FDAC), q_j is the atomic charge at the j ésimo site for neutral (N), anionic ($N+1$), or cationic ($N-1$) of the chemical species:

$$f_j^-(r) = q_{j(N-1)} - q_{j(N)} \quad (13)$$

$$f_j^+(r) = q_{j(N)} - q_{j(N+1)} \quad (14)$$

$$f_j^0(r) = \frac{1}{2}(q_{j(N-1)} - q_{j(N+1)}) \quad (15)$$

EXPERIMENTAL

The alliin structure was subjected to full geometric optimization in the aqueous phase employing the X/DGDZVP level of theory²¹ (where X is B3LYP,²² M06,²³ M06L²⁴ or ω B97XD²⁵). The solvent phase optimization was carried out using the continuous polarizable model (PCM) developed by Tomasi *et al.*²⁶ In all cases, vibrational frequencies were calculated to ensure that the stationary points were minimal on the potential energy surface. All quantum calculations reported in this research were performed with the Gaussian program 09²⁷ and visualized with the packages GaussView,²⁸ Gabedit²⁹ and Multwfn.³⁰ The docking study was performed through the Swiss Bioinformatics Institute website with the free software SwissDock.³¹ Visualizations of the ligand/receptor complex were performed by the programs Chimera³² and Discovery Studio Visualizer 2019.³³

RESULTS AND DISCUSSION

Reactivity parameters and molecular interactions

The alliin structure was optimized without restrictions at the X/DGDZVP level of theory at gas and aqueous phase³ (where X is B3LYP,²² M06,²³ M06L²⁴ or ω B97XD²⁵), as can be seen in Fig. 1. Here, it is important to mention that no significant differences were obtained, neither in distances nor in angles, when the

solvent effect was considered at the different levels of theory employed in this work. All the frequency values calculated at the theoretical level X/DGDZVP²¹ in both phases were positive and are in good agreement with the values reported in the literature, suggesting that the level of theory employed is able to predict the electronic properties of alliin. A summary of the main bands for the aqueous phase present in the alliin spectrum is shown in Fig. S-1 of the Supplementary material to this paper which are at 270 cm⁻¹ for the N–H bending out of plane, 580 cm⁻¹ O–H bending out of plane, 970 cm⁻¹ S=O stretching, 1160 cm⁻¹ N–C stretching, 3060 cm⁻¹ C–H stretching, 3500 cm⁻¹ N–H stretching and 3690 cm⁻¹ O–H stretching.

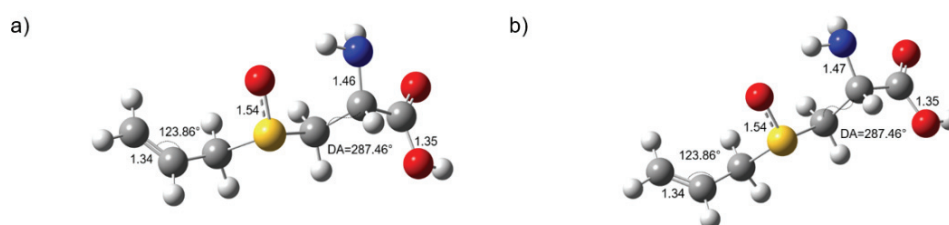


Fig. 1. Structure of alliin. a) Gas phase and b) aqueous phase, optimized at the B3LYP/DGDZVP level of theory in the aqueous phase using the PCM solution model. Bond distances are given in Å, DA = dihedral angle.

Global reactivity descriptors

The global reactivity descriptors for alliin were evaluated using Eqs. (1)–(6) and are reported in Table I. The electronic chemical potential values indicate that alliin is a good nucleophile. It is also a stable molecule according to the hardness values obtained at all levels of theory. Note that the presence of a solvent has no effect on the global chemical reactivity of alliin.

Local reactivity parameters

The local reactivity of a molecular system can be evaluated through the Fukui Function, using the FC and FD approximations. Fig. 2 shows the distribution of the electrophilic sites in alliin, using the FC approximation in the aqueous phase, it is worth mentioning that a similar behaviour was observed in the gas phase (see Fig. S-2 of the Supplementary material). Note that for alliin the HOMO distribution is localized over the sulfoxide and the alkene, while the LUMO distribution is localized over the whole molecule except for the nitrogen bonded hydrogens.

The evaluation of the Fukui Function using the FD approximation (Eqs. (10)–(12)) in the aqueous phase is reported in Fig. 3 for alliin. The most active sites towards nucleophilic attacks are found at 1C, 2C and 9C (Fig. 3a), on the alkene carbons. For electrophilic attacks, the most reactive sites are found at pos-

itions 3C, 4S and 5O (Fig. 3b), in the thioether region, while for free radical the attacks on the most reactive sites are the same sites as the total for nucleophilic and electrophilic attacks (Fig. 3c). It is clear from the FD approach that the most reactive sites are located in the same positions for the gas and aqueous phase, which is indicative that they are showing the same reactivity to the different types of attacks (see Fig. S-3 of the Supplementary material).

TABLE I. Global reactivity parameters calculated for alliin, evaluated at the X/DGDZVP level of theory (where X is B3LYP, M06, M06L or ω B97XD) in aqueous and gas phases, using Eqs. (1)–(6). Values in parentheses correspond to the values calculated using Koopmans theorem

Level type	I / eV	A / eV	μ / eV	μ / eV	μ^-	μ^+	χ / eV	ω / eV	ω^+ / eV	ω^- / eV
Aqueous										
B3LYP	6.76	0.94	-3.85	5.81	-6.76	-0.94	3.85	1.27	0.08	3.93
	(-0.83)	(-6.76)	(3.80)	(5.92)	(0.83)	(6.76)	(-3.80)	(1.22)	(3.85)	(0.06)
M06	6.89	0.82	-3.86	6.07	-6.89	-0.82	3.86	1.22	0.06	3.91
	(-0.51)	(-7.07)	(3.79)	(6.56)	(0.51)	(7.07)	(-3.79)	(1.09)	(3.81)	(0.02)
M06L	8.64	0.96	-4.80	7.68	-8.64	-0.96	4.80	1.50	0.06	4.86
	(0.96)	(-5.89)	(2.46)	(6.85)	(-0.96)	(5.89)	(-2.46)	(0.44)	(2.53)	(0.07)
WB97XD	6.92	0.33	-3.63	6.59	-6.92	-0.33	3.63	1.00	0.01	3.63
	(1.28)	(-8.90)	(3.81)	(10.18)	(-1.28)	(8.90)	(-3.81)	(0.71)	(3.89)	(0.08)
Gas										
B3LYP	6.75	0.96	-3.86	5.79	-6.75	-0.96	3.86	1.28	0.08	3.93
	(-0.86)	(-6.76)	(3.81)	(5.90)	(0.86)	(6.76)	(-3.81)	(1.23)	(3.87)	(0.06)
M06	6.90	0.83	-3.86	6.07	-6.90	-0.83	3.86	1.23	0.06	3.92
	(-0.51)	(-7.07)	(3.79)	(6.56)	(0.51)	(7.07)	(-3.79)	(1.09)	(3.81)	(0.02)
M06L	9.05	0.96	-5.01	8.09	-9.05	-0.96	5.01	1.55	0.06	5.06
	(-1.26)	(-5.89)	(3.58)	(4.62)	(1.26)	(5.89)	(-3.58)	(1.38)	(3.75)	(0.17)
WB97XD	6.92	0.33	-3.62	6.59	-6.92	-0.33	3.62	1.00	0.01	3.63
	(1.28)	(-0.89)	(-0.20)	(2.17)	(-1.28)	(0.89)	(0.20)	(0.01)	(0.18)	(0.38)

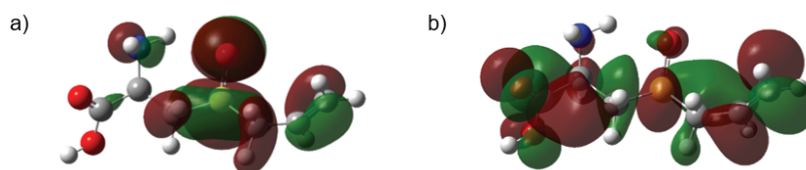


Fig. 2. HOMO and LUMO distributions on alliin obtained at the B3LYP/DGDZVP level of theory in the aqueous phase using the PCM solution model. In all cases the isosurfaces were obtained at 0.08 e/u.a.³

Furthermore, it is possible to condense the Fukui function through Eqs. (13)–(15) to identify the point distribution of the active sites because the highest values of CFF correspond to the most reactive atoms in the reference molecule.⁴ In the case of Eqs. (13)–(15), we used the Hirshfeld population analysis to evalu-

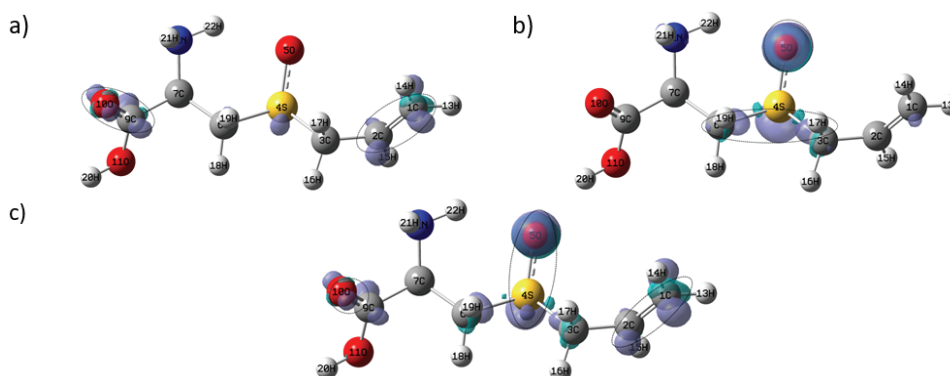


Fig. 3. Isosurfaces of Fukui Functions for aliin according to Eqs. (10)–(12) at the B3LYP/DGDZVP level of theory using the PCM solution model in the case of nucleophilic (a), electrophilic (b) and free radical attacks (c). In all cases, the isosurfaces were obtained at 0.008 e/a.u.^3 . The dotted circles show the most reactive zones in each molecule.

ate the CFF values because the values obtained are non-negative.^{35,36} The CFF values for nucleophilic attacks at the different levels of theory, for aliin calculated in aqueous phase, are shown in Fig. 4. Note that aliin exhibits the most susceptible sites towards nucleophilic attacks at 1C, 2C and 9C. In the case of electrophilic attack, the most reactive sites are 3C, 4S and 5O (Fig. S-4 of the Supplementary material). Whereas, the most reactive sites towards a free radical

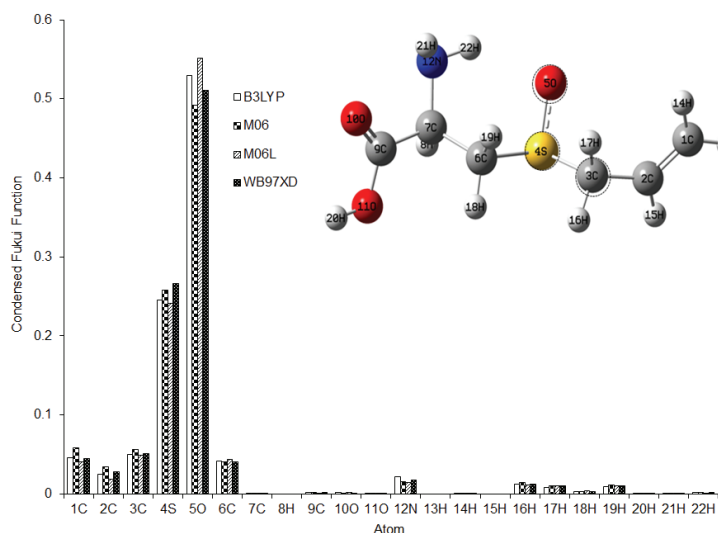


Fig. 4. Condensed Fukui function values for nucleophilic attacks on aliin at the X/DGDZVP level of theory (where X=B3LYP, M06, M06L and ω B97XD), in the aqueous phase using the Hirshfeld population and Eqs. (12)–(14), the dotted circles show the most reactive zones in each molecule.

attack are 1C, 9C, 4S and 5O (Fig. S-5 of the Supplementary material). It was also observed that the molecule has the same behaviour in the gas phase (Figs. (S-6)–(S-8) of the Supplementary material).

In addition to global and local reactivity descriptors, it is possible to analyse the chemical reactivity through molecular electrostatic potential (MEP) maps.³¹ Fig. 5 shows the MEPs of the alliin molecule. In this image, the negative potential areas (red colour) are characterized by an abundance of electrons while the positive potential areas (blue colour) are characterized by a relative lack of electrons. Alliin exhibits the highest potential values on hydrogen and nitrogen atoms compared to the other atoms, therefore they have a lower electron density around them, and show that oxygen atoms are the sites with the lowest potential and therefore are the most electrophilic active sites. The same occurred when the MEP for almotriptan in the gas phase was performed, as shown in Fig. S-9 of the Supplementary material.

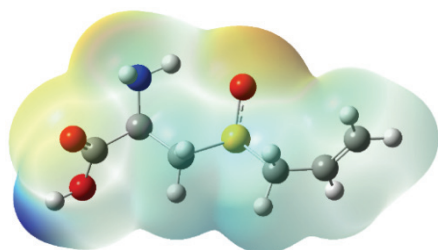


Fig. 5. Mapping of the electrostatic potentials evaluated at the B3LYP/DGDZVP level of theory using the PCM solvation model, on a density isosurface (value = 0.002 e/a.u.³) for alliin.

Non-covalent interactions

As expressed by the *NCI* index, in regions far from the molecule, the density decreases to zero exponentially and, consequently, the reduced gradient displayed large positive values, while in regions of covalent bonding and non-covalent interactions, the reduced gradient will have values close to zero:³⁷

$$s(r) = \frac{1}{2(3\pi^2)^{1/3}} \frac{|\nabla\rho(r)|}{\rho(r)^{4/3}} \quad (16)$$

Fig. 6 shows this plot for alliin, note that, in the low reduced gradient region, several interactions are observed, caused by the interactions in the amide. To verify this result, the isosurface $s(r)$ of the alliin structure was plotted, see Fig. S-10 of the Supplementary material.

Molecular docking

In order to analyse the influence of alliin structure on its role as an inhibitor of SARS-CoV-2 virus replication for the treatment of COVID-19 disease, the optimal ligand/protein configuration and binding affinity of alliin to M^{PRO} were analysed. Fig. 7 shows the alliin–M^{PRO} configuration, where the binding energy is

$-29.79 \text{ kJ mol}^{-1}$. This binding energy value is more negative than the previously reported in the literature ($-17.99 \text{ kJ mol}^{-1}$),³⁸ suggesting a higher affinity to the alliin to the active site of M^{pro} . Although, it was previously reported a molecular docking of alliin with the protease M^{pro} with a ΔG equal to $-40.57 \text{ kJ mol}^{-1}$, it is important to mention that it was done in the presence of the inhibitor N3, and this fact may decrease the number of interactions with the active site residues.⁷ To identify the interactions around 3 \AA , the interactions were plotted on a 2D map, as shown in Fig. S-11 of the Supplementary material, thus it is observed that alliin has van der Waals interactions at the catalytic site of the M^{pro} reported.³⁹ The interaction of alliin with the catalytic site of M^{pro} , at residues CYS145 and HSD164, considered the catalytic dyad, in addition to ASN142, MET165, HSD163, GLU166, HSD41, alkyl-type interaction with MET49 and by hydrogen bridging with PHE140.

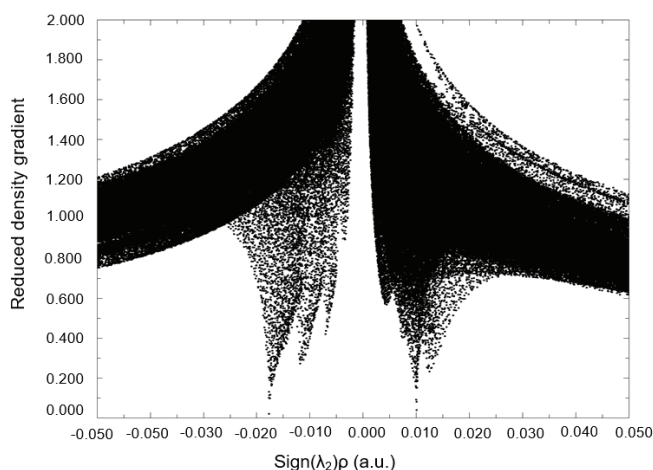


Fig. 6. Plot of the reduced density gradient vs. $\text{sign}(\lambda_2)\rho$ for alliin in the aqueous phase.

Molecular dynamics simulation study

The molecular dynamics simulation allows the docking study to be validated by evaluating the stability of the compounds docked to a protein, based on the description of the forces. Here it is important to mention that recently was reported in the literature a molecular dynamic study of 6lu7–alliin but with a RMSD larger than 2 \AA , (see Fig. 2 in reference 12),⁷ which is bigger than the average values of RMSD reported as reliable. In this work, the molecular dynamics simulation was performed for 20 ns for the M^{pro} alliin complex as shown in Fig. 9. The system reached equilibrium after 10 ns and fluctuated around the mean value of 0.8 \AA until the end of the simulation which suggest that

the formation of complex protein-ligand is stable and may inactive to the M receptor^{pro}.^{7,40}

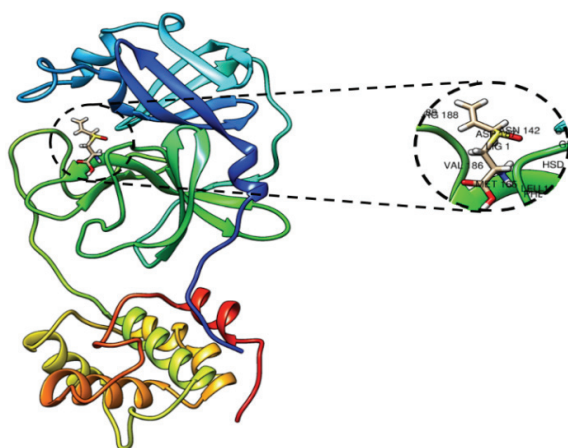


Fig. 7. Alliin binding site in the protease M^{pro} of SARS-CoV-2.

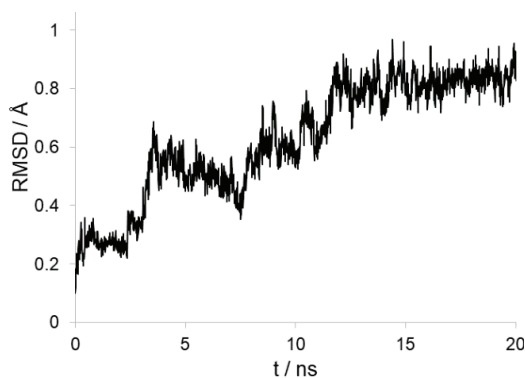


Fig. 9. RMSD diagram of the SARS-CoV-2 M^{pro}-alliin protease complex.

CONCLUSIONS

In the present work, the molecular chemical reactivity of the alliin structure was studied in aqueous and gas phase. Through the Fukui Function it was identified that the most active sites towards the nucleophiles are located at 1C, 2C and 9C the for electrophilic attacks 3C, 4S and 5O and for free radical attacks the most reactive sites are the same sites as for nucleophilic and electrophilic attacks and there was no significant change in the two phases. The ΔG of binding for the alliin-M^{pro} configuration was also calculated to be equal to $-29.79 \text{ kJ mol}^{-1}$. Alliin showed interactions with important residues of the active site of the M^{pro} receptor.

SUPPLEMENTARY MATERIAL

Additional data and information are available electronically at the pages of journal website: <https://www.shd-pub.org.rs/index.php/JSCS/article/view/12534>, or from the corresponding author on request.

Acknowledgements. WLO acknowledges CONACYT for the scholarship granted for Doctoral studies. Authors gratefully acknowledge financial support from CONACYT (project CB2015-257823) and to the Universidad Autónoma del Estado de Hidalgo. Guanajuato National Laboratory (CONACyT 123732) is acknowledged for supercomputing resources. LHMH acknowledges to the SNI for the distinction of his membership and the stipend received.

ИЗВОД

ХЕМИЈСКА РЕАКТИЦНОСТ АЛИИНА И ЊЕГОВА МОЛЕКУЛСКА ИНТЕРАКЦИЈА СА SARS-COV-2 PROTEASE M^{PRO}

WENDOLYNE LÓPEZ-OROZCO, LUIS HUMBERTO MENDOZA-HUIZAR, GIAAN ARTURO ÁLVAREZ-ROMERO, JESÚS MARTÍN TORRES-VALENCIA и MARICRUZ SANCHEZ-ZAVALA

Academic Area of Chemistry, Universidad Autónoma del Estado de Hidalgo, Carretera Pachuca-Tulancingo, 42184, Mineral de la Reforma, Hidalgo, Mexico

У овом раду је дата рачунарска студија хемијске реактивности алиина на X/DGhDZVP нивоу теорије (где је X B3LYP, M06, M06L или wB97XD). Расподела активних места на алиину одређена је на основу Fukui функције. За електрофилне нападе, најреактивнија места су на угљениковим атомима проп-2-енског дела. Реактивнија места за нуклеофилне нападе су лоцирана на тиоетарској групи. У случају слободно-радикалских напада, реактивнија места су на кабонилним, тиоетарским и проп-2-енским деловима. Додатно је студија молекулског докинга показала да је алиин у стању да пристане на protease M^{PRO} у SARS-CoV-2 кроз интеракцију са каталитичком CYS145-HSD164 дијадом, преко van der Waals интеракција, са MET49 преко интеракција са јонима алкил типа, и са PHE140 преко водоничних веза. Такође, студије молекулске динамике указују да се алиин задржава на месту цепа. Најновији резултати сугеришу да је овај молекул потенцијални кандидат за даљу *in vitro* евалуацију, као лек за третирање главног, на протеази заснованог, SARS-CoV-2 вируса.

(Примљено 17. августа, ревидирано 9. септембра, прихваћено 11. октобра 2023)

REFERENCES

1. B. Hughes, B. Murray, J. North, L. Lawson, *Planta Med.* **55** (1989) 114 (<https://www.thieme-connect.com/products/ejournals/abstract/10.1055/s-2006-961894>)
2. S. Quintero-Fabián, D. Ortuño-Sahagún, M. Vázquez-Carrera, R. I. López-Roa, *Mediators Inflamm.* **2013** (2013) (<https://doi.org/10.1155/2013/381815>)
3. M. G. Jones, J. Hughes, A. Tregova, J. Milne, A. B. Tomsett, H. A. Collin, *J. Exp. Bot.* **55** (2004) 1903 (<https://doi.org/10.1093/jxb/erh138>)
4. C. Jacob, A. Anwar, *Physiol. Plant.* **133** (2008) 469 (<https://doi.org/10.1111/j.1399-3054.2008.01080.x>)
5. N. D. Weber, D. O. Andersen, J. A. North, B. K. Murray, L. D. Lawson, B. G. Hughes, *Planta Med.* **58** (1992) 417 (<https://www.thieme-connect.com/products/ejournals/abstract/10.1055/s-2006-961504>)
6. A. Helen, K. Krishnakumar, P. L. Vijayammal, K. T. Augusti, *Pharmacology* **67** (2003) 113 (<https://doi.org/10.1159/000067796>)

7. D. A. Hanoush, A. H. Al-Auqaili, M. Mansour, A. Ghosh, *Trop. J. Nat. Prod. Res.* **6** (2022) 1233 (<http://www.doi.org/10.26538/tjnpr/v1i4.5>)
8. J. M. Casasnovas, T. A. Springer, *J. Biol. Chem.* **270** (1995) 13216 (<https://doi.org/10.1074/jbc.270.22.13216>)
9. P. Gale, *Microb. Risk Anal.* **21** (2022) 100198. (<https://doi.org/10.1016/j.mran.2021.100198>)
10. M. E. Popovic, *Microbiol. Res.* **270** (2023) 127337. (<https://doi.org/10.1016/j.micres.2023.127337>)
11. K. Rajagopal, G. Byran, S. Jupudi, R. Vadivelan, *Int. J. Heal. Allied Sci.* **9** (2020) 43 (http://www.doi.org/10.4103/ijhas.IJHAS_55_20)
12. W. Lopez-Orozco, L. H. Mendoza-Huizar, G. A. Álvarez-Romero, J. de J. M. Torres-Valencia, *Pädi Boletín Científico Ciencias Básicas e Ing. Del ICBI* **10** (2023) 126 (<https://repository.uaeh.edu.mx/revistas/index.php/icbi>)
13. M. B. M. Spera, F. A. Quintão, D. K. D. Ferraresi, W. R. Lustrì, A. Magalhães, A. L. B. Formiga, P. P. Corbi, *Spectrochim. Acta, A* **78** (2011) 313 (<https://doi.org/10.1016/j.saa.2010.10.012>)
14. P. Geerlings, F. De Proft, W. Langenaeker, *Chem. Rev.* **103** (2003) 1793 (<https://doi.org/10.1021/cr990029p>)
15. R. G. Pearson, *J. Chem. Educ.* **64** (1987) 561 (<https://doi.org/10.1021/ed064p561>)
16. R. G. Parr, R. A. Donnelly, M. Levy, W. E. Palke, *J. Chem. Phys.* **68** (1977) 3801 (<https://doi.org/10.1063/1.436185>)
17. R. G. Parr, R. G. Pearson, *J. Am. Chem. Soc.* **105** (1983) 7512 (<https://doi.org/10.1021/ja00364a005>)
18. R. G. Parr, W. Yang, *J. Am. Chem. Soc.* **106** (1984) 4049 (<https://doi.org/10.1021/ja00326a036>)
19. R. G. Parr, *Horizons Quantum Chem.* (1980) 5 (<https://link.springer.com/book/10.1007/978-94-009-9027-2>)
20. W. Yang, W. J. Mortier, *J. Am. Chem. Soc.* **108** (1986) 5708 (<https://doi.org/10.1021/ja00279a008>)
21. N. Godbout, D. R. Salahub, J. Andzelm, E. Wimmer, *Can. J. Chem.* **70** (2011) 560 (<https://doi.org/10.1139/v92-079>)
22. K. Raghavachari, *Theor. Chem. Accounts* **103** (2000) 361 (<https://link.springer.com/article/10.1007/s002149900065>)
23. Y. Zhao, D. G. Truhlar, *Theor. Chem. Acc.* **120** (2008) 215 (<https://link.springer.com/article/10.1007/s00214-007-0310-x>)
24. Y. Wang, X. Jin, H. S. Yu, D. G. Truhlar, X. He, *Proc. Natl. Acad. Sci. U.S.A.* **114** (2017) 8487 (<https://doi.org/10.1073/pnas.1705670114>)
25. J. Da Chai, M. Head-Gordon, *Phys. Chem. Chem. Phys.* **10** (2008) 6615 (<https://doi.org/10.1039/B810189B>)
26. S. Miertuš, E. Scrocco, J. Tomasi, *Chem. Phys.* **55** (1981) 117 ([https://doi.org/10.1016/0301-0104\(81\)85090-2](https://doi.org/10.1016/0301-0104(81)85090-2))
27. *Gaussian 09, Revision A.01*, Gaussian, Inc., Wallingford, CT, 2009 (<https://gaussian.com/g09citation/>)
28. *Gaussview Rev. 3.09, Windows version*, Gaussian Inc., Pittsburgh, PA (https://gaussian.com/508_gvw/)
29. A. Allouche, *J. Comput. Chem.* **32** (2012) 174 (<https://doi.org/10.1002/jcc.21600>)
30. T. Lu, F. Chen, *J. Comput. Chem.* **33** (2012) 580 (<https://doi.org/10.1002/jcc.22885>)

31. A. Jorge-Finnigan, S. Brasil, J. Underhaug, P. Ruíz-Sala, B. Merinero, R. Banerjee, L. R. Desviat, M. Ugarte, A. Martínez, B. Pérez, *Hum. Mol. Genet.* **18** (2013) (<https://doi.org/10.1093/hmg/ddt217>)
32. E. F. Pettersen, T. D. Goddard, C. C. Huang, G. S. Couch, D. M. Greenblatt, E. C. Meng, T. E. Ferrin, *J. Comput. Chem.* **25** (2004) 1605 (<https://doi.org/10.1002/jcc.20084>)
33. BIOVIA, *Discovery Studio Visualiser 2019*, Dassault Systèmes, San Diego, CA, 2019 (<https://discover.3ds.com/discovery-studio-visualizer-download>)
34. J. L. Gázquez, *J. Phys. Chem., A* **101** (1997) 4591 (https://www.scielo.org.mx/scielo.php?script=sci_arttext&pid=S1870-249X2008000100002)
35. P. K. Chattaraj, *Chemical Reactivity Theory: A Density Functional View*, CRC Press, Boca Raton, FL, 2009, p. 576 (https://books.google.com/books/about/Chemical_Reactivity_Theory.html?hl=es&id=n8JBNvF_2KAC)
36. F. L. Hirshfeld, *Theor. Chim. Acta* **44** (1977) 129 (<https://link.springer.com/article/10.1007/BF00549096>)
37. E. R. Johnson, S. Keinan, P. Mori-Sánchez, J. Contreras-García, A. J. Cohen, W. Yang, *J. Am. Chem. Soc.* **132** (2010) 6498 (<https://doi.org/10.1021/ja100936w>)
38. M. Chebaibi, D. Boust, R. F. B. Goncalves, H. Hoummani, S. Achour, *Res. Sq.* **1** (2021). (<https://doi.org/10.21203/rs.3.rs-679827/v1>)
39. Z. Jin, X. Du, Y. Xu, Y. Deng, M. Liu, Y. Zhao, *Nature* **582** (2020) 289 (<https://doi.org/10.1038/s41586-020-2223-y>)
40. A. Castro-Alvarez, A. M. Costa, J. Vilarrasa, *Molecules* **22** (2017). (<https://doi.org/10.3390/molecules22010136>).

SUPPLEMENTARY MATERIAL TO
**Chemical reactivity of alliin and its molecular interactions with
the protease M^{pro} of SARS-CoV-2**

WENDOLYNE LÓPEZ-OROZCO, LUIS HUMBERTO MENDOZA-HUIZAR*, GIAAN
ARTURO ÁLVAREZ-ROMERO, JESÚS MARTÍN TORRES-VALENCIA
and MARICRUZ SANCHEZ-ZAVALA

*Academic Area of Chemistry, Universidad Autónoma del Estado de Hidalgo, Carretera
Pachuca-Tulancingo, 42184, Mineral de la Reforma, Hidalgo, Mexico*

J. Serb. Chem. Soc. 89 (11) (2024) 1433–1445

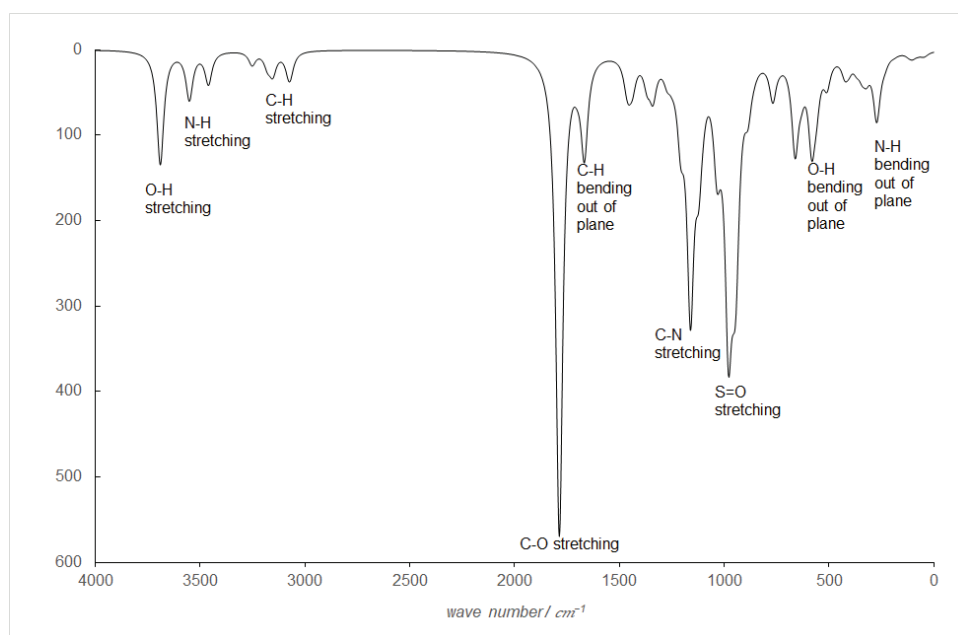


Figure S-1: Theoretical IR spectra of alliin in the aqueous phase obtained at the B3LYP/DGDZVP level of theory.

* Corresponding author. E-mail: hhuizar@uaeh.edu.mx

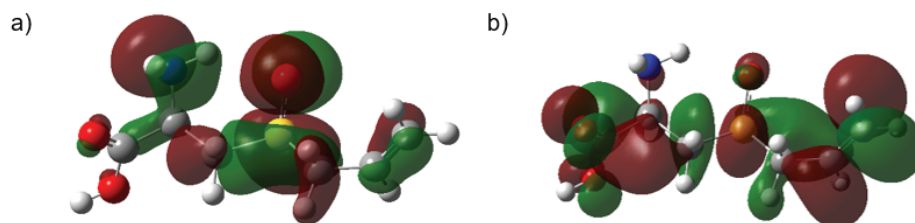


Figure S-2. HOMO and LUMO distributions on alliin obtained at the B3LYP/DGDZVP level of theory in the gas phase. In all cases the isosurfaces were obtained at 0.08 e/u.a.^3 .

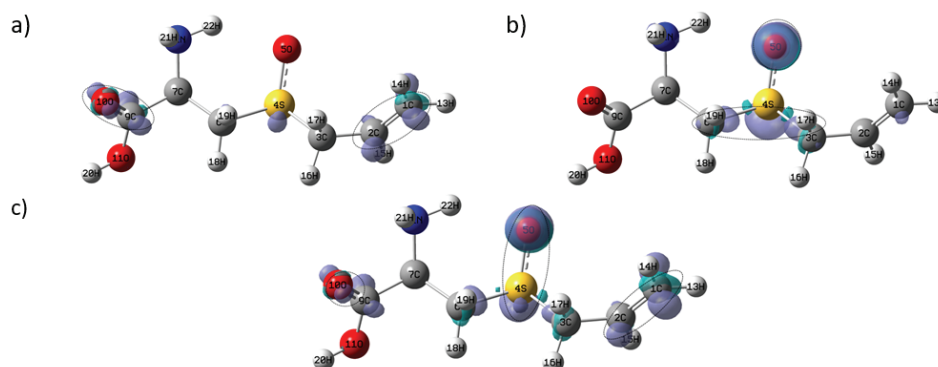


Figure S-3. Isosurfaces of Fukui Functions for alliin according to equations (9), (10) and (11) at the B3LYP/DGDZVP level of theory in the gas phase. In the case of (a) nucleophilic, (b) electrophilic and (c) free radical attacks. In all cases the isosurfaces were obtained at 0.008 e/u.a.^3 . The dotted circles show the most reactive zones in each molecule.

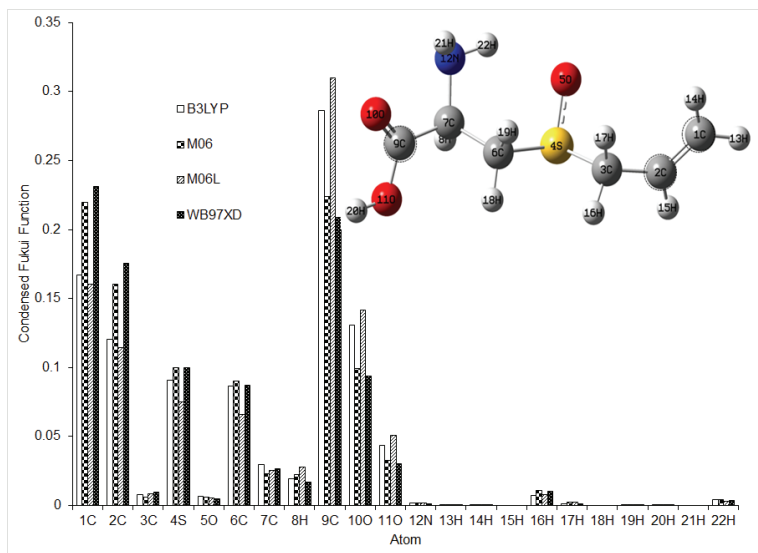


Figure S-4. Condensed Fukui function values for electrophilic attacks on alliin at the X/DGDZVP level of theory (where X=B3LYP, M06, M06L and ω B97XD), in the aqueous phase employing the Hirshfeld population and equations (12)-(14), the dashed circles show the most reactive zones in each molecule.

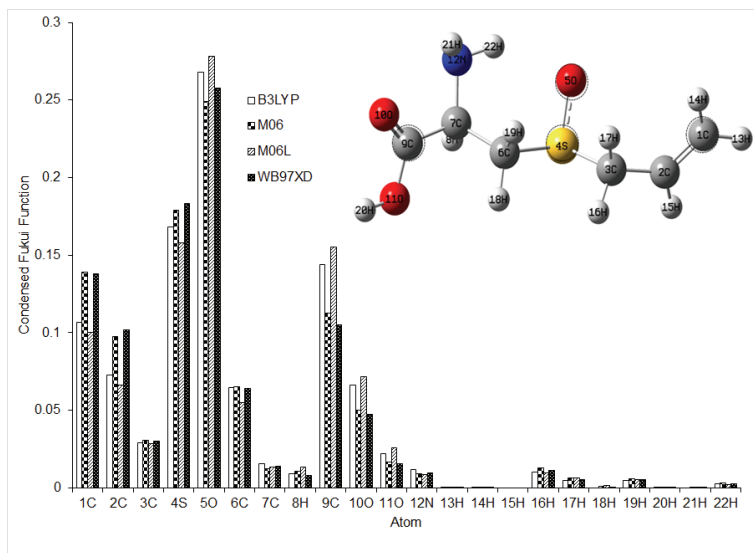


Figure S-5. Condensed Fukui function values for free radical attacks on alliin at the X/DGDZVP level of theory (where X=B3LYP, M06, M06L and ω B97XD), in the aqueous phase employing the Hirshfeld population and equations (12)-(14), the dashed circles show the most reactive zones in each molecule.

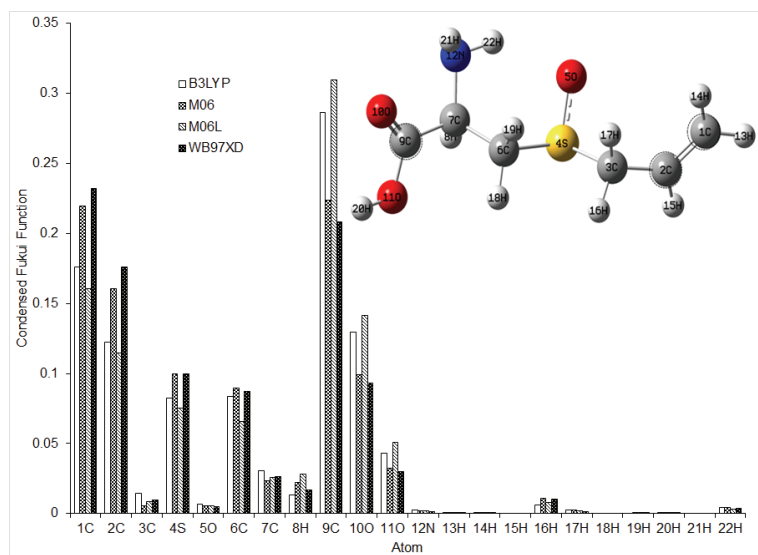


Figure S-6. Condensed Fukui function values for nucleophilic attacks on alliin at the X/DGDZVP level of theory (where X=B3LYP, M06, M06L and ω B97XD), in the gas phase employing the Hirshfeld population and equations (12)-(14), the dashed circles show the most reactive zones in each molecule.

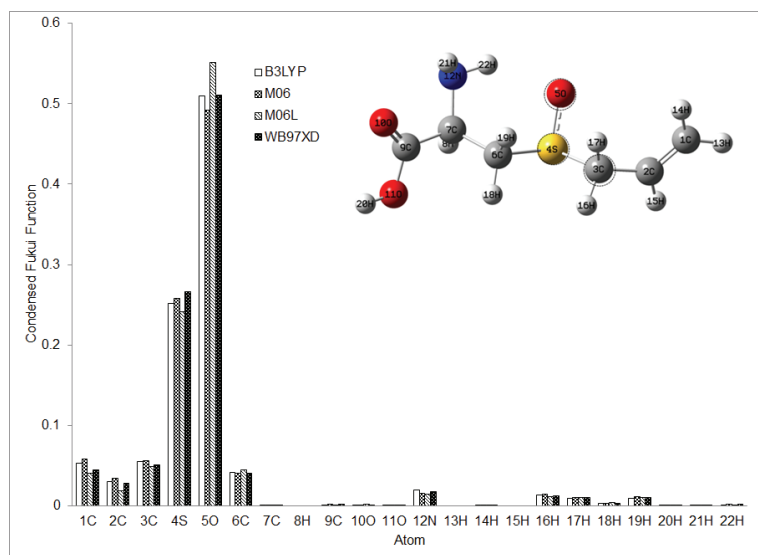


Figure S-7. Condensed Fukui function values for electrophilic attacks on alliin at the X/DGDZVP level of theory (where X=B3LYP, M06, M06L and ω B97XD), in the gas phase employing the Hirshfeld population and equations (12)-(14), the dashed circles show the most reactive zones in each molecule.

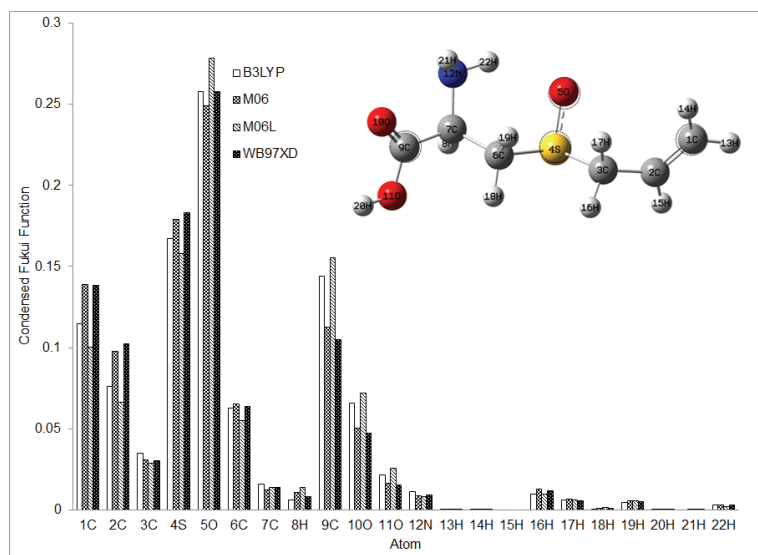


Figure S-8. Condensed Fukui function values for free radical attacks on alliin at the X/DGDZVP level of theory (where X=B3LYP, M06, M06L and ω B97XD), in the gas phase employing the Hirshfeld population and equations (12)-(14), the dashed circles show the most reactive zones in each molecule.

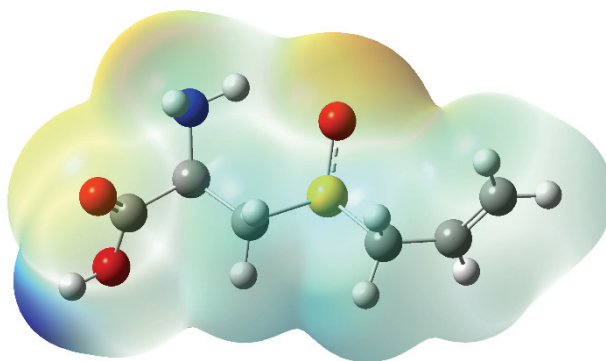


Figure S-9. Mapping of electrostatic potentials evaluated at the B3LYP/DGDZVP level of theory in the gas phase, over a density isosurface (value = 0.002 e/a.u.^3) for alliin.

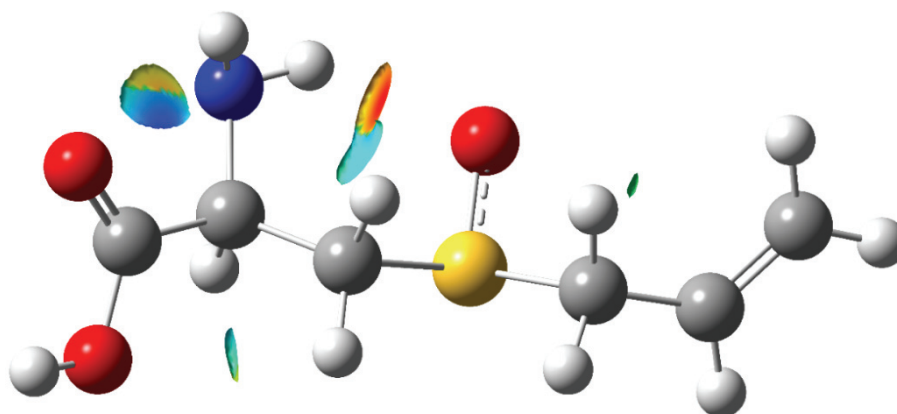


Figure S-10. Isosurface area of NCI = 0.2 for alliin in aqueous phase.

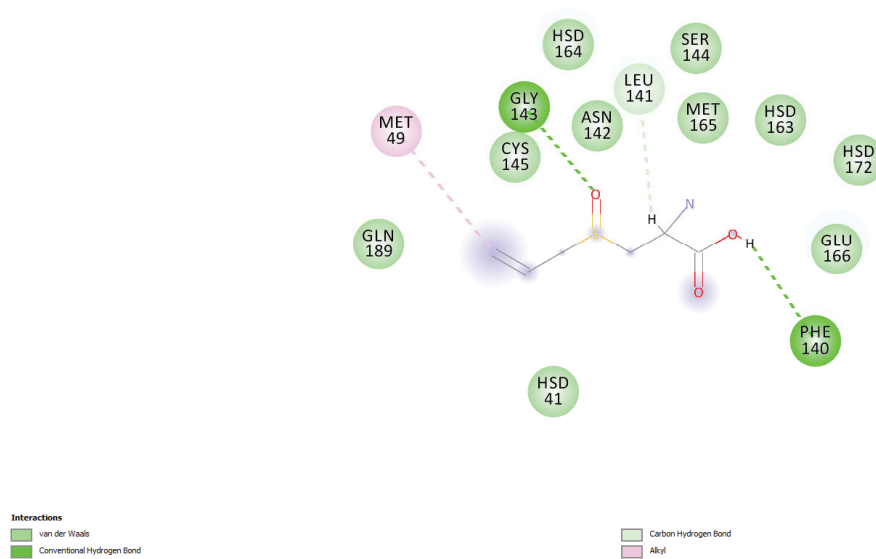


Figure S-11. 2D mapping of ligand/protein interactions for alliin.



J. Serb. Chem. Soc. 89 (11) 1447–1460 (2024)
JSCS–5799

Identification of musk compounds as inhibitors of the main SARS-CoV-2 protease by molecular docking and molecular dynamics studies

ASSIA BELHASSAN¹, GUILLERMO SALGADO², LUIS HUMBERTO MENDOZA-HUIZAR^{3*}, HANANE ZAKI⁴, SAMIR CHTITA⁵, TAHAR LAKHLIFI¹, MOHAMMED BOUACHRINE^{1,4}, LORENA GERLI CANDIA⁶ and WILSON CARDONA⁷

¹Molecular Chemistry and Natural Substances Laboratory, Faculty of Science, Moulay Ismail University of Meknes, Morocco, ²Facultad de Ciencias Químicas. Investigador Extramural, Universidad de Concepción, Concepción, Chile, ³Autonomous University of Hidalgo State. Academic Area of Chemistry. Mineral de la Reforma, Hidalgo. México, ⁴EST Khenifra, Sultan Moulay Sliman University, Benimellal, Morocco, ⁵Laboratory of Analytical and Molecular Chemistry, Department of Chemistry, Faculty of Sciences Ben M'Sik, Hassan II University of Casablanca, Casablanca, Morocco, ⁶Departamento de Química Ambiental, Facultad de Ciencias, Universidad Católica de la Santísima Concepción, Concepción, Chile and ⁷Facultad de Medicina y Ciencia, Universidad San Sebastián, Puerto Montt, Chile

(Received 25 November, revised 22 December 2023, accepted 19 February 2024)

Abstract: As new drug development is a long process, reuse of bioactives may be the answer to new epidemics; thus, screening existing bioactive compounds against a new SARS-CoV-2 infection is an important task. With this in mind, we have systematically screened potential odorant molecules in the treatment of this infection based on the affinity of the selected odorant compounds on the studied enzyme and the sequence identity of their target proteins (olfactory receptors) to the same enzyme (the main protease of SARS-CoV-2). A total of 12 musk odorant compounds were subjected to a molecular docking and molecular dynamics study to predict their impact against the main protease of SARS-CoV-2. In this study, we have identified two musk-scented compounds (androstenol and vulcanolide) that have good binding energy at the major protease binding site of SARS-CoV-2. However, the *RMSD* values recorded during dynamic simulation show that vulcanolide exhibits high stability of the protein–ligand complex compared to androstenol. The perspectives of this work are as follows: *in vitro*, *in vivo* and clinical trials to verify the computational findings.

Keywords: coronavirus; musk-smelling compounds; olfactory receptors; molecular docking; molecular dynamics.

* Corresponding author. E-mail: hhuizar@uaeh.edu.mx
<https://doi.org/10.2298/JSC231125012B>



INTRODUCTION

A new form of infection, the coronavirus caused by the SARS-CoV-2 virus, has spread rapidly around the world,^{1–5} and continues to kill thousands of people every day. This new form of coronavirus occurred in December 2019 in Wuhan, China,⁶ and to date no effective treatment against SARS-CoV-2 virus infection has been reported.^{7,8} The possible treatment of coronaviruses can be carried out in two different ways: the first by strengthening the human immune system, and the second by attacking the coronavirus itself.² This virus is a member of the beta-coronavirus family.⁹ It infects cells by binding to ACE2 by its spike glycoprotein (S). In order to complete the entry into the cell, the protease enzyme must prime the spike glycoprotein; this protease is called TMPRSS2. In fact, the activation of TMPRSS2 as a protease is needed to attach the spike protein of the virus to its human cellular ligand. The viral genome is transcribed and then translated after the virus enters the host cell and uncoats. Therefore, targeting and disturbing the operation of one or many of those enzymes involved in viral replication, transcription, or translation can be effective in stopping the emergency of this pandemic.² Here, it is important to mention that the structure-biology study of coronavirus (SARS-CoV-2) proteins is still at an early stage. The crystal structure of the main protease, also named 3CLpro or 3-chymotrypsin-like protease,² has many PDB structures (PDB code: 6LU7, 6M03, 6W4B, 6Y84, 6YB7, 5R7Y, 5R7Z, 5R80, 5R81, 6W63, 6M3M...).¹⁰ However, in this study, we are interested in the crystal structure of 3CLpro (PDB code: 6LU7) because the protease activity that is responsible for polyprotein cleavage is present in this enzyme (nsp5 protein).¹¹ This crystallographic structure is encoded within the viral genome in complex with the N3 inhibitor.¹² Here it is worth mentioning that the reuse of bioactive compounds can be a good option in the face of the outbreak of unexpected infectious diseases due to the long production time of new drugs.^{3,13} For example, the effect of chloroquine and hydroxychloroquine in the treatment of COVID-19 has been evaluated in many research papers,^{3,14–16} and in fact, these two drugs are used worldwide for the treatment of COVID-19 disease.^{17,18} Therefore, there is an urgent task to discover novel bioactives with new methodologies to combat COVID-19 disease; and consequently, the challenge is to detect chemical compounds with inhibitory effects on the SARS-CoV-2 main protease virus. Specifically, in the event of a pulmonary infection, volatile compounds are very useful since the respiratory system will positively support therapies of this kind.¹⁹ Thus, the chemical constituents present in aromatic plants have the potential to inhibit viral infections.^{19–23} Musk-smelling compounds are well known as a very odorous material, which is the secretion of the musk-carrying Chevrotin.²⁴ These musk-smelling compounds are able to activate the human musk receptors OR5AN1 and OR1A1, and they could activate other kinds of receptors if they have homology. In this sense, two receptors have homology when

their structures share a significant sequence similarity (a percentage of identity greater than 40 % is considered to be a sign of homology unless the sequences are of low complexity). Although a complete lack of similarity does not mean an absence of homology, Moreover, the significant increase in the number of known 3D structures has made it clear that in many cases, two sequences with sequence identities of the order from 20 to 40 % adopt similar folds and may have similar functions.²⁵ It is therefore important to look for possible structural analogies and determine if these can correspond to common biological functions.²⁵ To the best of our knowledge and based on exhaustive bibliographic research, the homology between the olfactory receptors (OR5AN1, OR1A1) and the 6LU7 has not been analyzed. Thus, in this paper, the goal is to evaluate the potential efficiency of 12 Musk-smelling compounds against novel coronaviruses by searching for the sequence identity of their biological targets (olfactory receptors) with the 6LU7 and comparing the affinity and stability of these molecules at the binding site by molecular docking and molecular dynamic methods, respectively.^{26,27}

EXPERIMENTAL

Data set

In this study, we have chosen 12 musk-smelling compounds based on the fact that their targets have a good sequence identity with 6LU7. These compounds are (3*R*)-3-methylcyclopentadecan-1-one (*R*-muscone), 1,4-dioxacycloheptadecane-5,17-dione (ethylene brassylate), 5 α -androst-16-en-3 α -ol (androstenol), (9*Z*)-cycloheptadec-9-en-1-one (civetone), (8*Z*)-1-oxa-cycloheptadec-8-en-2-one (ambrettolide), (6*R*,7*R*)-3,5,5,6,7,8,8-heptamethyl-5,6,7,8-tetrahydro-naphthalene-2-carbaldehyde (vulcanolide), as-hydrindacene-1-ol (hydrindacene), 1-(3,5,5,6,8,8-hexamethyl-6,7-dihydronaphthalen-2-yl)ethenone (fixolide), 1-tert-butyl-3,5-dimethyl-2,4,6-trinitrobenzene (musk xylene), 1,1,3,3,5-pentamethyl-4,6-dinitroindane (moskene), 1-(4-tert-butyl-2,6-dimethyl-3,5-dinitrophenyl)ethan-1-one (musk ketone) and 4-tert-butyl-3-methoxy-2,6-dinitrotoluene (musk ambrette). Fig. 1 shows the chemical structure of these compounds.

Sequence identity

The comparison between the sequence of SARS-CoV-2 main protease (PDB code 6LU7, chain A) and the selected olfactory receptors was carried out using the Swiss-Model modelling server (<http://swissmodel.expasy.org>).²⁸ To determine the sequence identity between SARS-CoV-2 main protease and these targets,²⁹⁻³² these targets are selected according to their sequence identity (ID) with SARS-CoV-2 main protease. All studied compounds were obtained from chemical structure databases such as ChemSpider (An Online Chemical Information Resource).³³

Molecular docking

We performed a molecular docking study of 12 odorant molecules (Fig. 1). The ligands (12 Musk-smelling compounds) of selected olfactory receptors (ORs) are indicated in the literature.³⁴ The computational study was carried out with two programs; Autodock vina and Autodock tools 1.5.6.³⁵ The ligands and macromolecule preparation was carried out by Discovery Studio 2016 program,³⁶ the structure of SARS-CoV-2 main protease (PDB code 6LU7, chain A)³⁷ was imported to detect the binding site of this enzyme.²⁷ The center coordinates of

the binding site are: $x = -10.782$, $y = 15.787$ and $z = 71.277$,³⁸ and the grid size was set at $20 \times 20 \times 20$ xyz points with a grid spacing of 1 Å using N3 (co-crystallized ligand) as the center for docking to determinate the accurate size.³⁸

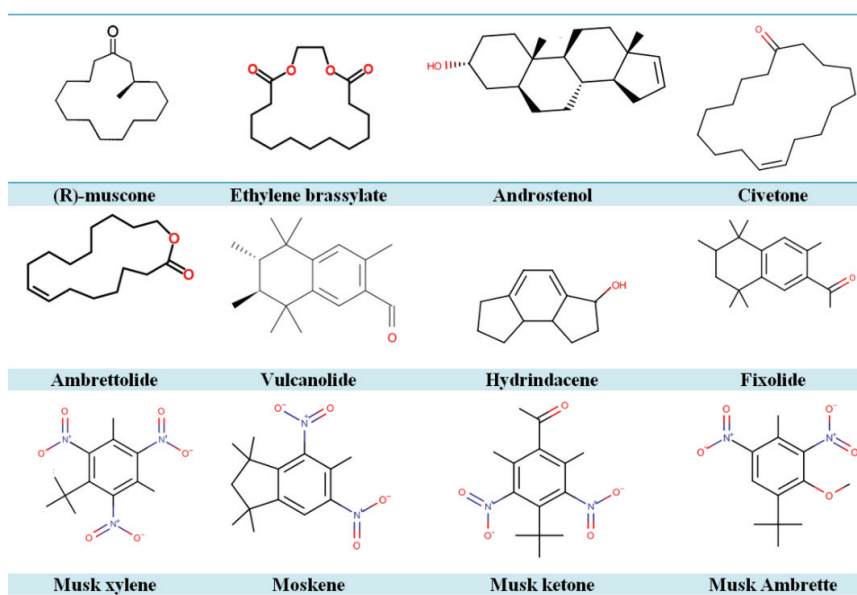


Fig. 1. Musk-smelling compounds used in this study (their targets are human olfactory receptors O5AN1 and OR1A1).

Molecular dynamic (MD) simulation

In order to validate whether the orientation and interaction energy in the active pocket predicted by molecular docking correspond to stable and biologically relevant binding, we performed a 100 ns molecular dynamics study of androstenol-3CLpro and vulcanolide-3CLpro. The water was modelled using the TIP3P equation and placed in the octahedron center for a 100 ns MD simulation. Molecular dynamics calculation and visualization were performed using the programs GROMACS³⁹ and UCSF-Chimera,⁴⁰ respectively. Prior to the MD simulation, an energy minimization process was performed and then equilibration process was conducted in two phases. The first one was conducted under an NVT ensemble (constant number of particles, volume, and temperature) and in the next step, the equilibrium of pressure was conducted under an NPT ensemble (isothermal-isobaric ensemble) for 1 ns. Then a MD for 100 ns was conducted to analyze the stability of the protein–ligand complex.

Molecular electrostatic potential (MEP)

It is widely recognized that MEP is capable of helping determine a molecule's relative polarity, which highlights a variety of interactions, including those involving chemical reactivity, hydrogen bonds and compounds that are biologically active.^{41,42} In this work, the basis set 6-31G(d) and the hybrid functional B3LYP^{43,44} have been used to calculate MEP using the Gaussian 09 package⁴⁵ and GaussView 5.08.⁴⁶

RESULTS AND DISCUSSION

Molecular docking

The top-scoring pose of each odorant molecule is presented according to the best energy of interaction in the binding pocket of the SARS-CoV-2 main protease (Table I), and their targets (olfactory receptors (ORs)) present a good ID with the SARS-CoV-2 main protease: human olfactory receptor O5AN1 has the code UniProtKB: Q8NGI8 and $ID = 31.08\%$ with the SARS-CoV-2 main protease; human olfactory receptor OR1A1 has the code UniProtKB: Q9P1Q5 and $ID = 35.29\%$ with SARS-CoV-2 main protease.

This methodology was performed to find potential drugs for the studied enzyme and the results are presented in Table I.

TABLE I. Binding free energies, binding equilibrium constant and dissociation equilibrium constant of Musk-smelling compounds in the binding site of the studied enzyme, and information about their protein targets (ORs)

N°	Potential drug	Binding free energies with 6LU7, kJ mol ⁻¹	Binding equilibrium constant, $K_B \times 10^{-4} / M^{-1}$	Dissociation equilibrium constant, $K_D \times 10^5 / M^{-1}$	Target and sequence identity with 6LU7
1	Androstenol	-28.0	8.1	1.2	
2	Vulcanolide	-25.9	3.5	2.9	Human olfactory receptor O5AN1
3	Fixolide	-25.5	3.0	3.4	code UniProtKB: Q8NGI8
4	Civetone	-25.5	3.0	3.4	ID = 31.08 %
5	Ambrettolide	-25.5	3.0	3.4	
6	Ethylene brassylate	-25.5	3.0	3.4	
7	(R)-Muscone	-25.1	2.5	4.0	Human olfactory receptor OR1A1
8	Moskene	-25.1	2.5	4.0	code UniProtKB: Q9P1Q5
9	Musk ambrette	-24.3	1.8	5.5	ID = 35.29 %
10	Hydrindacene	-24.3	1.8	5.5	
11	Musk xylene	-23.8	1.5	6.7	
12	Musk ketone	-23.0	1.1	9.3	

Here, it is important to mention that in a docking study, the scoring functions evaluate the binding affinity, which is directly related to the Gibbs energy change of binding ($\Delta_B G^0$),⁴⁷ and this energy is the driving force for the acceptor-receptor binding process.^{48,49} From this $\Delta_B G^0$ it is possible to evaluate the binding equilibrium constant (K_B) through the Eq. (1):⁵⁰

$$K_B = e^{-\frac{\Delta_B G^0}{RT}} \quad (1)$$

In addition, the binding strength of a ligand can also be evaluated by the thermodynamic dissociation constant, K_D , which measures the strength of binding of the ligand to the protein.⁵¹ Thus, K_D is the equilibrium constant of the

ligand–protein complex dissociation reaction in the free protein and the ligand and is defined as:⁵¹

$$K_D = \frac{1}{K_B} \quad (2)$$

In Table I, the values of K_B and K_D for the musk compounds docked to 6LU7 are reported. Note that the results indicate that androstenol and vulcanoide interacted the best with both studied receptors, with binding free energies equal to -28 and -25.9 kJ mol^{-1} , respectively. Also, the ligands androstenol and vulcanolide represent the highest binding equilibrium constant values, indicating a high binding affinity between 6LU7 and these ligands.⁵⁰ For androstenol and vulcanoide, the K_D values are 0.012 and 2.9 M^{-1} , respectively. These K_D values are lower than those found for the binding of glycans to the SARS-CoV-2 spike protein,⁵² suggesting a high affinity of androstenol and vulcanoide to 6LU7. Thus, it is clear that these two musk-smelling compounds present the best energies of interaction with the SARS-CoV-2 main protease, see Table I. We can also observe that their target has a good ID with the SARS-CoV-2 main protease. Based on the effect that structural homology is sometimes linked to functional homology,²⁵ two sequences with sequence identities of the order from 20 to 40 % adopt similar folds and may have similar functions. Thus, it is important to look for the selected musk-smelling compounds (androstenol and vulcanolide); these volatile molecules are very useful since the respiratory system will positively support therapies of this kind. The two selected molecules could have good inhibitory effects on the SARS-CoV-2 main protease.³⁰

The interaction results of androstenol in the binding site of the SARS-CoV-2 main protease (Fig. 2) show hydrogen bond interaction and a carbon-hydrogen bond with His163 and Met165, respectively.

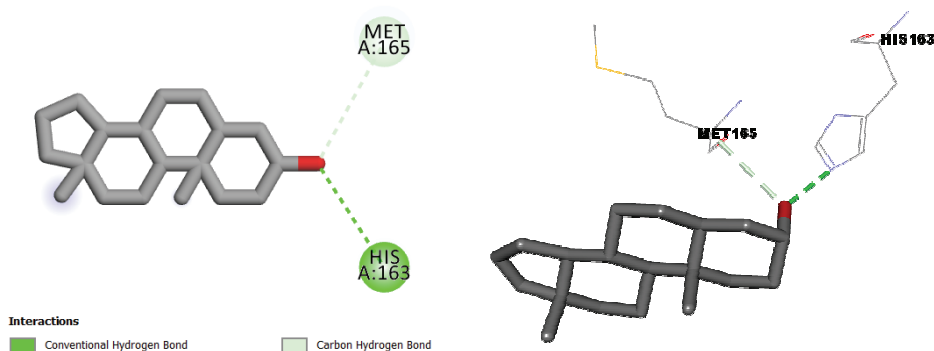


Fig. 2. Interactions between androstenol and the SARS-CoV-2 main protease.

The interaction results of vulcanolide in the binding site of the SARS-CoV-2 main protease (Fig. 3) show alkyl and π -alkyl interactions with Met49, Cys145, and His41.

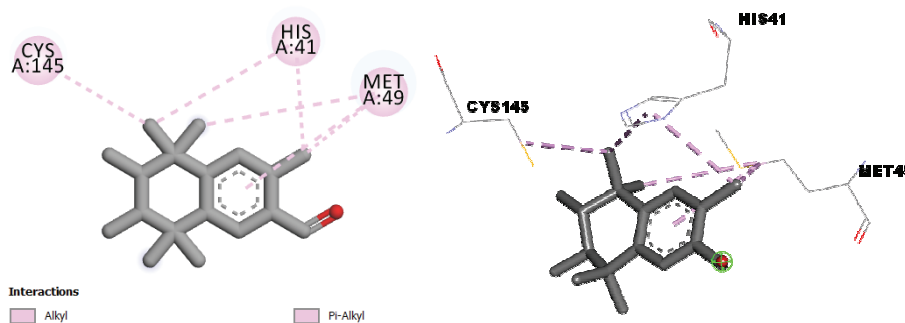


Fig. 3. Interactions between vulcanolide and the SARS-CoV-2 main protease.

Molecular dynamic (MD) simulation

The complex androstenol-3CLpro was unstable and after 1 ns of MD simulation androstenol compound get out from the pocket site of 3CLpro (not shown). The last one is probably due to the fewer interactions between this molecule and the pocket site (see Fig. 2). In the case of the vulcanoide-3CL procomplex, a MD simulation of 100 ns shows the complex is stable. In Fig. 4, the potential energy behavior of the complex is depicted during the MD simulation. It may be seen that the potential energy of the protein-ligand complex lies in the range from -2.86×10^5 to -2.88×10^5 kJ mol⁻¹ and reaches a constant level after approx. 10 ns.

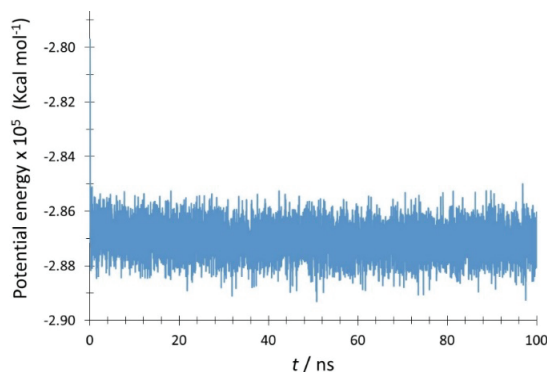


Fig. 4. Variation of the potential energy vs. simulation time.

Also, we mapped the interactions of vulcanolide with the closer residues in the pocket site of 3CLpro, and they are summarized in Table II. Note that at 0 ns, the main interactions are with the residues Cys145, His41 and Met49. However, at 10 ns, the main interactions are with His41, Met49 and Met165, suggesting a

modification of the vulcanolide position in the pocket site. At 40 ns, the ligand modifies its position again, but from 50 ns, in all cases, the ligand keeps strong interactions with His41, Met49 and Met165 to the end of the simulation, suggesting that a stable conformation was reached.

TABLE II. Interactions of vulcanolide with 3CLpro during the MD simulation

<i>t</i> / ns	Interacting residue				
0	Cis145	His41	Met49		
10		His41	Met49	Met165	
20		His41	Met49	Met165	
30		His41	Met49	Met165	
40	Cys44	His41		Met165	
50		His41	Met49	Met165	Leu167
60		His41	Met49	Met165	Gln189
70		His41	Met49	Met165	
80	Cys44	His41	Met49	Met165	
90		His41	Met49	Met165	
100		His41	Met49	Met165	

In Fig. 5, the variation of the distances of vulcanolide to the residues His41, Met49 and Met165 is depicted. Note that after 45 ns, the separation distance between His41, Met49 and Met165 drops drastically from 6 to 3 Å, and the distances are kept at the end of the simulation, indicating that a stable configuration is reached.

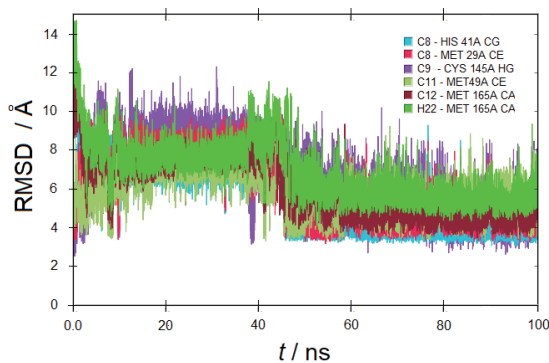


Fig. 5. *RMSD* of the characteristic distances between the ligand (purple) and the enzyme vs. simulation time.

Also, the *RMSD* plots of the drug and the complex were obtained separately, and they are depicted in Fig. 6. Note that vulcanolide equilibrates rather quickly than the protein, but the complex equilibrates until after 60 ns, and after this time, the complex is stable.

Also, the coulomb interaction energy was analyzed (Fig. 7). At the end of the simulation, this energy shows a value of -401 kJ mol^{-1} , suggesting a strong interaction between the protein and the ligand.

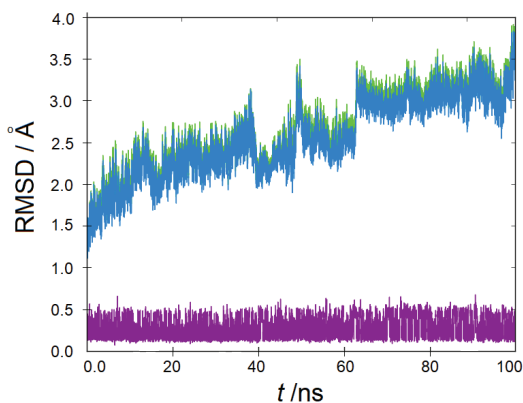


Fig. 6. *RMSD* of the ligand (purple), enzyme (green) and the ligand–enzyme complex (blue) vs. simulation time.

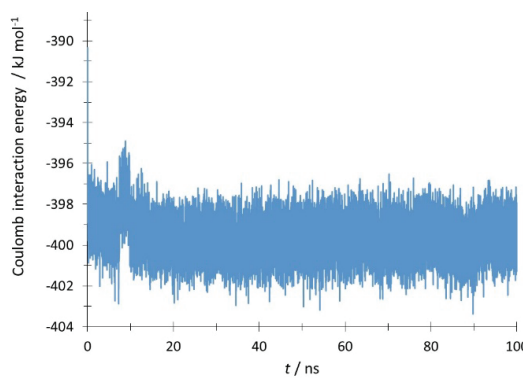


Fig. 7. Variation of the Coulomb interaction energy during the simulation.

Molecular electrostatic potential (MEP)

Fig. 8 shows the MEP for vulcanolide. The red color indicates the existence of a higher electron density site, while the blue color is associated with charge deficiency and the presence of a maximum positive charge, and these sites are primarily nucleophilic. If one compares the interactions observed in Fig. 3 between vulcanolide and SARS-CoV-2, note that vulcanolide is interacting with 3CLpro through its nucleophilic sites.

CONCLUSION

In this study, we have identified potential drugs that could have an effect on the studied enzyme. This research will provide new principal musk-smelling compounds that could have a good effect against SARS-CoV-2 main protease because of their affinity energy and stability in the binding site of the studied enzyme and their good sequence identity (*ID*) with the same enzyme (SARS-CoV-2 main protease). Androstenol and vulcanolide have the best energies of interaction with the SARS-CoV-2 main protease. We can also observe that their selected target has a good *ID* with the SARS-CoV-2 main protease. Based on the

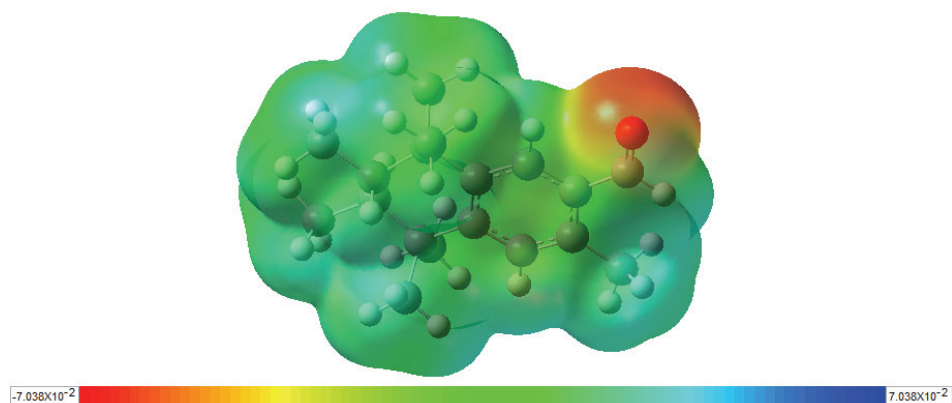


Fig. 8. Maps of molecular electrostatic potential obtained at the B3LYP/6-31G(d) level of theory onto a density isosurface of 0.002 e/u.a.^3 , for vulcanolide molecule.

fact that structural homology is sometimes linked to functional homology, it is important to look for the selected compounds that could have good inhibitory effects on the SARS-CoV-2 main protease. The *RMSD* values recorded during the simulation (for drug vulcanolide) and fairly low potential energy of $-2.88 \times 10^5 \text{ kJ mol}^{-1}$ show the high stability of the protein ligand complex and the likelihood of the vulcanolide molecule to be a drug-like candidate. Thus, the evaluation of the activity, *in vitro* and *in vivo*, of vulcanolide against COVID-19 could be interesting.

Acknowledgements. The authors would like to thank the Research Department of the Universidad Católica de la Santísima Concepción for its support through the DIREG 03/2020 project. L. H. Mendoza-Huizar thankfully acknowledges the computer resources, technical expertise and support provided by the Laboratorio Nacional de Supercómputo del Sureste de México, Consejo Nacional de Ciencia y Tecnología (CONACYT) member of the network of national laboratories through the project No. 202203072N and to the Universidad Autónoma del Estado de Hidalgo.

ИЗВОД

ИДЕНТИФИКАЦИЈА МОШУСНИХ ЈЕДИЊЕЊА КАО ИНХИБИТОРА ГЛАВНЕ SARS-COV-2 ПРОТЕАЗЕ, СТУДИЈАМА МОЛЕКУЛСКОГ ДОКИНГА И МОЛЕКУЛСКЕ ДИНАМИКЕ

ASSIA BELHASSAN¹, GUILLERMO SALGADO², LUIS HUMBERTO MENDOZA-HUIZAR³, HANANE ZAKI⁴, SAMIR CHTITA⁵, TAHAR LAKHLIFI¹, MOHAMMED BOUACHRINE^{1,4}, LORENA GERLI CANDIA⁶ и WILSON CARDONA⁷

¹Molecular Chemistry and Natural Substances Laboratory, Faculty of Science, Moulay Ismail University of Meknes, Morocco, ²Facultad de Ciencias Químicas. Investigador Extramural, Universidad de Concepción, Concepción, Chile, ³Autonomous University of Hidalgo State. Academic Area of Chemistry. Mineral de la Reforma, Hidalgo. México, ⁴EST Khenifra, Sultan Moulay Sliman University, Benimellal, Morocco, ⁵Laboratory of Analytical and Molecular Chemistry, Department of Chemistry, Faculty of Sciences Ben M'Sik, Hassan II University of Casablanca, Casablanca, Morocco, ⁶Departamento de Química Ambiental, Facultad de Ciencias, Universidad Católica de la Santísima Concepción, Concepción, Chile u ⁷Facultad de Ciencias Exactas, Departamento de Química. Universidad Andrés Bello. Concepción, Chile

Пошто је развој нових лекова дуготрајан процес, поновна употреба биоактивних супстанци би могла бити одговор на нове епидемије; тако је скрининг постојећих биоактивних једињења према новој SARS-CoV-2 инфекцији важан задатак. Са тиме на уму, ми смо систематски прегледали потенцијалне мирисне молекуле за третирање ове инфекције на бази афинитета одабраних мирисних једињења према проучаваном ензиму и идентичност секвенце њихових циљних протеина (олфакторни рецептори) према истом ензиму (главна протеаза SARS-CoV-2). Укупно је 12 мошусних мирисних једињења подвргнуто студији докинга и молекулске динамике да би предвидели њихов утицај на главну протеазу SARS-CoV-2. У овој студији идентификовали смо два једињења мошусног мириса (андростенол и вулканолид) која имају добру енергију везивања на везивно место главне протеазе SARS-CoV-2. Међутим, RMSD вредности забележене током симулације молекулске динамике показују да вулканолид испољава високу стабилност протеин-лигандног комплекса у поређењу са андростенолом. Перспективе овог рада су следеће: *in vitro*, *in vivo* и клиничка испитивања за потврђивање рачунарских налаза.

(Примљено 25. новембра, ревидирано 22. децембра 2023, прихваћено 19. фебруара 2024)

REFERENCES

1. R. Tosepu, J. Gunawan, D. S. Effendy, L. O. A. I. Ahmad, H. Lestari, H. Bahar, P. Asfian, *Sci. Total Environ.* **725** (2020) 138436 (<http://dx.doi.org/10.1016/J.SCITOTENV.2020.138436>)
2. C. Wu, Y. Liu, Y. Yang, P. Zhang, W. Zhong, Y. Wang, Q. Wang, Y. Xu, M. Li, X. Li, M. Zheng, L. Chen, H. Li, *Acta Pharm. Sin., B* **10** (2020) 766 (<http://dx.doi.org/10.1016/J.APSB.2020.02.008>)
3. A. K. Singh, A. Singh, A. Shaikh, R. Singh, A. Misra, *Diabetes Metab. Syndr. Clin. Res. Rev.* **14** (2020) 241 (<http://dx.doi.org/10.1016/J.DSX.2020.03.011>)
4. D. Kang, H. Choi, J. H. Kim, J. Choi, *Int. J. Infect. Dis.* **94** (2020) 96 (<http://dx.doi.org/10.1016/j.ijid.2020.03.076>)
5. P. Zhai, Y. Ding, X. Wu, J. Long, Y. Zhong, Y. Li, *Int. J. Antimicrob. Agents* **55** (2020) 105955 (<http://dx.doi.org/10.1016/J.IJANTIMICAG.2020.105955>)
6. Y. Shi, J. Wang, Y. Yang, Z. Wang, G. Wang, K. Hashimoto, K. Zhang, H. Liu, *Brain, Behav. Immun. – Heal.* **4** (2020) 100064 (<http://dx.doi.org/10.1016/J.BBIH.2020.100064>)
7. C. H. Parga-Lozano, *Biomed. J. Sci. Tech. Res.* **35** (2021) 28000 (<http://dx.doi.org/10.26717/bjstr.2021.35.005761>)

8. Z. Wang, X. Chen, Y. Lu, F. Chen, W. Zhang, *Biosci. Trends* **14** (2020) 64 (<http://dx.doi.org/10.5582/BST.2020.01030>)
9. A. A. Elfiky, *Life Sci.* **248** (2020) 117477 (<https://doi.org/10.1016/J.LFS.2020.117477>)
10. B. Robson, *Comput. Biol. Med.* **119** (2020) 103670 (<http://dx.doi.org/10.1016/J.COMPBIOMED.2020.103670>)
11. V. Pooladanda, S. Thatikonda, C. Godugu, *Life Sci.* **254** (2020) 117765 (<http://dx.doi.org/10.1016/J.LFS.2020.117765>)
12. R. Hatada, K. Okuwaki, Y. Mochizuki, K. Fukuzawa, Y. Komeiji, Y. Okiyama, S. Tanaka, *J. Chem. Inf. Model.* **60** (2020) 3593 (<https://doi.org/10.1021/acs.jcim.0c00283>)
13. X. Tang, R. H. Du, R. Wang, T. Z. Cao, L. L. Guan, C. Q. Yang, Q. Zhu, M. Hu, X. Y. Li, Y. Li, L. R. Liang, Z. H. Tong, B. Sun, P. Peng, H. Z. Shi, *Chest* **158** (2020) 195 (<http://dx.doi.org/10.1016/j.chest.2020.03.032>)
14. J. Fantini, C. Di Scala, H. Chahinian, N. Yahi, *Int. J. Antimicrob. Agents* **55** (2020) 105960 (<http://dx.doi.org/10.1016/J.IJANTIMICAG.2020.105960>)
15. Z. Sahraei, M. Shabani, S. Shokouhi, A. Saffaei, *Int. J. Antimicrob. Agents* **55** (2020) 105945 (<http://dx.doi.org/10.1016/J.IJANTIMICAG.2020.105945>)
16. A. C. Tsang, S. Ahmadi, J. Hamilton, J. Gao, G. Virgili, S. G. Coupland, C. C. Gottlieb, *Am. J. Ophthalmol.* **206** (2019) 132 (<http://dx.doi.org/10.1016/j.ajo.2019.04.025>)
17. P. Gautret, J. C. Lagier, P. Parola, V. T. Hoang, L. Meddeb, M. Mailhe, B. Doudier, J. Courjon, V. Giordanengo, V. E. Vieira, H. Tissot Dupont, S. Honoré, P. Colson, E. Chabrière, B. La Scola, J.-M. Rolain, P. Brouqui, D. Raoult, *Int. J. Antimicrob. Agents* **56** (2020) 105949 (<http://dx.doi.org/10.1016/J.IJANTIMICAG.2020.105949>)
18. J. B. Radke, J. M. Kingery, J. Maakestad, M. D. Krasowski, *Toxicol. Reports* **6** (2019) 1040 (<http://dx.doi.org/10.1016/J.TOXREP.2019.10.006>)
19. C. Colalto, *Drug Dev. Res.* **81** (2020) 950 (<http://dx.doi.org/10.1002/ddr.21716>)
20. E. O. Ojah, *Iberoam. J. Med.* **2** (2020) 322 (<http://dx.doi.org/10.53986/ibjm.2020.0056>)
21. N. Contreras-Puentes, M. Salas-Moreno, L. Mosquera-Chaverra, L. Córdoba-Tovar, A. Alviz-Amador, *J. Pharm. Pharmacogn. Res.* **10** (2022) 469 (http://dx.doi.org/10.56499/jppres21.1328_10.3.469)
22. P. T. Quy, T. Q. Bui, N. M. Thai, L. N. H. Du, N. T. Triet, T. Van Chen, N. V. Phu, D. T. Quang, D. C. To, N. T. A. Nhung, *Open Chem.* **21** (2023) 20230109 (<http://dx.doi.org/10.1515/chem-2023-0109>)
23. S. Dev, I. Kaur, *Kragujev. J. Sci.* **42** (2020) 29 (<http://dx.doi.org/10.5937/kgjsci2042029d>)
24. U. J. Meierhenrich, *Rev. Oenologues Tech. Vitivinic. Oenologiques Mag. Trimest. Inform.* **33** (2006) 19 (<https://dialnet.unirioja.es/servlet/articulo?codigo=3556037>)
25. V. Meyer, *Détection d'homologies lointaines à faibles identités de séquences : Application aux protéines de la signalisation des dommages de l'ADN*, Université Paris-Diderot – Paris VII, 2007 (<https://theses.hal.science/tel-00361212>)
26. I. Aanouz, A. Belhassan, K. El-Khatibi, T. Lakhliifi, M. El-Idrissi, M. Bouachrine, *J. Biomol. Struct. Dyn.* **39** (2021) 2971 (<http://dx.doi.org/10.1080/07391102.2020.1758790>)
27. H. Zaki, A. Belhassan, M. Benlyas, T. Lakhliifi, M. Bouachrine, *J. Biomol. Struct. Dyn.* **39** (2021) 2993 (<http://dx.doi.org/10.1080/07391102.2020.1759452>)
28. K. Arnold, L. Bordoli, J. Kopp, T. Schwede, *Bioinformatics* **22** (2006) 195 (<http://dx.doi.org/10.1093/BIOINFORMATICS/BTI770>)
29. A. Belhassan, H. Zaki, A. Aouidate, M. Benlyas, T. Lakhliifi, M. Bouachrine, *Moroccan J. Chem.* **7** (2019) 028 (<http://dx.doi.org/10.48317/IMIST.PRSM/MORJCHEM-V7I1.12247>)

30. A. Belhassan, S. Chtita, H. Zaki, T. Lakhlifi, M. Bouachrine, *Bioinformation* **16** (2020) 404 (<http://dx.doi.org/10.6026/97320630016404>)
31. M. Biasini, S. Bienert, A. Waterhouse, K. Arnold, G. Studer, T. Schmidt, F. Kiefer, T. G. Cassarino, M. Bertoni, L. Bordoli, T. Schwede, *Nucleic Acids Res.* **42** (2014) w252 (<http://dx.doi.org/10.1093/NAR/GKU340>)
32. N. Guex, M. C. Peitsch, T. Schwede, *Electrophoresis* **30** (2009) S162 (<http://dx.doi.org/10.1002/ELPS.200900140>)
33. H. E. Pence, A. Williams, *J. Chem. Educ.* **87** (2010) 1123 (<http://dx.doi.org/10.1021/ED100697W>)
34. L. Ahmed, Y. Zhang, E. Block, M. Buehl, M. J. Corr, R. A. Cormanich, S. Gundala, H. Matsunami, D. O'Hagan, M. Ozbil, Y. Pan, S. Sekharan, N. Ten, M. Wang, M. Yang, Q. Zhang, R. Zhang, V. S. Batista, H. Zhuang, *Proc. Natl. Acad. Sci. U. S. A.* **115** (2018) E3950 (<https://doi.org/10.1073/pnas.1713026115>)
35. O. Trott, A. J. Olson, *J. Comput. Chem.* **31** (2010) 455 (<http://dx.doi.org/10.1002/jcc.21334>)
36. BIOVIA, Dassault Systèmes, Discovery Studio Visualiser 2019, San Diego: Dassault Systèmes, 2019 (<https://discover.3ds.com/discovery-studio-visualizer-download>)
37. H. M. Berman, J. Westbrook, Z. Feng, G. Gilliland, T. N. Bhat, H. Weissig, I. N. Shindyalov, P. E. Bourne, *Nucleic Acids Res.* **28** (2000) 235 (<http://dx.doi.org/10.1093/nar/28.1.235>)
38. M. Hakmi, E. M. Bouricha, I. Kandoussi, J. El Harti, A. Ibrahim, *Bioinformation* **16** (2020) 301 (<http://dx.doi.org/10.6026/97320630016301>)
39. C. Kutzner, S. Páll, M. Fechner, A. Esztermann, B. L. De Groot, H. Grubmüller, *J. Comput. Chem.* **36** (2015) 1990 (<http://dx.doi.org/10.1002/JCC.24030>)
40. E. F. Pettersen, T. D. Goddard, C. C. Huang, G. S. Couch, D. M. Greenblatt, E. C. Meng, T. E. Ferrin, *J. Comput. Chem.* **25** (2004) 1605 (<http://dx.doi.org/10.1002/jcc.20084>)
41. M. Martínez-Cifuentes, B. E. Weiss-López, L. S. Santos, R. Araya-Maturana, *Molecules* **19** (2014) 9354 (<http://dx.doi.org/10.3390/MOLECULES19079354>)
42. A. Kumar, C. G. Mohan, P. C. Mishra, *J. Mol. Struct. Theochem* **361** (1996) 135 ([http://dx.doi.org/10.1016/0166-1280\(95\)04312-8](http://dx.doi.org/10.1016/0166-1280(95)04312-8))
43. K. Raghavachari, *Theor. Chem. Accounts* **103** (2000) 361 (<https://doi.org/10.1007/S002149900065>)
44. A. D. Becke, *Phys. Rev., A* **38** (1988) 3098 (<http://dx.doi.org/https://doi.org/10.1103/PhysRevA.38.3098>)
45. Gaussian 09, Revision A.01, Gaussian, Inc., Wallingford, CT, 2009. (<https://gaussian.com/g09citation/>)
46. Gaussview Rev. 3.09, Windows version, Gaussian Inc., Pittsburgh, PA (https://gaussian.com/508_gvw/)
47. T. Pantsar, A. Poso, *Molecules* **23** (2018) 1899 (<http://dx.doi.org/10.3390/molecules23081899>)
48. M. Popovic, *Microb. Risk Anal.* **23** (2023) 100250 (<http://dx.doi.org/10.1016/j.mran.2023.100250>)
49. M. Popovic, *Microb. Risk Anal.* **22** (2022) 100231 (<http://dx.doi.org/10.1016/j.mran.2022.100231>)
50. X. Du, Y. Li, Y. L. Xia, S. M. Ai, J. Liang, P. Sang, X. L. Ji, S. Q. Liu, *Int. J. Mol. Sci.* **17** (2016) 144 (<http://dx.doi.org/10.3390/ijms17020144>)
51. P. Gale, *Microb. Risk Anal.* **21** (2022) 100198 (<http://dx.doi.org/10.1016/j.mran.2021.100198>)

52. T. Maass, G. Ssebyatika, M. Brückner, L. Breckwoldt, T. Krey, A. Mallagaray, T. Peters, M. Frank, R. Creutzmacher, *Chem. - A Eur. J.* **28** (2022) e202202614 (<http://dx.doi.org/10.1002/chem.202202614>).



J. Serb. Chem. Soc. 89 (11) 1461–1473 (2024)
JSCS–5800

Fiber and microelements content in various types of wheat bread

AZRA REDŽEPOVIĆ-ĐORĐEVIĆ¹, MARGARITA DODEVSKA^{2*}, MILICA JOVETIĆ³
and MARIJANA AČANSKI⁴

¹Institute of Public Health of Belgrade, Belgrade, Serbia, ²Institute of Public Health of Serbia „Dr Milan Jovanovic Batut“, Belgrade, Serbia, ³Directorate for National Reference Laboratories, Ministry of Agriculture, Water Management and Forestry, Belgrade, Serbia and ⁴Faculty of Technology, University of Novi Sad, Novi Sad, Serbia

(Received 24 February, revised 4 April, accepted 21 August 2024)

Abstract: Various types of wheat bread are present in the Serbian market: white, brown, whole-wheat, wheat/rye, buckwheat/wheat, half-white and corn/wheat bread. This research included the quantification of the content of total fiber, fiber fractions, and microelements (manganese, copper, iron and zinc) in order to check whether the breads on the market contain the amounts that are proven beneficial for health. The aim was also to determine the contribution of these nutrients through the consumption of bread to the recommended daily intake. The results show that the bread from the Serbian market contains a large amount of arabinoxylan (1.2–2.6 g 100 g⁻¹) and that wheat/rye, brown and whole wheat bread are sources of dietary fiber (4.0–4.6 g 100 g⁻¹). Also, an important result is that all types of bread except white, contain more than 15 % of dietary reference values for copper and manganese. The intake of total fiber (+ 100 %), arabinoxylan (+ 117 %), copper (+ 118 %), and manganese (+ 85 %) increases by replacing white bread with whole wheat bread, therefore it is of great interest to raise awareness among consumers about the beneficial foods that should be included in the diet. Methods applied in this research showed acceptable precision and accuracy and also proved to be quite simple for routine analysis work.

Keywords: bread; total fiber; arabinoxylan; beta glucan; microelements.

INTRODUCTION

Recommendations on proper nutrition, as one of the basic prerequisites for a healthy and quality lifestyle, clearly refer to the use of vegetables, fruits, grains, dairy products, protein foods, and oils. These types of foods are good sources of energy and nutrients, but one must take into account the changes caused by their

* Corresponding author. E-mail: margarita_dodevska@batut.org.rs
<https://doi.org/10.2298/JSC240211075R>



processing, which can lead to the loss of important nutritionally active components. No less important are the consumers' habits that need to be adapted and directed in the function of health.¹

Bread is the basic component of the daily diet in Serbia – even 86.2 % of the population consume it, mostly white bread (60.1 %).^{2,3}

As bread belongs to the group of grain products, depending on whether it is made from whole or refined grains, it is declared as whole-wheat or white bread.¹ There is an important difference between these two types of bread regarding the content of biologically active compounds. In contrast to white bread, whole-wheat bread is rich in dietary fiber, vitamins and minerals.⁴

In whole grain cereals, dietary fiber in the rye is 15.5 % and in wheat, it is nearly 12 % (results are in % dry basis).⁵ The content of arabinoxylan, an important dietary fiber component, varies from 4.8 to 7.6 % in wheat and 7.6–12.1 % in rye.⁶ The whole grain is composed of 80–85 % endosperm, 12–18 % bran and 2–3 % germ.⁷ The total nonstarch polysaccharides of wheat bran consist of arabinoxylan (17–33 %), cellulose (9–14 %), fructan (3–4 %) and β -D-glucan (1–3 %).⁸ The higher the proportion of wheat bran in the flour, the higher will be the content of arabinoxylan and beta-glucans.⁹

Dietary fiber, vitamins, and minerals are associated with a reduced risk of various diseases.¹⁰ Many studies indicate the beneficial effects of dietary fiber and fiber fractions on health. Arabinoxylan, the most abundant dietary fiber fraction, has been found to be very effective in preventing diabetes and reducing postprandial glycemia.^{11,12} The meta-analysis of prospective studies confirmed an inverse relationship between the intake of wholegrain cereals and diabetes mellitus type 2.¹³ Also, the meta-analysis by Huang *et al.* showed that high consumption of whole grains or cereal fibers can be associated with a reduced risk of non-communicable diseases (NCD).¹⁴ Wolever *et al.* reported that beta glucan from oats is more effective on lowering LDL-cholesterol than beta glucan from wheat bran.¹⁵ Regular intake of an adequate amount of dietary fiber is considered good for controlling obesity and blood cholesterol levels.^{16,17}

Summarizing data from studies that dealt with the mineral composition of grain products, it can be concluded that the most abundant microelements in grains are iron, zinc, manganese and copper.^{18,19} The importance of microelements for the human organism is well known. Iron is a component of hemoglobin and, as well as zinc, is important for the functioning of a large number of enzymes.⁴ Copper participates in the synthesis of hemoglobin, as well as in redox reactions, while manganese is necessary for many metabolic functions.^{20,21} Due to the importance of these elements, their appropriate intake is necessary and for that reason, they are included in dietary reference values (DRVs) for nutrients.²²

There are three goals of this study: to examine the quality of bread present in the Serbian market from the aspect of the content of fibers and selected microele-

ments, to determine to what extent these types of bread contain fibers and microelements that were proven to be health beneficial and to determine what is the contribution of these nutrients to their recommended daily intakes.

EXPERIMENTAL

Samples and sample preparation

A total of 69 bread samples were obtained from local markets in Novi Sad. All products on sale in bakeries as well as unpacked products available in food shops were bought on the same day when they were made, while a number of products were prepacked breads with prolonged usage periods, bought within their expiration date.

Bread samples were classified into seven types, based on their characteristics, *i.e.*, main ingredients. This classification was made following Serbian regulations regarding the quality of cereals and cereal products.²³ These seven types were: brown bread (BB, 17 samples), whole-wheat bread (WWB, 12 samples), wheat/rye bread (WRB, 6 samples), buckwheat/wheat bread (BWB, 13 samples), half-white bread (HWB, 7 samples), white bread (WB, 11 samples) and corn/wheat bread (CWB, 3 samples).

The samples were ground and homogenized in a blender, then transferred in polyethylene containers (Lab Logistics Group GmbH, Germany) suitable for foodstuff according to the EU Regulations²⁴ and deep-frozen at $-18\text{ }^{\circ}\text{C}$ until analysis.

Determination of total dietary fiber

The content of total dietary fiber was determined by the enzyme–gravimetric method (AOAC method 985.29), as described by Proski *et al.* (1985)²⁵, using the K-TDFR enzyme assay kit (Megazyme, Bray, Ireland). Phosphate buffer, pH 6.0, and enzymes (heat-stable α -amylase, protease and amyloglucosidase) are required for analysis. Heat-stable α -amylase depolymerizes starch, protease depolymerizes and dissolves proteins, while amyloglucosidase converts starch to glucose. After treating the sample with the mentioned enzymes and adding ethanol to precipitate soluble fiber and remove depolymerized protein and glucose (from starch), the residue was filtered, 95 % ethanol and acetone were added to it, subsequently, and then dried and weighed. Protein content was determined in one part of the residue, using Turbotherm digestion unit Gerhard TT100 and System for protein analysis Gerhardt VAP40 Vapodest. The other part of the residue was incinerated at 525°C to determine the ash content (annealing furnace up to $1100\text{ }^{\circ}\text{C}$, Elektron, ELP-06, Banja Koviljača, Serbia, were used). The content of total dietary fiber was obtained by subtracting the mass of protein and ash from the mass of the filtered and dried residue. Memmert 400 dryer was used for drying.

Determination of β -glucan

Beta-glucan was quantified according to McCleary and Codd by a spectrophotometric method,²⁶ using the K-BGLU enzyme assay kit (Megazyme, Ireland). The samples were suspended and hydrated in a pH 6.5 buffer solution, incubated with the purified lichenase enzyme, and then filtered. An aliquot of the filtrate was completely hydrolyzed with purified β -glucosidase, yielding D-glucose, which was further assayed using the glucose oxidase/peroxidase reagent. The D-glucose thus formed was measured by absorption at 510 nm, by a UV–Vis spectrophotometer (Thermo Scientific Evolution 201, Waltham, MA, USA).

Determination of D-xylose including xylan and arabinoxylan

D-Xylose, including xylan and arabinoxylan, were determined by spectrophotometric method using the enzymatic assay kit K-Xylose (Megazyme, Ireland). The assay was per-

formed according to the producer instruction manual. The procedure is based on the interconversion of α -D-xylose to β -D-xylose later being oxidised by NAD^+ to D-xylonic acid. Interconversion of the α - and β -anomeric forms of D-xylose is catalyzed by xylose mutarotase. The β -D-xylose is oxidised by NAD^+ to D-xylonic acid in the presence of β -xylose dehydrogenase at pH 7.5. The amount of NADH formed in this reaction is proportional (directly correlated) to D-xylose concentration. NADH is measured by the increase of the absorbance at 340 nm, by a UV-Vis spectrophotometer (Thermo Scientific Evolution 201, Waltham, MA, USA). Arabinoxylan content is calculated according to the formula:

$$\text{Arabinoxylan (g 100 g}^{-1}\text{)} = 100 \times \text{D-xylose content (g 100 g}^{-1}\text{)} / 62 \quad (1)$$

The quality control of determination of total fiber content was conducted using the left-over of the test material from the proficiency testing Nutritional Components in Breadcrumbs (T2454, Fapas, UK). For the quality control of determination of fiber fractions – beta glucan and arabinoxylan quality control materials Barley flour control (Megazyme, Lot 60301e, Ireland) and D-xylose standard (Megazyme, Lot 141005c, Ireland) were analyzed.

Method performance parameters (precision and accuracy) are presented in Table I. The limit of quantification (*LOQ*) was 0.1 mg kg⁻¹ for total fiber, 0.3 mg kg⁻¹ for beta glucan and 0.1 mg kg⁻¹ for arabinoxylan.

TABLE I. Quality control of total dietary fiber, beta glucan and arabinoxylan content determination

Analyte	Precision ^a <i>RSD_r</i> / %	Recovery, %	Quality control material	
			Assigned value	Result
Total fiber	2.6	98	4.24 g 100 g ^{-1b}	4.16 g 100 g ⁻¹
Beta glucan	3.6	96	4.1 % ^c	3.9 %
Arabinoxylan	2.0	104	0.25 mg mL ^{-1d}	0.26 mg mL ⁻¹

^aPrecision under repeatability conditions; ^bbreadcrumbs (FAPAS T2454); ^cbarley flour control (Megazyme lot 60301e); ^dD-xylose standard (Megazyme lot 141005c)

Determination of microelements

Microelements: manganese, iron, copper and zinc were quantified by inductively coupled plasma mass spectrometry (ICP-MS) after microwave digestion of bread samples.

Test portions of about 0.5 g of grinded and homogenized bread samples were weighed into polytetrafluoroethylene (PTFE) vessels for microwave digestion. Nine mL of 65 % nitric acid (Suprapur[®], Merck, Germany) and 1 mL of 30 % hydrogen peroxide (Emsure[®], Merck, Germany) were added to the vessels and the mixture was mineralized in a microwave closed digestion system (Ethos Up, Milestone, Italy) by heating up to 200 °C for 15 min, followed by digestion at 200 °C for 20 min, and cooling for 30 min. The digested solutions were quantitatively transferred into 50 mL volumetric flasks and diluted with deionized water (electrical resistivity 18.2 M Ω cm) obtained using a Simplicity[®] water purification system (Merck Millipore, USA). The blank solution was prepared in the same way.

Trace element levels were determined by inductively coupled plasma mass spectrometer (iCAP RQ, Thermo Scientific, USA) in KED mode of operation. The entire system was controlled with the Qtegra Instrument Control Software (Thermo Scientific, USA). Instrumental conditions were as follows: RF power 1548 W; argon (≥ 99.999 %) flows: 14 L min⁻¹ (cooling); 1.1 L min⁻¹ (nebulizer); 0.8 L min⁻¹ (auxiliary gas); helium (≥ 99.9999 %) flow: 5 L min⁻¹ (CCT); acquisition time: 3 \times 60 s; points per peak: 3; dwell time: 10 ns; detector mode: pulse.

The measured isotopes were: ^{55}Mn , ^{56}Fe , ^{63}Cu and ^{66}Zn . For the quantification of these metals, stock solutions of iron, copper and zinc, concentration of $100\ \mu\text{g mL}^{-1}$ each, in 2–5 % nitric acid (AccuTrace™, AccuStandard, USA) and stock solution of manganese, concentration of $100\ \text{mg mL}^{-1}$ in 2 % nitric acid (CPAchem, Bulgaria) were used. The intermediate multi-element standard solutions were prepared from these stock solutions. The results were expressed as mg per 100 g of bread samples.

For the quality control of the entire analytical procedure the certified reference material (CRM) NIST® SRM® 1568b (National Institute of Technology, USA) was analyzed. Method performance parameters (precision and accuracy) are presented in Table II. The limit of quantification (*LOQ*) was $0.20\ \text{mg kg}^{-1}$ for manganese, $0.80\ \text{mg kg}^{-1}$ for iron, $0.16\ \text{mg kg}^{-1}$ for copper and $0.40\ \text{mg kg}^{-1}$ for zinc.

TABLE II. Quality control of the determination of microelement content

Analyte	Precision ^a <i>RSD_r</i> / %	Recovery, %	CRM	
			Certified value ^b , mg kg^{-1}	Result, mg kg^{-1}
Manganese	3.6	103	19.2 ± 1.8	19.7
Iron	4.7	101	7.42 ± 0.44	7.49
Copper	5.9	97	2.35 ± 0.16	2.27
Zinc	3.3	100	19.42 ± 0.26	19.36

^aPrecision under repeatability conditions; ^bNIST® SRM® 1568b rice flour

Data analysis

Results obtained in this experiment were analyzed using the SPSS version 20.0 program (Chicago, IL, USA). The sample size was shown and descriptive statistics (mean, median, minimum and maximum) were calculated. Principal component analysis (PCA) was applied to integrate the results of chemical parameters, discover the possible correlations among measured parameters, and classify them in a factor plane. The analyzed fiber, fiber fractions and microelements of breads were used to generate the PCA model. The level of significance was set at 0.05.

RESULTS AND DISCUSSION

The content of fibers and microelements in different bread types

The content of total dietary fiber, fiber fractions (arabinoxylan and β -glucan) and microelements determined in bread samples is presented in Table III. The results are expressed as g per 100 g for fiber and fiber fractions, and as mg per 100 g for microelements, wet weight both. The parameters of descriptive statistics are presented in the same Table III.

Total fiber, arabinoxylan and β -glucan

In Table III it can be clearly observed that BB, WWB and WRB did not substantially differ among themselves concerning total fiber, beta glucan and arabinoxylan contents, and the same was true for BWB, HWB, WB and CWB when compared among themselves. Therefore, based on these results the examined samples were divided into two aggregate groups: the first one (a total of 35

samples) included BB, WWB and WRB samples, while the second one (a total of 34 samples) included BWB, HWB, WB and CWB samples.

TABLE III. Content of fiber fractions, total fiber and microelements in different bread types; *SD* – standard deviation, BB – brown bread, WWB – whole-wheat bread, WRB – wheat/rye bread, BWB – buckwheat/wheat bread, HWB – half white bread, WB – white bread, CWB – corn/wheat bread (CWB)

Parameter	Value type	Bread type						
		BB (17)	WWB (12)	WRB (6)	BWB (13)	HWB (7)	WB (11)	CWB (3)
Arabinoxylan g 100 g ⁻¹	Mean	2.4	2.6	1.7	1.5	1.4	1.2	1.6
	<i>SD</i>	0.9	0.7	0.7	0.3	0.3	0.5	0.7
	Median	2.4	2.7	1.5	1.4	1.4	1.3	1.4
	Maximum	4.3	3.6	3.0	2.2	1.9	2.0	2.4
	Minimum	1.3	1.6	1.1	1.2	0.9	0.4	1.1
β -Glucan g 100 g ⁻¹	Mean	0.8	1.0	1.2	0.5	0.3	0.4	0.3
	<i>SD</i>	0.5	0.5	0.2	0.3	0.1	0.2	0.1
	Median	0.8	1.0	1.2	0.4	0.3	0.3	0.3
	Maximum	1.7	1.7	1.5	1.2	0.4	0.9	0.4
	Minimum	0.2	0.3	1.0	0.2	0.2	0.2	0.3
Total fiber g 100 g ⁻¹	Mean	4.4	4.6	4.0	2.9	2.6	2.3	2.3
	<i>SD</i>	1.4	1.1	1.1	0.7	0.5	0.8	0.6
	Median	4.0	4.5	4.0	3.0	3.0	2.0	2.0
	Maximum	7.0	6.0	6.0	4.0	3.0	4.0	3.0
	Minimum	3.0	3.0	3.0	2.0	2.0	1.0	2.0
Mn mg 100 g ⁻¹	Mean	1.08	1.05	1.26	1.01	0.71	0.54	0.73
	<i>SD</i>	0.48	0.68	0.99	0.68	0.18	0.40	0.40
	Median	0.92	0.85	1.05	0.69	0.79	0.51	0.52
	Maximum	1.96	2.71	2.62	2.45	0.95	1.42	1.29
	Minimum	0.31	0.21	0.20	0.30	0.44	0.11	0.38
Fe mg 100 g ⁻¹	Mean	1.90	1.51	1.96	1.51	1.60	1.01	1.15
	<i>SD</i>	0.65	0.66	1.15	0.57	0.40	0.63	0.37
	Median	1.67	1.40	1.78	1.35	1.53	0.85	0.95
	Maximum	3.22	3.15	4.02	2.90	2.43	2.38	1.66
	Minimum	0.94	0.71	0.51	0.86	1.14	0.39	0.84
Cu mg 100 g ⁻¹	Mean	0.22	0.22	0.18	0.34	0.19	0.12	0.16
	<i>SD</i>	0.10	0.16	0.15	0.27	0.11	0.10	0.04
	Median	0.18	0.16	0.15	0.26	0.16	0.10	0.15
	Maximum	0.42	0.56	0.40	1.11	0.42	0.37	0.21
	Minimum	0.10	0.03	0.02	0.07	0.05	0.02	0.13
Zn mg 100 g ⁻¹	Mean	1.28	1.14	1.14	1.20	0.88	0.72	1.07
	<i>SD</i>	0.57	0.75	0.74	0.63	0.44	0.44	0.29
	Median	1.19	0.88	0.93	0.86	0.82	0.56	1.26
	Maximum	2.48	3.20	2.13	2.61	1.64	1.86	1.29
	Minimum	0.43	0.44	0.31	0.56	0.25	0.22	0.67

The determined value of total fiber content in bread samples from the first aggregate group was around 4 g 100 g⁻¹, while in the second group, it was around 2 g 100 g⁻¹.

Data on fiber content in various types of bread were presented by many authors.^{4,27–30} Most of those results for WB^{4,28–30} were in agreement with the results of the current study, while Lee *et al.* have reported a slightly higher value (3.45 g 100 g⁻¹).²⁷ However, greater differences in fiber content were observed in case of wholegrain and wholemeal bread. Carochio *et al.* presented lower values (3.3 g 100 g⁻¹), while Kurek *et al.* obtained higher results (about g 100 g⁻¹).^{4,29} On the other hand, Benítez *et al.*, presented a content of total fibers similar to the content obtained in this study (4.9 g 100 g⁻¹).³⁰ In the case of WWB, WRB and CWB obtained results (4.6, 4.0 and 2.0 g 100 g⁻¹, respectively) were similar to those reported in the study of dietary fiber in Serbian diet, carried out by Dod-evska *et al.* (7.03±1.11, 6.16±0.89 and 3.41±0.57 g 100 g⁻¹ of dry matter, respectively), where a substantially smaller number of bread samples was analyzed.²⁸ Noorth *et al.* in their manuscript presented two healthy bread products that contained about 7 g of total fiber per 100 g of product.³¹

Based on the results of the current study, the claim “source of dietary fiber” according to the European Regulation (EC) no. 1924/2006³² may be applied to brown, integral and wheat/rye bread, since the total content of dietary fiber in these samples exceeded 3 g per 100 g.

Results for the arabinoxylan contents in the first aggregate group of bread samples were greater than those in the second one. Thus, for example, the values for arabinoxylan in BB and WWB (2.4 and 2.6 g 100 g⁻¹) were almost twice greater than in BWB, HWB and WB samples (1.5, 1.4 and 1.2 g 100 g⁻¹, respectively). Regarding arabinoxylan, the current study confirmed that wholemeal or rye bread are good source of it. The amounts of arabinoxylan were greater than those presented by Benitez *et al.*, because, in their study, the analyzed breads were made from different percentage compositions of white flour, cereal products and seeds.³⁰

Regarding the content of β -glucan, the first aggregate group of bread samples, especially WWB and WRB samples, stood out in comparison to the samples from the second group. The contents of beta-glucan in WWB and WRB samples were 2.5 to 3-fold greater than the average β -glucan content in the samples from the second group.

Microelements

Investigated microelements: Mn, Fe, Cu and Zn were quantified in all bread samples. The descending order of microelements according to their content was Fe > Zn > Mn > Cu. It is noticeable, comparing all tested samples, that the content of microelements was the lowest in WB. On the other hand, the highest content was observed in WRB in the case of Mn and Fe, and BB and BWB in the case of Cu and Zn.

Numerous authors have dealt with the analysis of microelements in various types of bread. Basaran included several types of bread in his research (multi-grain, wholemeal, whole wheat, rye and white bread), which were quite similar to those from the current study. However, he reported much higher values for Cu (from 0.27 to 0.65 mg 100 g⁻¹) and Mn (from 1.16 to 4.30 mg 100 g⁻¹).³³ Higher values for Cu (from 0.38 to 0.84 mg 100 g⁻¹) were also obtained by Carcho *et al.*⁴ In the current study, Cu content was relatively uniform in all bread types (Table III), except BWB, where it was the highest (0.34 mg 100 g⁻¹). A similar result for Cu content (0.38±0.01 mg 100 g⁻¹) was reported by Rogaska *et al.*³⁴ The highest content of Mn was found in WRB (1.26 mg 100 g⁻¹), as it was reported for Polish wheat-rye bread “Magnus”, which showed much higher Mn level (10.41±0.47 mg kg⁻¹).³⁵ Contrary to that, Mn content in WRB investigated in the current study was about 2.5-fold higher than those investigated by Carcho *et al.*⁴ Iron was the most abundant element in all bread types (1.01–1.96 mg 100 g⁻¹), which is in agreement with other studies.^{4,35,36} Fernandez-Canto *et al.* reported slightly different data for wholegrain bread, where Mn was the most abundant (4.8 mg 100 g⁻¹).¹⁹ The Zn content ranged from 0.72 in WB to 1.28 mg 100 g⁻¹ in BB samples, corresponding well with results reported for wholemeal and wheat/rye bread and refined bread.^{4,19} However, in the formulations of the so-called healthy breads (Salutello and HealthBread) developed by Noorth *et al.*, made from whole grains and with a high fiber content, the content of Zn (2.3 and 2.0 g 100 g⁻¹, respectively) and Fe (2.4 g 100 g⁻¹ for both breads) were much higher than those obtained in the current study.³¹

The intake (contribution to the recommended intake) of fibers and microelements from various bread types

The regulation of the Republic of Serbia³⁷ is aligned with the European Dietary Reference Values for Nutrients.²² The reference intakes for adults are Fe 14 mg per day, Zn 10 mg per day, Mn 2 mg per day, and Cu 1 mg per day. Based on the determined content of microelements in various bread types and dietary reference intakes (DRIs) for adults, Fig. 1 presents the contribution of one portion of bread, *i.e.*, 30 g, then of 100 g of bread, as well as of 166 g³⁸ of bread per day to the DRVs for minerals (Fig. 1a and b) and recommended intakes of fibers (Fig. 1c). If the intake of bread at the daily level is 166 g, only Mn from WRB and Cu from the BWB sample is near the 50 % of the respective DRV. However, they are not the type of bread traditionally represented in the daily diet of the Serbian population.³⁹ The upper Cu level for the adult population of the EU is set at 5 mg per day, making these breads contribute 11.3 % of this limit.⁴⁰

In relation to a portion of 30 g of bread, Cu contribution ranges from 2.82 to 9.36 % of its DRV, while Mn contribute in larger amounts, from 4.28 to 9.69 % of its DRV. This means that one portion of bread is not a source of either Cu or

Mn, but at a level of consumption of 100 g, all types of bread except WB contribute a minimum of 15 % of DRVs for these two elements. The contributions of Fe and Zn remain below 15 % of their respective DRVs even at the level of consumption of 100 g of bread (Fig. 1a).

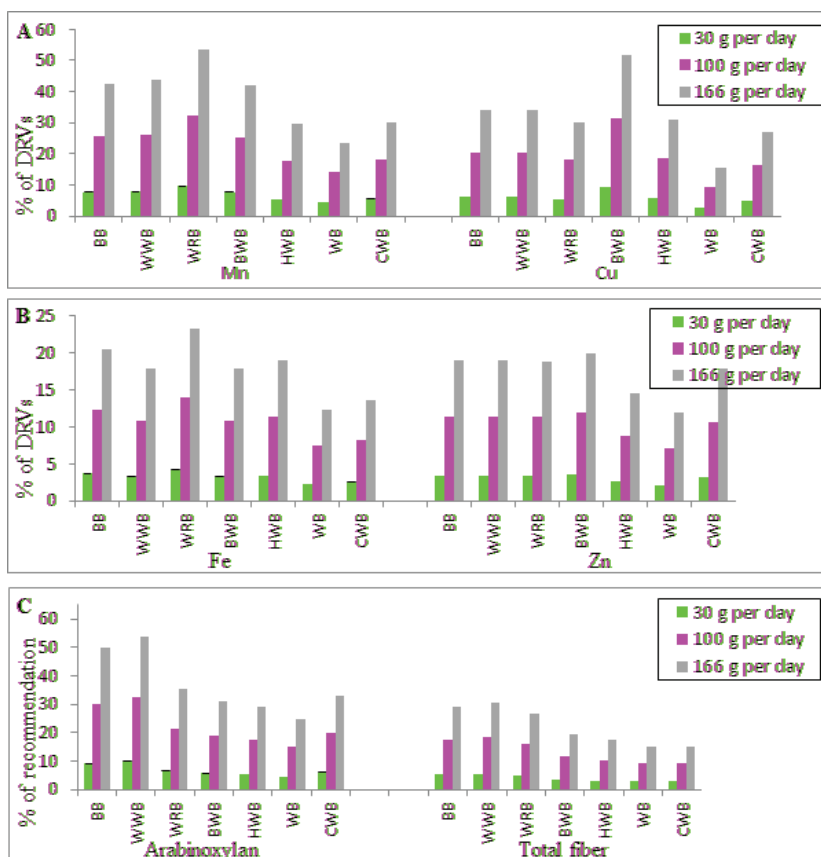


Fig. 1. Contribution of investigated bread types to the Dietary Reference Values (DRVs) of: a) manganese (Mn; 2 mg per day) and copper (Cu; 1 mg per day), b) iron (Fe, 14 mg per day) and zinc (Zn, 10 mg per day) as well as to the recommendations for intake of c) total fibers (25 g per day) and arabinoxylan (8 g per day), related to the intake of 30, 100 and 166 g of the tested bread types.

According to Regulation (EC) No. 1924/2006, a product could bear a nutritional claim of being a source of a nutrient if contains no less than 15 % of its respective DRV.³²

Total fiber (contribution range from 2.8 to 5.5 % of recommended intake) and arabinoxylan (contribution range from 4.5 to 9.8 % of recommended intake) do not reach 15 % of the recommended intake in case of consumption of one 30

g-portion of bread. If the consumption amount increases to 100 g, the contribution of arabinoxylan rises to 15–32.5 % of the recommended intake. For total fiber, higher contributions per 100 g of bread were observed in BBW, BB and WRB bread samples (18.4, 17.6 and 16 % of recommended intake).

Principal component analysis (PCA)

Principal component analysis was applied to integrate the results of chemical parameters, discover possible correlations among measured parameters and classify the parameters in a factor plane. The analyzed fiber, fiber fractions and microelements of breads were used to generate the PCA model.

According to PCA for bread samples (Fig. 2), the highest content of total fiber, arabinoxylane, Zn and Cu (which show a strong positive correlation with the first axis: 0.917, 0.848, 0.722 and 0.686, respectively) were observed in BB, WWB and BWB (it can also be seen from their position), while WRB is the most significant source of β -glucan, Mn and Fe (strong positive correlation with the second axis: 0.757, 0.709 and 0.664, respectively).

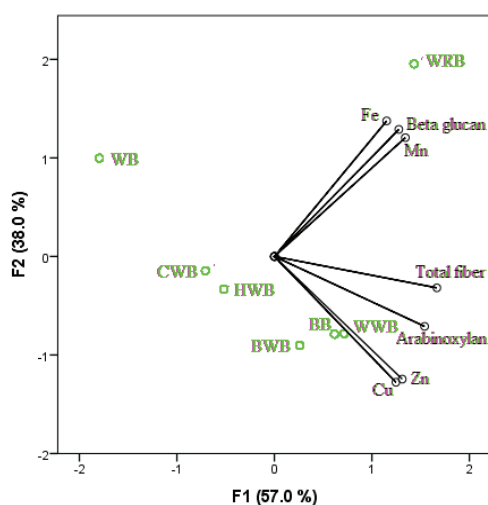


Fig. 2. The biplot of PC1 and PC2 of total fiber, fiber fractions and microelements content of various bread types.

CONCLUSION

Bread is present in the Serbian diet on daily basis, mostly as white bread. Considering that whole wheat bread, compared to refined, contains more fiber and microelements, and knowing the habit of consuming large amounts of bread in this region, if white bread were to be replaced with whole wheat, thus introduced fiber and microelements would have a significant contribution to the total daily intake of these nutrients. Just by replacing white with whole wheat bread, the intake of total fiber would increase by 100 %, especially arabinoxylan

(117 %). There would also be an increase in microelements intake, particularly copper (+ 118 %) and manganese (+ 85 %).

The increased intake of fiber and microelements through the consumption of staple food such as bread, supports, in the overall result, the intake of the amounts of nutrients that are proven to be adequate for maintaining health and which are associated with reduction of the risk of certain chronic diseases. Therefore, special attention must be paid to raising awareness among consumers about the food that should be consumed, as well as about its health impact.

ИЗВОД

САДРЖАЈ ВЛАКАНА И МИКРОЕЛЕМЕНАТА У РАЗЛИЧИТИМ ВРСТАМА ПШЕНИЧНОГ ХЛЕБА

АЗРА РЕЦЕПОВИЋ-ЂОРЂЕВИЋ¹, МАРГАРИТА ДОДЕВСКА², МИЛИЦА ЈОВЕТИЋ³ и МАРИЈАНА АЧАНСКИ⁴

¹Институт за јавно здравље Београд, Београд, ²Институт за јавно здравље Србије „Др Милан Јовановић Башић“, Београд, ³Дирекција за националне референтне лабораторије, Министарство пољопривреде, водопривреде и шумарства, Београд и ⁴Технолошки факултет Универзитета у Новом Саду, Нови Сад

На тржишту Србије присутне су различите врсте пшеничног хлеба: бели, црни, интегрални, пшенично/ражени, хељдино/пшенични, полубели и кукурузно/пшенични хлеб. Ово истраживање је обухватило одређивање садржаја укупних влакана, фракција влакана и микроелемената (мангана, бабра, гвожђа и цинка) како би се проверило да ли хлебови са тржишта садрже количине ових хранљивих материја за које је доказано да су корисне за здравље. Циљ је био и да се одреди колики је допринос ових хранљивих материја препорученом дневном уносу конзумирањем хлеба. Резултати показују да хлеб са тржишта Србије садржи велику количину арабинооксиана (1,2–2,6 g 100 g⁻¹), а да су пшенично/ражени, црни и интегрални хлеб извори дијететских влакана (4,0–4,6 g 100 g⁻¹). Такође, важан резултат је да све врсте хлеба осим белог садрже више од 15 % референтних вредности у исхрани за бабар и манган. Заменом белог хлеба интегралним повећава се унос укупних влакана (+ 100 %), арабинооксиана (+ 117 %), бабра (+ 118 %) и мангана (+ 85 %), стога је од великог интереса подизање свести потрошача о корисним намирницама које треба укључити у исхрану. Методе примењене у овом истраживању су показале прихватљиву прецизност и тачност и такође су се показале прилично једноставним за рутински аналитички рад.

(Примљено 11. фебруара, ревидирано 4. априла, прихваћено 21. августа 2024)

REFERENCES

1. https://www.dietaryguidelines.gov/sites/default/files/2021-03/Dietary_Guidelines_for_Americans-2020-2025.pdf (date accessed: 07.01.2024)
2. <https://www.batut.org.rs/download/publikacije/pub2022v1.pdf> (date accessed: 07.01.2024)
3. Regulation on the national program for the prevention of obesity in children and adults, *Sl. glasnik RS*, No. 9/2018 (In Serbian)
4. M. Carrocho, P. Morales, M. Ciudad-Mulero, V. Fernández-Ruiz, E. Ferreira, S. Heleno, P. Rodrigues, L. Barros, I. C F R, Ferreira, *Food Chem.* **310** (2020) 125954 (<https://doi.org/10.1016/j.foodchem.2019.125954>)

5. M. S. Izydorczyk, in: *Carbohydrates in Food*, 3. ed., A.-C. Eliasson, Ed., CRC Press, Boca Raton, FL, 2017, pp. 215–278
6. N. H. Maina, A. Rieder, Y. De Bondt, N. Mäkelä-Salmi, S. Sahlström, O. Mattila, L. M. Lamothe, L. Nyström, C. M. Courtin, K. Katina, K. Potanen, *Foods* **10** (2021) 2566 (<https://doi.org/10.3390/foods10112566>)
7. C. R. Babu, H. Ketanapalli, S. K. Beebi, V. C. Kolluru, *J. Adv. Biol. Biotechnol.* **9** (2018) 21 (<https://juniperpublishers.com/aibm/pdf/AIBM.MS.ID.555754.pdf>)
8. A. Kaur, M.P. Yadav, B. Singh, S. Bhinder, S. Simon, N. Singh, *Carbohydr. Polym.* **221** (2019) 166 (<https://doi.org/10.1016/j.carbpol.2019.06.002>)
9. P. Saini, M. Islam, R. Das, S. Shekhar, A. Sanjay, K. Sinha, K. Prasad, *J. Food Compos. Anal.* **116** (2023) 105030 (<https://doi.org/10.1016/j.jfca.2022.105030>)
10. S. Ragaei, I. Guzar, N. Dhull, K. Seetharaman, *Food Sci. Technol.* **44** (2011) 2147 (<https://doi.org/10.1016/j.lwt.2011.06.016>)
11. Z. X. Lu, K. Z. Walker, J. G. Muir, T. Mascara, K. O’Dea, *Am. J. Clin. Nutr.* **71** (2000) 1123 (<https://doi.org/10.1093/ajcn/71.5.1123>)
12. M. Müller, G. D. A. Hermes, C. Emanuel E, C, J. J. Holst, E. G. Zoetendal, H. Smidt, F. Troost, F. G. Schaap, S. O. Damink, J. W. E. Jocken, K. Lenaerts, A. A. M. Masclee, E. E. Blaak, *Gut Microbes* **12** (2020) 1704141 (<https://doi.org/10.1080/19490976.2019.1704141>)
13. The InterAct Consortium, *Diabetologia* **58** (2015) 1394 (<https://doi.org/10.1007/s00125-015-3585-9>)
14. T. Huang, M. Xu, A. Lee, S. Cho, L. Qi, *BMC Med.* **13** (2015) 59 (<https://doi.org/10.1186/s12916-015-0294-7>)
15. T. M. S. Wolever, S. M. Tosh, A. L. Gibbs, J. Brand-Miller, A. M. Duncan, V. Hart, B. Lamarche, B. A. Thomson, R. Duss, P. J. Wood, *Am. J. Clin. Nutr.* **92** (2010) 723 (<https://doi.org/10.1016/j.lwt.2013.12.004>)
16. Y. He, B. Wang, L. Wen, F. Wang, H. Yu, D. Chen, X. Su, C. Zhang, *Food Sci. Hum. Wellness* **11** (2022) 1 (<https://doi.org/10.1016/j.fshw.2021.07.001>)
17. W. Cheng, Y. Sun, M. Fan, Y. Li, L. Wang, H. Qian, *Crit. Rev. Food Sci. Nutr.* **62** (2022) 7269 (<https://doi.org/10.1080/10408398.2021.1913399>)
18. E. Suchowilska, M. Wiwart, W. Kandler, R. Krska, *Plant Soil Environ.* **58** (2012) 141 (<https://doi.org/10.17221/688/2011-PSE>)
19. M. N. Fernández-Canto, M. B. García-Gómez, S. Boado-Crego, M. L. Vázquez-Odériz, M. N. Muñoz-Ferreiro, M. Lombardero-Fernández, S. Pereira-Lorenzo, M. A. Romero-Rodríguez, *Foods* **11** (2022) 3176 (<https://doi.org/10.3390/foods11203176>)
20. C. Askwith, J. Kaplan, *Trends Biochem. Sci.* **23** (1998) 135 ([https://doi.org/10.1016/S0968-0004\(98\)01192-X](https://doi.org/10.1016/S0968-0004(98)01192-X))
21. M. Pirsaeheb, M. Hadei, K. Sharafi, *J. Food Compos. Anal.* **96** (2021) 103697 (<https://doi.org/10.1016/j.jfca.2020.103697>)
22. *Dietary Reference Values for Nutrients Summary report, European Food Safety Authority (EFSA)*, Approved: 4 December 2017, Amended: 23 September 2019 (<https://doi.org/10.2903/sp.efsa.2017.e15121>)
23. Rulebook on the quality of grain, mill and bakery products and pasta, *Sl. glasnik RS*, Nos. 68/2016 and 56/2018 (In Serbian)
24. *Regulation (EC) No. 1935/2004 of the European Parliament and of the Council of 27 October 2004 on materials and articles intended to come into contact with food and repealing Directives 80/590/EEC and 89/109/EEC*, OJ L 338, 13.11.2004, pp. 4–17

25. L. Prosky, N. G. Asp, I. Furda, J. W. DeVries, T. F. Schweizer, B. F. Harland, *J. Assoc. Off. Anal. Chem.* **68** (1985) 677 PMID: 2993226
26. B. V. McCleary, R. Codd, *J. Sci. Food Agric.* **55** (1991) 303 (<https://doi.org/10.1002/jsfa.2740550215>)
27. Y. Lee, HJ. Lee, HS. Lee, YA. Jang, C. Kim, *J Food Compost Anal.* **21** (2008) 35 (<http://dx.doi.org/10.1016/j.jfca.2007.07.008>)
28. M. S. Dodevska, B. I. Djordjevic, S. S. Sobajic, I. D. Miletic, P. B. Djordjevic, V. S. Dimitrijevic-Sreckovic, *Food Chem.* **141** (2013) 1624 (<http://dx.doi.org/10.1016/j.foodchem.2013.05.078>)
29. M. A. Kurek, J. Wyrwicz, S. Karp, M. Brzeska, A. Wierzbicka, *J. Cereal Sci.* **74** (2017) 210 (<http://dx.doi.org/10.1016/j.jcs.2017.02.011>)
30. V. Benítez, R. M. Esteban, E. Moniz, N. Casado, Y. Aguilera, E. Mollá, *J. Cereal Sci.* **82** (2018) 113 (<https://doi.org/10.1016/j.jcs.2018.06.001>)
31. M.W.J. Noort, O. Mattila, K. Katina, J. W. van der Kamp, *J. Cereal Sci.* **78** (2017) 57 (<http://dx.doi.org/10.1016/j.jcs.2017.03.009>)
32. *Regulation (EC) No 1924/2006 of the European Parliament and of the Council of 20 December 2006 on nutrition and health claims made on foods*, OJ L 404, 30.12.2006, pp. 9–25
33. B. Basaran, *J. Food Compos. Anal.* **108** (2022) 104443 (<https://doi.org/10.1016/j.jfca.2022.104443>)
34. A. Rogaska, J. Reguła, J. Suliburska, Z. Krejpcio, *Foods* **9** (2020) 1853 (<https://doi.org/10.3390/foods9121853>)
35. P. Bawiec, M. Halabis, Z. Marzec, A. Kot, J. Solski, K. Gawel, *Curr. Issues Pharm. Med. Sci.* **27** (2014) 71 (<https://doi.org/10.2478/cipms-2014-0016>)
36. A. Torrinha, M. Oliveira, S. Marinho, P. Paíga, C. Delerue-Matos, S. Morais, *Molecules* **24** (2019) 2787 (<https://doi.org/10.3390/molecules24152787>)
37. Rulebook on declaration, labeling and advertising of food, *Sl. glasnik RS*, Nos. 19/2017, 16/2018, 17/2020, 118/2020, 17/2022, 23/2022 i 30/2022 (In Serbian)
38. D. R. Živančev, M. S. Buljovčić, J. M. Ninković, I. B. Antić, S. Z. Mikić, S. Ž. Jaćimović, B. Đ. Jocković, *Food Feed Res.* **50** (2023) 13 (<https://doi.org/10.5937/ffr0-42946>)
39. S. Zivic, E. Golubovic, M. Zivic, *Acta Med. Medianae* **39** (2000) 29 (https://publisher.medfak.ni.ac.rs/AMM_1/amm-stari/2000-html/3-broj/STRUKTURA%20ISHRANE%20STANOVNISTVA....pdf)
40. *Re-evaluation of the existing health-based guidance values for copper and exposure assessment from all sources*, European Food Safety Authority (EFSA) Scientific Committee, adopted: 16 November 2022.



J. Serb. Chem. Soc. 89 (11) 1475–1487 (2024)
JSCS–5801

Thermal behavior of polymeric nickel(II) oxalate complex obtained through nickel(II) nitrate/ethylene glycol reaction

MIRCEA NICULESCU¹, MIHAI-COSMIN PASCARIU^{2,3*}, ANDREI RACU²
and BOGDAN-OVIDIU TARANU^{2**}

¹University Politehnica Timisoara, Faculty of Industrial Chemistry and Environmental Engineering, 6 Vasile Parvan Blvd., RO-300223 Timisoara, Romania, ²National Institute of Research and Development for Electrochemistry and Condensed Matter, 144 Dr. Aurel Paunescu-Podeanu, RO-300569 Timisoara, Romania and ³“Vasile Goldis” Western University of Arad, Faculty of Pharmacy, 86 Liviu Rebreanu, RO-310414 Arad, Romania

(Received 13 October, revised 25 December 2023, accepted 18 August 2024)

Abstract: This paper describes the analysis of the thermal decomposition of polymeric nickel (II) oxalate complex, a homopolynuclear coordination compound having the formula $[\text{Ni}(\text{C}_2\text{O}_4)(\text{H}_2\text{O})_2]_n \cdot x\text{nH}_2\text{O}$. The thermolysis was conducted in both dynamic oxidative and inert atmospheres by simultaneously applying thermogravimetry (TG), differential thermogravimetry (DTG) and differential thermal analysis (DTA). The proposed decomposition mechanism was confirmed using evolved gas analysis (EGA) technique *via* the Fourier transform infrared spectroscopy (FTIR) of the gaseous decomposition products. The solid-state decomposition products formed during heating were investigated by chemical analysis, FTIR, Raman spectroscopy and X-ray diffraction (XRD). The structure, morphology and properties of the final decomposition products were characterized by XRD, FTIR, energy dispersive X-ray spectroscopy (EDX) and transmission electron microscopy (TEM). These analyses show that the final decomposition product in oxidative atmosphere was nickel oxide, shaped as polygonal particles with widely distributed sizes. As for the results in inert atmosphere, they outlined a mixture of Ni and NiO as rhombohedral particles in a 3:2 mole ratio.

Keywords: homopolynuclear coordination compound; nickel oxide; evolved gas analysis.

INTRODUCTION

Oxide systems, generated through various methods, are nowadays required in increasing quantities because of the development of modern technologies in many

* Corresponding authors. E-mail: (*)mihai.cosmin.pascariu@gmail.com,
(**)b.taranu84@gmail.com
<https://doi.org/10.2298/JSC231013071N>

fields such as sensing, environmental remediation, energy storage and conversion, catalysis, optoelectronics, photonics and pharmaceuticals.¹ One of the synthetic pathways used for their preparation consists in the thermal conversion of homo- and heteropolynuclear metal complexes, which contain anions of carboxylic acids as ligands.²

Previous papers^{2–4} have described the products of the redox reactions between several diols, such as ethylene glycol, 1,2-propanediol and 1,3-propanediol and certain metal nitrates. All the coordination compounds obtained through this method contain carboxylate or hydroxycarboxylate anions as ligands (*i.e.*, glyoxylate, oxalate, lactate or 3-hydroxypropionate). These complexes, which contain simple organic ligands, have one main advantage over other coordination compounds: they undergo thermally induced degradation to metals, alloys and oxide structures at considerably low temperatures, with the release of gaseous species such as carbon oxides (CO, CO₂), hydrocarbons (*e.g.*, CH₄) and water. The composition of the obtained powders depends on both the structure of the coordination compound and the thermal treatment being applied.

A variety of preparative methods allow for the production of nickel oxides with specific properties regarding their crystallinity degree, particle size (from nm to mm), morphology and surface area.⁵

Nanosized materials have attracted many researchers because of their unusual properties based on the size-quantization effect and the large surface area. Nanosized nickel oxide is of great interest because it exhibits anomalous electronic⁶ and magnetic⁷ properties. The characteristic properties of nanosized NiO particles also enable one to tailor materials for various applications, including catalysis,⁸ electrochromic windows⁹ and sensors.¹⁰ These properties can be enhanced by decreasing the particle size, on which they are highly dependent. This is why precise control of the size and distribution in the nanometre regime is required. In addition, a facile preparation process that allows the convenient production of these particles is necessary for miscellaneous new applications. So far, many different methods have been attempted to synthesize nanosized NiO, such as thermal decomposition,^{11,12} microemulsion,¹³ precipitation,^{14,15} electrochemical deposition,¹⁶ sol-gel technique^{17,18} and surfactant-mediated method.¹⁹

The present paper aims to clarify the mechanism involved in the thermal decomposition of polymeric nickel(II) oxalate complex, namely nickel(II) oxalate dihydrate having the formula $[\text{Ni}(\text{C}_2\text{O}_4)(\text{H}_2\text{O})_2]_n \cdot x\text{nH}_2\text{O}$,²⁰ in both oxidative and inert atmospheres. Macklen²¹ analysed the thermal behaviour of the simple nickel (II) oxalate dihydrate obtained through classical methods. On the other hand, our study refers to a polynuclear compound obtained by an original method, starting from nickel (II) nitrate and ethylene glycol in the presence of nitric acid. The *in situ* generation of the ligand, the oxalate anion, simultaneously with its coordination to the complex generator, Ni²⁺, leads to a polynuclear structure, which pos-

sesses high stability: it is virtually insoluble in water and common organic solvents, and it can only be decomposed in a strongly acidic medium.²⁰ This study also shows that, following the thermal decomposition at relatively low temperatures of this complex compound, nickel oxide is obtained in oxidative atmosphere, while a mixture of nickel oxide and nickel is produced in inert atmosphere.

EXPERIMENTAL

$[\text{Ni}(\text{C}_2\text{O}_4)(\text{H}_2\text{O})_2]_n \cdot x\text{nH}_2\text{O}$ was prepared starting from nickel (II) nitrate hexahydrate (Merck) and ethylene glycol (Sigma–Aldrich), in the presence of nitric acid (Sigma–Aldrich), using an original method, as described in a previous paper.²⁰ The compound was purified by refluxing in a 5:1 by volume acetone/water mixture (acetone from Chimreactiv Bucharest) in an ultrasonic bath before being used.

For the thermal analysis, a Netzsch STA 409 PC coupled with a Bruker 27 FTIR instrument (for evolved gas detection) was used, with the following measuring conditions: $10\text{ }^\circ\text{C min}^{-1}$ heating speed, 100 mL min^{-1} synthetic air flow and 20.58 mg sample weight for the oxidative decomposition, as well as a gas flow rate of 100 mL min^{-1} and a 30.00 mg sample weight in dynamic atmosphere of argon.

The phase composition of the powders obtained through the complex's thermolysis at 400 and $1000\text{ }^\circ\text{C}$ was investigated by X-ray diffractometry (XRD) using a Rigaku Ultima IV diffractometer with CuK_α radiation ($\lambda = 1.5406\text{ \AA}$). The lattice parameters (a , b , c) and the average crystallite size (d) were calculated by using the whole pattern profile fitting (WPPF) method. The instrument influence over the lines' broadening was subtracted using the diffraction pattern of a Si standard recorded in the same conditions.

The FTIR spectra of the solid products were acquired on a Vertex 70 (Bruker, Germany) FT-IR spectrometer in the $4000\text{--}400\text{ cm}^{-1}$ domain, using KBr pellets.

The Raman spectra were measured at room temperature using a MultiView-1000 system (Nanonics Imaging, Israel) incorporating the Shamrock 500i Spectrograph (Andor, UK). A laser wavelength of 514.5 nm was used as the excitation source, with a 20 s exposure time and a 300 L mm^{-1} grating.

For the TEM analyses, the materials were deposited from ethanol on 200 mesh TEM copper grids covered with lacey carbon film. A Titan G2 80-200 TEM/STEM (FEI Company, The Netherlands) instrument with an image corrector was used to record the images at 200 kV accelerating voltage. Digital micrograph, ver. 2.12.1579.0 (for image recording), and TEM Imaging & Analysis, ver. 4.7 (for EDX analysis), were the software employed during the TEM investigation.

RESULTS AND DISCUSSION

Thermal decomposition in air

Thermoanalytical methods have been used to clarify the mechanism involved in the thermal decomposition of $[\text{Ni}(\text{C}_2\text{O}_4)(\text{H}_2\text{O})_2]_n \cdot x\text{nH}_2\text{O}$, in both air and argon, as well as the decomposition products formed during its heating.

The TG, DTG and DTA curves, corresponding to the thermal decomposition in flowing air of $[\text{Ni}(\text{C}_2\text{O}_4)(\text{H}_2\text{O})_2]_n \cdot x\text{nH}_2\text{O}$, are shown in Fig. 1a, while the FTIR curves of the gases evolved during the same process are shown in Fig. 1b.

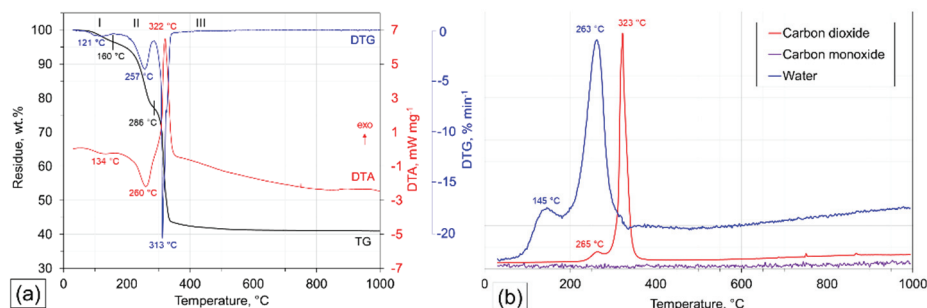


Fig. 1. Thermoanalytical curves for the thermolysis of $[\text{Ni}(\text{C}_2\text{O}_4)(\text{H}_2\text{O})_2]_n \cdot x\text{H}_2\text{O}$ in flowing air: a) TG, DTG and DTA results; b) FTIR analysis of generated gaseous products (not to scale): CO_2 2361 cm^{-1} , CO 2108 cm^{-1} , H_2O 1508 cm^{-1} .

The annealing was monitored by chemical analysis, XRD, FTIR, EDX and TEM.

Figs. 2 and 3 comparatively show the FTIR and Raman spectra of the coordination compound and its decomposition products.

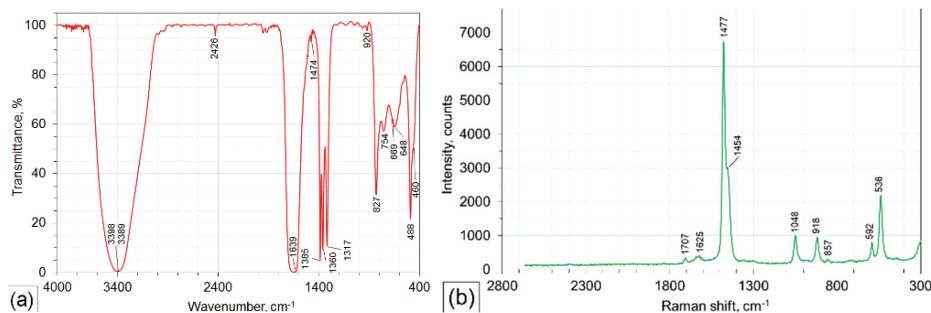


Fig. 2. FTIR (a) and Raman (b) spectra of the studied coordination compound.

The corresponding assignments of the FTIR and Raman spectra of $[\text{Ni}(\text{C}_2\text{O}_4)(\text{H}_2\text{O})_2]_n \cdot x\text{H}_2\text{O}$ are given in Table I.^{11,20–25}

The intense FTIR band at 1639 cm^{-1} (Fig. 2a) is attributed to the asymmetrical vibration of the carboxylate ion. The value shows that the resonance from the carboxylate group is maintained during complex formation since the metal–carboxylate bond is preponderantly ionic. The band with the maximum at 1385 cm^{-1} is attributed to the $\nu_{\text{sy}}(\text{OCO})$ symmetric vibration. The absence of the bands from the $1720\text{--}1660\text{ cm}^{-1}$ range, attributed to the $\nu_{\text{asy}}(\text{C}=\text{O})$ vibration in the case of coordination compounds in which $\text{C}_2\text{O}_4^{2-}$ is coordinated as bidentate chelate ligand, shows that, in the synthesized complex compound, the resonance of the carboxylate groups is achieved, and that the four oxygen atoms are equivalent, the oxalate anion being a bridging ligand.²⁵ At the same time, the value for $\nu_{\text{sy}}(\text{OCO})$,

i.e., 1385 cm^{-1} , along with the $\delta(\text{OCO})$ found at 1317 cm^{-1} , are in agreement with the positions of the corresponding absorptions in oxalate-bridged complexes.²¹ The very sharp and strong band at 488 cm^{-1} is attributed to the $\nu(\text{Ni-O})$ vibration and/or ring deformation.

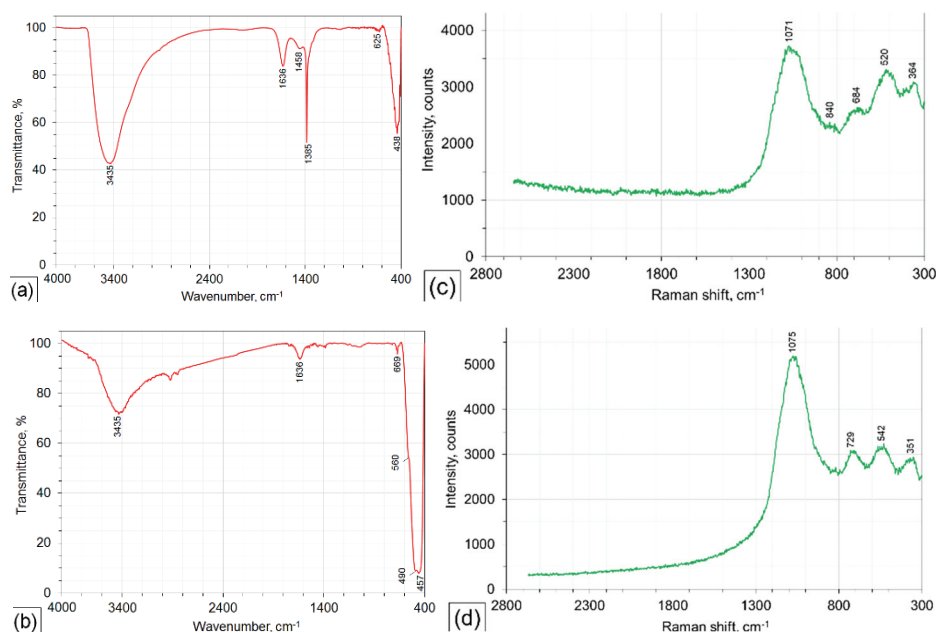


Fig. 3. FTIR (a, c) and Raman (b, d) spectra of the air decomposition products at 400 (a, c) and 1000 °C (b, d); the FTIR bands at 3435 and 1636 cm^{-1} are owned to traces of water.

TABLE I. Assignment of the FTIR and Raman spectra of $[\text{Ni}(\text{C}_2\text{O}_4)(\text{H}_2\text{O})_2]_n \cdot x\text{nH}_2\text{O}$ (band positions are expressed in cm^{-1}); *vs* – very strong; *s* – strong; *m* – medium; *w* – weak; *br* – broad; *sh* – shoulder; H_2O^* – coordinated water

FTIR	Raman	Assignments
3398/3389 <i>vs, br</i>		$\nu(\text{OH}) (\text{H}_2\text{O})$, hydrogen bonding
	1707 <i>w</i>	$\nu_{\text{asy}}(\text{C-O})$
1639 <i>vs, br</i>	1625 <i>w</i>	$\nu_{\text{sv}}(\text{OCO}) + \delta(\text{H}_2\text{O}^*)$
1474 <i>w</i>	1477 <i>vs</i>	$\nu_{\text{sv}}(\text{C-O}) + \nu(\text{C-C})$
	1454 <i>s, sh</i>	$\nu_{\text{sv}}(\text{C-O}) + \delta(\text{OCO})$
1385 <i>vs</i>		$\nu_{\text{sv}}(\text{OCO})$
1360 <i>vs, 1317 vs</i>		$\nu_{\text{sv}}(\text{C-O}) + \delta(\text{OCO})$
	1048 <i>m</i>	$\nu_{\text{sv}}(\text{C-O})$
920 <i>w</i>	918 <i>m</i>	$\nu(\text{C-C})$
	857 <i>w</i>	$\nu(\text{C-C})$
827 <i>s</i>		$\nu_{\text{sv}}(\text{C-C}) + \delta(\text{OCO})$
754 <i>m, 669 m, 648 m</i>		$\rho(\text{H}_2\text{O})$
	592 <i>m, 536 s</i>	δ_{ring} and/or lattice water
488 <i>vs, ~460 sh</i>		$\nu(\text{Ni-O})$ and/or δ_{ring}

The FTIR spectra of the thermal decomposition products show the characteristic bands of nickel oxide. In the case of the product obtained at 400 °C (Fig. 3a), besides the two absorption bands of NiO at 625 and 438 cm⁻¹, other bands also appear and indicate the presence of traces of the partially decomposed coordination compound. At the same time, the FTIR spectrum of the product synthesized at 1000 °C (Fig. 3b) shows the absorption bands at 669, 560 (shoulder) and 457 cm⁻¹, slightly shifted with respect to the characteristic bands of nickel(II) oxide mentioned in the literature.²⁶ The more relevant bands of [Ni(C₂O₄)(H₂O)₂]_n·*xn*H₂O, found at 1639, 1385, 1360, 1317, 827 and 488 cm⁻¹, are no longer present, leaving place for the two characteristic bands of nickel oxide. The other weak bands are not relevant for the decomposition of [Ni(C₂O₄)(H₂O)₂]_n·*xn*H₂O. Also, the broadness of the 457 cm⁻¹ band indicates that the NiO powder consisted of nanocrystals.²⁷

After analysing the Raman spectra of the same products (Fig. 3c,d), the disappearance of the characteristic bands for the coordination compound can be observed, confirming its degradation. The more relevant bands, found at 1477, 1454, 1048, 918 and 536 cm⁻¹ of [Ni(C₂O₄)(H₂O)₂]_n·*xn*H₂O (Fig. 2b), are replaced by the characteristic bands of nickel oxide. The Raman spectrum from Fig. 3d (for 1000 °C) shows the characteristic bands of nickel oxide (1075, 729, 542, 351 cm⁻¹) in accordance with literature data.^{22,24} Also, the Raman spectrum from Fig. 3c (400 °C) reveals the presence of slightly shifted bands, confirming that it is, to some extent, contaminated with the traces of the partially decomposed precursor.

Based on the FTIR and Raman spectra, it can be concluded that nickel oxide as the final solid-state product is formed and [Ni(C₂O₄)(H₂O)₂]_n·*xn*H₂O entirely decomposed.

The XRD patterns of the powders obtained by the annealing of coordination compound at 400 and 1000 °C are presented in Fig. 4. Both patterns record the diffraction lines of the single-phase NiO (rhombohedral, ICDD file 01-078-4374). The powder annealed at 400 °C was composed of much smaller crystallites (4.4 nm) compared to the one annealed at 1000 °C (37.4 nm). For the powder annealed at 1000 °C, the calculated values of the lattice parameters, $a = b = 2.9575 \text{ \AA}$, $c = 7.2464 \text{ \AA}$, are close to the values found in the ICDD file ($a = b = 2.9633 \text{ \AA}$, $c = 7.2553 \text{ \AA}$).

These results allow some conclusions to be drawn based on the thermoanalytical curves presented in Fig. 1. The TG profile shows, in the first two steps, the removal of the lattice water and of the coordinated water molecules (mass loss: calculated 22.74 %; experimental: 22.89 %). Two endothermic DTA peaks located between 25 and 160 °C (weak maximum at 134 °C), as well as between 160 and 286 °C (maximum at 260 °C) and a change on the DTG curve in the same temperature ranges correspond to the removal of water. A completely dehydrated compound is produced at around 300 °C, as confirmed in Fig. 1b. These results are in

good agreement with literature data for nickel (II) oxalate dihydrate obtained through classical methods.^{21,28} Also, the ratio between lattice water (3.57 % loss) and coordinated water (19.32 % loss), as calculated from the thermogravimetric analysis, shows for the $[\text{Ni}(\text{C}_2\text{O}_4)(\text{H}_2\text{O})_2]_n \cdot x\text{nH}_2\text{O}$ formula that $x \approx 0.4$, which is slightly less than previously reported.²⁰

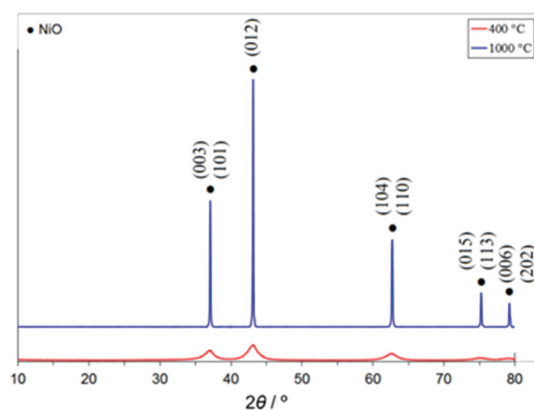


Fig. 4. XRD patterns of the powders obtained by the coordination compound's annealing at 400 and 1000 °C.

In the third step, the almost complete combustion of the anhydrous compound occurred within a narrow temperature range (286–345 °C), as shown by a steep slope on the TG curve with an inflexion point at 313 °C. The total experimental mass loss of 59.00 % (calculated 60.63 %) suggests NiO as the product of the conversion. The formation of this product was accompanied by a very sharp exothermic DTA peak located at 322 °C.

After analysing the FTIR curves from Fig. 1b, the water release can be confirmed due to the presence of two peaks: a weak one around 145 °C and the main one around 263 °C. The carbon dioxide shows a very intense peak at around 323 °C.

An EDX quantitative elemental analysis of very small areas revealed that, on the surface, the product obtained at 1000 °C in air is a non-stoichiometric oxide. The EDX profile for an area of the surface is presented in Fig. 5. It should be noted that the analysed area was smaller than 50 nm in diameter.

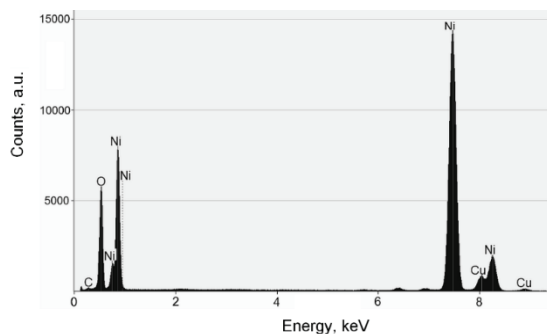


Fig. 5. EDX profile for a surface area (C and Cu peaks belong to the grid).

Table II shows the stoichiometry and composition of the nickel oxide analyzed by EDX.

TABLE II. Composition and stoichiometry of NiO obtained from EDX

Composition	wt. %	at. %
Ni	81.68	54.87
O	18.31	45.12
Ni:O (at. ratio)		1.2

The results indicate that, on the surface, the product is an oxygen-deficient non-stoichiometric nickel oxide.

The TEM analysis was performed to obtain useful information about the morphology and particle size of the nickel oxide originating from the thermal decomposition of the complex. TEM images recorded at different magnification values (Fig. 6) show that NiO was comprised of polygonal particles displaying some defined edges and faces, which appear to be further composed of small and conglomerated particles. The polygonal particles were piled up to form inter-particle pores of submicrometric sizes, corresponding to the spaces between them (Fig. 6a). The increase in magnification (Fig. 6b–d) did not allow for the improved particle differentiation. The formation of NiO aggregates, built from very small three-dimensional disordered primary particles, was clearly visible. The 2.07 nm value obtained from measurements performed on the TEM image shown in Fig. 6d corresponds to 10 interplanar spacings. The value for one interplanar spacing (2.07

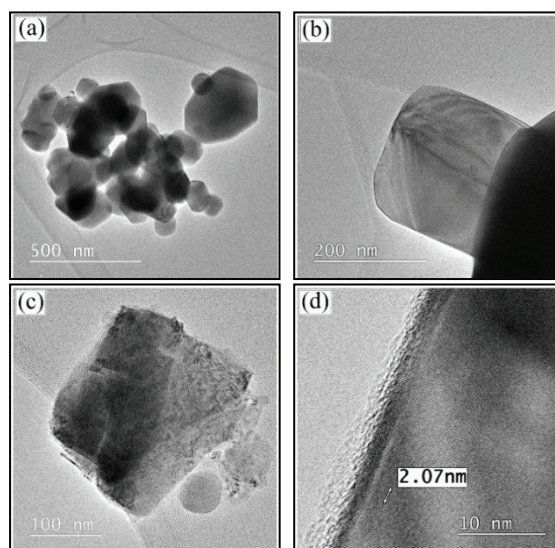


Fig. 6. TEM images of NiO obtained by decomposition of $[\text{Ni}(\text{C}_2\text{O}_4)(\text{H}_2\text{O})_2]_n \cdot x\text{nH}_2\text{O}$ at 1000 °C in air atmosphere.

Å) is very close to the *d*-spacing of 2.095050 Å from the previously mentioned ICDD file 01-078-4374, which corresponds to the (012) crystal plane. Thermal decomposition of $[\text{Ni}(\text{C}_2\text{O}_4)(\text{H}_2\text{O})_2]_n \cdot x\text{nH}_2\text{O}$ resulted in the formation of NiO with wide particle size distribution, from 4 nm to 1 μm .

Thermal decomposition in argon

The TG, DTG and DTA curves, corresponding to the thermal decomposition of $[\text{Ni}(\text{C}_2\text{O}_4)(\text{H}_2\text{O})_2]_n \cdot x\text{nH}_2\text{O}$ in argon atmosphere, are shown in Fig. 7a, while the FTIR curves of the gases evolved during the same process are shown in Fig. 7b.

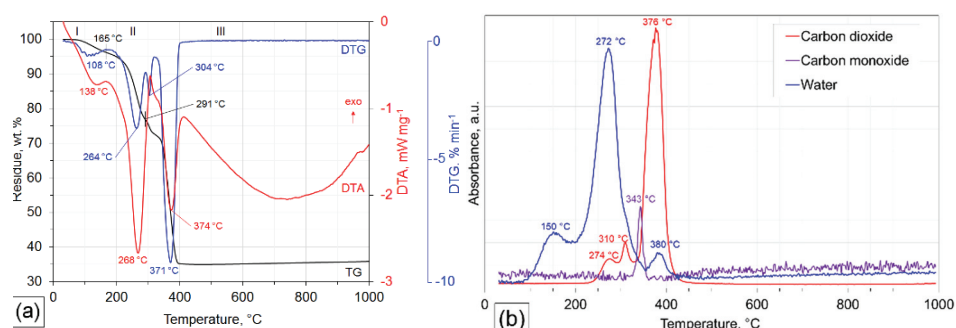


Fig. 7. Thermoanalytical curves for the thermolysis of $[\text{Ni}(\text{C}_2\text{O}_4)(\text{H}_2\text{O})_2]_n \cdot x\text{nH}_2\text{O}$ in argon: a) TG, DTG and DTA results; b) FTIR analysis of generated gaseous products (not to scale): CO_2 2361 cm^{-1} , CO 2108 cm^{-1} and H_2O 1508 cm^{-1} .

As can be seen in Fig. 7, the TG profile shows, in the first two steps, the removal of the lattice water and of the coordinated water molecules (mass loss: calculated 22.74 %; experimental: 23.17 %). The first mass loss, up until around 165 °C, has a maximum intensity recorded at 108 °C and a corresponding endothermic DTA peak located at 138 °C, as confirmed by the FTIR spectrum (maximum at 150 °C). The second mass loss, up until around 291 °C, has a process maximum intensity at 264 °C and a corresponding endothermic DTA peak at 268 °C. This mass loss is also confirmed by the FTIR spectrum (maximum at 272 °C), which shows that the breakdown of the C–C bonds begins in this step and continues in step three (up until around 400 °C), with CO_2 release. A weak trace of CO was recorded in the third step at around 343 °C. The total mass loss of 65.01 % (calculated 65.66 %) suggests that the conversion product was a biphasic Ni/NiO system in a 3:2 molar ratio. The following analyses confirm this result.

The FTIR spectrum of the decomposition product in argon atmosphere is presented in Fig. 8. The spectrum shows a few absorption bands at 663, 555 (shoulder) and 476 cm^{-1} , slightly shifted compared with those from Fig. 3b, probably due to the presence of metallic nickel.

The XRD pattern of the powder obtained by annealing the coordination compound in argon at 1000 °C can be seen in Fig. 9. The XRD pattern records the

diffraction lines of the NiO (rhombohedral, ICDD 01-089-3080) and metallic nickel (cubic, ICDD 00-004-0850).

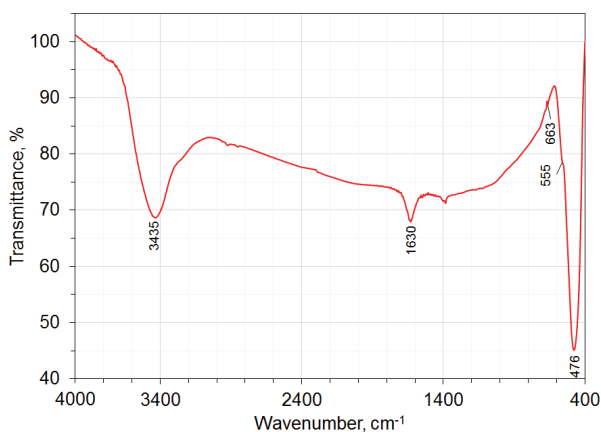


Fig. 8. FTIR spectrum of biphasic Ni/NiO system obtained by thermal decomposition at 1000 °C in argon atmosphere; the FTIR bands at 3435 and 1630 cm^{-1} are owned to traces of water.

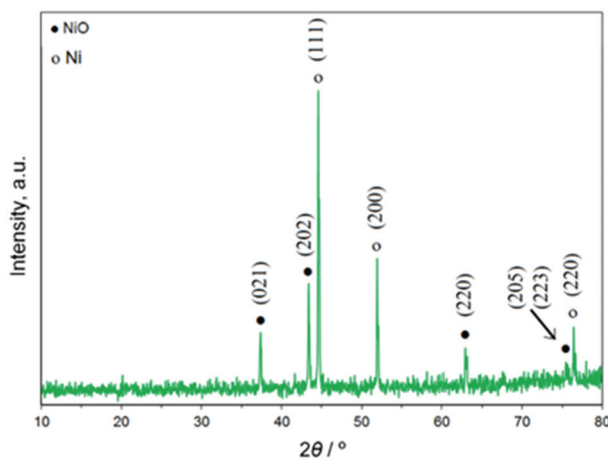


Fig. 9. XRD patterns of biphasic Ni/NiO system.

The TEM images of Ni/NiO at different magnification (Fig. 10) showed that the particles are of rhombohedral shape as well as the existence of submicrometric pores, which was already observed at NiO obtained in air atmosphere. The measurements performed on the TEM image presented in Fig. 10d show a value of 2.42 nm corresponding to 10 interplanar spacings. The value of 2.42 Å, corresponding to one interplanar spacing, is very close to the d -spacing of 2.412570 Å from the previously mentioned ICDD file 01-089-3080, which corresponds to the (021) crystal plane.

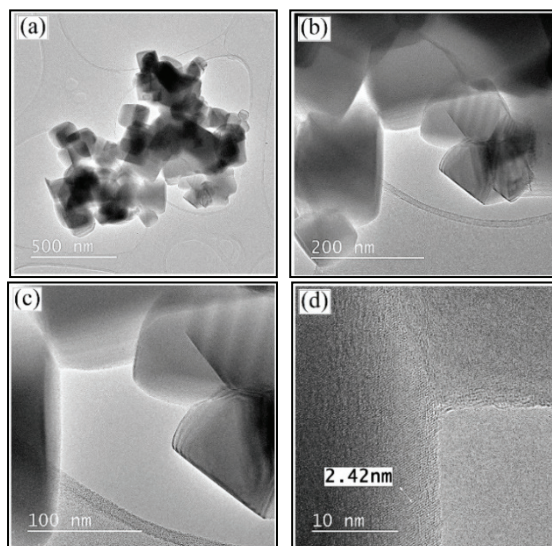


Fig. 10. TEM images of the NiO/Ni system obtained at 1000 °C in argon.

CONCLUSION

Three successive decomposition steps for $[\text{Ni}(\text{C}_2\text{O}_4)(\text{H}_2\text{O})_2]_n \cdot x\text{H}_2\text{O}$ were recorded during its thermal decomposition in dynamic air atmosphere, the first two being endothermic and the third exothermic.

The thermal conversion of this homopolynuclear coordination compound resulted in nickel oxide or a mixture of Ni and NiO in a 3:2 mole ratio, depending on the oxidative or inert atmosphere.

The XRD results reveal the rhombohedral crystallinity of the synthesized NiO phase and the cubic crystallinity of the metallic nickel phase. The TEM images at different magnification values show NiO particles obtained by the thermal decomposition of the coordination compound in air and consist of smaller particles. These particles exhibit polygonal shapes, and their size is widely distributed between 4 nm and 1 μm . The TEM images of the NiO/Ni system obtained in argon outline particles with rhombohedral shapes. For both oxidic systems, the particles were piled up and formed the inter-particle pores with sizes of tens of nanometers.

Acknowledgements. Part of this research was performed at the Center of Genomic Medicine of the “Victor Babes” University of Medicine and Pharmacy of Timișoara, POSCCE 185/48749, contract 677/09.04.2015. The authors wish to thank Prof. Dr. Zoltan Szabadai for some of the FTIR spectra and Dr. Maria Poienar for helping us obtain the ICDD files.

ИЗВОД

ТЕРМИЧКО ПОНАШАЊЕ ПОЛИМЕРНОГ КОМПЛЕКСА НИКЛ(II)-ОКСАЛАТА
ДОБИЈЕНОГ РЕАКЦИЈОМ НИКЛ(II)-НИТРАТ/ЕТИЛЕН-ГЛИКОЛMIRCEA NICULESCU¹, MIHAI-COSMIN PASCARIU^{2,3}, ANDREI RACU² и BOGDAN-OVIDIU TARANU²

¹University Politehnica Timisoara, Faculty of Industrial Chemistry and Environmental Engineering, 6 Vasile Parvan Blvd., RO-300223 Timisoara, Romania, ²National Institute of Research and Development for Electrochemistry and Condensed Matter, 144 Dr. Aurel Paunescu-Podeanu, RO-300569 Timisoara, Romania и ³“Vasile Goldis” Western University of Arad, Faculty of Pharmacy, 86 Liviu Rebreanu, RO-310414 Arad, Romania

Анализирано је термичко разлагање хомополинуклеарног координационог једињења $[\text{Ni}(\text{C}_2\text{O}_4)(\text{H}_2\text{O})_2]_n \cdot x\text{nH}_2\text{O}$, полимерног комплекса никл(II)-оксалата. Термолиза је урађена у динамичкој оксидативној и инертној атмосфери истовременом применом термогравиметрије (TG), диференцијалне термогравиметрије (DTG) и диференцијалне термичке анализе (DTA). Предложени механизам разлагања је потврђен употребом технике анализе еволуираног гаса (EGA) путем инфрацрвене спектроскопије Фуријеове трансформације (FTIR) гасовитих производа разлагања. Производи у чврстом стању, који настају током загревања, испитивани су хемијском анализом, FTIR, Рамановом спектроскопијом и Рендгенском дифракцијом (XRD). Структура, морфологија и својства финалних производа разлагања су окарактерисани XRD, FTIR, енергетско дисперзивном рендгенском спектроскопијом (EDX) и трансмисијском електронском микроскопијом (ТЕМ). Резултати анализа показују да је финални производ разлагања у оксидативној атмосфери никл-оксид, у облику полигоналних честица, док се у инертној атмосфери, добија смеша Ni и NiO у облику ромбоедарских честица у моларном односу 3:2.

(Примљено 13. октобра, ревидирано 25. децембра 2023, прихваћено 18. августа 2024)

REFERENCES

1. M. L. Grilli, *Metals* **10** (2020) 820 (<https://dx.doi.org/10.3390/met10060820>)
2. M. Niculescu, M. C. Pascariu, C. Muntean, V. Sasca, L. Lupa, M. S. Milea, M. Bîrzescu, *J. Therm. Anal. Calorim.* **131** (2018) 127 (<https://dx.doi.org/10.1007/s10973-016-6079-1>)
3. D. Roşu, M. Bîrzescu, M.-S. Milea, M.-C. Pascariu, V. Sasca, M. Niculescu, *Rev. Roum. Chim.* **59** (2014) 789 (<https://revroum.lew.ro/wp-content/uploads/2014/9/Art%2009.pdf>)
4. M. Niculescu, V. Sasca, C. Muntean, M.-S. Milea, D. Roşu, M.-C. Pascariu, E. Sisu, I. Ursoiu, V. Pode, P. Budrugaş, *Thermochim. Acta* **623** (2016) 36 (<https://dx.doi.org/10.1016/j.tca.2015.11.008>)
5. S. S. Narender, V. V. S. Varma, C. S. Srikar, J. Ruchitha, P. A. Varma, B. V. S. Praveen, *Chem. Eng. Technol.* **45** (2022) 397 (<https://dx.doi.org/10.1002/ceat.202100442>)
6. V. Biju, M. A. Khadar, *Mater. Sci. Eng., A* **304–306** (2001) 814 ([https://dx.doi.org/10.1016/S0921-5093\(00\)01581-1](https://dx.doi.org/10.1016/S0921-5093(00)01581-1))
7. F. Bødker, M. F. Hansen, C. B. Bender Koch, S. Mørup, *J. Magn. Magn. Mater.* **221** (2000) 32 ([https://dx.doi.org/10.1016/S0304-8853\(00\)00392-9](https://dx.doi.org/10.1016/S0304-8853(00)00392-9))
8. C. L. Carnes, K. J. Klabunde, *J. Mol. Catal., A* **194** (2003) 227 ([https://dx.doi.org/10.1016/S1381-1169\(02\)00525-3](https://dx.doi.org/10.1016/S1381-1169(02)00525-3))
9. G. Boschloo, A. Hagfeldt, *J. Phys. Chem., B* **105** (2001) 3039 (<https://dx.doi.org/10.1021/jp003499s>)
10. D. Das, M. Pal, E. Di Bartolomeo, E. Traversa, D. Chakravorty, *J. Appl. Phys.* **88** (2000) 6856 (<https://dx.doi.org/10.1063/1.1312835>)

11. Y. Wang, J. Zhu, X. Yang, L. Lu, X. Wang, *Thermochim. Acta* **437** (2005) 106 (<https://dx.doi.org/10.1016/j.tca.2005.06.027>)
12. X. Li, X. Zhang, Z. Li, Y. Qian, *Solid State Commun.* **137** (2006) 581 (<https://dx.doi.org/10.1016/j.ssc.2006.01.031>)
13. D. Y. Han, H. Y. Yang, C. B. Shen, X. Zhou, F. H. Wang, *Powder Tech.* **147** (2004) 113 (<https://dx.doi.org/10.1016/j.powtec.2004.09.024>)
14. X. Y. Deng, Z. Chen, *Mater. Lett.* **58** (2004) 276 ([https://dx.doi.org/10.1016/S0167-577X\(03\)00469-5](https://dx.doi.org/10.1016/S0167-577X(03)00469-5))
15. X. Xin, Z. Lü, B. Zhou, X. Huang, R. Zhu, X. Sha, Y. Zhang, W. Su, *J. Alloy Compd.* **427** (2007) 251 (<https://dx.doi.org/10.1016/j.jallcom.2006.02.064>)
16. A. Dierstein, H. Natter, F. Meyer, H.-O. Stephan, C. Kropf, R. Hempelmann, *Scr. Mater.* **44** (2001) 2209 ([https://dx.doi.org/10.1016/S1359-6462\(01\)00906-X](https://dx.doi.org/10.1016/S1359-6462(01)00906-X))
17. C. Lin, S. A. Al-Muhtaseb, J. A. Ritter, *J. Sol–Gel Sci. Tech.* **28** (2003) 133 (<https://dx.doi.org/10.1023/A:1025653607374>)
18. Y. R. Park, K. J. Kim, *J. Cryst. Growth* **258** (2003) 380 ([https://dx.doi.org/10.1016/S0022-0248\(03\)01560-4](https://dx.doi.org/10.1016/S0022-0248(03)01560-4))
19. Y. Wang, C. Ma, X. Sun, H. Li, *Inorg. Chem. Commun.* **5** (2002) 751 ([https://dx.doi.org/10.1016/S1387-7003\(02\)00546-4](https://dx.doi.org/10.1016/S1387-7003(02)00546-4))
20. M. Birzescu, M. Milea, D. Roşu, I. Ledeti, M. Rafailă, V. Sasca, M. Niculescu, *Rev. Roum. Chim.* **59** (2014) 555 (<https://revroum.lew.ro/wp-content/uploads/2014/6/Art%2024.pdf>)
21. E. D. Macklen, *J. Inorg. Nucl. Chem.* **30** (1968) 2689 ([https://dx.doi.org/10.1016/0022-1902\(68\)80396-3](https://dx.doi.org/10.1016/0022-1902(68)80396-3))
22. N. Mironova-Ulmane, A. Kuzmin, I. Steins, J. Grabis, I. Sildos, M. Pärs, *J. Phys.: Conf. Ser.* **93** (2007) 012039 (<https://dx.doi.org/10.1088/1742-6596/93/1/012039>)
23. A. Wladimirsky, D. Palacios, M. C. D'Antonio, A. C. González-Baró, E. J. Baran, *J. Argent. Chem. Soc.* **98** (2011) 71 (https://notablesdelaciencia.conicet.gov.ar/bitstream/handle/11336/151619/CONICET_Digital_Nro.1f79f00b-4945-4466-aff5-917bfc14f1da_A.pdf)
24. M. Nowsath Rifaya, T. Theivasanthi, M. Alagar, *Nanosci. Nanotechnol. (Rosemead, CA, U.S.)* **2** (2012) 134 (<https://dx.doi.org/10.5923/j.nn.20120205.01>)
25. N. N. Dass, S. Sarmah, *J. Therm. Anal. Calorim.* **58** (1999) 137 (<https://dx.doi.org/10.1023/A:1010148022032>)
26. *Spectral Database for Organic Compounds, SDBS*, https://sdb.sdb.aist.go.jp/sdbs/cgi-bin/direct_frame_top.cgi (accessed 25.09.2023)
27. H. Qiao, Z. Wei, H. Yang, L. Zhu, X. Yan, *J. Nanomater.* **2009** (2009) 795928 (<https://dx.doi.org/10.1155/2009/795928>)
28. X. M. Fu, Z. Z. Yang, *Adv. Mater. Res. (Durnten-Zurich, Switz.)* **228–229** (2011) 34 (<https://dx.doi.org/10.4028/www.scientific.net/AMR.228-229.34>).



J. Serb. Chem. Soc. 89 (11) 1489–1506 (2024)
JSCS–5802

Thermophysical investigation of glycol ethers in mannitol solutions at various temperatures

NABAPARNA CHAKRABORTY^{1,2*}, PRIYA THAKUR¹, KAILASH CHANDRA JUGLAN¹ and ABRAR HUSSAIN SYED³

¹Department of Physics, Lovely Professional University, Phagwara, 144401, Punjab, India, ²Central Instrumentation Facility, Research and Development Cell, Lovely Professional University, Phagwara, 144401, Punjab, India and ³Research and Development, Saputo Dairy Australia, Freshwater Place, 3006, Victoria, Australia

(Received 15 September 2023, revised 21 February, accepted 20 August 2024)

Abstract: Ultrasonic analysis can be very helpful to comprehend the molecular dynamics and interactions in liquid systems. Employing the Anton-Paar (DSA 5000 M) at concentrations and 0.1 MPa, sound speed as well as density of glycol ethers, *i.e.*, phenoxyethanol (PE) and butoxyethanol (BE) in solutions of a well-known sugar alcohol (D-mannitol), were measured at 288.15–303.15 K. A variety of advanced acoustic-thermodynamic parameters, including apparent molar parameters, partial molar parameters and transfer molar properties, were estimated using the experimentally attained the velocity and density values. These derived values are used to express the interactions between solutes and their solvents. The propensity of the solute to generate or destroy structures in a solvent is also a subject of research. Analysis was done on the interactions between the molecules in the ternary mixture of D-mannitol and glycol ethers in aqueous medium.

Keywords: phenoxyethanol; butoxyethanol; kosmotropes; chaotropic; acoustic and volumetric.

INTRODUCTION

Every industry has recognized the usage of chemicals. By examining the physicochemical characteristics of diverse liquids and mixtures using ultrasonic techniques, numerous studies into the molecular interactions have been conducted. The pharmaceutical, healthcare, cosmetic, food, leather, textile and automotive industries all heavily rely on the use of ultrasonic technology to characterize various thermophysical properties of liquid mixtures as well as their behavior. Details about the character and intensity of molecular interactions occurring within the mixture, is obtained from this technique since it is a non-destructive

*Corresponding author. E-mail: nabaparnac@gmail.com
<https://doi.org/10.2298/JSC230915073C>

for describing the liquid systems.^{1–4} The binding forces that form between the molecules in a liquid directly affect the ultrasonic speed at which sound travels through it.^{5–9}

Phenoxyethanol, commonly known as 2-phenoxyethanol, is an aromatic alcohol that is colorless and has a pleasant smell. Phenoxyethanol serves as an antibacterial and is a common preservative in cosmetic goods. It works well against a variety of bacteria and yeasts. The US Food and Drug Administration has given 2-butoxyethanol permission for use as an adhesive, antibacterial agent, defoamer, stabilizer, and preservative in food additives.^{9–12}

Mannitol is a sugar alcohol or polyol with the chemical formula $C_6H_{12}O_6$ that is used as a sweetener and in medicine. Mannitol is a member of the class of medications known as diuretics. D-Mannitol is readily available, reasonably priced, and available in a variety of granular and powder forms. Water molecules interact hydrophilically with mannitol. Due to the creation of H-bonds, D-mannitol and water molecules become associated molecularly. It is critically important for biological reasons because polyhydroxy chemicals assist stabilize globular proteins.^{13–17}

Glycol ethers (PE/BE) have been the subject of extensive research, for instance, Scognamiglio *et al.* had analysed the toxic and dermatological behaviour of phenoxyethanol, which finds application as an ingredient in fragrances.¹⁸ Whereas, Lowe and Southern had investigated the antibacterial properties of phenoxyethanol and thiomersal, two preservatives.¹⁹ Both substances demonstrated equal effectiveness at inactivating challenge doses of yeast, Gram-positive and Gram-negative microorganisms, and reported that phenoxyethanol had no effect on Gram-positive bacteria, but the yeast and both Gram-positive challenge strains were rendered inactive by the vaccines as they were created.

Raman *et al.* had studied the intermolecular association in aqueous mannitol solutions at multiple temperatures by evaluating various thermo-acoustic parameters from the experimental values of density and velocity. These properties advocate the strong molecular interlinkage in the system.²⁰

The literature review on mannitol and glycol ethers indicates that no volumetric and acoustic investigations for their combination have been published yet. Based on the experimental findings, several thermodynamic parameters were calculated to uncover the physical and chemical characteristics of the liquid system. Glycol ethers and mannitol are commonly utilized in industries such as medicine, cosmetics and chemicals. This present study aims to elucidate the intermolecular interactions occurring in liquid mixtures, providing an opportunity to assess the mixture and explore different attributes and properties that enhance the quality of the product.

EXPERIMENTAL

Materials used

Phenoxyethanol, butoxyethanol and D-mannitol are the chemicals employed in the current experiment; their molar masses are 118.16, 138.16, and 182.172 g·mol⁻¹, respectively. The solvent mixtures were made using the sugar alcohol D-mannitol and degassed, triple-distilled water. Table I presents the characteristics of the compounds utilized in the study. The mass fraction purities of, PE, BE and D-mannitol are all greater than 0.99. Although the chemicals were dried and stored in desiccators over P₂O₅ for two days before usage, they were employed without additional purification.

Methods used

The Anton-Paar DSA 5000 M instrument provides a reliable and accurate data for the density and speed of sound. The high level of precision and accuracy required in the measurements is crucial to ensure the validity of the results. The obtained measurements of different concentration calculation methods that are included into the DSA use density and sound speed as inputs. Degassed, triple-distilled water with a specific conductance of less than 10⁻⁶ S·cm⁻¹ was used to create the solutions. The Sartorius CPA 225D was used to weigh the samples and the precision was within ±0.00001 g. The density and sound speed measurements have precisions of ±0.001 kg·m⁻³ and ±0.01 m·s⁻¹, respectively. The corresponding measurement uncertainties were ±0.001 K, ±0.15 kg·m⁻³ and ±0.01 m·s⁻¹, respectively for temperature, density and speed of sound.

TABLE I. Specifications of the chemicals utilized in this present investigation

Chemical	Butoxyethanol	Phenoxyethanol	D-Mannitol
Source	Loba Chemie Pvt. Ltd., India		Sigma–Aldrich
Mass fraction purity (supplier)	≥0.99	≥0.99	≥0.99
Purification method	Used as such	Used as such	Used as such

RESULTS AND DISCUSSION

Density

Experimental density values (ρ) for butoxyethanol (BE) and phenoxyethanol (PE) in aqueous solutions of mannitol with 0.00, 0.02, 0.06 and 0.1 mol·kg⁻¹ concentrations, were obtained at temperatures of 288.15–303.15 K and 0.1 MPa pressure. The experimental density values for (water + mannitol) were cross-referenced with values from literature at 288.15, 293.15, 298.15 and 303.15 K, which is shown in Fig. 1a, and the consistency between the experimental results and the values found in the literature is demonstrated.^{21,22} For this binary system, Fig. 2 plots the deviation in density between the experimental density values and those reported^{21,22} at 288.15, 293.15, 298.15 and 303.15 K. It finds a good agreement, with the maximum deviation falling within the reported experimental error.

By measuring the density of pure components, each experimental chemical used in this work was verified, and the data were compared to the values found in the literature,^{23,24} which are listed in Table II along with the percentage deviation between the data from the experiment and reported data. In Table III the

density values of glycol ethers at a specific concentration of mannitol are recorded, and it can be observed that the ρ values are exhibiting linear trend, *i.e.*, increasing with the rising values of mannitol concentrations as well as with the molality of glycol ethers. This behavior implies that the water molecules form a new structure, in existence that is more when projecting at higher concentrations. The decline in ρ values occurs when the kinetic energy of solution molecules exceeds the binding energy at high temperatures.^{25–27} Overall, the study provides a comprehensive analysis of the density values of BE and PE in mannitol solutions at different temperatures and mannitol concentrations in aqueous medium.^{28,29}

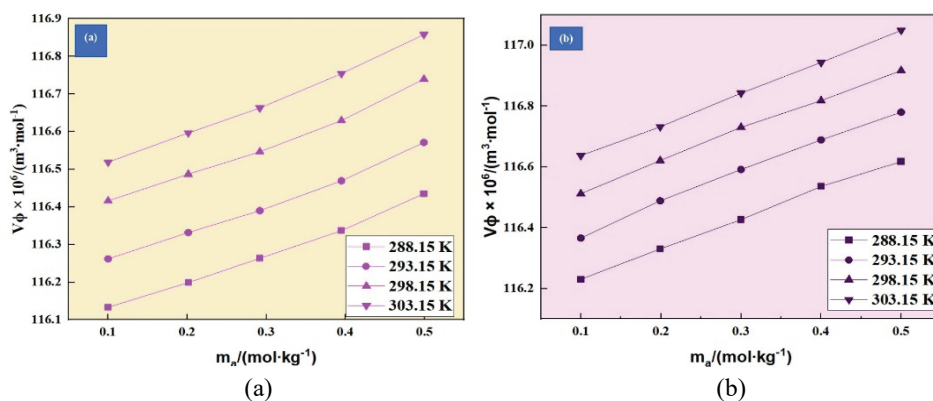


Fig. 1. The comparison graph between the experimental and literature^{21,22} values for: a) density and b) speed of sound for the binary solution of (D-mannitol + water) at different temperatures against molality of D-mannitol.

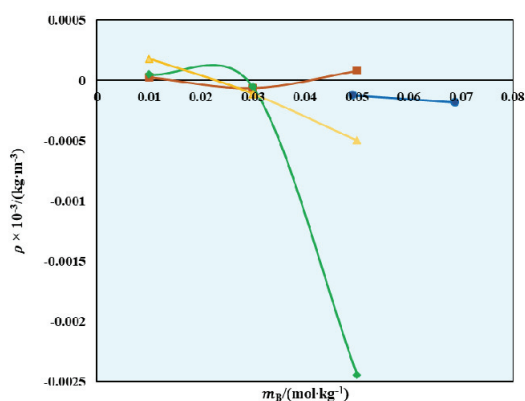


Fig. 2. Plot of deviation in densities, ρ , of binary mixture (D-Mannitol + water) with the literature data at different temperatures; circle-blue: 288.15 K²²; square-brown: 293.15 K²¹, diamond-green: 298.15 K²¹, triangle-yellow: 303.15 K²¹.

Speed of sound

For the binary system of (water + mannitol), Fig. 3 plots the deviation in speed of sound between the experimental and literature^{21,22} at 293.15, 298.15 and 303.15 K. It reaches a satisfactory agreement, with the highest difference fall-

TABLE II. Comparison of experimental densities (ρ) and ultrasonic velocities (v) with literature values for pure chemicals at different temperatures

Chemical	T / K	$\rho \times 10^{-3} / \text{kg} \cdot \text{m}^{-3}$			$v / \text{m} \cdot \text{s}^{-1}$		
		Exp.	Lit.	% Deviation	Exp.	Lit.	% Deviation
Butoxyethanol (BE)	288.15	0.9032	–	–	1341.04	–	–
	293.15	0.9001	0.9001 ²³	0.00000	1322.45	1322.50 ²³	0.00378
	298.15	0.8960	0.8959 ²³	0.01116	1305.06	1304.94 ²³	0.03218
	303.15	0.8917	0.8917 ²³	0.00000	1288.52	1288.02 ²³	0.03
Phenoxyethanol (PE)	288.15	1.1150	–	–	1608.56	–	–
	293.15	1.1080	1.1070 ²⁴	0.09033	1592.00	1591.80 ²⁴	0.0020
	298.15	1.1020	1.1030 ²⁴	0.09066	1575.02	1574.60 ²⁴	0.0042
	303.15	1.0970	1.0990 ²⁴	0.18198	1557.80	1557.40 ²⁴	0.0040

TABLE III. Values of density ($\rho / \text{g} \cdot \text{cm}^{-3}$) of (BE/PE) in aqueous solutions of D-mannitol at different temperatures 288.15–303.15 K; m_a is the molality of glycols in the aqueous solution D-mannitol, standard uncertainties, u , are $u(m) = 1\%$, $u(T) = 0.001 \text{ K}$ and $u(\rho) = 0.15 \text{ kg} \cdot \text{m}^{-3}$

m_a	T / K				m_a	T / K			
	288.15	293.15	298.15	303.15		288.15	293.15	298.15	303.15
mol·kg ⁻¹	0.00 mol·kg ⁻¹ D-mannitol + BE				mol·kg ⁻¹	0.02 mol·kg ⁻¹ D-mannitol + BE			
0.00000	0.9992	0.9982	0.9970	0.9956	0.00000	1.0006	0.9997	0.9984	0.9970
0.10016	0.9994	0.9984	0.9972	0.9958	0.09978	1.0008	0.9999	0.9986	0.9972
0.20147	0.9996	0.9986	0.9974	0.9960	0.19899	1.0009	1.0001	0.9988	0.9974
0.29196	0.9998	0.9987	0.9976	0.9962	0.30003	1.0011	1.0002	0.9989	0.9975
0.39510	0.9999	0.9989	0.9977	0.9963	0.40010	1.0012	1.0003	0.9990	0.9976
0.49928	1.0001	0.9990	0.9978	0.9965	0.50003	1.0013	1.0004	0.9991	0.9977
	0.06 mol·kg ⁻¹ D-mannitol + BE					0.1 mol·kg ⁻¹ D-mannitol + BE			
0.00000	1.0031	1.0021	1.0009	0.9996	0.00000	1.0056	1.0045	1.0034	1.0021
0.10034	1.0032	1.0023	1.0010	0.9998	0.09894	1.0057	1.0046	1.0035	1.0022
0.20009	1.0034	1.0024	1.0011	0.9999	0.19880	1.0058	1.0046	1.0035	1.0022
0.30012	1.0035	1.0025	1.0012	1.0000	0.30001	1.0058	1.0047	1.0036	1.0023
0.39990	1.003	1.0026	1.0013	1.0001	0.39959	1.0059	1.0047	1.0036	1.0024
0.50023	1.003	1.0026	1.0014	1.0001	0.50005	1.0059	1.0048	1.0037	1.0024
	0.00 mol·kg ⁻¹ D-mannitol + PE					0.02 mol·kg ⁻¹ D-mannitol + PE			
0.00000	0.9992	0.9982	0.9970	0.9956	0.00000	1.0006	0.9997	0.9984	0.9970
0.09102	0.9996	0.9986	0.9974	0.9961	0.09983	1.0010	1.0002	0.9989	0.9975
0.20047	1.0002	0.9991	0.9979	0.9966	0.20034	1.0015	1.0006	0.9993	0.9979
0.29106	1.0005	0.9995	0.9983	0.9969	0.30010	1.0019	1.0010	0.9997	0.9983
0.39951	1.0009	0.9999	0.9987	0.9974	0.39990	1.0022	1.0014	1.0001	0.9987
0.49928	1.0013	1.0002	0.9991	0.9977	0.50004	1.0026	1.0017	1.0004	0.9991
	0.06 mol·kg ⁻¹ D-mannitol + PE					0.1 mol·kg ⁻¹ D-mannitol + PE			
0.00000	1.0031	1.0021	1.0009	0.9996	0.00000	1.0056	1.0045	1.0034	1.0021
0.10028	1.0035	1.0025	1.0013	1.0001	0.09999	1.0060	1.0049	1.0038	1.0025
0.19996	1.0039	1.0029	1.0017	1.0004	0.19973	1.0063	1.0052	1.0041	1.00282
0.30056	1.0042	1.0033	1.0020	1.0008	0.29880	1.0066	1.0055	1.0044	1.0031
0.40031	1.0045	1.0036	1.0023	1.0011	0.40050	1.0069	1.0058	1.0047	1.0034
0.50009	1.0048	1.0039	1.0027	1.0015	0.50009	1.0072	1.0061	1.0050	1.0037

ing within the expected experimental margin of error. The speed of sound of these chemicals used in this study was confirmed by measuring the speed of sound of pure components, and the results were compared to values from previous studies^{23,24} listed in Table II, including the percentage difference between experimental and reported data. At 288.15–303.15 K, the speed of sound (v) of glycol ethers in aqueous mannitol solutions, at different temperatures (and mannitol concentrations 0.00, 0.02, 0.06 and 0.1 mol·kg⁻¹), are expressed in Table IV. For the experimentally acquired speed of sound values for (water + mannitol), a comparison was made between the obtained values and the values documented in the literature for at certain temperatures. The experimental v measurements align with the velocity values reported in the literature for various temperatures, as illustrated in Fig 1b.²¹ Results showed that speed of sound values increased with temperature and (BE/PE) molality, and there was an observable rise in speed of sound with an increase in mannitol concentration, which can be attributed to the presence of a three-dimensional network of hydrogen bonds within the water structure. Intramolecular and intermolecular hydrogen bonds in solute–solvent molecules caused a hike in speed of sound values, while hydrogen bond formation between water and mannitol degraded with the acceleration in the molar mass of glycol ethers. The formation of a hydrogen bond network occurs between the solute and aqueous mannitol molecules resulted in a rise of speed of sound values with mannitol concentration, and new H-bonds were created between glycol ethers and mannitol molecules. The study provided a comprehensive analysis of factors influencing speed of sound values in glycol ethers in aqueous mannitol solutions at different temperatures and mannitol concentrations.^{30–36}

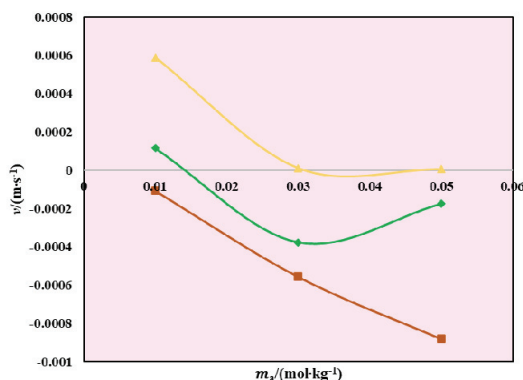


Fig. 3. Plot of deviation in speed of sound, v , of binary mixture (D-mannitol + water) with the literature data at different temperatures; square-brown: 293.15 K²¹; diamond-green: 298.15 K²¹; triangle-yellow: 303.15 K²¹.

Apparent molar volume

The experimental density values were employed in the calculation of the apparent molar volume (V_{Φ}) for binary mixtures of glycol ethers (BE/PE) and

TABLE IV. Values of Speed of sound ($v / \text{m}\cdot\text{s}^{-1}$) of BE/PE in aqueous solutions of D-mannitol at different temperatures 288.15–303.15 K; m_a is the molality of glycols in the aqueous solution D-mannitol, standard uncertainties, u , are $u(m) = 1 \%$, $u(T) = 0.001 \text{ K}$, $u(v) = 1.0 \text{ m}\cdot\text{s}^{-1}$

T / K					T / K				
m_a	288.15	293.15	298.15	303.15	m_a	288.15	293.15	298.15	303.15
$\text{mol}\cdot\text{kg}^{-1}$	0.00 $\text{mol}\cdot\text{kg}^{-1}$ D-mannitol + BE				$\text{mol}\cdot\text{kg}^{-1}$	0.02 $\text{mol}\cdot\text{kg}^{-1}$ D-mannitol + BE			
0.00000	1466.6	1482.6	1495.9	1508.8	0.00000	1469.5	1485.1	1499.0	1511.4
0.10016	1467.6	1483.5	1497.0	1509.6	0.09978	1470.4	1485.9	1500.2	1512.2
0.20147	1468.6	1484.5	1498.2	1510.5	0.19899	1471.5	1486.8	1501.4	1513.1
0.29196	1469.5	1485.4	1499.5	1511.4	0.30003	1472.5	1487.9	1502.8	1514.0
0.39510	1470.9	1486.6	1501.0	1512.4	0.40010	1473.6	1488.9	1504.0	1515.1
0.49928	1472.1	1487.7	1502.6	1513.6	0.50003	1474.9	1489.9	1505.4	1516.2
0.06 $\text{mol}\cdot\text{kg}^{-1}$ D-mannitol + BE					0.1 $\text{mol}\cdot\text{kg}^{-1}$ D-mannitol + BE				
0.00000	1473.4	1489.3	1503.1	1516.0	0.00000	1476.8	1492.8	1507.4	1520.6
0.10034	1474.4	1490.2	1504.1	1516.8	0.09894	1477.8	1493.7	1508.4	1521.3
0.20009	1475.4	1491.0	1505.4	1517.7	0.19880	1478.8	1494.5	1509.6	1522.4
0.30012	1476.2	1492.0	1506.5	1518.5	0.30001	1479.7	1495.3	1510.7	1523.4
0.39990	1477.4	1492.9	1507.6	1519.6	0.39959	1480.8	1496.3	1511.7	1524.5
0.50023	1478.5	1493.8	1508.8	1520.7	0.50005	1481.9	1497.4	1512.8	1525.6
0.00 $\text{mol}\cdot\text{kg}^{-1}$ D-mannitol + PE					0.02 $\text{mol}\cdot\text{kg}^{-1}$ D-mannitol + PE				
0.00000	1466.6	1482.6	1495.9	1508.8	0.00000	1469.5	1485.1	1499.0	1511.4
0.09102	1468.3	1484.2	1497.5	1510.5	0.09983	1471.2	1487.0	1500.6	1513.4
0.20047	1470.3	1486.3	1499.5	1512.7	0.20034	1473.1	1489.1	1502.6	1515.5
0.29106	1472.3	1488.2	1501.2	1514.4	0.30010	1475.3	1491.1	1504.4	1517.4
0.39951	1474.7	1490.3	1503.4	1516.5	0.39990	1477.6	1493.0	1506.7	1519.5
0.49928	1476.6	1492.2	1505.4	1518.6	0.50004	1479.5	1495.1	1508.8	1521.4
0.06 $\text{mol}\cdot\text{kg}^{-1}$ D-mannitol + PE					0.1 $\text{mol}\cdot\text{kg}^{-1}$ D-mannitol + PE				
0.00000	1473.4	1489.3	1503.1	1516.0	0.00000	1476.8	1492.8	1507.4	1520.6
0.10028	1475.3	1491.0	1505.0	1518.0	0.09999	1478.7	1494.8	1509.2	1522.6
0.19996	1477.3	1493.1	1507.0	1520.0	0.19973	1480.5	1496.8	1511.3	1524.5
0.30056	1479.4	1495.1	1509.1	1522.1	0.29880	1482.6	1498.8	1513.2	1526.5
0.40031	1481.5	1497.1	1511.0	1524.1	0.40050	1484.8	1500.8	1515.4	1528.5
0.50009	1483.5	1499.2	1513.0	1526.0	0.50009	1486.8	1502.8	1517.3	1530.6

mannitol. The equation used for this calculation included the densities of the solution (ρ) and solvent (ρ_0), the molality of the solute per kg of solvent (m_A), and molar mass (M) of the solute:

$$V_{\Phi} = M / \rho - (\rho - \rho_0) / m_A \rho \rho_0 \quad (1)$$

Table V illustrates the positive values of V_{Φ} calculated for different mannitol concentrations and temperatures. As the temperature and mannitol concentration increased, the V_{Φ} values also increased. The observed increase in the apparent molar volume values with temperature implies a strong interaction between the solute and solvent in the mixture, as depicted in Fig. 4.^{37–39} This suggests that

the solvent exhibits a higher affinity for the solute at elevated temperatures, leading to enhanced solute-solvent interactions.

TABLE V. Values of apparent molar volumes ($V_{\Phi} / \text{m}^3 \cdot \text{mol}^{-1}$) of BE/PE in aqueous solutions of D-mannitol at different temperatures 288.15–303.15 K; m_a is the molality of glycols in the aqueous solution D-mannitol, standard uncertainties, u , are $u(m) = 1 \%$, $u(T) = 0.001 \text{ K}$, $u(V_{\Phi}) = (0.023\text{--}0.028) \times 10^6 \text{ m}^3 \text{ mol}^{-1}$

m_a mol·kg ⁻¹	T / K				m_a mol·kg ⁻¹	T / K			
	288.15	293.15	298.15	303.15		288.15	293.15	298.15	303.15
	0.00 mol·kg ⁻¹ D-mannitol + BE					0.02 mol·kg ⁻¹ D-mannitol + BE			
0.10016	116.13	116.26	116.42	116.52	0.09978	116.23	116.37	116.51	116.64
0.20147	116.20	116.33	116.49	116.60	0.19899	116.33	116.49	116.62	116.73
0.29196	116.26	116.39	116.55	116.66	0.30003	116.43	116.59	116.73	116.84
0.39510	116.34	116.47	116.63	116.75	0.40010	116.54	116.69	116.82	116.94
0.49928	116.44	116.57	116.74	116.86	0.50003	116.62	116.78	116.92	117.05
0.10016	116.13	116.26	116.42	116.52	0.09978	116.23	116.37	116.51	116.64
	0.06 mol·kg ⁻¹ D-mannitol + BE					0.1 mol·kg ⁻¹ D-mannitol + BE			
0.10034	116.35	116.46	116.60	116.73	0.09894	116.43	116.56	116.69	116.81
0.20009	116.45	116.56	116.71	116.82	0.19880	116.54	116.67	116.81	116.91
0.30012	116.54	116.66	116.81	116.93	0.30001	116.64	116.78	116.92	117.02
0.39990	116.65	116.76	116.91	117.03	0.39959	116.74	116.88	117.01	117.12
0.50023	116.76	116.87	117.03	117.15	0.50005	116.84	116.97	117.11	117.22
0.10034	116.35	116.46	116.60	116.73	0.09894	116.43	116.56	116.69	116.81
	0.00 mol·kg ⁻¹ D-mannitol + PE					0.02 mol·kg ⁻¹ D-mannitol + PE			
0.10034	116.35	116.46	116.60	116.73	0.09894	116.43	116.56	116.69	116.81
0.20009	116.45	116.56	116.71	116.82	0.19880	116.54	116.67	116.81	116.91
0.30012	116.54	116.66	116.81	116.93	0.30001	116.64	116.78	116.92	117.02
0.39990	116.65	116.76	116.91	117.03	0.39959	116.74	116.88	117.01	117.12
0.50023	116.76	116.87	117.03	117.15	0.50005	116.84	116.97	117.11	117.22
0.10034	116.35	116.46	116.60	116.73	0.09894	116.43	116.56	116.69	116.81
	0.06 mol·kg ⁻¹ D-mannitol + PE					0.1 mol·kg ⁻¹ D-mannitol + PE			
0.10028	133.70	133.78	133.88	133.96	0.09999	133.82	133.89	133.98	134.09
0.19996	133.82	133.89	133.98	134.06	0.19973	133.91	133.98	134.07	134.18
0.30056	133.91	133.98	134.08	134.16	0.29880	134.00	134.07	134.16	134.27
0.40031	133.99	134.07	134.17	134.25	0.40050	134.08	134.17	134.26	134.37
0.50009	134.09	134.17	134.27	134.35	0.50009	134.18	134.26	134.36	134.48
0.10028	133.70	133.78	133.88	133.96	0.09999	133.82	133.89	133.98	134.09

Corresponding to the co-sphere overlapping model, when ionic species interact in solutions, the volume of the solution increases, indicating the presence of molecular interactions within the system through the formation of cavities among the solution molecules.^{4,5} These cavities expand as the temperature rises, facilitating the interaction between solute and solvent molecules. However, at lower temperatures, solute molecules encounter difficulties in fitting into the water structure, resulting in stronger interactions between solute and solvent molecules in solutions.^{40–42} Similarly, at higher mannitol concentrations, more solute–solvent

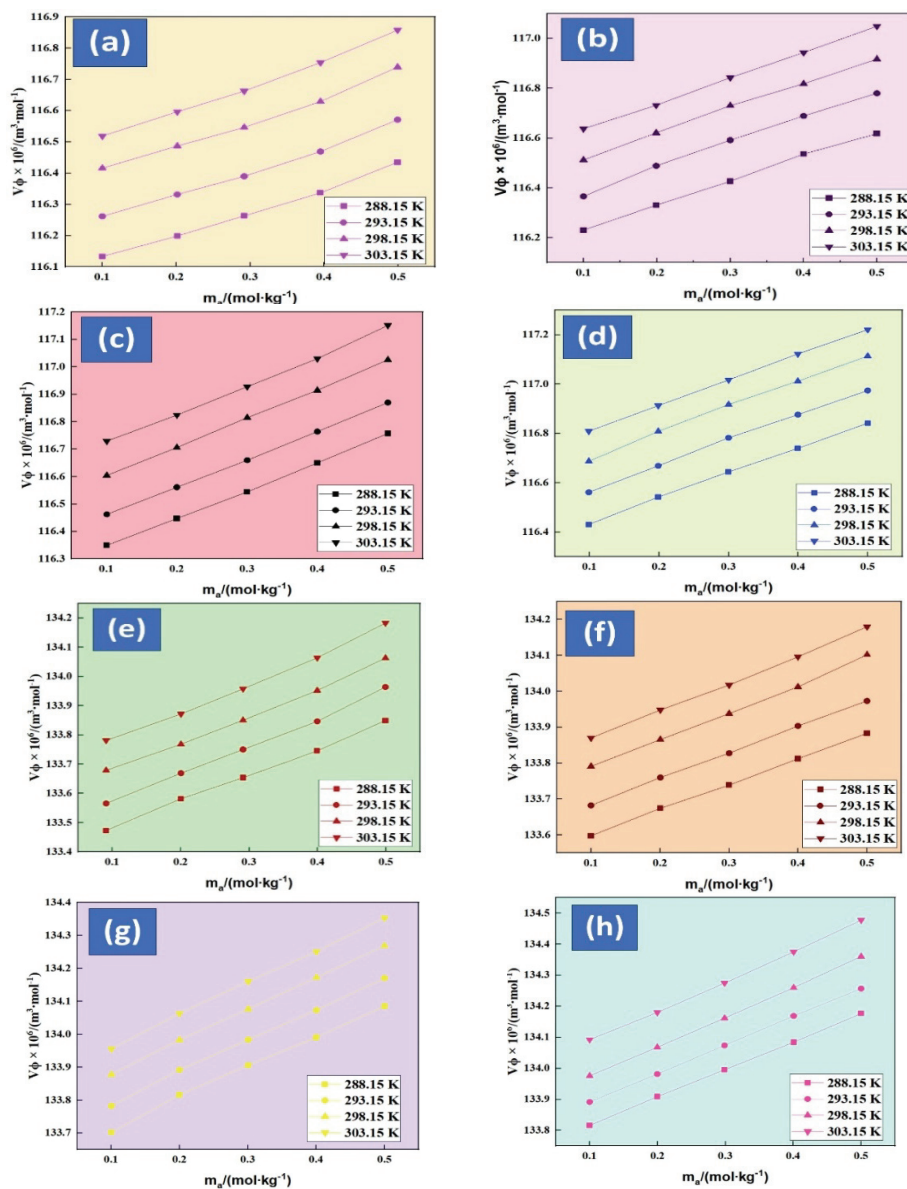
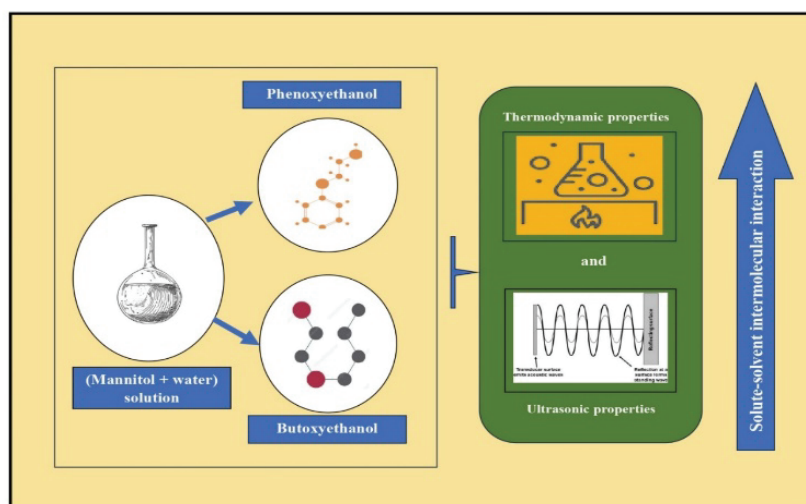


Fig. 4. Graphical illustration of apparent molar volume (V_{ϕ}) against the molality of BE/PE (m_A) at different temperatures: a) 0.00 D-mannitol + BE + water, b) 0.02 D-mannitol + BE + water, c) 0.06 D-mannitol + BE + water, d) 0.1 D-mannitol + BE + water, e) 0.00 D-mannitol + PE + water, f) 0.02 D-mannitol + PE + water, (g) 0.06 D-mannitol + PE + water and h) 0.1 D-mannitol + PE + water.

interactions can occur as water constituents are held in place by strong hydrogen bonds instead of being directly attached to the surfaces of solute molecules. This leads to the formation of gaps or cavities in the solutions, consequently increasing the apparent molar volume.⁴⁰

Moreover, the presence of glycol ethers in the mixture with water induces a combination of inter- and intramolecular hydrogen bonding, hydrophobic hydration, and dipole–dipole as well as dipole–induced dipole interactions.^{21–23} The increase in solute–solvent interactions in the sample compositions, as the molar mass of glycol ethers increases from BE to PE, corresponds to the phenomenon of solvation in the mixture at high temperatures and a greater affinity of the solvent as depicted in the Scheme 1.^{6–8}



Scheme 1. Representation of BE/PE and mannitol interactions.

Apparent molar isentropic compressibility

The undermentioned formula is utilized to determine the isentropic compressibility of glycol ethers in aqueous mannitol solutions:

$$K_{\Phi,S} = (Mk_S / \rho) - \{(k_{S,0}\rho - k_{S,0}\rho_0) / m_A\rho\rho_0\} \quad (2)$$

which takes into account various parameters such as densities of solution (ρ) and solvent (ρ_0), molar mass of solute (M), molality of solute (m_A), and isentropic compressibility of pure solvent ($k_{S,0}$) and solution (k_S).

The following Laplace–Newton formula is used to compute the isentropic compressibility:⁸

$$k_S = 1 / v^2\rho \quad (3)$$

The values of apparent molar isentropic compressibility ($K_{\Phi,S}$) are presented in Table VI, depicting their variation with temperature, glycol ethers molality, and mannitol concentration. These relationships are also visually represented in Fig. 5. The negative values of $K_{\Phi,S}$ decrease as temperature and mannitol concentration increase, but they increase with higher glycol ethers molality. This behavior can be attributed to the expulsion of solute molecules by thermal agitation, leading to volume expansion and an increase in compressibility. The negative values indicate that water molecules near the ionic charge groups of glycol ethers are more compressible than the solute molecules, resulting in a reduction in the structural compressibility of water.^{6–10} The presence of charged particles, such as ions, contributes to the overall rigidity of the solution, explaining the negative values of apparent molar isentropic compressibility in the presence of glycol ethers. As the temperature of the solution rises, the solution becomes more compressible due to the faster movement of ions and solvent molecules, which overcomes the resistance of the charged particles, resulting in enhanced compressibility.^{10–13} The intermolecular hydrogen bonding between glycol ethers and mannitol molecules forms compact structures, contributing to the reduction in compressibility. Additionally, as compressibility increases at higher temperatures, the average distance between molecules increases. The significant solvent–solvent interactions are evident through the dipole–dipole interactions between nearby water molecules and the –OH groups of glycol ethers.^{12–14}

TABLE VI. Values of apparent molar isentropic compressibility ($K_{\Phi} \times 10^6 / \text{m}^3 \text{mol}^{-1} \text{GPa}^{-1}$) of BE/PE in aqueous solutions of D-mannitol at different temperatures 288.15–303.15 K; m_a is the molality of glycols in the aqueous solution D-mannitol, standard uncertainties, u , are $u(m) = 1\%$, $u(T) = 0.001 \text{ K}$, $u(K_{\Phi}) = 0.11 \times 10^6 \text{ m}^3 \cdot \text{mol}^{-1} \cdot \text{GPa}^{-1}$

m_a	T / K				m_a	T / K			
	288.15	293.15	298.15	303.15		288.15	293.15	298.15	303.15
$\text{mol} \cdot \text{kg}^{-1}$	0.00 $\text{mol} \cdot \text{kg}^{-1}$ D-mannitol + BE				$\text{mol} \cdot \text{kg}^{-1}$	0.02 $\text{mol} \cdot \text{kg}^{-1}$ D-mannitol + BE			
0.10016	–46.04	–45.05	–44.25	–43.49	0.09978	–45.85	–44.90	–44.06	–43.34
0.20147	–46.28	–45.28	–44.48	–43.72	0.19899	–46.09	–45.13	–44.29	–43.57
0.29196	–46.36	–45.36	–44.56	–43.80	0.30003	–46.18	–45.21	–44.37	–43.65
0.39510	–46.41	–45.41	–44.60	–43.85	0.40010	–46.22	–45.26	–44.42	–43.69
0.49928	–46.44	–45.44	–44.63	–43.87	0.50003	–46.25	–45.28	–44.44	–43.72
0.10016	–46.04	–45.05	–44.25	–43.49	0.09978	–45.85	–44.90	–44.06	–43.34
	0.06 $\text{mol} \cdot \text{kg}^{-1}$ D-mannitol + BE					0.1 $\text{mol} \cdot \text{kg}^{-1}$ D-mannitol + BE			
0.10034	–45.61	–44.64	–43.83	–43.08	0.09894	–45.40	–44.43	–43.57	–42.82
0.20009	–45.85	–44.87	–44.06	–43.31	0.19880	–45.63	–44.66	–43.80	–43.04
0.30012	–45.93	–44.95	–44.13	–43.38	0.30001	–45.71	–44.74	–43.87	–43.12
0.39990	–45.97	–44.99	–44.17	–43.42	0.39959	–45.75	–44.78	–43.91	–43.16
0.50023	–45.99	–45.02	–44.20	–43.45	0.50005	–45.78	–44.80	–43.94	–43.18
0.10034	–45.61	–44.64	–43.83	–43.08	0.09894	–45.40	–44.43	–43.57	–42.82

TABLE VI. Continued

T / K					T / K				
m_a $\text{mol}\cdot\text{kg}^{-1}$	288.15	293.15	298.15	303.15	m_a $\text{mol}\cdot\text{kg}^{-1}$	288.15	293.15	298.15	303.15
0.00 $\text{mol}\cdot\text{kg}^{-1}$ D-mannitol + PE					0.02 $\text{mol}\cdot\text{kg}^{-1}$ D-mannitol + PE				
0.09102	-46.00	-45.01	-44.21	-43.46	0.09983	-45.87	-44.91	-44.08	-43.35
0.20047	-46.30	-45.31	-44.50	-43.75	0.20034	-46.12	-45.16	-44.32	-43.60
0.29106	-46.39	-45.40	-44.59	-43.83	0.30010	-46.21	-45.25	-44.41	-43.69
0.39951	-46.46	-45.46	-44.65	-43.89	0.39990	-46.27	-45.31	-44.47	-43.74
0.49928	-46.50	-45.50	-44.69	-43.93	0.50004	-46.31	-45.34	-44.50	-43.78
0.09102	-46.00	-45.01	-44.21	-43.46	0.09983	-45.87	-44.91	-44.08	-43.35
0.06 $\text{mol}\cdot\text{kg}^{-1}$ D-mannitol + PE					0.1 $\text{mol}\cdot\text{kg}^{-1}$ D-mannitol + PE				
0.10028	-45.63	-44.66	-43.84	-43.10	0.09999	-45.42	-44.45	-43.59	-42.84
0.19996	-45.87	-44.90	-44.08	-43.33	0.19973	-45.66	-44.68	-43.82	-43.07
0.30056	-45.96	-44.99	-44.17	-43.42	0.29880	-45.75	-44.77	-43.91	-43.15
0.40031	-46.02	-45.04	-44.22	-43.47	0.40050	-45.80	-44.82	-43.96	-43.20
0.50009	-46.05	-45.07	-44.26	-43.50	0.50009	-45.83	-44.86	-43.99	-43.23
0.10028	-45.63	-44.66	-43.84	-43.10	0.09999	-45.42	-44.45	-43.59	-42.84

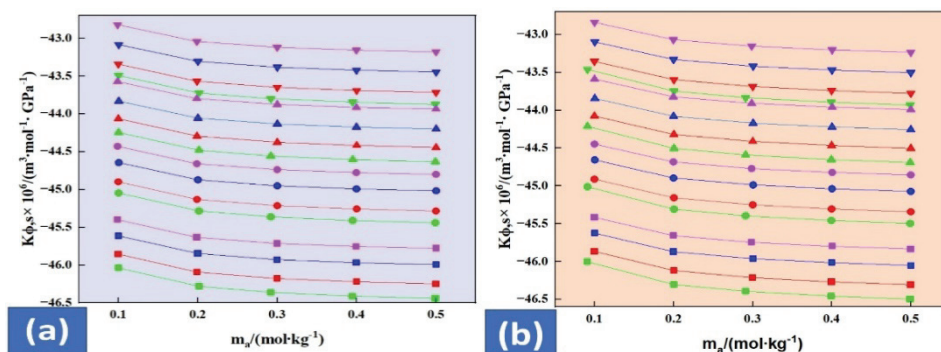


Fig. 5. Graphical illustration of apparent molar isentropic compressibility ($K_{\Phi,S}$), against the molality of BE/PE (m_A) at different temperatures: a) BE and b) PE (green, 0.00 D-mannitol; red, 0.02 D-mannitol; blue, 0.06 D-mannitol; purple, 0.1 D-mannitol; square, 288.15 K; circle, 293.15 K; triangle, 298.15 K; inverted triangle, 303.15 K).

Partial molar properties

Partial molar volume. The undermentioned formula used to attain the partial molar volume of solution containing mannitol and glycol ethers. The partial molar volume (V_{Φ}^0) values and experimental slope (S_V^*) along with their standard errors corresponding to experimental temperatures and mannitol concentrations, obtained using the least square fitting method, are demonstrated in Table VII. The equation used is:

$$V_{\Phi} = V_{\Phi}^0 + S_V^* m_A \quad (4)$$

The positive values of V_{Φ}^0 increase with the concentration of mannitol and temperature, indicating the solute-solvent interactions in the liquid mixture which is shown in Fig. 6. According to the co-sphere overlap model, the overlap of the hydration co-sphere between two ionic species results in an increase in volume, whereas the overlap of ion-hydrophobic and hydrophobic-hydrophobic groups leads to a decrease in volume.^{4,5} Thus, the positive values of V_{Φ}^0 indicate that ion-hydrophilic interactions prevail over hydrophobic-hydrophobic and ion-hydrophobic interactions, providing evidence for the strong hydrogen bond formation between water molecules and the hydroxyl (-OH) groups of glycol ethers.¹²⁻¹⁵ The increase in V_{Φ}^0 values with temperature can be attributed to several factors, such as the release of solvation molecules from the relaxed solvation layers of the solute into the mixture, thermal expansion, and the formation of hydrogen bonds. Additionally, as the molecular mass of the glycol ethers (BE < PE) increases, the solute-solvent interaction becomes stronger, as evidenced by the increase in V_{Φ}^0 values with longer solute chain lengths.²³⁻²⁵

The S_V^* values for each temperature and mannitol concentration are found to be positive, representing the semiempirical solute-solute interaction parameter. This indicates the presence of solute-solute interactions within the mixture, although their magnitude is smaller compared to the V_{Φ}^0 values. This suggests that solute-solvent interactions dominate over solute-solute interactions in the solution.^{18,32-34}

TABLE VII. Values of partial molar volumes, (V_{Φ}^0), and experimental slopes, (S_V^*), of BE/PE in aqueous solution of D-mannitol at different temperatures (288.15–303.15 K); m_b is the concentration of D-mannitol, standard uncertainties, u , are $u(m) = 1\%$, $u(T) = 0.001\text{ K}$, $u(\rho) = 0.15\text{ kg}\cdot\text{m}^{-3}$, $u(v) = 1.0\text{ m}\cdot\text{s}^{-1}$, $u(V_{\Phi}^0) = \pm 0.01 \times 10^6\text{ m}^3\cdot\text{mol}^{-1}$ and $u(S_V^*) = \pm 0.03 \times 10^6\text{ m}^3\cdot\text{kg}\cdot\text{mol}^{-2}$

m_b mol·kg ⁻¹	$V_{\Phi}^0 \times 10^6 / \text{m}^3\cdot\text{mol}^{-1}$				$S_V^* \times 10^6 / \text{m}^3\cdot\text{kg}\cdot\text{mol}^{-2}$			
	T / K							
	288.15	293.15	298.15	303.15	288.15	293.15	298.15	303.15
BE								
0.00	116.05 (±0.010)	116.18 (±0.012)	116.33 (±0.010)	116.43 (±0.010)	0.7484 (±0.032)	0.7634 (±0.037)	0.7975 (±0.046)	0.8437 (±0.032)
0.02	116.14 (±0.007)	116.28 (±0.011)	116.42 (±0.008)	116.53 (±0.003)	0.9783 (±0.021)	1.0266 (±0.034)	1.0059 (±0.024)	1.0332 (±0.011)
0.06	116.24 (±0.004)	116.36 (±0.003)	116.50 (±0.002)	116.62 (±0.008)	1.0179 (±0.014)	1.0176 (±0.008)	1.0511 (±0.008)	1.0490 (±0.025)
0.10	116.34 (±0.004)	116.46 (±0.006)	116.59 (±0.009)	116.71 (±0.002)	1.0176 (±0.014)	1.0304 (±0.020)	1.0553 (±0.028)	1.0310 (±0.006)
PE								
0.00	133.39 (±0.007)	133.48 (±0.009)	133.59 (±0.010)	133.68 (±0.012)	0.9026 (±0.023)	0.9587 (±0.028)	0.9370 (±0.031)	0.9800 (±0.038)
0.02	133.53 (±0.002)	133.61 (±0.002)	133.71 (±0.006)	133.79 (±0.004)	0.7092 (±0.008)	0.7259 (±0.008)	0.7682 (±0.018)	0.7679 (±0.013)

TABLE VII. Continued

m_b mol·kg ⁻¹	$V_{\Phi}^0 \times 10^6 / \text{m}^3 \cdot \text{mol}^{-1}$				$S_{\Phi}^* \times 10^6 / \text{m}^3 \cdot \text{kg} \cdot \text{mol}^{-2}$			
	T / K							
	288.15	293.15	298.15	303.15	288.15	293.15	298.15	303.15
PE								
0.06	133.62 (±0.010)	133.69 (±0.006)	133.78 (±0.003)	133.86 (±0.005)	0.9415 (±0.030)	0.9579 (±0.019)	0.9713 (±0.010)	0.9832 (±0.015)
0.10	133.73 (±0.002)	133.80 (±0.001)	133.88 (±0.003)	133.99 (±0.005)	0.8956 (±0.006)	0.9168 (±0.004)	0.9609 (±0.009)	0.9636 (±0.016)

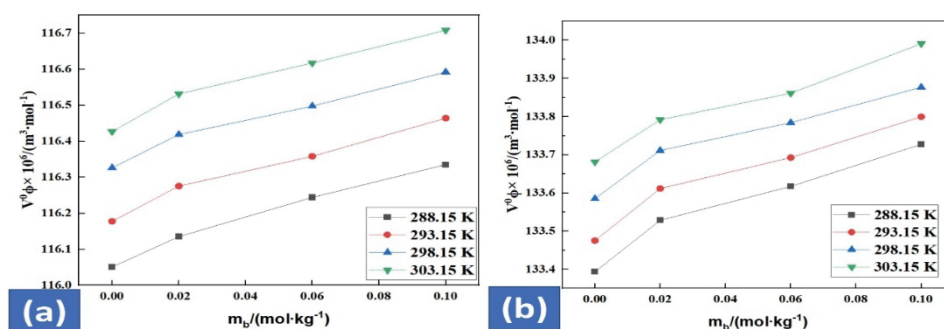


Fig. 6. Graphical illustration of partial molar volume (V_{Φ}^0) against the concentration of mannitol (m_b) at different temperatures: a) BE and b) PE (square, 288.15 K; circle, 293.15 K; triangle, 298.15 K; inverted triangle, 303.15 K).

Partial molar isentropic compressibility

The partial molar isentropic compressibility of liquid mixtures containing mannitol and glycol ethers is determined using as:

$$k_{\Phi,S} = K_{\Phi,S}^0 + S_k^* m_A \quad (5)$$

Table VIII presents the values of partial molar isentropic compressibility ($K_{\Phi,S}^0$) and experimental slope (S_k^*). In Fig. 7 the $K_{\Phi,S}^0$ values are represented graphically. These values are acquired by applying the method of least square fitting.

The $K_{\Phi,S}^0$ values are negative and decrease with increasing mannitol concentration and temperature. This trend implies the existence of strong interaction in water and glycol ethers in the mixture, causing some water molecules to be released into the bulk. The compressibility of water around glycol ethers is less at lower mannitol concentrations, but more at higher concentrations because of dominant interaction between mannitol and water, which dehydrates the glycol ethers molecules. The $K_{\Phi,S}^0$ values are affected by intermolecular interactions and is connected to the partial volume change of a solution. Ion dipole and hydrogen bonding occur, and are brought about by electrostatic forces between the polar group of mannitol, water and the ions of glycol ethers.^{20–26} This shows that

the molecules in the solutions are tightly packed and well organized as the temperature drops, the strength of these connections increases, and partial molar compressibility values decrease. It showed that ions developed their structure-forming or structure-deforming behavior as a result of their strong interactions with water particles, such as H-bonding with water particles. Greater molecular interactions are present in the system with a lower compressibility value and *vice versa*.^{40–43} According to the S_k^* values in the table, solute–solute interactions are minimal in a liquid mixture while they predominate in a solution.³⁹

TABLE VIII. Values of Partial molar isentropic compressibility, ($K_{\phi,S}^0 / \text{m}^3 \cdot \text{mol}^{-1} \cdot \text{GPa}^{-1}$) and experimental slopes, ($S_k^* \times 10^6 / \text{kg} \cdot \text{m}^3 \cdot \text{mol}^{-2} \cdot \text{GPa}^{-1}$) of BE/PE in aqueous solution of D-mannitol at different temperatures; m_b is the concentration of D-mannitol, standard uncertainties, u , are $u(m) = 1 \%$, $u(T) = 0.001 \text{ K}$, $u(\rho) = 0.15 \text{ kg} \cdot \text{m}^{-3}$, $u(v) = 1.0 \text{ m} \cdot \text{s}^{-1}$, $u(K_{\phi,S}^0) = \pm 0.01 \times 10^6 \text{ m}^3 \cdot \text{mol}^{-1}$ and $u(S_k^*) = \pm 0.24 \times 10^6 \text{ m}^3 \cdot \text{kg} \cdot \text{mol}^{-2}$

m_b $\text{mol} \cdot \text{kg}^{-1}$	$K_{\phi,S}^0$				S_k^*			
	T / K							
	288.15	293.15	298.15	303.15	288.15	293.15	298.15	303.15
BE								
0.00	-46.03	-45.04	-44.24	-43.48	-0.9353	-0.9163	-0.9008	-0.8891
0.02	-45.84	-44.89	-44.05	-43.33	-0.9162	-0.8958	-0.8822	-0.8714
0.06	-45.60	-44.64	-43.82	-43.08	-0.8841	-0.8668	-0.8527	-0.8412
0.10	-45.39	-44.42	-43.57	-42.82	-0.8712	-0.8544	-0.8392	-0.8289
PE								
0.00	-46.00	-45.01	-44.21	-43.45	-1.1271	-1.1058	-1.0907	-1.0772
0.02	-45.84	-44.89	-44.06	-43.33	-1.0338	-1.0141	-0.9998	-0.9899
0.06	-45.61	-44.64	-43.82	-43.08	-0.9959	-0.9782	-0.9650	-0.9538
0.10	-45.40	-44.43	-43.57	-42.82	-0.9705	-0.9542	-0.9395	-0.9274

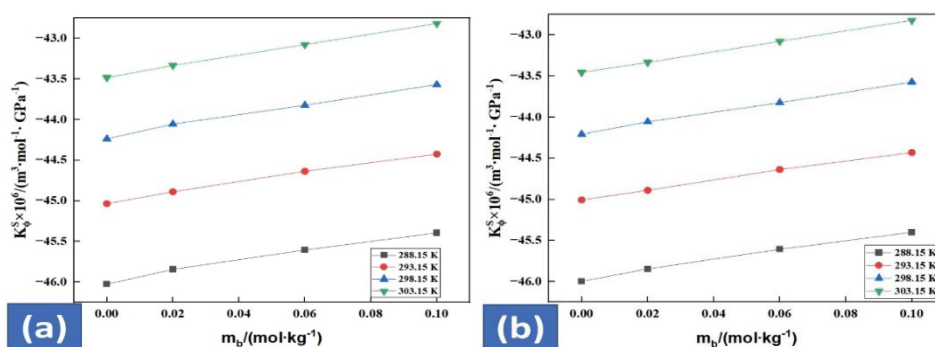


Fig. 7. Graphical illustration of partial molar isentropic compressibility ($K_{\phi,S}^0$) against the concentration of mannitol (m_b) at different temperatures: a) BE and b) PE (square, 288.15 K; circle, 293.15 K; triangle, 298.15 K; inverted triangle, 303.15 K).

CONCLUSION

The Anton-Paar DSA 5000 M was employed in the experimental setup to measure both the density and speed of sound. This data was pivotal in exploring the volumetric and acoustic properties of the solutions. The substances under investigation, glycol ethers, and D-mannitol, have diverse applications in industries like pharmaceuticals, cosmetics, leather and food. Examining the mixture's thermodynamics allows us to understand the molecular interactions between these liquids. Using the DSA system is advantageous as it prevents structural deformations in glycol ethers within aqueous D-mannitol, avoiding potential errors from suspension formation. Analyzing the acoustical properties and their variations with different molar concentrations of D-mannitol provides crucial insights into the intermolecular forces in the mixtures. Measuring the speed of sound is an effective means to characterize the physicochemical behavior of D-mannitol, reflecting solute-solvent interactions that lead to attractive forces contributing to structure formation. Additionally, interactions such as dipole-dipole, dipole-induced dipole and electrostatic forces enhance the structure-forming tendency in this medium. The data obtained from this study lays a solid foundation for future research aimed at refining our understanding of these molecular interactions. Further investigations could delve into optimizing the mixture's properties for specific industrial applications, thus contributing to advancements in various sectors.

SUPPLEMENTARY MATERIAL

Additional data and information are available electronically at the pages of journal website: <https://www.shd-pub.org.rs/index.php/JSCS/article/view/12593>, or from the corresponding author on request.

Acknowledgements. The authors express their gratitude to the Department of Physics at Lovely Professional University (Punjab, India) and the Department of Chemistry at Dr. BR Ambedkar NIT (Punjab, India) for their kind provision of the necessary laboratory equipment.

ИЗВОД

ТЕРМОФИЗИЧКО ИСПИТИВАЊЕ ГЛИКОЛ-ЕТАРА У РАСТВОРИМА МАНИТОЛА НА РАЗЛИЧИТИМ ТЕМПЕРАТУРАМА

NAVAPARNA CHAKRABORTY^{1,2}, PRIYA THAKUR¹, KAILASH CHANDRA JUGLAN¹ и ABRAR HUSSAIN SYED³

¹Department of Physics, Lovely Professional University, Phagwara, 144401, Punjab, India, ²Central Instrumentation Facility, Research and Development Cell, Lovely Professional University, Phagwara, 144401, Punjab, India и ³Research and Development, Saputo Dairy Australia, Freshwater Place, 3006, Victoria, Australia

Ултразвучна анализа може бити од велике помоћи за разумевање молекуларне динамике и интеракција у течним системима. Применом Anton-Paar инструмента (DSA 5000 M), измерене су брзина звука и густина гликол-етара, као што су феноксietанол (PE) и бутоксиетанол (BE), у растворима добро познатог шећерног алкохола (D-манитол), при различитим концентрацијама и 0,1 МПа, у опсегу температура 288,15–303,15

К. Израчунати су различити акустично–термодинамички параметри, укључујући привидне моларне параметре, парцијалне моларне параметре и преносна моларна својства, коришћењем експериментално добијених вредности брзине и густине. Ове изведене величине су искоришћене за изражавање интеракција између растворених материја и растварача. Предмет истраживања је и склоност растворене супстанце да изгради или разори структуре у растварачу. Урађена је анализа интеракција између молекула у тернарној смеси d-манитола и гликол етара у воденој средини.

(Примљено 15. септембра 2023, ревидирано 21. фебруара, прихваћено 20. августа 2024)

REFERENCES

1. M. S. Raman, M. Kesavan, K. Senthilkumar, V. Ponnuswamy, *J. Mol. Liq.* **202** (2015) 115 (<https://doi.org/10.1016/j.molliq.2014.12.014>)
2. S. Emiliani, M. V. Bergh, A. S. Vannin, J. Biranane, Y. Englert, *Hum. Reprod.* **15** (2000) 905 (<https://doi.org/10.1093/humrep/15.4.905>)
3. C. Zhu, X. Ren, Y. Ma, *J. Chem. Eng. Data* **62** (2017) 477 (<https://doi.org/10.1021/acs.jced.6b00766>)
4. N. Chakraborty, K. C. Juglan, H. Kumar, *J. Chem. Thermodyn.* **154** (2021) 106326 (<https://doi.org/10.1016/j.jct.2020.106326>)
5. A. Ali, P. Bidhuri, S. Uzair, *Indian J. Phys.* **88(7)** (2014) 715 (<https://doi.org/10.1007/s12648-014-0461-2>)
6. N. Chakraborty, K. C. Juglan, H. Kumar, *J. Mol. Liq.* **337** (2021) 116605 (<https://doi.org/10.1016/j.molliq.2021.116605>)
7. H. Kumar, M. Singla, R. Jindal, *Monatsh. Chem.* **145** (2014) 1063 (<https://doi.org/10.1007/s00706-014-1183-z>)
8. P. Pradhan, R.S. Sah, M. N. Roy, *J. Mol. Liq.* **144** (2009) 149 (<https://doi.org/10.1016/j.molliq.2008.11.001>)
9. S. K. Lomesh, M. Bala, D. Kumar, *J. Mol. Liq.* **289** (2019) 109479 (<https://doi.org/10.1016/j.molliq.2018.08.034>)
10. J. Wawer, J. Krakowiak, W. Grzybkowski, *J. Chem. Thermodyn.* **40** (2008) 1193 (<https://doi.org/10.1016/j.jct.2008.04.008>)
11. R. Rani, A. Kumar, T. Sharma, T. Sharma, R. K. Bamezai, *J. Chem. Thermodyn.* **135** (2019) 260 (<https://doi.org/10.1016/j.jct.2019.03.039>)
12. H. Zarei, S. M. Asl, *Fluid Phase Equilib.* **457** (2018) 52 (<https://doi.org/10.1016/j.fluid.2017.10.027>)
13. X. Jiang, C. Zhu, Y. Ma, *J. Chem. Eng. Data* **58** (2013) 2970 (<https://doi.org/10.1021/je400395u>)
14. N. G. Tsierkezos, I. E. Molinou, *J. Chem. Eng. Data* **43** (1998) 989 (<https://doi.org/10.1021/je9800914>)
15. I. Gheorghe, C. Stoicescu, F. Sirbu, *J. Mol. Liq.* **218** (2016) 515 (<https://doi.org/10.1016/j.molliq.2016.02.033>)
16. B. Sinha, A. Sarkar, P. K. Roy, D. Brahman, *Int. J. Thermophys.* **32** (2011) 2062 (<https://doi.org/10.1007/s10765-011-1060-5>)
17. M. Liu, L. L. Wang, G. Q. L. N. Dong, D. Z. Sun, L. Y. Zhu, Y. Y. Di, *J. Chem. Thermodyn.* **43** (2011) 983 (<https://doi.org/10.1016/j.jct.2011.02.005>)
18. M. Scognamiglio, L. Jones, C. S. Letizia, A. M. Api, *Food Chem. Toxicol.* **50** (2012) 244 (<https://doi.org/10.1016/j.fct.2011.10.030>)
19. I. Lowe, J. Southern, *Lett. App. Microbiol.* **18** (1994) 115 (<https://doi.org/10.1111/j.1472-765X.1994.tb00820.x>)

20. M. S. Raman, G. Amrithaganesan, *Indian J. Phys.* **78**(12) (2004) 1329
21. D. Chawla, N. Chakraborty, K. C. Juglan, H. Kumar, *Chem. Papers* **75** (2021) 1497 (<https://doi.org/10.1007/s11696-020-01403-y>)
22. P. K. Banipal, S. Arti, T. S. Banipal, *J. Chem. Eng. Data* **60** (2015) 1023 (<https://doi.org/10.1021/je500886a>)
23. I. Mozo, I. G. de la Fuente, J. A. Gonzalez, J. C. Cobos, N. Riesco, *J. Chem. Eng. Data* **53** (2008) 1404 (<https://doi.org/10.1021/je8000975>)
24. H. Makhlauf, N. Munoz-Rujas, F. Aguilar, B. Belhachemi, E. A. Montero, I. Bahadur, L. Negadi, *J. Chem. Thermodyn.* **128** (2019) 394 (<https://doi.org/10.1016/j.jct.2018.08.029>)
25. X. U. Wang, R. Fu, Y. Gua, L. Rusin, *J. Mol. Liq.* **197** (2014) 73 (<https://doi.org/10.1016/j.molliq.2014.04.028>)
26. J. G. Kirkwood, *Chem. Rev.* **24** (1939) 233 (<https://doi.org/10.1021/cr60078a004>)
27. Z. Yan, J. J. Wang, H. Zheng, D. Liu, *J. Solut. Chem.* **27** (1998) 473 (<https://doi.org/10.1023/A:1022608906767>)
28. H. L. Friedman, C. Krishnan, *J. Solut. Chem.* **2** (1973) 119 (<https://doi.org/10.1007/BF00651969>)
29. S. Li, W. Sang, R. Lin, *J. Chem. Thermodyn.* **34** (2002) 1761 ([https://doi.org/10.1016/S0021-9614\(02\)00125-8](https://doi.org/10.1016/S0021-9614(02)00125-8))
30. A. Salabat, L. Shamschiri, F. Sahrakr, *J. Mol. Liq.* **118** (2005) 67 (<https://doi.org/10.1016/j.molliq.2004.07.014>)
31. A. K. Mishra, J. C. Ahluwalia, *J. Phys. Chem.* **88** (1984) 86 (<https://doi.org/10.1021/j150645a021>)
32. L. G. Hepler, *Can. J. Chem.* **47** (1969) 4613 (<https://doi.org/10.1139/v69-762>)
33. B. Naseem, I. Arif, M. A. Jamal, *Arab. J. Chem.* **14** (2021) 103405 (<https://doi.org/10.1016/j.arabjc.2021.103405>)
34. A. K. Nain, R. Pal, *J. Chem. Thermodyn.* **60** (2013) 98 (<https://doi.org/10.1016/j.jct.2013.01.008>)
35. R. A. Miranda- Quintana, J. Smiatek, *ChemPhysChem* **21** (2020) 2605 (<https://doi.org/10.1002/cphc.202000644>)
36. Z. Yan, X. Wen, Y. Kang, S. Zhang, S. Wu, *J. Chem. Thermodyn.* **93** (2016) 172 (<https://doi.org/10.1016/j.jct.2015.10.004>)
37. F. J. Millero, in *Water and Aqueous Solutions: Structure, Thermodynamics, and Transport Processes*, R. A. Horne, Ed., Wiley, New York, 1972
38. W. G. McMillan, Jr., J. E. Mayer, *J. Chem. Phys.* **13** (1945) 276 (<https://doi.org/10.1063/1.1724036>)
39. C. V. Krishnan, H. L. Friedman, *J. Solut. Chem.* **2** (1973) 37 (<https://doi.org/10.1007/BF00645870>)
40. F. Franks, M. Pedley, D. S. Reid, *J. Chem. Soc., Faraday Trans. 1* **72** (1976) 359 (<https://doi.org/10.1039/F19767200359>)
41. N. Chakraborty, K. C. Juglan, H. Kumar, *J. Chem. Thermodyn.* **163** (2021) 106584 (<https://doi.org/10.1016/j.jct.2021.106584>)
42. R. K. Wadi, P. Ramasami, *J. Chem. Soc., Faraday Trans.* **93** (1997) 243 (<https://doi.org/10.1039/A604650I>)
43. N. Chakraborty, P. Thakur, K. C. Juglan, *E3S Web Conf.* **453** (2023) 01051 (<https://doi.org/10.1051/e3sconf/202345301051>).



SUPPLEMENTARY MATERIAL TO
Thermophysical investigation of glycol ethers in mannitol solutions at various temperatures

NABAPARNA CHAKRABORTY^{1,2*}, PRIYA THAKUR¹, KAILASH CHANDRA JUGLAN¹ and ABRAR HUSSAIN SYED³

¹Department of Physics, Lovely Professional University, Phagwara, 144401, Punjab, India,

²Central Instrumentation Facility, Research and Development Cell, Lovely Professional University, Phagwara, 144401, Punjab, India and ³Research and Development, Saputo Dairy Australia, Freshwater Place, 3006, Victoria, Australia

J. Serb. Chem. Soc. 89 (11) (2024) 1489–1506

Partial molar volume of transfer

To determine the Transfer of partial molar volume of glycol ethers from water to aqueous solutions of mannitol at infinite dilution, the formula used is

$$\Delta V_{\phi}^0 = V_{\phi}^0(\text{in aqueous d-Mannitol}) - V_{\phi}^0(\text{water}) \quad (\text{SEq1})$$

The partial molar volume of transfer allows for qualitative and quantitative studies of solvent and solute interactions within the mixture, excluding interactions resulting from solute-solute molecules. The results of this parameter are presented in **Table S-I**, revealing that all ΔV_{ϕ}^0 values are positive. This indicates the presence of strong ion-ion interactions between mannitol and glycol ethers, both of which contain polar groups. According to the co-spheres overlap theory, the solute's ability to form structures is enhanced through their interactions in the solution, resulting in a positive value that is attributed to the structural interactions between the two co-spheres.¹⁻² The ΔV_{ϕ}^0 values reflect the different types of interactions in the solution, such as ion-hydrophilic interactions, ion-hydrophobic interactions, hydrophilic-hydrophilic interactions, and hydrophobic-hydrophobic interactions. These values primarily control the solute-solute interactions, which are almost nonexistent in this case. The positive ΔV_{ϕ}^0 values suggest the presence of ion-hydrophilic and hydrophilic-hydrophilic contacts, as indicated by the co-spheres overlap model. On the other hand, ion-hydrophobic and hydrophobic-hydrophobic interactions would have a negative impact on the partial molar volume of transfer. Based on the current investigation of the mannitol-water-glycol ethers system, the findings support the existence of ion-hydrophilic and hydrophilic-hydrophilic interactions.

* Corresponding author. E-mail: nabaparnac@gmail.com

Consequently, the results are interpreted as the following interactions-

- i. (hydrophobic-hydrophobic) interactions:
Between the alkyl groups of mannitol and glycol ethers
- ii. (hydrophilic- hydrophobic) interactions:
Between -OH group of mannitol and alkyl group of glycol ethers.
- iii. (hydrophilic-hydrophilic) interactions:
Between -OH group of mannitol and hydrophilic group of glycol ethers
- iv. (ion-hydrophobic) interactions:
Between alkyl groups of mannitol and zwitterions of glycol ethers
- v. (ion- hydrophilic) interactions:
Between -OH group of mannitol and zwitterions of glycol ethers.

It can be seen that the ΔV_{ϕ}^0 values of the solutions are increasing along the concentrations of mannitol at specific temperature. The dominance of (ion-hydrophilic) interactions in the system is established and is increasing with the molar mass of the glycol ethers i.e., from BE to PE as $\Delta V_{\phi}^0(\text{BE}) < \Delta V_{\phi}^0(\text{PE})$.³⁻¹²

Partial molar isentropic compression of transfer

The transfer of partial molar isentropic compression is determined using the undermentioned formula at infinite dilution

$$\Delta K_{\phi,s}^0 = K_{\phi,s}^0(\text{in aqueous d- Mannitol}) - K_{\phi,s}^0(\text{in water}) \quad (\text{Seq 2})$$

The results presented in **Table S-I** reveal that all ($\Delta K_{\phi,s}^0$) values are positive and exhibit an increasing trend with increasing mannitol concentration. However, these values do not follow a consistent pattern with temperature. These findings suggest that the interaction between the zwitterionic center of glycol ethers and mannitol contributes to a structure-making tendency in the ions. This tendency becomes more pronounced as the mannitol concentration increases and the electrostriction decreases. The compressibility of bulk water experiences a significant decrease as the mannitol concentration increases, resulting in positive ($\Delta K_{\phi,s}^0$) values. In contrast, for (BE/PE) at different concentrations of mannitol, the $K_{\phi,s}^0$ values are negative. The cause of this behavior is due to incorporation of more solute water molecules with solvent molecules, leading to increased interactions within the ions. At lower mannitol concentrations and temperatures, the water molecules are more likely to interact with each other, contributing to the negative $K_{\phi,s}^0$ values for (BE/PE).¹³⁻¹⁵

Table S-I. Values of Partial molar volumes of transfer (ΔV_{ϕ}^0), and partial molar isentropic compression transfer, ΔK_{ϕ}^0 of (BE/PE) in aqueous solution of d-Mannitol at different temperatures.

mb/ (mol·kg ⁻¹)	$\Delta V_{\phi}^0 * 106/(\text{m}^3 \cdot \text{mol}^{-1})$				$\Delta K_{\phi}^0 * 106/(\text{m}^3 \cdot \text{mol}^{-1} \cdot \text{GPa}^{-1})$			
	288.15 K	293.15 K	298.15 K	303.15 K	288.15 K	293.15 K	298.15 K	303.15 K
	BE							
0.02	0.0844	0.0979	0.0921	0.1046	0.1836	0.1474	0.1824	0.1503
0.06	0.1934	0.1803	0.1713	0.1906	0.4224	0.4000	0.4138	0.4073
0.10	0.2843	0.2864	0.2655	0.2812	0.6328	0.6109	0.6695	0.6671
	PE							
0.02	0.1348	0.1362	0.1262	0.1107	0.1523	0.1165	0.1520	0.1202
0.06	0.2237	0.2174	0.1990	0.1800	0.3909	0.3691	0.3833	0.3771
0.10	0.3339	0.3244	0.2920	0.3097	0.5974	0.5761	0.6350	0.6331

m_b is the concentration of d-mannitol

Temperature dependent partial molar volume

The given equation describes the change in the apparent molar volume at finite dilution corresponding the temperature

$$V_{\phi}^0 = a + b(T - T_{ref}) + c(T - T_{ref})^2 \quad (\text{SEq 3})$$

The constants a , b , and c represent empirical values, and the values of these constants for three types of glycol ethers, where T is the experimental temperature and T_{ref} is the reference temperature, i.e., 298.15 K.

Utilizing these empirical parameters to derive deviations known as ARDs (σ), estimated and experimental values of V_{ϕ}^0 are used to obtain the deviations. These deviations (ARD) are obtained by applying the following relation.

$$\sigma = (1/n) \sum [\text{abs}((Y_{\text{Exptl.}} - Y_{\text{Calc.}})/Y_{\text{Exptl.}})] \quad (\text{SEq 4})$$

Here, $Y = V_{\phi}^0$

After this above-mentioned substitution, equation (9) becomes-

$$\sigma = (1/n) \sum [\text{abs}((V_{\phi, \text{Exptl.}}^0 - V_{\phi, \text{Calc.}}^0)/V_{\phi, \text{Exptl.}}^0)] \quad (\text{SEq 5})$$

To calculate the deviations, we employed equation (10). The present investigation's R^2 results demonstrate that the polynomial equation is fully appropriate, and the deviation values are considerably lower.¹⁶ **Table S-II** displays the values of the empirical parameters (a , b , and c), ARDs (σ), and R^2 . The theoretical values of V_{ϕ}^0 are evaluated using these empirical constants, and they are then compared with the outcomes of the experiments.¹² With regard to temperature, the values of partial molar expansibility E_{ϕ}^0 is obtained by differentiating equation (8) which becomes equation (11), mentioned as below:

$$E_{\phi}^0 = (\partial E_{\phi}^0 / \partial T)_n = b + 2c(T - T_{ref}) \quad (\text{SEq 6})$$

These values are used to determine the partial molar expansibilities at infinite dilution, which is considered to be a significant property for characterizing the interactions between solute and solvent that take place in solution.¹⁴⁻¹⁷ The values of E_{ϕ}^0 are not showing any discrete trend but are all positive, as shown in **Table S-III**, indicating that the volume is decreased following the between the glycol ethers and aqueous mannitol solution.

In order to determine whether solute molecules tend to support or intervene with the structure of the solvent molecules, Hepler proposed a mathematical relationship that is assessed by the following equation.¹⁷

$$\left(\frac{\partial E_{\phi}^0}{\partial T}\right)_{\infty} = \left(\frac{\partial^2 V_{\phi}}{\partial T^2}\right)_{\infty} = 2c \quad (\text{Seq 7})$$

according to Hepler's constant $\left(\frac{\partial^2 V_{\phi}}{\partial T^2}\right)_{\infty}$, even a solute in a solution can operate as a structural forming or deforming agent. Values with positive $\left(\frac{\partial^2 V_{\phi}}{\partial T^2}\right)_{\infty}$ values revealed the structure making property in the solutions. **Table S-III** summarizes the computed $\left(\frac{\partial^2 V_{\phi}}{\partial T^2}\right)_{\infty}$ data for all mixes under investigation. The results showed that $\left(\frac{\partial^2 V_{\phi}}{\partial T^2}\right)_{\infty}$ values for aqueous mannitol solutions containing glycol ethers are positive, demonstrating the solute's ability to promote structure. This is shown by the fact that water molecules develop weak intermolecular contacts with single charged ions with low charge densities, and that these interactions have only a minimal impact on H-bonding. These ions are classified as "structure deformer" or chaotropic ions. On the other hand, stronger interactions with water molecules are produced by charged ions with higher charge densities and can strengthen the H bonding in water structure. These ions are referred to as kosmotropes or "structure-former" ions.¹⁸⁻²¹ Positive or small negative values of $\left(\frac{\partial E_{\phi}^0}{\partial T}\right)_{\infty}$ implies the structure making capability solute, while negative values imply a structure breaker. In summary, the thermodynamic equation provides a measure of the solute's ability to influence the structure of the solution, and the sign of the partial molar expansibility derivative determines whether the solute breaks or builds structures. In Table 8 values of $\left(\frac{\partial E_{\phi}^0}{\partial T}\right)_{\infty}$ are found to be positive which implies the structure making property of glycol ethers in aqueous mannitol solutions.¹⁶⁻²⁵

Table S-II. Values of Empirical parameters (a, b, c) of (BE/PE) in aqueous solution of d-Mannitol.

${}^a m_B / (\text{mol} \cdot \text{kg}^{-1})$	$a \cdot 10^6 / (\text{m}^3 \cdot \text{mol}^{-1})$	$b \cdot 10^6 / (\text{m}^3 \cdot \text{mol}^{-1} \cdot \text{K}^{-1})$	$c \cdot 10^6 / (\text{m}^3 \cdot \text{mol}^{-1} \cdot \text{K}^{-2})$	R^2	ARD
BE					
0.00	116.18813	0.01343	-0.00007	0.9999	0.00043
0.02	116.28039	0.01400	-0.00007	0.9999	0.00044
0.06	116.36480	0.01244	0.00002	0.9999	0.00041
0.10	116.46561	0.01279	-0.00003	0.9999	0.00055
PE					
0.00	133.48155	0.00937	0.00004	0.9999	0.00027
0.02	133.61688	0.00897	-0.00001	0.9999	0.00025
0.06	133.69722	0.00819	0.00000	0.9999	0.00023
0.10	133.79504	0.00764	0.00010	0.9999	0.00029

m_b is the concentration of d-mannitol

Table S-III. Values of Partial molar expansibilities, (E_ϕ^0), and its first derivatives ($(\partial E_\phi^0 / \partial T)_p$) for (BE/PE) in aqueous solution of d-Mannitol at different temperatures.

${}^a m_B / (\text{mol} \cdot \text{kg}^{-1})$	$E_\phi^0 \cdot 10^6 / (\text{m}^3 \cdot \text{mol}^{-1} \cdot \text{K}^{-1})$				$(\partial E_\phi^0 / \partial T)_p / (\text{m}^3 \cdot \text{mol}^{-1} \cdot \text{K}^{-2})$
	288.15 K	293.15 K	T298.15 K	303.15 K	
BE					
0.00	0.01474	0.01408	0.01343	0.01277	-0.00013
0.02	0.01537	0.01469	0.01400	0.01332	-0.00014
0.06	0.01214	0.01229	0.01244	0.01259	0.00003
0.10	0.01343	0.01311	0.01279	0.01247	-0.00006
PE					
0.00	0.00864	0.00900	0.00937	0.00973	0.00007
0.02	0.00909	0.00903	0.00897	0.00891	-0.00001
0.06	0.01474	0.01474	0.01474	0.01474	-0.00013
0.10	0.00555	0.00659	0.00764	0.00868	0.00021

m_b is the concentration of d-mannitol

Pair and triplet coefficients

The partial molar volume of transfer (ΔV_ϕ^0) and partial molar isentropic compression of transfer (ΔK_ϕ^0) can be calculated using the given equation, where A represents glycol ethers, B represents d-mannitol, and m_B is the molality of the aqueous d-mannitol solution. The interaction between the glycol ethers and d-mannitol is characterized by pair and triplet interaction coefficients, denoted by V_{AB} , V_{ABB} , K_{AB} , and K_{ABB} , which are listed in **Table S-IV** and calculated by the undermentioned formula-

$$\Delta V_\phi^0(\text{water to aqueous d- Mannitol solution}) = 2V_{AB}m_B + 3V_{ABB}m_B^2 \quad (\text{Seq 8})$$

$$\Delta K_\phi^0(\text{water to aqueous d- Mannitol solution}) = 2K_{AB}m_B + 3K_{ABB}m_B^2 \quad (\text{Seq 9})$$

The separation of effects in liquid mixtures is examined using the McMillan and Mayer hypothesis, which has been later studied by Krishnan-Friedman, and Franks.²³⁻²⁵ At all temperatures for all glycol ethers, the triplet interaction

coefficient V_{ABB} is negative and the pair interaction coefficient V_{AB} is positive. For, the pair interaction coefficient K_{AB} is positive; however, K_{ABB} it is negative for both glycol ethers, except at 303.15 K for PE. According to this hypothesis of co-sphere, the water is released and enters the bulk, changing the volume.⁴⁻⁵ Given that the water molecules are grouped in distinct structures, the change is positive when the bulk is more structured than the co-sphere and it is negative when the reverse is true. Additionally, because the interaction that took place was a non-bonding one, the water molecules from the hydration co-spheres are released into the bulk. The dominance of pair-wise interactions in the current investigation is established by the higher positive values of the pair interaction coefficients in the mixture of (mannitol + water + PE/ BE) compared to the triplet interaction coefficients.^{26, 27}

Table S-IV. Pair (V_{AB} , K_{AB}) and triplet (V_{ABB} , K_{ABB}) of (BE/PE) in aqueous solutions of d-Mannitol at different temperatures

T/K	$V_{AB} * 10^6$ ($m^3 \cdot mol^{-2} \cdot kg$)	$V_{ABB} * 10^6$ ($m^3 \cdot mol^{-3} \cdot kg^2$)	$K_{AB} * 10^6$ ($m^3 \cdot mol^{-2} \cdot kg \cdot GPa^{-1}$)	$K_{ABB} * 10^6$ ($m^3 \cdot mol^{-3} \cdot kg^2 \cdot GPa^{-1}$)
BE				
288.15	2.02	-4.08	4.35	-8.04
293.15	1.97	-3.75	3.78	-4.86
298.15	1.90	-3.95	4.02	-4.66
303.15	2.21	-5.53	3.61	-1.87
PE				
288.15	2.70	-7.10	3.78	-5.33
293.15	2.68	-7.29	3.22	-2.21
298.15	2.49	-7.12	3.47	-2.04
303.15	1.97	-3.06	3.06	0.71

T/K is the temperature

REFERENCES

1. N. Chakraborty, K. C. Juglan, H. Kumar, *J. Chem. Thermodynamics* **154** (2021) 106326 (<https://doi.org/10.1016/j.jct.2020.106326>)
2. Ali, P. Bidhuri, S. Uzair, *Indian J Phys.* **88** (2014) 715 (<https://doi.org/10.1007/s12648-014-0461-2>)
3. N. Chakraborty, K. C. Juglan, H. Kumar, *J. Mol. Liq.* **337** (2021) 116605 (<https://doi.org/10.1016/j.molliq.2021.116605>)
4. H. Kumar, M. Singla, R. Jindal, *Monatsh Chem.* **145** (2014) 1063 (<https://doi.org/10.1007/s00706-014-1183-z>)
5. P. Pradhan, R.S. Sah, M.N. Roy, *J. Mol. Liq.* **144** (2009) 149 (<https://doi.org/10.1016/j.molliq.2008.11.001>)
6. S. K. Lomesh, M. Bala, D. Kumar, *J. Mol. Liq.*, **289** (2019) 109479 (<https://doi.org/10.1016/j.molliq.2018.08.034>)
7. J. Wawer, J. Krakowiak, W. Grzybkowski, *J. Chem. Thermodyn.* **40** (2008) 1193 (<https://doi.org/10.1016/j.jct.2008.04.008>)
8. Lowe, J. Southern, *Lett. App. Microbiol.* **18** (1994) 115 (<https://doi.org/10.1111/j.1472-765X.1994.tb00820.x>)

9. M. S. Raman, G. Amrithaganesan, *Indian J. Phys.* **78**(12) (2004) 1329
10. D. Chawla, N. Chakraborty, K. C. Juglan, H. Kumar, *Chem. Papers* **75** (2021) 1497 (<https://doi.org/10.1007/s11696-020-01403-y>)
11. P. K. Banipal, S. Arti, T. S. Banipal, *J Chem Thermodyn.* **60** (2015) 1023 (<https://doi.org/10.1021/je500886a>)
12. X. U. Wang, R. Fu, Y. Gua, L. Rusin, *J. Mol. Liq.* **197** (2014) 73 (<https://doi.org/10.1016/j.molliq.2014.04.028>)
13. H.L. Friedman, C. Krishnan, *J. Solut. Chem.* **2** (1973) 119 (<https://doi.org/10.1007/BF00651969>)
14. S. Li, W. Sang, R. Lin, *J. Chem. Thermodyn.* **34** (2002) 1761 ([https://doi.org/10.1016/S0021-9614\(02\)00125-8](https://doi.org/10.1016/S0021-9614(02)00125-8))
15. Salabat, L. Shamshiri, F. Sahrakr, *J. Mol. Liq.* **118** (2005) 67 (<https://doi.org/10.1016/j.molliq.2004.07.014>)
16. K. Mishra, J. C. Ahluwalia, *J. Phys. Chem.* **88** (1984) 86 (<https://doi.org/10.1021/j150645a021>)
17. L. G. Hepler, *Can J Chem.* (1969) (<https://doi.org/10.1139/v69-762>).
18. Naseem, I. Arif, M. A. Jamal, *Arab. J. Chem.* **14** (2021) 103405 (<https://doi.org/10.1016/j.arabjc.2021.103405>)
19. K. Nain, R. Pal, *J. Chem. Thermodyn.* **60** (2013) 98 (<https://doi.org/10.1016/j.jct.2013.01.008>)
20. R. A. Miranda- Quintana, J. Smiatek, *Chem. Phys. Chem.* **21** (2020) 2605 (<https://doi.org/10.1002/cphc.202000644>)
21. Z. Yan, X. Wen, Y. Kang, S. Zhang, S. Wu, *J. Chem. Thermodyn.* **93** (2016) 172 (<https://doi.org/10.1016/j.jct.2015.10.004>)
22. F. J. Millero, in: *Structure and Transport Process in Water and Aqueous Solutions*. Horne, R.A. (Ed.), Wiley, New York, 1972
23. W. G. Jr. McMillan, J. E. Mayer, *J. Chem. Phys.* **13** (1945) 276 (<https://doi.org/10.1063/1.1724036>)
24. V. Krishnan, H. L. Friedman, *J Solution Chem.* **2** (1973) 37 (<https://doi.org/10.1007/BF00645870>).
25. F. Franks, M. Pedley, D. S. Reid, *J. Chem. Soc., Faraday Trans.* **1** (1976) (<https://doi.org/10.1039/F19767200359>)
26. N. Chakraborty, K. C. Juglan, H. Kumar, *J. Chem. Thermodyn.* **163** (2021) 106584 (<https://doi.org/10.1016/j.jct.2021.106584>)
27. R. K. Wadi, P. Ramasami, *J Chem Soc.* **93** (1997) 243 (<https://doi.org/10.1039/A604650I>).



J. Serb. Chem. Soc. 89 (11) 1507–1524 (2024)
JSCS–5803

Chemistry educational outcomes and standards in Serbia and Montenegro. Analysis of the teachers' attitudes and high school students' achievements

FILIP STAŠEVIĆ^{1#}, ANDREA BUBANJA², ALEKSANDRA MAKSIMOVIĆ¹
and JELENA ĐURĐEVIĆ NIKOLIĆ^{1#*}

¹University of Kragujevac, Faculty of Science, Kragujevac, Serbia and ²Grammar school „Panto Mališić“, Berane, Montenegro

(Received 27 December 2023, revised 21 February, accepted 9 July 2024)

Abstract: Standards and outcomes-based education led to significant adjustments in school organizations and contributed to the in-depth analysis of teachers' professional identity. This research aimed to examine the chemistry teachers' attitudes in the context of the implementation of the educational outcomes and standards in educational policy and in the school practice, as well as to ascertain the level of accomplished learning outcomes for the selected teaching topic “Lipids”. The research sample included both, chemistry teachers ($N = 4$) and high school students ($N = 172$) from two countries, Serbia and Montenegro. The data were analyzed qualitatively jointly for two countries using mixed-methods research and constant comparison of the data. There are no significant differences in teachers' attitudes as well as in achievements among students between these two educational systems. All teachers emphasized the importance of learning outcomes and standards and confirmed that they help them in organizing lessons and monitoring students' assessments. However, interviewed teachers pointed out the need for support and consideration of teachers' opinions about implementing educational changes. The results obtained on the knowledge test have highlighted that knowledge about “Lipids” among students is not at the expected level.

Keywords: chemistry teaching; educational policies; students' assessments, teachers' perspectives.

INTRODUCTION

Changes in education and educational systems are common occurrences and demand monitoring, examining and analysing in certain ways.¹ Introducing innovation is not an easy process, and the success of the novelty depends on numer-

* Corresponding author. E-mail: jelena.djurdjevic@pmf.kg.ac.rs

Serbian Chemical Society member.

<https://doi.org/10.2298/JSC231227069S>



ous factors.^{2,3} For decades, the Serbian educational system has been criticized as highly centralized, while the most important shortcomings of the chemistry curriculum refer to its extensiveness, generalization and abstraction.^{4–6} Related to this, the educational reforms based on standards and outcomes started in the 2000s⁷ but outcomes were not implemented until 2018/2019 when they were first applied in the first and the fifth grade of primary school and in the first year of general secondary education.^{8–10} Meanwhile, in 2009, the National Education Council of the Republic of Serbia announced educational standards for the end of compulsory education.¹¹ The standards for the end of the first cycle of compulsory education were defined in 2011, whereas the standards of students' achievement for the end of general secondary education and general education subjects in secondary vocational education were created in 2013.^{12,13} In Montenegro educational reforms were also intensively conducted since the 2000s, and along with respecting the principle of individuation, imposed in 2017 the development of curriculum based on learning outcomes.^{14,15} Revised educational programs that included outcomes were put into practice in 2019 for primary and vocational schools, and in 2020 for grammar schools.^{16,17} In both countries, there has been trainings that should help teachers realize education based on standards/learning outcomes.^{18–20} In Serbia, training for the implementation of achievement standards started in 2016 and for outcomes in 2017 both by the Institute for the Improvement of Education and Training. In Montenegro, training began with the realization in 2019–2021 by the Institute for Education of Montenegro. Since then, every year there has been trainings on this theme.

In Serbian and Montenegrin educational systems, outcomes have the same meaning and show the desired and expected results expressed in the form of skills and knowledge that the student possesses at the end of a certain school year.^{21,22} In terms of outcomes, neither quality nor quantity is specified. On the other hand, the crucial quality of implementing standards in educational policy and practice is that they are expressed in terms of measurable students' behavior.^{23,24} In Serbia standards of achievements define the required knowledge, skills and attitudes for solving different social challenges. Accordingly, standards can be understood as both, mandatory and recommendative, depending on the educational context. For example, at the primary school level, it is specified that 80 % of students should achieve chemical knowledge at the basic level of standards of achievement.²⁵ As the standards of achievement for secondary school represent expanded knowledge, skills and attitudes relative to those determined for primary school, it is expected that all high school students should achieve a basic level of standards of achievement.¹¹ In Montenegro, educational standards and outcomes are used interchangeably, and they are set in educational programs for each subject by the Institute for Education of Montenegro, as well as in assessment catalogues, adopted by the National Council for Education.^{26,27}

The choice of a document depends on the teacher since standards/learning outcomes are defined very similarly in both. Both Institutions are part of the Ministry of Education, Science, Culture and Sports.

There are certain similarities but also differences between outcomes and standards. The main similarity is that both define what the student should know at the end of the educational process (the outcomes refer to the end of the school year, and the standards to the end of the educational cycle). The difference is that the outcomes are broader (the teachers could choose teaching methods and how they will present the material) while the standards are limited to a certain extent (teachers receive detailed instructions for work).²⁸ To evaluate students in a useful and correct way, it is necessary to use outcomes and standards. Outcomes show what students learned, while achievement standards show how successful learning was.²⁹

Proper usage of educational outcomes and standards is not a simple activity. For the appropriate management of outcomes and standards, the teacher must understand and know how to apply the outcomes and standards in the right way. Teaching outcomes and standards can help both, teachers to organize teaching that is adequate for the realization of the potential of each student, as well as students and parents as guidelines for them to follow during studying. In all countries, during the creation and implementation of standards, one of the biggest problems was disagreement among experts on what are the most important concepts in certain areas, as well as the content of the standards. Also, there were problems with teachers' training and designing and enforcement of procedures for monitoring and measuring the achievement of standards. Furthermore, in Serbia, there are no chemistry educational outcomes and standards that include knowledge of certain areas, and some basic chemical terms and laws.³⁰

In light of this, the authors wanted to explore how the Serbian and Montenegrin chemistry teachers understand and apply the educational outcomes and standards, as well as to discover the level of accomplished outcomes among high school students for the selected teaching topic. Accordingly, the aim of the research is not to evaluate the reform or any educational change. The authors emphasize that every idea that starts from the creators of educational policy arrives in the classroom, and at the end, the main protagonists are students and teachers. The value of this research lies precisely in including the perspectives of both, teachers and students.

EXPERIMENTAL

Research aims and research questions

The change in teaching based on standards and outcomes led to significant adjustments in school organizations and the perception of teachers' professional identity.³¹ The educational outcomes and standards emphasize the conditions that are prerequisite for unfolding of the learning process. Students cannot have a high level of achievement without qualified teachers

who constantly upgrade their competencies through professional development, adequate time for learning, necessary equipment and materials for learning, and an appropriate school environment. This research aimed to examine the chemistry teachers' attitudes in the context of the application of educational outcomes and standards, as well as to ascertain the level of achieved learning outcomes for the selected teaching topic "Lipids". Furthermore, the paper contrasts teachers' attitudes towards educational outcomes and standards in Serbian and Montenegrin secondary education with the teachers' attitudes in other parts of the world.

Due to strong historical ties education in Serbia and Montenegro is structurally similar. Education in both countries is divided into four cycles: pre-primary, primary, secondary and tertiary.^{21,32} Primary education in Serbia is compulsory, it lasts for eight years, starting from the age of 7, and is divided into two cycles, each one lasting four years. Before primary school, a pre-primary educational period of one year is mandatory. Secondary education is provided in high schools, grammar or vocational. In Montenegro, the duration of primary (compulsory) education is extended to nine years, starting from the age of 6. Nine-year primary education is divided into three cycles, each one lasting three years. General secondary education (grammar schools) is not compulsory and lasts for four years. After the completion of secondary education, students can start education at the tertiary level choosing between high schools of applied studies (lasting 3 years) and universities (Bachelor programs lasting 4–6 years, Master programs lasting 1–2 years and PhD programs lasting 3 years) in both countries. Although the two countries share some educational features and have a similar educational structure, each has an independent educational program. After 2006 each country strived to find its own educational *milieu* (participation in PISA, increase in the number of university graduates, adoption of educational outcomes and standards). The teaching curriculums for the grammar school (general stream of studies) in Serbia and Montenegro include the same content. Students in both states firstly elaborate on general chemistry with thermochemistry (first grade), then inorganic chemistry (second grade), organic chemistry (third grade) and in final year biochemistry (fourth grade). Also, both curriculums propose learning outcomes for each topic and the same number of classes (2) per week. More details about proposed learning outcomes in the curriculum will be given in the section Instrument/Design.

Accordingly, the following research questions were posed:

1. What are the attitudes of chemistry teachers, from Serbia and Montenegro, hold in regard to educational outcomes and standards?
2. To what extent are educational outcomes for the teaching topic "Lipids" which is elaborated in the fourth grade of grammar schools, accomplished in Serbia and Montenegro?
3. What is the difference in the level of accomplished chemistry educational outcomes for the teaching topic "Lipids" between the fourth-grade grammar-school students from Serbia and Montenegro?

Sample/Participants

The research sample included both chemistry teachers and grammar school students. A convenience sampling design was applied for the teachers' sample. The sample size corresponds to the availability of teachers at the moment of research. A heterogeneous sample ($N = 172$) encompassed grammar school students from grammar school in Kragujevac, Serbia ($N = 83$) and grammar school in Berane, Montenegro ($N = 89$). All students attended the 4th grade of the grammar school, the general stream of studies. The curriculum of the two countries encompasses a similar number of lessons per year, 68 in the grammar school in Montenegro and 66 in the grammar school in Serbia. For the topic "Lipids", all four teachers planned 5 lessons and similar learning outcomes, hence, all participants were equipped with

the necessary knowledge and skills for solving the knowledge test. The four teachers, two from both countries, were involved in the research. The sample included 3 female and 1 male chemistry teacher with 10–20 years of teaching experience. Based on years of experience, only one was employed after implementing standards and outcomes-based education, whereas three were in a transition phase and had to adapt to a new concept of education.

Instrument/Design

The data were collected by means of an interview and specially designed knowledge test in the 2022/2023 school year. Two instruments were used for a deeper understanding of the phenomenon of standards- and outcomes-based education. The first should give insight into teachers' perspectives and second unveil how successfully the idea of introducing outcomes was realized from the aspect of improving students' achievements. A semi-structured interview protocol was created to examine teachers' attitudes toward standards- and outcomes-based education. The interviews were conducted in person with each respondent individually, in the schools where the teachers are employed. Participation in interviews was voluntary, and their duration was between 50 and 70 min. both in Serbia and in Montenegro. The participants were guaranteed confidentiality, and interviews were recorded and transcribed. The authors emphasize that the results reported in this paper do not represent all teachers' opinions and practices regarding the implementation of educational outcomes and standards in Serbia and Montenegro. Still, they do provide some information about teachers' attitudes related to the educational standards and outcomes. In order to explore to what extent the educational outcomes for the teaching topic "Lipids" in the fourth grade the two above-mentioned grammar schools are accomplished, a knowledge test was created based on outcomes defined in teachers' lesson plans. Teachers from both schools define and state educational outcomes in their lesson plans, which is not done with the standards, and only for that reason the knowledge test contained questions grounded on outcomes and not standards. The committee of experts (high school chemistry teachers and university chemistry teachers) who were not involved in its design confirmed the instruments validity. Based on the evaluations, the revised items were held in the instrument. The framework formulations of questions from the interview and knowledge test are given in Supplementary material to this paper.

Learning outcomes for all teaching topics for the subject Chemistry could be found in educational documents proposed by corresponding institutions from both states.^{10,26} The teaching curriculum for fourth grade grammar schools (general stream studies) in both countries includes the same content, biochemistry and biologically important compounds. Regarding content, the only difference among curriculums is the period of elaboration on the teaching content. For example, according to the curriculum, students from Montenegro learn about the "Lipids" in November, whereas Serbian students study "Lipids" in April/May. Both curriculums define learning outcomes for each teaching topic but in a different way. In Serbia, outcomes are broadly defined, and teachers must specify them for personal lessons. However, within the Montenegrin document outcomes are already specified. Accordingly, differences in defined outcomes in teachers' personal lesson plans are expected. Learning outcomes for the topic "Lipids" defined by teachers from both schools are given in Supplementary material. The outcomes predicted by teachers from Montenegro are more detailed than outcomes defined by Serbian teachers, which is probably the effect of the curricula they use. Furthermore, noticeable is the difference in the levels of knowledge defined by these outcomes (defines, states, recognizes, knows, connects *vs.* observes, explains, writes, analyses).

The reason for choosing the topic "Lipids" was the presence and role of the selected compounds in daily life, as well as a similar number of lessons regarding this teaching topic in

both schools. A set of questions covered by the instrument was chosen under previously defined learning outcomes by teachers. The instrument was designed with the intention to examine whether students achieve predicted learning outcomes and to what extent. Students should get the necessary knowledge and skills to solve the test within the same number of lessons in both schools. The first category of questions (first two questions) relates to the knowledge about the chemical structure of lipids and covers the following outcomes: “defines lipids according to their chemical composition” and “knows the structure of chemical compounds that make up the composition of triacylglycerol, phospholipids and sphingolipids”. The second category of questions (third and fourth) relates to the role and importance of fats and oils in everyday life. The outcomes that shaped these questions are: “connects the structure of lipids with properties and roles in living organisms” and “analyses the biological role of triacylglycerol, phospholipids and sphingolipids”.

RESULTS AND DISCUSSION

The data were analysed jointly for Serbia and Montenegro, using mixed methods research.³³ The data obtained from the interview were analysed using a thematic analysis approach and the method of constant comparison.^{34,35} Understanding teachers' perceptions of their roles and competencies is critical for designing systems of support that can improve teachers' practices. A lot of attention is devoted to studying the perspective of teachers, taking into consideration that everyday school practice critically depends on teachers' understanding of specified requirements.^{36,37} The results from the knowledge test were analysed qualitatively. Answers were scored as correct, partially correct, wrong, and without answer, and descriptive statistics will be provided in the form of percentages.

Furthermore, this section will describe Serbian and Montenegrin chemistry teachers' responses to questions from interviews in four categories: teachers' perspectives of educational outcomes and standards, teachers' understanding of educational outcomes and standards, teachers' attitudes about the adequacy of educational outcomes and standards and teachers' personal assessment of the implementation of outcomes and standards in teaching. Along with the analysis of the answers, some of the responses of all four teachers will be shown using abbreviations (*e.g.*, CTS1/2-Chemistry Teacher from Serbia 1 and 2; CTM1/2-Chemistry Teacher from Montenegro 1 and 2).

Teachers' perspectives of educational outcomes and standards

The first category of questions was related to teachers' information about the implementation of educational standards and outcomes. Analysis of these responses should give an insight into whether and in what way chemistry teachers were informed about standards and outcomes-based education. Also, the involvement of teachers in the process of creating learning outcomes and standards was examined.

All teachers stated that although they were informed about the outcomes and standards, this was not done in a sufficient and adequate way. The teachers from

Montenegro point out that they were not informed specifically, except through a general lecture by the agent from the Ministry of Education with explanations of how and in what way the standards/learning outcomes can be useful to the teacher. Some of the answers were:

“They informed us about it in such a way, that I remember for a long time I didn't even know how to use standards properly.” (CTM1)

“The standards are something that I remember from the first day of my work experience. To the greatest extent, it was my colleagues who explained to me how learning outcomes and standards work, and because of that, it was easier for me to catch up on things.” (CTM2)

Teachers in Serbia were informed about outcomes and standards through practical training, carried out at the national level. They emphasized that every year there are trainings for novice teachers. One of the teachers particularly emphasized the importance of the training:

“In my opinion, without that training, teachers who are just starting to do this job, would not be able to start working.” (CTS1)

None of the interviewees was involved in the process of creating outcomes and standards. They all were informed about the outcomes and standards only when they were included in educational policy and school practice, which is illustrated by some of the responses:

“Teachers were given the right to vote after the implementation of outcomes and standards, then a public discussion was opened, but then, most of my colleagues and I did not want to comment.” (CTS1)

“As far as I remember, it was only served to us as something ready, it was up to us to adhere to it, no one honestly asked us about our opinion, and even if they did so, it would only have been done pro forma.” (CTM1)

Based on these answers, the authors established that teachers were informed about the introduction of outcomes and standards, but believed that the process of defining and creating standards and outcomes should have been implemented differently.

“Outcomes and standards should have been crafted by teachers who know what the real situation is in schools, not by someone who has no experience as a teacher.” (CTS2)

“The people who are responsible for introducing outcomes and standards should be available to all teachers, to answer any questions that teachers have.” (CTS1)

Reasons for such teachers' perspectives could be changes in education policy without their active participation in creating reforms. The collected results regarding teachers' awareness of educational outcomes and standards and participation in the process of their implementation are in line with the results of prior studies.^{4,38,39} Teachers worldwide generally feel disappointed because they do

not have the opportunity to participate in the creation of standards and because their role is reduced to applying standards that are defined by educational policy makers. As mentioned, the findings of previous studies have shown that one of the ways to successfully overcome these problems is to involve teachers, „practitioners“, in the process of designing standards, instead of just informing them that the standards have been defined and that their task is to apply them in the classroom.^{30,40,41} Also, it is essential to address the quality of teacher instructors because teachers demand well-trained instructors who can disseminate useful information about educational changes and transfer examples of good practice.⁴²

Teachers' understanding of educational outcomes and standards

The second category of questions aimed to unveil teachers' comprehension of learning standards and outcomes. Moreover, this sub-section outlines teachers' understanding of the importance of outcomes and standards and their opinion about their function and purpose. Some of the questions were related to the impact of outcomes and standards on lesson preparation and the usage of the outcomes and standards for monitoring student achievements.

All respondents acknowledged the significance of the outcomes and standards and their necessity for lifelong education. On questions about similarities and differences among outcomes and standards, teachers provided different answers, such as:

“The standards are the framework that determines the lesson plans, while the outcomes are the goal that should be achieved by teaching, at the end of a certain period, such as one particular class.” (CTM2)

“Novice teachers can only learn to apply outcomes and standards properly after a few years, at the beginning it is tough, if not impossible.” (CTS1)

“In my opinion, there should only be either standards or outcomes, in the end, both have the same function.” (CTM1)

Such teachers' opinions are not isolated, since the majority of teachers worldwide, find the implementation of outcomes and standards to be problematic and confusing.^{38,43} Also, teachers expressed concerns about the amount of administrative work required for the teaching profession, which encompasses defining outcomes and standards and their operationalization.^{44,45} These concerns are expected due to very broadly defined learning outcomes in the Serbian teaching curriculum.

All respondents viewed teachers as someone for whom educational standards and outcomes are intended. Some of them stated that through using educational standards and outcomes teachers can monitor the progress of each student as well as organize their lessons. Also, teachers confirmed that with outcomes and standards, they are able to improve their lessons and ensure better achievement of their students. One of the interesting answers was:

“Educational standards and outcomes represent the roof of education, based on them the teacher can see how to build a house, how high and wide, and no house can be functional without a roof.” (CTS1)

They also mentioned the students and the school, as potential users of outcomes and standards, but pointed out that “if the teacher adheres to the outcomes and standards properly, then the results achieved by the school are better” (CTS1). The teacher’s role in the process of accomplishing learning outcomes and standards is important and highlighted in a similar study.⁴⁶

The teaching outcomes and standards eliminate uncertainties among teachers in evaluating students as well as give insight to students and their parents in the evaluation criteria. At the same time, it is easier to compare the marks between students from different schools when educational standards are defined at the national level. An overall positive response from teachers about the impact of educational outcomes and standards on students’ achievements and organization of the teaching process is complementary with results of similar studies.^{4,38,47}

Teachers’ attitudes about the adequacy of educational outcomes and standards

This sub-section is related to the teachers’ perceptions of the adequacy of educational standards and outcomes. The teachers were asked whether they think that the defined standards and outcomes are good or not, how useful they are, and as the most important item, whether education based on standards and outcomes adequately meets the needs of all students.

Summed teachers’ opinions indicate the positive as well as negative sides of standards and outcome-based education. As a positive side, teachers stated that outcome-based education facilitated the planning and realization of teaching and improved monitoring of the progress of each student. The following several answers describe the downside of this form of education:

“They are bad due to not following the development of society, science, the same has been taught for the last who knows how many years.” (CTS2)

“The teaching process must be modernized, the defined standards and outcomes must be constantly revised, and the volume of material must be reduced.” (CTS1)

In earlier studies, teachers reacted differently when confronted with a new curriculum.⁴⁸ However, adequate support could contribute to the teachers’ easy assimilation and accommodation with new pedagogies.⁴⁹ Also, there are plenty of examples of additional materials that show potential to improve the level of students’ understanding, ability to think critically, and level of students’ science literacy.^{50,51} Experiences from countries where teaching standards have been part of educational policy for many years indicate that, for the acceptance of standards by teachers and the inclusion of standards in everyday teaching practice, it is also important how the standards are formulated.⁵² Furthermore, it is important

to understand them and that the way in which they are applied depends on whether the standards will be “a good servant or an evil master”.⁵³

Teachers' personal assessment of the implementation of outcomes and standards in teaching

In this research, the authors explored the teachers' self-assessment of their success in implementing the standards and outcomes. The teachers were asked about the knowledge and skills required for implementing education based on standards and outcomes. Furthermore, teachers' self-assessment of competence to deal with the demands of outcomes-based education was examined. Also, ways of support that teachers see as essential for applying the concept of education based on standards and outcomes in school practice have been identified.

Some of the answers about self-success in the implementation of teaching based on educational standards and outcomes are given below:

“I will be able to assess that at the end of education of one generation, after four years at least.” (CTS2)

“I think that after so many years, I can successfully apply the outcomes and standards, and recognize what is most important for their achievement. Based on the results achieved by the students, I can say that I am on the right path.” (CTM1)

The first response in this sub-section is expected due to the fact one teacher from the sample is a novice, and, hence, in need of support and experience. The teachers believe that they can strengthen their knowledge and skills by constantly revising standards and outcomes and that they should constantly be trained to recognize what is most important for achieving outcomes and standards. On the question about the knowledge and skills required for implementing educational standards and outcomes, one of the teachers explained that “no matter how many years a teacher works in education, no one is ever ready for all pedagogical situations that may occur in class, and hence, support is always welcome” (CTS1). Also, teachers emphasized the need for defining correlation among subjects within outcomes and standards as an assistance for more efficient teaching.

“Several teachers from different subjects should teach the same or similar material in the same time period, this should be acknowledged within outcomes and standards, not just with a verbal agreement between the teachers.” (CTS2)

Based on this, it can be concluded that teachers should also have the competence for cooperation with their colleagues. For successful teaching, with all the changes that are being introduced, it is necessary to strengthen the competencies of the teacher, both the competencies for cooperation with students and for cooperation with other teachers.⁵⁴

Regarding the competencies that need to be strengthened, all of them cited Information and Communication Technologies (ICT) competencies. This finding

overlaps with other natural sciences teachers' opinions and indicates that teachers are interested in the opportunities offered by ICT.⁵⁵ ICT learning tools can be useful for understanding many chemical phenomena. Thus, teachers need adequate support from schools and faculties to use technology in teaching through different pedagogical and technical trainings.

Analysis of the students' achievements on the knowledge test

The data collected with the knowledge test are presented in Table I. The students' achievements on the knowledge test were presented to chemistry teachers and interpreted in tandem with them.

TABLE I. Distribution of answers (%) on the knowledge test; GS – grammar school from Serbia; GM – grammar school from Montenegro

Question No. (Table S-III of the Supplementary material)	Answer							
	Correct		Partially correct		Wrong		Without answer	
	GS	GM	GS	GM	GS	GM	GS	GM
1	12.4	21.7	73.0	61.4	14.6	14.5	–	2.4
2	10.1	16.9	–	–	–	–	89.9	83.1
3	82.0	81.9	18.0	14.5	–	–	–	3.6
4	68.5	69.9	31.5	30.1	–	–	–	–

The first question investigated whether students know how to classify lipids depending on their structure. Based on the given chemical representations, students needed to determine which listed lipids could be saponified. In both grammar schools, students did not show satisfactory knowledge about the structure of lipids. In Serbia, out of a total of 89 students, only 12.4 % of them (11 students) answered correctly, whereas that number was similar in Montenegro, 21.7 % (18 students) of a total of 83 students. Chemistry teachers point out that throughout the elaboration on this topic, they paid little attention to the structure of phospholipids, terpenes and other lipids, whilst they focused on fats and oils. Furthermore, they justify the above-mentioned result with the insufficient number of classes and short class duration. The teacher from Kragujevac especially highlights the period of elaboration on this topic (April/May) as a cause of the low number of correct answers, as during these months students are more focused on preparation for faculty entrance exams. The majority of students partially answered this question correctly and circled only the answer c). A small number of students circled the answer a) and not the answer c).

The second question examined students' knowledge of physical properties of lipids. Students were supposed to give an adequate explanation of the solvation of fatty acids based on their structure. This question had the lowest number of correct answers, in both countries. Based on the obtained data, it can be seen that the majority of students did not attempt to answer this question. The teacher from

Montenegro stated that he did not require students to know this explanation, whereas the teachers from Serbia the low percentage of correct answers explained in the same way as in regard to the previous question, and they pointed out students' lack of interest. Based on correct answers, it can be concluded that this content does not have to be abstract for students, it is only important to connect the previously acquired knowledge with the new one. As an illustration of the previous statement, the authors list the following answers:

“A large hydrocarbon chain is non-polar, so fatty acids dissolve in non-polar solvents and not in water.” and “Fatty acids do not dissolve in water because of their non-polarity.”

With the third question, the authors examined whether students know basic chemical concepts related to real life. Students were asked to state the roles of fats and oils in human organism, as well as to name food sources that are rich in fats and oils. This question had the highest number of correct answers (in both grammar schools over 80 % of students). It should be pointed out also that none of the students answered incorrectly to this question. Mostly, students cited an energetic role, but a majority of students marked also a thermoregulatory role of fats and oils. Almost all students listed food sources that are rich in fats and oils (bacon, cheese, seeds, salmon, flax, almonds, avocados, dairy products, cream, fish oil, butter, fish, nuts, *etc.*). On the other hand, some of them did not mention the role of fats and oils in the human body and, hence, such answers are accepted as partially correct. This result could relate to the abundance of the respective compounds in everyday life. Food packages contain this information, and this topic is often discussed in the media and their social environment. One of the teachers states that this was an “easy question”, because as she says, “as prom night celebration draws nearer, most students go to the gym and know how much they can take into their body, what role food plays in their body, as well as how it affects their weight” (CTS1).

The fourth question is an extension of the previous question. The authors were interested in whether the students could explain why polar bears survive at extremely cold temperatures. About 70 % of students answered this question correctly (in Serbia 68.5 % and in Montenegro 69.9 %), stating that the thermoregulatory role of fat in animal organism is responsible, as well as the role of fat as a heat insulator. Answer such as the following: “Because of the large layer of fat” and similar, are accepted as partially correct, due to this response being correct in a certain way but unspecified. None of the students left the question unanswered or answered incorrectly.

The following figure (Fig. 1) presents the percentages of correct answers of students from both grammar schools on each of the four questions in the knowledge test.

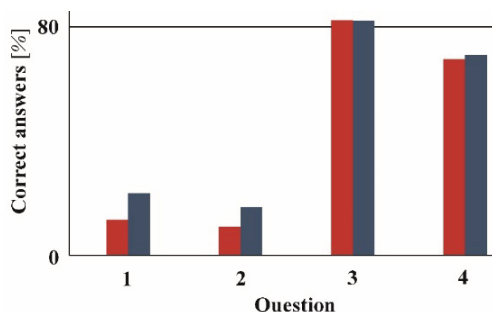


Fig 1. Distribution of respondents' correct answers to questions per grammar school; red – grammar school, Serbia and blue – grammar school, Montenegro.

Fig. 1 suggests that for the two questions (1st and 2nd), defined learning outcomes do not exceed 25 % of achievement among students. On the other hand, outcomes on which questions number 3 and 4 were accomplished by nearly 80 % of students. The level of achieved learning outcomes concerning the structure and properties of lipids is concerning and needs improvement, in contrast to accomplished outcomes about the role and importance of lipids for the living world. Students from the Montenegrin grammar school show somewhat better results but overall, there is no significant difference between the results of students from two states.

The collected data by a knowledge test could relate to earlier similar research that examined the level of achievement standard. Respective research included not only grammar schools but also vocational school students and indicated better achievements among vocational school students, hence, a lower level of accomplished outcomes among students from the two grammar schools could be expected.⁵⁶ Through the preparation of the knowledge test, teachers already knew which questions students would and would not be able to answer correctly. Some reasons cited were that they did not ask the students to know certain content, while for other content, even though it is defined by the plan and program, there is not enough time and classes during one school year. According to the present and other prior research, the teachers are links between the defined outcomes and the students.⁵⁷ The teachers also state that the students did not give correct answers to certain questions as majority of them do not want to study, they lack interest, and if some students learn even the basic things it is a success. There is a study with similar answers from their respondents.⁵⁸ As a problem in the realization of evaluating student achievements, the teachers state that the students are not motivated to work in class, they do not have sufficiently developed work habits, they are not focused on what the teacher presents during the class, and the main problem is that the students learn only to get the desired grade.

CONCLUSION

The conducted study aimed to explore the teachers' attitudes toward educational outcomes and standards in the two countries, Serbia and Montenegro, as

well as to assess the level of students' accomplished outcomes for the teaching topic „Lipids“. The key findings of this research can be summarized as follows. Although research included teachers from two educational systems, Serbian and Montenegrin, there are no significant differences in their attitudes and perspectives. They all point out that it is essential to take into consideration teachers' opinions about implementing educational changes, and thus, make reforms more realistic and easier to implement in everyday school practice. Otherwise, teachers may not consider themselves potential leaders in the process of changing contemporary educational practices. Teachers from both grammar schools emphasize the importance of learning outcomes and standards and affirm that they help them in organizing lessons and monitoring students' assessments. It is important to support teachers in their demands referring to constant revising of standards and outcomes, defining correlation among subjects within outcomes and standards, reinforcing ICT competencies, etc., all in service to more efficient teaching.

The results gathered from the knowledge test have highlighted that knowledge about „Lipids“ among students is not on an enviable level. Responses obtained show that students recognize the importance of chemistry and lipids in everyday life, and their presence in diet and environment. On the other hand, percentage of correct answers was lower on questions related to the physical properties of fats and oils, and their structure. There are no significant differences in achieved accomplishments between students from two countries, Serbia and Montenegro. There could be plenty of reasons for that, similar curriculum, teachers' initial education, pandemic effects and online learning, the individual characteristics of both, teachers and students and the quality of the teaching process. Collected data are in disagreement with teaching curriculum and defined outcomes, and imply the need to make some changes in the two educational systems. Above all, learning activities that promote knowledge acquisition need to be developed. This result can trigger the educational community to inspect the existing curriculum and bring adequate changes to it. The teaching curriculum needs to be innovative and it has to take into account new discoveries, students' needs and the needs of society as well as support students in their professional development.

SUPPLEMENTARY MATERIAL

Additional data and information are available electronically at the pages of journal website: <https://www.shd-pub.org.rs/index.php/JSCS/article/view/12747>, or from the corresponding author on request.

Acknowledgement. This work was supported by the Serbian Ministry of Science, Technological Development and Innovation (Agreement No. 451-03-47/2023-01/200122).

ИЗВОД

ОБРАЗОВНИ ИСХОДИ И СТАНДАРДИ ЗА ПРЕДМЕТ ХЕМИЈА У СРБИЈИ И ЦРНОЈ ГОРИ. АНАЛИЗА СТАВОВА НАСТАВНИКА И ПОСТИГНУЋА УЧЕНИКА

ФИЛИП СТАШЕВИЋ¹, АНДРЕА БУБАЊА², АЛЕКСАНДРА МАКСИМОВИЋ¹ И ЈЕЛЕНА БУРЂЕВИЋ НИКОЛИЋ¹

¹Универзитет у Крагујевцу, Природно-математички факултет, Крагујевац и ²Гимназија „Пантић Малишић“, Беране, Црна Гора

Реформе у образовању су уобичајена појава и захтевају детаљну анализу. Реализација образовања заснованог на стандардима и исходима довела је до прилагођавања школа и наставног процеса и остваривања професионалног идентитета наставника. Ово истраживање је имало за циљ да испита ставове наставника хемије у контексту примене образовних исхода и стандарда, као и да открије ниво остварених исхода учења за одабрану наставну тему „Липиди“. Истраживањем су обухваћени и наставници хемије ($N = 4$) и ученици гимназија ($N = 172$) из две земље, Србије и Црне Горе. Подаци су квантитативно и квалитативно анализирани коришћењем микс-методског приступа истраживања и константног поређења података. Анализом резултата уочено је да нема значајних разлика у ставовима наставника, као ни у постигнућима ученика између две земље. Сви наставници су истакли значај исхода учења и стандарда постигнућа и потврдили да им помажу у организовању часова и праћењу оцењивања ученика. Међутим, истакли су захтеве за подршку и уважавање мишљења наставника о спровођењу образовних реформи. Резултати са теста знања су показали да знање о „Липидима“ код ученика није на очекиваном нивоу.

(Примљено 27. децембра 2023, ревидирано 21. фебруара, прихваћено 9. јула 2024)

REFERENCES

1. A. Hargreaves, A. Lieberman, M. Fullan, D. Hopkins, *Second International Handbook of Educational Change*, Springer, Berlin, 2009 (<https://doi.org/10.1007/978-90-481-2660-6>)
2. D. K. Cohen, H. C. Hill, *Learning policy: When state education reform works*, Yale University Press, New Haven, CT, 2001
3. D. A. Spencer, *Educ. Res.* **25** (1996) 15 (<https://doi.org/10.2307/1177154>)
4. J. Radišić, J. Raković, N. Pantić, J. Marković, A. Maksimović, M. Marković, in *Research, Policy and Practice in Teacher Education in Europe*, J. Madalinska-Michalak, H. Niemi, S. Chong, Eds., University of Lodz, Lodz, 2012, p. 223
5. P. Rado, *Governing Decentralized Education Systems: Systemic Change in South Eastern Europe*, Open Society Foundations, Budapest, 2010
6. L. J. Dull, *Comp. Educ. Rev.* **56** (2012) 511 (<https://doi.org/10.1086/664993>)
7. *The national core curriculum for general education*, Ministry of Education and Sports, Belgrade, Serbia, 2003 (in Serbian)
8. *Curriculum for the first grade of compulsory education and upbringing (10/2017-1, 12/2018-1)*, Official Gazette, Belgrade, Serbia (<https://www.pravno-informacioni-sistem.rs/SlGlasnikPortal/eli/rep/pg/ministarstva/pravilnik/2017/10/1/reg>) (6.11.2023) (in Serbian)
9. *Curriculum for the fifth grade of compulsory education and upbringing (15/2018)*, Official Gazette, Belgrade, Serbia (<https://www.pravno-informacioni-sistem.rs/SlGlasnikPortal/eli/rep/pg/ministarstva/pravilnik/2018/15/2/reg>) (6.11.2023) (in Serbian)

10. *Curriculum for the general secondary education and upbringing (12/2018)*, Official Gazette, Belgrade, Serbia (<https://www.pravno-informacioni-sistem.rs/SlGlasnikPortal/eli/rep/pg/ministarstva/pravilnik/2017/10/1/reg>) (6.11.2023) (in Serbian)
11. *General standards of achievement for the end of compulsory education*, Institute for the Evaluation of the Quality of Education, Belgrade, Serbia, 2009 (in Serbian) (<https://ceo.edu.rs/стандарди-у-образовању/>) (6.11.2023)
12. *General standards of achievement for the end of the first cycle of compulsory education*, Institute for the Evaluation of the Quality of Education, Belgrade, Serbia, 2011 (in Serbian) (<https://ceo.edu.rs/стандарди-у-образовању/>) (6.11.2023)
13. *General standards of achievement for the end of general secondary education and upbringing and secondary vocational education and education in the field of general education subjects for the subject – Chemistry*, Institute for the Evaluation of the Quality of Education, Belgrade, Serbia, 2013 (in Serbian) (<https://ceo.edu.rs/стандарди-у-образовању/>) (6.11.2023)
14. Z. Lalović, *Assessment in the function of student development and improvement of teaching and learning in school*, Institute for Education, Podgorica, Montenegro, 2020 (ISBN 978-9940-24-078-3) (in Serbian)
15. V. Mićanović, *J. Elem. Educ.* **12** (2019) 245 (<https://doi.org/10.18690/rei.12.3.245-265.2019>)
16. *Work report for 2019 (01/1-077/20-122/1)*, Institute for Education, Podgorica, 2020 (<https://wapi.gov.me/download-preview/8139a44a-aced-4b5e-a43b-66d2a6408ff4?version=1.0>) (8.4.2024) (in Serbian)
17. *Work report for 2020 (01/1-077/21-99/1)*, Institute for Education, Podgorica, 2021 (<https://wapi.gov.me/download/d3cc484f-58ce-400b-89ba-4076a1eb2eb1?version=1.0>) (8.4.2024) (in Serbian)
18. *Institute for the Improvement of Education and Training, Ministry of Education, Science and Innovation (150-00-6/2016-06)* (<https://zuov.gov.rs/obuka-za-realizaciju-nastave-orijentisane-ka-ishodima-ucenja-21-11-2022-godine/>) (8.4.2024.) (in Serbian)
19. *Institute for the Improvement of Education and Training, Ministry of Education, Science and Innovation (150-00-6/2016-06)* (<https://shorturl.at/uwAI2>) (8.4.2024.) (in Serbian)
20. *Professional program catalog teacher trainings for the school year 2019/20 and 2020/21*, Institute for Education, Podgorica, 2019 (<https://profesionalnirazvoj.edu.me/2024/01/23/katalozi-programa-strucnog-usavrsavanja-nastavnika-ca/>) (8.4.2024.) (in Serbian)
21. *Referencing the Montenegrin Qualifications Framework to the European Qualifications Framework for Lifelong Learning and the Qualifications Framework for the European Higher Education Area*, Ministry of Education, 2014 (<https://europa.eu/europass/system/files/2020-06/Montenegrin%20Referencing%20Report.pdf>) (13.11.2023)
22. B. Tomašević, D. Trivić, S. Bojović, *Pedagogija* **63** (2008) 261
23. A. Maksimović, *Nastava vasp.* **65** (2016) 279 (<https://doi.org/10.5937/nasvas1602279m>)
24. D. Trivić, R. Jankov, M. Ranđelović, M. Marković, G. Zindović-Vukadinović, *Nastava vasp.* **56** (2007) 30
25. D. Trivić, R. Jankov, M. Ranđelović, V. Vukotić, M. Marković, R. Kovačević, M. Nikolić, *Educational standards for the end of compulsory education for the subject - chemistry*, Ministry of Education, Science and Technological Development of the Republic of Serbia, Belgrade, Serbia, 2010 (ISBN 978-86-86715-22-7) (in Serbian)

26. *Curriculum for the fourth grade of general secondary education and upbringing*, Institute for Education, Podgorica, 2020, (<https://www.gov.me/dokumenta/0b6e9e24-768e-4237-a5c7-4e1434cfc992>) (8.4.2024.) (in Serbian)
27. *Examination center*, Ministry of Education, Science and Innovation (<https://iccg.co.me/>) (8.4.2024.) (in Serbian)
28. A. Maksimović, *Inov. Nastavi* **30** (2017) 98 (<https://doi.org/10.5937/inovacije1702098M>)
29. N. Havelka, E. Hebib, A. Baucel, *Assessment for Student Development: A Handbook for Teachers*, Center for evaluation of quality in education and upbringing, Belgrade, 2003 (in Serbian)
30. A. Pešikan, *Inov. Nastavi* **25** (2012) 5 (<http://www.inovacijeunastavi.rs/wp-content/uploads/arhiva/2012/Inovacije-1-12.pdf>)
31. S. J. Ball, *J. Educ. Policy* **18** (2003) 215 (<https://doi.org/10.1080/0268093022000043065>)
32. *OECD Reviews of Evaluation and Assessment in Education: Serbia* (<https://www.oecd-ilibrary.org/sites/72483fab-en/index.html?itemId=/content/component/72483fab-en>) (13.11.2023)
33. R. B. Johnson, A. J. Onwuegbuzie, *Educ. Res.* **33** (2004) 14 (<https://doi.org/10.3102/0013189X033007014>)
34. V. Braun, V. Clarke, *Qual. Res. Psychol.* **3** (2006) 77 (<https://doi.org/10.1191/1478088706qp063oa>)
35. S. B. Merriam, *Qualitative research and case study applications in education*, Jossey-Bass, San Francisco, CA, 1998
36. A. Hargreaves, P. Woods, *Classrooms and Staffrooms: The Sociology of Teachers and Teaching*, Routledge, London, 1984 (<https://doi.org/10.4324/9780367823221>)
37. T. Ferguson, C. Rooft, L. D. Cook, *Environ. Educ. Res.* **27** (2021) 1343 (<https://doi.org/10.1080/13504622.2021.1921113>)
38. A. Maksimović, I. Ćosić, *Psihološka istraživanja* **22** (2016) 189 (<https://doi.org/10.5937/PSISTRA22-20024>)
39. J. Pieters, J. Voogt, N. P. Roblin, *Collaborative Curriculum Design for Sustainable Innovation and Teacher Learning*, Springer, Berlin, 2019 (<https://doi.org/10.1007/978-3-030-20062-6>)
40. D. Stanković, I. Đerić, V. Milin, *J. Inst. Educ. Res.* **45** (2013) 86
41. N. Vujisić Živković, J. D. Vranješević, *Inov. Nastavi* **32** (2019) 13 (<https://doi.org/10.5937/inovacije1903013V>)
42. J. Teodorović, D. Stanković, B. Bodroža, V. Milin, I. Đerić, *Educ. Assess. Evaluation Account.* **28** (2016) 347 (<https://doi.org/10.1007/s11092-015-9221-x>)
43. D. Malinić, Đ. Komlenović, J. Stanišić, *Nastava Vasp.* **62** (2013) 576
44. S. Horvat, V. Popović, D. Rodić, T. Rončević, *J. Serb. Chem. Soc.* **88** (2023) 793 (<https://doi.org/10.2298/JSC220822039H>)
45. B. Tomašević, D. Trivić, *Pedagogija* **4** (2014) 605
46. V. F. Savec, B. Urankar, M. Aksela, I. Devetak, *J. Serb. Chem. Soc.* **82** (2017) 1193 (<https://doi.org/10.2298/JSC161221083S>)
47. Đ. Komlenović, D. Malinić, J. Stanišić, *Nastava vasp.* **63** (2014) 401
48. R. Dolfing, A. Bulte, A. Pilot, J. D. Vermunt, *Res. Sci. Educ.* **42** (2012) 567 (<https://doi.org/10.1007/s11165-011-9211-z>)
49. R. Dolfing, G. T. Prins, A. M. W. Bulte, A. Pilot, J. D. Vermunt, *Sci. Teach. Educ.* **105** (2020) 127 (<https://doi.org/10.1002/sce.21603>)
50. J. Korolija, S. Rajić, M. Tošić, Lj. Mandić, *J. Serb. Chem. Soc.* **80** (2015) 1567 (<https://doi.org/10.2298/JSC150522072K>)

51. K. Putica, D. D. Trivić, *Chem. Educ. Res. Pract.* **17** (2016) 172 (<https://doi.org/10.1039/C5RP00179J>)
52. V. Klenowski, *Oxf. Rev. Educ.* **39** (2013) 36 (<https://doi.org/10.1080/03054985.2013.764759>)
53. A. Baucal, *Inov. Nastavi* **26** (2013) 7 (<http://www.inovacijeunastavi.rs/wp-content/uploads/Inovacije3-13/01-Baucal.pdf>)
54. N. Zobenica, A. Stipančević, *Pedagoška stvarnost* **63** (2017) 107 (<https://doi.org/10.19090/ps.2017.2.107-119>)
55. M. Aksela, J. Lundell, *Chem. Educ. Res. Pract.* **9** (2008) 301 (<https://doi.org/10.1039/B818464J>)
56. F. Stašević, N. Miletić, J. Đurđević Nikolić, I. Gutman, *J. Serb. Chem. Soc.* **88** (2023) 343 (<https://doi.org/10.2298/JSC211126083S>)
57. H. C. Hill, M. Chin, *Am. Educ. Res. J.* **55** (2018) 1076 (<https://doi.org/10.3102/0002831218769614>)
58. B. Tomašević, K. Putica, D. Trivić, *Hemijski pregled* **57** (2016) 99.



SUPPLEMENTARY MATERIAL TO
**Chemistry educational outcomes and standards in Serbia and
Montenegro. Analysis of the teachers' attitudes and high school
students' achievements**

FILIP STAŠEVIĆ¹, ANDREA BUBANJA², ALEKSANDRA MAKSIMOVIĆ¹
and JELENA ĐURĐEVIĆ NIKOLIĆ^{1*}

¹University of Kragujevac, Faculty of Science, Kragujevac, Serbia and ²Grammar school
„Panto Mališić“, Berane, Montenegro

J. Serb. Chem. Soc. 89 (11) (2024) 1507–1524

TABLE S-II. Defined learning outcomes for the subject Chemistry, topic “Lipids” per a school

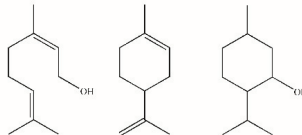
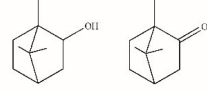
Educational outcomes	
Grammar school in Serbia	Grammar school in Montenegro
-defines lipids according to their chemical composition; -states the role of fats, oils and waxes; -recognizes biologically important compounds as reserve building and energy value compounds; -knows the meaning of essential fatty acids; -knows food sources of biologically important compounds; -connects the structure of lipids with properties and roles in living organisms.	-knows the structure of chemical compounds that make up the composition of triacylglycerols, phospholipids and sphingolipids; -observes and explains experiments (acid-base hydrolysis of fats, acrolein test, and proving cholesterol); -writes the chemical formula of cholesterol and describes its important metabolites; -analyses the biological role of triacylglycerol, phospholipids and sphingolipids; -presents on the topic: "Fats and oils in the diet - advantages and disadvantages".

* Corresponding author. E-mail: jelena.djurdjevic@pmf.kg.ac.rs

TABLE S-II. Framework formulations of questions from the interview

Questions
<p>Are you informed about educational standards and outcomes? How are you informed about the changes that have occurred during the transition to standards and outcomes-based education? Were teachers sufficiently involved in the process of determining standards and student achievement outcomes? Why do you think so?</p> <p>From your point of view, what is the main purpose of implementing educational standards and outcomes? What innovations bring the application of educational standards and outcomes? Do you consider the implementation of outcomes and standards as a positive change in the education process? In your opinion, why they are good or bad?</p> <p>Teaching should enable the realization of the potential of each student. Do educational standards and outcomes enable this? What is the main intention of stating educational standards and objectives? Who do you think is most responsible for fulfilling the defined outcomes and then the standards?</p> <p>Who benefits from education based on educational standards and outcomes? In what way? Do you think that you are successful/unsuccessful in implementing teaching based on standards and outcomes?</p>

TABLE S-III. Question from the knowledge test

Question No.	Question
1.	<p data-bbox="587 555 1225 582">Based on the given structures, which lipids can be saponified?</p> <div data-bbox="582 616 1236 1064"> <p>a)</p> $\begin{array}{c} \text{CH}_2-\text{O}-\overset{\text{O}}{\parallel}{\text{C}}-(\text{CH}_2)_{16}-\text{CH}_3 \\ \\ \text{CH}-\text{O}-\overset{\text{O}}{\parallel}{\text{C}}-(\text{CH}_2)_{14}-\text{CH}_3 \\ \\ \text{CH}_2-\text{O}-\overset{\text{O}}{\parallel}{\text{C}}-(\text{CH}_2)_7-\text{CH}=\text{CH}-(\text{CH}_2)_7-\text{CH}_3 \end{array}$ <p>b)</p>  <p>c)</p> $\begin{array}{c} \text{CH}_3-\text{O}-\overset{\text{O}}{\parallel}{\text{P}}(\text{OH})-\text{CH}_2-\text{CH}_2-\text{N}(\text{CH}_3)_2 \\ \\ \text{CH}-\text{NH}-\overset{\text{O}}{\parallel}{\text{C}}-\text{R} \\ \\ \text{CH}_2-\text{CH}=\text{CH}-(\text{CH}_2)_{12}-\text{CH}_3 \end{array}$  </div>
2.	Based on the chemical structure of fatty acids, explain why they dissolve in non-polar solvents and not in water.
3.	What is the main role of fats and oils in our body? List a few food sources that are rich in fats and oils.
4.	Polar bears can survive in extreme cold. One of the reasons is?